The Geological Evolution and Regional Significance of the Mesozoic to Tertiary Païkon Massif, Northern Greece.

Sally A. M. Brown

Thesis submitted for the degree of Doctor of Philosophy

University of Edinburgh

1997



DECLARATION

I declare that this thesis has been written by myself and is the result of my own research, except where contributions have been stated and duly acknowledged.



SALLY A. M. BROWN

ABSTRACT

This thesis investigates a critical part of the Tethyan orogenic system in northern Greece and, based on new stratigraphic, structural, sedimentological and geochemical data, a new tectonic model for the area is proposed. The main unit investigated is the Païkon Massif which is situated centrally within the Vardar/Axios zone of the Internal Hellenides, which is part of the Alpine-Himalayan belt. The area is bounded to the west and east by ophiolitic units of the Almopias (western Vardar/Axios) and Peonias (eastern Vardar/Axios) subzones, respectively. During the break-up of the northern margin of Gondwana in the Permo-Triassic, the Païkon Massif formed the western margin of the Serbo-Macedonian continental unit, where a deep-water mixed carbonate-clastic slope succession (the Gandatch Formation) accumulated. At this time the Serbo-Macedonian zone was bordered to the west by the Triassic-Jurassic Almopias Ocean.

Inferred onset of eastward subduction of the Almopias Ocean beneath the western margin of Serbo-Macedonia (Middle Jurassic) led to the eruption of Island Arc Tholeiites, which are basic to intermediate in composition at their base and become progressively more acidic upwards. A relatively wide Almopias Ocean is envisaged. Back-arc spreading is believed to have generated the Guevgueli back-arc basin (Peonias subzone) in the late-Middle to Late Jurassic, separating the Païkon Massif from its parent continent, leaving a remnant arc in its wake (the Chortiatis Group of the Circum-Rhodope zone). Continued subduction culminated in collision of the Pelagonian continental unit with the southern margin of Eurasia. Regional contractional (Eohellenic) deformation ensued and emplaced the Guevgueli Ophiolite westward onto the Païkon Massif. Deep burial of the Païkon Massif at this time is recorded by blueschist to upper greenschist facies mineral assemblages and pervasive ductile folding and fabric development (D1).

A switch to inferred extensional/transtensional tectonics (E0 - pre-Kimmeridgian) exhumed the Païkon blueschists which were exposed at the surface by Kimmeridgian times, and overlain by the shallow-water Khromni Limestones. E0 extension generated inferred transtensional pull-apart basins on either side of the Païkon Massif (i.e. the Meglenitsa and western Guevgueli Ophiolites). Subsequent tectonic uplift and/or regression induced a switch in sedimentation from marine to continental and the fluvial Ghrammos Formation was then deposited. These clastics were transgressed in the Aptian/Albian by a shallow-

water carbonate platform which persisted until the Turonian (the Cretaceous Transgressive Limestones). Renewed regional extension in the Turonian (E1) resulted in platformal collapse, immediately preceded by flexural uplift, marked by the deposition of the deep-water Buff Pelagic Carbonates. These were then followed by foreland basin-type sediments of the Tchouka Flysch which were deposited as a result of Tertiary compression (D2 - Neohellenic event). Final suturing of the Pelagonian continental block with southern Eurasia initiated this contractional tectonic regime across the Internal Hellenides. The Païkon Massif underwent simultaneous bi-vergent brittle compression due to overthrusting by the Guevgueli and Meglenitsa Ophiolites on both its eastern and western margins, respectively. The Païkon Massif was folded into a large anticline during D2, characterised by west-vergent structures on its eastern flank and east-vergent structures on its western flank. Later in the Tertiary (pre-Eocene), suturing of the Pindos ocean to the west instigated dextral transpressional shear along the Païkon-Guevgueli and Pelagonian-Almopias contacts (D3).

Further north, the Voras Massif holds a key position along the border between Greece and former Yugoslavia and contains invaluable geological information concerning the regional evolution of the Internal Hellenides. The Voras Massif documents a complete transect through the Pelagonian, Almopias and Païkon zones, exposed directly to the south, and is unlikely to be a far-travelled nappe of Peonias and Serbo-Macedonian zone affinity as previously suggested. Finally, new evidence from the Païkon Massif and the Voras Massif are integrated into a revised regional tectonic synthesis of the area of study in an Eastern Mediterranean context.

ACKNOWLEDGEMENTS

I would firstly like to thank my supervisors, Alastair Robertson and John Dixon, for all their help and guidance both in the field and in Edinburgh. Thanks particularly to Alastair for tirelessly reading and re-reading each page of this thesis and to John for teaching me about the machanics of a Volkswagen Golf.

This thesis was funded by the Natural Environment Research Council, without whose backing this project, and many enjoyable trips to Greece, would not have been possible. Additional thanks must go to the manager and staff of the Royal Bank of Scotland in Nairn, whose co-operation made my financial life as a postgraduate student significantly easier.

Many people have contributed to work in this thesis. In particular I am grateful to Dr Sarandis Dimitriadis (Thessaloniki University) who helped considerably in the field and who has been a good friend in Greece; Dr Brian Rosen (Natural History Museum) for his assistance with coral identification; Dr Taniel Danelian (Edinburgh University) for his help and advice concerning radiolarian extraction and identification and Professor Hsin Yi Ling (Illinois University) for his on-going help with radiolarian identification.

A large number of people from the Department of Geology and Geophysics at Edinburgh University have also been invaluable during the course of this project and none more than Gordon Waugh. Gordon has been wonderful and I am sure that certain aspects of this PhD, both in the field and in Edinburgh, would have been much more difficult without his constant assistance. Much thanks also to Roger Scrutton, Ian Parsons, Dodie James, Yvonne Cooper, Mike Hall and Geoff Angel who have all helped considerably, as have Peder Aspen, Diana Baty, Alex Jackson, Helena Jack, Nicky McEwan, Heather Hooker, Lisa Thorburn and Simon Harley. Enormous thanks to you all.

Some of the most important people to help during this project, and who cannot really be thanked enough for their time, patience, encouragement and company are those who field assisted for me during some long, hot field seasons in Greece. Gordon - thanks for drinking my share of Ouzo at "Why Not", I would have done considerably less fieldwork otherwise. Ian - thanks for all your help, advice and friendship and for introducing me to Chamonix. Mike B - the best tyre-changer and early morning tea-maker I have ever met; it wasn't your fault that the car kept breaking down....honest ! Ned - your spider deterrent is second to none, a transferable

skill that will certainly get you places. Dave - I bet you never want to see another compass-clino in your life; thanks for getting up early each morning and for Eastern Europe.

In Greece, the friends I made will never be forgotten for their help, kindness and hospitality. Sitiri and Tasu are among the most wonderful people I have met and field work would have been much less enjoyable, and tasty, had they not been around. Harris, Jim, Panegiotis, Fotes, Cristos and Vangelis are also thanked very much for their company during many evenings in cafe-pub "Why Not" and cafe "Hobby", and for a constant fruit supply.

Coleen and Nicky have been very dear friends throughout my PhD and their support and joviality have kept me going through thick and thin. Both are also thanked for their company at various times in Greece and countless times in Edinburgh. Coleen and Ian are also thanked for the Baffin Expedition, which I will never forget, and for being great flat-mates.

Karen and Pauline are worthy of considerable gratitude for managing to share a very small office with someone as messy as I am, and for being great friends. A special thankyou also to Alan for much-needed coffee breaks and for inviting me on a fantastic trip to Turkey. My office-mates have been the best anyone could hope for - thankyou Harriet, Babs, Jon, Chris, Mark H, Mark L, Paula, Allison and Keerthi. Big thanks also to Kevin for chumming me to Alien Rock so many times (in the name of stress relief, of course), and to all the other folk who have made life great; Chil, Sandra G, Paul & Allison, J.T., Dianne, Amy, Alyson, Phil, Amanda, Clare, Ally, Rodney and all the inmates of the Mouse-house. I apologise profusely if there is anyone I have forgotten!

It is impossible to express how grateful I am for all the help I have had recently from Mike. I know that the final stages of thesis-production would have been so much more stressful and lengthy without all the time and effort that he contributed, not to mention the moral-support and bananas. Thankyou so, so much.

This thesis is dedicated to my family (Mum, Dad, Sandra, Chloe, Jim, Meg, Susan and Michael) who always have an endless supply of love, encouragement and support and who have continued to have faith in my ability to finish this task. I could never have done this without you all. Finally, a big thankyou prod to "Wee Jock" for giving me the best incentive in the world to finish!

CONTENTS

CHAPTER 1 - INTRODUCTION **1**

1.1 Location and Geographical Setting of the Study Area **1**
1.2 Regional Geological Setting **4**
1.2.1 Palaeogeographic Reconstructions of the Tethyan Belt **4**
1.2.2 The Isopic Zones of the Hellenides **8**
1.2.3 The External Hellenides **8**
Pre-Apulian zone **8**
Ionian zone **8**
Gavrovo-Tripolitza zone **9**
Pindos zone **9**
Parnassus zone **9**
Sub-Pelagonian/Othris/Maliac zone **10**
1.2.4 The Internal Hellenides **10**
Pelagonian zone **10**
Vardar/Axios zone **11**
Circum-Rhodope zone **12**
Serbo-Macedonian zone **13**
Rhodope zone **13**
1.2.5 The Tectonic Zones of Turkey **14**
1.3 The Païkon Massif **15**
1.3.1 Previous Work in the Païkon Massif **15**
1.3.2 Geotectonic Models for the Evolution of the Païkon Massif **16**
The Thrust Imbricate Model - Mercier (1968) **16**
The Tectonic Window Model - Godfriaux and Ricou (1991) **18**
The Multi-shell Model - Bonneau et al. (1994, in press) **18**
1.3.3 Project Rationale, Objectives and Methodology **19**
Rationale and Objectives **19**
Methodology **21**

CHAPTER 2 - STRATIGRAPHY **22**

2.1 Previous Stratigraphy **22**
2.2 Revised Stratigraphy **27**
2.2.1 Gandatch Formation **27**
2.2.2 The Païkon Volcanic Group - Livadia Formation **32**
2.2.3 Gropi Formation **33**
2.2.4 The Païkon Volcanic Group - Kastaneri Formation **37**
2.2.5 Khromni Limestones **38**
2.2.6 Ghrammos Formation **39**
2.2.7 Cretaceous Transgressive Limestones **43**
2.2.8 Buff Pelagic Carbonates **46**
2.2.9 Tchouka Flysch **48**
2.3 Discussion and Conclusions **49**

CHAPTER 3 - LITHOLOGICAL DESCRIPTIONS 52

3.1 Introduction 52
3.2 Previous Work 53
3.3 Basement Lithologies 53
3.4 Gandatch Formation 55
3.4.1 Introduction 55
3.4.2 Stratotype 1: Marbles 57
3.4.3 Stratotype 2: Interbedded Marbles and Schists 58
3.4.4 Stratotype 3: Schists 59
3.4.5 Stratotype 4: Calcirudites 63
3.4.6 Discussion 63
3.5 The Païkon Volcanic Group: Livadia Formation 68
3.5.1 Introduction 68
3.5.2 Volcanics 69
3.5.3 Volcaniclastics 71
3.5.4 Discussion 72
3.6 The Païkon Volcanic Group: Kastaneri Formation 74
3.6.1 Introduction 74
3.6.2 Volcanics 75
3.6.3 Volcaniclastics 79
Tuffs and lapilli-tuffs 81
Chlorite-mica schists 84
Breccio-conglomerates 84
3.6.4 Plutonic Rocks 86
3.6.5 Interbedded Carbonates 86
3.6.6 Discussion 87
3.7 Khromni Limestones 89
3.7.1 Introduction 89
3.7.2 Biomicrites 89
3.7.3 Bioturbated Micrites 92
3.7.4 Coquina Packstones 94
3.7.5 Algal Biomicrites 94
3.7.6 Marls 96
3.7.7 Discussion 96
3.8 Ghrammos Formation 99
3.8.1 Introduction 99
3.8.2 Rudites 102
3.8.3 Arenites 106
3.8.4 Siltstones and Mudstones 106
3.8.5 New Key Localities 106
3.8.6 Discussion 109
3.9 Cretaceous Transgressive Limestones 112
3.9.1 Introduction 112
3.9.2 Palaeontology 113
3.9.3 Facies 116

Calcarenites 118
Biopelmicrites 118
Biomicrites and Sparry-biomicrites 118
Bioclastic-packstones 120
3.9.4 New Key Localities 124
3.9.5 Discussion 128
3.9.6 Transition to Deep-Water Sedimentation 131
3.10 Buff Pelagic Carbonates 131
3.10.1 Introduction 131
3.10.2 Transitional Iron Crust Horizon 132
3.10.3 Carbonate-Clastic Facies 132
3.10.4 Discussion 135
3.11 Tchouka Flysch 136
3.11.1 Introduction 136
3.11.2 Sedimentary Facies 136
3.11.3 New Key Localities 138
3.11.4 Biostratigraphy 142
3.11.5 Discussion 142
3.12 Summary and Regional Correlations 143

CHAPTER 4 - DEFORMATION 147

4.1 Introduction and Previous Work 147
4.2 Upper Jurassic Compression - D1 "Eohellenic" Deformation 151
4.2.1 Field and Petrological Observations 151
Folds 153
Foliation and Lineation 156
4.2.2 Discussion 162
4.3 Upper Jurassic Extension - E0 166
4.3.1 Tectonic Unroofing and Core Complex Exhumation 166
4.3.2 Discussion and Regional Implications 167
4.4 Lower Cretaceous Compression - A JE2 Event? 171
4.4.1 Previous Conclusions 171
4.4.2 Recent Findings and New Key Localities 173
4.4.3 The Regional Picture 174
4.5 Upper Cretaceous (Turonian) Extension - E1 175
4.5.1 Platform to Basin Transition : the Cretaceous Transgressive Limestones and Buff Pelagic Carbonate 175
4.5.2 Eustatic versus Tectonic Controls 176
4.5.3 Discussion and Conclusions 176
4.6 Early Tertiary Compression - D2 "Neohellenic" Deformation 177
4.6.1 Introduction 177
4.6.2 Field Observations 178
Folds 181
Lineation 188
Planar Structures 188
Thrust-Imbrication and Flexural Foredeep Deposition 190

4.6.3 Petrological Observations and Metamorphism 199
4.6.4 Discussion and Conclusions 205
4.7 Later Tertiary Compression - D3 206
4.7.1 Field Relations 206
4.7.2 Discussion 210
4.8 Late-stage Extension - E2 214
4.9 Conclusions 215
4.10 Summary 219

CHAPTER 5 - GEOCHEMISTRY 220

5.1 Introduction and Previous Work 220
5.2 Methodology 221
5.2.1 Screening Samples 222
Elimination of Sedimentary Samples 222
Elimination of Highly Altered Samples 222
5.2.2 Screening Elements 229
Major Elements 230
Trace Elements 230
5.3 Tectonic Discrimination 231
5.3.1 Screening Discrimination Diagrams 231
5.3.2 The Livadia Formation 233
5.3.3 The Kastaneri Formation 242
5.4 Discussion and Conclusions 249

CHAPTER 6 - THE VORAS MASSIF 253

6.1 Introduction 253
6.2 Previous Work 253
6.3 Tectono-Stratigraphy of the Voras Massif 258
6.3.1 Unit 1 - the Loutra-Arideas Unit 258
Stratigraphy, Petrology and Field Relations 258
Interpretation 270
Regional Comparisons 272
Structure 274
Summary 277
6.3.2 Unit 2 - the Likostomo-Promachi Unit 277
Stratigraphy, Petrology and Field Relations 278
Structures 278
Interpretation 282
Regional Correlations 288
Summary 289
6.3.3 Unit 3 - the Livadia Unit 289
Stratigraphy, Petrology and Field Relations 289
Interpretation and Regional Correlations 293
Structure 294
Summary 298

6.3.4 Unit 4 - the Ano Garefi Unit **298**
Stratigraphy, Petrology and Field Relations **301**
Interpretation and Regional Correlations **306**
Structures **309**
Summary **310**
6.3.5 Unit 5 - the Pinovon Unit **310**
Stratigraphy and Petrology **310**
Interpretation and Regional Correlations **315**
Structures **316**
6.3.6 Unit 6 - the Porta-Tzena Unit **317**
Interpretation and Regional Correlations **326**
Structures **329**
6.4 Discussion **333**
6.5 Conclusions **339**

CHAPTER 7 - CONCLUSIONS **340**

7.1 Introduction **340**
7.2 Previous Models **340**
7.2.1 The Thrust-Imbricate Model (Mercier, 1968) **340**
7.2.2 The Tectonic Window Model (Godfriaux and Ricou, 1991) **342**
7.2.3 The Multi-Shell Model (Bonneau et al., in press) **344**
7.3 Proposed Tectonstratigraphic Evolution of the Study Area **345**
7.3.1 Introduction **345**
7.3.2 ?Triassic-Jurassic Continental Margin Deposits and the Onset of Arc Volcanism **346**
7.3.3 The Onset of Subduction, Arc Volcanism and Back-Arc Basin Genesis **348**
7.3.4 Eohellenic Deformation - the D1 Event **349**
7.3.5 Extensional Exhumation and Pull-Apart Basin Formation **350**
7.3.6 Upper Jurassic and Lower Cretaceous Transgressions **352**
7.3.7 Portlandian-Aptian/Albian Fluvial Deposition **353**
7.3.8 Lower Cretaceous Compressional Deformation (JE2)? **354**
7.3.9 Aptian/Albian Transgression **354**
7.3.10 Turonian Regional Extension and Platform Collapse **355**
7.3.11 Uppermost Cretaceous Flysch Deposition: Fault Scarp Degradation and Foreland Basin Formation **357**
7.3.12 Neohellenic Deformation: The D2 Event **357**
7.3.13 Renewed Contraction in the Later Tertiary: D3 Transpression **359**
7.3.14 Neotectonic Extension **359**
7.4 Summary **360**
7.5 Wider Implications **363**
7.6 Possible Future Work **364**

REFERENCES **365**
APPENDIX

ACKNOWLEDGEMENTS

I would firstly like to thank my supervisors, Alastair Robertson and John Dixon, for all their help and guidance both in the field and in Edinburgh. Thanks particularly to Alastair for tirelessly reading and re-reading each page of this thesis and to John for teaching me about the machanics of a Volkswagen Golf.

This thesis was funded by the Natural Environment Research Council, without whose backing this project, and many enjoyable trips to Greece, would not have been possible. Additional thanks must go to the manager and staff of the Royal Bank of Scotland in Nairn, whose co-operation made my financial life as a postgraduate student significantly easier.

Many people have contributed to work in this thesis. In particular I am grateful to Dr Sarandis Dimitriadis (Thessaloniki University) who helped considerably in the field and who has been a good friend in Greece; Dr Brian Rosen (Natural History Museum) for his assistance with coral identification; Dr Taniel Danelian (Edinburgh University) for his help and advice concerning radiolarian extraction and identification and Professor Hsin Yi Ling (Illinois University) for his on-going help with radiolarian identification.

A large number of people from the Department of Geology and Geophysics at Edinburgh University have also been invaluable during the course of this project and none more than Gordon Waugh. Gordon has been wonderful and I am sure that certain aspects of this PhD, both in the field and in Edinburgh, would have been much more difficult without his constant assistance. Much thanks also to Roger Scrutton, Ian Parsons, Dodie James, Yvonne Cooper, Mike Hall and Geoff Angel who have all helped considerably, as have Peder Aspen, Diana Baty, Alex Jackson, Helena Jack, Nicky McEwan, Heather Hooker, Lisa Thorburn and Simon Harley. Enormous thanks to you all.

Some of the most important people to help during this project, and who cannot really be thanked enough for their time, patience, encouragement and company are those who field assisted for me during some long, hot field seasons in Greece. Gordon - thanks for drinking my share of Ouzo at "Why Not", I would have done considerably less fieldwork otherwise. Ian - thanks for all your help, advice and friendship and for introducing me to Chamonix. Mike B - the best tyre-changer and early morning tea-maker I have ever met; it wasn't your fault that the car kept breaking down....honest ! Ned - your spider deterrent is second to none, a transferable

skill that will certainly get you places. Dave - I bet you never want to see another compass-clino in your life; thanks for getting up early each morning and for Eastern Europe.

In Greece, the friends I made will never be forgotten for their help, kindness and hospitality. Sitiri and Tasu are among the most wonderful people I have met and field work would have been much less enjoyable, and tasty, had they not been around. Harris, Jim, Panegiotis, Fotes, Cristos and Vangelis are also thanked very much for their company during many evenings in cafe-pub "Why Not" and cafe "Hobby", and for a constant fruit supply.

Coleen and Nicky have been very dear friends throughout my PhD and their support and joviality have kept me going through thick and thin. Both are also thanked for their company at various times in Greece and countless times in Edinburgh. Coleen and Ian are also thanked for the Baffin Expedition, which I will never forget, and for being great flat-mates.

Karen and Pauline are worthy of considerable gratitude for managing to share a very small office with someone as messy as I am, and for being great friends. A special thankyou also to Alan for much-needed coffee breaks and for inviting me on a fantastic trip to Turkey. My office-mates have been the best anyone could hope for - thankyou Harriet, Babs, Jon, Chris, Mark H, Mark L, Paula, Allison and Keerthi. Big thanks also to Kevin for chumming me to Alien Rock so many times (in the name of stress relief, of course), and to all the other folk who have made life great; Chil, Sandra G, Paul & Allison, J.T., Dianne, Amy, Alyson, Phil, Amanda, Clare, Ally, Rodney and all the inmates of the Mouse-house. I apologise profusely if there is anyone I have forgotten!

It is impossible to express how grateful I am for all the help I have had recently from Mike. I know that the final stages of thesis-production would have been so much more stressful and lengthy without all the time and effort that he contributed, not to mention the moral-support and bananas. Thankyou so, so much.

This thesis is dedicated to my family (Mum, Dad, Sandra, Chloe, Jim, Meg, Susan and Michael) who always have an endless supply of love, encouragement and support and who have continued to have faith in my ability to finish this task. I could never have done this without you all. Finally, a big thankyou prod to "Wee Jock" for giving me the best incentive in the world to finish!

Chapter 1

Introduction

CHAPTER 1 - INTRODUCTION

1.1 - LOCATION AND GEOGRAPHICAL SETTING OF THE STUDY AREA

This thesis is concerned with the Païkon Massif, and to a lesser extent the Voras Massif, located in a critical, little-studied area of northern Greece. The Païkon Massif is situated in the far north of eastern, mainland Greece (Macedonia) and forms a roughly N-S trending mountainous massif bordered to the west and south by the plains of Aridea and Thessaloniki respectively (Figure 1.1). To the north lies the spectacular Voras Massif, which extends across the border into former Yugoslavia and the low-lying hills of the Vardar/Axios river valley lie to the east (Figure 1.1). The Païkon Massif constitutes rounded, rolling mountains of moderate height (Gola Tchouka 1650 m), which rise abruptly from surrounding low-lying plains (<100 m). Deep river valleys and gorges intervene, with scattered areas of relatively flat arable land. Vegetation cover varies across the massif. In the west (from Ida to Mandalon; Figure 1.2) the study area is relatively barren comprising scorched, rocky limestone hillsides with a sparse scrubby floral cover. Northerly areas (from Archangelos to Livadia) are characterised by a more open, undulating landscape, where large tracts alluvium-covered agricultral land are punctuated by patches of dense forest and/or stark limestone. However, most of the Païkon Massif, particularly central, southern and eastern areas, is forested and dense beech woods cover the hillsides from their summits to the depths of the river valleys below. The quality and quantity of rock exposure in any given area depends largely on the vegetation cover which is, in turn, dictated primarily by lithology. Consequently, the most extensive exposure can be found in the far west of the study area, which is dominantly limestone, whereas exposure in many central, southern and eastern areas are largely restricted to dirt-track road cuttings and polished goat and sheep tracks.

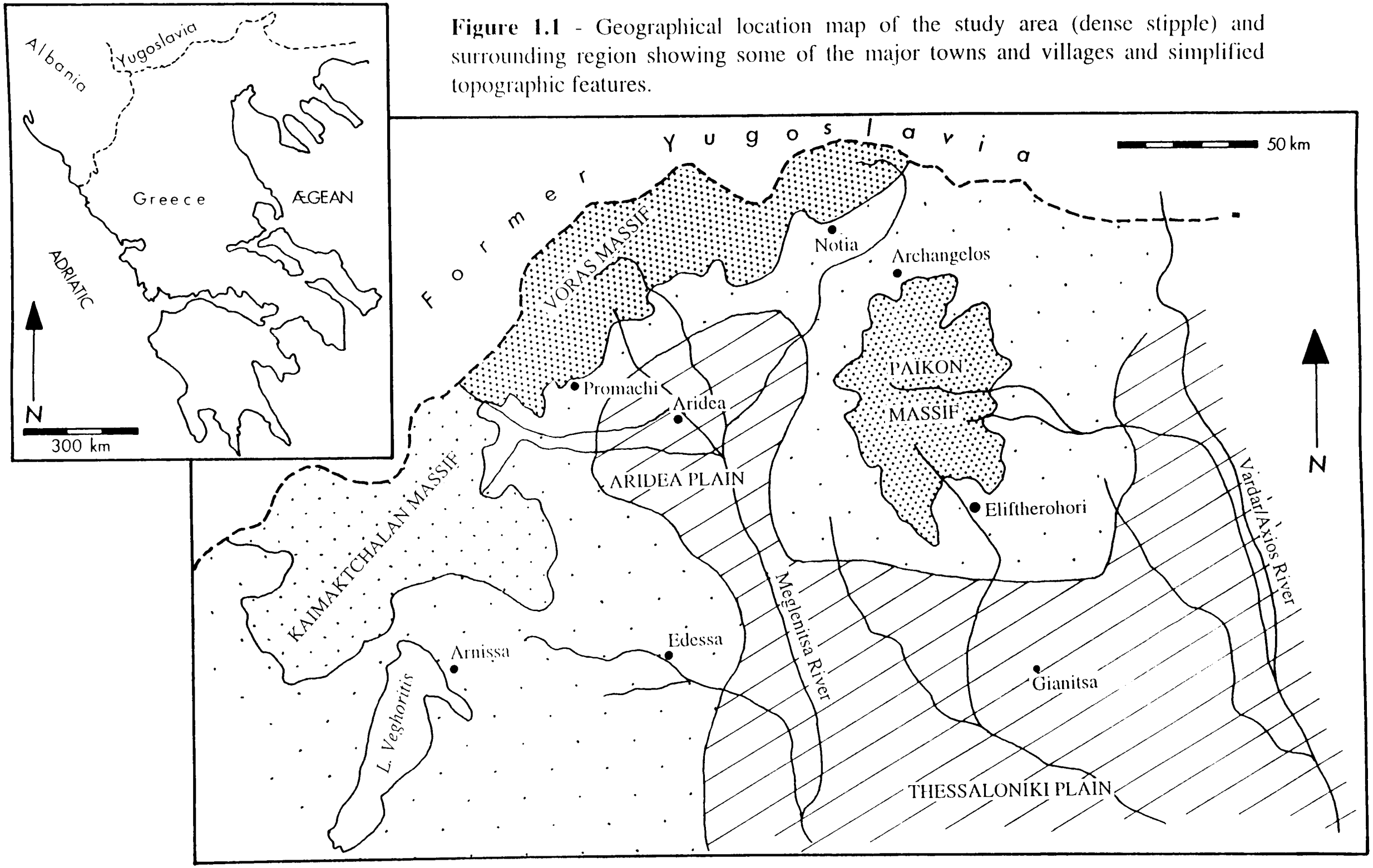


Figure 1.1 - Geographical location map of the study area (dense stipple) and surrounding region showing some of the major towns and villages and simplified topographic features.

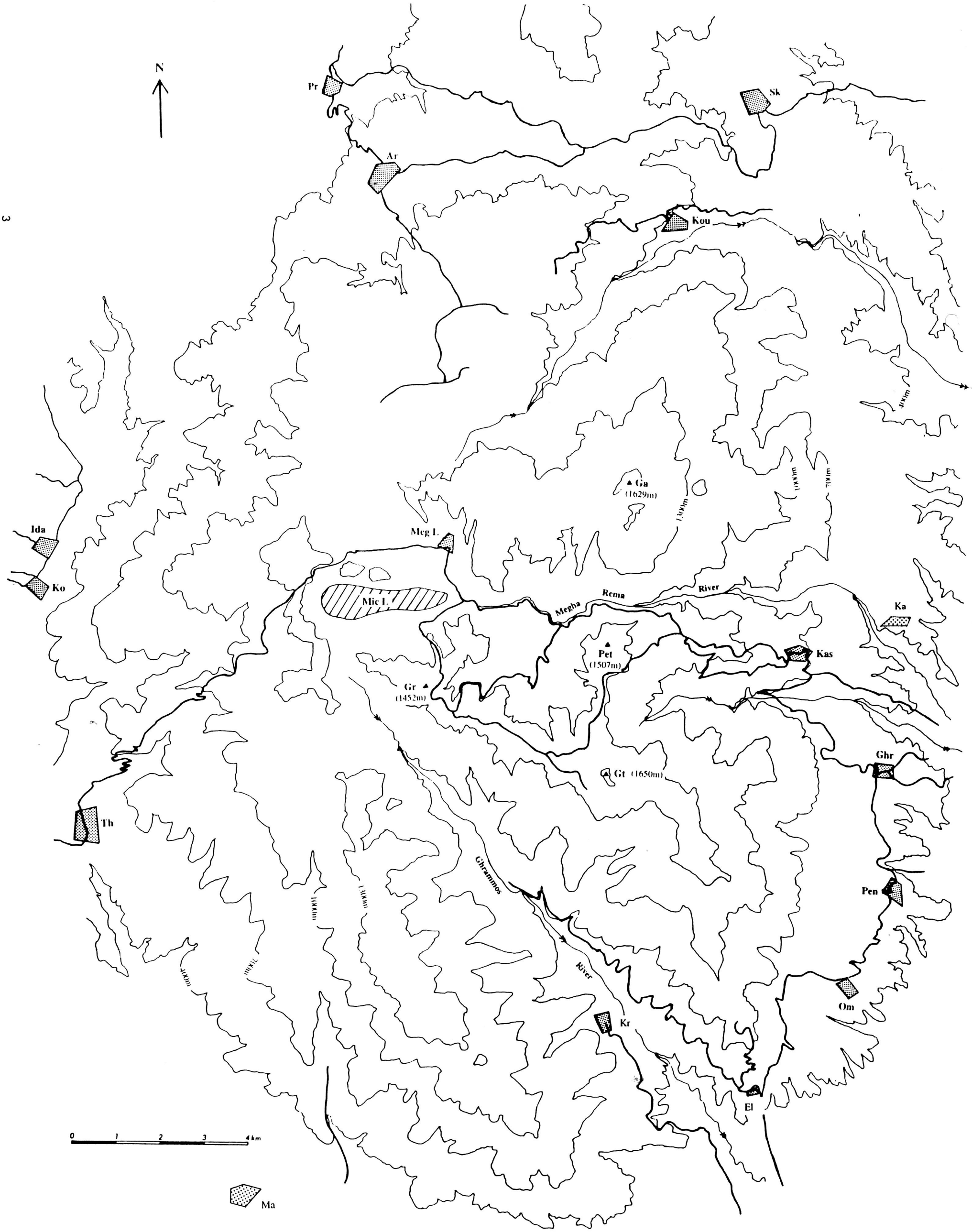


Figure 1.2 - Topographic map of the Païkon Massif.

1.2 - REGIONAL GEOLOGICAL SETTING

1.2.1 - *Palaeogeographic Reconstructions of the Tethyan Belt*

The Païkon Massif is part of the Hellenide orogen, which is an extension of the Alpine mountain chain to the west, the Dinarides to the north and the Pontides, Anatolides and Taurides to the east. These orogens, together with the Himalayan chain, constitute the Tethyan realm. The Hellenides have been classically sub-divided into a number of NNW-SSE trending tectono-stratigraphic or "isopic" zones, each seperated from those adjacent by significant tectonic lineaments (Kosmatt, 1924; Aubouin, 1959; Figure 1.3A).

Large-scale palaeogeographic reconstructions of the Tethyan realm remain somewhat contentious (e.g. Smith, 1971; Dewey *et al.*, 1973; Sengör *et al.*, 1984; Robertson & Dixon, 1984; Robertson *et al.*, 1991, 1996), but it is now generally accepted that the Alpine-Himalayan belt formed by the gradual closure of a westward-narrowing ocean basin (Palaeotethys; Sengör, 1979b; Robertson & Dixon, 1984) which separated the southern margin of the Eurasian continental mass from the northern margin of Gondwana during the late Palaeozoic, Mesozoic and Tertiary (Neumayr, 1875). As the Palaeotethyan ocean basin progressively closed, numerous elongate blocks of continental crust rifted off the African continental margin in the Permo-Triassic, and small Mesozoic ocean basins formed in their wake (Figure 1.4; Robertson & Dixon, 1984). The micro-continental blocks drifted northwards with continued subduction of the Palaeotethys ocean and were ultimately accreted to the southern margin of Eurasia, as the intervening ocean basins closed, in the Jurassic and Cretaceous (Figure 1.5; Robertson & Dixon, 1984). The landmass produced by the accretion of these continental and oceanic terranes forms Greece, Turkey and parts of Yugoslavia and Albania. The Païkon Massif is potentially one such accreted terrane and it is situated within the eastern "Internal" Hellenides (Figure 1.3; Brunn, 1956).

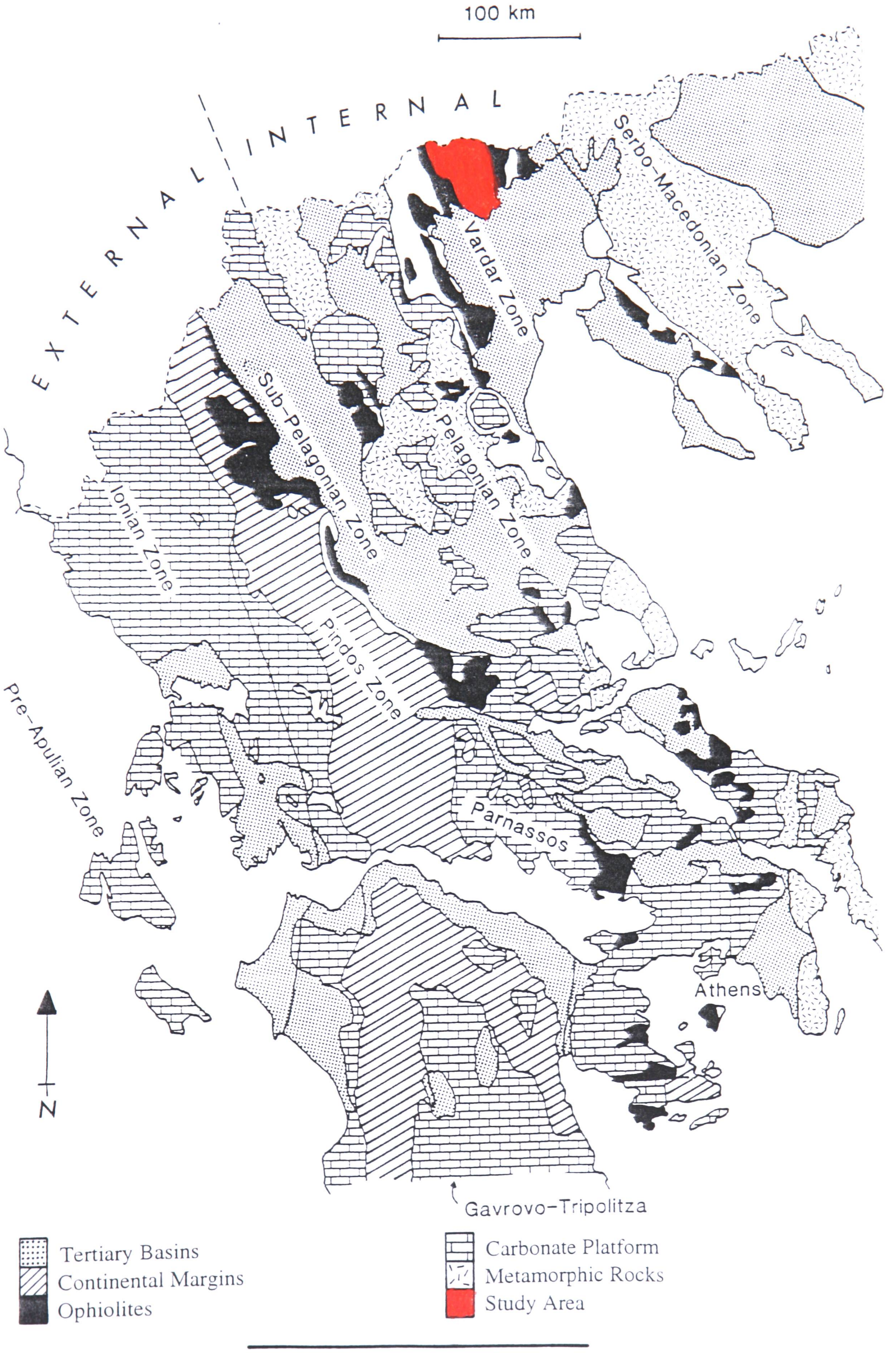


Figure 1.3 A Map of the tectonostratigraphic ("isopic") zones of the Hellenides.

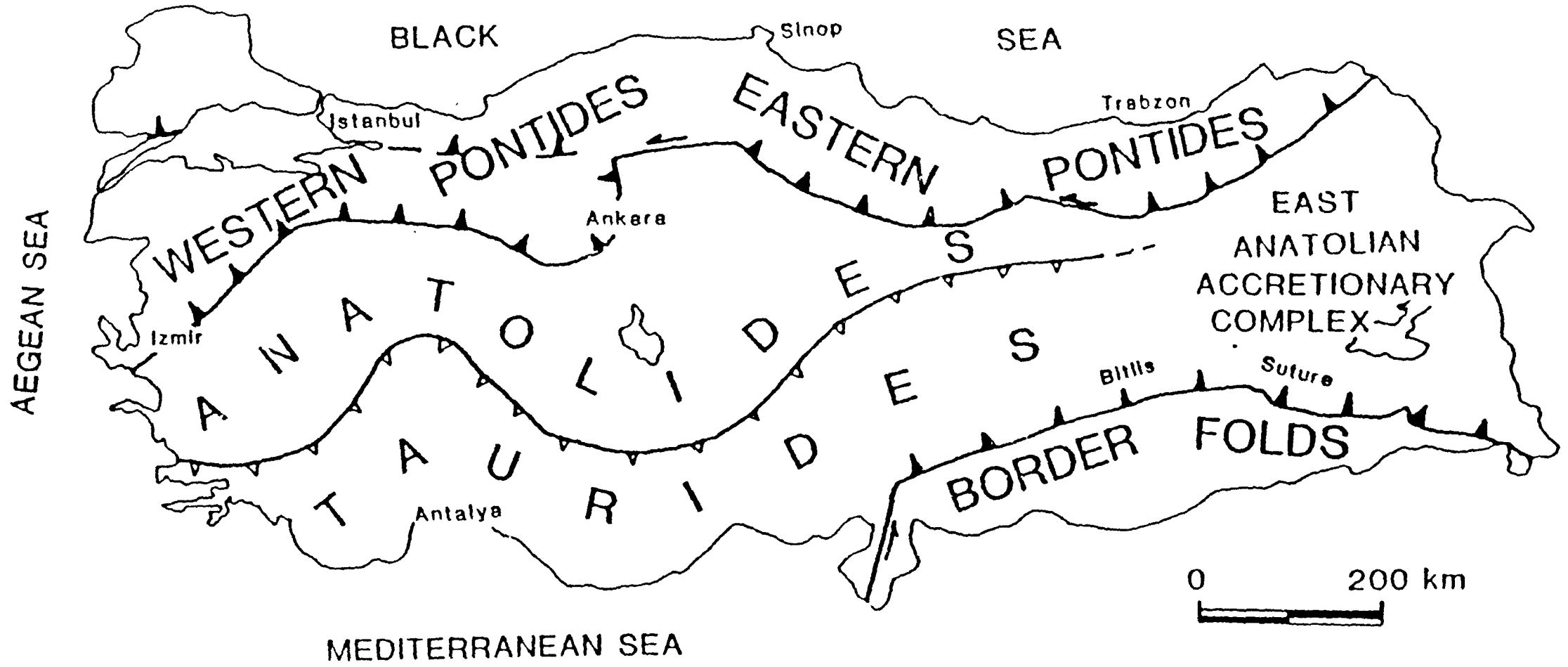


Figure 1.3 B - The tectonic zones of Turkey (after Sengör *et al.*, 1982).

Figure 1.4

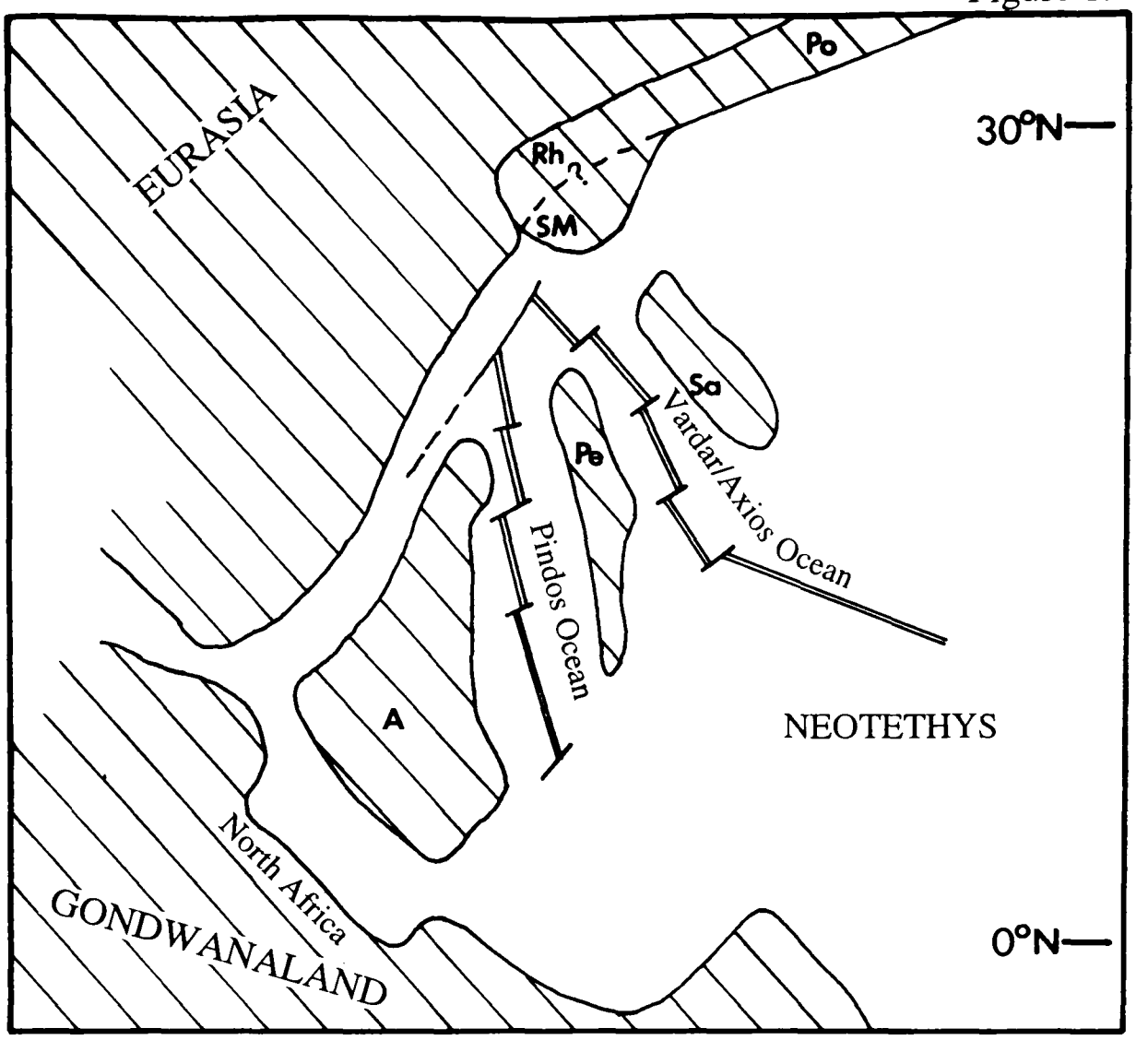


Figure 1.5

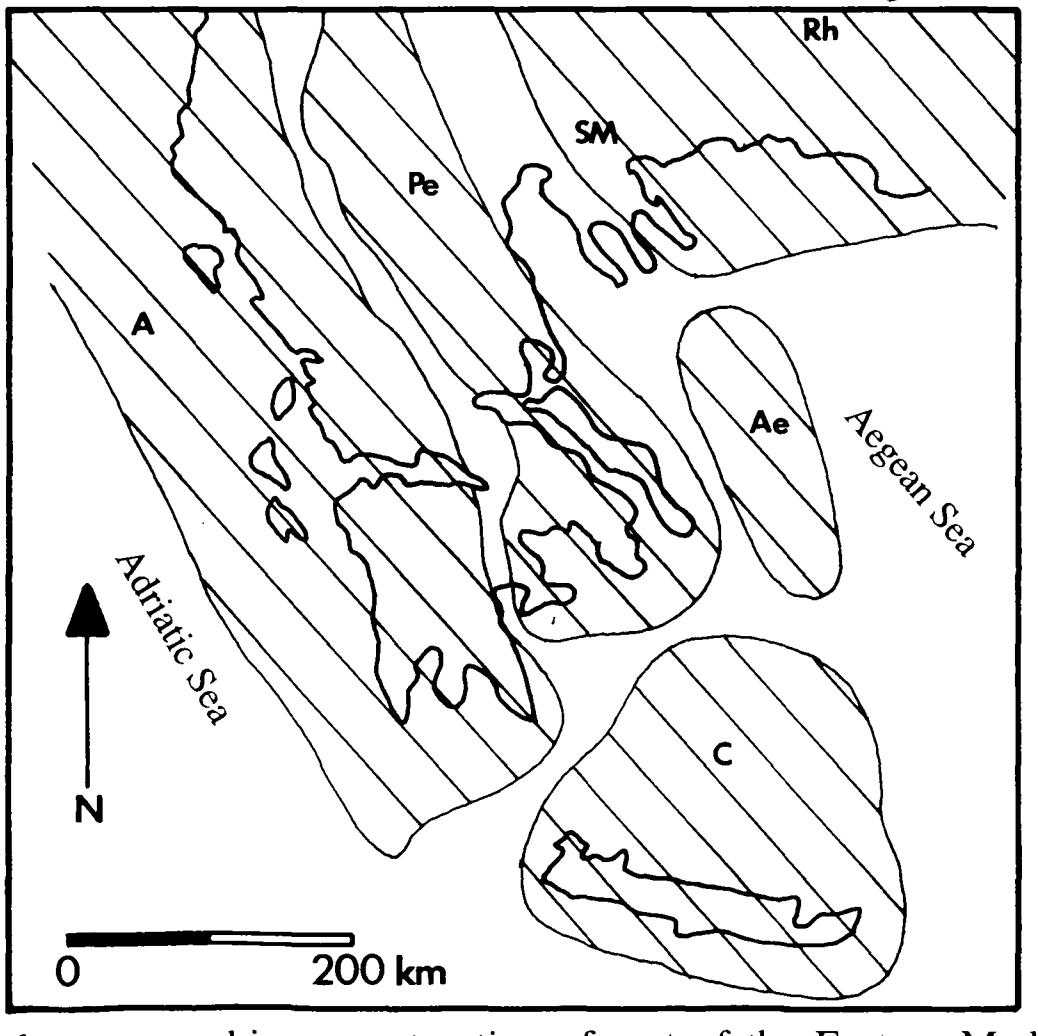


Figure 1.4 - Palaeogeographic reconstruction of part of the Eastern Mediterranean during the Early Jurassic. Modified after Robertson *et al.* (1991). Po = Pontides; Rh = Rhodope; SM = Serbo-Macedonian; Pe = Pelagonian; A = Apulia; Sa = Sakarya.

Figure 1.5 - Present-day configuration of the micro-continental blocks which constitute the Hellenides. Rh = Rhodope; SM = Serbo-Macedonian; Pe = Pelagonian; A = Apulia; C = Crete; Ae = Aegean.

1.2.2 - *The Isopic Zones of the Hellenides*

A brief summary is now given of the Isopic zones which constitute Greece and Turkey as background for the setting of the Paikon Massif in the eastern Mediterranean. The Isopic zones which constitute Greece can be divided into the External Hellenides and the Internal Hellenides (Brunn, 1956). The Internal Hellenides constitute the eastern half of Greece and were subjected to a phase of Upper Jurassic "Eohellenic" compressional deformation (chapter 4): the Pelagonian, Vardar/Axios, Serbo-Macedonian and Rhodope zones from west to east respectively. The External Hellenides did not experience "Eohellenic" orogenesis and have only been affected by Tertiary "Neohellenic" tectonism: the Pre-Apulian, Ionian, Gavrovo-Tripolitza, Pindos and Parnassos zones from west to east respectively (Figure 1.3). The Sub-Pelagonian (or Othris or Maliac zone) is also classed as an External zone, although this terrane underwent compressional deformation during the Upper Jurassic-Lower Cretaceous.

1.2.3 - *The External Hellenides*

Pre-Apulian zone

The Pre-Apulian zone is the most westerly isopic zone in the Hellenides, cropping out on the islands of Kephallonia, Zakinthos, Paxos and Lefkas in the eastern Adriatic, and it forms the eastern margin of the Apulian continental block. It essentially comprises Jurassic carbonates and evaporites overlain by a neritic platform of Cretaceous to Tertiary age.

Ionian zone

This is the most westerly tectonostratigraphic zone on the mainland of Greece. It represents a basinal terrane comprising evaporites, carbonates, cherts and clastics (flysch) of Mesozoic to Tertiary age situated between the platformal Pre-Apulian and Gavrovo-Tripolitza zones (Fleury, 1980; Thiebault, 1982; Underhill, 1985; Clews,

1989). Miocene overthrusting of the Gavrovo-Tripolitza zone to the east resulted in the formation of salt domes (Underhill, 1985, 1988, 1989).

Gavrovo-Tripolitza zone

The Gavrovo-Tripolitza zone can be subdivided into two subzones which comprise neritic carbonates of Mesozoic and early Tertiary age overlain by deep-water flysch (the Gavrovo subzone) and metamorphic continental basement rocks overlain by evaporites and a Mesozoic to Tertiary-aged shallow-water carbonate platform (the Tripolitza subzone). Much of these rocks have been overthrust by the Pindos thrust sheets (derived from the east) and are now exposed as tectonic windows (Poisson, 1984). The Gavrovo-Tripolitza zone is interpreted as the passive margin between the Apulian continent and the Pindos ocean (Robertson *et al.*, 1991; Degnan, 1992).

Pindos Zone

The Pindos zone, as classically defined, comprises deep-water sediments (turbidites, cherts, carbonates) of Mesozoic to early Tertiary age (Aubouin, 1959). However, more recent work suggests that the associated ophiolitic rocks (the Pindos or Othris Ophiolite) should be included in this terrane also (Smith *et al.*, 1975; Green, 1982; Jones, 1990; Robertson *et al.*, 1991; Degnan, 1992). The Pindos ophiolitic and sedimentary rocks are largely preserved as a series of imbricate sheets which overlie the Gavrovo-Tripolitza zone to the west. The ophiolitic rocks are thought to represent the vestiges of a Neotethyan ocean basin (the Othris ocean of Smith *et al.*, 1975; Green, 1982; the Pindos ocean of Jones, 1990; Robertson *et al.*, 1991; Degnan, 1992) which separates the Apulian (west) and Pelagonian (east) continental blocks.

Parnassus zone

The Parnassus zone covers a small area to the south of the Pindos and Sub-Pelagonian zones and essentially comprises shallow-water deposits of Triassic to Upper Cretaceous age (Celet, 1962; Johns, 1978), interpreted as a small block of continental crust which rifted from the Aplulian continental margin during the break-up of Gondwana (Robertson *et al.*, 1991; Robertson & Degnan, 1992a)

Sub-Pelagonian/Othris/Maliac zone

This subzone (Aubouin, 1959; Smith *et al.*, 1975, 1979; Ferriere, 1976; Vergely, 1984) is dominated by platformal sequences of essentially Permian and early Mesozoic age which overlie a pre-Permian continental basement. Ophiolitic rocks were overthrust from the west (Smith *et al.*, 1979) during the Upper Jurassic and unconformably overlain by an Upper Cretaceous neritic carbonate platform; this conflicts with earlier interpretations which envisage emplacement from the east (Aubouin, 1959).

1.2.4 - *The Internal Hellenides*

Pelagonian zone

The Pelagonian zone comprises metamorphic continental basement rocks, including meta-ophiolitic rocks (Nance, 1976) and granites of Upper Palaeozoic age overlain by Triassic platformal carbontes that are interpreted to represent a micro-continental block that rifted from the northern African margin during the Permo-Triassic (Aubouin *et al.*, 1970; Dercourt *et al.*, 1986; Robertson *et al.*, 1991). At this time the Pelagonian continental block is interpreted to have been separated from the Apulian Platfrom by the Pindos ocean and from the Serbo-Macedonian continent by the Vardar/Axios ocean. Contractional deformation in the Upper Jurassic led to the emplacement of ophiolitic rocks onto the Pelagonian margin from both the west, in some models (Pindos ocean; Robertson *et al.*, 1991), and east (Vardar or Almopias ocean; Sharp, 1995). The remains of these dismembered ophiolites were subsequently overlain by uppermost Jurassic, ophiolite-derived sediments and carbonates which were themselves transgressed by platform carbonate rocks during the Creatceous. Renewed compression in the early Tertiary caused the obduction of Upper Jurassic-Lower Cretaceous ophiolites from the western Almopias subzone (see below), which created a flexural foredeep that was infilled by deep-water flysch deposits (Brunn, 1956; Celet & Ferriere, 1978; Sharp, 1995). Mount Olympos is inferred to represent

a tectonic window of Pelagonian rocks, which is exposed beneath an allochthonous metamorphic nappe (Barton, 1975).

Vardar/Axios zone

The Vardar/Axios zone lies to the east of the Pelagonian continent and can be divided into three distinct tectonostratigraphic subzones; the Almopias, Païkon and Peonias subzones from west to east respectively (Mercier, 1968; Filbrandt, 1985).

Almopias subzone : This ophiolitic suture zone comprises the remains of an ophiolite of Triassic to Jurassic age which is inferred to represent a branch of Neotethys in the Hellenide orogen. It is still debated as to whether the main suture of the Palaeotethyan ocean is located in this zone or not. These Triassic/Jurassic ophiolitic rocks were subducted beneath the Païkon subzone to the east during the Upper Jurassic, and subsequent extension in the Upper Jurassic-Lower Cretaceous led to renewed ocean floor spreading and the formation of the Meglentisa Ophiolite (Sharp & Robertson, 1991; Sharp, 1995). These ophiolitic rocks are unconformably overlain by Lower Cretaceous shallow-water carbonates and clastics.

Païkon subzone : Until this work the Païkon subzone was little studied since the initial research of Mercier (1968) and so has remained rather poorly understood. The Païkon subzone is situated centrally within the Vardar/Axios zone and includes a thick sequence of bi-modal volcanics of ~Middle to Upper Jurassic age unconformably overlain by a shallow-water mixed carbonate/clastic succession of Upper Jurassic to Upper Cretaceous age. Deeper-water carbonates and flysch depopsits of Upper Cretaceous and early Tertiary age overlie the shallower-water rocks. The Païkon subzone was folded into a roughly north-south-trending anticline during Tertiary compression. The volcanic rocks of the Païkon subzone have been interpreted as an arc sequence (Mercier, 1968; Bebien, 1982; Vergely, 1984; Bebien *et al.*, 1987; Dimitriadis & Asvesta, 1993; Bebien *et al.*, 1994, in press).

Peonias subzone : The Peonias subzone forms part of an elongate ophiolite belt which extends southeastwards to Chalkidiki on the north Aegean coast. This ophiolite zone is known as the Innermost Hellenic Ophiolite Belt or IMHOB (Haenel-Remy & Bebien, 1985; Bebien *et al.*, 1986; Dimitriadis & Asvesta, 1993; Dimitriadis *et al*, in press; Zachariadou & Dimitriadis, in press). The IMHOB comprises a series of small ophiolites including the Guevgueli Ophiolite (and the Oreokastro, Thessaloniki-Metamorphosis and Sithonia-Kassandra complexes) which lies directly to the east of the Païkon subzone (i.e. to the east of the study area). The Guevgueli Ophiolite is estimated to be between 166 and 146 Ma in age and is associated with migmatites and granites (e.g. the Fanos Granite; De Wet, 1989) of the same age. The Guevgueli ophiolitic rocks are unconformably overlain by Upper Jurassic to Lower Cretaceous sediments, which are in turn unconformably overlain by Eocene limestones. Mercier (1968), Bebien (1982) Bebien *et al.* (1987) and Baroz *et al.* (1987) interpret the Guevgueli Ophiolite as having formed in a back-arc basin setting. Prior to this sea floor speading, however, the Peonias subzone formed as an aulacogen during the Triassic break-up of Gondwana (Stais & Ferriere, 1991; Stais, 1994).

Circum-Rhodope zone

The eastern part of the Peonias subzone is known as the Circum-Rhodope zone (Kauffmann *et al.*, 1976). It comprises three main units (Kockel *et al.*, 1977) which from east to west are: The Deve-Koran Doubia unit - Triassic ?rift sediments, acidic volcanics and overlying shallow-water marbles unconformably overlain by neritic limestones of Upper Jurassic age (Mercier, 1968). The Melissochori-Cholomon unit - moderate to deep-water sediments (the Permian to Jurassic Svoula Group) interthrusted with slices of metamorphic continental basement rocks of Serbo-Macedonian zone affinity. The Aspro Vrisi-Chortiatis unit - deeper-water sediments overlain by volcanic rocks of the Chortiatis Group and the IMHOB ophiolites. The three units indicate progressive deepening from east to west. Dixon & Dimitriadis (1984) suggest that the Circum-Rhodope zone represents the western margin of the

Serbo-Macedonian continent. Shunemann (1985) and Mussallam & Jung (1986) suggest that the Chortiatis Group is of volcanic arc affinity and is contemporaneous with formation of the Thessaloniki-Metamorphosis Ophiolite, but pre-dates the pre-Kimmeridgian Sithonia-Kassandra Ophiolite.

Serbo-Macedonian zone

The Serbo-Macedonian zone is floored by poly-phase deformed continental basement rocks which have been intruded by numerous Middle Jurassic granitic bodies (e.g. the Arnea Granite; Dixon & Dimitriadis, 1984; De Wet, 1989). The metamorphic rocks are overlain by Triassic marbles and Jurassic carbonates. Strike-slip motions are inferred to have induced the formation of small pull-apart basins within the Serbo-Macedonian basement (Dixon & Dimitriadis, 1984; Batty, 1993) which resulted in the formation of the Neotethyan Thermi, Volvi and Gomati ultramafic bodies (Batty, 1993). Although the Serbo-Macedonian and Pelagonian continental basement rocks have endured similar Upper Palaeozoic to Mesozoic histories, it is postulated that they were never part of the same basement area (Mountrakis, 1986; De Wet, 1989). The origin of the Serbo-Macedonian metamorphic rocks is thus thought to be internal (i.e. Eurasian) while those of the Pelagonian zone are postulated to be of north African derivation, although this requires further study.

Rhodope zone

The contact between the Serbo-Macedonian zone and the more internal Rhodope zone remains contentious, with debate centered around the presence, or lack thereof, of an oceanic suture (the Palaeotethyan suture) between the two. The Rhodope zone is generally correlated with the southern margin of Eurasia, including the Istranca Massif in northwest Turkey and adjacent areas (Sengör *et al.*, 1991). However, it has also been suggested that a Palaeotethyan suture could lie within or to the north of the Rhodope zone in Bulgaria (Sandulescu, 1989). The Rhodope zone was originally thought to be in thrust contact with the adjacent Serbo-Macedonian zone along the Strimon Line (Mercier, 1968; Smith & Moores, 1974). However, more recent studies suggest that a low-angle normal detachment separates the two metamorphic massifs,

and that the Rhodope zone formed as a metamorphic core complex during Tertiary regional extension (Dinter, 1994).

1.2.5 - *The Tectonic Zones of Turkey*

Like Greece, Turkey has been classically subdivided into a series of elongate tectonic facies belts, which are likely to be lateral continuations of some of the tectonostratigraphic zones of Greece. For this reason it is important to mention the main tectonostratigraphic components present in the Turkish region, as they may include lateral equivalents of the study area. Turkey essentially constitutes four tectonic belts (Ketin, 1966; Sengör *et al.*, 1982; Figure 1.3B), which are now separated by ophiolitic suture zones of late Mesozoic and Tertiary age. The **Pontides**, which include the Karakaya Complex (Pickett, 1994; Pickett *et al*, in press) and the Intra-Pontide suture (Ustaömer, 1993), form the most northerly zone and are separated from the more southerly **Anatolides** and **Taurides** by an inferred northern branch of Neotethys, represented by the **Izmir-Ankara-Erzincan** ophiolitic suture. This oceanic suture may be an along-strike equivalent to the Vardar/Axios zone in Greece (Robertson *et al.*,1996). The Anatolide and Tauride (or Menderes-Taurus) blocks are separated by a more southerly suture zone (the Inner-Tauride suture). To the east, the Anatolide block pinches out and the Inner-Tauride and Izmir-Ankara-Erzincan sutures merge (Sengör & Yilmaz, 1981).

The most southerly tectonic belt in Turkey is the Arabian Platform or Border Folds region, which collided with the Menderes-Taurus block during the closure of the southern branch of Neotethys in the Tertiary (Sengör & Yilmaz, 1981; Aktas & Robertson, 1984). The Bitlis ophiolitic suture formed between the Border folds and the Tauride block at this time.

1.3 - THE PAÏKON MASSIF

1.3.1 - *Previous Work in the Païkon Massif*

The Païkon Massif was first classified as an area of distinct geological composition during Mercier's classic research that encompassed the whole of the Internal Hellenides (1958-1968). This work subdivided the Vardar/Axios zone into three distinct units: The Almopais subzone to the west, the central Païkon subzone (which was further divided into the Païkon subzone proper and the Prepeonian subzone) and the Peonias subzone to the east (see Figure 2.1). Mercier outlined the first stratigraphy of his Païkon and Prepeonias subzones (which together form the Païkon Massif; chapter 2.1) and undertook extensive palaeontological investigations of the carbonate units therein, dating many stratigraphic units very accurately. Mercier's work was carried out prior to the plate tectonic revolution.

Bebien (1982) completed a detailed petrological and geochemical investigation of the Guevgueli Ophiolite (in the Peonias subzone to the east) during which he studied the contact between the Prepeonias subzone (Mercier, 1968) and the Guevgueli Ophiolite and determined its conformable nature (see Figure 4.48). Bebien *et al.* (1987) then carried out preliminary geochemical analyses of some of the Païkon and Prepeonias volcanics and sediments, concluding that both supra-subduction zone and abyssal signatures existed and could be related very closely to signatures obtained from the neighbouring Guevgueli Ophiolite.

Following on from Mercier's pioneering work in the Païkon Massif, Vergely (1984) subsequently undertook a detailed structural investigation of the Internal Hellenides which incorporated the first tectonic history of the Païkon Massif. Vergely recognised three major contractional events within the Païkon Massif and these will be discussed in detail in chapter 4. Vergely also concluded that the contact between the Prepeonias subzone and the Peonias subzone (or Guevgueli Ophiolite) was in fact tectonic and not conformable, as Bebien had implied (see Figure 4.49).

Baroz *et al.* (1987) studied and analysed the metamorphic mineral assemblages present in the lowermost stratigraphic units of the Païkon Massif and determined that these units had been subjected to a phase of blueschist to upper greenschist facies metamorphism (see chapters 3 and 5 for details). Some time later, Godfriaux & Ricou (1991) carried out reconnaissance research in the Païkon Massif and proposed an alternative tectonic model (the Tectonic Window model, see section 1.3.2 below) for the area based on their findings. Their findings are discussed in section 1.3.2 below and in chapters 2 and 7.

The most recent work in the area, besides this, was carried out by Bebien *et al.* (in press) who likened the volcanics of the Prepeonias subzone to those of the Guevgueli Ophiolite and not the Païkon subzone, and Bonneau *et al.* (in press) who proposed a further geotectonic model for the evolution of the Païkon Massif based on some new biostratigraphical data. The findings and conclusions of Bebien *et al.* (in press) are more fully explored in chapter 5, and those of Bonneau *et al.* (in press) are discussed in section 1.3.2 and in chapters 2, 4 and 7.

1.3.2 - *Geotectonic Models for the Evolution of the Païkon Massif*

The Thrust Imbricate Model - Mercier (1968)

Mercier (1968) envisaged the Païkon Massif (which is synonymous with the Païkon subzone of this work, see chapter 2) as comprising two tectonically juxtaposed terranes of distinct tectonostratigraphic origin. The westerly of these terranes he named the Païkon subzone and the easterly he named the Prepeonian subzone. In this model each terrane was separated from its neighbours by a major east-dipping tectonic contact; i.e. the Païkon subzone (of Mercier, 1968) rests with east-dipping tectonic contact upon the Almopias subzone to the west, the Prepeonian subzone rests upon the Païkon subzone and the Guevgueli Ophiolite of the Peonias

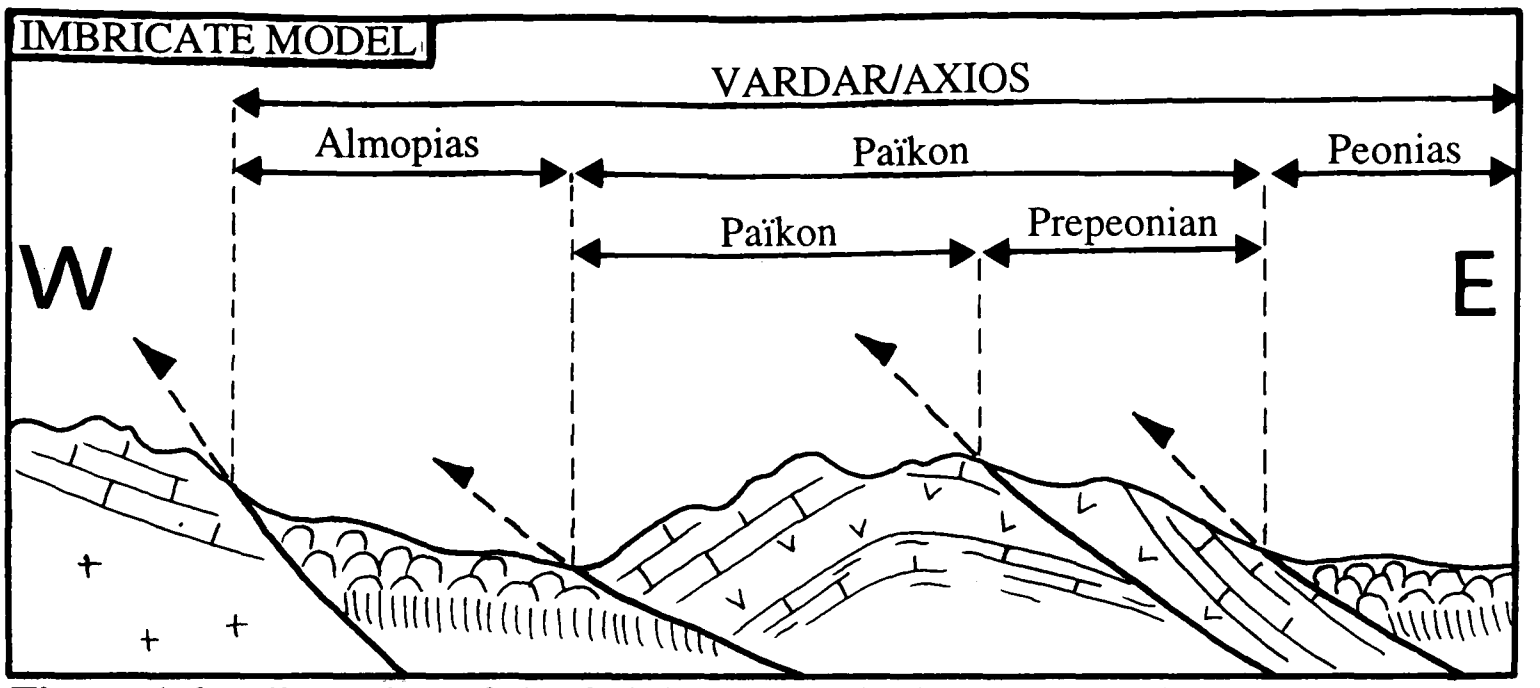


Figure 1.6 - Illustration of the Imbricate Model of Mercier (1968). A westward-propagating thrust stack was envisaged across the Internal Hellenides.

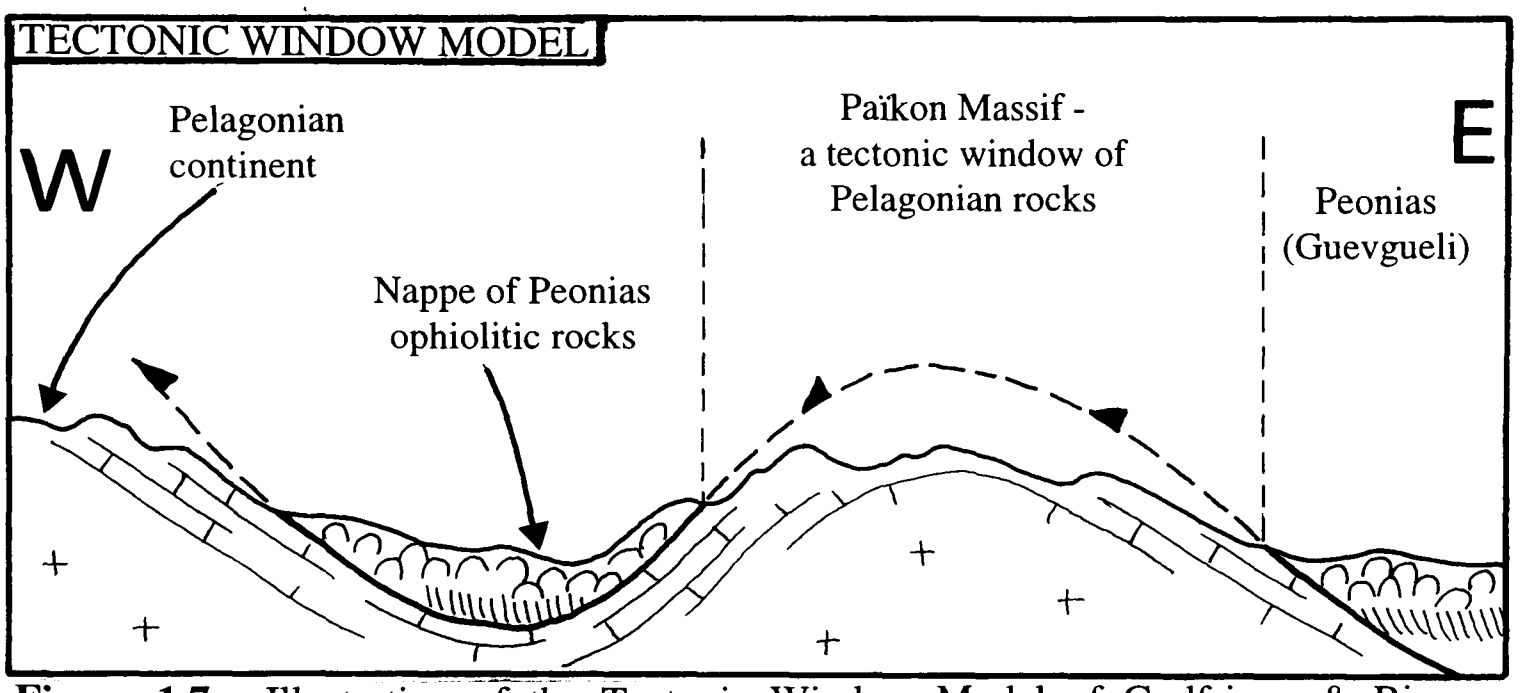


Figure 1.7 - Illustration of the Tectonic Window Model of Godfriaux & Ricou (1991). An ophiolitic "nappe" overlies the western Païkon with west-verging contact

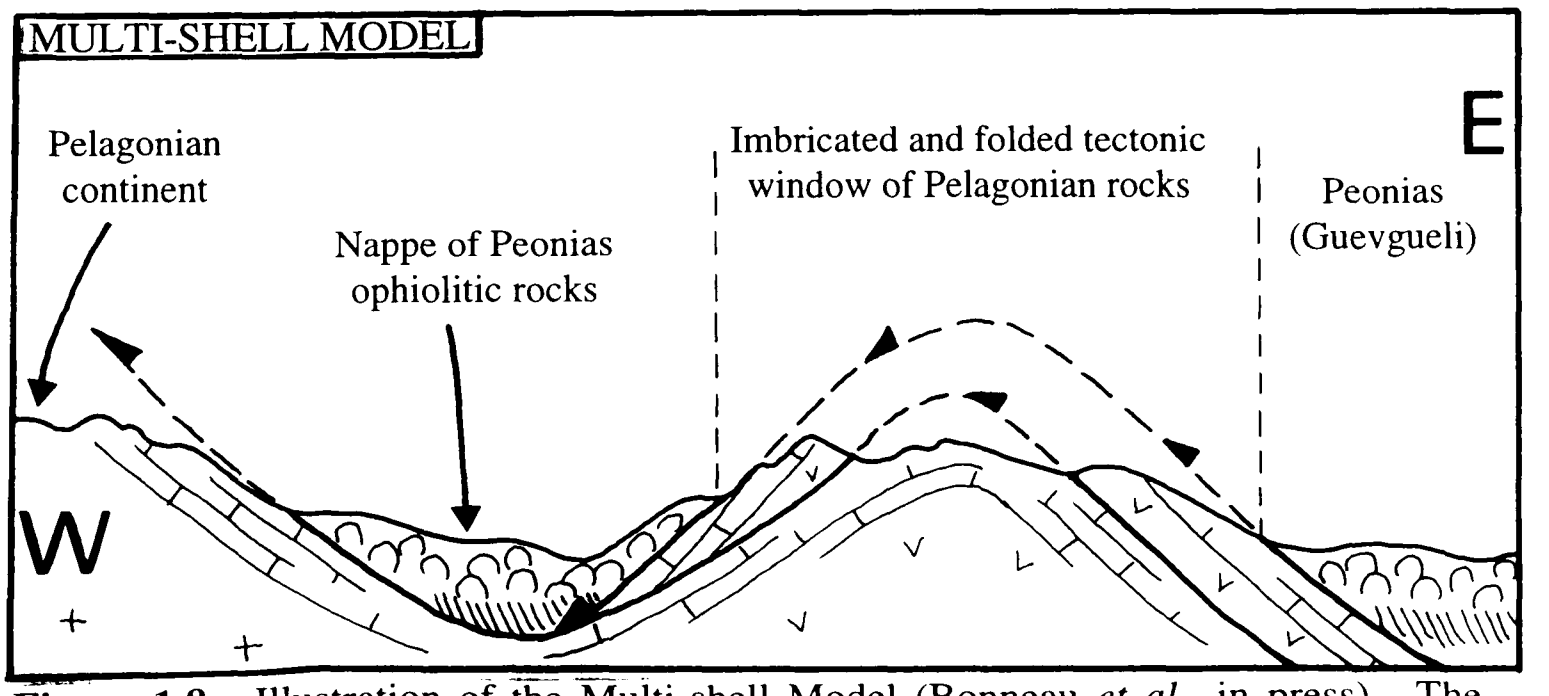


Figure 1.8 - Illustration of the Multi-shell Model (Bonneau *et al.*, in press). The Eastern Pelagonian zone is exposed as an upfolded and imbricated window beneath a nappe of ophiolitic rocks derived from the Peonias subzone.

subzone rests upon the Prepeonian subzone, again with an east-dipping tectonic contact (Figure 1.6). The Prepeonian subzone, in this model, is thought to represent the early Mesozoic succession which underlies the late-Middle to Upper Jurassic Guevgueli Ophiolite (see Figure 2.3), while the Païkon subzone represents a separate terrane including volcanic outpourings of arc affinity.

The Tectonic Window Model - Godfriaux & Ricou (1991)

The concept of a tectonic window of Pelagonian zone rocks within the Vardar/Axios zone was first described by Papanikalaou (1984) and, more recently, Godfriaux & Ricou's (1991) discovery of new biostratigraphical data (see chapter 2.2) in the Prepeonias subzone led to renewed interest in this model (Figure 1.7). In this model the Païkon and Prepeonias subzones represent opposing limbs of a large anticline comprising rocks of the Pelagonian zone (far to the west; Figure 1.3) which have been exposed as a "window". Godfriaux & Ricou (1991) believe that ophiolitic rocks from the Peonias subzone (namely the Guevgueli Ophiolite) overthrust the eastern margin of the Pelagonian zone during the Tertiary, hence, the ophiolitic rocks of the Almopias zone are visualised as an isolated nappe of rocks thrust westward from the Peonias subzone, or IMHOB, to the east.

The Multi-shell Model - Bonneau *et al.* (1994, in press)

This model is a variation of the Tectonic Window model outlined above. Bonneau *et al.* (1994, in press) propose that the Païkon Massif is of Pelagonian zone affinity and that the Almopias subzone ophiolitic rocks are a far-travelled nappe, but structurally more complex than envisaged in the Tectonic Window model. The discovery of a Cretaceous fauna in central parts of the Païkon Massif (see chapter 2.1 and 2.2.3) has been interpreted in terms of a multi-shell structure developed as ophiolitic rocks from the Peonias subzone were thrust west onto the eastern Pelagonian margin (Figure 1.8). During this thrusting and nappe formation, the eastern margin of Pelagonia was itself imbricated and the stratigraphic succession therein repeated vertically and folded into an anticlinal structure.

1.3.3 - *Project Rationale, Objectives and Methodology*

Rationale and Objectives

Following initial exploratory geological research within the Hellenides during the 1950s and 1960s (e.g. Brunn, 1956, 1959; Aubouin, 1959; Mercier, 1968) many regions of Greece have been re-studied. The External Hellenides have received a considerable amount of attention in recent years and are now relatively well understood, while the Internal Hellenide regions have remained relatively unknown. Although the Vardar/Axios zone (Figure 1.3) has been the focus of some attention since the onset of the plate tectonic era, many key areas in this important suture zone have been neglected until very recently. The Païkon Massif of the central Vardar/Axios zone is one such area. As discussed in section 1.2.3, the Païkon Massif (or Païkon subzone) is bordered to the west and east by mainly ophiolitic units of the Almopias and Peonias subzones respectively. The Pelagonian and Almopias zones were the subject of a recently completed PhD project at the University of Edinburgh (I. Sharp, 1995), which has shed some light on the tectonic evolution of the western part of the Vardar/Axios zone. The Peonias subzone, of the eastern Vardar/Axios zone, has also been reviewed in the last decade or so (e.g. Bebien, 1982; Haenel-Remy & Bebien, 1985; Bebien *et al.*, 1986; De Wet, 1989; Stais & Ferriere, 1991; Dimitriadis & Asvesta, 1993; Stais, 1994; Dimitriadis *et al*, in press; Zachariadou & Dimitriadis, in press) and hence the geological history of this area is similarly well constrained. The Païkon subzone, on the other hand, has not been the subject of a thorough, multi-disciplinary study since the ground-breaking work of Mercier (1968), which, as stated above, was undertaken prior to the implementation of present-day plate tectonic theories. The Païkon Massif holds a key, central position in the Vardar/Axios zone and effectively represents the missing, or unstudied, piece in the otherwise nearly complete Hellenide jigsaw, hence its selection for this research project.

Arc volcanism is effectively absent from the Pindos oceanic suture zone situated to the west (in the External Hellenides) but has been reported from east of the

Vardar/Axios zone (i.e. the Chortiatis Group of the Circum-Rhodope zone). The Païkon Massif, around which this study is centered, is known to contain a thick succession of Jurassic volcanics and volcaniclastics, which were previously speculated as being of volcanic arc affinity, based on limited data.

An additional objective of this study is to re-assess the validity and applicability of the existing geotectonic models (see section 1.3.2) concerning the Mesozoic and early Tertiary evolution of the Païkon subzone within its regional framework. Such re-evaluation necessitates thorough petrological, palaeontological, structural and geocheochemical investigations of the rock units exposed within the study area, taken together with up-to-date information from adjacent terranes to generate a complete picture of the regional geology.

As a supplement to detailed work in the Païkon Massif, a reconnaissance study of the Voras Massif (directly to the north; Figure 1.1) was undertaken. Due to its strategic position along the frontier between Greece and former Yugoslavia, the Voras Massif has been little studied, but its regional significance has been the subject of recent debate. The rock units therein have been variably assigned to the Pelagonian, Almopias, Païkon, Peonias and Serbo-Macedonian zones, although no detailed research has been carried out across the entire Massif since the preliminary studies of Mercier (1968). Although a thorough investigation of all geological aspects of the Voras Massif is outside the scope of this thesis, the new data gathered in this area do shed light on its regional geological significance and hence provide invaluable information concerning the tectonic evolution of the Internal Hellenides as a whole.

Methodology

In order to achieve the objectives outlined above, extensive field studies were carried out over the course of three seasons (total 7 months). Field work was concentrated in the main study area (the Païkon Massif; chapters 2 to 5) but also incorporated comprehensive reconnaissance work within the subsidiary Voras Massif (chapter 6). The neighbouring tectono-stratigraphic terranes (i.e. the Pelagonian, Almopias,

Peonias, Circum-Rhodope and Serbo-Macedonian zones) were also briefly visited in order to complete the picture of the regional geological setting of the Païkon Massif.

Detailed re-mapping of the entire Païkon Massif was not undertaken during the course of this project due to the size of the area and to the quality of work already available (Mercier, 1968). However, key areas of stratigraphic and/or structural interest were investigated thoroughly and mapped in detail. In the field, a revised tectono-stratigraphy of the Païkon Massif was established by careful consideration of crucial contact areas (chapter 2) and the structural framework of the area was re-assessed (chapter 4). Each stratigraphic unit was systematically examined and detailed logs and geotraverses of key sections recorded (chapter 3). Samples from each stratigraphic unit were collected for subsequent palaeontological, geochemical, petrological and sedimentological investigation, and oriented samples were collected to allow the study of microscopic structural relationships and fabrics.

Back in Edinburgh, samples of the volcanic successions were prepared and analysed using the X-ray fluorescence technique outlined in the Appendix, and the data obtained was used to assess their geochemical signature and tectonic environment of eruption (chapter 5). X-ray diffraction analyses of selected samples was performed in order to constrain mineralogical assemblages, and a comprehensive petrological study of all rock units was undertaken using thin-sections and oriented thin-sections of selected samples. New palaeontological data collected in the field were identified with the assistance of experts (i.e. B. Rosen, T. Danelian and H. Y. Ling) and previously identified faunal determinations were checked and confirmed in order to date stratigraphic units as accurately as possible. These data were then used to constrain the tectonic evolution of the Païkon and Voras Massifs, as detailed in the concluding chapter (chapter 7).

Chapter 2

Stratigraphy

CHAPTER 2 - STRATIGRAPHY

The stratigraphy of the Païkon Massif was initially described by Mercier (1968) and was later modified by Bebien (1982), Vergely (1984), Godfriaux & Ricou (1991), Sharp & Robertson (1992) and Bonneau *et al.* (in press). The following is a brief outline of the original stratigraphy of the study area and its subsequent modifications, followed by a revised stratigraphy, which has been erected during the course of this work. All stratigraphic terminology is consistent with the most recent conventions, as outlined by Whittaker *et al.* (1991).

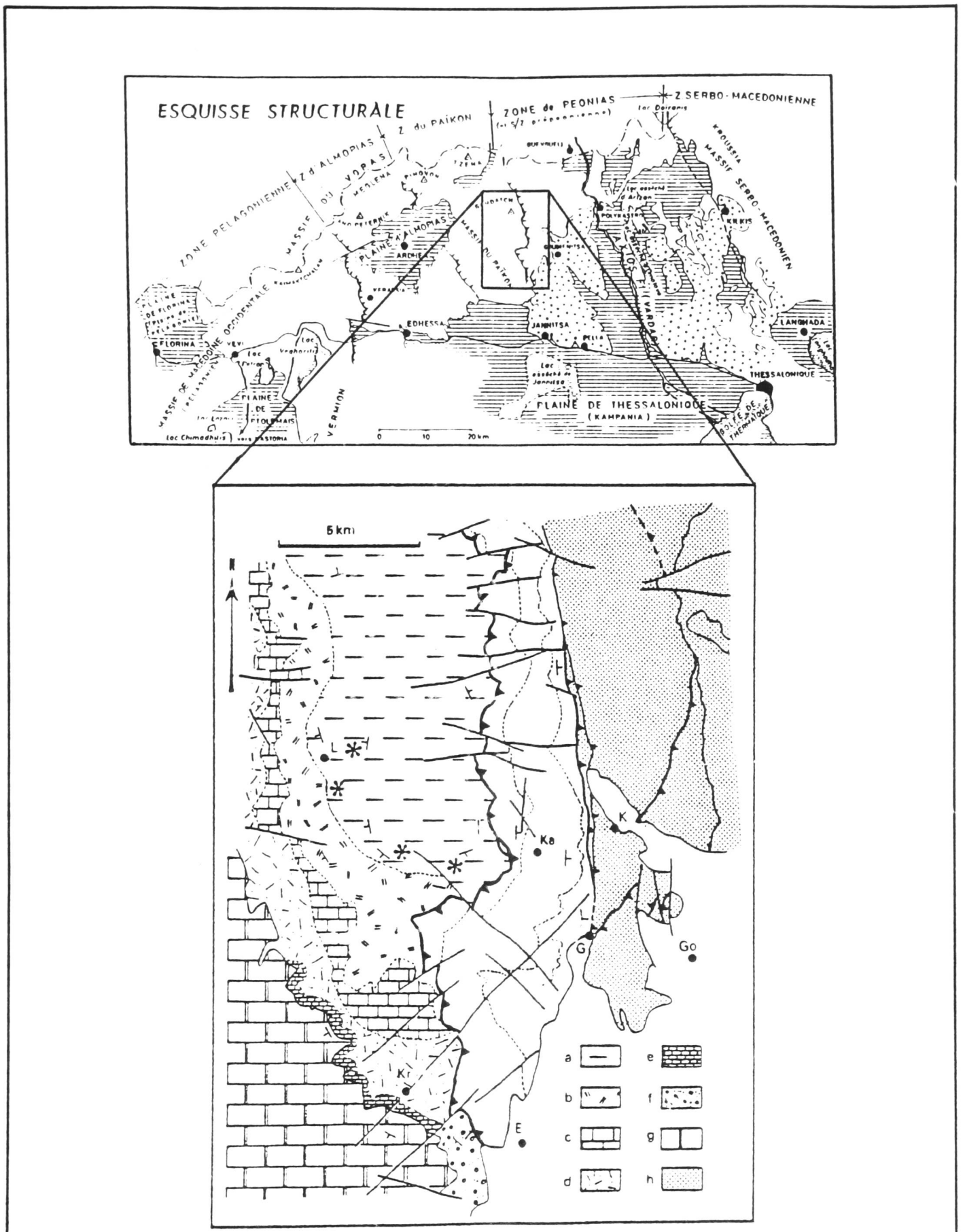
2.1 - PREVIOUS STRATIGRAPHY

Mercier (1968) subdivided the Païkon Massif into two distinct parts separated by a major east-dipping reverse fault (Figure 2.1). The western, more extensive part he named the Païkon subzone (la sous zone du Païkon), while the smaller, eastern part he termed the Prepeonian subzone (la sous zone Prépéonienne). Based on his mapping, Mercier stated that, in the west, the Païkon subzone lies structurally above the more westerly Almopias subzone and in the east the Serbo-Macedonian Massif rests tectonically upon the Prepeonian subzone with an east-dipping tectonic contact: a regional southwest-propagating imbricate stack was envisaged.

The original stratigraphy of the Païkon subzone, as devised by Mercier (1968), is illustrated in Figure 2.2. In this arrangement the Païkon subzone was split into 11 lithostratigraphic units (série) ; Pa1 to Pa11, from base to top, respectively. Pa6 is not exposed within the Païkon subzone[1].

[1] Mercier (1968) correlated all lithostratigraphic units of the Païkon zone with those of the Prepeonian subzone. Ppé6 has no stratigraphic equivalent in the Païkon subzone and so Pa6 was omitted from the stratigraphic column (see Mercier, 1968, p 156).

Figure 2.1 - Mercier's (1968) simplified map of the Païkon Massif showing the Païkon subzone to the west and the Prepeonian subzone to the east.



a - Gandatch Formation marbles; b - volcano-sedimentary Livadia Formation; c - Jurassic Gropi marbles; d - volcano-sedimentary spilites & keratophyres; e - Khromni Limestones (Portlandian - Basal Cretaceous); f - Eocretaceous Flysch; g - Mid - Upper Cretaceous Transgressive Limestones; h - Guevgueli ophiolite complex.

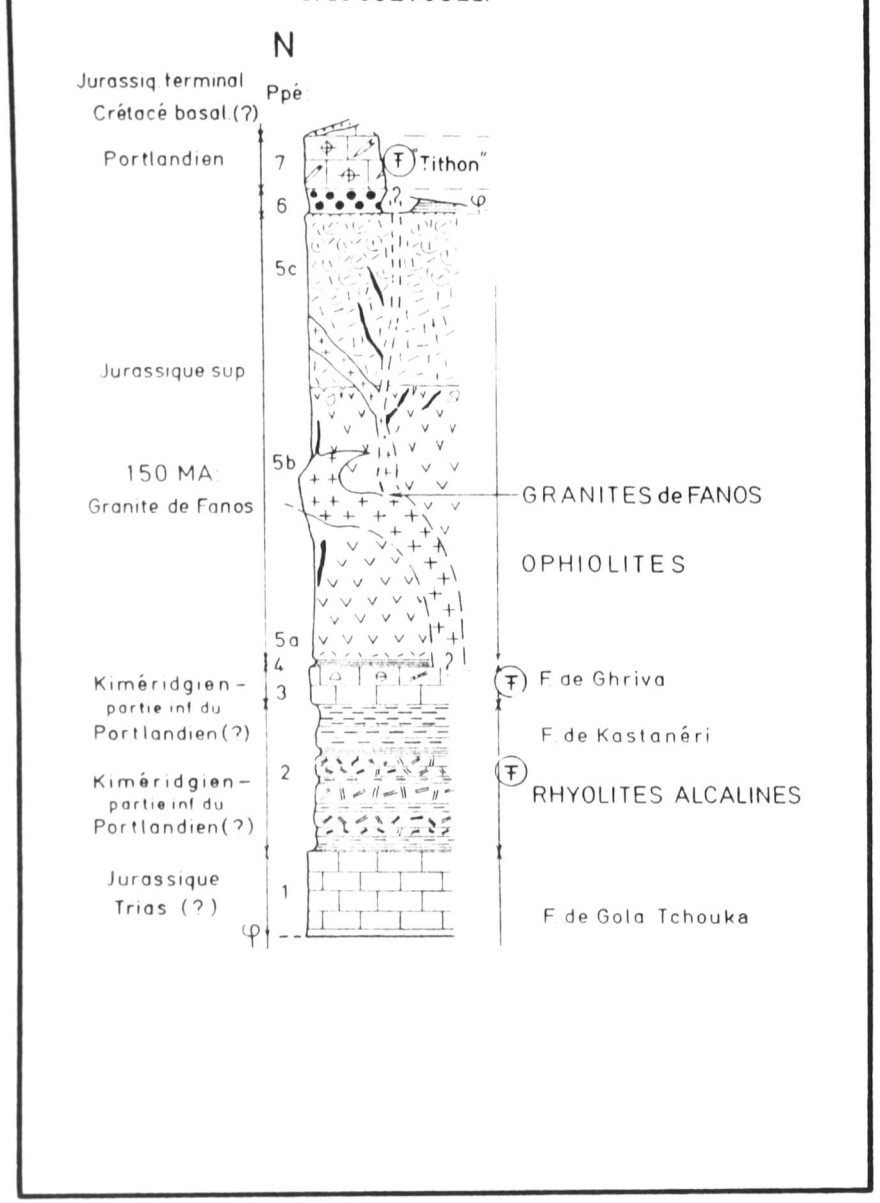


Figure 2.3 - Mercier's straigraphy of the Prepeonian subzone. After Mercier (1968).

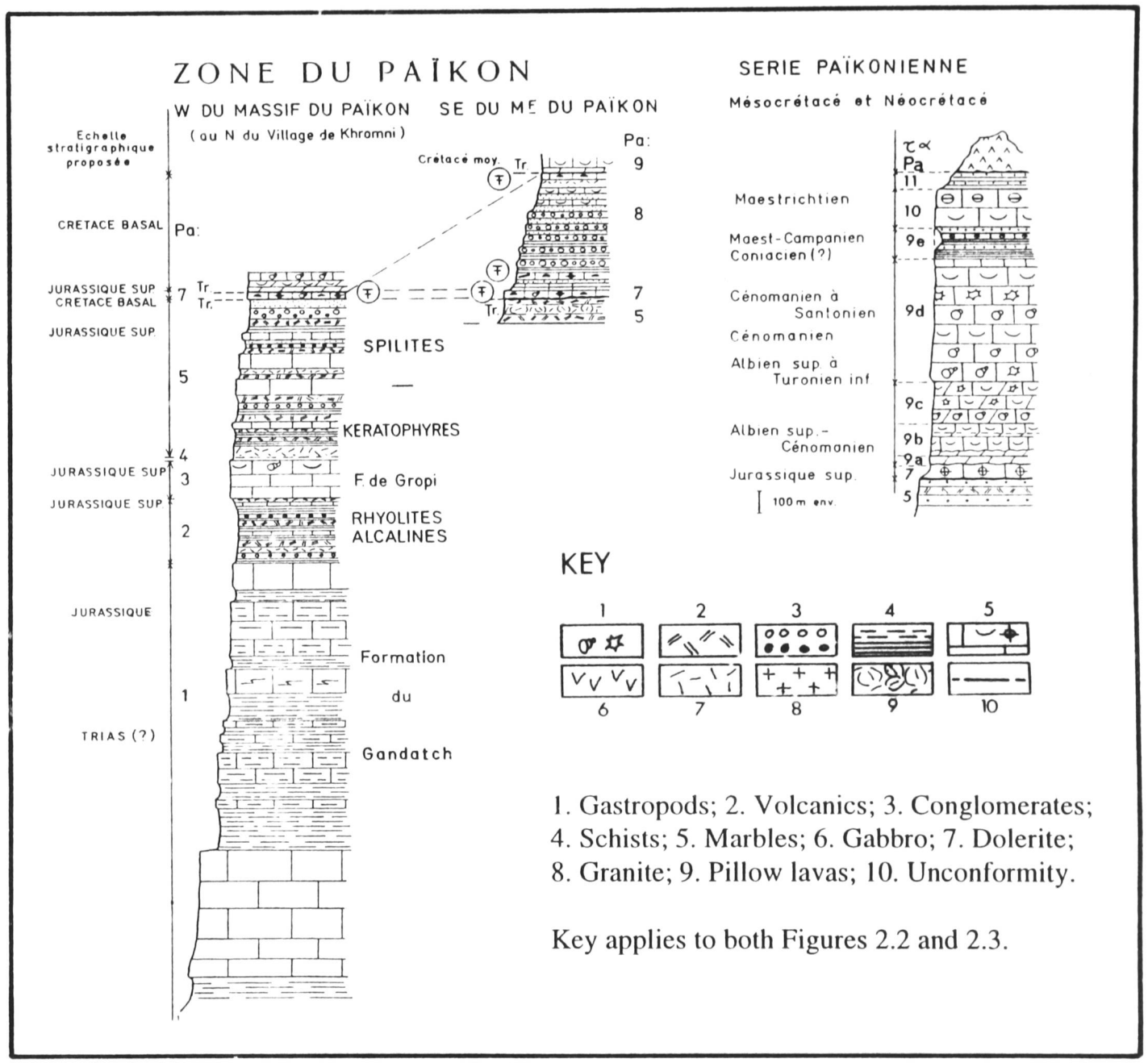


Figure 2.2 - Mercier's stratigraphy of the Païkon subzone. After Mercier (1968).

Similarly, Mercier (1968) separated the more easterly Prepeonian subzone into 8 lithostratigraphic units, ranging from ?Triassic-Lower Jurassic at its base (Ppé1 - Calcaires de Gola Tchouka) to Basal Cretaceous at its top (Ppé8 - Flysch). The internal stratigraphy, as originally proposed, is set out in Figure 2.3. Although Mercier subdivided the Païkon Massif into these two distinct tectonostratigraphic[2] components, he did note that stratigraphic successions exposed within them were likely to be associated, as summarised in Figure 2.4.

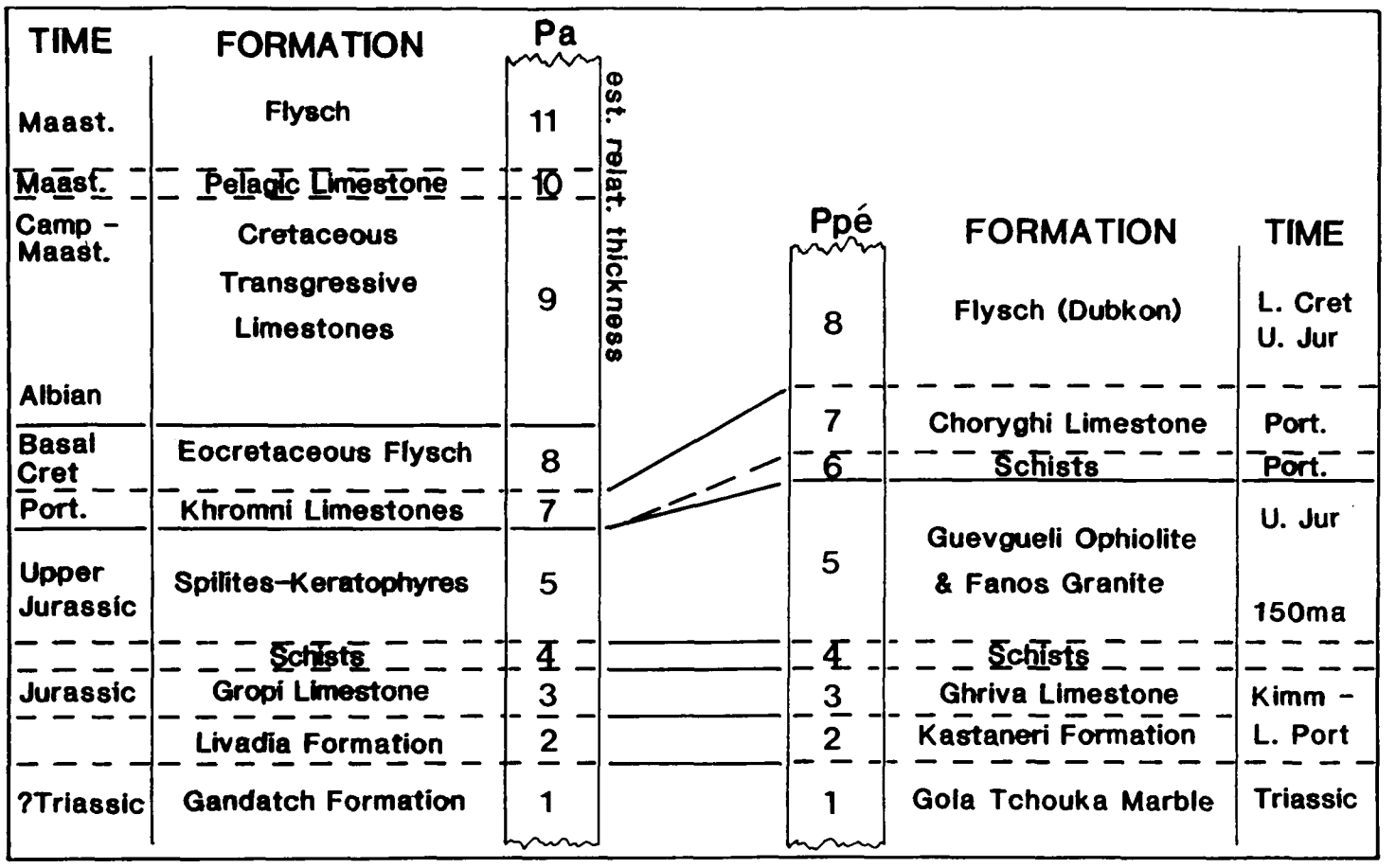


Figure 2.4 - Stratigraphic correlation between the Païkon zone and the Prepeonian subzone, as proposed by Mercier (1968),.

Bebien (1982) modified Mercier's original stratigraphy by recording two previously unidentified volcanic/pyroclastic units at the base of Pa1 (Série du Gandatch) and at the top of Pa8 (Le Flysch Éocrétacé). During the course of this study, these units were seen to be the result of structural duplication and are thus abandoned.

---

[2] Tectonostratigraphy is here defined as. 1- The vertical structural ordering of stratigraphic formations by tectonic processes (e.g. thrust-bound sequences). 2-The sedimentary succession produced by the operation of tectonic processes (e.g. foreland basin sequences). 3-The creation of a stratigraphy based on the structural history of each unit (e.g. Unit 4 has undergone 3 phases of deformation whereas Unit 5 has only experienced 2 etc.).

A further modification was introduced by Vergely (1984), who noted that the contact between Ppé4 and Ppé5 is tectonic, as shown by the presence of an east-dipping reverse fault.

The discovery by Godfriaux & Ricou (1991) of Cretaceous fauna within Ppé3, previously dated as ?Mid Jurassic, led to a revision of the correlations made between the Païkon subzone and the Prepeonian subzone (Figure 2.5). Also, new age data based on a radiolarian fauna within Pa9e (Sharp & Robertson, 1992) indicate a Turonian age for this unit, as opposed to the post-Maastrichtian age previously assigned. Sharp & Robertson (1992) also noted that units Pa10 & 11 are structural repeats of Pa9d & Pa9e, hence stratigraphically obsolete, and that locally conformable contacts exist between Pa8 and Pa9, where a major unconformity was previously inferred (Mercier, 1968; Vergely, 1984).

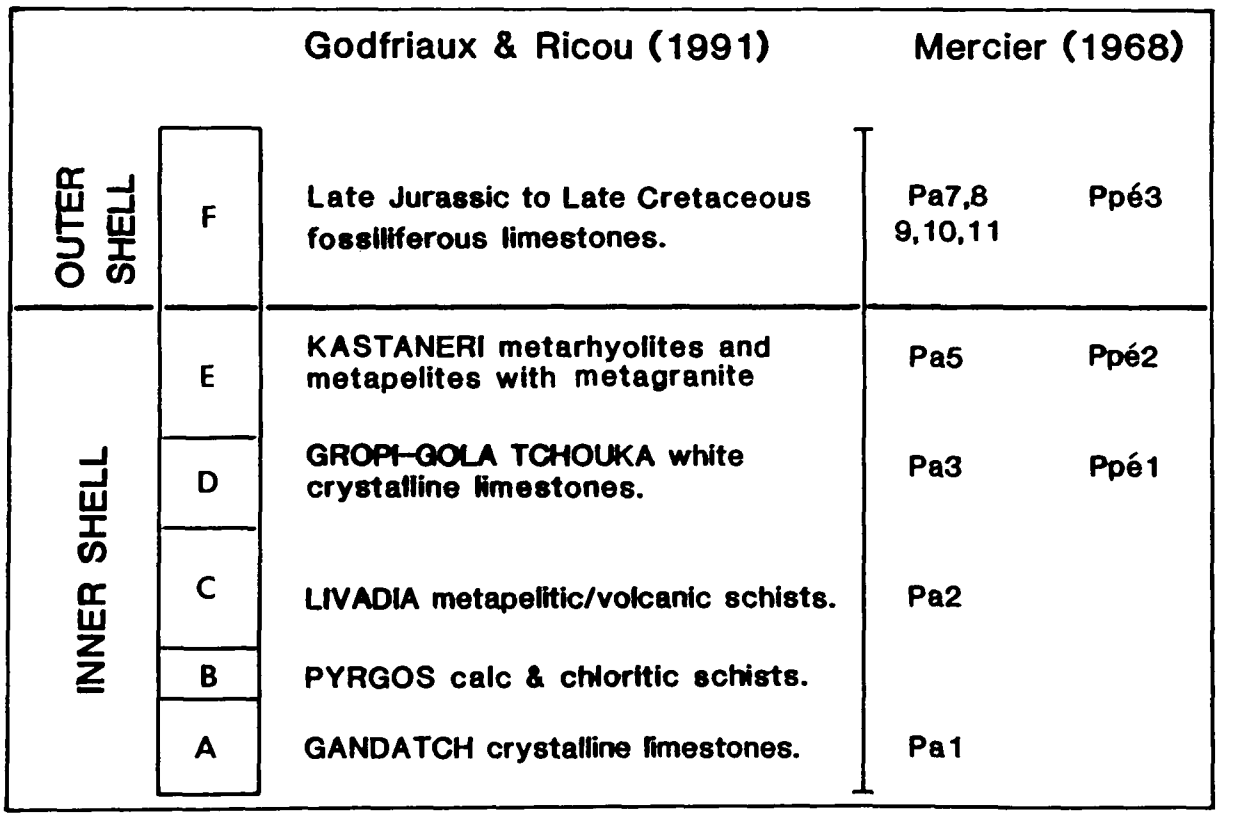


Fig. 2.5 - Stratigraphic succession and correlations within the Païkon subzone proposed by Godfriaux & Ricou (1991).

Finally, Bonneau *et al.* (in press) reported a Cretaceous fauna within Ppé1 (Calcaires de Gola Tchouka) in the central Païkon Massif. These Cretaceous dates have been confirmed during the course of this work, and additional units, not dated by Bonneau *et al.*(in press) and previously thought to be Middle Jurassic (Mercier, 1968), have also been assigned a Cretaceous age. These modifications are detailed in sections 2.2.3 and 3.9.

2.2 - REVISED STRATIGRAPHY.

Field studies within the Païkon Massif reveal that lithostratigraphic units exposed on its western side (Païkon subzone of Mercier, 1968) are equivalent in age and facies to those exposed on its eastern side (Prepeonian subzone of Mercier, 1968). The Païkon Massif is therefore envisaged as a SSE-plunging anticline, each side of which exhibits a nearly identical stratigraphic succession from core to flank (Figures. 2.6 & 2.7). Thus, the Païkon subzone, as redefined here, involves the entire Païkon Massif and combines both the western Païkon subzone and eastern Prepeonias subzone of Mercier (1968). The revised lithostratigraphic succession within the Païkon Massif is as follows:

THE LOWER PAÏKON MEGASEQUENCE

2.2.1 - *Gandatch Formation*

Nomenclature - Named after Mount Gandatch (1629m; Figure 2.7), one of the highest peaks within the Païkon Massif, which is composed entirely of this formation.

Equivalents - Equivalent to the **Série du Gandatch** of Mercier (1968) and to the **Gandatch** and **Pyrgos** units of Godfriaux & Ricou (1991). The latter two-fold

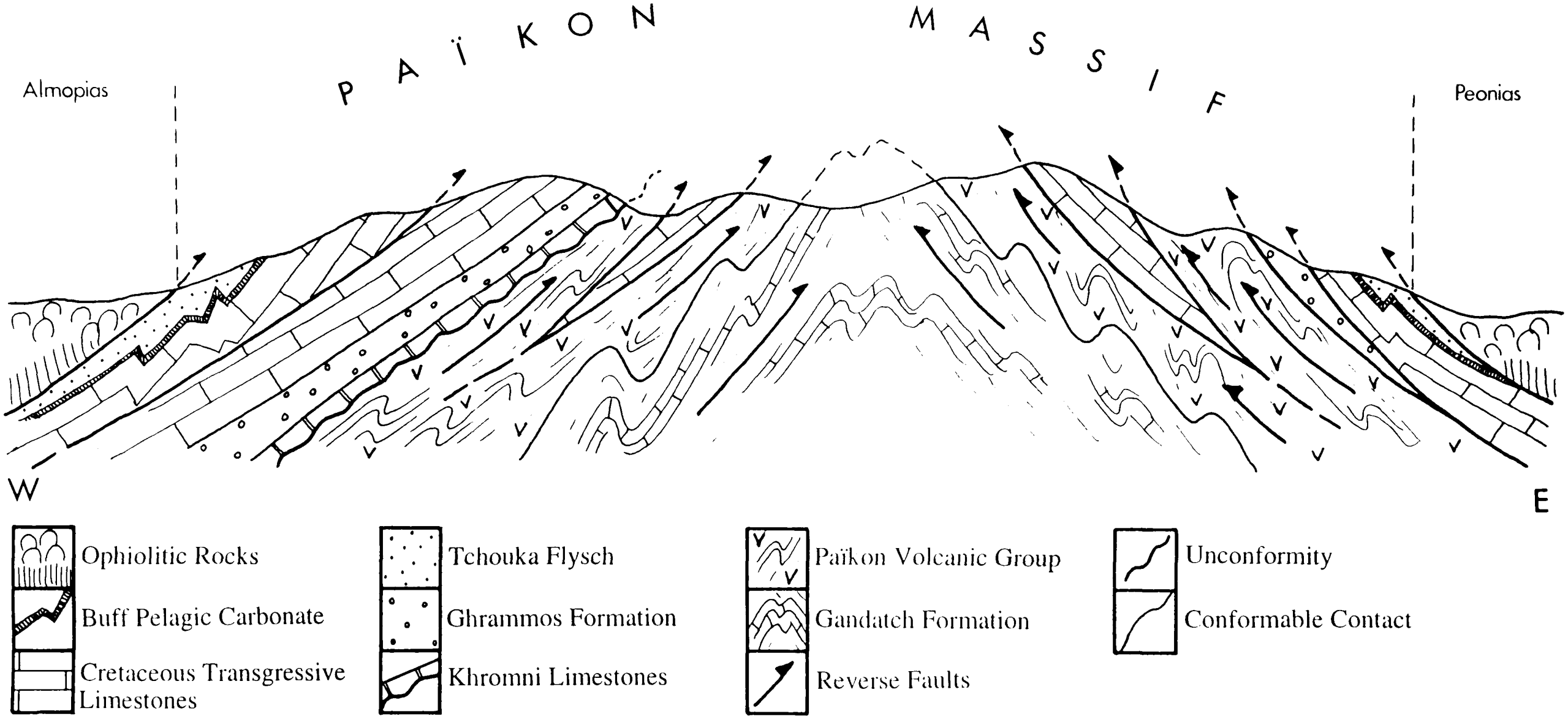


Figure 2.6 - Schematic cross-section through the anticlinal Païkon Massif. The stratigraphic succession on either side of the massif is identical, although reverse faulting has caused considerable disruption (see chapter 4).

KEY

to all colour maps in thesis

Villages

Pr - Periklia

Ar - Archangelos

Sk - Skra

Kou - Koupa

Ka - Karpi

Kas - Kastaneri

Ghr - Ghriva

Pen - Pentalofos

El - Eliftherohori

Kr - Khromni

Ma - Mandalon

Th - Theodoraki

Ko - Konstantia

Ida - Ida

Meg L - Meghala Livadia

Mic L - Micra Livadia

Mountains

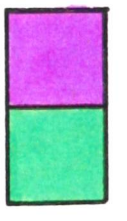
Pet - Petrades

Gr - Gropi

Gt - Gola Tchouka

Ga - Gandatch

Lithologies

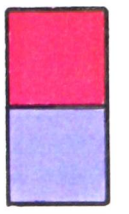


Gandatch Fm

Paikon Volcanic Group

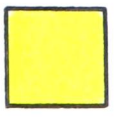


Khromni Limestone



Ghrammos Fm

Cret. Transgress. Limestones



Tchouka Flysch & Buff Pelagic Carb.

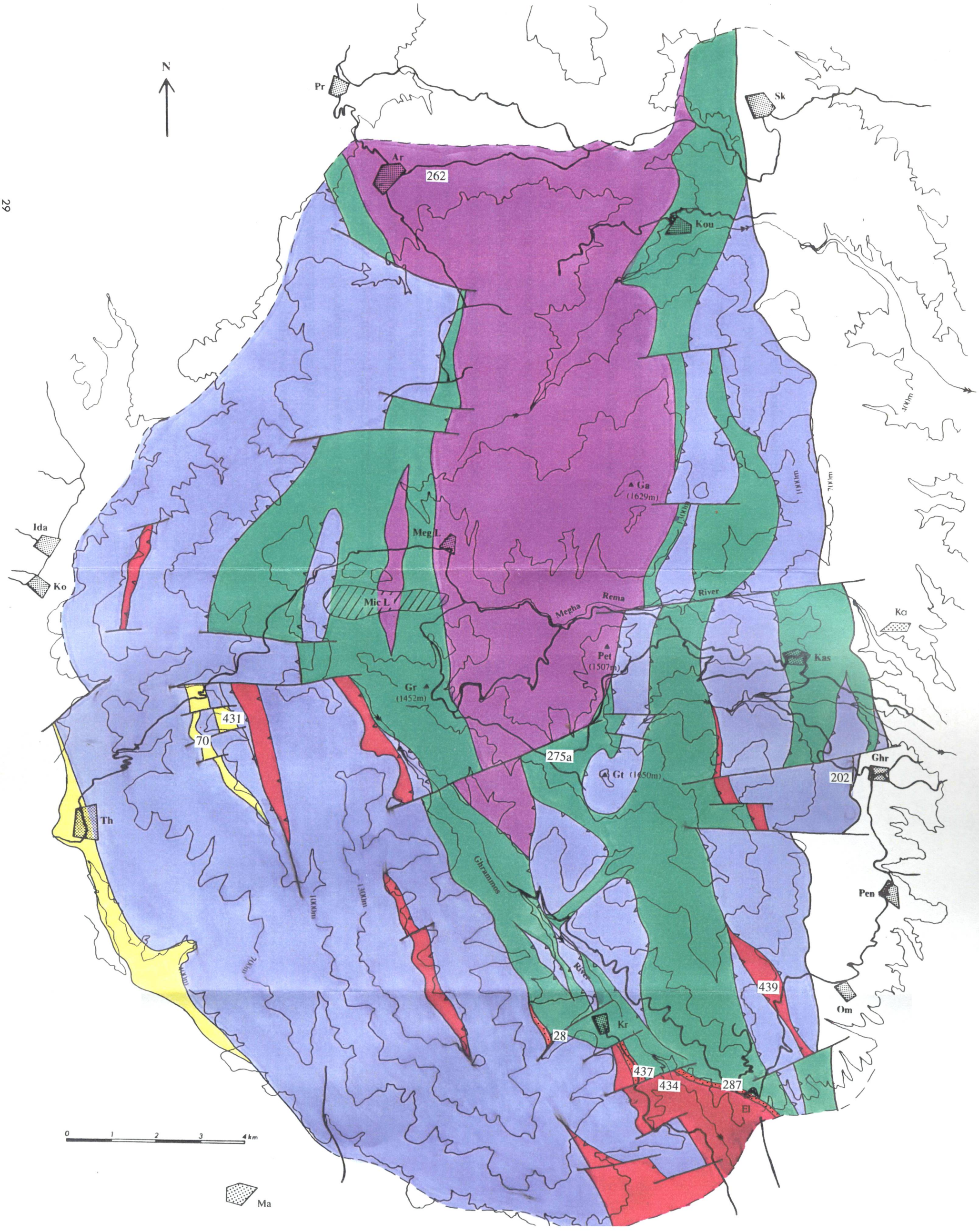


Figure 2.7 - Geological map of the Païkon Massif showing all localities mentioned in the text of chapter 2.

division has been relinquished, as the Pyrgos unit was found merely to represent a more schistose component, which has been observed throughout the Gandatch Formation and not exclusively along its upper margin. The Gandatch Formation is not equated to the Calcaires de Gola Tchouka (Ppé1; section 2.2.3) of Mercier (1968).

Characteristics **- ? Upper Triassic to Middle Jurassic** interbedded chloritic schists, calc-schists and marbles, which vary in relative abundance between localities. The thickness of this unit is difficult to assess due to extensive structural repetition, however, an estimated thickness in the order of 500 metres is likely.

Distribution - The Gandatch Formation constitutes the core of the anticlinal Païkon Massif and crops out in a ~5 km wide band between Archangelos village in the northwest and Mount Petrades (1507 m) in the south (Figures 2.6 & 2.7).

Contacts - The lower contact of the Gandatch Formation is not exposed within the Païkon Massif but is exposed further north within the Voras Massif (Figure 2.7, section 6.3.6), where a depositional contact exists between the schists and marbles of this unit and the underlying gneisses and mica-schists (Mercier, 1968; Brown *et al.,* in prep; chapter 3.3). The upper contact is depositional, passing from the chloritic and calc-schists of the Gandatch Formation into the Livadia Formation above (Figure 2.8). This contact is rarely preserved intact, but is well exposed between Mount Petrades and Gola Tchouka (Figure 2.7). At most localities where this contact is exposed (e.g. Micra Livadia, Meghala Livadia, Archangelos, see Figure 2.7), the contact between these two units is folded and often tectonically re-activated due to a significant competency contrast.

GANDATCH - LIVADIA CONTACT
NW GOLA TCHOUKA
CENTRAL PAÏKON

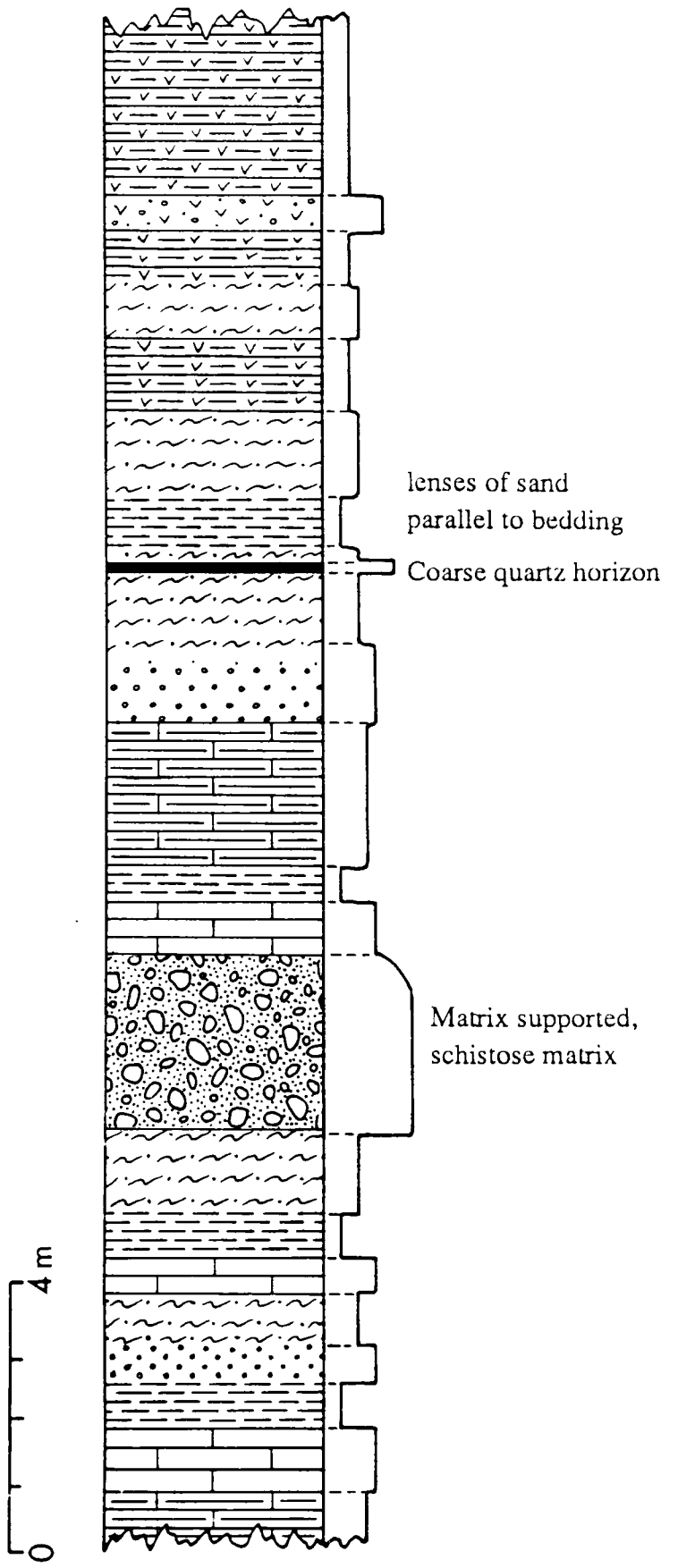


Figure 2.8 - Logged section through the contact between the Gandatch Formation and the Livadia Formation. The contact is conformable and marked by a progressive increase in volcaniclastic and chloritic schists and a decrease in clac-schists and marbles (locality 275a between Mount Petrades and Gola Tchouka; see Figure 2.7).

2.2.2 - *The Païkon Volcanic Group - Livadia Formation*

Due to a reassessment of the stratigraphic significance of the Gropi Formation (see sections 2.2.3 and 3.9) the Livadia and Kastaneri Formations (sections 2.2.2 and 2.2.4 respectively) are now considered as two distinct formations which together constitute the Païkon Volcanic Group (see chapter 5 for details of geochemistry).

Equivalents - Equivalent to the **Série de Livadia** of Mercier (1968). Represents the lower, more basic formation of the Païkon Volcanic Group.

Nomenclature - The type locality of this formation is exposed on the low-lying hills around Micra and Meghala Livadia in the central Païkon Massif and it is from this area that the formation takes its name.

Characteristics - **?Middle Jurassic.** The lower, more basic formation of the Païkon Volcanic Group: rust-brown, fine-grained, chloritic, pyroclastic schists interbedded with occasional basic to intermediate composition lava flows.

Distribution - The Livadia Formation crops out sporadically in a narrow, folded zone around the underlying Gandatch Formation. Exposure is relatively poor due to its low absolute volume, its susceptibility to weathering (much of the surficial exposure has been cultivated) and due to tectonic cut-out.

Contacts - As described above, the lower contact of this formation is normal and folded. The nature of the contact with the overlying Kastaneri Formation is gradational and marked by an increase in more evolved volcanic and volcaniclastic horizons and a greater proportion of pyroclastic rocks relative to volcanic flows (sections 3.5, 3.6 and chapter 5).

2.2.3 - *Gropi Formation*

Nomenclature - Named after the type locality designated by Mercier (1968) near Mount Gropi (1452m, Figure 2.7).

Equivalents - The **Calcaires de Gropi** (Pa3) and **Calcaires de Gola Tchouka** (Ppé1) of Mercier (1968). These two units are facies and lithostratigraphic equivalents (as noted by Godfriaux & Ricou, 1991; this work) which are exposed on opposing sides of the anticlinal Païkon Massif (i.e. Gropi on west flank, Gola Tchouka on east flank).

Characteristics - **?Middle Jurassic** massively-bedded white recrystallised limestone with a highly deformed fauna. On a road section which passes below the summit of Gola Tchouka (1650m, Figure 2.7) more calcarenitic horizons, characteristic of the base of this unit, can be observed, as can the remains of deformed and recrystallised fauna, mainly unidentifiable gastropods and possibly bivalves.

Boundaries - Both the upper and lower contacts of the Gropi Formation are tectonic.

The age and stratigraphic significance of the Gropi Formation has been the subject of much recent debate. Three possible scenarios can be envisaged:

1 - The Gropi Formation is a stratigraphic unit of Middle Jurassic age, which occurs conformably between the Livadia Formation and the Kastaneri Formation (Mercier, 1968; Figure 2.9).

2 - The Gropi Formation is Cretaceous in age and is the inner shell of a multi-layered tectonic window which formed during Tertiary compression (Godfriaux & Ricou, 1991; Bonneau *et al.*, in press; Figure 2.10).

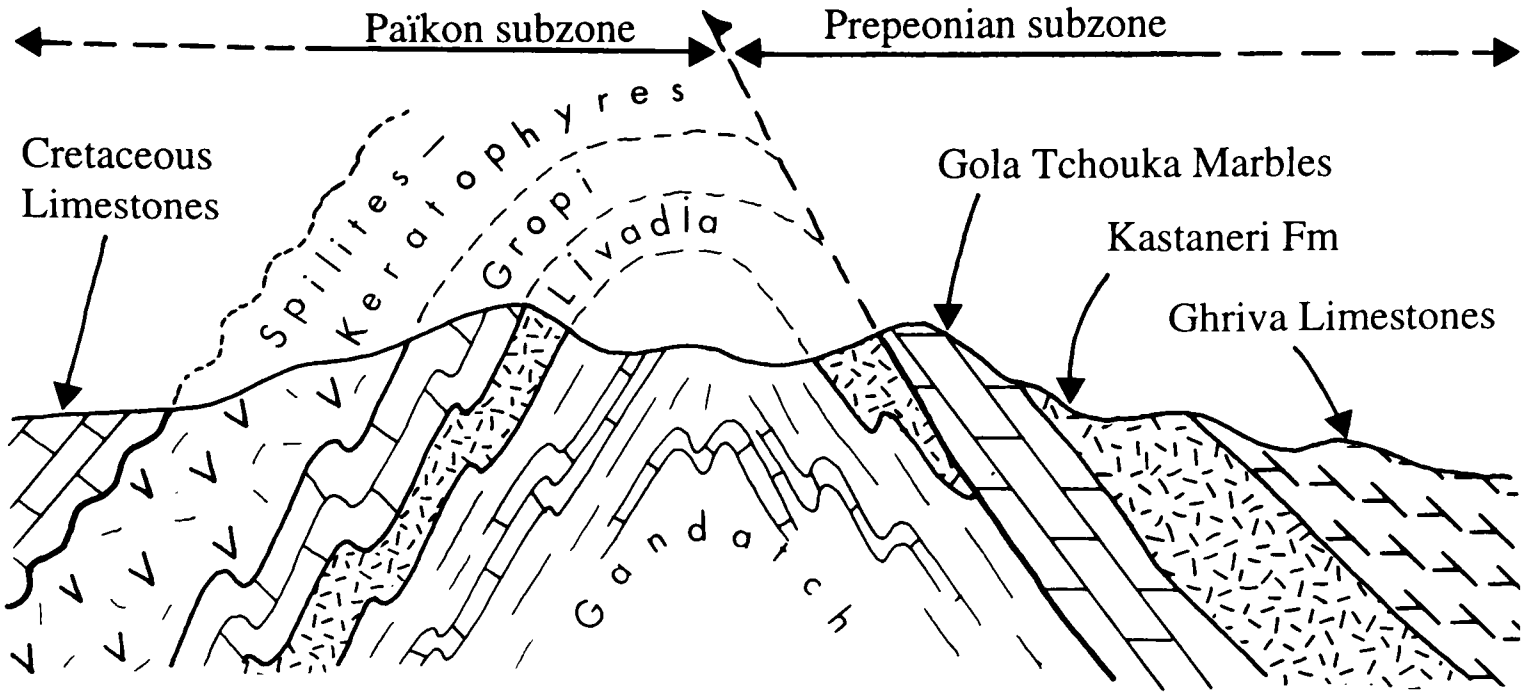


Figure 2.9

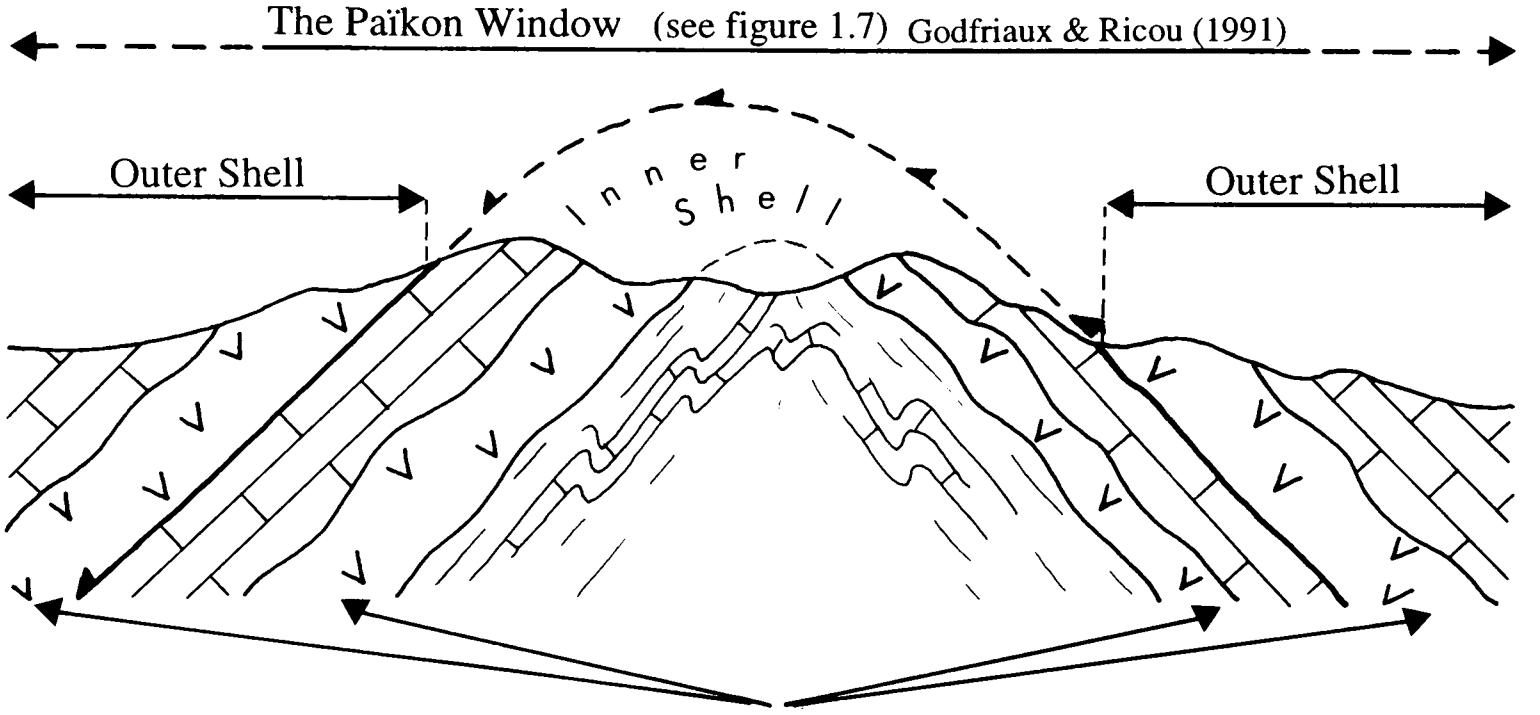


Figure 2.10

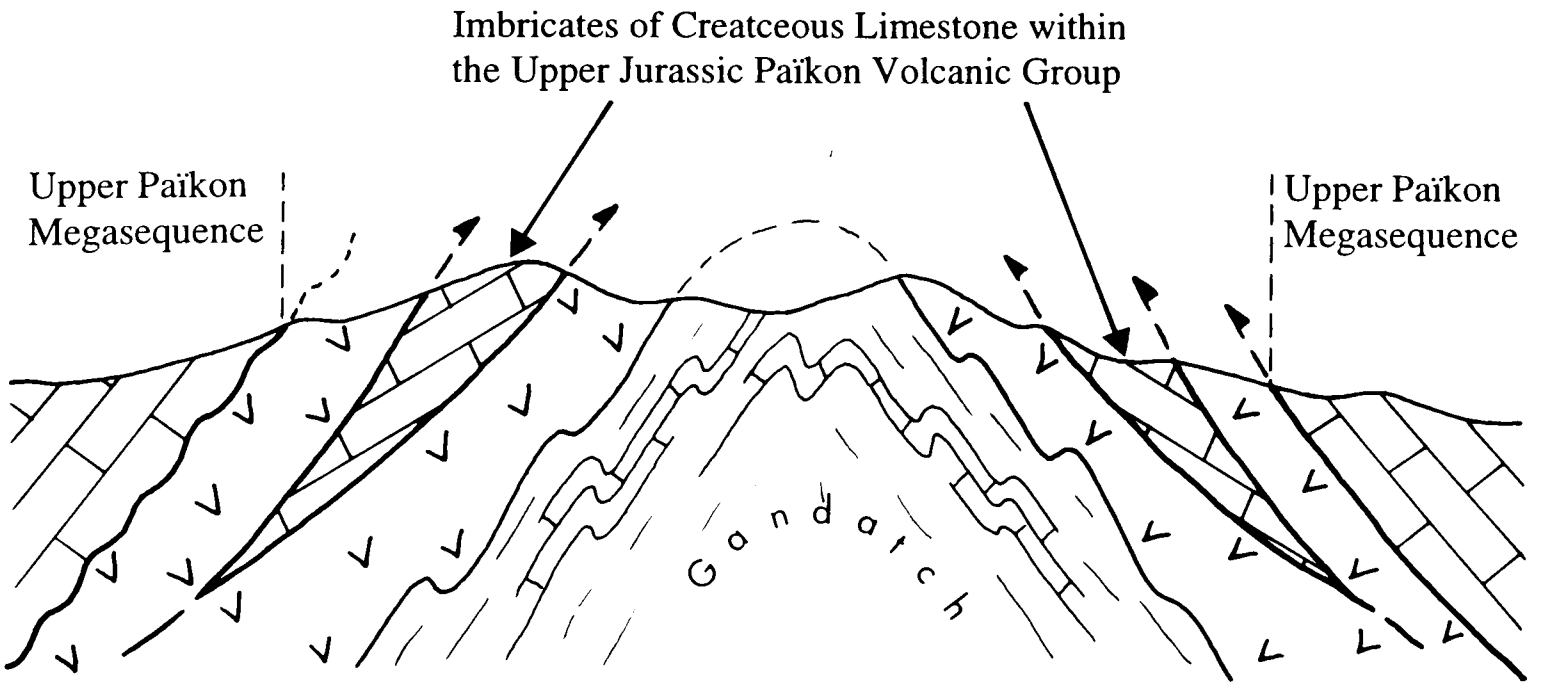


Figure 2.11

3 - The Gropi Formation is a thrust slice of the Cretaceous Transgressive Limestones (section 2.2.7) incorporated within a single, bi-modal volcanic group which is basic to intermediate at its base (Livadia Formation) and intermediate to acidic at its top (Kastaneri Formation) (Figure 2.11).

As described earlier, these carbonates were originally dated as ?Middle Jurassic based on a poorly-preserved gastropod fauna. However, more recent work carried out by Bonneau *et al.* (in press), and during the course of this study, indicate that both the *Calcaires de Gropi* (this work) and the *Calcaires de Gola Tchouka* (this work and Bonneau *et al.*, in press), which together constitute the Gropi Formation, (Godfriaux & Ricou, 1991; this work) are Cretaceous in age.

From outcrops between Kastaneri and Micra Livadia, and north of Eliftherohori village, large, deformed lamellibranchs were found (this work; Figure 2.12), and near summit of Gola Tchouka a fauna including *Radiolitidae sp.* (Albian-Maastrichtian) and *Requieniidae sp.* (Tithonian-Maastrichtian) rudist bivalves was extracted (Bonneau *et al.*, in press). Based on the findings in these areas a Cretaceous age is now envisaged for the Gropi Formation.

The new age data imply that Scenario 1 is unlikely. In addition, Scenario 1 suggests that the Gropi Formation formed as a limestone build-up within the Païkon Volcanic Group, either during a lull in volcanism (i.e. between the Livadia and Kastaneri Formations) or in an isolated area which was fully marine yet protected from the influx of volcanic material. The absence of any volcanogenic material within the Gropi Formation would be surprising if Scenario 1 were correct, and thus Scenario 1 is abandoned.

The complex layer-cake model proposed by Bonneau *et al.* (in press) is unlikely due to the structural relationships observed between the Gropi Formation and the volcanic succession within which it occurs and between the Païkon Massif as a whole and the Almopias subzone to the west (this matter will be explored further in



Figure 2.12 - Field photograph of deformed rudist bivalves in a thrust slice of Cretaceous limestone (originally dated as Middle Jurassic) from west of Kastaneri village.



Figure 2.13 - Field photograph of the sheared unconformable contact between the Kastaneri Formation and the Khromni Limestones. The top of the Kastaneri Formation is lateritic and deeply weathered (locality 28, north of Khromni village).

section 2.2.9 and in chapters 4 and 7). In all areas, including the localities of Bonneau *et al.* (in press) both upper and lower contacts of these newly-dated Cretaceous carbonate units are tectonic, and it is postulated here that they are thrust slices of the overlying Cretaceous Transgressive Formation, which were incorporated into the underlying volcaniclastic succession of the Livadia and Kastaneri Formations during bi-vergent Tertiary deformation (see chapter 4.6). Therefore, Scenario 3 is adopted here and the Gropi Formation is no longer considered as a separate stratigraphic unit, but as a series of thrust slices of Cretaceous Transgressive Limestone which were incorporated into the Païkon Volcanic Group during Tertiary compression. Further evidence of this interpretation is given in chapters 4 and 7.

2.2.4 - *The Païkon Volcanic Group - Kastaneri Formation*

Nomenclature - The nomenclature of this unit is in keeping with that of Mercier (1968) for the eastern component of this formation (Ppé2). The name was taken from the village of Kastaneri, around which this formation crops out in abundance.

Equivalents - Represents the upper, more acidic formation of the Païkon Volcanic Group. **Le Cortège Spilites-Keratophyres** (Pa5), and **Formation de Kastaneri** (Ppé2) of Mercier (1968), and also to the **Kastaneri Meta-rhyolites** of Godfriaux & Ricou (1991). The two-fold subdivision made by Mercier was found to be incorrect as Pa5 and Ppé2 are equivalent units which respectively crop out on western and eastern limbs of the anticlinal Païkon Massif.

Characteristics - **Middle to Upper Jurassic (pre-Kimmeridgian).** Interbedded acidic and intermediate-composition pyroclastic and volcanic rocks. Highly weathered andesites are common, as are quartz and feldspar porphyries and fine-grained tuffs. There are also rare, deformed granites. In certain sections, hydrothermal alteration and massive sulphide impregnation is well-developed, while other areas remain relatively well preserved. The Kastaneri Formation is one of the

most voluminous in the Païkon Massif, with an estimated thickness of around 500 metres (structural repetition increases the apparent thickness considerably). An Upper Jurassic (pre-Kimmeridgian) age has been assigned to this formation due to its relative stratigraphic position below the Kimmeridgian Khromni Limestones (chapters 2.2.5 and 3.7).

Distribution - The Kastaneri Formation dominates the eastern flank of the Païkon Massif where it crops out sporadically along heavily forested road cuttings, and is disrupted by lensoid thrust slices of recrystallised Cretaceous limestone (see sections 2.2.3 and 2.2.7). In the west it crops out along, and on either side of, the Ghrammos river valley in the south and extends north as a band of irregular thickness towards Ida village (Figure 2.7). The type locality of this formation can be seen along the road that leads north out of Eliftherohori village (Figure 2.7).

Contacts - Its lower contact is tectonic, as described in section 2.2.3. The upper contact is unconformable. There is a marked structural and metamorphic break between the Kastaneri Formation and the overlying Khromni Limestones (section 2.2.5), as well as a small angular discordance. This is exposed south of Khromni village and north of Eliftherohori (Figures 2.6 & 2.7). The former area also exposes lateritic surfaces, the presence of which suggests that some degree of subaerial exposure and weathering (Figure 2.13) has taken place. From a tectonostratigraphic perspective the Kastaneri Formation, and the two formations which underlie it, have undergone a phase of ductile, compressional deformation which did not affect the overlying units (see chapter 4.2).

THE UPPER PAÏKON MEGASEQUENCE

2.2.5 - *Khromni Limestones*.

Nomenclature - Translated from Mercier (1968).

Equivalents - Equivalent to the **Calcaires de Khromni** of Mercier (1968).

Characteristics - Highly bioturbated, shallow-water carbonates of rapidly changing facies. Accurately dated as **Kimmeridgian to Portlandian** by an abundant fauna of *Cladocoropsis mirabilis* algae and *Psuedocyclammina* foraminifera (Mercier, 1968; this work Figure 2.14). Horizons rich in detrital terrigenous material are common (chapter 3.7).

Distribution - The Khromni Limestones are limited in extent, either due to structural cut-out during Tertiary tectonism and/or to restricted deposition. The Khromni Limestones were originally documented only from the western central Païkon Massif (south of Khromni village, Mercier, 1968), but this unit has also been identified in southwestern and southeastern areas of the Païkon Massif during the course of this work (see chapter 3.7).

Contacts - The Khromni Limestones unconformably overlie the Kastaneri Formation but have a normal gradational contact with the Ghrammos Formation above (section 2.2.6). This normal contact was observed along the road that leads north out of Eliftherohori village (Figure 2.15).

2.2.6 - *Ghrammos Formation*

Equivalents - Equivalent to **Le Flysch Éocrétacé** of Mercier (1968).

Nomenclature - This unit has been renamed the Ghrammos Formation to avoid any confusion with the Tchouka Flysch (section 2.2.9) and because the type locality of this formation lies along the western side of the Ghrammos river valley, south of Khromni village (Figures 2.6 & 2.7).

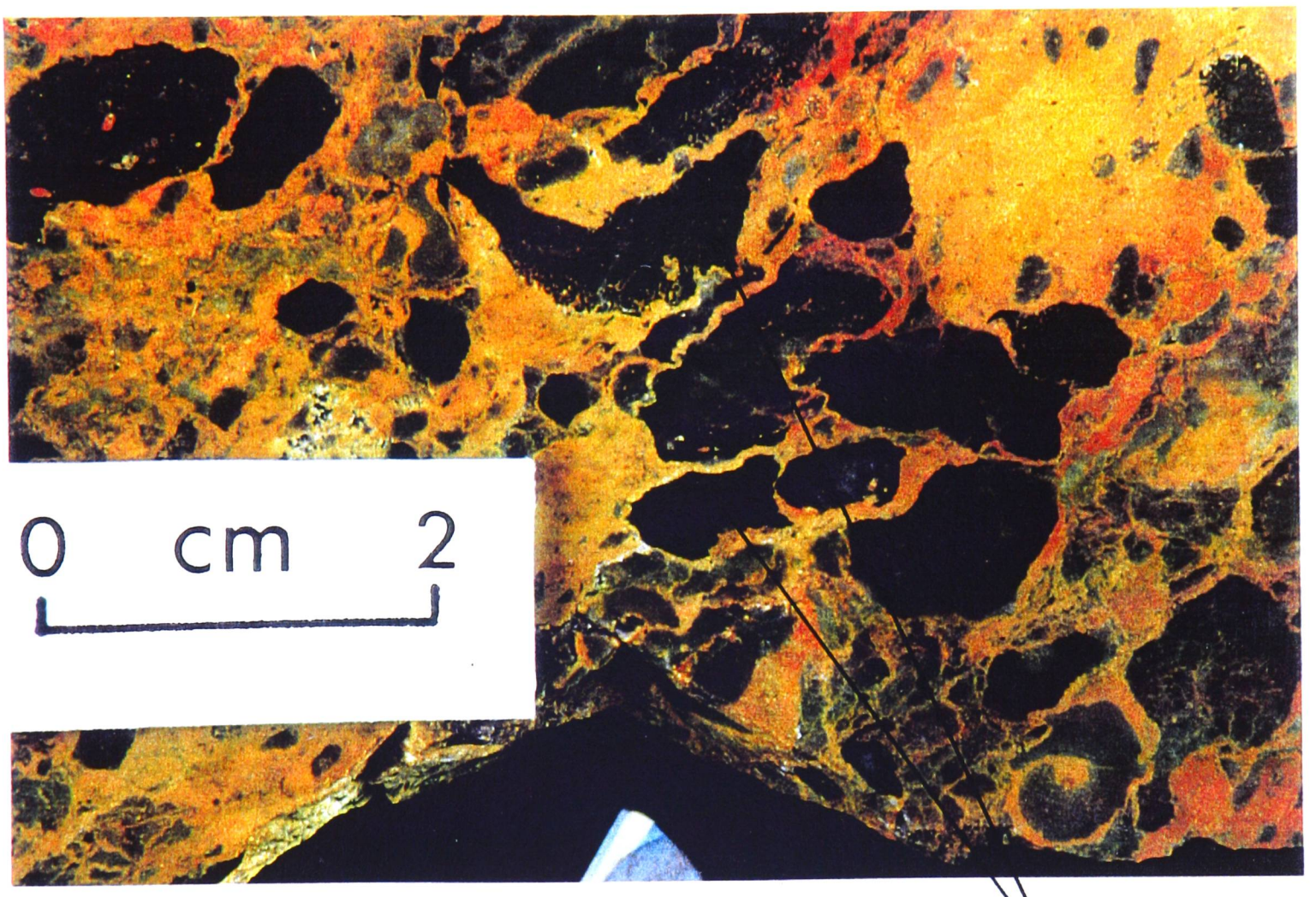


Figure 2.14 - Photograph of a polished hand specimen from the Khromni Limestones. *Cladocoropsis* algae structures can be picked out in dark patches and are surrounded by buff marl. From locality 437 north of Khromni village.

KHROMNI - GHRAMMOS CONTACT
ELIFTHEROHORI
CENTRAL SOUTHERN PAÏKON

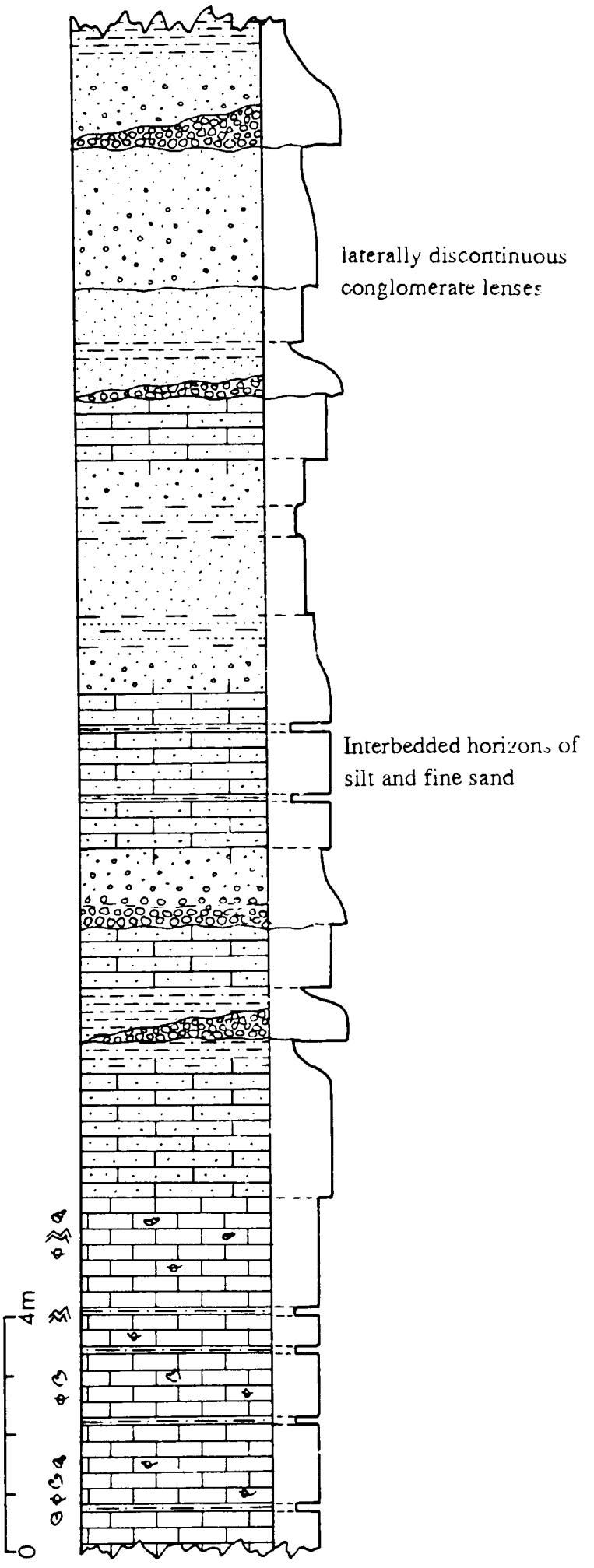


Figure 2.15 - Logged section of the contact between the Khromni Limestones and the Ghrammos Formation. The carbonate component decreases up-section and eventually gives way to a wholly clastic sequence (locality 287 just north of Eliftherohori village; see Figure 2.7).

Distribution - Previously thought to crop out solely in the southwestern corner of the Païkon Massif, south of Khromni village, as the Khromni Limestones. Detailed field studies, however, have shown that the Ghrammos Formation is considerably more extensive than previously recognised, cropping out along the entire length of the western Païkon Massif and in central and southern parts of the eastern flank. In the southeast it is extremely difficult to distinguish it from the Kastaneri Formation of the Païkon Volcanic Group and has been wrongly identified by previous workers as a result. Due to poor exposure the Ghrammos Formation has not been identified in the northeast of the study area, although it may exist.

Characteristics - **Portlandian to Albian** interbedded wine-red sands, silts and conglomerates. The conglomerates form lenticular, laterally discontinuous bodies within finer-grained horizons. In all areas other than the type locality, the Ghrammos Formation has been reduced to a pale green colour and is often difficult to distinguish from the Kastaneri Formation.

Contacts - As described above (section 2.2.5) the contact between the Ghrammos Formation and the underlying Khromni Limestones is conformable. The uppermost contact is, however, contentious. Mercier (1968) did not identify the Ghrammos Formation or Khromni Limestones in any area other than the southwest corner of the Païkon Massif, and therefore postulated that these units were unconformably overlain by the extensive Cretaceous Transgressive Limestones above. This, however, is incorrect, as outlined above. Vergely (1984) also inferred that an unconformable contact existed at this stratigraphic position, as he had identified a phase of compressional deformation (JE2) within the Ghrammos and Khromni units which he did not recognise within the limestones above (chapter 4.2). This is also erroneous, as all structures displayed within the Ghrammos Formation and Khromni Limestones structures also affect the overlying Cretaceous Transgressive Limestones and can thus be attributed to Tertiary tectonism (chapter 4.6).

Close inspection of the contact in question has revealed that a conformable transition from one unit to the other can be demonstrated with certainty (Figure 2.16). Locally, horizons of non-deposition characterised by caliche formation have developed (Sharp & Robertson, 1992; this work), which may be the result of periodic non-deposition. Hence it is postulated here that the contact between the Ghrammos Formation and the Cretaceous Transgressive Limestones is conformable, with occasional, regionally insignificant unconformities formed as a result of local non-deposition. As with many contacts in the study area, which separate two units of contrasting competency, the Ghrammos Formation/Cretaceous Transgressive Limestone contact is commonly tectonically reactivated.

2.2.7 - *Cretaceous Transgressive Limestones*

Nomenclature - Translated from the **Calcaires Transgressif** of Mercier (1968).

Equivalents - Mercier (1968) subdivided the "Calcaires Transgressif" into five parts: the Cretaceous Transgressive Limestones are equivalent to the first three of these; Pa9a, Pa9b and Pa9c. They are also comparable to the **Calcaires de Gropi** and **Calcaires de Gola** Tchouka, as discussed in section 2.2.2 and the **Calcaires de Ghriva** of Mercier's Prepeonian subzone (Ppé3; 1968).

Distribution - This unit was originally thought to occur only on the western side of the study area (Mercier, 1968), but the discovery of a deformed rudist fauna near Ghriva village indicates their presence in eastern areas also (Godfriaux & Ricou, 1991; this work). Such a Cretaceous fauna has also been identified both northwest and northeast of Kastaneri village (this work; Figure 2.17), and in more central parts of the Païkon Massif (Bonneau *et al.*, in press; this work; Figure 2.12), from carbonate units that were previously assigned to the Gropi Formation. These more central outcrops are now interpreted as thrust slices of the Cretaceous Transgressive

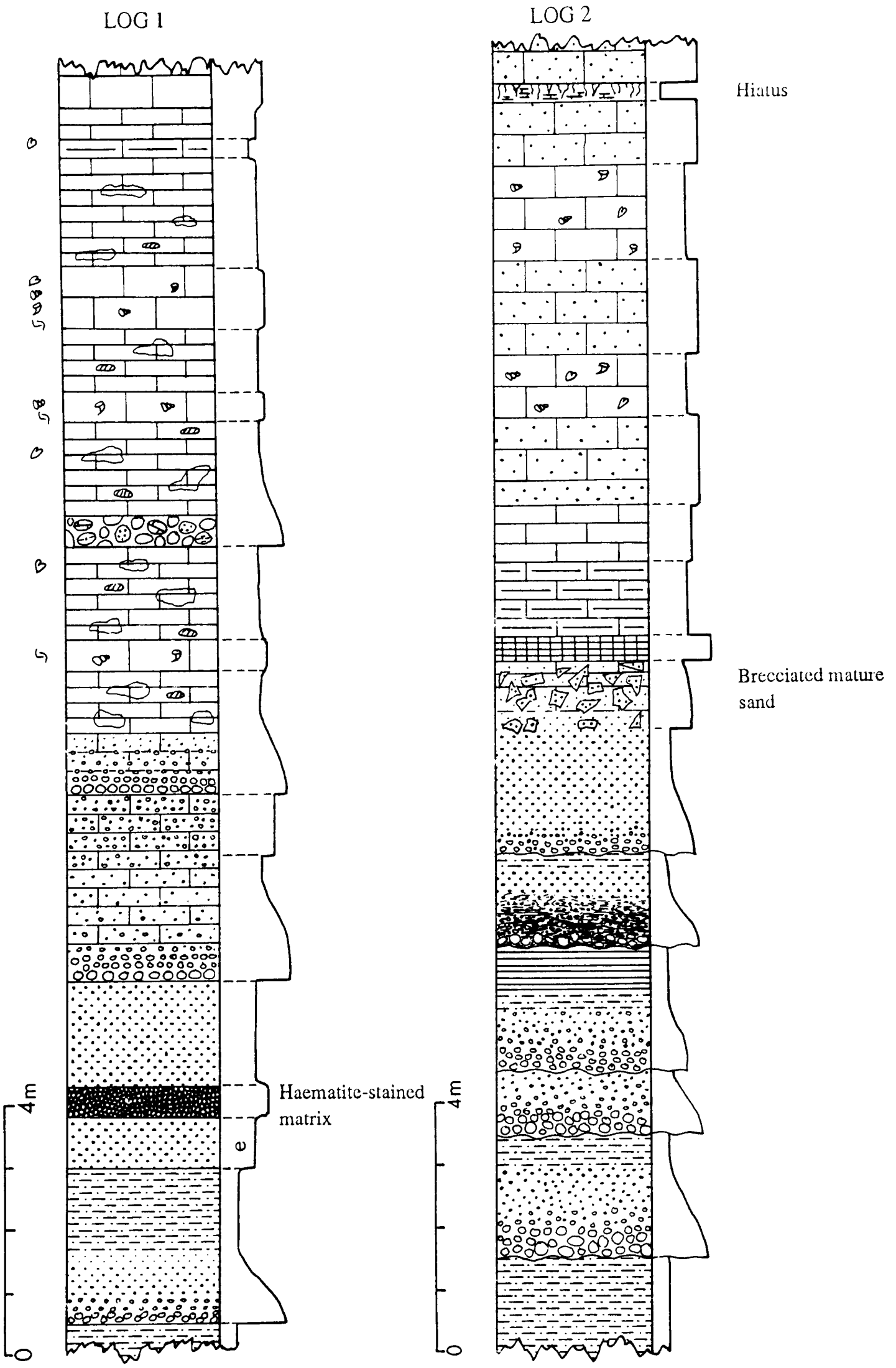


Figure 2.16 - Two logged sections of the contact between the Ghrammos Formation and the overlying Cretaceous Transgressive Limestones. The Ghrammos sediments become more mature towards their top and ultimately give way to calc-arenites and nodular carbonates. Log 1 is from locality 439 north of Khromni village and Log 2 is from locality 434 south of Khromni village (see Figure 2.7).



Figure 2.17 - Field photograph of a deformed rudist bivlave from the Cretaceous Transgressive Limestones on the eastern side of the Païkon Massif (north of Karpi village).

Limestones which were incorporated into the Païkon Volcanic Group during Tertiary deformation.

Characteristics - Albian to Turonian grey shallow-water carbonates (Mercier, 1968; Sharp & Robertson, 1992; this work). The limestones are calcarenitic at their base, passing up into grey, sparse and packed biomicrites with periodic horizons rich in terrigenous silt, mud and occasionally sand. Rudist bivalve and *Nerineid* gastropod packstones are common; solitary and colonial corals are rare. The unit has an estimated total thickness of approximately 300 m, although the apparent thickness is considerably more due to structural repetition. A complete section through the entire Cretaceous Transgressive Limestones was not observed due to extensive faulting and chevron folding and a composite section was thus compiled (illustrated and discussed in chapter 3.9.)

Contacts - For discussion of the lower contact see section 2.2.6 above. The upper contact of the Cretaceous Transgressive Formation is conformable, with the grey limestones of this unit passing up into the Buff Pelagic Carbonates above, over a distance of approximately 2 metres. This contact can be seen in both the vicinity of Theodoraki village (Sharp & Robertson, 1992) and west of Ghriva village (this work; Figures 2.7 & 2.18).

2.2.8 - ***Buff Pelagic Carbonates***

Nomenclature - Unchanged from Sharp & Robertson, 1992.

Equivalents - Equivalent to stratigraphic divisions **Pa9d** and **Pa10** of Mercier's Calcaires Transgressif.

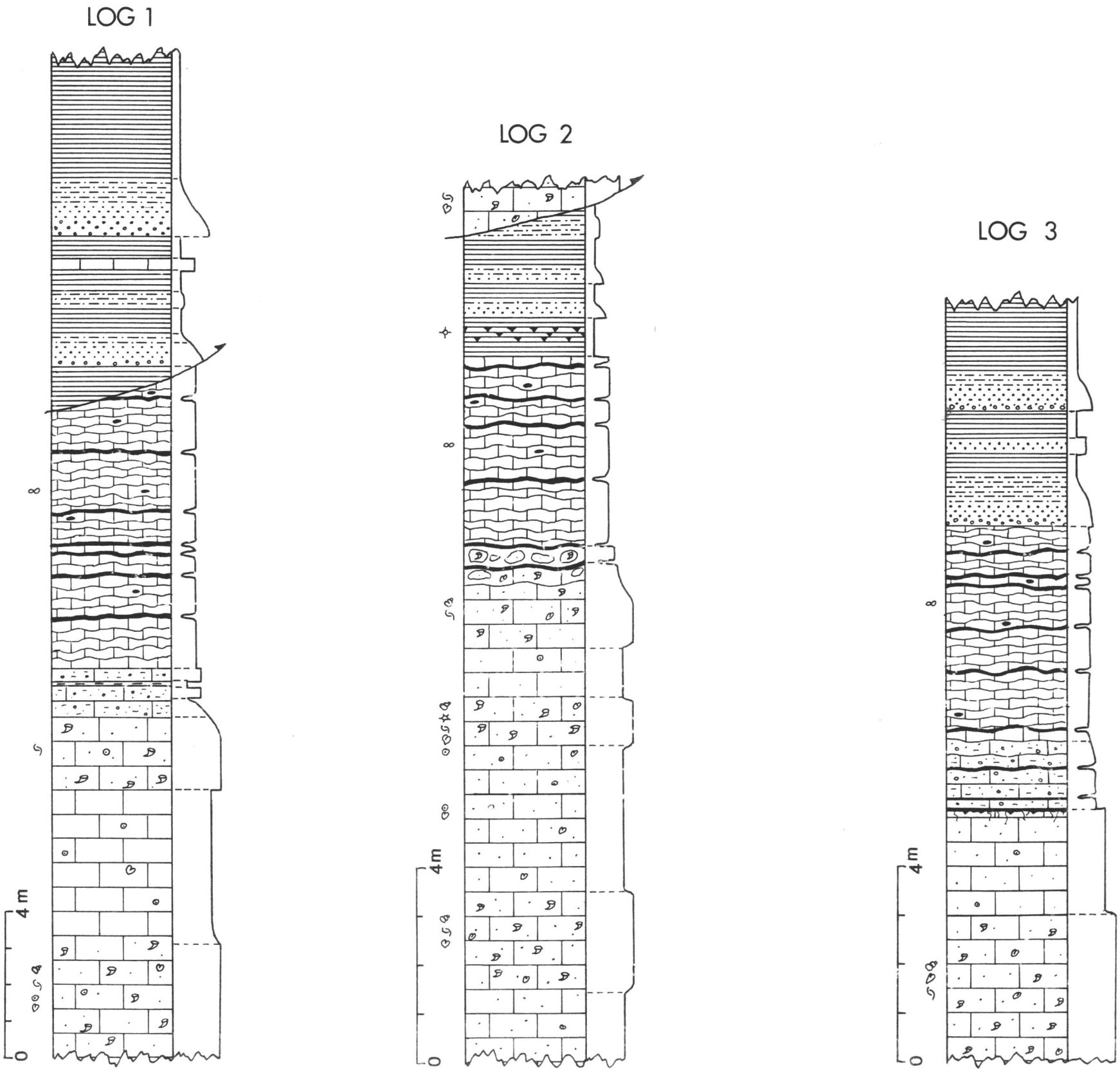


Figure 2.18 - Three logged sections across the contact between the Cretaceous Transgressive Limestones and the Buff Pelagic Carbonates. Log 1 is from locality 431; Log 2 is from locality 70 (both in the western Paikon Massif) and Log 3 is from locality 202 just south of Ghriva in the eastern Paikon Massif (see Figure 2.7).

Distribution - Crops out predominantly around the village of Theodoraki but can be traced south as far as Mandalon. It also crops out directly to the west of Ghriva village on the eastern side of the study area (Figure 2.7).

Characteristics - Pink/buff, fine-grained, *Globotruncana*-bearing carbonates. Thinly-bedded (0.25-1 cm). The unit thickness varies between 5 and 10 metres. Stylolitic clay/mud horizons commonly occur parallel to bedding. The clastic component increases up-section.

Contacts - Conformable contacts with both the underlying Cretaceous Transgressive Formation and the overlying Tchouka Flysch (Figure 2.18). The lower contact is marked by a red iron-stained crust, 0.1 to 5 cm thick (Sharp, 1995; this work).

2.2.9 - *Tchouka Flysch*

Nomenclature - After Sharp & Robertson (1992).

Equivalents - Equivalent to **Pa9e** and **Pa11** of Mercier (1968).

Distribution - The Tchouka Flysch can be found on both western and eastern sides of the Païkon Massif. Its presence in the west was first noted by Mercier (1968), and this work has revealed that the Tchouka Flysch is also present in the east of the study area, as previously unrecognised, principally to the west and south of Ghriva village.

Characteristics - Interbedded sands, silts and micro-conglomerates, intercalated periodically with detrital carbonates and green ribbon-radiolarite. Preliminary studies by Sharp & Robertson (1992) indicated a **Turonian to post-Maastrichtian** age for the radiolarian fauna present (chapter 3.11).

Contacts - The lowermost contact is conformable. The contact between the Tchouka Flysch and the overlying units is tectonic, with the Almopias (Sharp & Robertson, 1992; Brown & Robertson, in press) and Guevgueli (Vergely, 1984; Brown & Robertson, in press) volcanic rocks fold and thrust over the western and eastern flanks of the Païkon Massif, respectively.

The westward vergence of the Almopias subzone over the western Païkon margin does not support the complex layer-cake model proposed for the Païkon Massif by Bonneau *et al.* (in press; Scenario 2, section 2.2.3). The layer cake model requires the outer Païkon shell (Figure 2.10) to have been thrust from east to west over the inner Païkon shell during the Tertiary, which would produce west-verging structures of this age. However, as detailed in chapter 4.6 such Tertiary structures verge consistently towards the east and northeast in the western Païkon and thus the layer cake model is inappropriate.

2.3 - DISCUSSION AND CONCLUSIONS

The stratigraphy of the Païkon Massif can be described in terms of two essentially conformable megasequences, separated by a significant structural and metamorphic discontinuity (chapter 4; Figure 2.19). The **lower Païkon megasequence**, which crops out in the centre of the Païkon Massif, comprises three formations of ?Triassic to pre-Kimmeridgian age. From base to top these are the **Gandatch Formation** (?Triassic interfoliated schists and marbles), the **Livadia Formation** (Jurassic basic and intermediate volcanics) and the **Kastaneri Formation** (pre-Kimmeridgian rhyolites and acidic pyroclastics). Together the Livadia and Kastaneri Formations constitute the **Païkon Volcanic Group**.

The **upper Païkon megasequence** constitutes the flanks of the Païkon Massif anticline. From base to top it consists of the Kimmeridgian to Portlandian

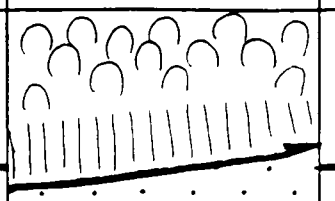
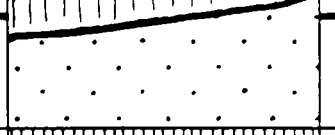
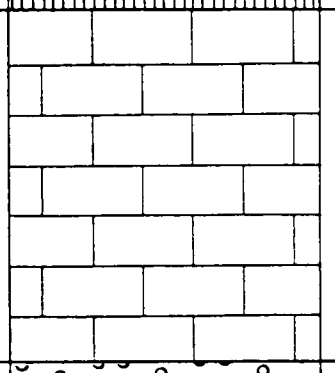
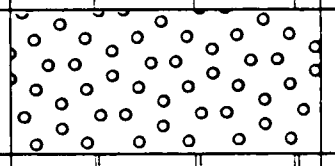
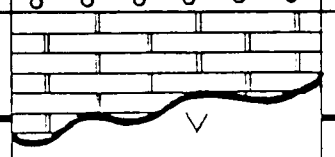
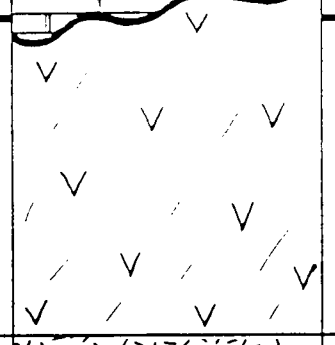
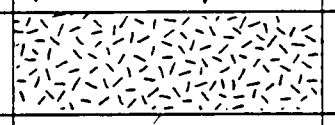
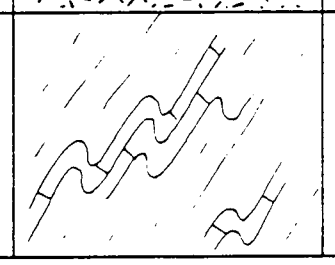
AGE	LITHOLOGY	FORMATION	DESCRIPTION	
Upper Jurassic to Lower Cretaceous		Overthrust ophiolites	Sheeted dykes, pillow lavas & radiolarian cherts	
Turonian to Maastrichtian		Tchouka Flysch	Deep-water sands, silts & radiolarite	UPPER PAÏKON MEGASEQUENCE
Turonian		Buff Pelag Carbonate	Pelagic limestones	
Turonian Aptian/Albian		Cretaceous Transgressive Limestones	Shallow-water carbonate platform	
post-Kimmeridgian - pre-Aptian/Albian		Ghrammos Formation	Red-bed sands, silts and conglomerates	
Kimmeridgian/ Tithonian		Khromni Limestones	Shallow marine algal limestones	
Middle to Upper Jurassic		Kastaneri Formation	Intermediate to acidic volcanics and volcaniclastics	LOWER PAÏKON MEGASEQUENCE
?Middle to Upper Jurassic		Livadia Formation	Basic to intermediate volcanics	
? Lower to Middle Jurassic		Gandatch Fortmation	Marbles, chloritic schists and calc-schists	

Figure 2.19 - Composite stratigraphic log of the Païkon Massif.

Khromni Limestones, the **Ghrammos Formation** (Uppermost Jurassic to Basal Cretaceous red-bed clastics), the **Cretaceous Transgressive Limestones** (Aptian/Albian to Turonian), the **Buff Pelagic Carbonates** and the Turonian to post-Maastrichtian **Tchouka Flysch**.

Chapter 3

Lithological Descriptions

CHAPTER THREE - LITHOLOGICAL DESCRIPTIONS

3.1 - INTRODUCTION

In this chapter, detailed lithological descriptions of each formation within the Païkon Massif are presented, from the base to the top of the succession in turn. In doing so, the sedimentological, biostratigraphical and petrological information necessary to draw conclusions concerning the depositional environments and/or environments of genesis of these lithologies will be outlined, thus enabling a picture of the spatial and temporal geological evolution of the Païkon Massif to emerge. Structural and geochemical data, that are also essential to the construction of an evolutionary model, will be presented and discussed in the succeeding two chapters (i.e. chapters 4 and 5 respectively). Location maps identify the principal areas of study and pinpoint the topographic features, roads and settlements used for orientation.

3.2 - PREVIOUS WORK

The fundamental anatomy of each lithological component which constitutes the Païkon subzone was initially documented by Mercier (1968). Within the Païkon Massif (which equates to the Païkon subzone of this work and to both the Païkon and Prepeonian subzones of Mercier, 1968; chapters 1 & 2) Mercier's work included a preliminary investigation of the volcanic successions and excellent palaeontological work on the carbonate formations present. This pioneering work laid the foundations for all subsequent research and provided invaluable age determinations of the post-volcanic cover sediments of the Païkon Massif.

Bebien (1982) and Godfriaux & Ricou (1991) later proposed alternative litho-tectonic models for the Païkon Massif (as detailed in chapters 1 & 2) but did not provide a comprehensive study of each, or indeed of any, of the lithological units. Their

conclusions were instead drawn from their interpretation of relationships *between* different rock types, as opposed to the petrological, biostratigraphical or geochemical characteristics inherent in each.

Baroz *et al.* (1987) studied the metamorphic petrology of the lowermost formations within the Païkon Massif (i.e. Gandatch, Livadia and Kastaneri Formations) which was previously lacking. Thermobarometric work by these authors identified mineral assemblages indicative of both blueschist and high-pressure greenschist facies metamorphism, with profound implications for the tectonic evolution of the Païkon Massif. The work of Baroz *et al.* (1987) is discussed in greater detail in chapter 4.

A recent study in the area involved biostratigraphical work by Bonneau *et al.* (in press). They discovered a Cretaceous fauna in carbonate rocks situated centrally within the Païkon Massif which led to a new, but controversial, tectonic model for the study area; this work is discussed in chapter 2. Although many researchers have published new information and have proposed alternative evolutionary models based on their own data, no thorough study embracing all stratigraphic units, and thus the Païkon subzone as a whole, has been carried out since that of Mercier (1968).

3.3 - BASEMENT LITHOLOGIES

The pioneering work of Mercier (1968) and more recent studies by Brown *et al.* (in prep.) in the Voras Massif, which lies directly to the north of the Païkon Massif (chapter 6, Figure 6.1), have identified the spatial, temporal, lithological and tectonic affinities of its eastern part (i.e. from Pinovon to east of Tzena, Figure 6.6) and the Païkon Massif. From these studies it has been concluded that the basal Gandatch Formation of the Païkon Massif (section 3.4; Figure 3.1) is equivalent to the Tzena schists and marbles of the Voras Massif (chapter 4 & chapter 6.3.6).

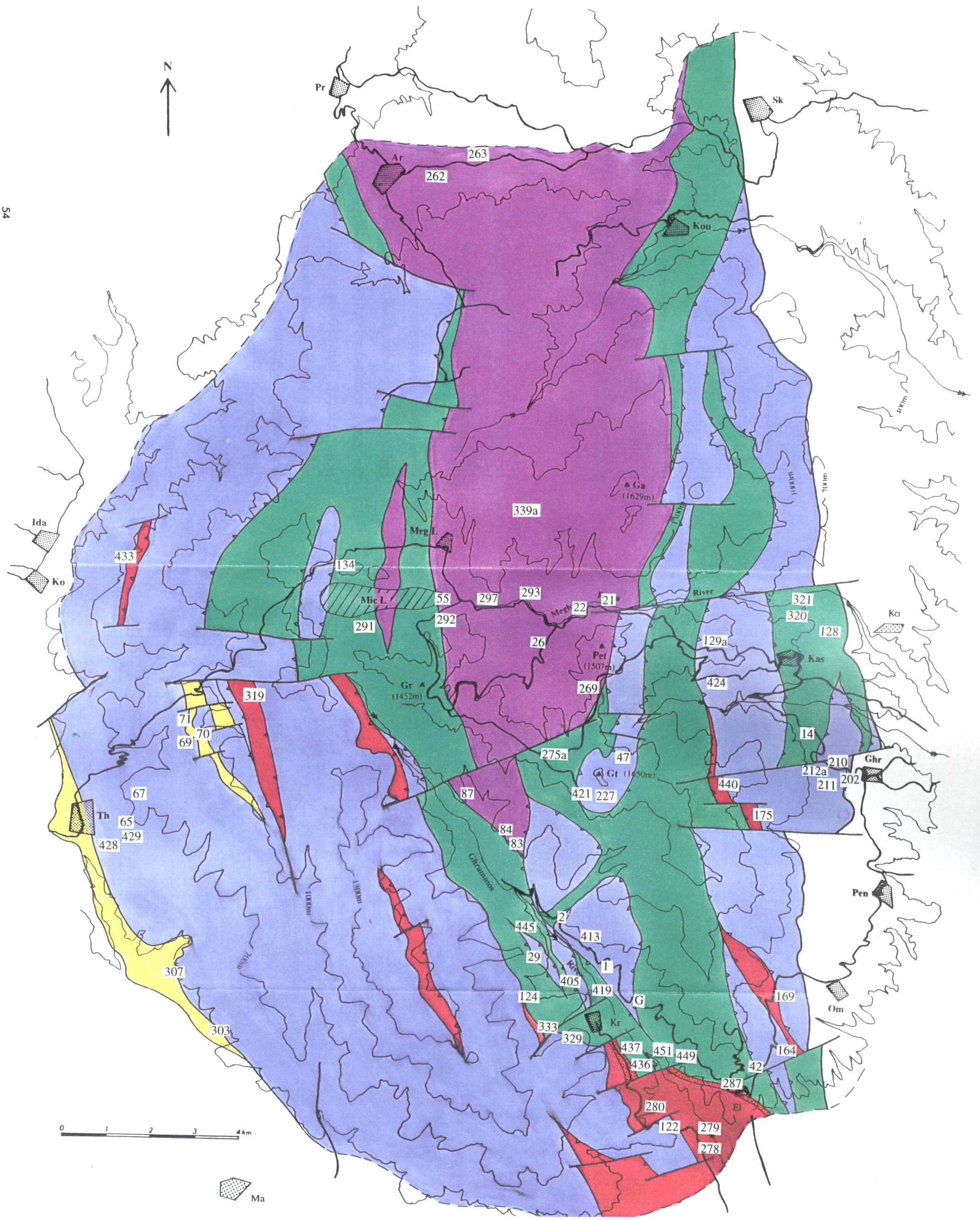


Figure 3.1 - Geological map of the Païkon Massif showing all localities mentioned in the text of chapter 3.

In the Voras Massif these meta-sediments (Tzena Formation) clearly overlie a thick succession of gneisses, marbles and mica-schists of pre-Alpine age with a depositional contact (Figure 3.2). These metamorphic rocks are believed to represent a fragment of continental basement onto which meta-sediments were deposited in Triassic to early Jurassic times (Mercier, 1968; Brown *et al.*, in prep). Given the striking similarity, in all respects, between the Tzena (Voras) and Gandatch (Païkon) Formations it is highly probable that similar pre-Alpine basement rocks also underlie the Païkon Massif although, unfortunately, they are not exposed (Mercier, 1968; Brown *et al.*, in prep).

Due to the enigmatic nature of these gneisses, mica-schists and marbles within the Païkon Unit they will not be discussed in any great detail here and the reader is referred to chapter 6 for more information and discussion.

3.4 - GANDATCH FORMATION

3.4.1 - *Introduction*

The type section of the Gandatch Formation (as defined in chapter 2) is exposed along a road cutting between Micra Livadia and the village of Kastaneri (Figure 3.1). Here the whole range of lithological variations which occur within the Gandatch Formation are well exposed in steep embankments which reach up to 10 m high. Scattered areas of no exposure and ubiquitous meso- and macro-scale folding, as well as significant reverse and normal faulting (chapter 4) hinder correlation of individual exposures and thus the relative stratigraphic position of each section is difficult to determine. The Livadia Formation of the Païkon Volcanic Group, which conformably overlies the Gandatch Formation, first crops out at localities 84 and 87 in the west, at locality 55 near Micra and Meghala Livadia (central Païkon Massif) and at locality 275a further east (Figure 3.1).



Figure 3.2 - Field photograph of the contact between the Tzena Formation metasediments and the pre-Alpine continental basement (Kalivia Socrati Gneisses; chapter 6.3.6) of the Voras Massif. The contact is depositional and isoclinally folded.



Figure 3.3 - Field photograph of Stratotype 1 (Marbles) of the Gandatch Formation. The clean white marbles are interbedded with thin horizons of chloritic schist and are chevron folded (see chapter 4.6). Locality 297, directly east of Micra Livadia.

Four main stratotypes can be used to describe the lithological variability within the Gandatch Formation, each of which varies internally and passes gradationally into each of the other three stratotypes. In order of decreasing carbonate content (% by outcrop area) they are :

Marbles >95% white, grey and lesser pink marbles interbedded on a decimetric scale with <5% chloritic schists and calc schists.

Interbedded Marbles and Schists ~50% white-grey marbles which alternate with ~50% calc-schists, calcarenites, calcilutites and chloritic schists.

Schists 75-90% chloritic schists, micaceous schists and calcarenitic schists and calcilutites with considerably lesser amounts of white-grey marble.

Calcirudites Matrix-supported and less clast-supported calcirudites.

3.4.2 - *Stratotype 1*: *Marbles*

A spectacular example of the *Marbles* is exposed at locality 297 (Figure 3.3), just east of Micra Livadia, where it has been deformed by Tertiary chevron folds (chapter 4.6). This stratotype forms the rounded summit of Mount Gandatch (1629 m), from where Mercier (1968) coined the term *Formation du Gandatch.*

The Gandatch Formation *Marbles* vary from clean white, often sugary marbles to slightly finer-grained grey to pink interbeds. The pink/grey horizons are commonly thinner-bedded and display a mottled, pearly appearance (as seen at localities 297 and 269; Figure 3.1). Although folded, all marble beds can be traced laterally for considerable distances and no channel-like, pinched horizons were observed.

The white marbles comprise almost entirely coarse recrystallised calcite and less common quartz, whereas darker marbles are finer-grained and include a wider variety of detrital and secondary phases. A more varied assemblage of detrital and secondary

minerals was observed within thin, schistose interbeds, which commonly separate marble horizons, and include quartz, chlorite, albite, white mica (phengite, Baroz *et al.*, 1987) and epidote. Polygonal, microcrystalline calcite grains have intragranular angles of 120° and often have strained and sutured margins.

The size of constituent calcite crystals varies markedly from locality to locality, as well as from bed to bed, but generally falls in the range 0.025 mm - 0.25 mm. The calcite crystals often have a preferred orientation, marked by crystal elongation parallel to bedding planes. Sutured grains, embayed and pitted grains and less frequently stylolites (the results of pressure dissolution) are largely responsible for anhedral crystal forms and give the rock a rather cloudy, blurred appearance in thin section. Stylolitic sutures within the Gandatch marbles generally occur parallel to bedding. However, no consistent peak orientation has been observed and hence such stylolites are of no value in determining the directions of maximum and minimum principal stress (Bathurst, 1995).

As a general rule the marbles have a granular texture, most metamorphic fabrics being limited to the intervening horizons of less competent chloritic and micaceous schists, which have acted as layers of weakness, concentrating the strain during deformation.

Any faunal components that may have been present on deposition have now been completely destroyed.

3.4.3 - *Stratotype 2: Interbedded Marbles and Schists*

This stratotype is more abundant than both the *Marbles* (section 3.4.2) and the *Schists* (section 3.4.4), and is exposed principally at the transition between these neighbouring units. Typical examples crop out directly north of Meghala Livadia at locality 263 (Figure 3.4) and sporadically along the Gandatch Formation type section (e.g. locality 293).

Together with an increase in terrigenous clastic material within this and the succeeding two stratotypes, there is a corresponding increase in chemical and mineralogical diversity. Minerals including chlorite, albite, quartz, white mica (phengite), biotite, epidote, stilpnomelane and rare amphibole occur within interbeds of chloritic and micaceous schist, whereas calcite, quartz, phengite, chlorite and albite provide the main constituents of arenitic schists and calc-schists. Marble interbeds are detrital in nature and encompass a wide range of grain sizes from gravel-grade calcarenites to very fine-grained calcilutites. They are often thinner-bedded than the *Marbles* (Stratotype 1), although beds commonly reach up to 30 cm thick (Figure 3.4).

All facies types of Stratotype 2 alternate on a centimetre to decimetre scale with rare, thicker beds of >50 cm. Primary sedimentary structures and textures have been destroyed in all horizons, whether clastic or carbonate, and fabrics now present are a function of post-depositional deformation (chapter 4).

Relatively rare D1 folds are best preserved within this stratotype (Figure 3.5; see chapter 4.2 for details).

3.4.4 - *Stratotype 3*: *Schists*

This is a highly deformed sequence of interbedded mafic chloritic schists, calc-schists, calcilutites and micaceous schists (see Figure 4.19). Bedding is on a centimetre and rarely decimetre scale, within which the carbonate component is present only as thin (0.5-5.0 cm), relatively sparse interbeds. The most extensive exposure occurs towards the flanking Gandatch-Livadia contacts (for example at localities 83 and 292, respectively on the western and eastern limbs of the Païkon

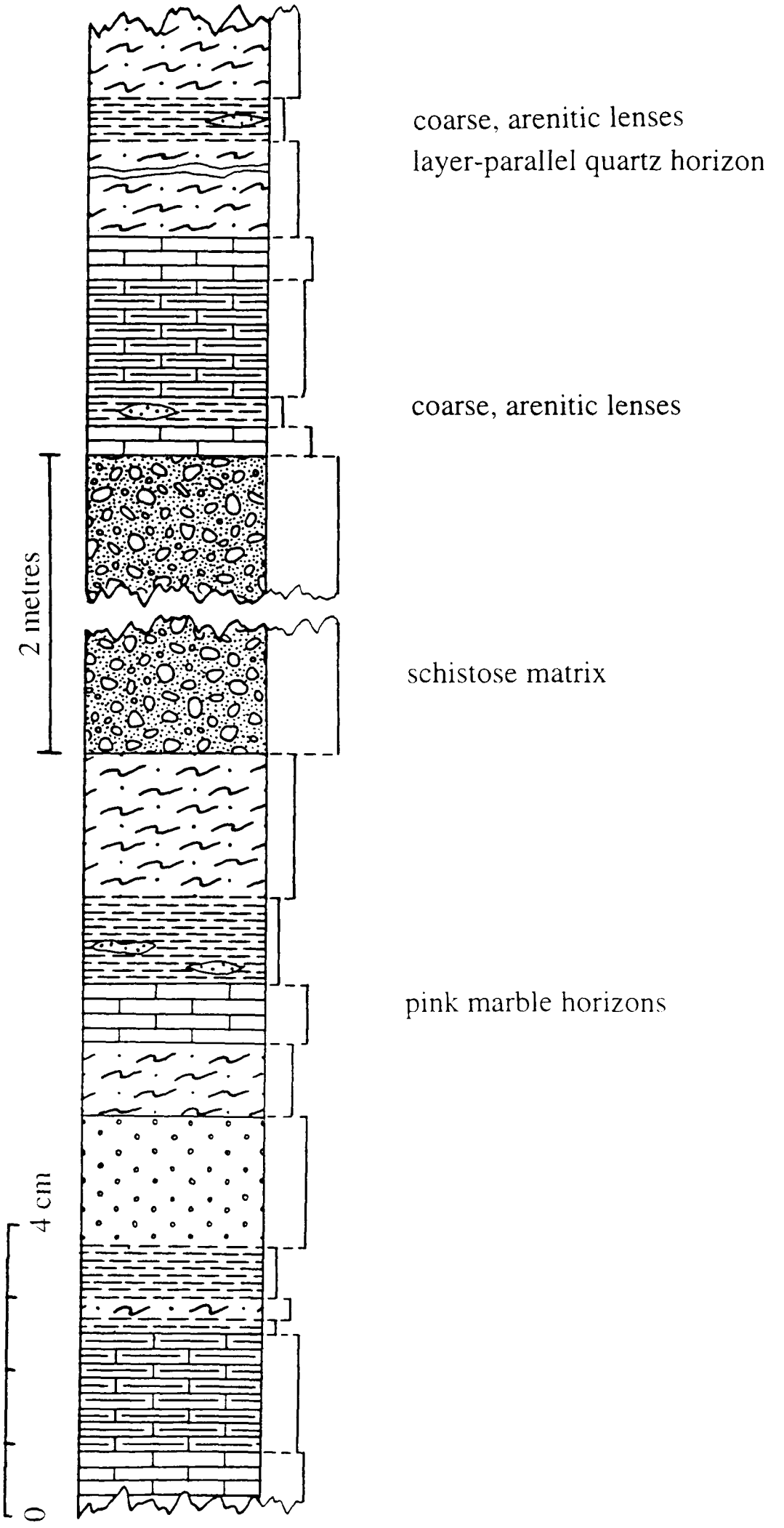


Figure 3.4 - Log through a representative section of Stratotype 2 (Interbedded Marbles and Schists) of the Gandatch Formation (section 3.4.3). Locality 263, east of Archangelos village. Chloritic schists, calc-schists and arenites dominate.



Figure 3.5 -Field photograph of isoclinally folded Stratotype 2 of the Gandatch Formation. Darker horizons are rich in phyllosilicate minerals (chlorite and mica), whereas the lighter horizons comprise dominantly calcite +/- quartz (locality 339a, Meghala Livadia).

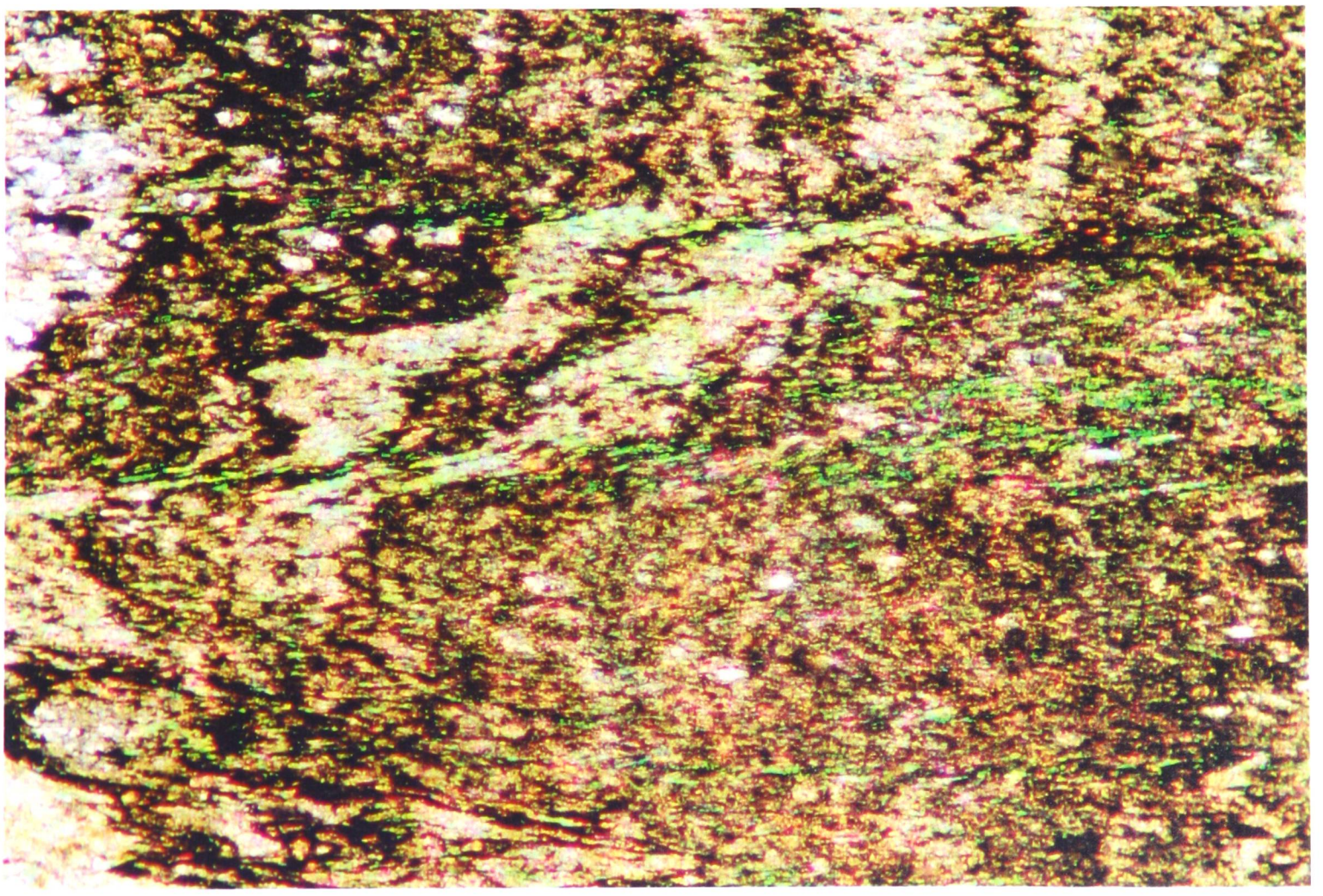


Figure 3.6 -Photomicrograph of a chlorite-mica-schist from Stratotype 3 (Schists) of the Gandatch Formation. Fine-grained chlorite and mica laths are aligned parallel to an early fabric which has been folded. These early micas are overgrown by larger, later-formed micas, which are oriented sub-horizontally on the photograph.

anticline), but less exposure occurs in more central areas. Again this may be used to infer the relative timing of deposition of this stratotype, with respect to neighbouring stratotypes (i.e. deposition after Stratotypes 1 and 2), although tectonic processes have greatly complicated this.

Phases that formed during post-depositional metamorphic events, include albite, chlorite, epidote, white mica, quartz, iron oxide (magnetite) and rare stilpnomelane and biotite. Chlorite is the main constituent phase of the bulk of the Gandatch Formation schists and has formed during more than one mineral growth phase. Chlorites form platy crystals which define the metamorphic fabrics and also occur as euhedral, randomly-orientated grains, which presumably crystallised subsequent to generation of the dominant schistose fabrics.

White micas are most commonly encountered in arenitic schist horizons, but occur throughout all horizons of this stratotype. They are fine-grained and are often aligned parallel to schistosity planes, as described in chapter 4. Electron microprobe analyses carried out by Baroz *et al.* (1987) indicate that they belong to the phengite series with rare, cross-cutting ferri-muscovites developed at a later stage (Figure 3.6). Epidote crystals are also commonly aligned along schistosity surfaces but may also occur as poikiloblastic phenocrysts and aggregate grains. Quartz crystals can be large (<0.5 cm) and often strongly flattened into cigar-shaped "blebs". The quartz crystals are highly strained, display undulose extinction and have commonly been affected by pressure dissolution, producing pressure solution shadows, stylolites and microcrystalline quartz.

A rare coexistence of radial stilpnomelane and euhedral biotite was documented by Baroz *et al.,* (1987). The metamorphic implications of this assemblage are discussed in chapter 4.

3.4.5 - *Stratotype 4: Calcirudites*

The distribution of calcirudites is seemingly random within the Gandatch Formation, although this is almost certainly a consequence of later tectonic disturbances. Such deformation has also caused significant flattening which has resulted in all but a few clasts becoming elliptical in configuration. Good examples crop out at locality 21 (type section) and locality 263 (between Archangelos and Skra, northern Païkon Massif; Figure 3.4).

Clasts range in size from 0.5-10 cm in diameter. The calcirudites are clast- and matrix-supported, massively-bedded and internally chaotic. The majority of clasts are calcareous and closely resemble stratotypes present elsewhere in the Gandatch Formation (i.e. white and grey-pink marbles, calc-schists and calc-arenites). Clasts of arenite, arenitic schist and chlorite/mica schist are generally smaller but are also common and similarly flattened. Some clasts have been subjected to poly-phase deformation and are consequently crenulated (these are possibly basement-derived), while others have been disrupted by brittle fracturing. The detrital carbonate matrix is moderately schistose and medium- to coarse-grained. Its principal constituents are calcite, quartz, chlorite, clay minerals (including kaolinite), white mica and epidote, some of which have become preferentially orientated along schistosity planes.

Areally, this is the least significant Gandatch Formation stratotype, representing <5% of the total exposure. However, the lateral and vertical extent of each occurrence is quite considerable reaching several metres in thickness by many tens to hundreds of metres in length.

3.4.6 - *Discussion*

The main stratotypes described for the Gandatch Formation comprise redeposited, randomly distributed interbeds of marble, calcarenite, calcilutite and conglomerate. No primary sedimentary structures (e.g. graded bedding, laminations, slumps, ripples)

have been preserved in any of these facies. The facies associations of the Gandatch Formation meta-sediments are typical of sedimentation in a carbonate-dominated, deep-water slope setting, where beds of redeposited shoal-water carbonates, conglomerates and mudstones are characteristic (Jenkyns, 1986). Deposition takes place mainly by mass-transport processes, such as turbidity currents, debris- and sheet-flows (Cook & Mullins, 1983). The alternating carbonate-clastic interbeds which characterise the Gandatch Formation may reflect pulsed derivation from carbonate platform and terrigenous sources respectively, induced by tectonic and/or eustatic processes. Alternatively, they may form due to fluctuating availability of a source, interbedded with hemipelagic deep-water sediments.

Marble horizons (Stratotype 1) have probably been deposited as sheet-like gravity flow deposits derived from a platform (Cook, 1983). This is evidenced by their extensive lateral continuity and their redeposited nature. The thin interbeds of fine chloritic and micaceous schist may represent background hemipelagic "clay drape" sedimentation as described from the Lower Carboniferous Dimple Limestone of the Marathon Region, Texas (Thomson & Thommason, 1969). Calcarenites, calc-schists and chloritic-schists (Stratotypes 1, 2 and 3) are believed to have been derived from platform and/or terrigenous sources, and deposited as turbidity currents. No characteristic turbidite sedimentary structures (c.f. Bouma, 1962; Postma *et al.*, 1988) have been preserved, but the laterally extensive alterations of calcarenite, calc-schist and chloritic-schist are very similar to turbidite deposits described from other locations. One such example is the Upper Cambrian Lower Hales Limestone, Nevada, which comprises non-channelised limestone turbidite sheets interbedded with lime mudstone and wackestone slope turbidites (Cook & Mullins, 1983; Cook, 1983). Although the Gandatch Formation calcirudites (Stratotype 4) preserve no primary sedimentary structures they can nonetheless be interpreted as debris-flow and debris-sheet deposits. This is suggested by their clast-supported nature and their vertical and lateral continuity (Leigh & Hartley, 1992). The calcirudites can be likened to the debris sheet deposits of the Upper Devonian Ancient Wall carbonate complex,

Alberta, Canada (Cook *et al.*, 1972), which comprise laterally extensive debris-flow sheets of clast-supported conglomerate within a largely turbiditic sequence. Calcilutite and mica-schist horizons within the Gandatch Formation may represent background hemipelagic sedimentation taking place in the slope environment during times of low mass-transport influx.

Two possible models exist to explain deposition in the slope environment; the submarine fan model (Walker, 1966; Mutti & Ricci Lucchi, 1972) and the apron model (Cook *et al*, 1972; Mullins & Cook, 1986). The submarine fan model has been successfully applied to both modern and ancient siliciclastic slope deposits (e.g. Bouma *et al*, 1985), but it has been less successfully related to carbonate margin deposits (Mullins & Cook, 1986). The apron model was thus devised as an alternative to the submarine fan model (Mullins & Cook, 1986) and deals primarily with the facies associations observed at carbonate-dominated platfrom-margin settings (e.g. the Little Bahama Bank, Mullins *et al.*, 1984). Carbonate margin deposits are characterised by gravity-flow sedimentation of unchannelised calcilutite, calcarenite, conglomerate and megabreccia sheets, derived from line sources and deposited as wedge-shaped "aprons" (Mullins & Cook, 1986; Figure 3.7).

As the Gandatch Formation is dominated by redeposited carbonate sediments it can thus be related more successfully to the apron model than to the submarine fan model. This is supported by the fact that no remnant channels were identified within the Gandatch Formation, with most interbeds forming laterally-continuous, sheet-like horizons. Had submarine fan deposition been dominant, it is likely that a significant proportion of channelised deposits would have been recognised within the redeposited Gandatch Formation, despite the deformation it has undergone, which is clearly not the case. Furthermore, the Gandatch Formation is largely composed of similar facies types to those described as characteristic of slope aprons by Mullins & Cook (e.g. conglomerates, calcarenites, calcilutites). It is therefore likely that the Gandatch Formation was deposited by sheet flow (marbles), turbidity current (calcarenites, calc-schists, chloritic-schists) and debris-flow/sheet (calcirudites) processes, alternating

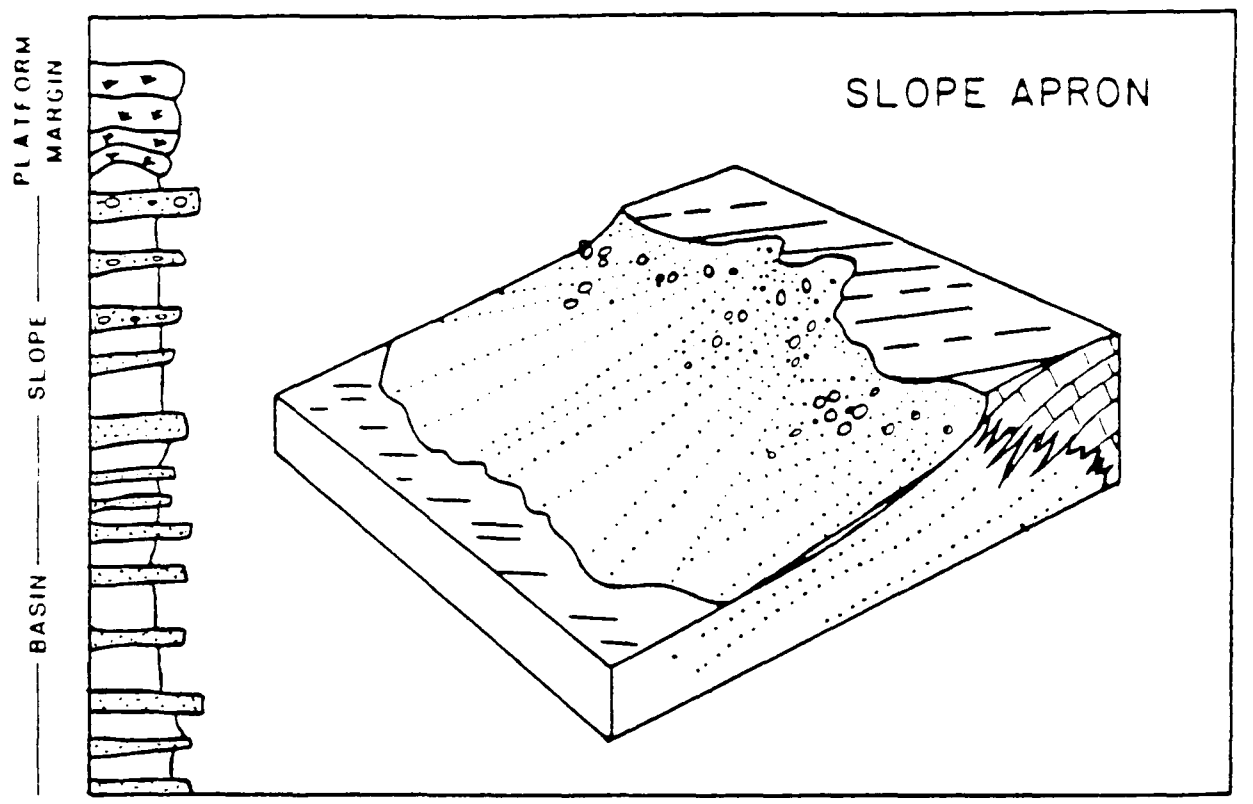


Figure 3.7 - Schematic block diagram model of a carbonate Slope Apron (after Cook, 1983). On the left hand side a generalised logged section shows the seaward prograding stratigraphic sequence produced in the Slope Apron setting.

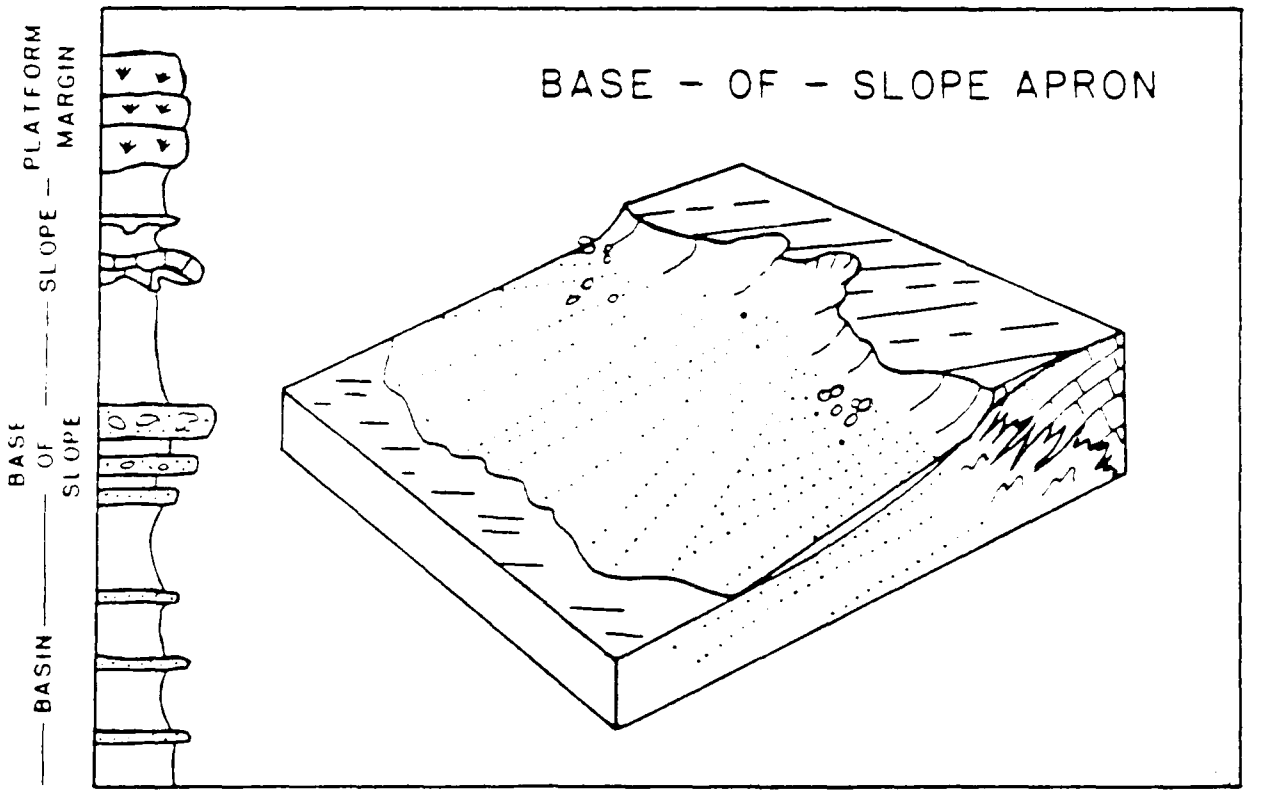


Figure 3.7A - Schematic block diagram model of a carbonate Base-of-slope Apron (after Cook, 1983). On the left hand side a generalised logged section shows the seaward prograding stratigraphic sequence produced in the Base-of-slope Apron setting.

(calcarenites, calc-schists, chloritic-schists) and debris-flow/sheet (calcirudites) processes, alternating with background hemipelagic sedimentation (calcilutites and mica-schists), in a slope apron setting.

The slope apron setting has been divided into slope aprons proper and base-of-slope aprons (Cook, 1983; Mullins & Cook, 1986; Figures 3.7 and 3.7A). Slope aprons are dominated by carbonate turbidite and debris-flow deposits with a high proportion of relatively coarse-grained megabreccia and conglomeratic horizons, whereas base-of-slope aprons are dominated by relatively finer-grained sheet-flow and turbidite deposits (Mullins & Cook, 1986; Figure 3.8). In the Gandatch Formation, the calcirudite stratotype, which represents the conglomerate and debris-flows units of Mullins & Cook (1986), is relatively subordinate while laterally continuous calcarenites, calcilutites, chloritic schists and redeposited marbles are dominant. The Gandatch Formation facies associations are therefore likely to represent the turbidite and sheet-flow deposits of Mullins & Cook (1986), and it is thus proposed here that the Gandatch Formation was deposited in a lower slope apron or base-of-slope apron (outer apron) setting (Figure 3.8).

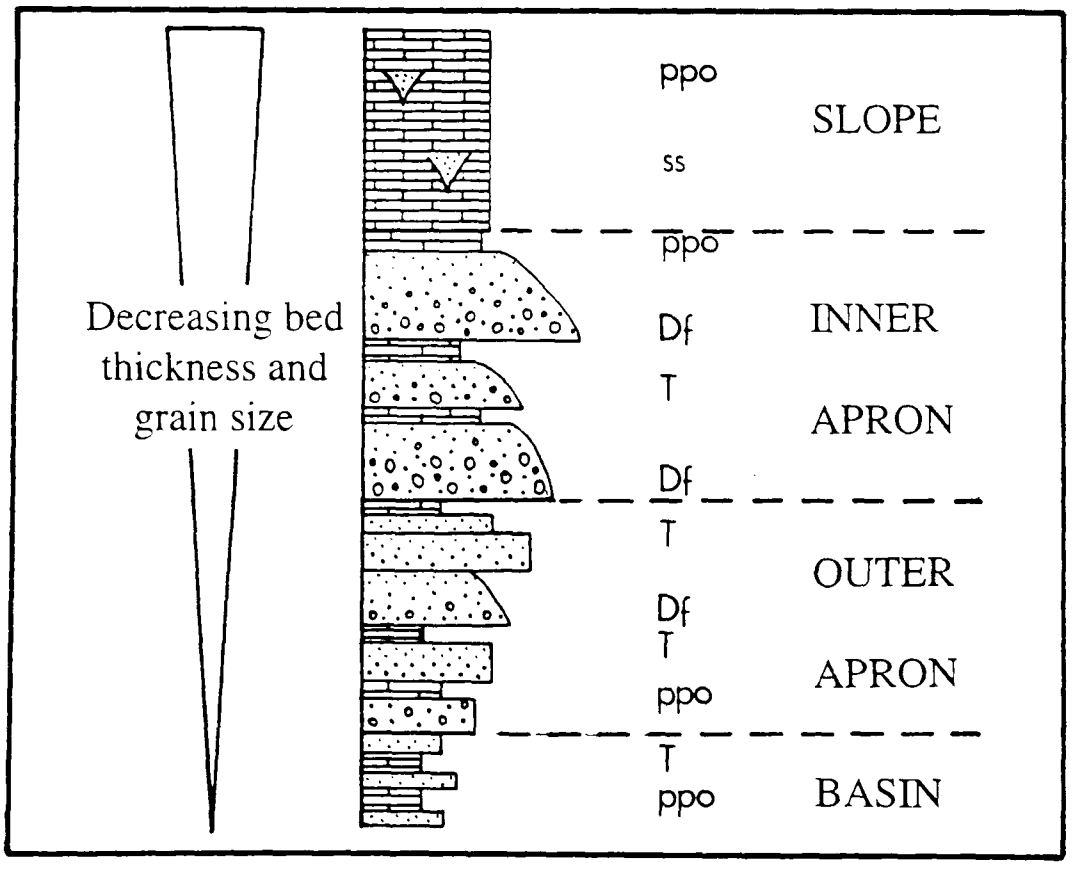


Figure 3.8 - Schematic, idealised stratigraphic sequence for a seaward prograding base-of-slope carbonate apron (modified after Mullins & Cook, 1986). ppo = peri-platform ooze; T = classical turbidites; Df = debris flow and megabreccia; ss = slumps, slides and truncation surfaces.

A possible modern equivalent to the Gandatch Formation is the deep-water sequence described from Exuma Sound in the Bahamas, where the sedimentary sequence is similar in both facies and facies association to the Gandatch Formation. The Exuma Sound area is characterised by calcirudites, calcarenites and calcisiltites which have been interpreted as turbidites and sheet-flow deposits deposited in a lower slope apron setting (Crevello, 1978; Crevello & Schlager, 1980). Similarly, the present day northern Little Bahama Bank has been interpreted as including a lower slope distal apron succession derived from a line source (Schlager & Chermak, 1979), comprising thin (<1 m) coarse-grained turbidites as well as thin (<30 cm) fine-grained turbidites and thin grain-supported debris-flows interbedded with subordinate amounts of peri-platform ooze (Mullins *et al.*, 1984). The Middle Devonian Prongs Creek Formation (Northern McKenzie Mountains, Yukon Territory, Canada) also closely resembles the Gandatch Formation. The Prongs Creek Formation comprises carbonate turbidites (c.f. the calcarenites, calc-schists and chloritic schists of the Gandatch Formation) and debris-flow sheets (c.f. the calcirudites of the Gandatch Formation) interbedded with hemipelagic lime mudstones (c.f. calcilutites of the Gandatch Formation), which are interpreted to have been deposited in a lower slope apron setting (Cook & Mullins, 1983).

3.5 - THE PAÏKON VOLCANIC GROUP : LIVADIA FORMATION

3.5.1 - *Introduction*

There is a gradational stratigraphic contact between the calcareous meta-sediments of the Gandatch Formation and the overlying Livadia Formation (chapter 2, Figure 2.8). The Livadia Formation is one of the most poorly exposed and volumetrically subordinate units within the Païkon Massif. In many areas the fissile nature, low competency and comparatively high fertility of soils generated from this unit have resulted in many areas of potential exposure being weathered into thick soils, now cultivated for fruit and grain crops. The Livadia Formation forms a thin band which

flanks the Gandatch Formation to the west, south and also to some extent in the east. Of these, the westernmost outcrops provide the best and most continuous exposure, from Gola Tchouka to the village of Archangelos (Figure 3.1). Eastern outcrops are comparatively poor and relatively rare, due to tectonic cut-out during subsequent deformation and to a widespread lack of exposure resulting from extensive woodland cover. The Livadia Formation is particularly well exposed in the vicinity of Micra and Meghala Livadia (central Païkon Massif, Figure 3.9) and it is after this area that the unit has been named.

Lithologically, the Livadia Formation consists of fine-grained, fissile volcaniclastics interbedded with basic to intermediate volcanic flows. Non-clastic volcanics are relatively minor, comprising 15-20% of the exposure, with the best examples being recorded at locality 26, to the south of Micra Livadia and locality 291, which lies along a dirt-track road adjoining Micra Livadia and Gola Tchouka. By contrast, volcaniclastic schists, which dominate the Livadia Formation, are well exposed all along the western margin of the Gandatch Formation.

3.5.2 - *Volcanics*

The geochemical characteristics of the relatively minor volcanic component of the Livadia Formation are discussed in detail in chapter 5. Essentially they represent a highly depleted and much altered intermediate-composition, extrusive succession.

The original mineralogy of these igneous rocks has been almost entirely transformed during deformation events, which occurred subsequent to their extrusion, and as a result primary textures have been largely obliterated. Where the majority of volcanic rocks crop out they are highly brecciated and thus fresh, unweathered samples are rarely found. Petrological analyses reveal that the more compositionally basic members of the Livadia Formation volcanics have been altered to a secondary

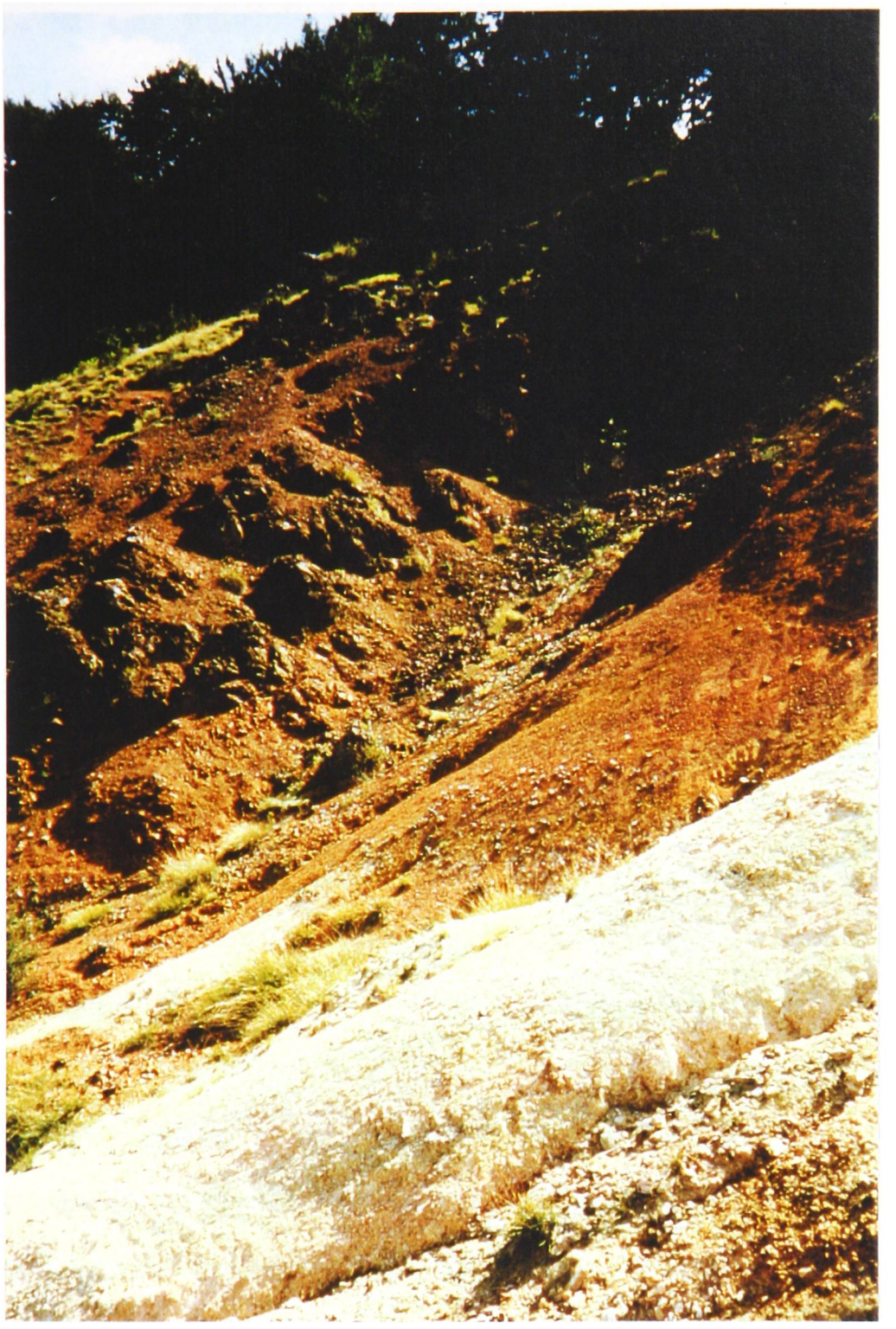


Figure 3.9 - Field photograph of the Livadia Formation (lower Païkon Volcanic Group). The dark brown/rust rocks in the middle ground are highly fractured, rubbley volcanics interbedded with lesser volcaniclastic schists (Micra Livadia, central Païkon Massif).

mineralogy dominated by chlorite, phengite, albite and iron oxides, with less abundant and variably occurring epidote. Many of these minerals are themselves altered to later phases of sericite, clay minerals and chlorite, giving the rock a cloudy, pitted appearance. The more intermediate-composition members of the volcanics are albite- and occasionally quartz-phyric.

Many exposures of the volcanics contain variable concentrations of disseminated massive sulphide minerals, principally pyrite with minor iron oxides such as goethite. The massive sulphide deposits are most abundant in samples which have undergone considerable metasomatism, which will be discussed in chapter 5.

Texturally, most of the samples studied show only secondary features which have been disrupted and occasionally overprinted. Rarely, however, glomeroporphyritic and variolitic primary textures were observed, as shown by the presence of albite phenocrysts in a fine matrix and by devitrified basic-intermediate glass, respectively.

3.5.3 - *Volcaniclastics*

The volcaniclastic component of the Livadia Formation is by far the most dominant. It occurs everywhere as highly sheared chloritic and micaceous schist which is commonly interbedded and interdigitated with volcanic flows on a centimetre to metre scale. The majority of the Livadia Formation volcaniclastics are very fine grained and schistose, hindering detailed petrological analyses. XRD analyses reveal the presence of albite, kaolinite, quartz and muscovite. Horizons of considerably coarser breccio-conglomerate crop out locally. Such coarse intercalations vary between 0.1 and 2.0 metres thick and are more chaotic than their finer-grained neighbours. They are generally matrix-supported, with clasts reaching up to 5 cm in diameter. The margins of these coarse horizons are always highly sheared, preventing the nature of contacts with surrounding fine volcaniclastics from being determined (e.g. erosional, gradational). These breccio-conglomerate horizons, as well as the Livadia Formation

as a whole, cannot be traced laterally for any distance due to extensive reverse and normal faulting.

In the majority of Livadia Formation volcaniclastics the matrix has a moderately schistose fabric sometimes interrupted by the presence of large, competent siliceous clasts. The clasts themselves, when not silicified, exhibit an array of altered igneous textures such as porphyritic and glomeroporphyritic.

3.5.4 - *Discussion*

The Livadia Formation forms the lowermost formation of the Païkon Volcanic Group. Constituent basaltic-andesites/andesites and fine-grained tuffs represent the eruption of intermediate composition lava flows and pyroclastic ejecta respectively. Post-eruption deformation has altered the primary mineralogy of the volcanics, thus original petrological and textural features are largely unobserved.

The Livadia Formation conformably overlies the deep-water meta-sediments of the Gandatch Formation (chapter 2.2.2), suggesting that the volcanic and volcaniclastic rocks were deposited, at least in their lower part, in a marine environment. A lack of any eutaxitic textures supports this hypothesis, although any evidence of subaerial welding may have been obliterated by subsequent deformation and alteration. The high proportion of volcaniclastic horizons relative to lava-flow horizons in the Livadia Formation may indicate an explosive eruptive regime involving magmas rich in water and/or volatile components (Walker, 1982). Caution is required, however, when making such inferences, as it is petrologically impossible to assess the relative amounts of pyroclastic versus epiclastic deposits within the volcaniclastic succession, due to the very small grain size of the rocks and the intense deformation and alteration that they have undergone. True pyroclastic horizons may therefore be less voluminous than is immediately apparent, and the volatile content of their magmatic source may be similarly difficult to assess by this means alone. If the volcaniclastic

rocks *are* pyroclastic in nature, it is not known whether they were deposited by pyroclastic fall, flow or surge deposits (Smith & Roobol, 1982; Best, 1982; Fisher & Schmincke, 1984), as all relevant depositional structures have been destroyed. It is therefore very difficult to assess the type of eruption that characterised the Livadia Formation (e.g. Strombolian, Vulcanian, Plinian or Peléan; Wilson, 1989).

Nonetheless, general comparisons can be drawn between the Livadia Formation and intermediate composition volcanic/volcaniclastic successions reported from elsewhere. Similar interdigitating lava-tuff associations of intermediate composition are commonly found at destructive plate boundaries such as the Andes, New Zealand, the Cascades of the Western USA and in other parts of the Tethyan belt. The Taupo Arc of New Zealand, and more specifically the presently active Mount Ruapehu (North Island, New Zealand), comprises interbedded intermediate (andesitic) flows and thick pyroclastic eruptive units (as described here for the Livadia Formation), deposited on the flanks of a classical stratovolcano (Cole, 1981; Cas & Wright, 1987). An ancient volcanic/volcaniclastic equivalent, in terms of the igneous rocks produced, can be found in the Central Pontides of Turkey. The Late Palaeozoic to Early Mesozoic-aged Çangaldag Complex of the Central Pontides comprises an imbricated pile of porphyritic andesites, basaltic-andesites and more evolved volcanics which alternate with fine-grained epiclastic and pyroclastic interbeds (Ustaömer, 1993). Both Mount Ruapehu and the Çangaldag Complex represent volcanic arc-type successions and thus the Livadia Formation may have erupted in a similar setting. The geochemical characteristics and tectonic environment of eruption of the Livadia Formation is discussed further in chapter 5.

3.6 - THE PAÏKON VOLCANIC GROUP : KASTANERI FORMATION

3.6.1 - *Introduction*

The Kastaneri Formation is one of the most volumetrically abundant lithologies within the study area, as it crops out extensively in most parts of the Païkon Massif. It is most commonly exposed along road cuttings. Thick woodland and scrubby, thorny flora obscure it elsewhere.

Where exposed, the Kastaneri Formation is disrupted by numerous Tertiary and Cainozoic faults (chapter 4) which preclude preservation of a complete transect through this unit from base to top. Instead, the unit is present as thin (20 m maximum) tectonically-bound slices, stacked one above the other to form a significantly over-thickened rock pile. Such tectonic disturbances not only render the relative stratigraphic position of each Kastaneri thrust slice impossible to determine, but also complicate estimation of the original thickness of the unit (chapter 2). Other effects of late-stage thrust-imbrication and folding are that slices and slivers of all the other units present in the Païkon Massif have been tectonically incorporated into and interdigitated with the Kastaneri Formation and, indeed, many other formations. The most striking examples of this are numerous thrust slices of the Cretaceous Transgressive Limestones which occur from Archangelos in the north to Eliftherohori in the south and from Theodoraki in the west to Ghriva in the east (Figures 3.1 and 4.29, 4.30, 4.32 & 4.33). These Cretaceous imbricates were originally interpreted by Mercier (1968) as Upper Jurassic, forming part of the Gropi, Gola Tchouka and Ghriva Limestones (Chapter 2) and as *in situ* sedimentary interbeds within the Kastaneri Formation (*Formation du Khromni* of Mercier) east of Khromni village. However, work carried out during this study and by Bonneau *et al* (in press) and Godfriaux and Ricou (1991) now conclusively prove their Cretaceous age. These Cretaceous imbricates will be discussed in greater detail in section 3.9.

The Kastaneri Formation is composed of highly altered, intermediate to acidic volcaniclastics interbedded with andesitic and rhyolitic volcanic flows (Figure 3.10; see chapter 5 for details of geochemical analyses).

The majority of the Kastaneri Formation is volcaniclastic, with 10 to 15% of the rocks exposed being rhyolitic to andesitic volcanic flows. Although disrupted by both normal and reverse faults (as discussed above), representative sections of the Kastaneri Formation are well exposed along the road which leads northwards out of Eliftherohori village, along the road between Ghriva and Kastaneri in the east, along the track which winds southwards out of Ida in the north and between the villages of Theodoraki and Micra Livadia in western-central areas (Figure 3.1).

3.6.2 - *Volcanics*

The volcanic component of the Kastaneri Formation is exposed as isolated flows within the dominantly volcaniclastic succession. Typically these are medium- to coarse-grained and relatively competent, with their competency often being enhanced by later silicification. Dacitic to andesitic flows are grey-blue to green-grey in colour and are often highly weathered (e.g. localities 1 and 124, north of Eliftherohori, Figure 3.11). Pitting is probably due to the alteration of feldspars, mainly albite, to clays, which were eroded.

Andesitic flows are often albite and quartz phyric with large aligned phenocrysts set in a fine-grained matrix (locality G; Figure 3.12), now partially replaced by a secondary assemblage including quartz, albite, chlorite, phengite and minor epidote, lawsonite (Baroz *et al.*, 1987) and iron oxides (haematite, goethite). Albite phenocrysts are often pitted and altered, especially around their rims, and display strained, undulose extinction. Quartz phenocrysts are similarly strained and embayed and often reduced to microcrystalline quartz. Intergrowths of quartz and feldspar are present sporadically, forming granophyric textures.

KEY - to Figure 3.10

Quartz/feldspar-phyric rhyolites

Feldspar-phyric andesites

Chloritic schists

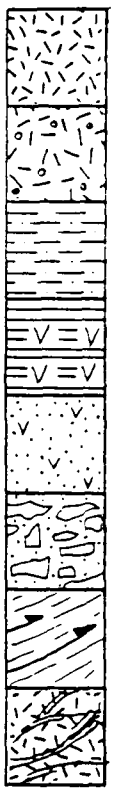
Coarse quartzose schists

Quartz & chlorite-rich tuffs

Volcaniclastic breccio-conglomerates

Shear zone

Sheared rhyolites



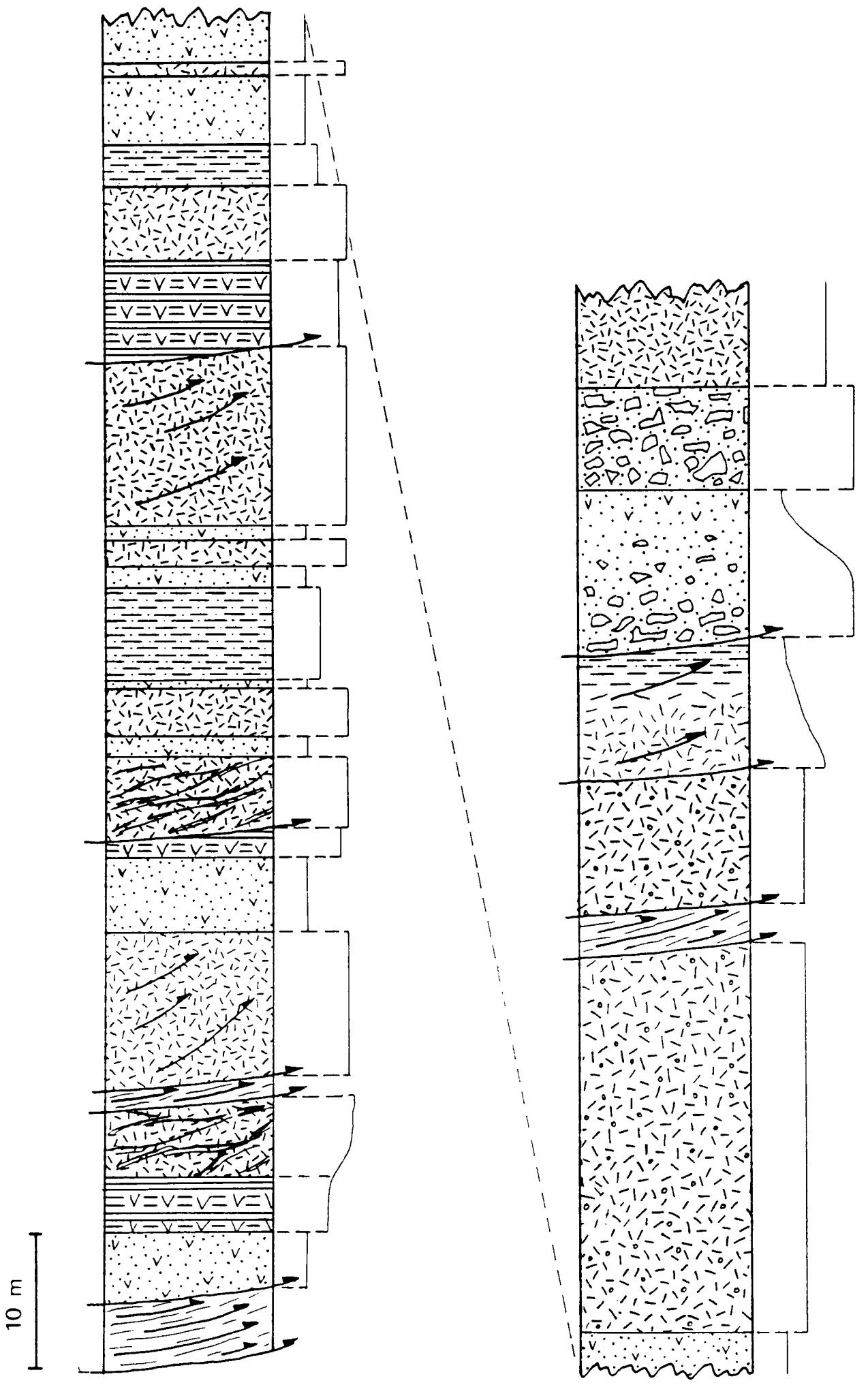


Figure 3.10 - Log of a representative section of the Kastaneri Formation. Quartz-feldspar porphyries, chloritic volcaniclastic schists, tuffs and breccio-conglomerates dominate (see key on opposite page). The succession is highly sheared throughout (locality 419, north of Eliftherohori village).



Figure 3.11 - Field photograph of a deformed and weathered andesitic flow within the Kastaneri Formation. Feldspar phenocrysts have been removed by weathering processes leaving sub-rectangular pits on the exposed surface (locality 1, north of Eliftherohori village).



Figure 3.12 - Field photograph of andesitic rocks from within the Kastaneri Formation. The andesites shown are feldspar- and occasionally quartz-phyric. Phenocrysts are often aligned and reach up to 0.5 cm long (locality G, north of Eliftherohori village).



Figure 3.13 - Field phtogoraph of a quartz-bearing rhyolitic flow from the Kastaneri Formation (locality 14, west of Ghriva village).

Lawsonite crystals were documented and analysed by Baroz *et al.*, (1987) and indicate that this unit has undergone high pressure-low temperature blueschist facies metamorphism; however, no examples of this mineral were found during this study (further discussion in chapter 4).

Rhyolitic and ultra-acidic flows are white to creamy-yellow in colour and comprise abundant quartz, much being secondary, with albite, phengite and chlorite (Figure 3.13). Flows of this type are variable in thickness, locally reaching up to 4 m. Large quartz phenocrysts are replaced by secondary microcrystalline quartz. The phenocrysts are often highly sheared into both delta and sigma wing structures which are excellent indicators of palaeo-shear sense (Figure 3.14; see chapter 4 for details). Quartz crystals are commonly affected by pressure-solution processes which result in embayment and stylolite formation as well as the silicification and strain-hardening of these and surrounding horizons. No lawsonite was observed in these ultra-acidic volcanics although Baroz *et al.* (1987) have reported the presence of this mineral.

Both andesitic and rhyolitic flows are impregnated with disseminated massive sulphides. As in the Livadia Formation, the massive sulphides (principally pyrite) are most abundant within horizons that have undergone considerable alteration (see chapter 5).

3.6.3 - *Volcaniclastics*

The volcaniclastic component of the Kastaneri Formation is highly variable. Volcaniclastics commonly occur as: 1- Tuffs and lapilli-tuffs; 2- Chloritic and phengitic schists; 3- Coarse breccio-conglomerates. The volcaniclastics are closely associated with detrital arenites and calcarenites in their upper part. The majority of volcaniclastic horizons are incompetent and consequently highly schistose and/or strongly cleaved (chapter 4; Figures 3.15 and 4.23). This, along with their extensive

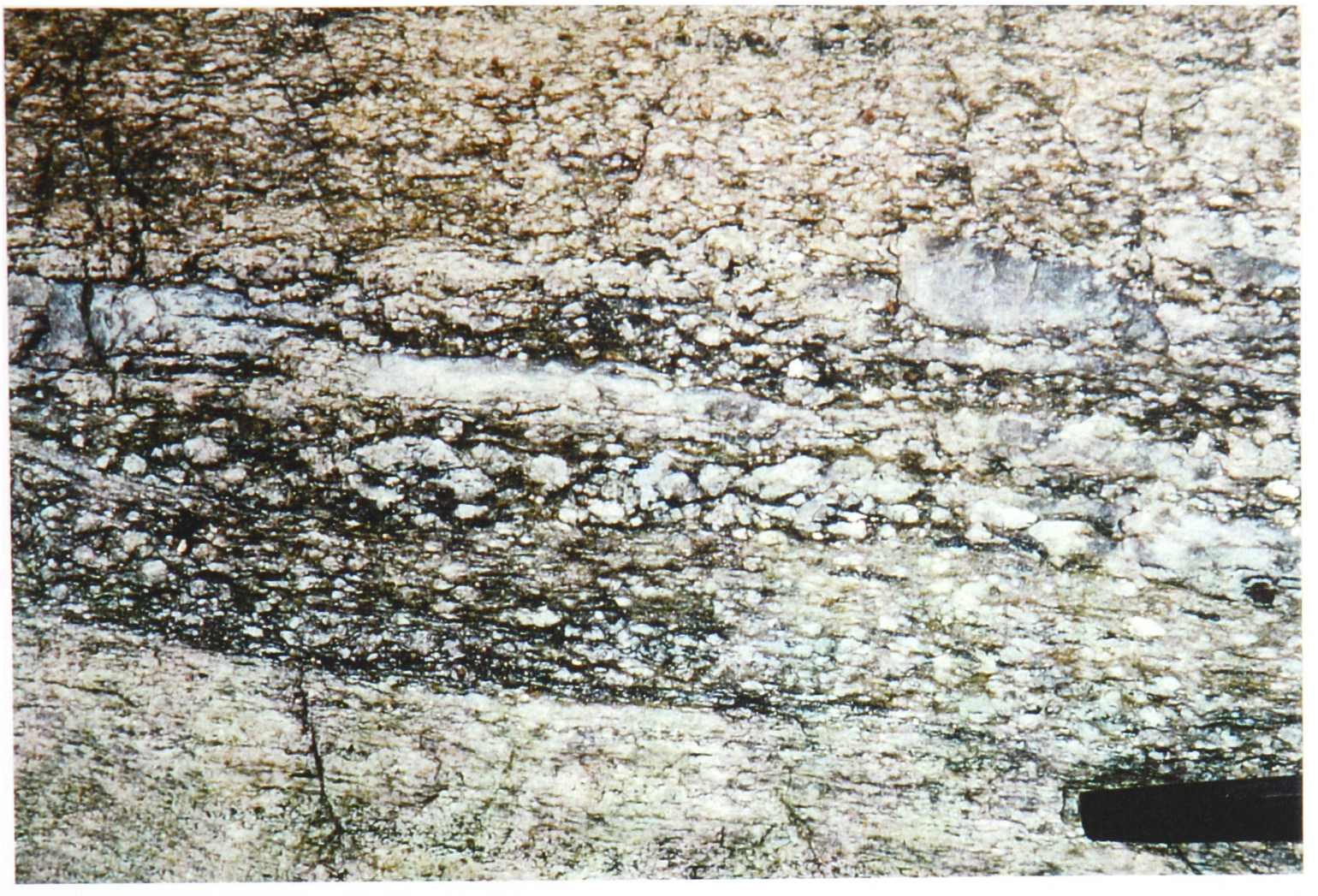


Figure 3.14 - Close-up field photograph of sheared quartz phenocrysts from an ultra-acidic rhyolitic flow within the Kastaneri Formation. The phenocrysts often form δ and σ-type structures which can be used to deduce palaeo-shear sense (see chapter 4). Pen lid is 2 cm long.



Figure 3.15 - Interbedded volcaniclastics and volcanic flows from the Kastaneri Formation. The slightly darker volcaniclastic horizons are fine-grained, often highly sheared and foliated by a penetrative scistosity and/or cleavage (locality 1, north of Eliftherohori village).

alteration, has obliterated most of their primary mineralogy and their original textures. Quartz, albite, phengite and chlorite are now the main constituent phases.

Tuffs and lapilli-tuffs

These lithologies are rich in quartz, albite, chlorite, sericite, epidote and phengite. More than one phase of mica growth has occurred, and micas are commonly aligned parallel to schistosity (S1 and S2) surfaces forming a distinct lineation (chapter 4), or form aggregate clusters (sericite) which have developed as pseudomorphs after flattened, primary albite (Figure 3.16). Secondary albite is also common and locally forms aggregate clusters with calcite. These albite-calcite clusters are usually square to rectangular in shape and may have formed as pseudomorphs after lawsonite (J.E. Dixon, pers. comm, 1997; Figure 3.17). Chlorite is abundant in many samples and is one of the principal constituents of the fine-grained tuffaceous matrix and of some highly altered clasts. Some chloritised clasts are themselves very fine-grained and may have formed during the devitrification of intermediate-composition volcanic glass (Figure 3.18). Clay minerals (smectite, kaolinite) are also common secondary phases, particularly in the fine-grained matrix, forming from the breakdown of albite phenocrysts and volcanic glass.

Epidote is very common as a secondary phase within the fine-grained matrix, as large porphyroblasts and in hydrothermal vein systems which intrude the rocks (Figure 3.19). Epidote porphyroblasts bend and displace the schistosity (usually S2, chapter 4), while the vein epidote overgrows this prominent fabric. The epidote-rich veins also contain abundant calcite and chlorite, all of which alter the albite, quartz and mica-bearing tuffs within a wide (0.5 - 1.5 times the thickness of the vein) hydrothermal aureole (Figure 3.19).

Tuffaceous horizons are highly schistose and preserve no primary depositional structures, whereas the coarser-grained lapilli-tuff beds preserve poorly-sorted, angular to sub-rounded grains. The tuffs and lapilli-tuffs are often closely associated with quartz-phyric rhyolitic flows and minor interbeds of chlorite-mica schist.

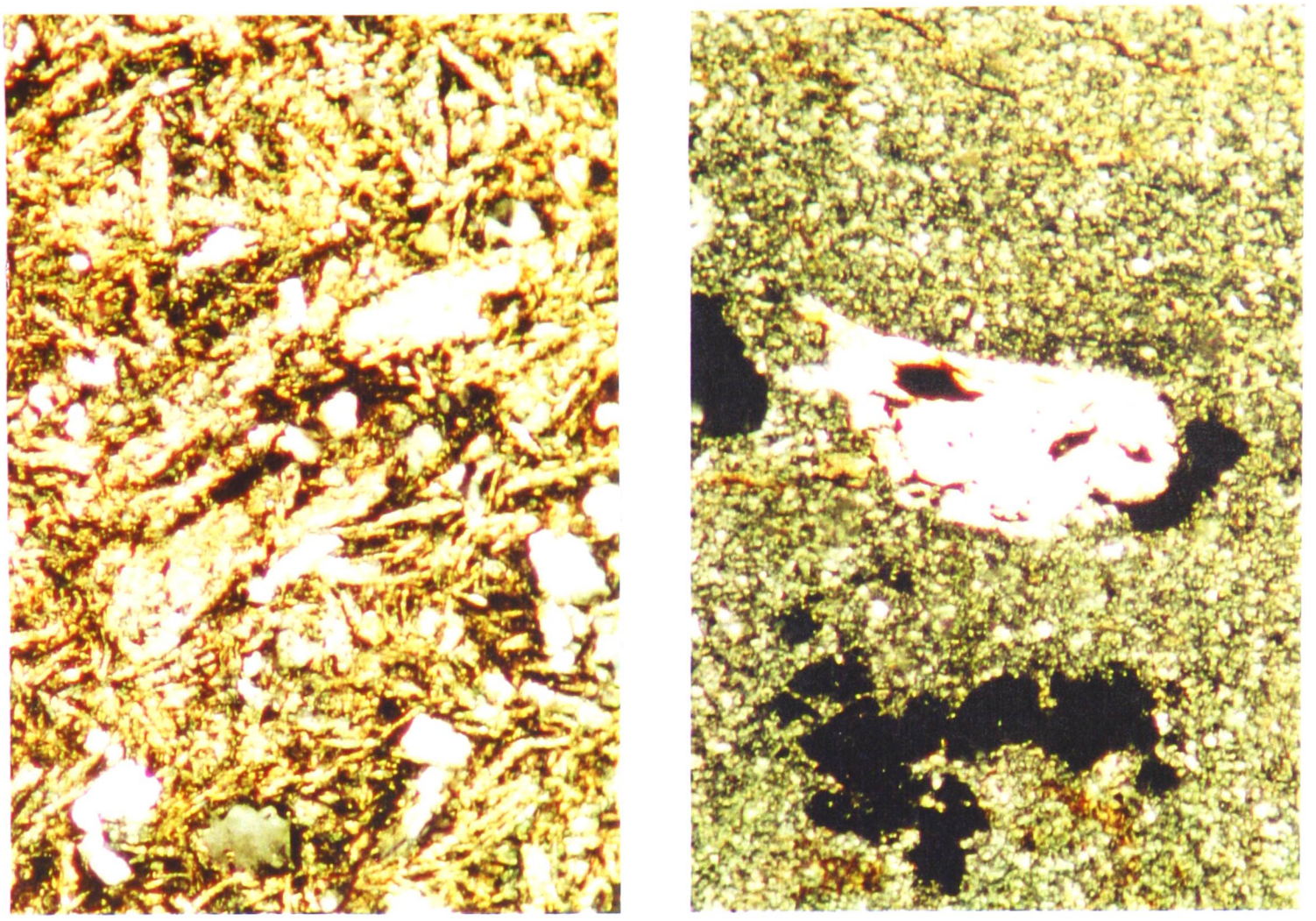


Figure 3.16 -Photomicrograph of two samples of porphyritic andesite (left x30 magnification; right x15 magnification) from the Kastaneri Formation. Many of the albite phenocrysts are at least partially altered to or pseudomorphed by aggregate clusters of fine-grained mica (probably sericite). Locality 449 and 435 from left to right respectively.

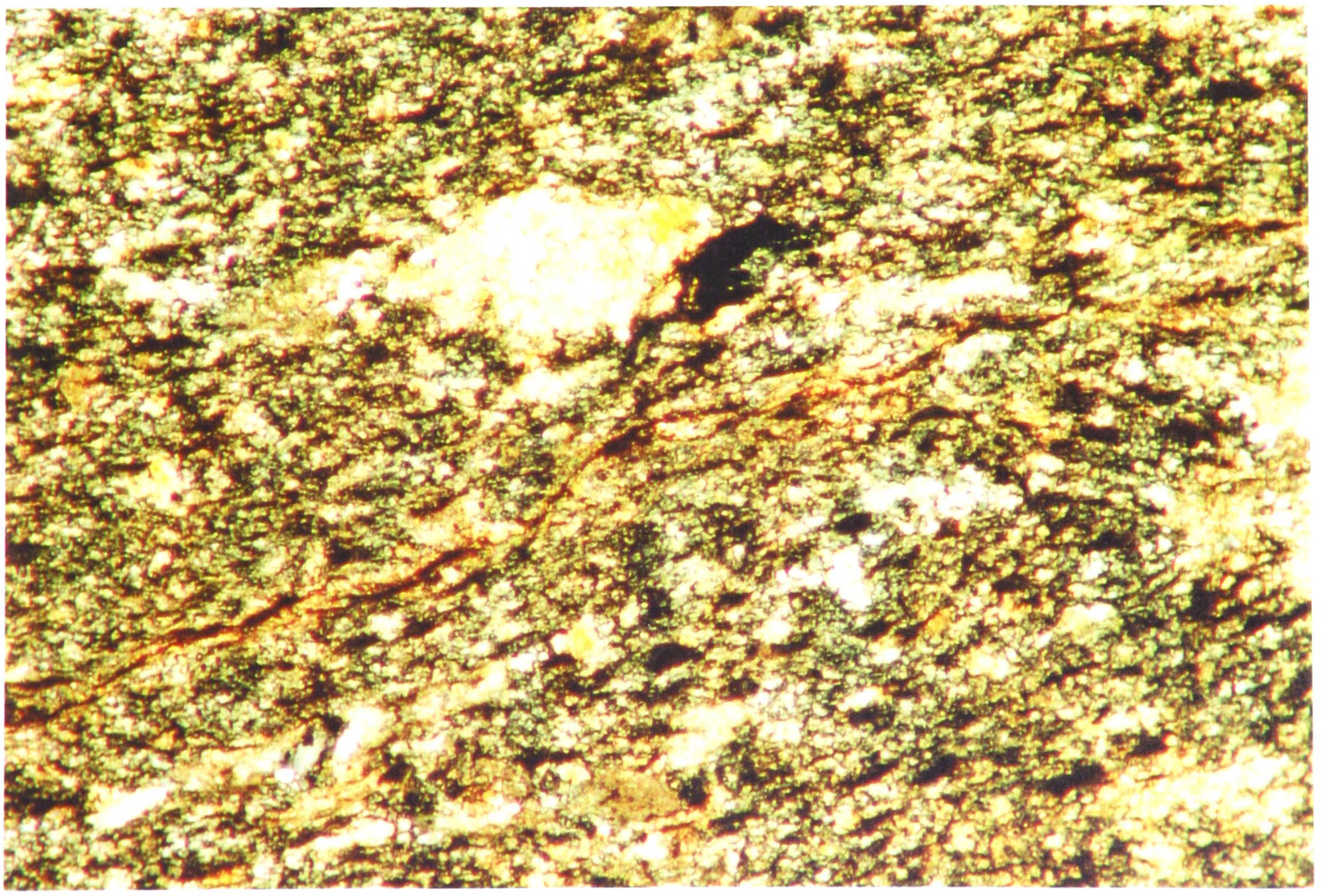


Figure 3.17 -Photomicrograph (x30 magnification) of a fine-grained chloritic volcaniclastic schist from the Kastaneri Formation. Sub-rhombic aggregates of calcite and albite are likely to have formed as pseudomorphs after lawsonite. Locality 451, north of Eliftherohori village).

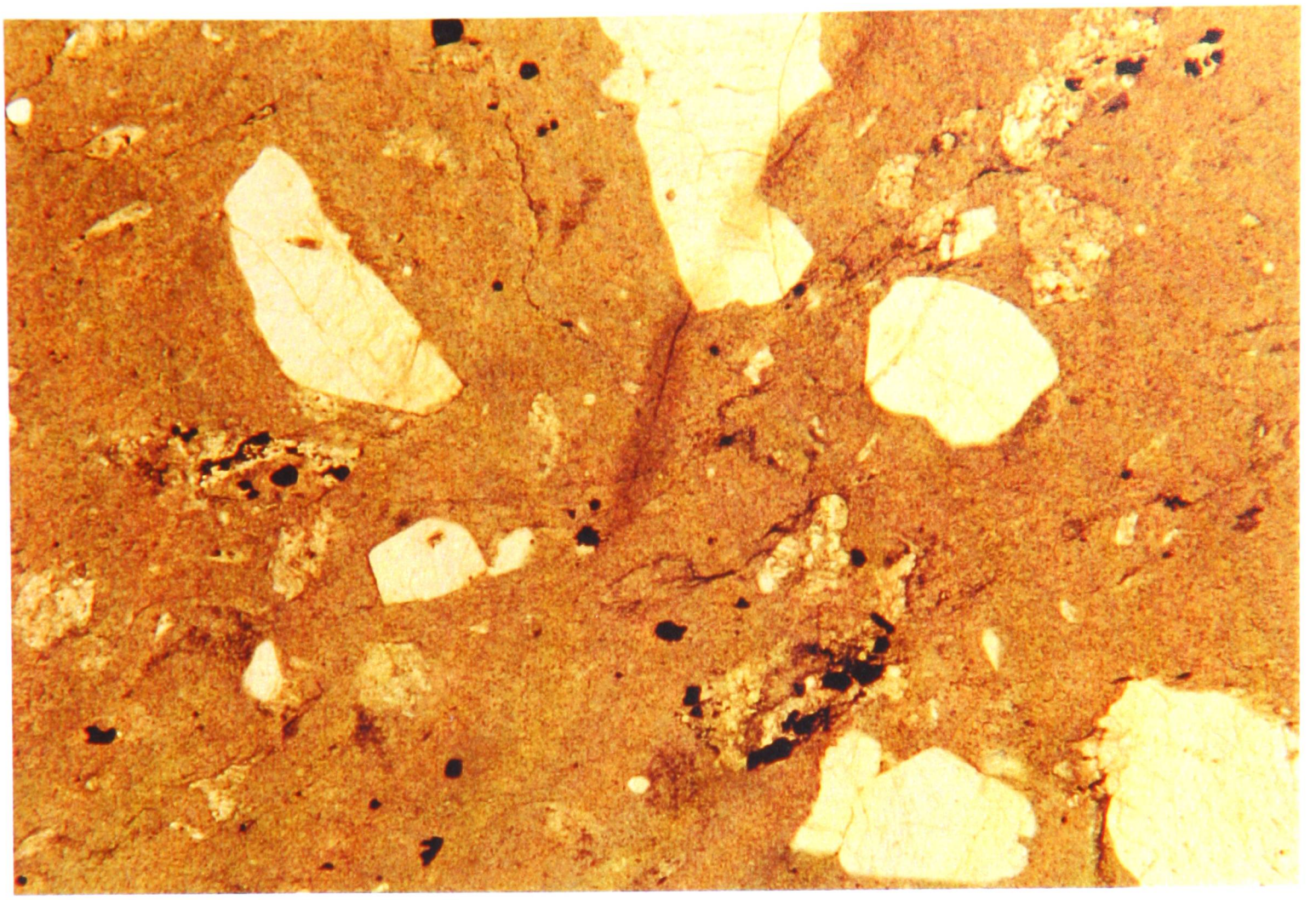


Figure 3.18 - Photomicrograph (x10 magnification) of a very fine-grained altered clast within the volcaniclastics of the Kastaneri Formation. It is possible that a rock of such fine grain size was originally a volcanic glass which has now devitrified into sub-microscopic crystals (probably of chlorite, epidote, quartz, mica and feldspar). Large feldspar porphyroblasts are also present.

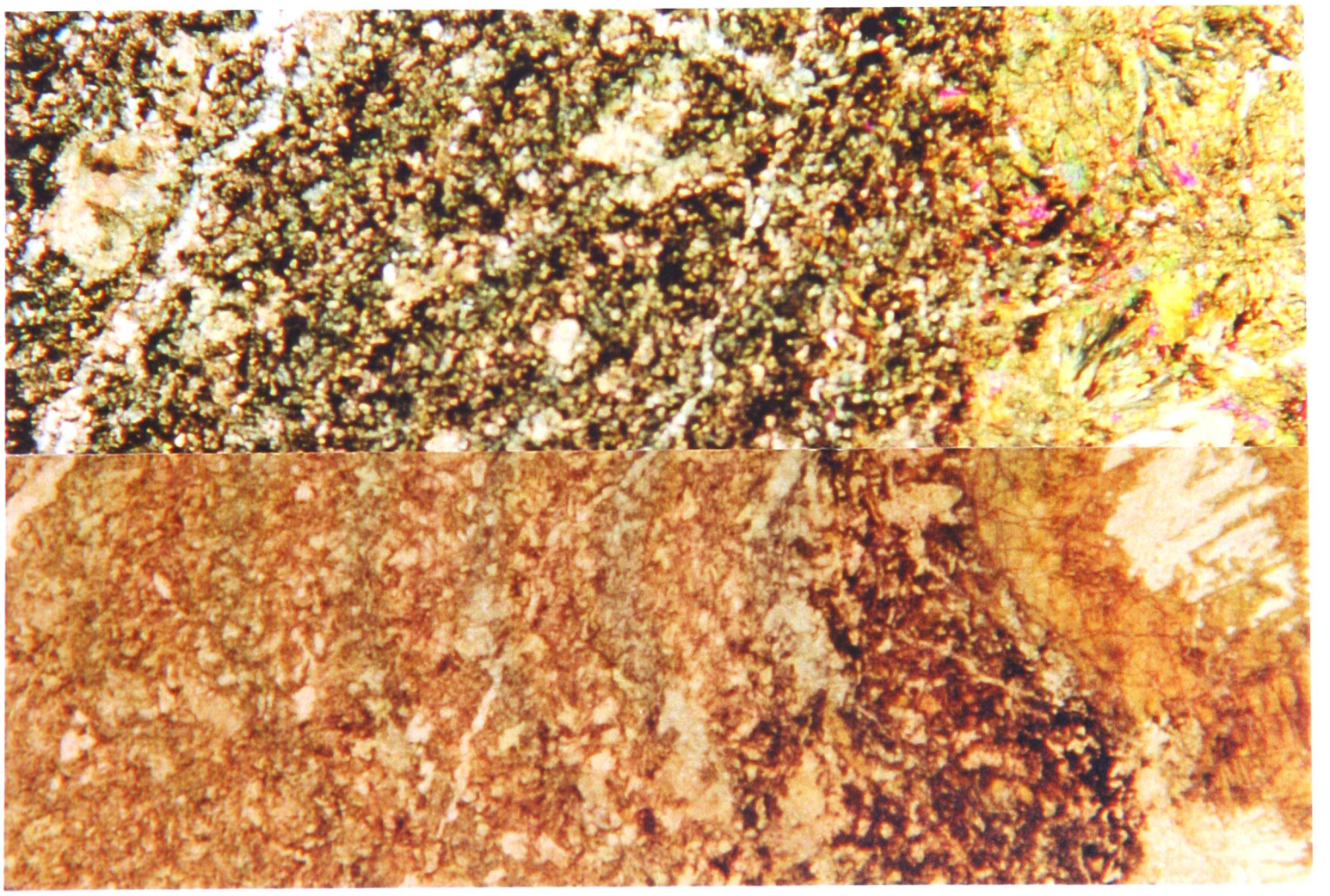


Figure 3.19 - Photomicrograph of a vein of epidote (x6 magnification) within the Kastaneri Formation. The top half of the picture is taken under crossed polars and oicks out the elongate laths of vein epidote on the right-hand-side. The lower half is taken in plane polarised light and more clearly shows the alteration aureole associated with the intrusion of the vein.

Chlorite-mica schists

The chlorite-mica schists are very fine-grained and greenish-grey in colour, with a pronounced schistose fabric (usually S2 and occasionally S1; see Figures 3.15 and 4.23). They are rich in chlorite, micas (phengite and sericite), both of which have grown during at least two distinct metamorphic events, and secondary clays, as well as ubiquitous, fine-grained quartz and albite. Small porphyroblastic epidotes are relatively common, with minor iron oxide minerals. Disseminated massive sulphides are frequently present and associated with extreme alteration to kaolinite, limonite and occasionally goethite.

The chlorite-mica schists are too fine-grained to preserve any primary igneous or volcano-sedimentary structures.

Breccio-conglomerates

Breccio-conglomeratic horizons are common throughout the Kastaneri Formation, where they tend to form laterally-discontinuous lensoid bodies, as opposed to blanket deposits (Figure 3.20). Clasts are typically sub-angular to sub-rounded, poorly sorted and for the most part matrix-supported, although clast-supported horizons are fairly common. A large range of grain sizes was recorded, from 1-2 mm in finer-grained beds to thick (0.5 m) horizons comprising large clasts and rare cobbles up to 6 cm in diameter. On average the clasts are around 0.5-1.5 cm in diameter. Clasts vary markedly in composition and texture from variolitic to glomeroporphyritic, and from tuffaceous to spherulitic, but all those in which primary textures are preserved are volcanic in origin. Many of the primary textures were wholly destroyed and primary mineralogical components are replaced by secondary mica (sericite), chlorite, clay minerals (e.g. kaolinite and smectite) and porphyroblastic albite, quartz, epidote and hydrothermal calcite. Many clasts are surrounded by an oxidised iron envelope and they are frequently invaded by an anastomosing network of haematite, epidote, calcite and quartz veins. This veining is common in all Kastaneri Formation volcaniclastics.



Figure 3.20 - Breccio-conglomeratic horizon from within the Kastaneri Formation. The horizon pinches out laterally. Clasts are wholly volcanic in origin, including quartz and feldspar porphyries, devitrified glass shards and fine-grained tuff.

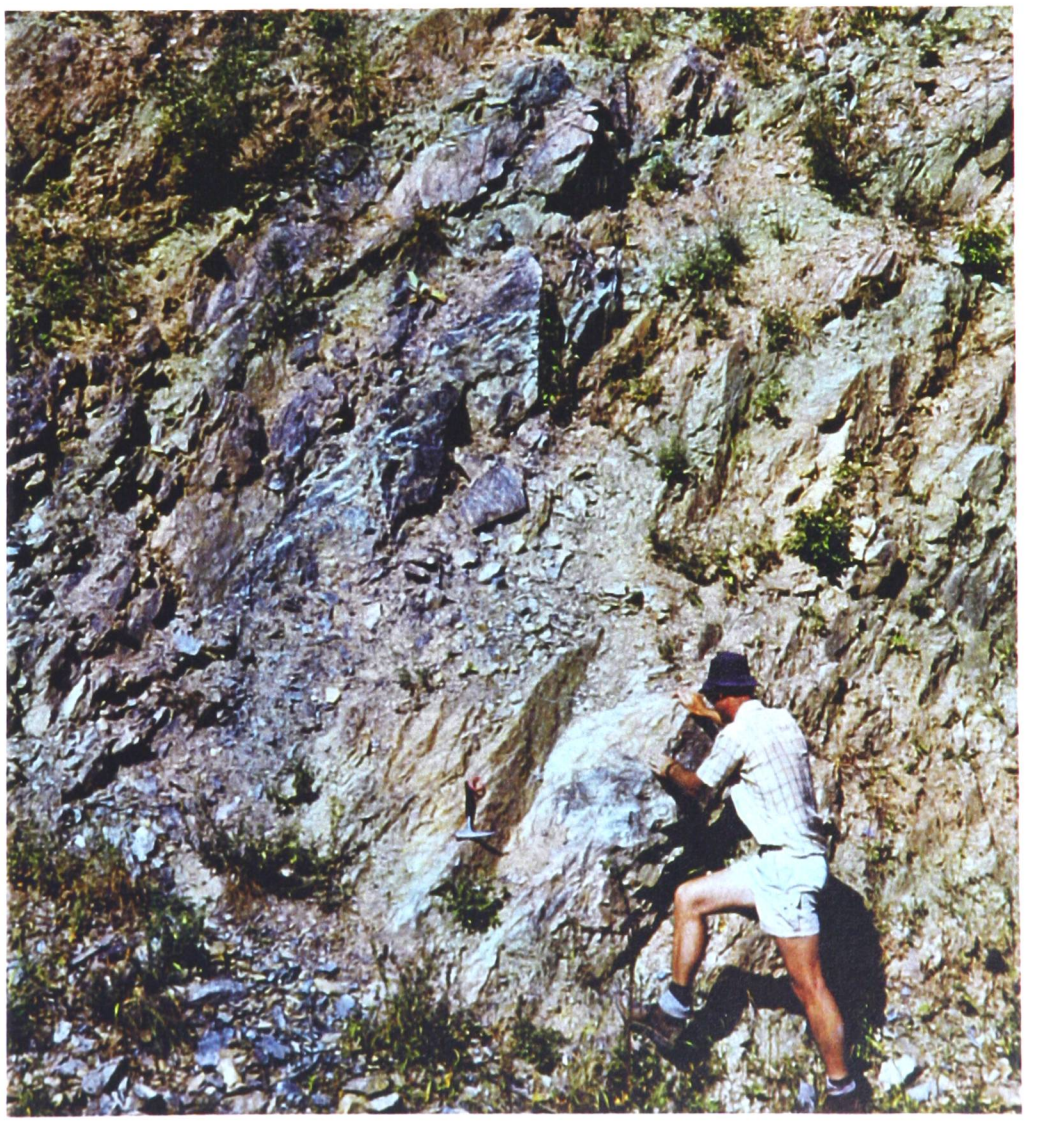


Figure 3.21 - Sheared and recrystallised limestone horizon within the volcanics and volcaniclastics of the Kastaneri Formation. The limestones contain abundant volcanic-derived detritus and a deformed shallow-water fauna (locality 212a, west of Ghriva village).

3.6.4 - *Plutonic Rocks*

At three principal localities the volcanics and volcaniclastics of the Kastaneri Formation are intruded by coarse-grained plutonic bodies. A few kilometres to the northwest of Kastaneri village small, sheared and deformed metagranitic bodies crop out (localities 320, 321 and 128, Figure 3.1). At locality 128 the meta-granite is severely altered and weathered and has been sheared and strained during multi-phase deformation. Large quartz crystals are variably strained (from undulose extinction to microcrystalline) and neighbouring quartz crystals are invariably sutured. Occasional primary quartz-feldspar granophyric intergrowths are preserved, however, in most cases the feldspar (usually albite, Baroz *et al.*, 1987) is at least partially replaced by kaolinitic clay.

3.6.5 - *Interbedded Carbonates*

Intermittent interbeds of detrital calcarenites and neritic carbonates are associated with the Khromni volcanic-volcaniclastic succession (Figure 3.21; this work, also Mercier, 1968; Sharp, 1995). The carbonates are dark grey and commonly rich in detrital and volcanic quartz. They are pervasively veined and frequently highly recrystallised and silicified. A poorly preserved fauna of indeterminate bivalves, gastropods and foraminifera is preserved as secondary calcite spar within a fine-grained pelmicritic matrix. Calcarenitic horizons are generally fauna-free and contain clasts of volcanic-derived material, such as chloritic schist, white tuff and quartz porphyry. Many of the shelly components are incomplete and some are bored. Isopachous fringe cements enclose debris of faunal fragments, and ooids were observed in one sample.

3.6.6 - *Discussion*

Field, petrological (see above) and geochemical (chapter 5) investigations of the Kastaneri Formation reveal that they constitute the uppermost eruptive units of the Païkon Volcanic Group, of which the Livadia Formation is the lower, more basic part.. The more acidic composition of the Kastaneri Formation, relative to the Livadia Formation below, is marked by a lower abundance of green/grey, chlorite-rich basaltic-andesite and basaltic lava flows within the rock pile, and a higher abundance of cream/white quartz-rich horizons. With respect to the underlying Livadia Formation, the Kastaneri Formation contains less primary lava flow horizons and is thus dominated by pyroclastic and/or epiclastic volcano-sedimentary rocks, which are very difficult to distinguish due to alteration. It also contains numerous breccio-conglomerate and detrital carbonate horizons which are lacking in the Livadia Formation.

The Kastaneri Formation has been severely affected by at least one phase of metasomatism. This is evidenced by the extensive hydrothermal vein systems which invade the rocks, massive sulphide alteration and the silicification and induration seen in many areas. This metasomatism is explored in greater detail in chapter 5.

Andesitic to rhyo-dacitic lava horizons represent primary flows. Their vesicularity and relative volumetric scarcity, with respect to volcaniclastic rocks, may reflect the existence of a viscose source magma with a high volatile content (Fisher & Schminke, 1984; Cas & Wright, 1987).

Tuff and lapilli-tuff horizons within the Kastaneri Formation are interpreted here as pyroclastic and/or epiclastic deposits, because primary igneous textures dominate the less deformed clasts. It is virtually impossible to determine whether the volcaniclastics are truly pyroclastic in origin, or whether they have been subsequently reworked into epiclastic deposits. However, because the Kastaneri Formation is likely to have been deposited in a shallow-marine environment, as evidenced by interbeds of

neritic carbonate, it is probable that at least some of the pyroclastic deposits have undergone epiclastic reworking in the shallow-marine environment. Breccio-conglomeratic horizons represent locally-occurring beds of considerably coarser-grained ejecta, which may have formed as primary pyroclastic flow/surge deposits (Fisher & Schminke, 1984; Best, 1982; Cas & Wright, 1987) and/or as secondary epiclastic debris flows and lahars (Cas & Wright, 1987). The lack of lateral continuity and limited vertical extent of the breccio-conglomerates suggest that they have been deposited in channels up to 10 m wide.

A similar eruptive setting to that described for the Livadia Formation is envisaged for the Kastaneri Formation; i.e. a composite or stratovolcano comprising intermediate to acidic composition pyroclastic rocks (tuffs, lapilli-tuffs and breccio-conglomerates) interbedded with subordinate lava flows (vesicular andesites and quartz/feldspar porphyritic rhyo-dacites). The successions described in section 3.5.4 from Mount Ruapehu (New Zealand) and the Çangaldag Complex (Central Pontides, Western Turkey) can be equally well compared to the Kastaneri Formation as to the Livadia Formation. In particular, the Çangaldag Complex resembles the Kastaneri Formation, in that both comprise a significant proportion of more evolved effusive and pyroclastic rocks. The Tithonian rocks of the Coast Range Ophiolite (central California) are also similar to the Kastaneri Formation, as they too comprise intermediate to acidic lava flows, submarine lahars and silicic pyroclastic sediments (Robertson, 1989).

The fact that the Kastaneri Formation lies above the Livadia Formation, with little or no break in volcanism, suggests that the magmatic system which affected the Païkon Massif and generated the eruptive units, became progressively more evolved throughout its volcanic history. This is a common occurrence in many volcanic centres, and particularly in supra-subduction zone settings such as the Coast Range Ophiolite (Robertson, 1989) and the Çangaldag Complex described above (Ustaömer, 1993). The same progression to more evolved rocks with time is reported from Santorini Island in the Aegean Sea (Nicholls, 1971a; Gill, 1981), many of the Japanese volcanic centres (Aramaki & Ui, 1982) and the Tongan Island of Fonualei (Cole,

1981), all of which are of volcanic arc origin. The geochemical characteristics of Kastaneri Formation and its tectonic environment of eruption are discussed more thoroughly in chapter 5.

3.7 - KHROMNI LIMESTONES

3.7.1 - *Introduction*

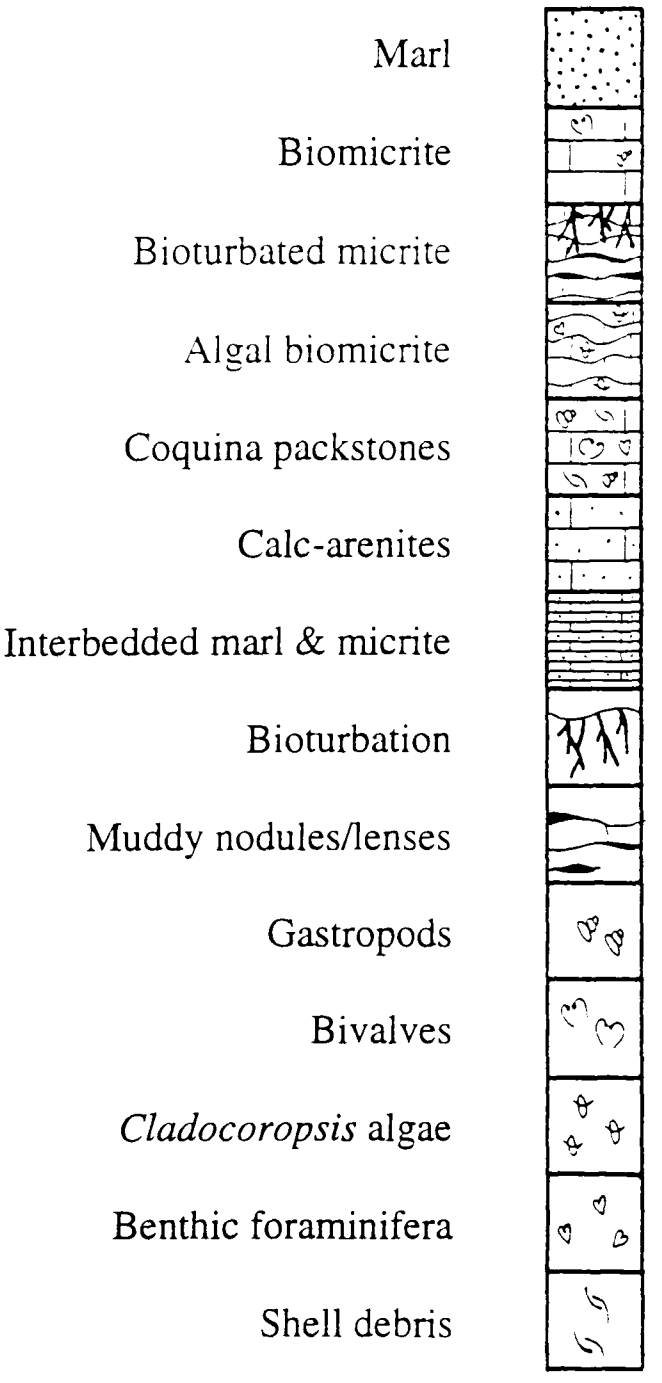
The Khromni Limestones are one of the least exposed stratigraphic units in the Païkon Massif. A strong metamorphic and structural discontinuity exists between the Khromni Limestones and the underlying Kastaneri Formation (upper Païkon Volcanic Group) in the form of an unconformity that is locally marked by a lateritic erosion surface (chapter 2.2.4; Figure 2.13).

The Khromni Limestones are highly variable from bed to bed and from locality to locality. Essentially, they comprise a thin (<40 m) sequence of grey neritic limestones interbedded with calcarenites, marls and buff mudstones (Figure 3.22). Bed thickness varies considerably with mean values at around 0.2-0.5 m. The neritic carbonates which dominate the Khromni Limestones are marked by rapidly changing facies, each of which is characterised by a unique faunal assemblage and mode of deposition. The succeeding paragraphs detail the principal features of each carbonate facies.

3.7.2 - *Biomicrites*

The biomicrite facies comprises grey, shallow-water micrites with a rich fauna including *Nerineid* gastropods, bivalves, *Cladocoropsis mirabilis* algae, benthic foraminifera and scarce corals (Figure 3.23). Benthic foraminifera species include

KEY to Figure 3.22



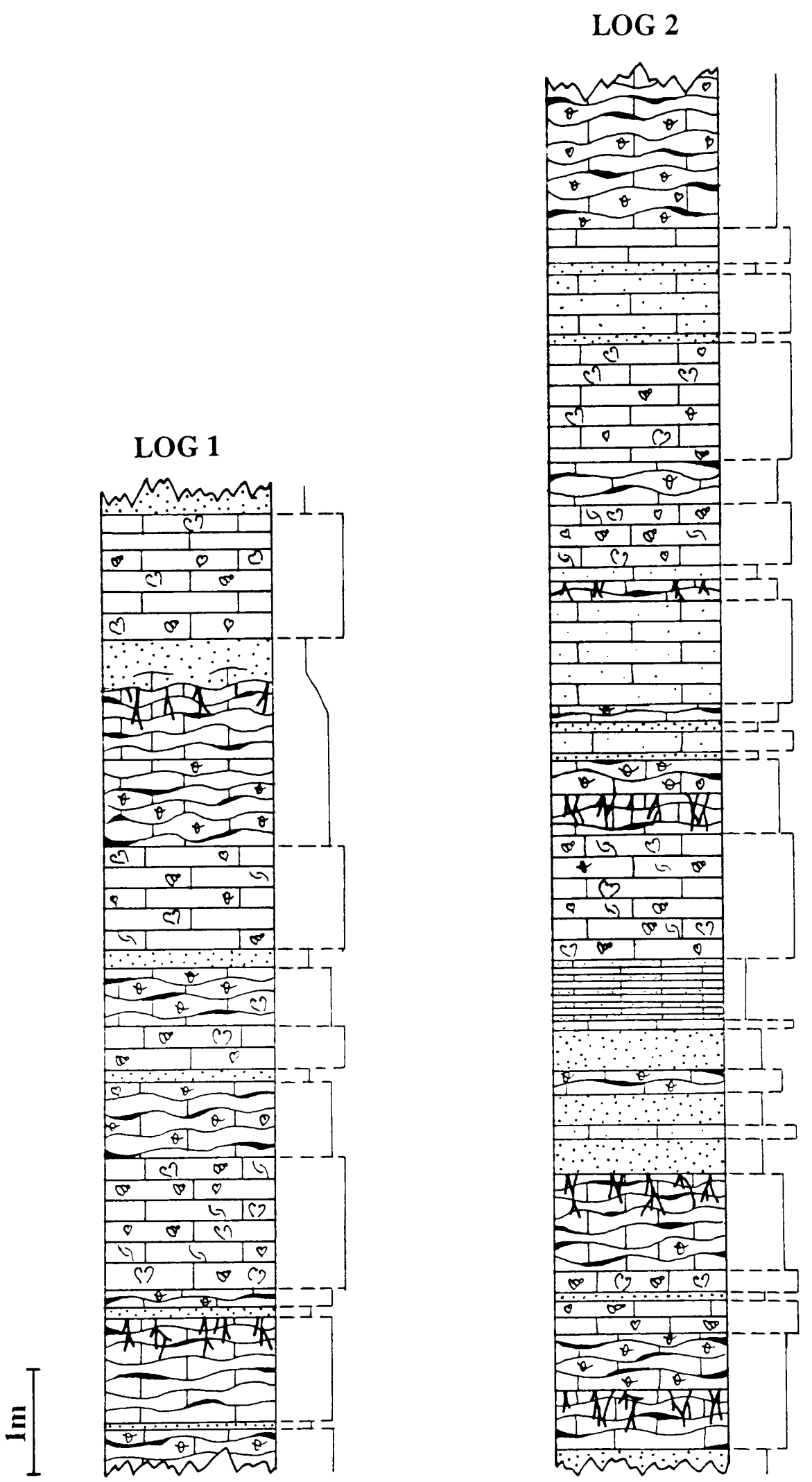


Figure 3.22 - Two representative logged sections through the Khromni Limestones. Log 1 is from locality 437 (south of Khromni village) and Log 2 is from locality 333 (north of Khromni village). The key on the opposite page indicates the main facies and their faunal constituents.



Figure 3.23 - Field photograph of the biomicrite facies of the Khromni Limestones (locality 436, south of Khromni village). The surface shown contains elliptical bivalves (centre), multi-chambered gastropods (centre right) and scarce algae (dark patch to bottom right) in a micritic matrix.



Figure 3.24 - Bioturbated micrite facies of the Khromni Limestones. The photograph shows disrupted buff, marl/sand-filled burrows within a host grey micrite. When undisturbed, the buff blebs form a branching burrow system (locality 437, south of Khromni village).

Actinoporella sp., Ammobaculites sp., Miliolidae and *Texturalidae. Trocholina sp.* and *Salpingoporella sp.* are particularly common. *Pseudocyclammina lituus* and *Cuneolina sp.* were also identified by Mercier (1968), and the coexistence of these foraminifera and *Cladocoropsis* algae infer a Kimmeridgian to Portlandian age for the Khromni Limestones (Mercier, 1968; chapter 2).

Micritic peloids are abundant in such horizons, with fewer ooids. Many bioclasts and bioclastic fragments are surrounded by isopachous fringe cements and/or micritic envelopes, and are sometimes partially replaced by recrystallised calcite spar.

3.7.3 - ***Bioturbated Micrites***

Buff, muddy nodules and partitions are commonly present within the grey micritic matrix and the study of key localities reveals that these are the remains of disrupted bioturbation structures, principally *Thalassinoides*. The buff, muddy partitions are concentrated towards the top of the micritic beds where faunal remains (predominantly gastropods and bivalves) are fractured and disarticulated. Subsequent phases of bioturbation and/or tectonic disturbances sever burrow trails and leave isolated patches of mudstone infilling (Figures 3.24 & 3.25). This highly bioturbated facies was likened to the Buff Nodular Carbonate (BNC facies) of the Pelagonian zone by Sharp (1995, see section 3.7.6 below).

In some areas, similar grey micrite horizons, which have undergone considerable bioturbation, lack the buff, muddy patches that characterise the rest of this facies. Instead the burrows and disrupted burrows in these horizons are infilled with finer and paler grey micritic material (Figure 3.26). On weathered bedding surfaces such micrite-filled burrows stand proud.



Figure 3.25 - Transverse section through a distorted burrow within the Khromni Limestones. The buff marl ring represent the burrow lining which has been infilled with coarse calcite spar. The burrows are set in a fine-grained micritic matrix (locality 437, south of Khromni village).



Figure 3.26 - Fine grey micrite-filled ramifying burrows within the Bioturbated Micrite facies of the Khromni Limestones (locality 437, south of Khromni village).

Macrofossils are rarely preserved in this facies and, where seen, are always fragmentary.

3.7.4 - *Coquina Packstones*

Many of the macro- and microfaunal species elsewhere in the Khromni Limestones are concentrated in micritic and calcarenitic packstones. Both whole and fragmentary bivalves, oysters and *Nerineid* gastropods are common, as are a wide variety of benthic foraminifera. Coral debris is more limited. The bases of many bioclastic packstone horizons are very sharp and/or erosive, abruptly truncating burrow systems. They are packed with randomly-orientated faunal fragments from base to top, which represent death assemblages or coquinas.

As in the biomicritic facies above, many bioclasts are partially replaced by calcite spar and are occasionally surrounded by micritic envelopes and isopachous fringe cements. The packstones are often associated with thick (0.5-1.0 m) horizons of calcarenite, which contain only minor, small faunal fragments. They are often erosive-based and internally massive, grading in their upper parts into succeeding limestone horizons.

3.7.5 - *Algal biomicrites*

This distinctive biofacies is characterised by the presence of dark, radiating *Cladocoropsis mirabilis* algae, which can be highly concentrated and reach up to 5 cm in diameter (Figure 3.27). The algae are set in a buff, laminated, cryptocrystalline carbonate matrix which has well developed dolomitic fenestrae. Abundant benthic foraminifera include *Cuneolinae, Textulariidae, Miliolidae* (this work) and possibly *Verneuilliidae, Spirophtalmidium sp., Lituolidae* and *Valvulinidae* (Mercier, 1968). Associated *Nerineid* gastropods and bivalves are rare (Figure 3.28).



Figure 3.27 - Fine-grained micritic limestones containing abundant algae. The algae (*Cladocoropsis mirabilis*) form dark, undulose patches within the paler micrite matrix (locality 436, south of Khromni village).

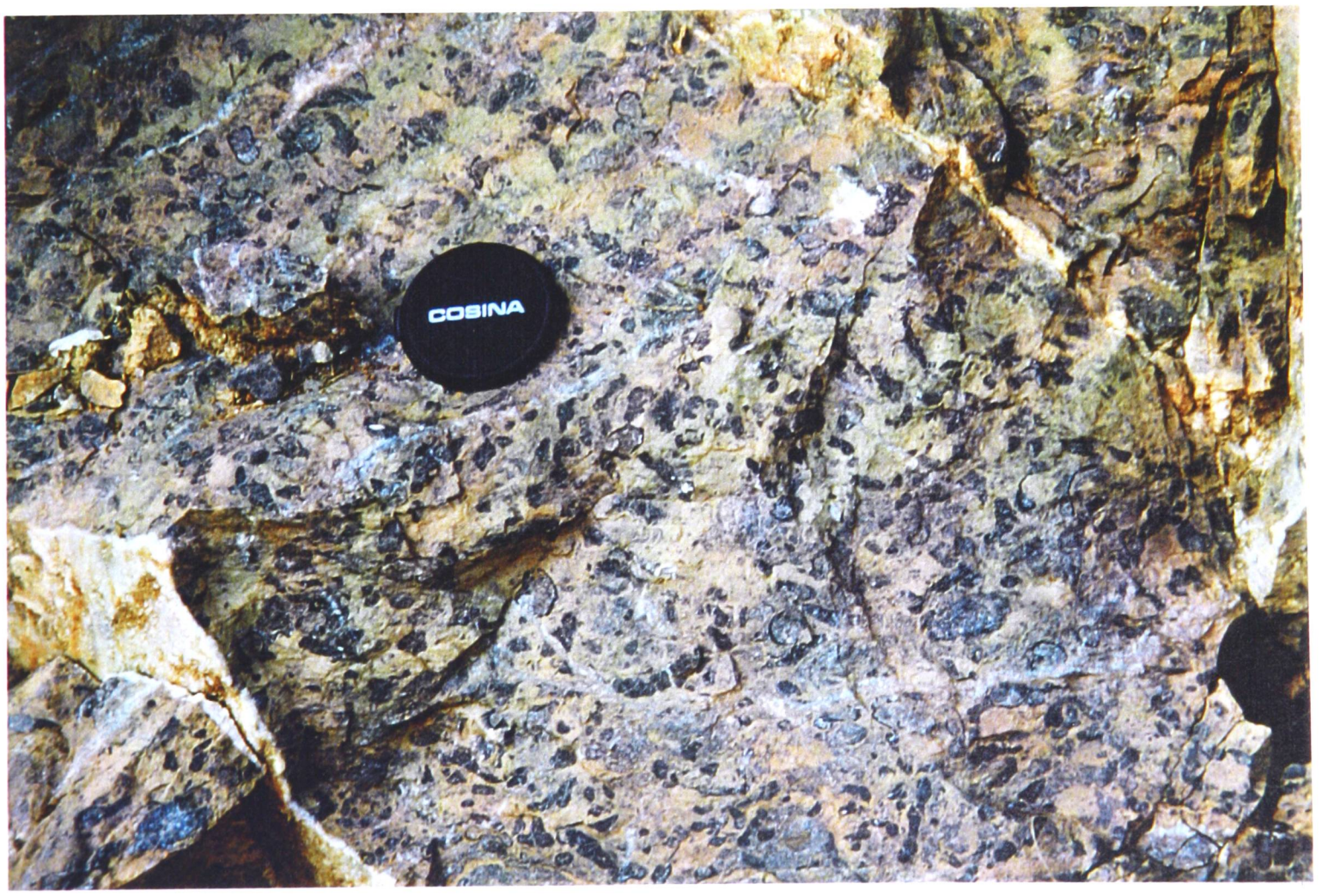


Figure 3.28 - Field photograph of the Algal Biomicrite facies of the Khromni Limestones (locality 333, north of Khromni village). The algae (elongate dark patches) are set in a grey micritic to buff marly matrix. Scarce gastropods and bivalves, infilled by coarse calcite spar, are also present.

3.7.6 - *Marls*

Many biofacies of the Khromni Limestones pass sharply, but gradationally, into pink/buff-yellow marl horizons which reach up to 2 m thick (Figure 3.29). The marls then end abruptly at contacts with succeeding carbonate horizons (Figure 3.30). They are typically fine- grained and devoid of bioclastic components. Occasional coarser, arenitic horizons rich in rounded volcanic and metamorphic quartz grains were observed, as were thin, haematite-stained lenticles and pods. Marly beds are often considerably more deformed than adjacent carbonate beds, due to their relative incompetency which allows them to assimilate tectonically-induced strain.

3.7.7 - *Discussion*

Horizons bearing *Cladocoropsis sp.* algae suggest that relatively quiescent shallow-marine conditions prevailed during their formation. A restricted platform or lagoonal setting is thus postulated (Sellwood, 1986). Disarticulated bivalve/gastropod packstones were most probably deposited by rather higher-energy currents, possibly generated during periodic storm events. During such catastrophic events, bioclastic material was entrained along with terrigenous clastic material and dumped off-shore as massively-bedded coquina. Ramifying burrow systems and extensive bioturbation indicate periods of non-deposition during which recently deposited biomicritic beds were aerated and internally disrupted. The presence of *Thalassinoides* burrows and beds rich in peloids and ooids indicate that much of the Khromni Limestone deposition took place in shallow-water marine conditions, namely an open and/or restricted platform or littoral setting during Kimmeridgian to Portlandian time (Sellwood, 1986; Wilson, 1975). The marl horizons, on the other hand, indicate the introduction of terrigenous clastic material to the dominantly carbonate system, due possibly to periodic input from a nearby deltaic system or to pulsed tectonically/eustatically-induced sea level changes.

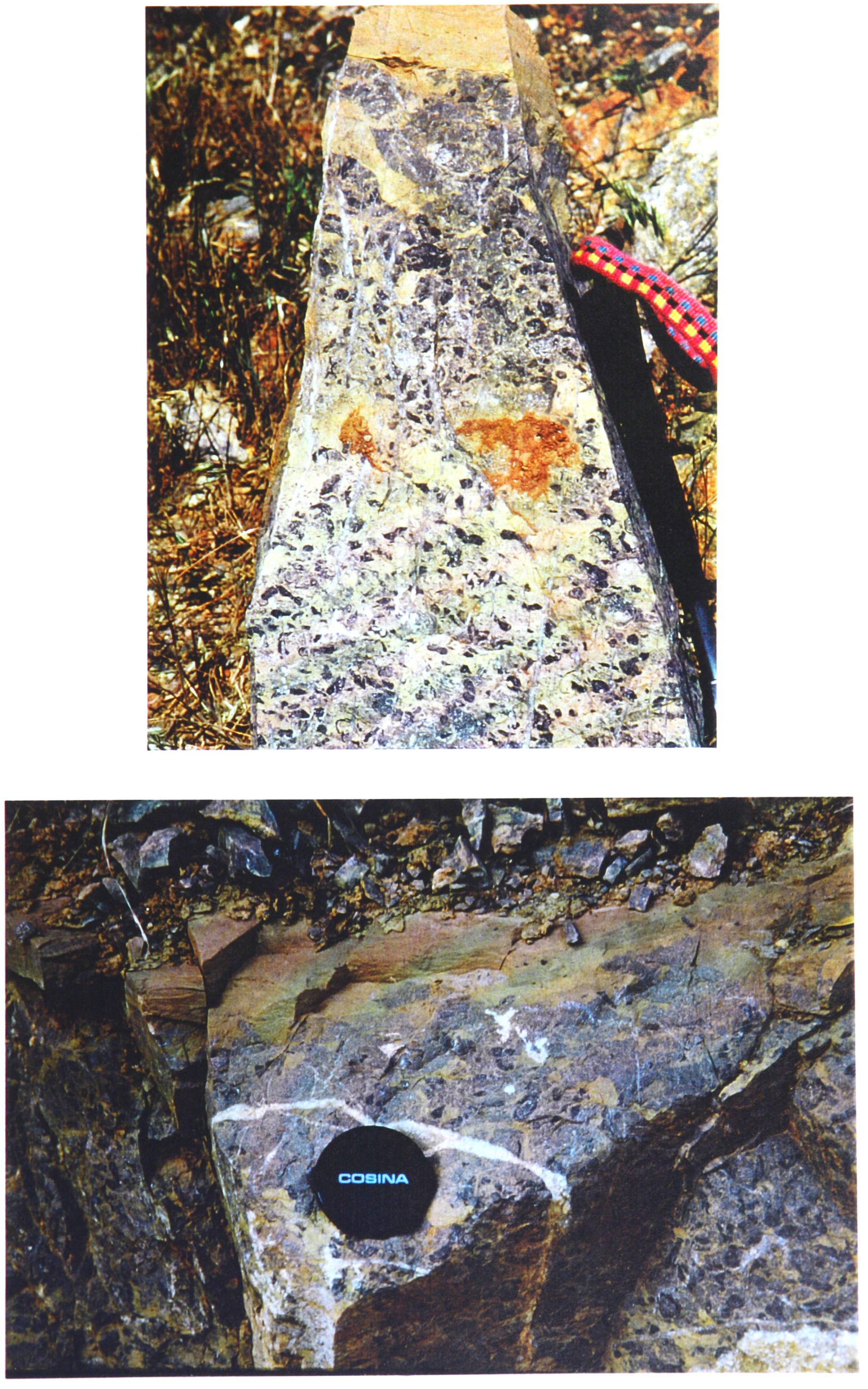


Figure 3.29 - Field photographs showing the gradational transition from grey biomicritic limestones into buff/pink marls (Khromni Limestones; locality 333, north of Khromni village).

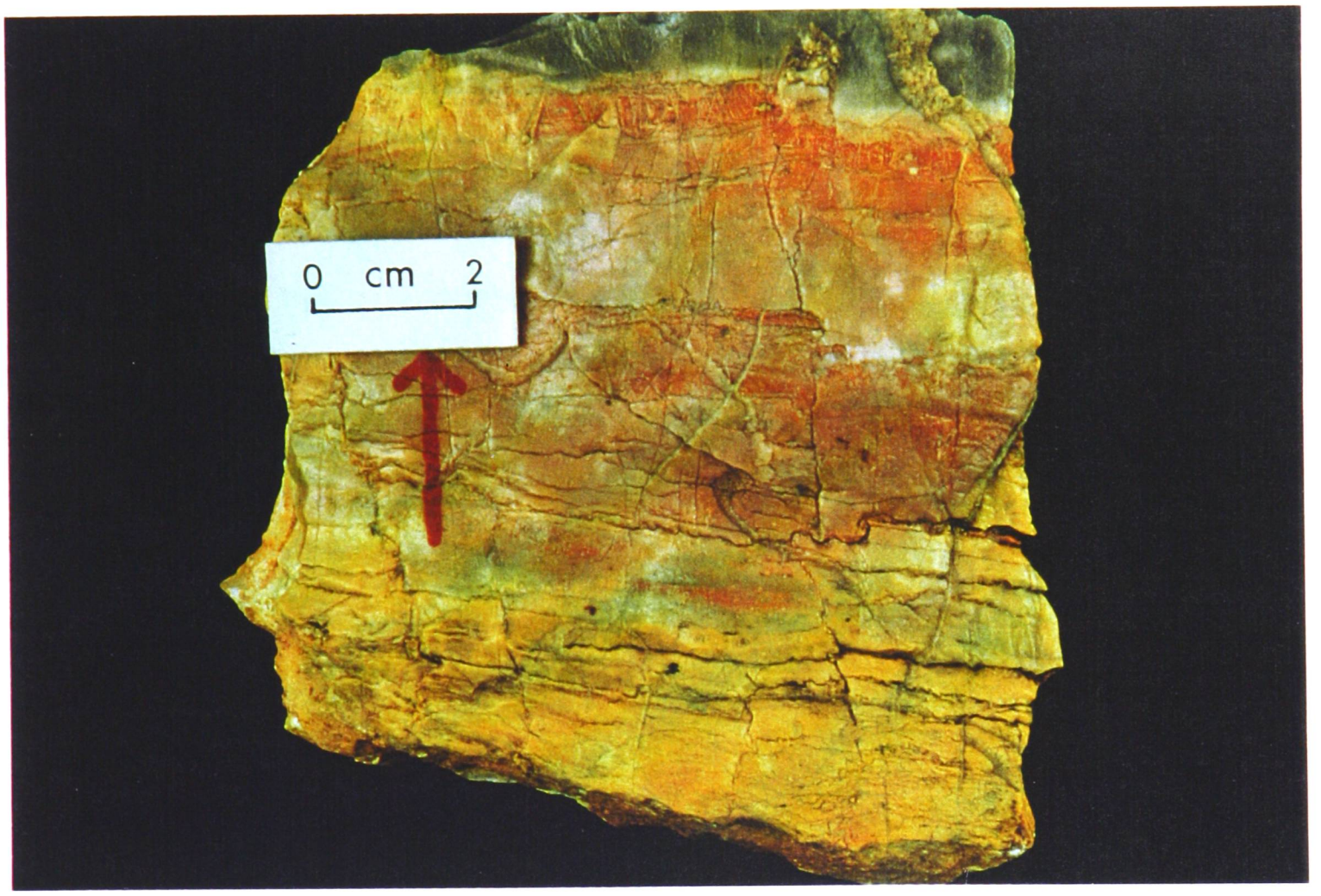


Figure 3.30 - Photograph of a hand specimen from the Khromni Limestones (locality 436, south of Khromni village). The pink/buff marls pass rapidly up into grey micritic limestones. The carbonate content of the marls varies from bed to bed.

No primary volcanic/volcaniclastic horizons were observed within the Khromni Limestone succession, therefore, the extensive volcanism associated with the underlying Khromni and Livadia Formations had ceased prior to their deposition.

3.8 - GHRAMMOS FORMATION

3.8.1 - *Introduction*

The Ghrammos Formation is primarily exposed in southern central areas of the Païkon Massif (road to Khromni, road north of Eliftherohori) but is also present much further to the northwest and in eastern parts of the Païkon Massif south of Ghriva (section 3.9.5, Figure 3.1). This unit lies conformably above the Khromni Limestones, where these carbonates are exposed, and elsewhere unconformably on the Kastaneri Formation. It grades depositionally into the Cretaceous Transgressive Limestone sequence above, as discussed in chapter 2.

As with most other lithological units within the Païkon Massif, the Ghrammos Formation has been severely affected by Tertiary tectonic disturbances which have segmented this sedimentary succession into laterally discontinuous, thrust-bound packages up to 30 m thick. Consequently, many individual and piggy-back imbricates at numerous localities have been studied in order to obtain a complete lithological and petrological picture of the Ghrammos Formation.

North of Eliftherohori village a gradational transition between the Khromni Limestones and the Ghrammos Formation is beautifully exposed (discussed in detail in chapter 2; Figure 2.15). On the section of road which winds southwards from Khromni village excellent exposures of the Ghrammos Formation *sensu stricto* crop out, as along the Ghrammos River valley, after which this unit has been named (Brown & Robertson, in press). In such areas the Ghrammos Formation is represented by rudites, arenites (coarse clast-supported sandstones, medium clast- and

matrix-supported sandstones), siltstones and mudstones which alternate on a decimetre to metre scale (Figure 3.31). All sediments are characteristically wine-red in colour, although many horizons, particularly the siltstones and mudstones, have been variably reduced to pale green-white and are thus mottled in appearance. The sediments are moderately consolidated with the more fine-grained, fissile members being the most friable. The Ghrammos Formation sediments are everywhere poorly-sorted but moderately-rounded, with clasts reaching up to 30 cm in diameter in some rudite horizons (e.g. locality 287).

The clasts which constitute the Ghrammos sediments, from coarse to fine, were derived from a siliceous volcanic and volcaniclastic source, almost without exception. Granophyric and glomeroporphyritic textures (also rarely microlitic textures) are occasionally preserved, and sub-angular to rounded cobbles of quartz porphyry, perlitic rhyolites, rotten, vesicular andesites, phengitic/cholritic schists (epidote-bearing) and white fine-grained tuff abound. Carbonate clasts also occur, containing fragments of *Cladocoropsis* algae and benthic foraminifera.

Many clasts, particularly those within rudite horizons, are surrounded by a rind of iron oxide and/or clay minerals. Locally veins of remobilised quartz or calcite invade the sediments and have been injected along fault planes. Rudite and arenite horizons have a fine to medium-grained, haematite-stained matrix which is itself composed of fragments of silicified tuff, volcanic and metamorphic quartz, abundant phengite, epidote and chlorite, pitted, altered feldspars (invariably albite) and clay minerals. Lithification has been achieved predominantly through the precipitation of siliceous cements, although carbonate cements are also present locally.

In this area (south of Khromni village) the conformable contact between the Ghrammos Formation and the overlying Cretaceous Transgressive Limestones (first documented by Sharp, 1995) is well exposed (see chapter 2; Figure 2.16). The poorly sorted, immature sediments which constitute the bulk of the Ghrammos Formation pass gradationally upwards into medium- to coarse-grained, moderately to

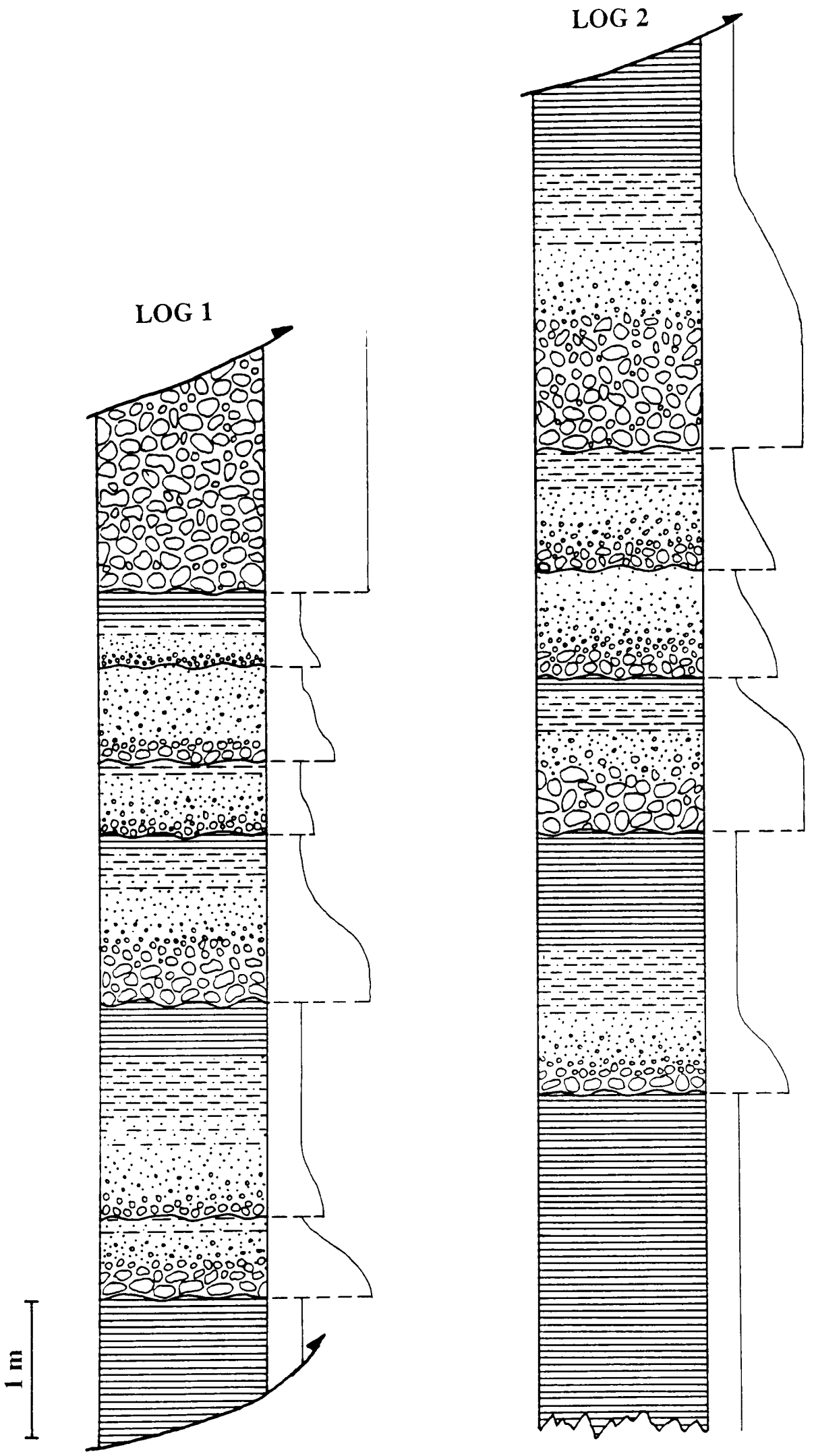


Figure 3.31 - Two representative logged sections through the Ghrammos Formation. Log 1 is from locality 169 (south of Omalo village, eastern Païkon Massif) and Log 2 is from locality 440 (south of Pentalofos village). The symbols used in the logs are explained by the key in chapter 2.

well sorted, relatively mature, buff sandstones. The arenites are flaser-bedded and clast-supported with a sparse, fine clay matrix. At some localities (e.g. locality 122) the transition into the Cretaceous Transgressive Limestones is marked by a 5-10 cm layer of nodular caliche overlain by coarse arenitic limestones with limonitic nodules. Other sections are devoid of caliche and simply grade into the basal calcarenites of the Cretaceous limestones via a progressive increase in carbonate content (Figure 2.16).

3.8.2 - ***Rudites***

The rudaceous elements of the Ghrammos Formation are always present as lensoid, laterally discontinuous horizons enclosed within a dominantly finer-grained sedimentary succession. Their bases are erosive, cutting down into the finer sandstones and siltstones below (Figure 3.31). The rudite beds vary in thickness from 10 cm to 3 m and in lateral extent from 1 m to 10 m.

Rudite horizons are usually clast-supported, but not exclusively so, and fine upwards from their base to where they grade over a short interval (1-5 cm) into clast- and matrix-supported arenites (Figure 3.31 & 3.32). Rip-up clasts of the underlying siltstones and mudstones are common and range in size from 0.5x1 cm to 10x4 cm. Such rip-ups are normally angular and tabular in shape, in contrast to moderately/well rounded pebbles in the rudite itself. The erosive-based rudite horizons mark the base of successive fining-upwards units which, when complete, grade from rudite through clast-supported arenite to matrix-supported arenite, siltstone and finally mudstone (Figures 3.31 & 2.16). Not all of the individual fining-up units are complete, but a notable degree of gradational grain size reduction is always seen (Figure 3.33). In some cases coarse, erosive-based arenites form the basal deposit of a fining-up unit; in others they make up the top, and so on. Fining-up units vary between 10 cm and 10 m in thickness. Clast-count analyses from many localities show the rudites to be almost wholly of volcanic derivation (Figure 3.34).



Figure 3.32 - Field photograph of an erosive-based rudite horizon within the Ghrammos Formation (locality 278, south of Khromni village). The rudites cut down into an arenitic bed below and pass gradationally upwards into coarse- then fine-grained sands. The rudites are clast-supported and pinch out laterally.

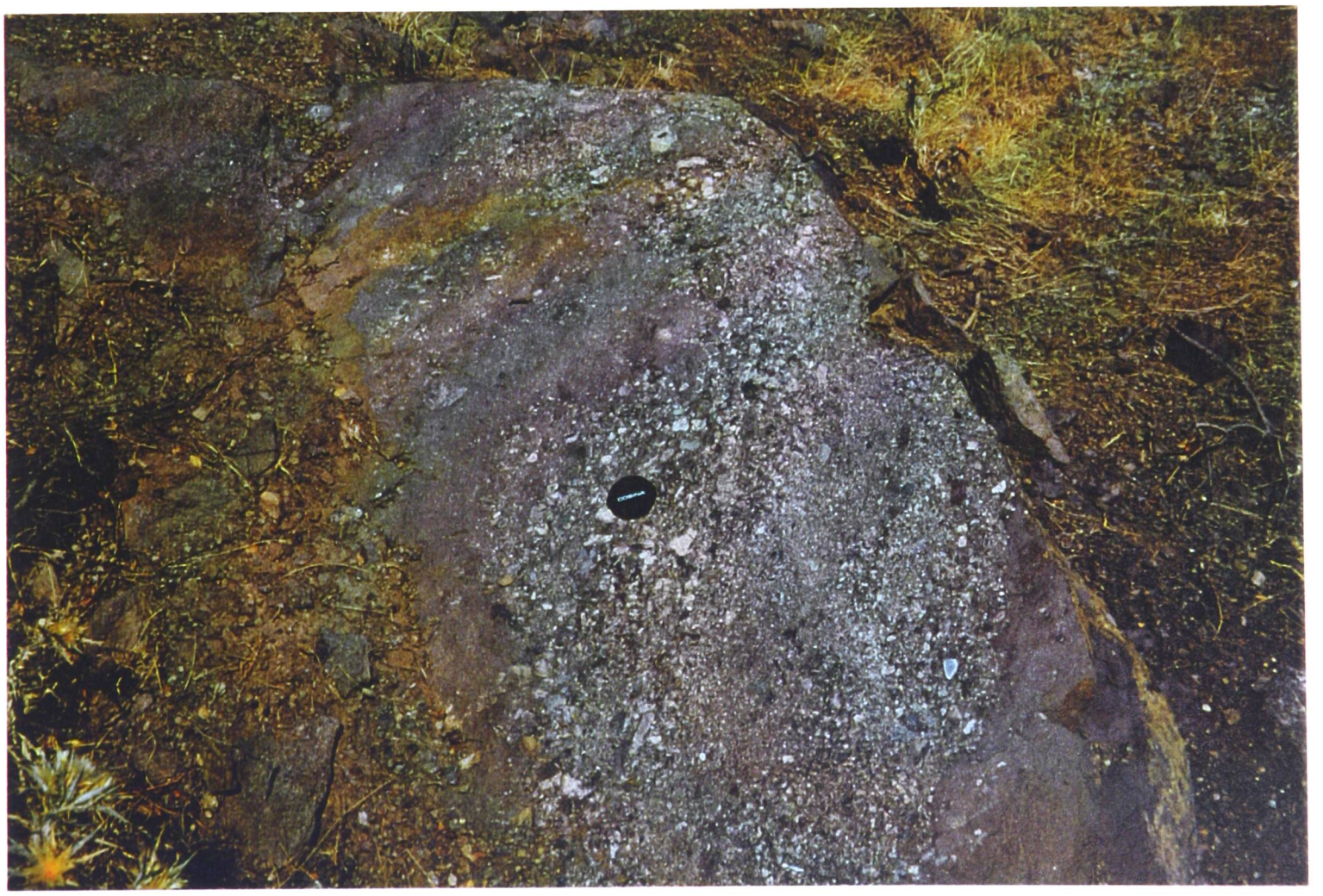
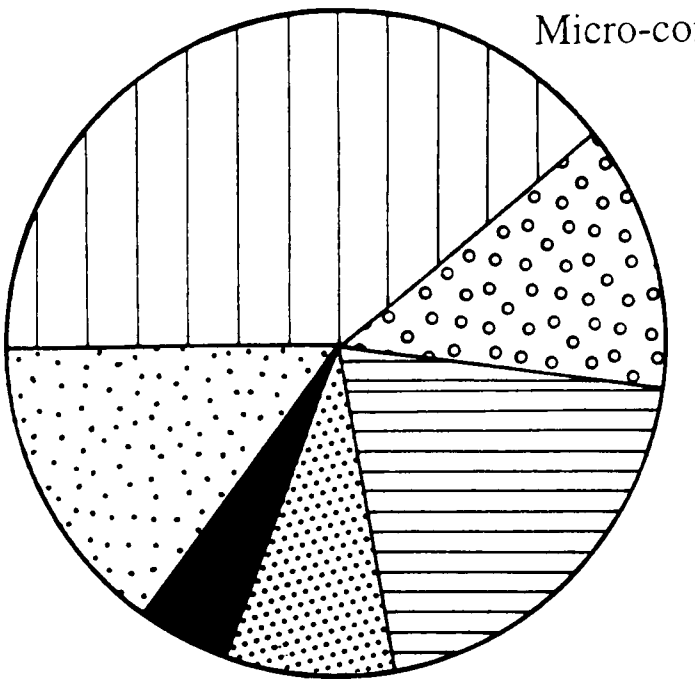
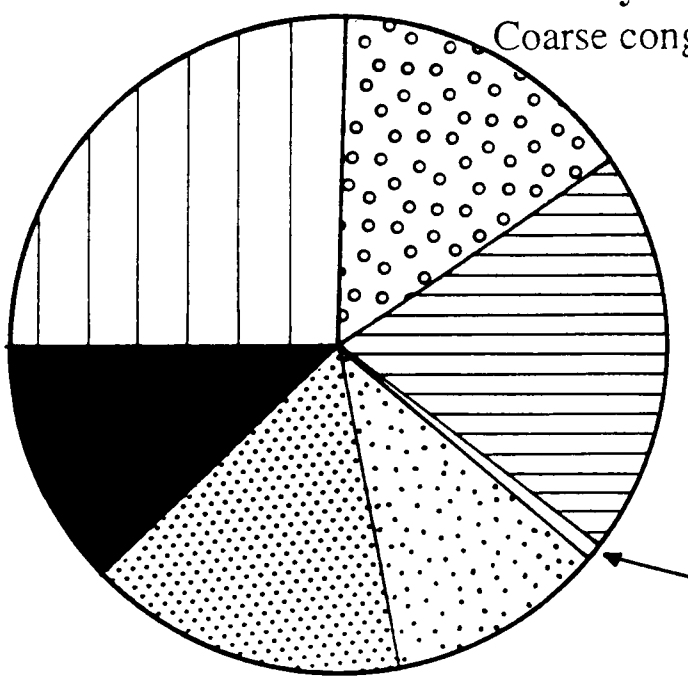


Figure 3.33 - Characteristically wine-red sediments of the Ghrammos Formation (locality 169, NE of Theodoraki village). The photograph shows two fining-up units (fine from bottom right to top left) resting upon fine-grained arenites. The lower fining-up unit grades into very coarse arenites/micro-conglomerates, while the second grades into fine-grained sands.

Locality 287 (south of Khromni)
Micro-conglomerate



Locality 280 (south of Khromni)
Coarse conglomerate



Locality 169 (south of Omalo)
Coarse conglomerate

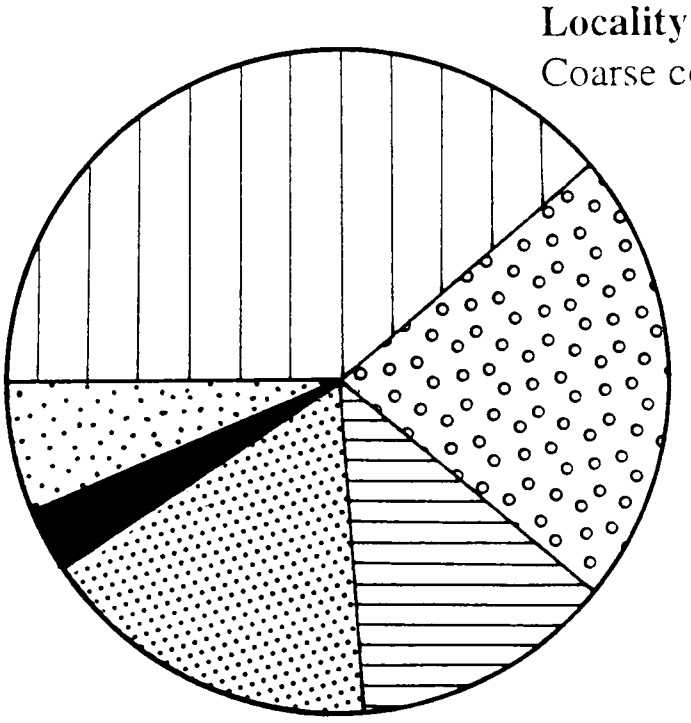
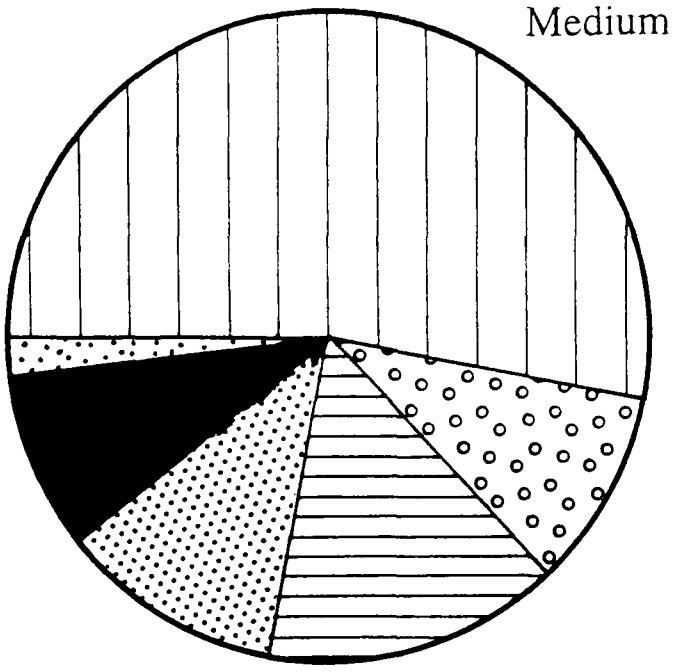
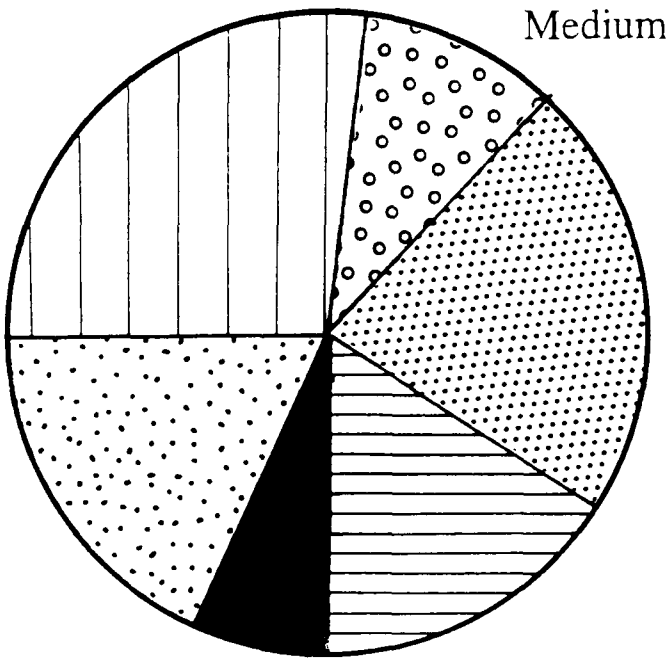


Figure 3.34 - continued on next page.....

Locality 319 (NE of Theodoraki)
Medium conglomerate



Locality 440 (south of Pentalofos)
Medium conglomerate



KEY

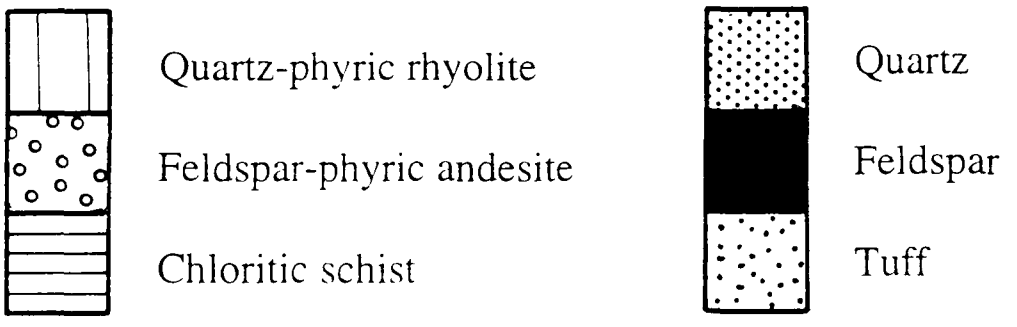


Figure 3.34 - Pie charts showing the composition of clasts from the Ghrammos Formation. Each pie charts represents the findings from one locality, where an average of 100 clasts were counted. Each shaded segment is proportional in size to the percentage of clasts counted of a given lithological type.

3.8.3 - *Arenites*

The arenitic component of the Ghrammos Formation is by far the most voluminous and the most lithologically variable. Clast-supported, coarse sandstones dominate, although matrix-supported coarse sandstones, medium-grained clast- and matrix-supported sandstones and fine-grained sandstones are also present. Petrological and provenance studies confirm that their source is correspondingly volcanic/volcaniclastic. Thin section studies reveal the principal components of the arenites to be volcanic and metamorphic quartz, pitted albites, epidote, chlorite and iron oxides set in a haematite-stained matrix (Figure 3.35).

3.8.4 - *Siltstones and Mudstones*

This sedimentary facies is dominated by wine-red, pale-green to white mottled siltstones and mudstones. Spheroidal weathering is characteristic and the sediments are always poorly consolidated and highly friable (Figure 3.36). XRD analyses of these fine-grained sediments reveal the dominant mineralogical components as quartz, albite, illite, phengite, montmorillite, kaolinite and chlorite. They commonly form the uppermost deposits of a fining-upwards unit (e.g. Figure 3.31) and can reach up to 4 m in thickness. Locally, nodular caliche occurs within the mudstones, as do ferruginous/limonitic concretions.

3.8.5 - *New Key Localities*

Previously unidentified outcrops of the Ghrammos Formation have been found in the western Païkon Massif (locality 134) during the course of this work. They were previously mistaken by former researchers as acidic volcanics and volcaniclastics of the Kastaneri Formation. This confusion arose because outcrops of Ghrammos

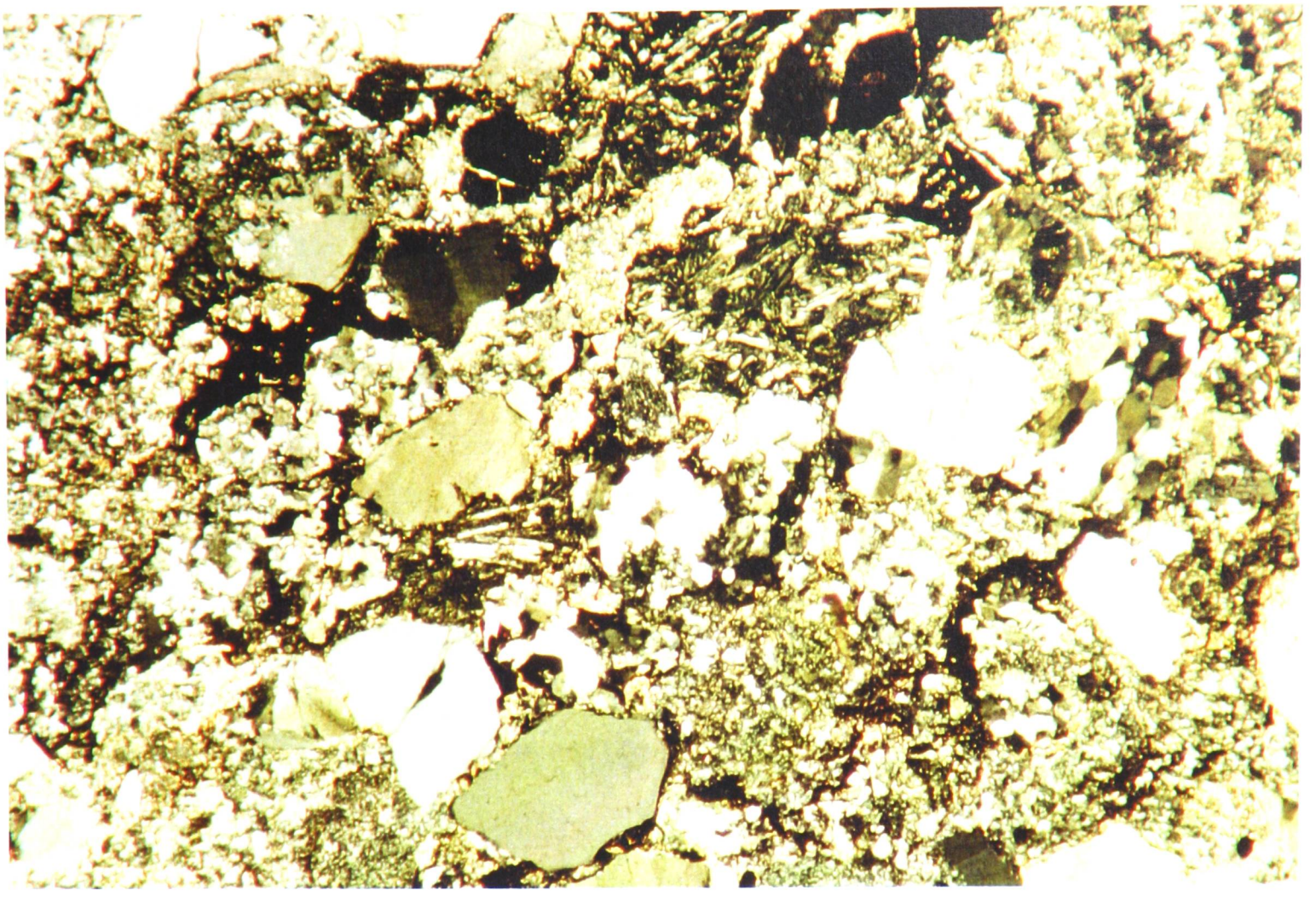


Figure 3.35 - Photomicrograph of arenites from the Ghrammos Formation. The majority of clasts are strained and microcrystalline quartz, with clasts of altered volcanics also. The altered volcanics still retain their primary porphyritic textures (randomly-oriented feldspar laths). Locality 279, south of Khromni village.



Figure 3.36 - Field photograph of mudstones from the Ghrammos Formation. The mudstones are often nodular in appearance due to spheroidal weathering (locality 278, south of Khromni village).

sediments in this area are almost completely weathered to a pale-green/white colour and hence closely resemble the quartz porphyries and white tuffs of the Kastaneri Formation. However, on close inspection in the field, the apparent "quartz porphyries" were found to be highly altered coarse arenites and fine rudites, while the "white tuffs" are in fact fine-grained Ghrammos Formation arenites and siltstones. Pockets of characteristically wine-red Ghrammos matrix which have evaded reduction are scarce but diagnostic. East of Konstantia, the Ghrammos Formation was encountered again, identified by wine-red mottled patches and its distinctly sedimentary texture.

Outcrops of the Ghrammos Formation on the eastern side of the anticlinal Païkon Massif were also recorded for the first time during the course of this study. It is in fact quite common there. Outcrops of pale-green/ white and rarely wine-red poorly-sorted sediments can be traced all the way north from localities 164 and 169 (between Eliftherohori and Omalou) and locality 175 (between Pentalofos and Ghriva; Figure 3.1). Many of the sediments identified in this area are now attributed to coarser members of the Ghrammos Formation, with lesser highly sheared siltstones and mudstones.

Everywhere on the eastern flank of the Païkon Massif the Ghrammos Formation sediments are considerably more sheared, silicified, indurated and altered than their western counterparts. This is due to the effect of the Tertiary D3 deformation event which is documented in chapter 4. As in northwestern areas of the Païkon Massif, the Ghrammos Formation in the east was formerly mapped as part of a Jurassic volcanic and volcaniclastic unit (Kastaneri Formation of Mercier, 1968).

In the northeastern quadrant of the Païkon Massif poor exposure due to extensive aforestation prevented the identification of the Ghrammos Formation in this area, should it exist.

3.8.6 - *Discussion*

The Ghrammos Formation sediments were almost certainly deposited over the whole of the Païkon unit, as opposed to merely the southwest corner as previously supposed (Mercier, 1968; Bebien, 1982; Godfriaux & Ricou, 1991; Bonneau *et al*, in press). Deposition took place subsequent to that of the limited Khromni Limestones (i.e. post Kimmeridgian/Portlandian) and prior to the Cretaceous Transgressive Limestone series (i.e. pre Aptian/Albian; see section 3.9). The Ghrammos Formation is postulated here to represent a continentally-derived braided fluvial system. The rationale behind this interpretation is given below.

The earliest Ghrammos Formation deposits reflect sedimentation in a shallow-marine environment, possibly deltaic, documented by the interbedded relationship of Ghrammos Formation clastic sediments and the conformably underlying Khromni Limestones. Carbonate sedimentation then ceased and the purely clastic sedimentation of the Ghrammos Formation commenced.

The erosive-based rudite horizons which pinch-out laterally are interpreted as migrating channel deposits, which are characteristically floored by coarse rudites and/or bar deposits, and which are formed by the vertical accretion of coarse clastic material (Collinson, 1986). Both channels and bars form laterally discontinuous, lensoid features (Leeder, 1982; Collinson, 1986), as typically seen in the Ghrammos Formation rudites. No sedimentary structures have been preserved in these channel/bar complexes and thus no conclusions relating to palaeocurrent directions can be drawn. The gradational passage of these rudites up into finer units, ultimately siltstones and mudstones, could reflect channel avulsion and/or change to a lower energy flood plain environment, as described by Collinson (1986; Figure 3.37). In the Donjek River system (Yukon, Canada), very coarse material of high-energy channels grades up into sands, which represent channel-fill deposits, and ultimately low-energy silts and muds of abandoned channel top or flood plain environments (Figures 3.38; Williams & Rust, 1969). These facies

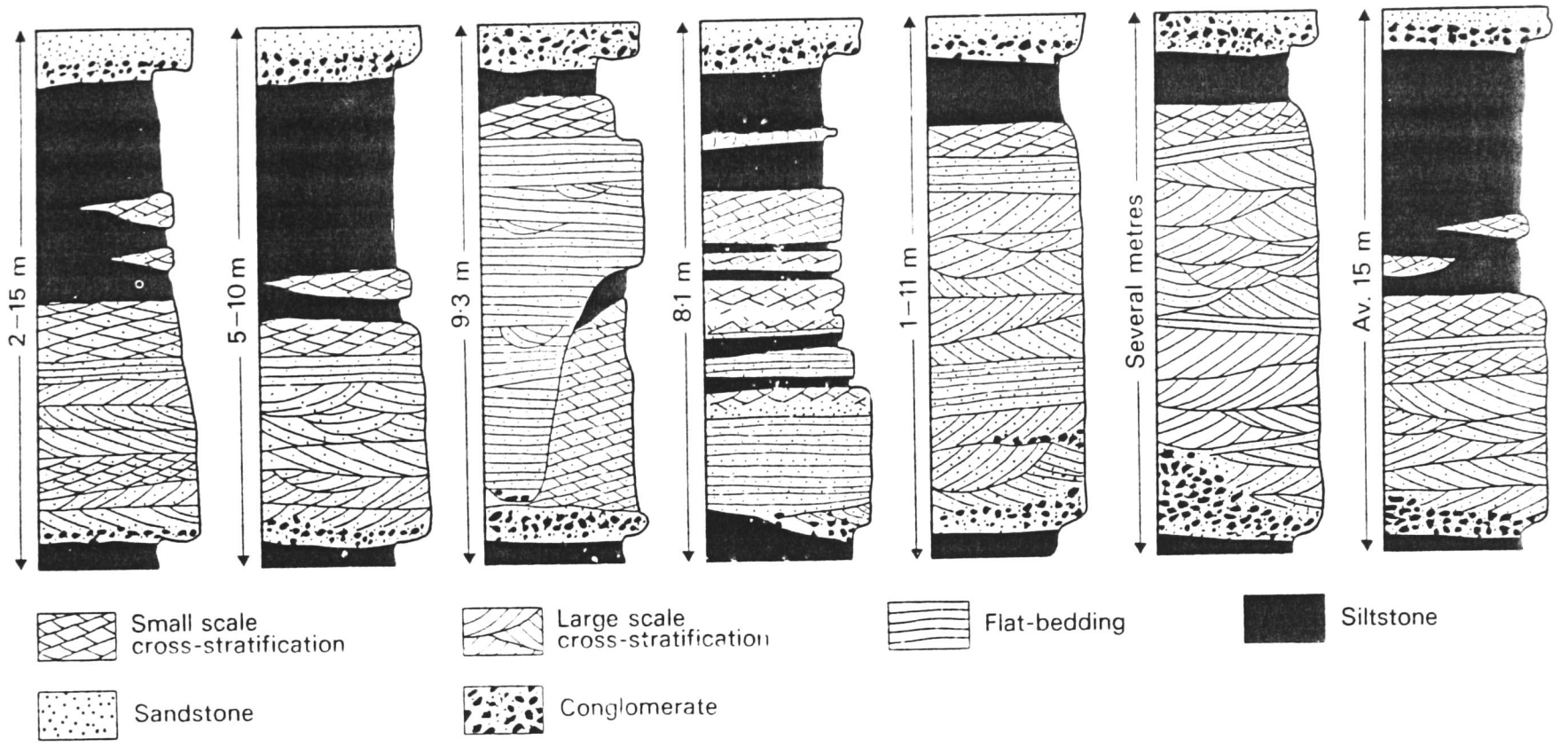


Figure 3.37 - Representative logs through fining-up sequences from various migrating channel systems (after Collinson, 1986). Coarse conglomeratic horizons are erosive-based and fine gradationally into sands and silts. The size of fining-up units varies from 1-15 m.

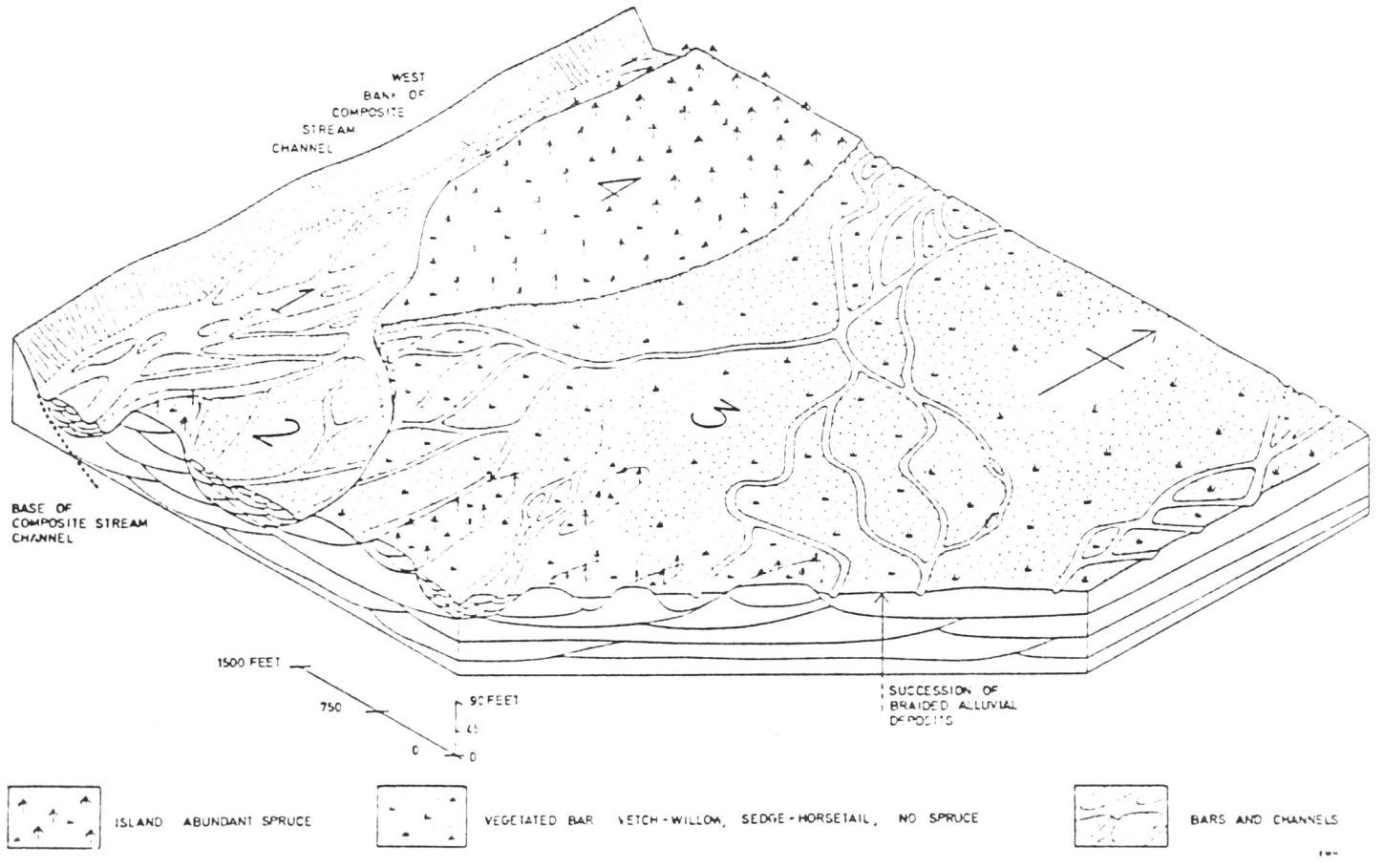


Figure 3.38 - Three-dimensional block diagram showing the anatomy of a braided river system. The Donjek River, Yukon/Alaska (after Williams & Rust, 1969). The anastomosing channels produce laterally-discontinous conglomerate horizons which fine up due to channel avulsion and waning flow.

associations correspond very closely to the fining-up units described from the Ghrammos Formation.

Periodic nodular caliche horizons suggest a subaerial environment dominated by evaporation and chemical precipitation (Leeder, 1982; Collinson, 1986). Caliche usually forms on non-depositional surfaces (Leeder, 1982; Sellwood, 1986) and so it is likely that the caliche horizons within the Ghrammos Formation represent periods of no sediment accumulation, perhaps atop an abandoned channel or in a flood plain setting. This hypothesis is supported by the semi-arid palaeogeographical setting of the Hellenic Tethyan region at this time (Robertson & Dixon, 1984; chapter 1). The calcium carbonate which formed the caliche may have been derived from calcium carbonate-saturated groundwaters (as also evidenced by local calcite cements), the rare carbonate clasts within the Ghrammos Formation, or from the Khromni Limestones below.

Provenance and petrological studies indicate that the Ghrammos Formation was almost wholly derived from the underlying Kastaneri Formation. Clasts of altered andesite, quartz porphyry and tuff abound, and their geochemical signature matches that of the volcanic-volcaniclastic series below. Rare carbonate clasts contain the algae *Cladocoropsis sp.* and are thus very likely to be sourced from the conformably underlying Khromni Limestones.

The braided fluvial environment of deposition and the derivation of these sediments from underlying units suggest that sedimentation took place on a relatively high gradient, and that a significant degree of extensional faulting and unroofing must have taken place prior to deposition of the Ghrammos Formation to allow the underlying blueschist facies Kastaneri Formation to be sourced.

3.9 - CRETACEOUS TRANSGRESSIVE LIMESTONES

3.9.1 - *Introduction*

The Cretaceous Transgressive Limestones are characterised by shallow-water, fossiliferous limestones which overlie the Ghrammos Formation with a normal, depositional contact (chapter 2.2.6). Palaeontological evidence (Mercier, 1968) indicates an Upper Albian age for the base of the unit and a Maastrichtian age for the upper limit of the neritic platform. However, recent work by Sharp & Robertson (1992) suggests that platformal collapse and the onset of pelagic carbonate deposition occurred during Cenomanian-Turonian time on the western flank of the Païkon Massif, indicated by the presence of a radiolarian assemblage of this age in the Tchouka Flysch (section 3.11).

The recent discovery of extremely deformed rudist lamellibranchs near Karpi (Figure 2.17) indicates that the Cretaceous Transgressive Limestones also occupy the easternmost parts of the Païkon Massif (Brown & Robertson, in press; Godfriaux & Ricou, 1991) and that they are not Jurassic in age as previously concluded (Mercier, 1968; Bebien, 1982). In fact, field research during this study has revealed the presence of a complete Kimmeridgian to early Tertiary conformable succession (i.e. Khromni Limestones to Tchouka Flysch) in the east, as well as on the west of the Païkon Massif, as will be discussed in the following sections (see 3.7.7, 3.8.5, 3.9.4, 3.10.3, 3.11.4 and chapter 2).

Due to Tertiary deformation, a complete, uninterrupted section through the Cretaceous Transgressive Limestones was not observed. Instead, many sections were studied and logged in detail in order to determine the relative stratigraphic position of each carbonate facies.

3.9.2 - *Palaeontology*

Mercier (1968) carried out extensive, detailed palaeontological and biostratigraphical investigations of the Cretaceous limestone fauna. During the course of this work (and in Sharp, 1995) many of the foraminiferal and mollusc species identified by Mercier have been confirmed and are listed in the succeeding text. Some new findings are noted and discussed below.

The fauna of the Cretaceous Transgressive Limestones are moderately to poorly preserved depending on their proximity to major tectonic contacts. In general, those of the western Païkon are in a somewhat better state of preservation than their equivalents on the east of Païkon, although imbricate slices in the west are highly recrystallised (e.g. localities 2, 47, 329 and 405; Figure 3.1). The dominant faunal constituents of the limestones are benthic foraminifera, bivalves, gastropods, rudist lamellibranchs and rare corals. A diverse benthic foraminiferal assemblage is present throughout the Cretaceous limestone series (Figure 3.39) and is dominated by *Textulariidae sp., Cuneolina sp., Nezzazata simplex, Nezzazatinella picardi* (Sharp, 1995), *Valvulinidae sp., Ophtalmidiidae sp., Cyclolina sp.* and *Miliolidae*, which indicate Lower Albian to Cenomanian-Turonian ages. Mercier also documented the presence of *Haplophragmoïdes sp., Textulariella sp.* and *Pseudolituonella sp.*, which were not observed during this study.

Macrofauna are again common throughout the limestone series, although they are chiefly concentrated in biomicritic and biosparmicritic-packstone horizons. Bivalve species may include fragmentary *Inoceramus sp.* (Sharp, 1995) and indeterminable oyster species (Figure 3.40). Both articulated and disarticulated bivalves are common in sparse biomicritic horizons and packstone-coquina: in the latter they are commonly flat-lying and fragmented. The bivalves often occur in association with high-spiral *Nerineid* gastropods which can reach up to 6 cm in length (Figure 3.41). *Nerineids* are also commonly found as the main macrofaunal constituents of some biopelmicritic horizons, in which they are highly recrystallised.

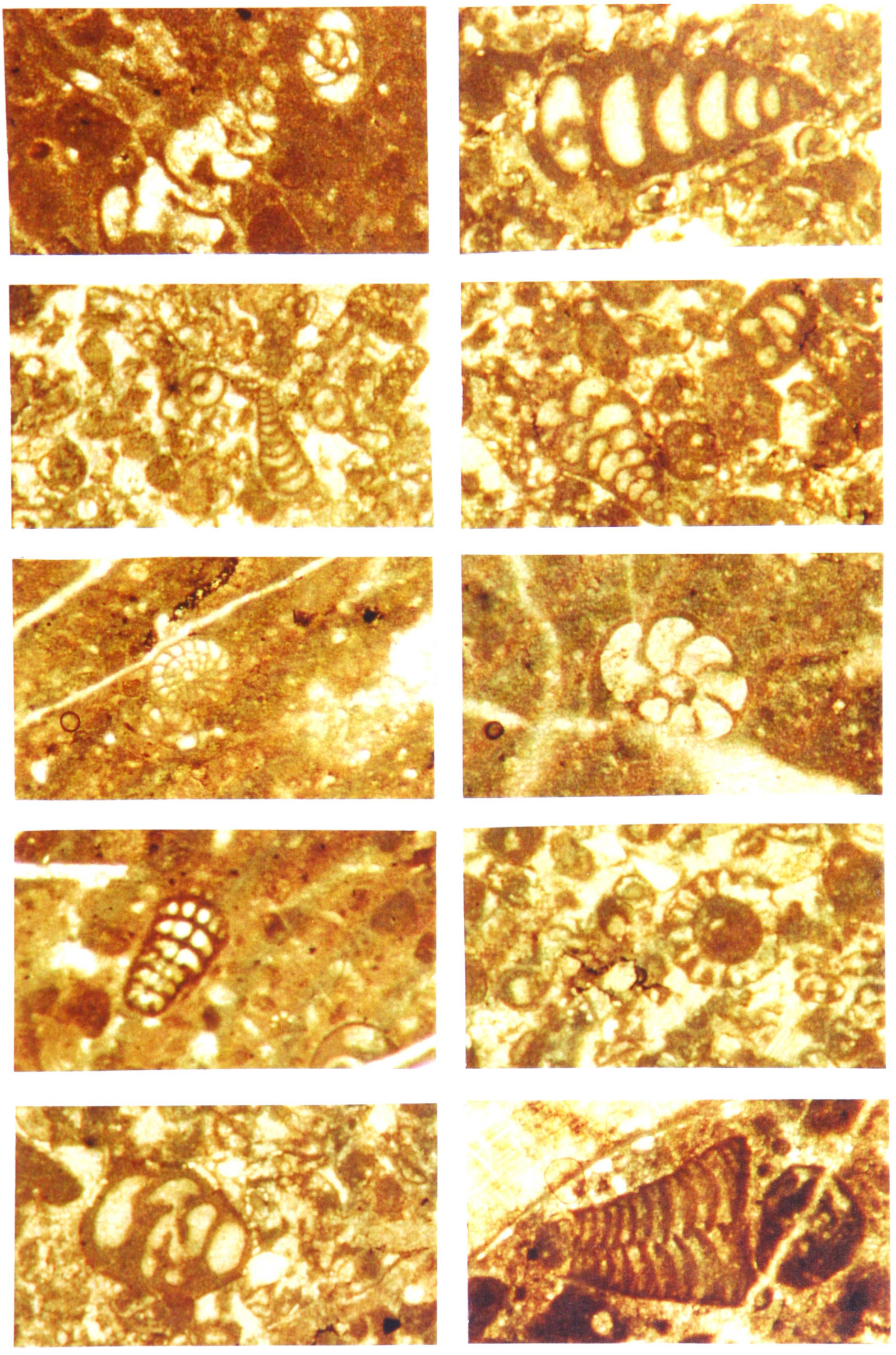


Figure 3.39 - Photomicrographic plates of benthic foraminifera within the Cretaceous Transgressive Limestones (various localities). The foraminifera species are given in the text (page 113). The foraminifera are set in a bioclastic pel-spar-micritic matrix. All photographs are taken at x30 magnification.



Figure 3.40 - Field photograph of an oyster packstone horizon within the Cretaceous Transgressive Limestones (locality 65, by Theodoraki village).



Figure 3.41 - Large, high-spiral *Nerinea* gastropods from a thrust-imbricate of the Cretaceous Transgressive Limestones (loclaity 445, north of Khromni village).

At a few localities (e.g. localities 29 & 2; Figure 3.1), small, isolated coral colonies were encountered. They are limited in extent due to shearing and tectonic cut-out, and were only observed in thrust-bound pods up to 10 cm in diameter. The colonies are exclusively inhabited by the scleractinian corals *Diplocoenia polygonalis* and *Diplocoenia dolfussi* (Figure 3.42) which indicate a Cenomanian age (B. Rosen, pers. comm., 1996). Rare, indeterminate solitary corals are also occasionally found.

Towards the top of the Cretaceous Transgressive Limestone series, assemblages including small, possibly *Monopleurid* rudist bivalves occur in association with poorly preserved *Nerineid* gastropod and bivalve species (Figure 3.43). Very rarely, larger rudist families are encountered in western parts of the Païkon Massif, predominantly within thrust-bound Cretaceous imbricates, for example at localities 129a and 424 (Figure 3.1). Large rudists, such as these, are invariably fragmentary and highly recrystallised or deformed with only outline morphological features remaining. Consequently, accurate classification was unsuccessful and only tentative identification of *Requieniidae* and *Radiolitidae* genera can be proposed. Similar large *Requieniidae* and *Radiolitidae* rudist remains have also been identified in the central, eastern Païkon Massif (this work; Bonneau *et al.*, in press), and unidentified rudist bivalves were reported from the extreme east (Godfriaux & Ricou, 1991). These limestones, as stated above, are often severely recrystallised hindering accurate determinations.

3.9.3 - ***Facies***

The Cretaceous Transgressive Limestones undergo a number of changes in depositional facies from calcarenitic limestones, biopelmicrites, biomicrites/sparites, biomicritic packstones and intraclastic packstones to pelagic carbonates, from base to top respectively. Basal calcarenites (10-20 m) grade conformably from the underlying Ghrammos Formation with a rapid increase in carbonate content (Figure 2.16).



Figure 3.42 - Photograph of a hand specimen showing colonial coral species from the Cretaceous Transgressive Limestones. The corals are *Diplocoenia dolfussi* and *D. polygonalis* (Cenomanian, B. Rosen, pers. comm.). Locality 28, north of Khromni village.



Figure 3.43 - Field photograph of a bioclastic packstone horizon within the Cretaceous Transgressive Limestones. The macrofauna present include *Nerineid* gastropods, bivlaves and rudist bivalves (*Monopleuridae*). Locality 65, by Theodoraki village.

Calcarenites

Calcarenitic beds are poorly-sorted and massively-bedded. Clasts are predominantly of volcanic and metamorphic quartz with lesser amounts of volcanic and sedimentary intraclasts. Microfaunal components are rare but some *Miliolida sp.* were noted, and macrofauna are entirely absent.

Biopelmicrites

Above the calcarenites lies a distinctive nodular-biopelmicrite facies. The micrites are dark-grey and individual beds are between 30 cm and 50 cm thick. They are characterised by distinctive elliptical to nodular black concretions which are putrid-smelling on fracture. The concretions range from 0.5 cm to 5.0 cm in diameter and often form bedding-parallel aggregates (Figure 3.44). On weathered surfaces they form distinctive protuberances that are significantly darker than the host micrite. Such putrid-smelling micritic nodules have been reported in similar neritic carbonates from the Pelagonian Zone to the west (Sharp, 1995). Thin-section studies reveal that the biopelmicrites are poor in faunal components but contain benthic foraminifera dominated by *Miliolidae* and *Cuneolina sp., Nerineid* gastropods and sparse algae and bivalves (possibly *Inoceramus*, Sharp, 1995). Fenestral textures in the micritic matrix are formed by bedding-parallel dolomitic lenticles. Dolomite concentration then decreases up-section.

Biomicrites and Sparry-biomicrites

The bulk of the Cretaceous Transgressive Limestones are characterised by a relatively thick succession of biomicrites and sparry-biomicrites. These facies are pale-grey, medium-grained and occasionally brecciated (Figure 3.45). Sparry horizons are significantly less voluminous than their micritic equivalents and are slightly coarser grained. These limestones accommodate much of the macrofauna present in the unit, as well as a diverse range of benthic foraminifera. Bivalves and *Nerineid* gastropods are common, as are *Monopleurid* (Figure 3.43) and possibly *Schiozia* (Mercier, 1968) rudists towards the top of the neritic succession, together with rare coralline build-ups (Figure 3.42). Where a macrofaunal assemblage is



Figure 3.44 - Field photograph of dark, nodular concretions within the biopelmicrite facies of the Cretaceous Transgressive Limestones. The concretions run in chains sub-parallel to bedding and are proud-weathering (locality 433, northeast of Kanstantia village).



Figure 3.45 - Brecciated biomicrite within the Cretaceous Transgressive Limestones. The breccia clasts contain fragments of coral, gastropods and bivalves and are set in a coarse brown calcite-spar matrix (locality 42, north of Eliftherohori village).

lacking, benthic foraminifera are still reasonably abundant, *Cuneolina sp.*, *Textulariidae* and *Miliolidae* being the most dominant.

A distinctive feature of this thick succession of biomicrites is the local occurrence of heavily bioturbated pink micritic horizons (Figures 3.46 and 3.47). Where these occur, the pale-grey biomicrites become progressively pink and fine-grained towards the top of beds and end in an abrupt contact with succeeding grey biomicritic beds. The contacts are commonly marked by thin, ferruginous crusts and always by a significant increase in both bioturbation and terrigenous mud content. Large ramifying burrows, probably *Thalassinoides,* are common and never penetrate the contact between the pink marls and the overlying grey micrites. Occasionally, bioturbated hiatus horizons are not accompanied by an increase in pink marls as demonstrated on Figure 3.48.

Occasional oolitic horizons have been observed in biomicritic beds, often occurring directly above a pink hiatus horizon. They have also been noted sporadically throughout the biomicritic facies *sensu stricto*, although they are usually limited in extent. The presence of sporadic oyster packstones has also been noted at a few isolated localities within the biomicritic facies, although, unlike the bioclastic-packstones described below, these horizons preserve oyster associations in life position.

Bioclastic-packstones

Bioclastic-packstones occur locally throughout the Cretaceous Transgressive Limestones as solitary beds. These have sharp basal and upper contacts and are between 30 and 120 cm thick (Figure 3.49). They are internally massive. Faunal components (bivalves, gastropods, oysters and rudists) are invariably fractured and flat-lying. Carbonate and terrigenous intraclasts were also observed and many such horizons have calcarenitic matrices.

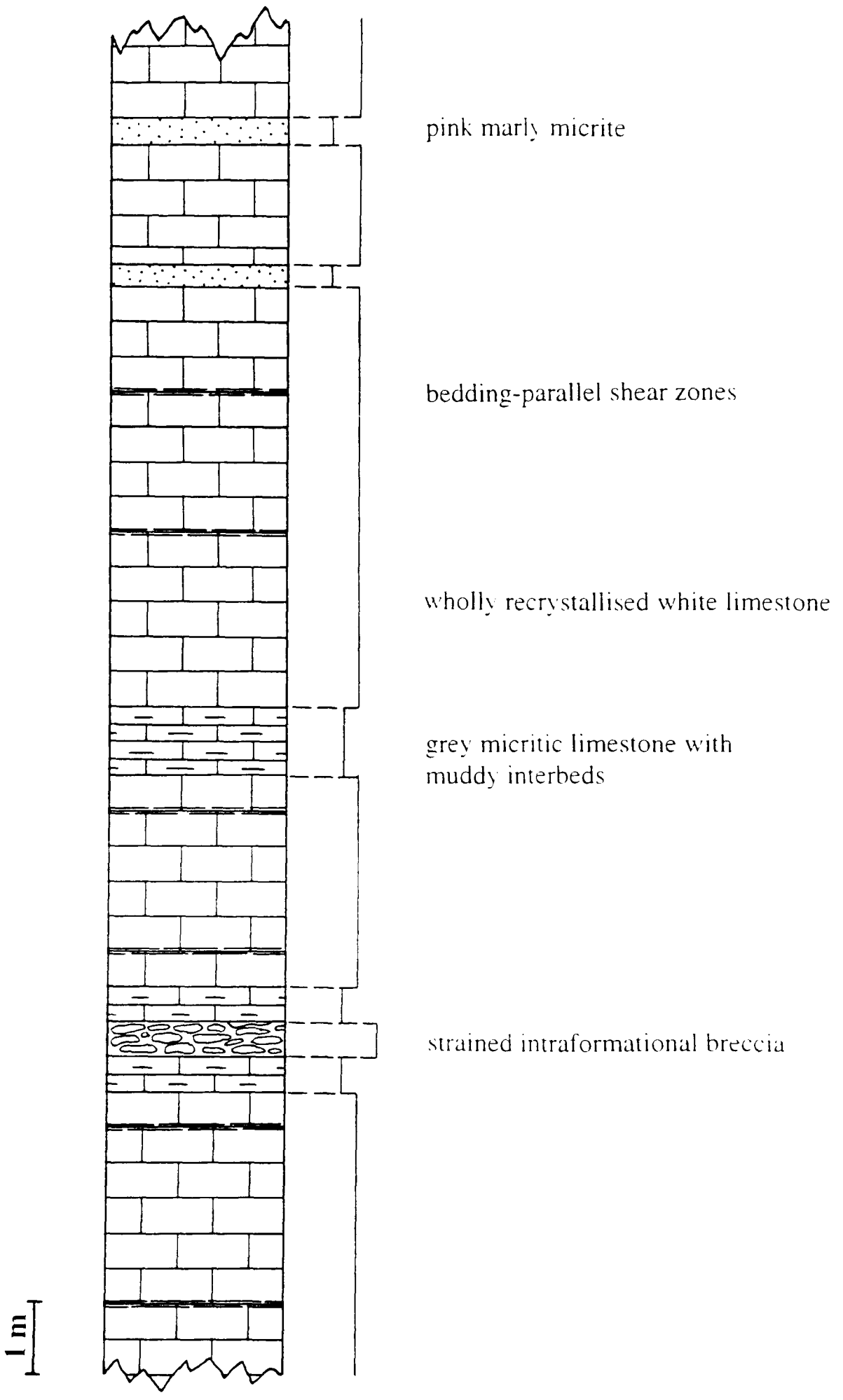


Figure 3.46 - Log through a thrusted imbricate of the Cretaceous Transgressive Limestones from just below the summit of Gola Tchouka (1650 m; locality 227, central Païkon Massif). The recrystallised limestones contain vestiges of indeterminable faunal components within grey micritic beds (possibly gastropods, bivlaves and benthic foraminifera). Pink marly horizons occur occasionally and are fine-grained and highly-sheared.

KEY to Figure 3.47

Sparse biomicrite

Packed biomicrite

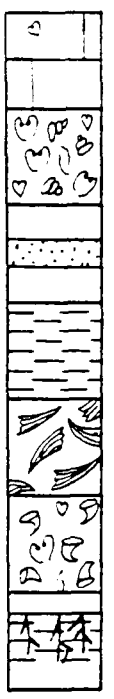
Calc-arenite

Marl

Oyster packstone

Rudist packstone

Bioturbation



Gastropods

Bivalves

Rudists

Shell debris

Foraminifera

Arenitic matrix



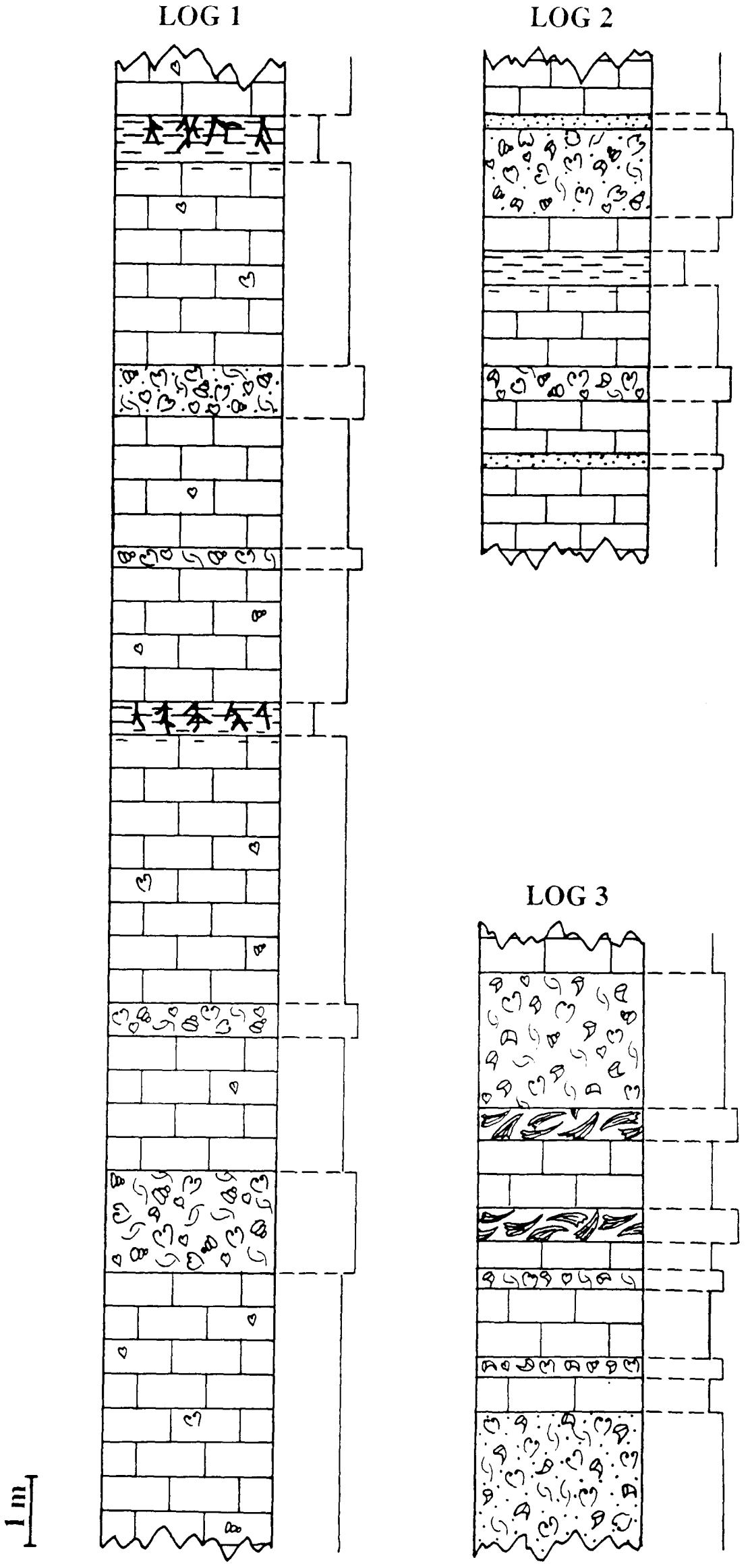


Figure 3.47 - Three logs of representative sections through the Cretaceous Transgressive Limestones. Log 1 shows interbedded sparse and packed biomicrites with periodic marl horizons (locality 428, by Theodoraki village). Log 2 also contains calc-arenitic horizons (locality 429, northeast of Theodoraki village) and Log 3 includes packstone horizons rich in oysters and oyster debris (locality 429).



Figure 3.48 - Field photograph of a hiatus horizon within the biomicrite facies of the Cretaceous Transgressive Limestones (locality 65, by Theodoraki village). Coarse sparry calcite-filled burrows extend down from the hiatus surface, which in many other localities is marked by a horizon of pink marl.



Figure 3.49 - Field photograph of a bioclastic packstone horizon within the Cretaceous Transgressive Limestones (locality 67, northeast of Theodoraki village). The packstone contains whole and fractured bivalves, gastropods, and the matrix is often calc-arenitic.

All the Cretaceous shallow-water facies display an unusual patchy/nodular texture. The patches are highly irregular in shape, reaching up to 0.5 m in lateral extent, and cross-cut bedding plane boundaries and facies types. The patches are characterised by coarse, recrystallised, dark-grey sparite, which stands proud on weathered surfaces (Figure 3.50). This texture is here interpreted to be diagenetic in origin, formed where recrystallisation has nucleated and spread to form sparite patches or nodules. It is not clear why diagenesis should nucleate in this fashion and no evidence was seen to indicate the nuclei responsible.

3.9.4 - *New Key Localities*

As discussed in chapter 2 (sections 2.2.3 and 2.2.7) many thrust-bound packages of limestone within the central Païkon Massif have been reinterpreted during this work as imbricate slices of Cretaceous Transgressive Limestone, which were tectonically incorporated into underlying stratigraphic units, namely the Païkon Volcanic Group (i.e. the Livadia and Kastaneri Formations). For example, the limestones which crop out in the vicinity of Gola Tchouka (Calcaires de Gola Tchouka of Mercier, 1968). These carbonates closely resemble the Cretaceous Transgressive Limestones, although they are considerably more deformed, in that they comprise white/pink recrystallised limestones, lesser marble breccias, minor, pink, chloritic schists and calcarenites (Figures 3.46 and 3.51). The white marbles commonly form interbeds between 0.5 and 1.5 m thick, which are variably pink and micritic along bedding horizons. Chloritic and buff schists are often present as thin (1 to 5 cm) horizons between neighbouring marble beds. Internally, the marbles are clean, white and highly recrystallised into medium-grained calcite. In certain beds, patches of coarser, recrystallised calcite are interpreted here as vestiges of a faunal assemblage which may have included foraminifera, gastropods, bivalves and perhaps corals (Figure 3.52). Such inferences are based on the present size, shape and structure of sparry calcite patches. Interbedded with the white marble beds are thick (up to 1 m) horizons of strained intraformational breccia (Figure 3.53). Clasts within this marble



Figure 3.50 - Coarse, sparry, diagenetic patches within the Cretaceous Transgressive Limestones. The upper photograph is a field photograph which shows the diagenetic recrystallisation crossing bedding surfaces. The lower photomicrograph is of a thin section and shows the crystallisation front of coarse calcite spar within a finer micritic matrix.

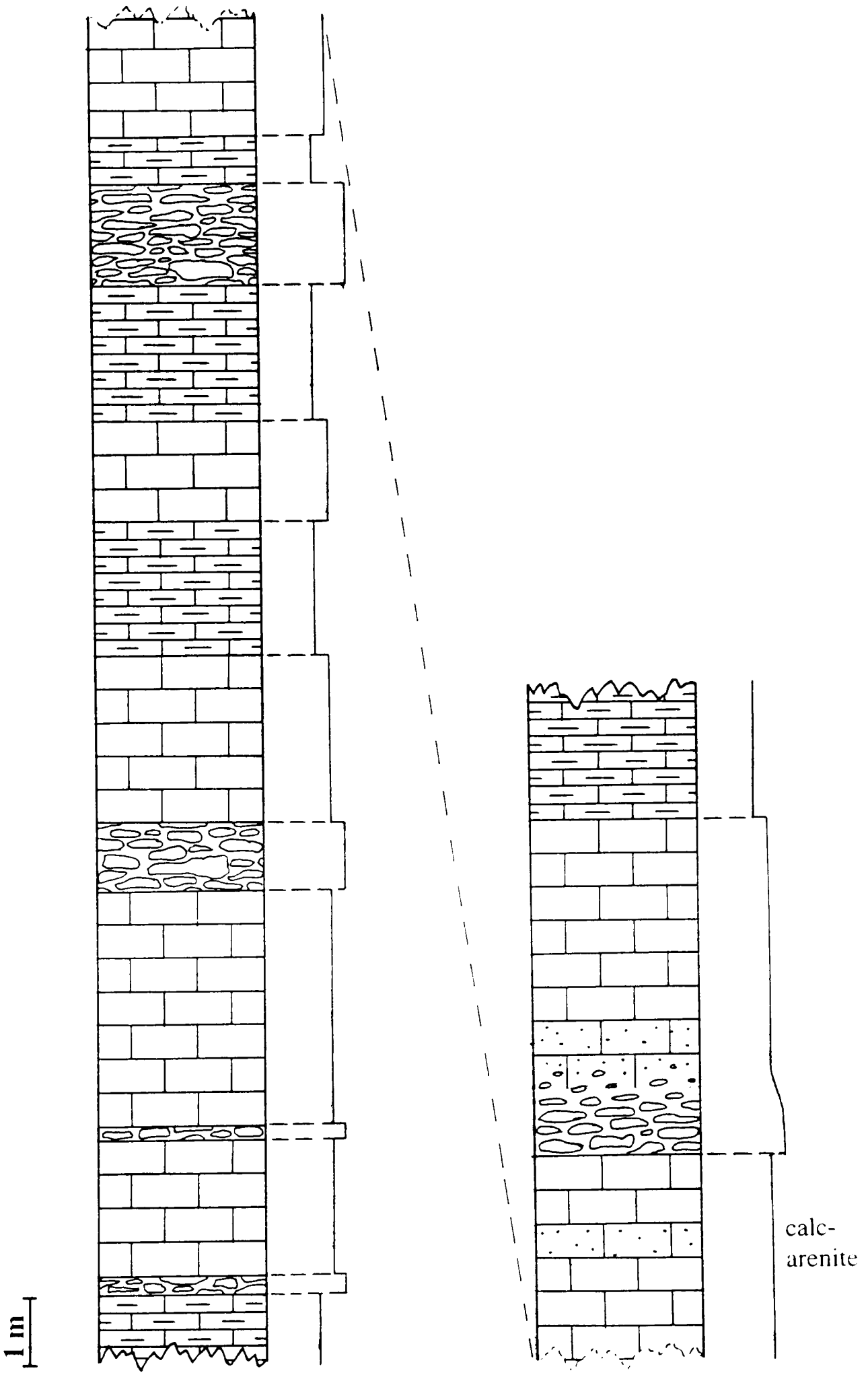


Figure 3.51 - Thrust imbricate of Cretaceous Transgressive Limestone from locality 421 (by Gola Tchouka, 1650 m). The limestones are completely recrystallised and contain no identifiable fauna. Strained breccia horizons are common and calc-arenites occur locally. For lithological descriptions see Figure 3.46.

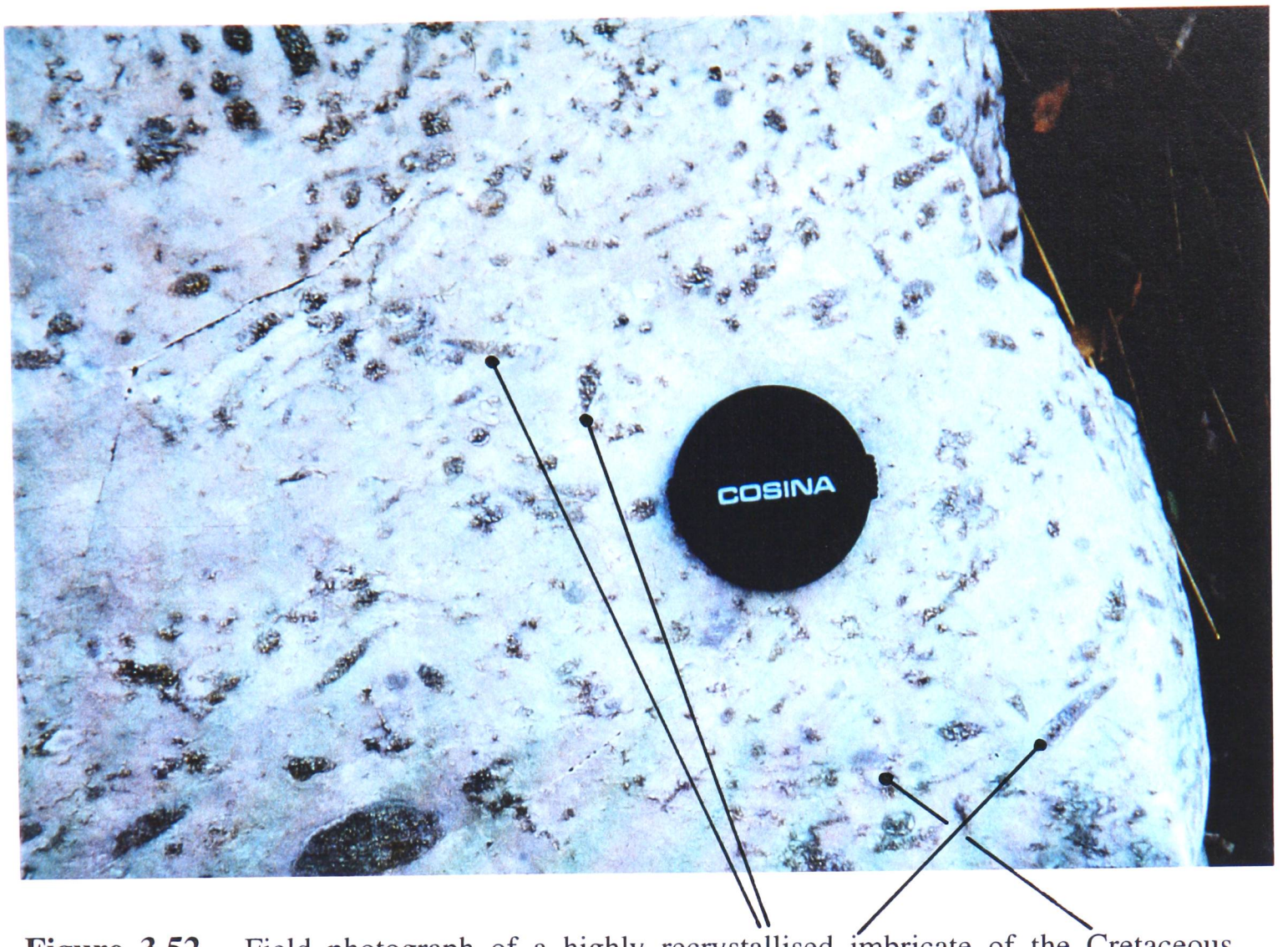


Figure 3.52 - Field photograph of a highly recrystallised imbricate of the Cretaceous Transgressive Limestones containing vestiges of gastropods (abundant) and bivalves (scarce). Locality 413, north of Khromni village).

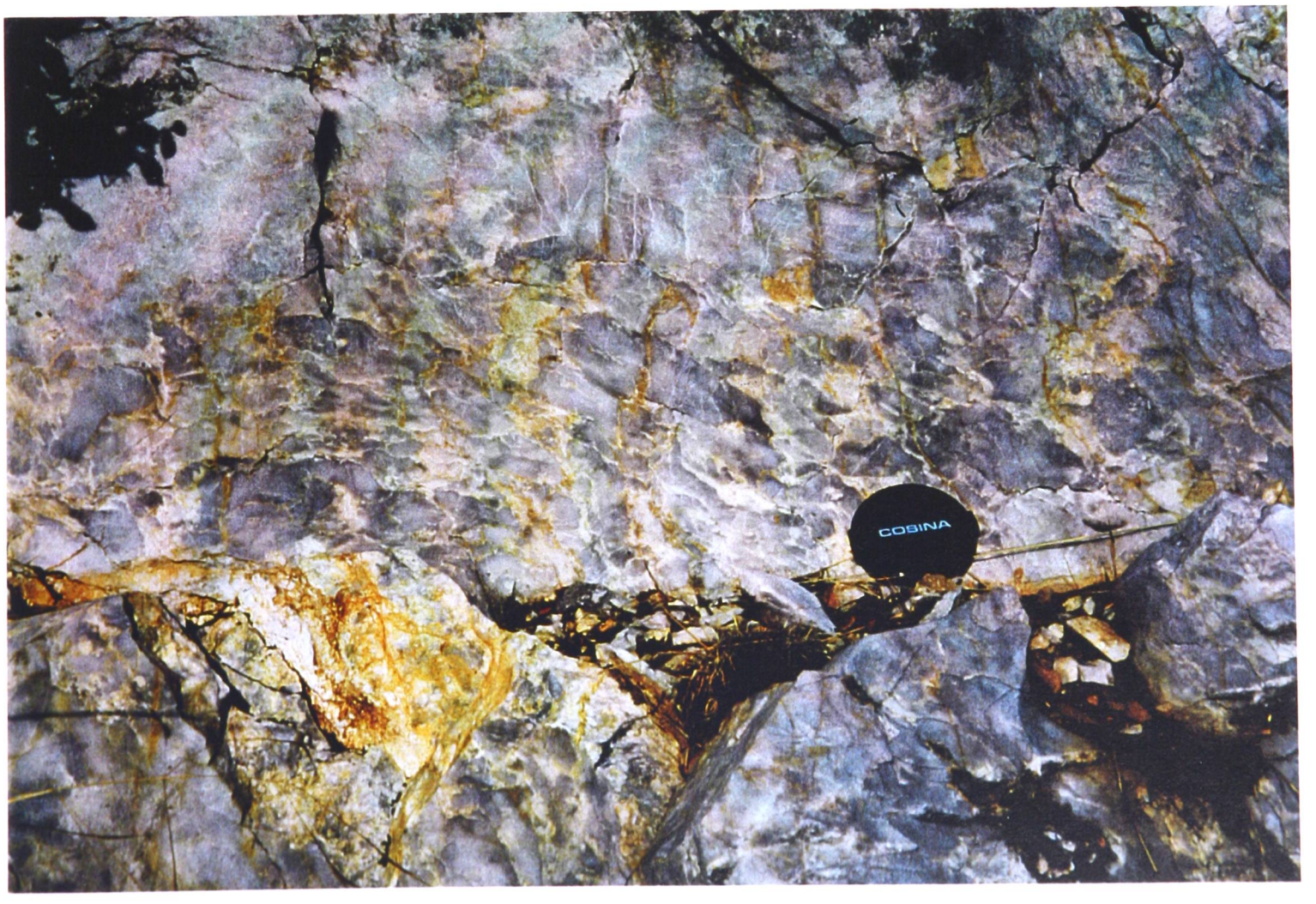


Figure 3.53 - Field photograph of a strained intraformational breccia within a thrust-imbricate of the Cretaceous Transgressive Limestones (locality 421, by Mount Gola Tchouka, central Païkon Massif).

breccia vary markedly in size (0.3-10.0 cm in diameter) and have been flattened subsequent to their deposition.

The white marbles with faunal vestiges, pink calc-schists horizons and intraformational breccias can be equated with the biomicrites and/or biomicritic packstones, bioturbated hiatus horizons and breccias of the Cretaceous Transgressive Limestones, respectively. This similarity in facies is supported by biostratigraphic data from directly along strike of Gola Tchouka, implying that the Gropi Formation (or the Calcaires de Gola Tchouka) are of Cretaceous age (see section 2.2.3).

3.9.5- *Discussion*

During the course of this work it was found that the Cretaceous Transgressive Limestones are much more extensive in the Païkon Massif than previously recognised. Besides cropping out all along the western side of the study area, the Cretaceous Transgressive Limestones also flank the massif to the east, and form conspicuous imbricate slices throughout internal parts of the Païkon Massif (see Figure 4.33).

The transgressive, depositional contact between the Ghrammos Formation and the Cretaceous Transgressive Limestones marks a switch from continental red-bed fluvial sedimentation (section 3.8.6) to fully marine deposition. Initial calcarenitic deposits record continued clastic sedimentation within a largely carbonate system in a marginal shelf setting (Sellwood, 1986). This died out up-section over a short interval, and carbonate sedimentation dominated throughout the Middle Cretaceous.

The abundance of fine-grained micrites containing a faunal assemblage of gastropods, *Miliolidae*, benthic foraminifera and algae indicate that the biopelmicrite facies may have formed in a restricted shelf or lagoonal setting (Wilson, 1975). The presence of dolomitic fenestrae and putrid concretions support this hypothesis (Sellwood, 1986). The overlying biomicrites/sparites are more akin to a marine shelf (Sellwood, 1986) or

open platform (Wilson, 1975; Figure 3.54), as indicated by their more diverse yet robust fauna of bivalves, rudists, benthic foraminifera and gastropods, and their abundance of shell lags and calcarenites, which are interpreted as storm deposits. Oyster and rudist packstones are almost certainly marginal patch reef build-ups which formed periodically along the shallow shelf or platform, and which were subsequently disrupted by faulting. Limited oolitic carbonates indicate agitated or turbulent shallow-water conditions and were probably generated as back-reef deposits (James & Ginsburgh, 1979) or platform margin sands (Wilson, 1975; Figure 3.54). Brecciated packstone facies are postulated to represent deposition in an unstable fore-reef setting (Figure 3.54; Wilson, 1975; James, 1983a).

The pink, marly beds record times of increased clastic input, possibly from a nearby landmass. This resulted in the carbonate facies being swamped by fine, terrigenous material. A period of non-deposition, marked by strong bioturbation of the subsurface material and local ferruginous crusts, tended to follow such swamping events. Reinstigation of the carbonate platform was initiated by the deposition of oolite-rich deposits, suggesting agitated, possibly littoral conditions, as observed in the present day Bahama Banks (Scoffin, 1987). This then passed up into biomicritic and/or nodular micritic facies as the platform re-established itself. Hiatuses in carbonate deposition were periodic and could reflect an increase in clastic input due to: 1. Pulsed terrigenous input; 2. Pulsed tectonic uplift and subsidence or 3. Eustatically-induced transgression and regression. A rapid transition from one shallow-marine carbonate facies to the other throughout the Cretaceous Transgressive Limestones, without any clastic influence, suggests that option 1 is unlikely.

Similar, shallow, carbonate shelf deposits, dominated by mollusc-rich skeletal sands and coquinas, oolitic and peloidal limestones and intervening patch reefs have been described from the northwest Yucatan Shelf in the Gulf of Mexico (Logan *et al.*, 1969; Sellwood, 1986).

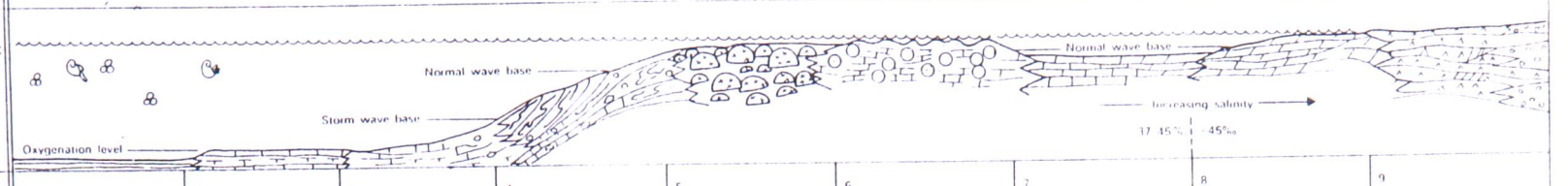
DIAGRAMMATIC CROSS SECTION									
FACIES NUMBER	1	2	3	4	5	6	7	8	9
FACIES AND GENERAL ENVIRONMENT	Basin (euxinic or evaporitic) (a) Fine clastics (b) Carbonates (c) Evaporites	Open marine neritic (a) Carbonates (b) Shale	Toe of slope carbonates	Foreslope (a) Bedded lime grained sediments with slumps (b) Foreset debris and lime sands (c) Lime mud masses	Organic build up (reef) (a) Boundstone (b) Encrusting masses (c) Bafflestone	Sands on edge of platform (a) Shoal lime sands (b) Islands with dune sands	Open platform (a) Lime sand bodies (b) Wackestone mudstone areas bioherms (c) Areas of terrigenous clastics	Restricted platform (a) Bioclastic wackestone lagoons and bays (b) Litho bioclastic sand in tidal channels (c) Lime mud on tidal flats (d) Fine grained terrigenous clastic interbeds	Platform evaporites (a) Nodular anhydrite and dolomite on salt flats (b) Laminated evaporites in desiccated ponds
LITHOLOGY	Dark shale or silt: thin limestones (starved basin) Evaporites fill basin if dessiccation occurs	Very fossiliferous limestone with marl interbeds	Fine grained limestone, locally cherty	Variable depending upon water turbulence: upslope sedimentary breccias and lime sands	Massive limestone dolomite	Calcarenitic oolitic lime sand or dolomite	Variable carbonates and terrigenous clastics	Often dolomite and dolomitic limestone.	Irregularly laminated dolomite and anhydrite locally may grade into red beds
COLOUR	Dark brown, black and red	Grey, green, red, brown	Dark to light	Dark to light	Light	Light	Dark to light	Light	Red, yellow, brown
GRAIN TYPE AND DEPOSITIONAL TEXTURE	Lime mudstones, fine calcisiltites	Bioclastic and whole fossil wackestones, some calcisiltites	Dominantly lime mudstone with some calcisiltites	Limesilt and bioclastic wackestone, packstone lithoclasts.	Boundstones and pockets of grainstone packstones	Grainstones well sorted, rounded	Variable textures in grainstone and mudstone Bioturbation	Clotted pelleted mudstone and grainstone, laminated mudstone, coarser wacke stones in channels	
BEDDING AND SEDIMENTARY STRUCTURES	Very even lamination on mm scale Rhythmic bedding, occasional ripple cross lamination	Bioturbated, thin to medium bedded with nodular layers	Minor lamination Often massive beds, lenses of graded sediment. Lithoclasts and exotic blocks.	Slumps, foreset bedding slope build ups, exotic blocks	Massive organic structure or open framework with roofed cavities Injection dykes Sometimes stromatactis	Medium to large scale cross bedding	Intense bioturbation	Birdseye, stromatolites, fine laminations, dolomite crusts Cross bedded sand in channels	Anhydrite after gypsum, nodular rosettes, chicken wire and blades, irregular lamination, caliche
TERRIGENOUS CLASTIC COMPONENT	Quartz silt and shale, fine grained siltstone, often cherty	Quartz silt and shale in well segregated beds	Some shales, silt and fine grained sandstone	Some shales and silts	None	Local quartz sand	Terrigenous and calcareous beds well segregated	Interbedded terrigenous and calcareous beds possible.	Aeolianites and terrigenous interbeds may be important
BIOTA	Planktonic and nektonic only Occasional mass mortality deposits	Diverse. Shelly fauna and trace fossils represent both infauna and epifauna	Bioclastic debris derived mostly from upslope	Colonies of whole fossil organisms and bioclastic debris	Major frame building colonies and communities associated with them	Few indigenous organisms Specialised community Mostly abraded shell debris from other platform environments	Fauna dominated by more tolerant groups (e.g. bivalves gastropods, sponges, forams some algae) less tolerant groups (e.g. cephalopods brachiopods and echinoderms) often restricted	Limited fauna Mostly grazing gastropods algae and some forams (e.g. miliolids) and ostracodes	Stromatolitic algae almost the only indigenous biota

Figure 3.54 - Table showing the standard facies belts across a carbonate platform and margin (after Wilson, 1975).(see following page)



Figure 3.55 - Field photograph of the top of the Cretaceous platform, which is marked by a red ferruginous crust (locality 202, by Ghriva village).

3.9.6- *Transition to Deep-water Sedimentation*

At the very top of the Cretaceous shallow-water sequence, Lower Turonian platform carbonates pass over a short interval (<5 m) into a thin unit of Buff Pelagic Carbonates (section 3.10), which in turn give way to the deep-water sediments of the Tchouka Flysch (section 3.11). The transition from neritic to pelagic deposition on the western side of the Païkon Massif is described in detail by Sharp (1995), who identified a transitional unit, the "*Bioturbated and Iron-encrusted facies*", which is developed locally. This unit reaches up to 10 m thick and comprises micritised lithoclasts and bioclasts set in a heavily bioturbated wackestone matrix. This unit is locally topped by ferruginous intraformational conglomerates, which grade into a relatively thick iron-stained crust horizon before giving way to wholly pelagic deposition. In many areas, however, this transitional wackestone unit (unit 2 of Sharp, 1995) is absent and the Lower Turonian neritic carbonates (unit 1 of Sharp, 1995) pass directly into the overlying Buff Pelagic Carbonate facies (unit 3 of Sharp, 1995). Where this occurs, units 1 and 3 are always separated by a thin 0.5-5.0 cm ferruginous crust or hardpan horizon, as described in section 3.10.

Nowhere on the eastern side of the Païkon Massif was the transitional wackestone unit (unit 2) encountered, and neritic carbonates always proceed directly to pelagic deposition by way of the ubiquitous ferruginous crust surface (e.g. just west of Ghriva, Figure 3.55).

3.10 - BUFF PELAGIC CARBONATES

3.10.1 - *Introduction*

The Buff Pelagic Carbonates form a distinctive, but relatively limited, unit exposed on both the western and eastern margins of the study area, where the stratigraphically highest units of the study area are tectonically overlain by rocks of the Meglenitsa

(Almopias subzone) and Guevgueli (Peonias subzone) ophiolites respectively. The unit was first described by Sharp (1995) for the western side of the Païkon Massif only (Figure 3.56), and it was not until this study that similar carbonates were also discovered on the eastern margin of the Païkon Massif. The best exposure of the Buff Pelagic Carbonates can be found directly west of Ghriva village (Figure 3.57) and due south of this between Ghriva and Pentalofos.

3.10.2 - *Transitional Ferruginous Crust Horizon*

As described in section 3.9.5, the uppermost platform carbonates of the Cretaceous Transgressive Limestones are always separated from the Buff Pelagic Carbonates by a thin (up to 5 cm) iron-encrusted surface. This crust is characterised by alternating layers of haematite-rich, laminated hardpans and calcite cements, pisolitic and rhizolithic hardpans and a network of acicular calcite crystals, all punctuated by pseudomorphic rhombic calcite and authigenic albite (Sharp, 1995; this work). In eastern exposures this hardpan horizon reaches a maximum thickness of only 1.0 cm (Figure 3.55) and is nowhere as thick as that observed in the west.

3.10.3 - *Carbonate-Clastic Facies*

Around Ghriva, transition into entirely pelagic deposition is gradual over an interval of approximately 20-50 cm. The pelagic carbonates become progressively more pink in colour and contain ever increasing amounts of buff, muddy laminations up-section. The muddy partitions are usually 2-8 mm thick and become progressively closer-spaced as the total mud content increases. The muddy partitions are aligned parallel to the stylolitic bedding surfaces of the pelagic carbonates and are variably rich in red-stained, siliceous, ferruginous material (Figure 3.58).



Figure 3.56 - Field photograph of the contact between the Cretaceous Transgressive Limestones and the Buff Pelagic Carbonate on the western side of the Païkon Massif (locality 71, northeast of Theodoraki village).



Figure 3.57 - Field photograph of the conformable contact between the Cretaceous Transgressive Limestones and the Buff Pelagic Carbonates on the eastern side of the Païkon Massif (locality 211, west of Ghriva village).

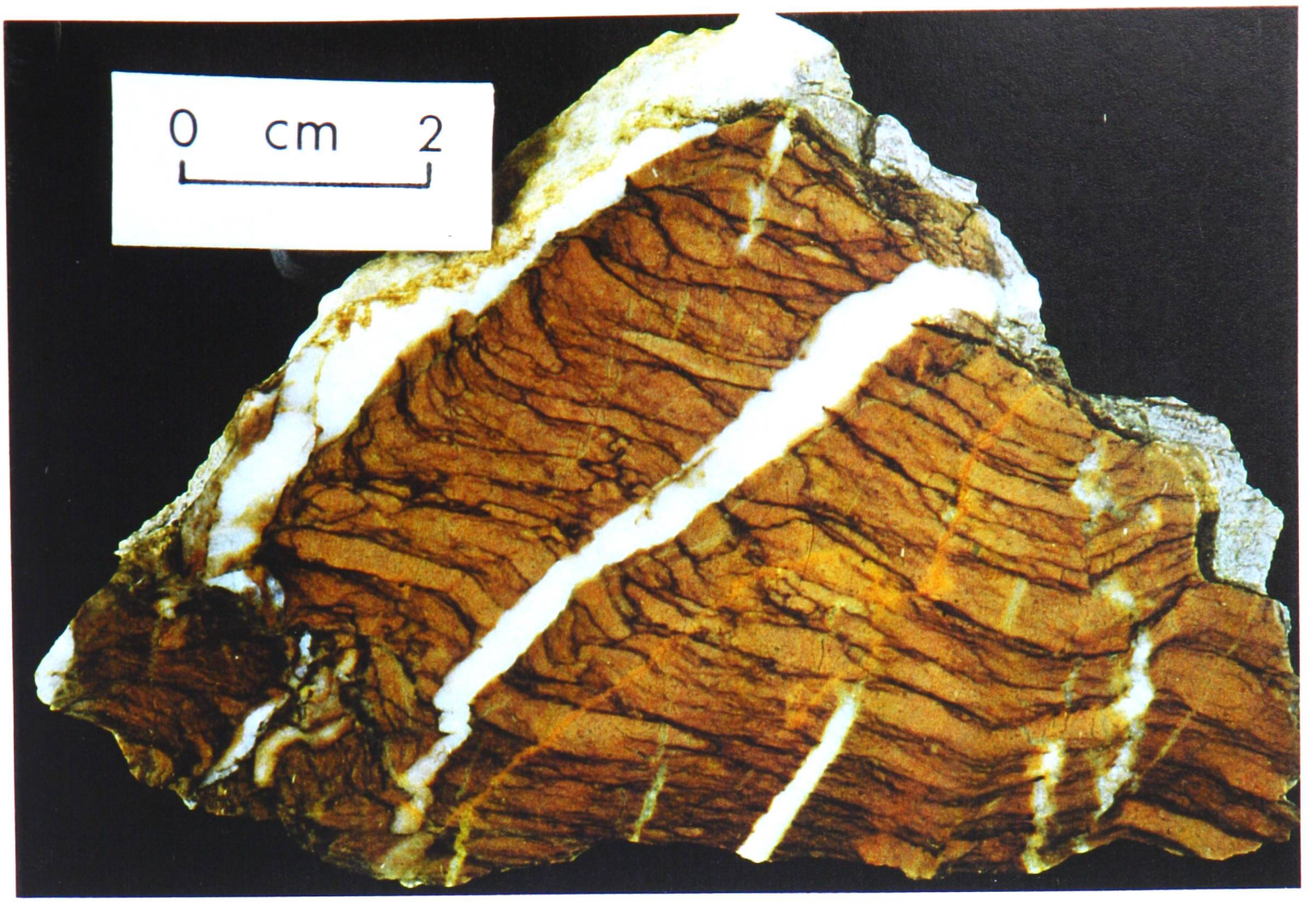


Figure 3.58 - Photograph of a hand specimen of the Buff Pelagic Carbonates from locality 210 (west of Ghriva village). The carbonates are folded and finely-bedded and adjacent beds are commonly separated by buff, muddy horizons (dark layers). Calcite veins intrude the carbonates parallel to fold axial planes (white layers).

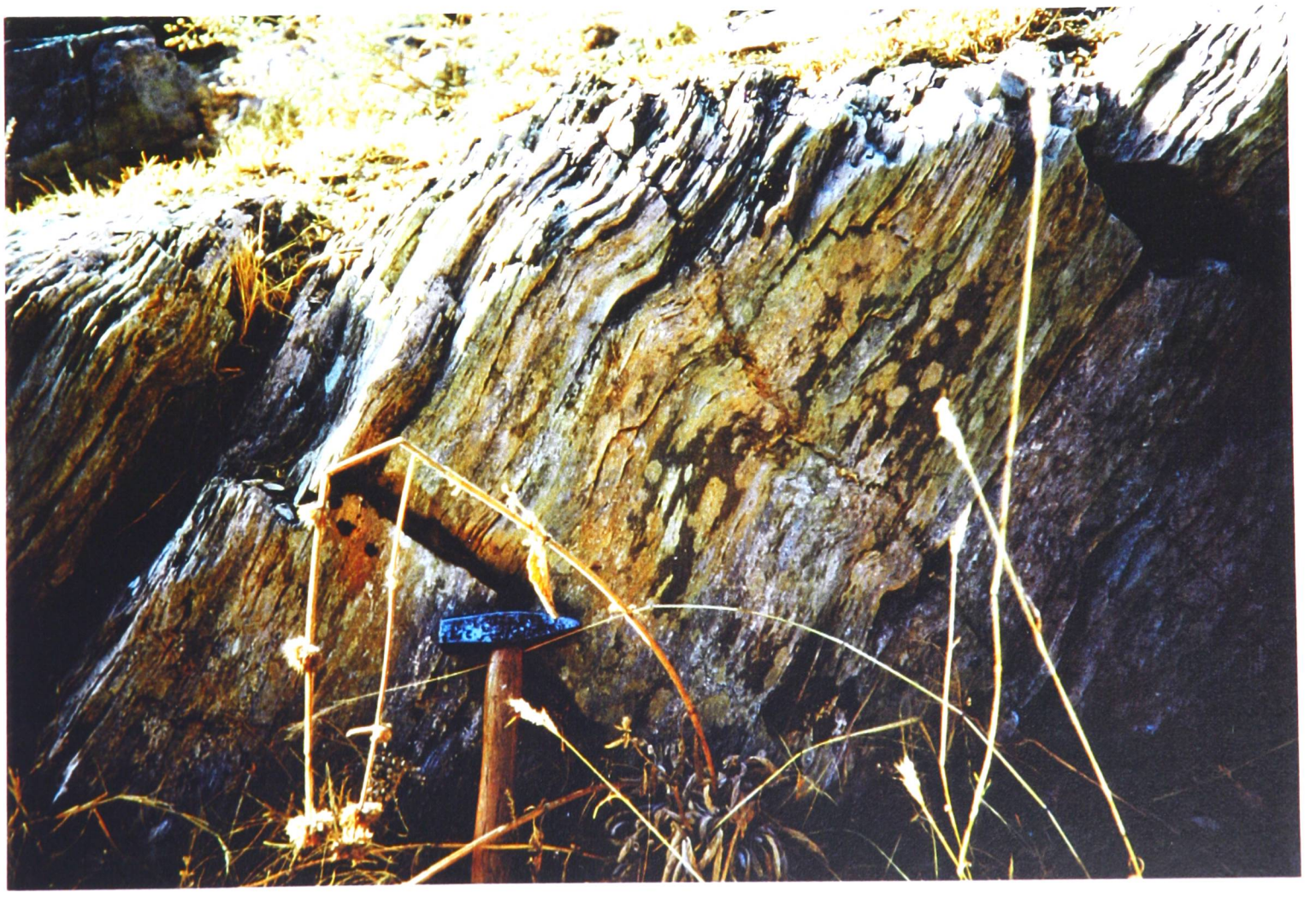


Figure 3.59 - Field photograph of the thinly-bedded Buff Pelagic Carbonate unit from locality 69 (northeast of Theodoraki village). The carbonates are folded by Tertiary kink folds (see chapter 4).

The pelagic carbonates themselves are very fine-grained and micritic. They are very finely-laminated (Figures 3.58 and 3.59) and contain pelagic foraminifera such as *Globotruncana sp., Calcisphaerulae* and *Globigerinids.* This is identical to fauna reported from western Païkon Massif (Sharp, 1995), only a little less diverse, probably owing to the effects of D3 deformation along the Païkon-Guevgueli margin (chapter 4).

Although the Buff Pelagic Carbonates lie above the platform carbonates of the Cretaceous Transgressive Limestones in most areas, Mercier (1968) noted the presence of a shallow-water Maastrichtian fauna at a few localities and so it is possible that shallow-water platformal highs persisted locally until the onset of Tertiary compression (see chapter 4.5 for further discussion).

3.10.4 - *Discussion*

Field studies carried out during this work have revealed for the first time that the Campanian-Maastrichtian pelagic carbonates known to flank the western Païkon Massif also occur in the easternmost Païkon Massif. An iron-rich hardpan surface succeeds the Lower Turonian neritic carbonate succession and is interpreted to indicate that a period of subaerial emersion occurred prior to rapid subsidence and the onset of pelagic sedimentation (Sharp, 1995). The more comprehensive faunal assemblage identified in the west has been interpreted to indicate an Upper Cretaceous age for the Buff Pelagic Carbonates (Mercier, 1968; Sharp, 1995) and it is postulated here that the similar carbonates exposed in the east are of the same age.

3.11 - TCHOUKA FLYSCH

3.11.1 - *Introduction*

Excellent examples of the Tchouka Flysch are exposed on the western flank of the Païkon Massif at Theodoraki, Nerostoma and in the Tchouka region, after which this unit has been named (Sharp & Robertson, 1992). All along the western margin of the Païkon Massif, thrust faulting and chevron/box folding (chapter 4) have repeated, cut-out and disrupted the Tchouka Flysch and as a result it is now of indeterminable thickness and is strongly deformed. Such deformation also precluded preservation of a complete transect through the flysch-type succession, from base to top.

The contact between the Buff Pelagic Carbonates (chapter 3.10) and the Tchouka Flysch is gradational, marked by a progressive increase in terrigenous clastic material over an interval of 0.5-1.5 m. Due to the contrasting competencies of these two units, however, shearing and reverse faulting often disrupt this contact. The upper contact of the flysch is always faulted, with the clastics being tectonically overlain by either the Cretaceous Transgressive Limestones, the Buff Pelagic Carbonates, the flysch itself or, in the extreme west and east by the basic volcanic rocks of the Almopias Meglenitsa Ophiolite or the Peonias Guevgueli Ophiolite, respectively (Figures 4.22, 4.47 and 3.65).

3.11.2 - *Sedimentary Facies*

The Tchouka Flysch comprises a deformed sequence of fine- to coarse-grained arenites, litharenites, siltstones and micaceous mudstones interbedded with minor detrital carbonates and radiolarian cherts (Figures 3.60 and 3.61). The sequence is moderately consolidated and is buff, rust-brown, red and locally green in colour. The sediments are interbedded on a millimetre to centimetre scale, with some thicker beds



Figure 3.60 - Field photograph of the Tchouka Flysch (locality 70, northeast of Theodoraki village). The flysch comprises both arenaceous and argillaceous rocks interbedded with radiolarian-bearing ribbon chert.



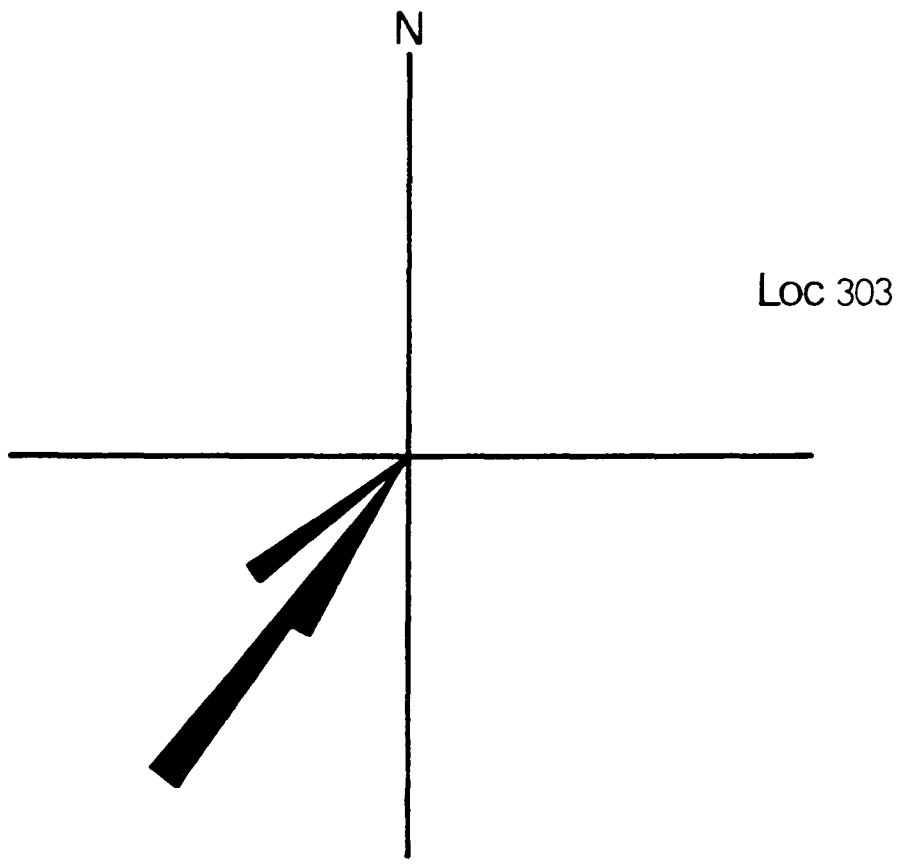
Figure 3.61 - Field photograph of bedded radiolarian cherts interbedded with the fine-grained red mudstones of the Tchouka Flysch (locality 70, northeast of Theodoraki village).

of relatively coarse litharenite reaching up to 10 cm. They are texturally immature and consist of poorly sorted, sub-angular to sub-rounded clasts of quartz, lithic fragments and rare marbles set in a ferruginous matrix and/or calcareous cement. In the west, relatively undeformed sections contain many arenitic beds which have sharp, possibly erosional, basal contacts and grade upwards into overlying siltstones and mudstones. Small-scale planar cross-bedding was also observed in these areas, suggesting a palaeocurrent direction to the present-day southwest or west (Figure 3.62; this is based on the results of a very small data set only from the western Païkon Massif).

Figure 3.63 and 6.64 are photomicrographs of arenitic horizons within the Tchouka Flysch. The dominant clastic constituents include microcrystalline quartz, strained quartz, chloritic schist, limestone, marble, quartz porphyry, altered volcanics (both basic and acidic) and rare pitted feldspars. Metamorphic quartz clasts and total lithic fragments are about equally represented, while limestone, marble and feldspar clasts are relatively scarce (Figure 3.64).

3.11.3 - *New Key Localities*

The most important new discovery of the Tchouka Flysch lies directly to the west of Ghriva village on the eastern side of the Païkon Massif. It was previously identified as being part of the Guevgueli Ophiolite, which tectonically overlies the Païkon lithologies to the east (Bebien, 1982). The eastern outcrops are identical in composition, facies and provenance to those described from the west (Figures 3.60, 3.61 and 3.56), but have experienced significantly more deformation. The flysch is often highly cleaved and disrupted by duplex structures, and preserves none of the graded or cross-bedded horizons seen in its western counterparts. Ribbon chert horizons are occasionally preserved as intact units but radiolarian tests extracted during this work are wholly recrystallised (T. Danelian, pers. comm., 1997).



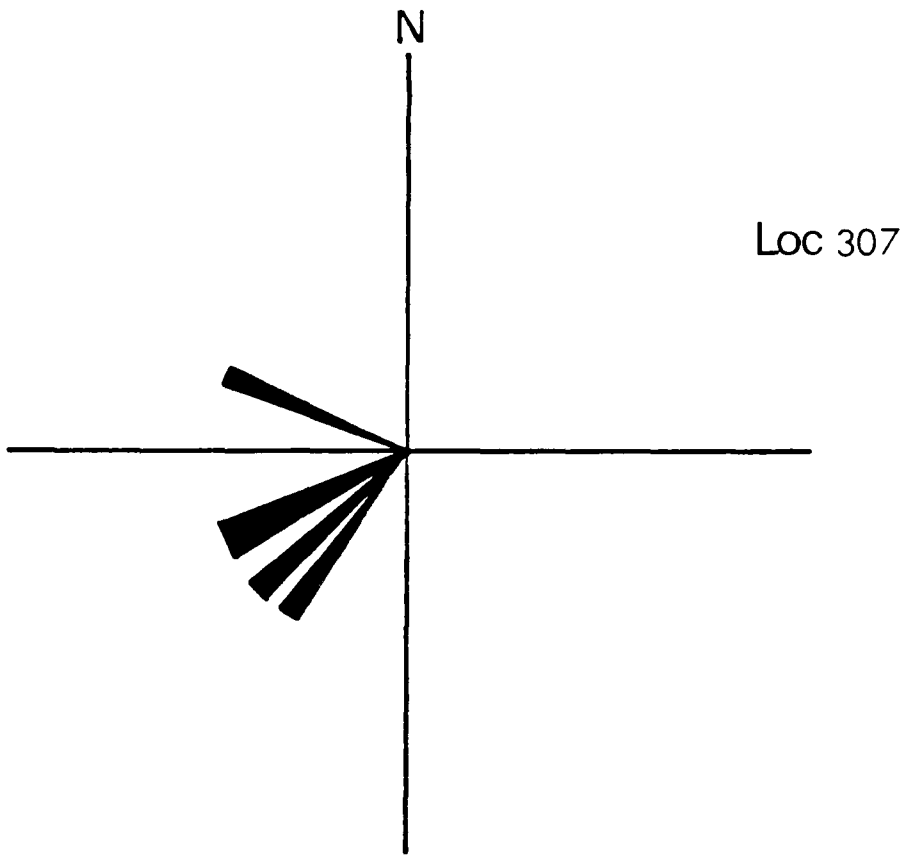


Figure 3.62 - Palaeocurrent data from the Tchouka Flysch (south of Theodoraki village). The limited data (9 total) suggest southwest- to west-directed palaeocurrents and thus sediments derived from the northeast to east.

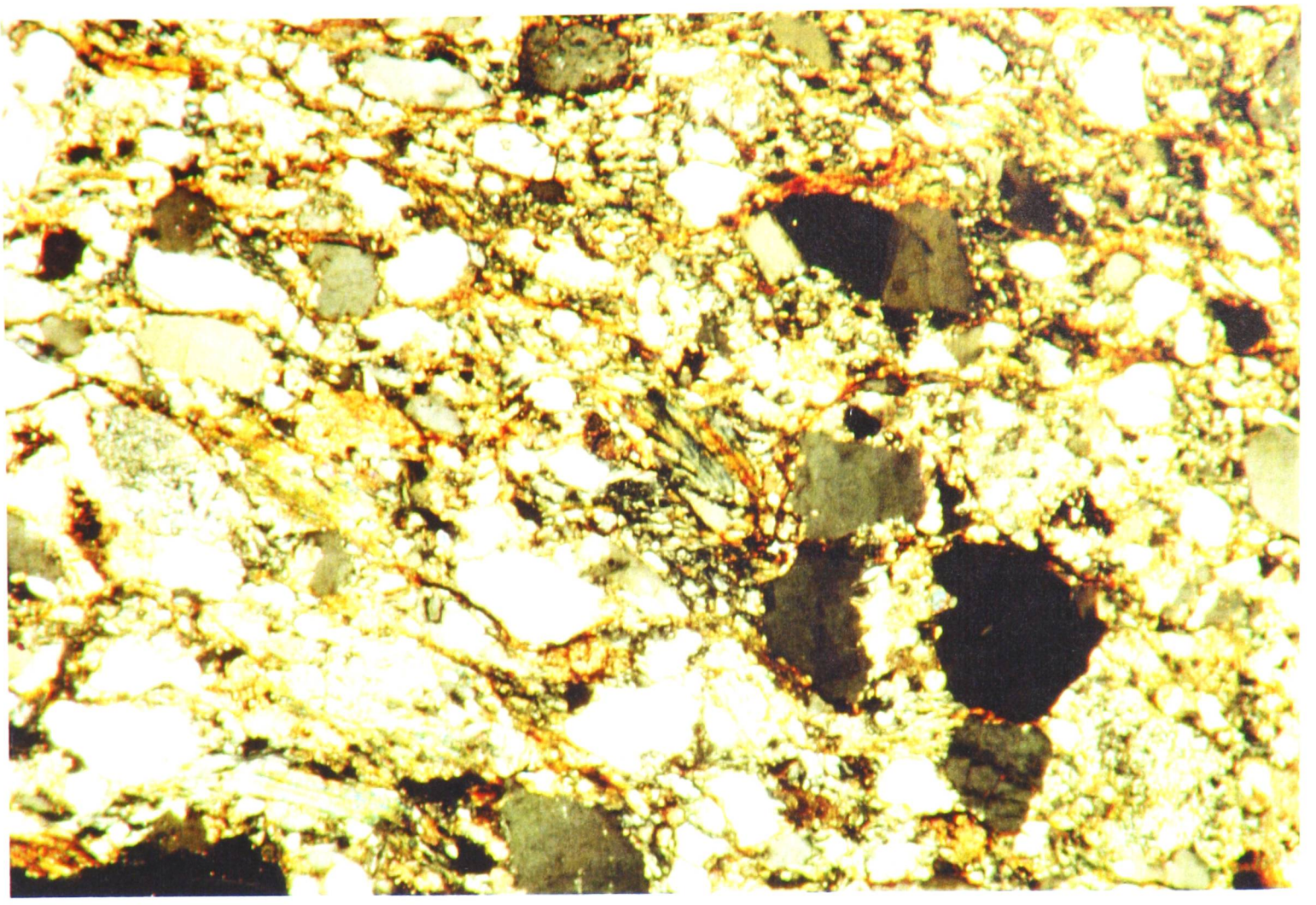


Figure 3.63 - Photomicrograph of the Tchouka Flysch from the western side of the Païkon Massif (near Thodoraki village). The poorly-sorted flysch is rich in clasts of quartz (bright clasts in picture), carbonate and lithoclasts of altered basalt, quartz porphyry and cloritic schist set in a fine-grained quartz- and clay-rich matrix. Magnification x10.

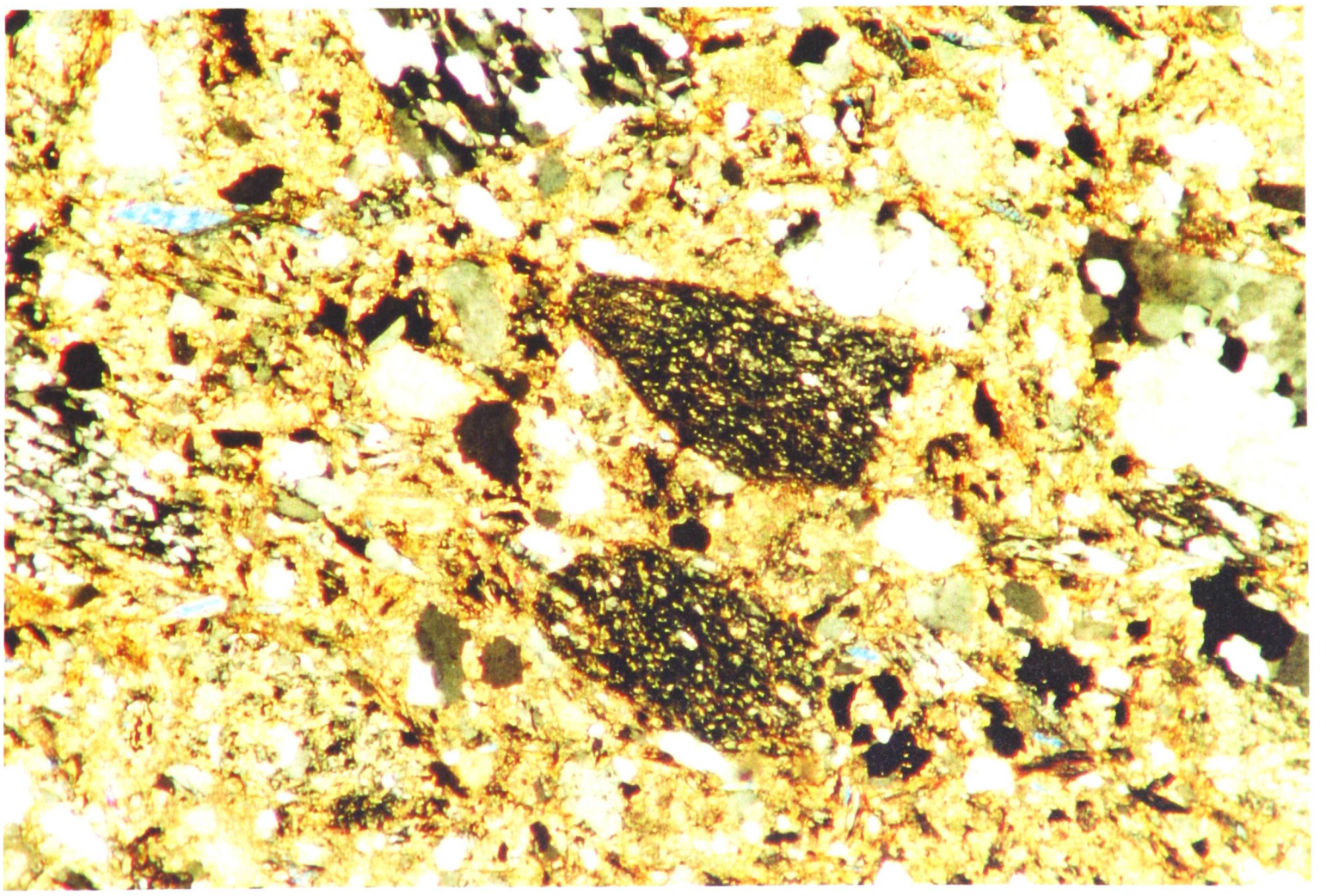


Figure 3.64 - Photomicrograph of the Tchouka Flysch from the eastern side of the Païkon Massif (near Ghriva village). The flysch in this area is very similar to that seen on the western side of the study area and is correspondingly rich in clasts of strained quartz and lithic fragments. Magnification x10.

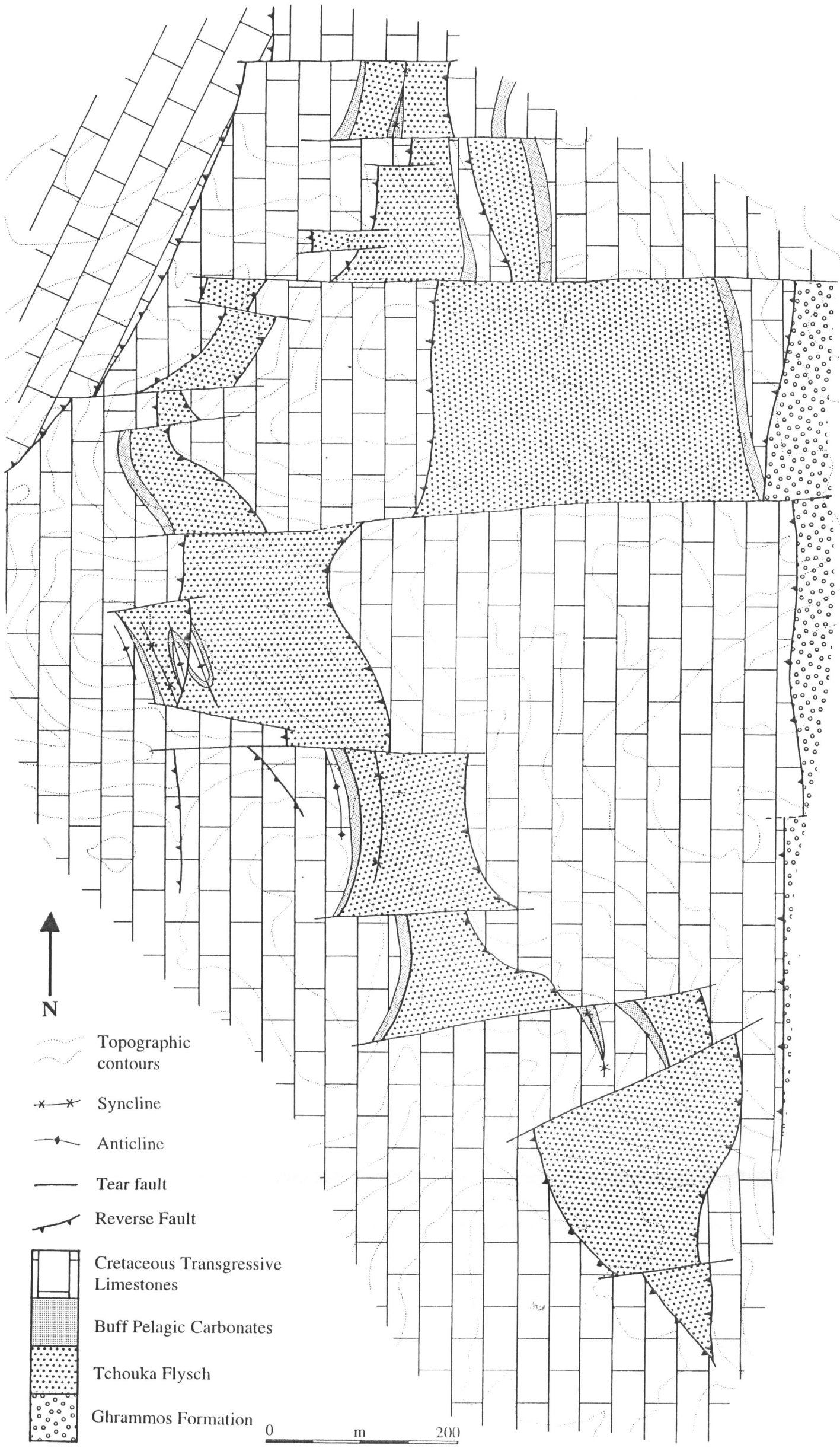


Figure 3.65 - Geological map of the area 2km northeast of Theodoraki village (western Païkon Massif). The Creatceous Transgressive Limestones dominate but are interrupted by upfolded and upthrusted bands of Buff Pelagic Carbonate and Tchouka Flysch. Thrust and fold propagation is towards the east and is off-set by E-W-trending tear faults.

Examples of the Tchouka Flysch have also been found some distance east of Theodoraki village (western Païkon Massif), where they have been up-thrust by Tertiary faulting. In this area the flysch is tectonically overlain by neritic carbonates of the Cretaceous Transgressive Formation (Figure 3.65) and not by Maastrichtian reworked limestones as suggested by Mercier (1968).

3.11.4 - *Biostratigraphy*

Sharp (1995) inferred a Turonian to Maastrichtian age for the Tchouka Flysch based on the identification of the species *Pseudodictymitra pseudomacrocephala* (P. De Wever pers. comm. to I. Sharp, 1992). Further radiolarians extracted from samples on both western and eastern sides of the Païkon Massif (this work) are presently being studied at the University of Illinois by Prof. H. S. Ling, but the results are not yet available. The results of this work will be discussed elsewhere in due course.

3.11.5 - *Discussion*

The finely interbedded arenites and mudstones of the Tchouka Flysch are interpreted as deep-water base-of-slope deposits. The deep-water environment is implied by the presence of radiolarian-bearing cherts within the dominantly thin-bedded silt succession and the thin-bedded, graded sand and silt horizons. The centimetre-scale rhythmic fining-up units of coarse, erosive-based arenites, cross-bedded arenites, siltstones and parallel-bedded mudstones are characteristic of medium-grained turbidity currents (Bouma, 1962; Stow, 1986; Pickering *et al.*, 1989). In turn, the graded coarse sands, cross-bedded sands, siltstones and parallel-bedded mudstones may represent T_a, T_c, T_d and T_e divisions of the classic Bouma sequence (Bouma, 1962). Radiolarian cherts are likely to have accumulated during time of low terrigenous clastic input.

The Tchouka Flysch deposits are closely followed by significant compressional deformation of Tertiary age and thus are likely to have formed at the onset of collision as foreland basin-type deposits. The Uppermost Cretaceous flysch sediments of the Pelagonian zone are also interpreted in this way (Sharp, 1995).

Petrological study and point-count data suggest that the Tchouka Flysch sediments may have been sourced from the Païkon Massif (e.g. Kastaneri and Ghrammos Formations; quartz porphyry, deformed volcanics, metamorphic quartz), which is tentatively supported by the limited SW to W-directed palaeocurrent data from the Tchouka Flysch in the west of the Païkon Massif, and from an ophiolitic source (basalt clasts and radiolarian chert).

3.12 - SUMMARY AND REGIONAL CORRELATIONS

One of the most important conclusions of this chapter, derived from both field and laboratory observations, is the recognition that identical stratigraphic successions exist on **both** sides of the anticlinal Païkon Massif, from the Gandatch Formation to the Tchouka Flysch. This refutes the original geotectonic model for the area, as proposed by Mercier (1968), which suggested that the Païkon Massif comprises two distinct but tectonically juxtaposed tectonostratigraphic terranes, namely the Païkon subzone and the Prepeonian subzone (chapter 1). The Païkon Massif can therefore be seen simply as a single tectonostratigraphic unit which was folded into an anticlinal structure during early Tertiary deformation (i.e. folded subsequent to the deposition/formation of all principal stratigraphic units).

The Païkon Massif can be sub-divided into two conformable megasequences, the lower Païkon megasequence and the upper Païkon megasequence, which are separated by a significant structural and metamorphic discontinuity of pre-Kimmeridgian age (chapters 2 & 4). Accurate ages for the lower Païkon megasequence (i.e. the Gandatch, Livadia and Kastaneri Formations) are lacking, constrained only by the age of the unconformably overlying Khromni Limestones. It

is likely, however, that the earliest units were deposited during the Lower to Middle Jurassic, prior to the genesis of the late-Middle to Upper Jurassic (166-146 Ma) Guevgueli Ophiolite, which flanks the Païkon Massif to the east. If this is the case then one would expect to encounter units equivalent to the Gandatch, Livadia and perhaps Kastaneri Formations on the opposing, eastern side of the Guevgueli Ophiolite. Potential counterparts exposed on the eastern side of the Guevgueli Ophiolite are discussed briefly below and then in more detail in chapter 7.

The Gandatch Formation schists and marbles form the lowest exposed stratigraphic unit of the Païkon subzone and are very likely to be underlain by poly-phase deformed continental basement, as exposed in the more northerly Voras Massif (chapter 6.3.6). The Gandatch meta-sediments have been interpreted here as lower slope apron or base-of-slope apron detrital carbonates and clastics and, given their regional situation, were most probably deposited on the west to southwest-facing continental margin of the Serbo-Macedonian continent which lies to the present day east (chapter 1; Figure 1.3). In light of this it may be possible to correlate the Païkon Gandatch Formation with the Svoula Group of the Circum-Rhodope zone, which is variably dated as Late Triassic to Middle Jurassic (Kauffmann *et al.,* 1976; Mussallam, 1991; Dimitriadis & Asvesta, 1993). The Svoula Group also records deposition in a continental slope and rise setting, was derived from the Serbo-Macedonian continental margin and is conformably overlain by the volcanic rocks of the Chortiatis Group, which are in turn overlain by the eastern Guevgueli Ophiolite (Bebien *et al.*, 1986; Dimitriadis & Asvesta, 1993).

Volcanism related to eruption of the Païkon Volcanic Group is estimated to have begun sometime in the Middle Jurassic(Mercier, 1968; Bebien, 1982; this work). The Livadia Formation is more basic in composition than the Kastaneri Formation, is finer-grained and comprises a greater proportion of primary volcanic flows. Previous workers concluded that the Livadia Formation volcanic rocks were erupted in an arc setting, based on a limited amount of data, and this hypothesis will be rigorously tested in chapter 5. A likely equivalent to these intermediate extrusives is the

Chortiatis Group of the Circum-Rhodope zone to the east (chapter 1), which is of Lower to Middle Jurassic age and has been interpreted as an arc-related volcanic succession (Mussallam, 1991). The comparison between the Livadia Formation and the Chortiatis Group will be further discussed in chapter 7.

The Kastaneri Formation records the eruption of intermediate to acidic volcanic rocks. They are generally more acidic than the Livadia Formation below and comprise a higher proportion of coarse- to medium-grained volcaniclastic rocks. The geochemical nature of the Kastaneri Formation and its environment of eruption is discussed in chapter 5.

A major structural and metamorphic discontinuity separates the pre-Kimmeridgian lower Païkon megasequence from the Kimmeridgian to Maastrichtian upper Païkon megasequence. The structural and metamorphic implications of this unconformity are discussed in detail in chapter 4.

The Khromni Limestones may have been deposited only in southerly parts of the Païkon Massif, in a shallow-marine setting characterised by rapidly changing facies and periodic clastic input. Regression then ensued and resulted in the Khromni restricted platform passing gradationally upwards through deltaic conditions into a fully continental fluvial system represented by the Ghrammos Formation. The sediments of the Ghrammos Formation were almost certainly reworked from the underlying Kastaneri Formation, and rarely the Khromni Limestones, which suggests that some kind of uplift had taken place (discussed further in chapter 4). Work carried out by Sharp (1995) and during this study suggests that the Ghrammos Formation may be a more proximal equivalent to Mavrolokkos Flysch of the central Almopias subzone. The Ghrammos Formation and the Mavrolokkos Flysch are similar in age and both are largely derived from a siliceous volcanic source (?the Kastaneri Formation of the Païkon Volcanic Group) and deposited by a fluvial system.

An Aptian/Albian marine transgression resulted in the deposition of the shallow-water Cretaceous Transgressive Limestones on top of the fluvial Ghrammos Formation. Such transgressive events are common throughout the Hellenides at this time and reflect a sea level high stand which continued throughout the Middle Cretaceous. Similar carbonate platforms have been reported from the southern Pelagonian zone (Argolis peninsula, Greece; Clift, 1990), the northern Pelagonian zone and western/central Almopias subzone (Edessa area, northern Greece; Sharp, 1995) and similar-aged continental platforms which flank the margins of the Menderes Metamorphic Massif and the Bey Daglari Unit in western Turkey (Dürr, 1976; Poisson, 1977; Collins, 1997).

The abrupt yet gradational passage from neritic (Cretaceous Transgressive Limestones) to pelagic sedimentation (Buff Pelagic Carbonates) suggests that the Païkon Massif underwent subsidence in Lower Turonian time. A similar deepening event of Turonian age has been reported from other parts of the Hellenides, for example in Argolis (Clift, 1990) and in the northern Pelagonian zone (Sharp, 1995). In addition, the *Microcodium*-bearing Iron-encrusted Facies of Sharp (1992, 1995) has been interpreted to indicate that flexural uplift preceded collapse, suggesting that extensional tectonic processes were active at this time (Sharp, 1995; this work chapter 4).

Some time later in the Upper Cretaceous the pelagic carbonates were succeeded by deep-water turbidites and radiolarite deposits (the Tchouka Flysch), which reflect the input of terrigenous clastic material into a deep-water basin. It is likely that the turbidites were derived from outcrops present in the underlying Païkon Massif, particularly the Kastaneri Formation, the Ghrammos Formation and the Cretaceous Transgressive Limestones.

Chapter 4

Deformation

CHAPTER 4 - DEFORMATION

4.1 - INTRODUCTION AND PREVIOUS WORK

Mercier (1966, 1968) first outlined the structural history of the Païkon Massif and recognised that the area had been folded into a broad north-south-trending anticline in post-Upper Cretaceous times: this has been confirmed by subsequent workers (Godfriaux & Ricou, 1991; Brown & Robertson, in press). Mercier also inferred the existence of two major structural breaks; one between the Middle-Upper Jurassic Kastaneri Formation and the overlying Kimmeridgian-Portlandian Khromni Limestones and the other between the post-Portlandian Ghrammos Formation and the Aptian/Albian Cretaceous Transgressive Limestones. Mercier envisaged the Païkon Massif as comprising two distinct tectonostratigraphic terranes, the Païkon subzone and the Prepeonian subzone, (chapters 1 and 2.1), which were tectonically juxtaposed along a major ~N-S-trending reverse fault (Figure 1.6).

Some time later, Vergely (1984) synthesised the structural history of the Païkon Massif and concluded that, in common with the "internal" Hellenides as a whole, three distinct phases of regional deformation had affected the Païkon Massif (Figure 4.1). These he named:

JE1 - A contractional event of Upper Jurassic age, involving isoclinal folding (Figure 4.2A)

JE2 - A contractional event of Lower Cretaceous age, characterised by folding with SE-ward vergence (Figure 4.2B).

CT1/2 - A series of Tertiary compressional events with westward vergence (Figure 4.2C).

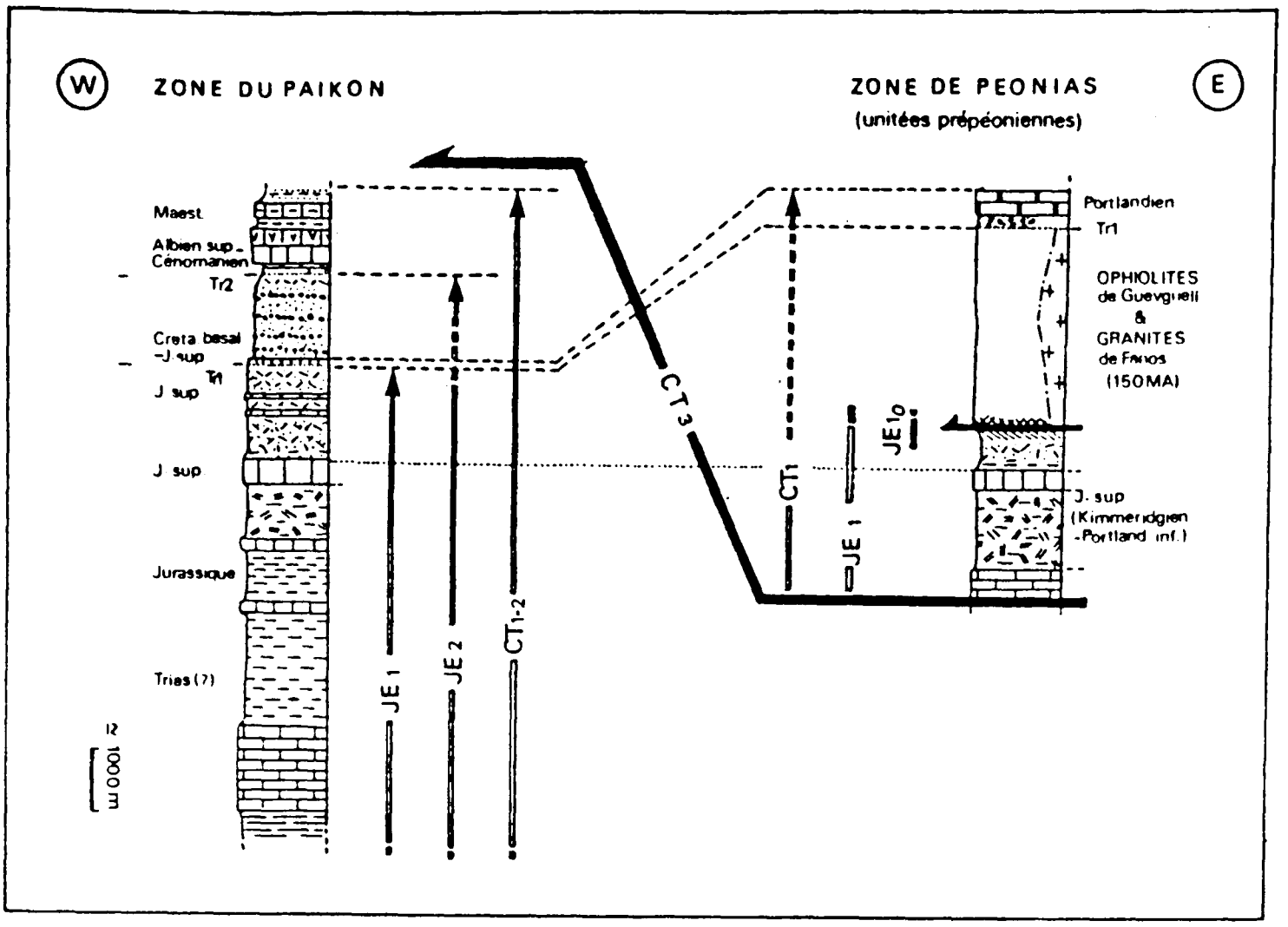


Figure 4.1 - Schematic log through the "Païkon" and "Prepeonian" subzones showing the relative timing of each of Vergely's (1984) proposed contractional deformation events. JE1 = Upper Jurassic; JE2 = Lower Cretaceous; CT1-3 = Tertiary. After Vergely (1984).

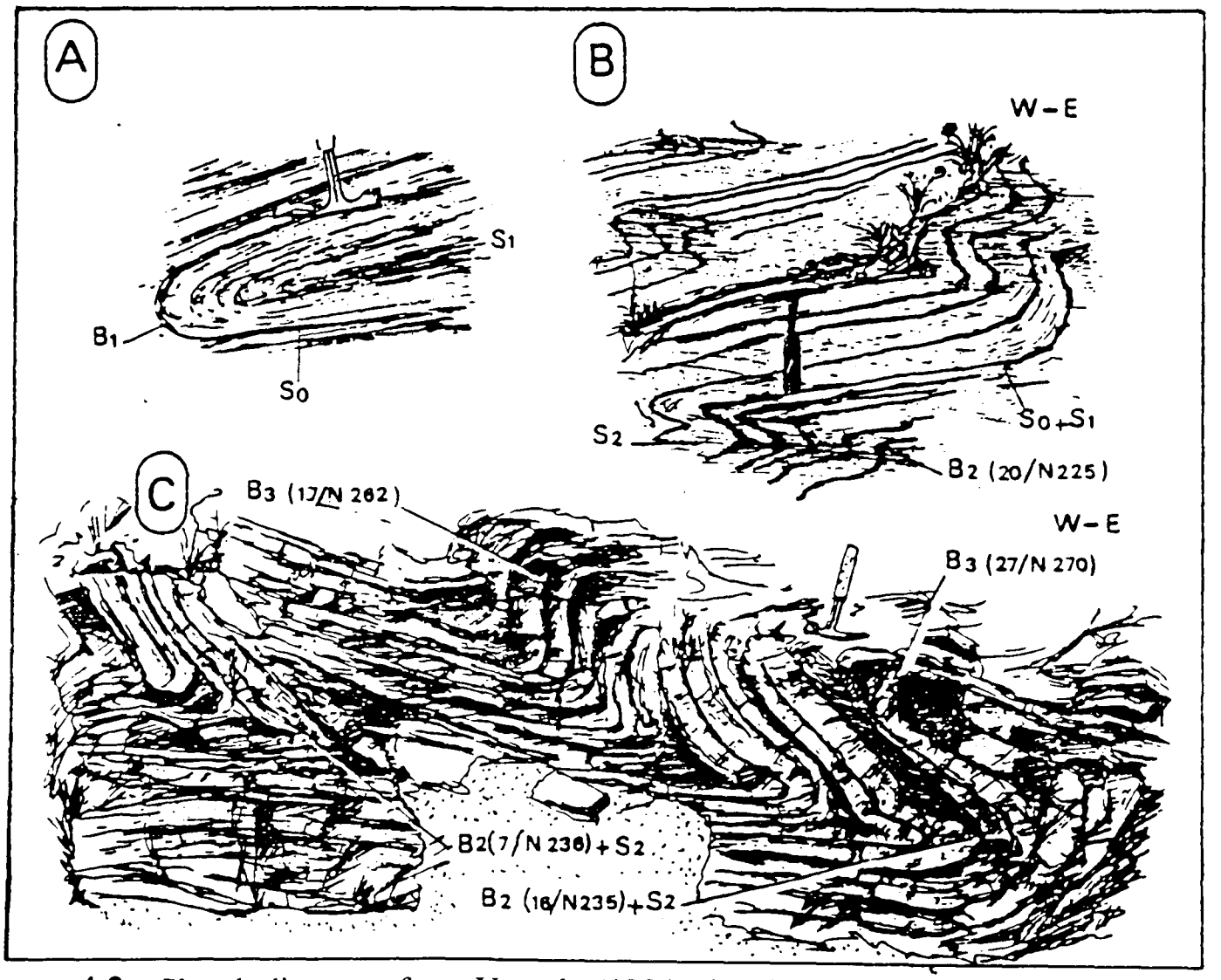


Figure 4.2 - Sketch diagrams from Vergely (1984) showing the style of folding associated with each of the main contractional deformation events to affect the Païkon Massif. A = JE1 isoclinal folds; B = JE2 asymmetrical folds; C = Tertiary chevron folds.

Godfriaux & Ricou (1991) proposed a theory which envisages the Païkon Massif as a "tectonic window", exposing rocks of the Pelagonian zone to the west (Figures 1.7 and 2.10). In this hypothesis the western margin of the Pelagonian zone (now the Païkon Massif) was over-ridden by an ophiolitic nappe derived from the east, and folded into an anticlinal structure during Tertiary compression (chapter 1). The validity of the "tectonic window" model has been assessed during this work and will be discussed further in section 4.8 and in chapter 7.

In this chapter I will present new structural data from within the Païkon Massif that lead to a significant revision of the original structural history, as outlined by Vergely (1984). In contrast to the findings of Vergely (1984; Figures 4.1 & 4.2), three distinct compressional events (D1, D2 & D3) and three extensional events (E0, E1 & E2) have been recognised. D1 compression took place during the Upper Jurassic and affected all stratigraphic units which underlie the pre-Kimmeridgian unconformity (i.e. the lower Païkon megasequence). Although the Gandatch, Livadia and Kastaneri Formations were all greatly affected by D1 compression, related structures are preserved in only a few key areas due to overprinting by successive phases of deformation. E0 extension occurred subsequent to D1 and was followed by a long period of tectonic stability, during the uppermost Jurassic and Lower Cretaceous, before further extension, E1, occurred in Turonian time. D2 and D3 compressional events occurred within a relatively short time of one another at some, poorly constrained, period in the early Tertiary. D2 affected the whole of the Païkon Massif, whereas D3 structures are mainly concentrated along the eastern margin of the study area, at the contact with the Guevgueli Ophiolite (Figure 4.3). Finally, the neotectonic E2 phase comprises a number of extensional events which remained active up to the present day. Each of the deformational events, and their related structures, are discussed in turn below.

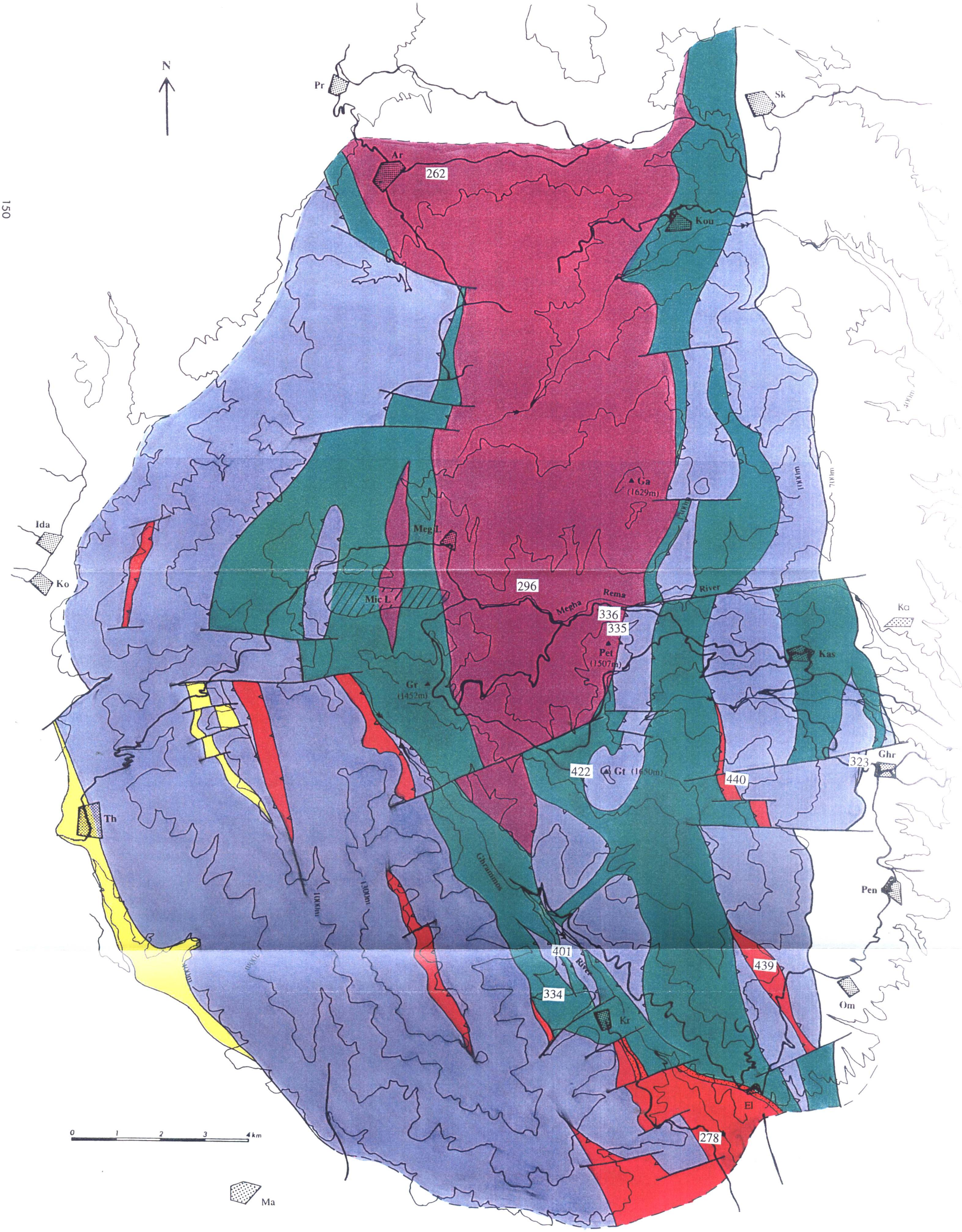


Figure 4.3 - Geological map of the Païkon Massif showing all localities mentioned in the text of chapter 4.

4.2 - UPPER JURASSIC COMPRESSION - D1 "Eohellenic" Deformation

4.2.1 - *Field and Petrological Observations*

D1 is the earliest phase of compressional deformation recorded within the Païkon Massif and it affects all of the lithologies which lie below the major Upper Jurassic unconformity. All stratigraphic units which overlie the Kastaneri Formation (chapter 3.7) are unaffected by D1 and, thus, the D1 event is "sealed" by the unconformably overlying Khromni Limestones (i.e. the upper Païkon megasequence), which are known to be of Kimmeridgian to Portlandian age (chapters 2.2.5 and 3.7). In short the D1 phase of compression took place subsequent to eruption of the Kastaneri Formation volcanics and prior to deposition of the Khromni Limestones.

A detailed investigation of the metamorphic evolution of the Païkon Massif is outside the scope of this work, but a previous study of the metamorphic assemblages present within the lower Païkon megasequence was undertaken by Baroz *et al.* (1987). Lawsonite-bearing assemblages, indicative of high pressure-low temperature blueschist facies conditions, were reported from the Kastaneri Formation, and co-existing biotite and stilpnomelane, indicative of upper greenschist facies conditions, were reported from the underlying Gandatch Formation (Baroz *et al.*, 1987; Figure 4.4). Assemblages such as these suggest that, during D1, the lower Païkon megasequence was subjected to pressure and temperature conditions in the range 5-7 kb and ~450°C in the basal Gandatch Formation to 3-6 kb and <330°C in the overlying Kastaneri Formation (Baroz *et al.*, 1987). No evidence of this high pressure/low temperature metamorphism exists in any of the units which overlie the Upper Jurassic unconformity (i.e. the upper Païkon megasequence; chapter 2).

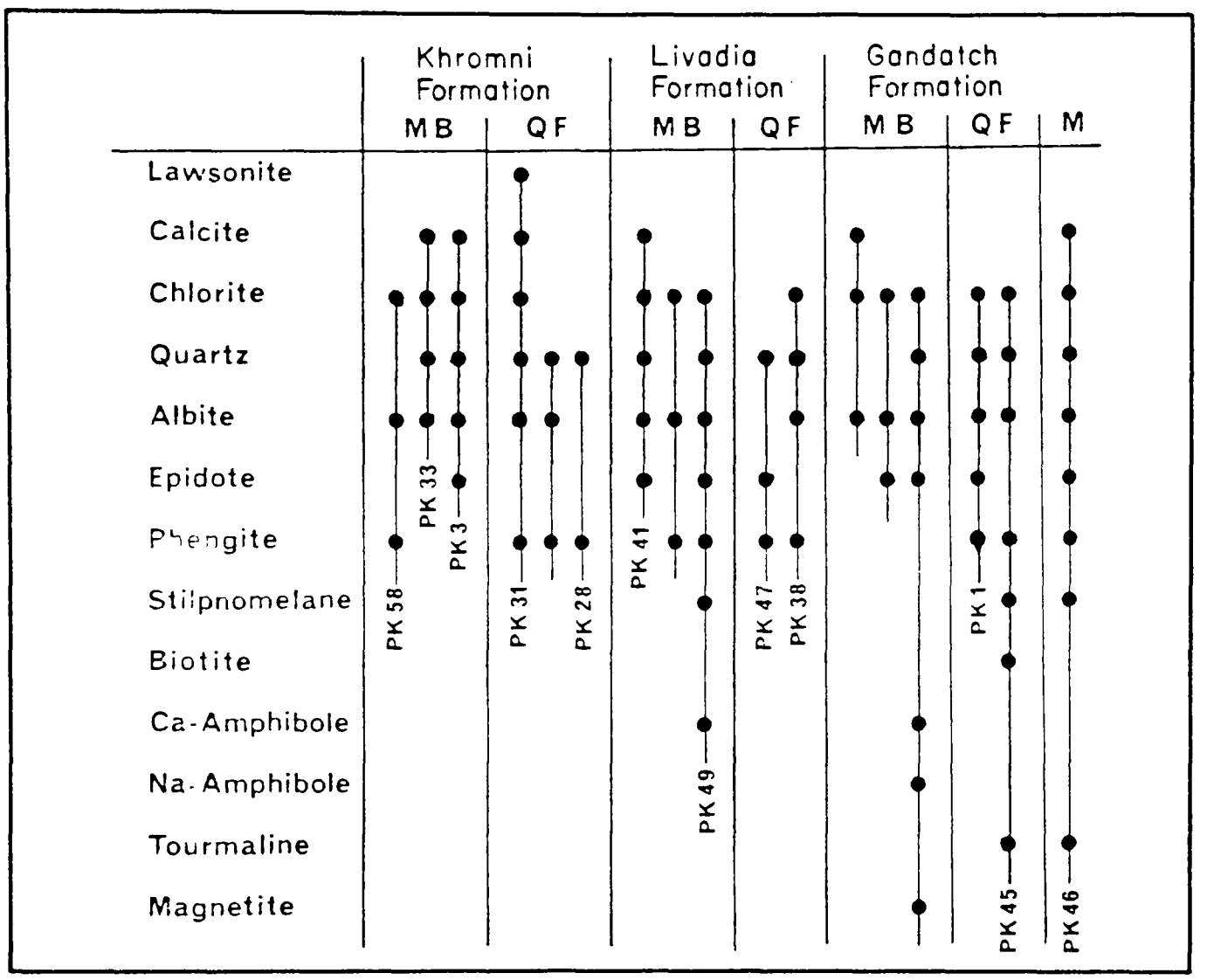


Figure 4.4 - Table showing the metamorphic mineral assemblages in the Gandatch, Livadia and Kastaneri (Khromni) Formations (after Baroz *et al.*, 1987). MB = Metabasic rocks; QF = Quartz-feldspar rocks; M = Marble.

Folds

In outcrop, the most conspicuous indication of D1 compression is the presence of tight to isoclinal folds. During later deformation events, many D1 fold structures were destroyed, particularly in less competent units such as the Livadia and Kastaneri Formations, where lineations and a remnant schistosity (S1) are the only remaining evidence of D1 compression. The marbles, calc-schists and chloritic schists of the Gandatch Formation preserve D1 fold structures the best, as observed around Micra and Meghala Livadia in the centre of the Païkon Massif (Figure 4.3).

Within the Gandatch Formation, folds associated with D1 have fairly consistent east-west fold axial trends (Figure 4.5A) and are typical of deep-level, essentially ductile deformation. They are associated with a marked axial planar cleavage, most prevalent in schistose, phyllosilicate-rich horizons, and an axis-parallel lineation (Figure 4.5B). Folds vary in wavelength and amplitude from 2 cm to over 10 m; they are distinctly asymmetrical and can be flat-lying, inclined or upright. Hinge thickening and limb attenuation are common and rare rootless isoclines were observed.

Figures 4.6 and 4.7 illustrate the style of folding which characterises D1 and clearly demonstrate the ductile nature of this phase of deformation. Figure 4.6 (and Figure 3.5) shows slightly inclined, tight D1 folds within Stratotype 2 of the Gandatch Formation. The folds have an associated axial planar fabric (S1). In the field it is evident that the D1 folds and S1 foliation are crenulated and overprinted by later D2 structures (section 4.6). Figure 4.7 shows D1 folds within the Gandatch Formation at locality 83 (base of Kopria ridge; Figure 4.3). Doubly vergent asymmetrical folds are picked out by the tightly-folded compositional layering (S0) and by a thin, siliceous layer, possibly produced during pre-D1 hydrothermal metasomatism (chapter 5). The primary D1 foliation can be picked out running roughly parallel to the fold limbs and to the axial planes of folds (Figure 4.7). The later D2 fabric is not evident on this photograph but,

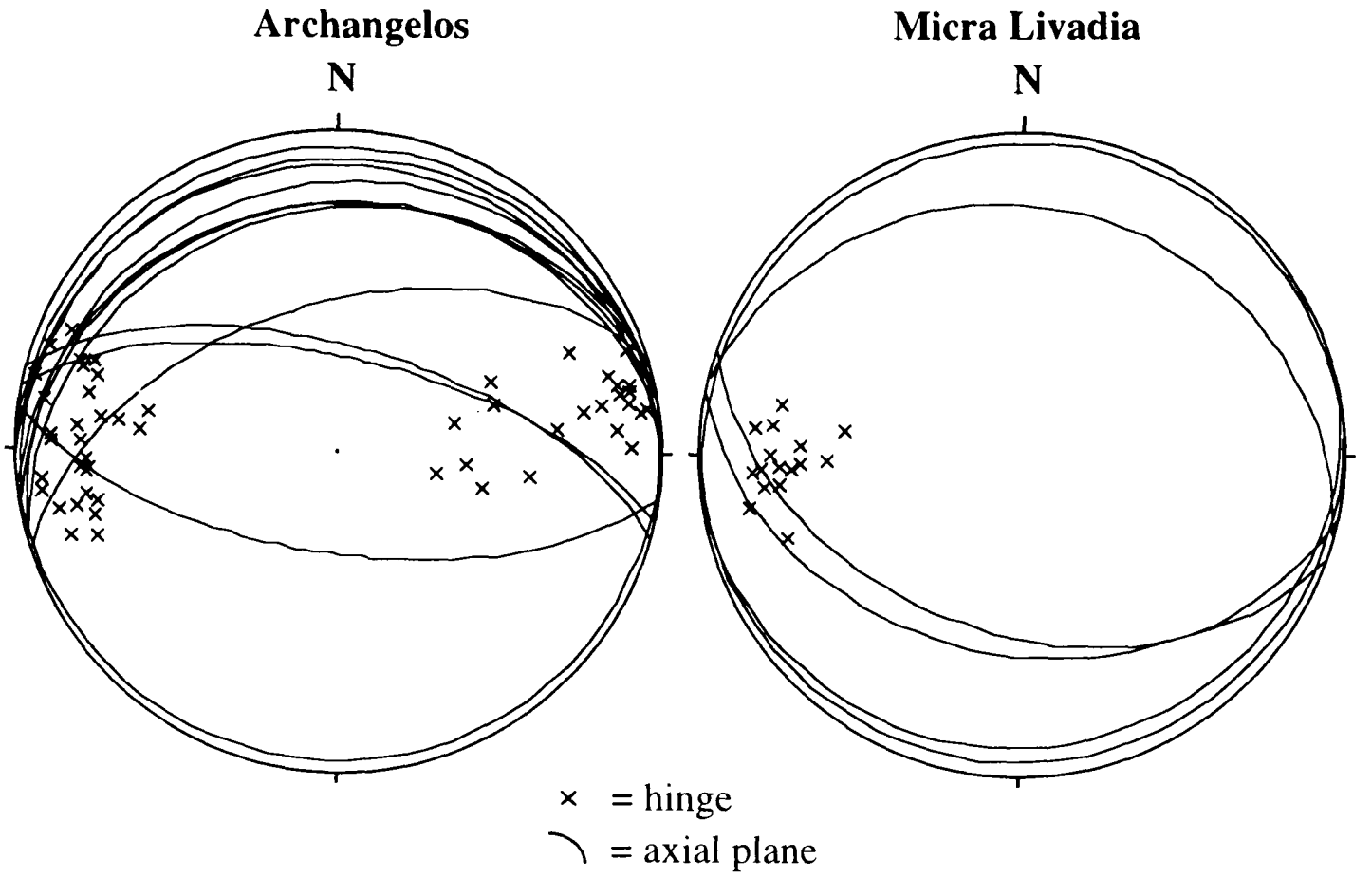


Figure 4.5A. Stereographic projections showing the orientation of D1 fold axes and axial planes within the Gandatch Formation. Data from Archangelos (left) and Micra Livadia (right).

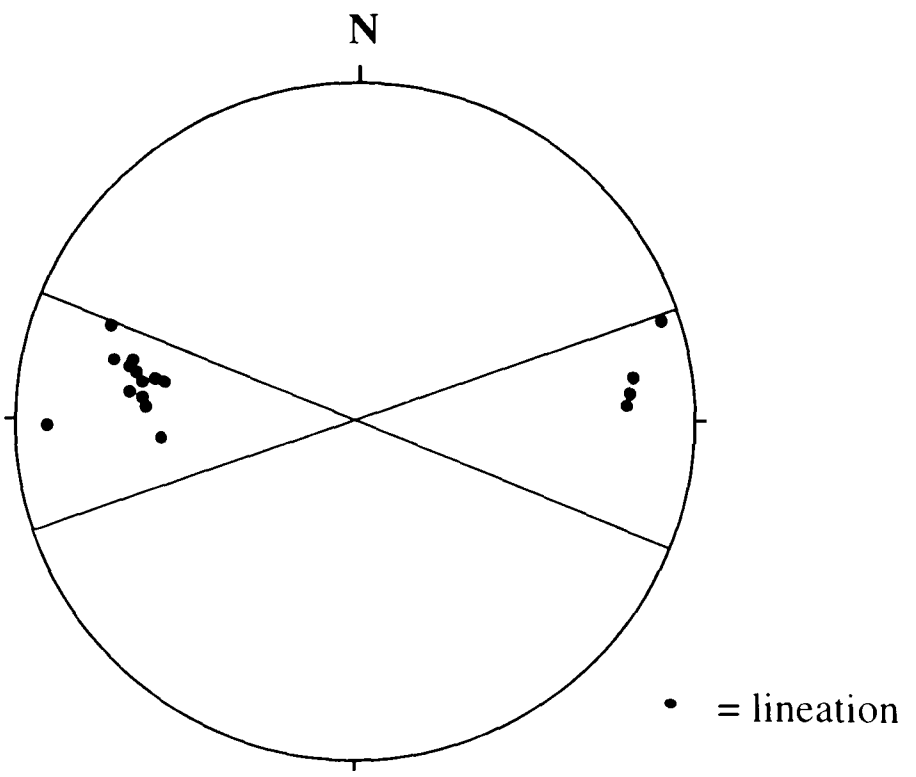


Figure 4.5B. Stereographic projection of the lineation produced during D1 deformation within the Gandatch formation (various localities). The lineation trends roughly E-W and is parallel to D1 fold axial directions.



Figure 4.6 - Field photograph showing inclined isoclinal D1 folds within Stratotype 2 (schists and marbles) of the Gandatch Formation. The folds are associated with a fold axis-parallel foliation.

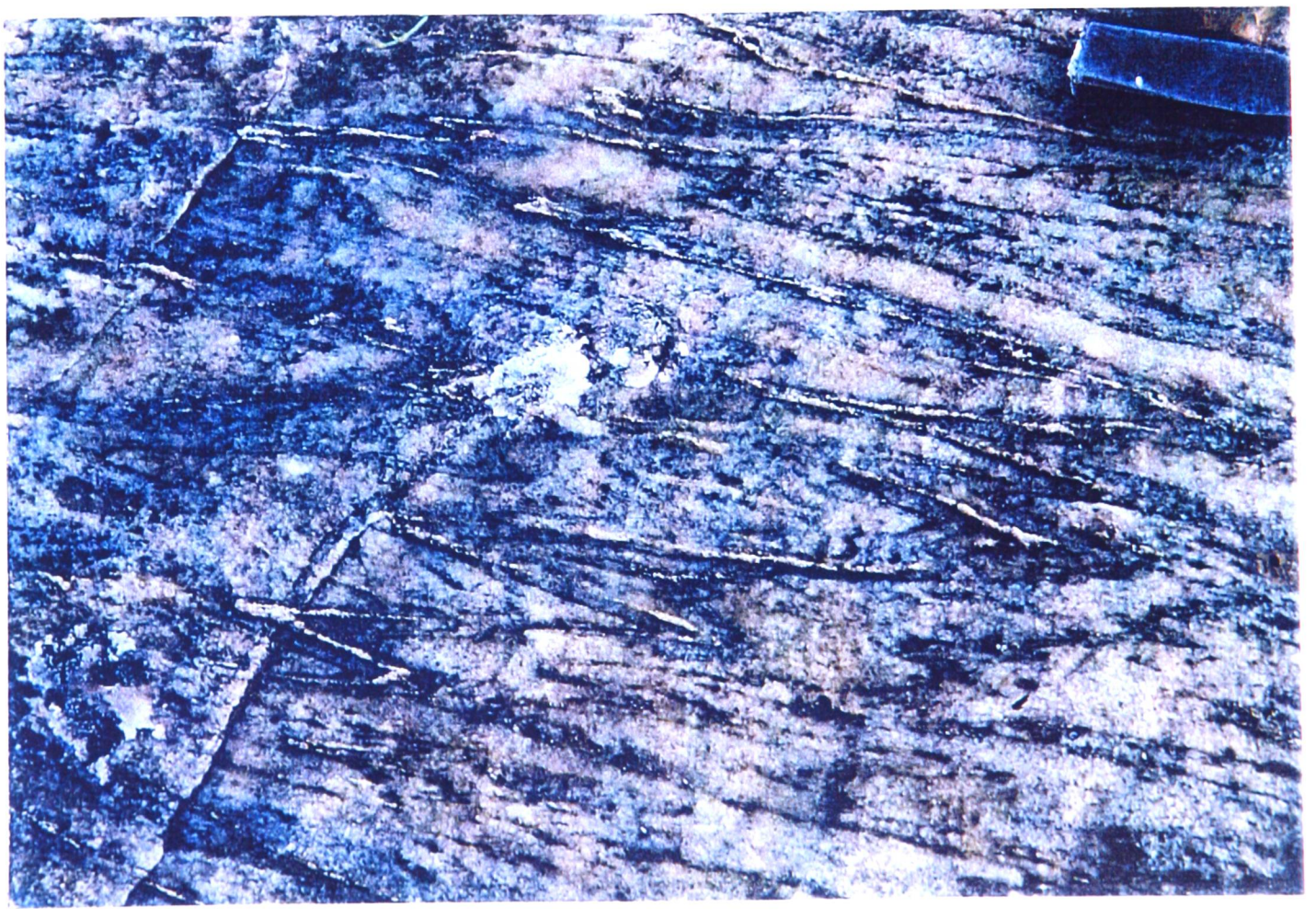


Figure 4.7 - Field photograph of D1 isoclinal folds being picked out by a folded quartz vein in the Gandatch Formation.

on close inspection in the field, cuts across the D1 structures in a more upright orientation. At the same outcrop, a few metres away from the site of the photograph, the D2 foliation dominates and D1 structures are somewhat obscured. A faint D3 lineation (chapter 4.7) can also be picked out at this locality.

Additionally, Figure 4.8 illustrates an asymmetrical, rootless isoclinal D1 fold pair in the Gandatch Formation from locality 23, between Micra Livadia and Kastaneri (Figure 4.3). The S0 layering is thickened in the vicinity of the fold noses and strongly attenuated along both long limbs. The short or overturned limb has been crenulated by numerous small parasitic isoclines. The remnant D1 fabric is faint here and has been almost entirely overprinted by a later-stage fabric, which is parallel to the dominant D2 schistosity (chapter 4.6).

In the Kastaneri Formation, rare D1 folds are also picked out by siliceous veins, such as at locality 230a (uphill north of Eliftherohori; Figure 4.9). The Kastaneri Formation here comprises finely interbedded chloritic schists with sparse vesicular andesitic flows. The veins occur predominantly within the schistose horizons and have been folded by isoclinal and sheath folds. The D1 fabric is flat-lying and parallel to fold axial surfaces. On three-dimensional surfaces, upright D2 folds, and their associated axial-planar foliation, refold and crenulate D1 structures.

In most localities, the S1 foliation developed during D1 compression is orientated parallel to primary bedding surfaces (S0) due to the isoclinal nature of D1 folding. Exceptions to this occur around the vicinity of D1 fold noses, where cleavage planes and bedding surfaces meet at high angles (Figure 4.10).

Foliation and Lineation

The D1 lineation is invariably oriented parallel to D1 fold hinges and, therefore, parallel

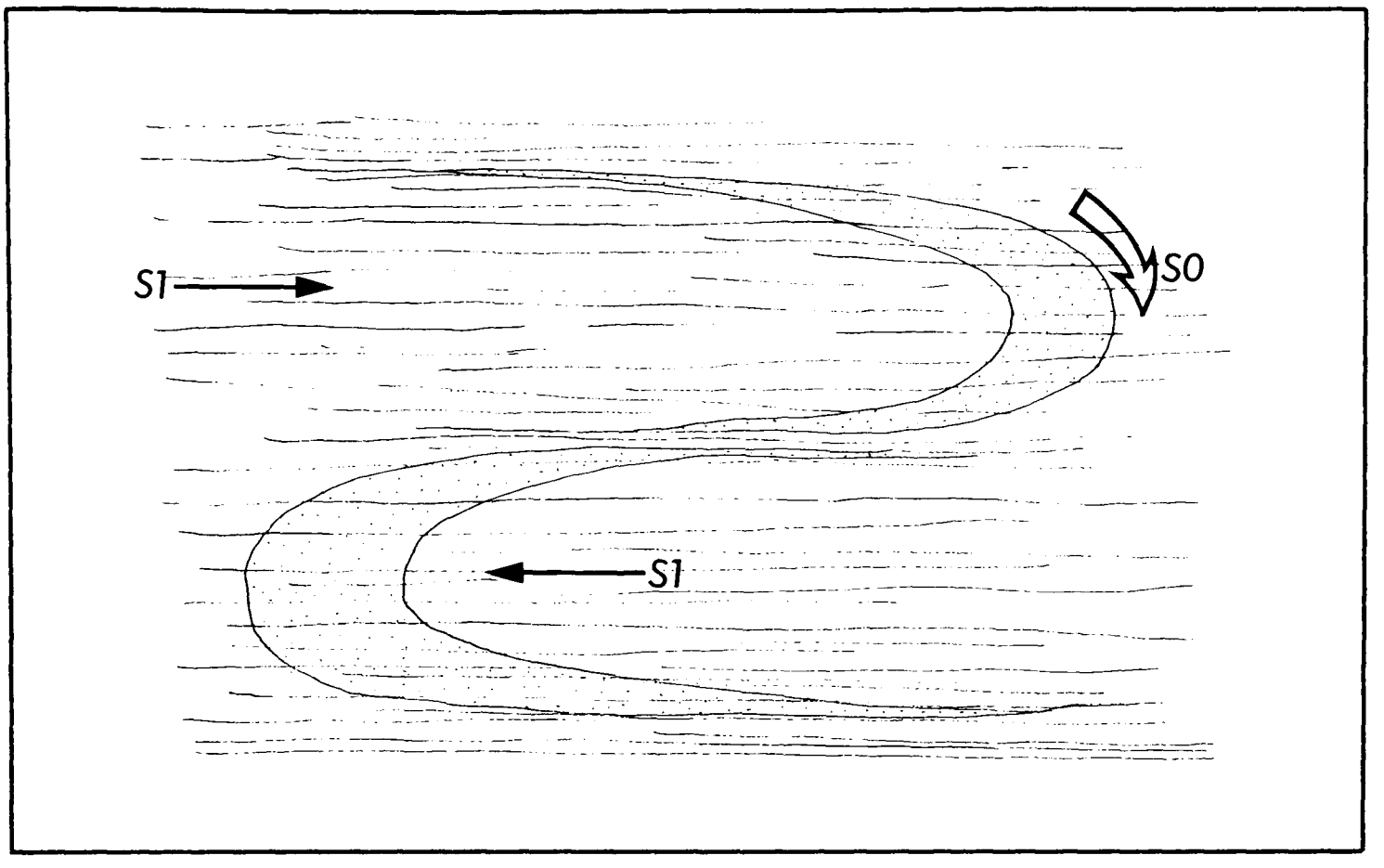


Figure 4.8 - Sketch of a rootless D1 isoclinal fold pair within the Gandatch Formation. The S1 fabric is axial-planar to the isoclines and parallel to S0 along the fold limbs. Locality 23, near Micra Livadia).

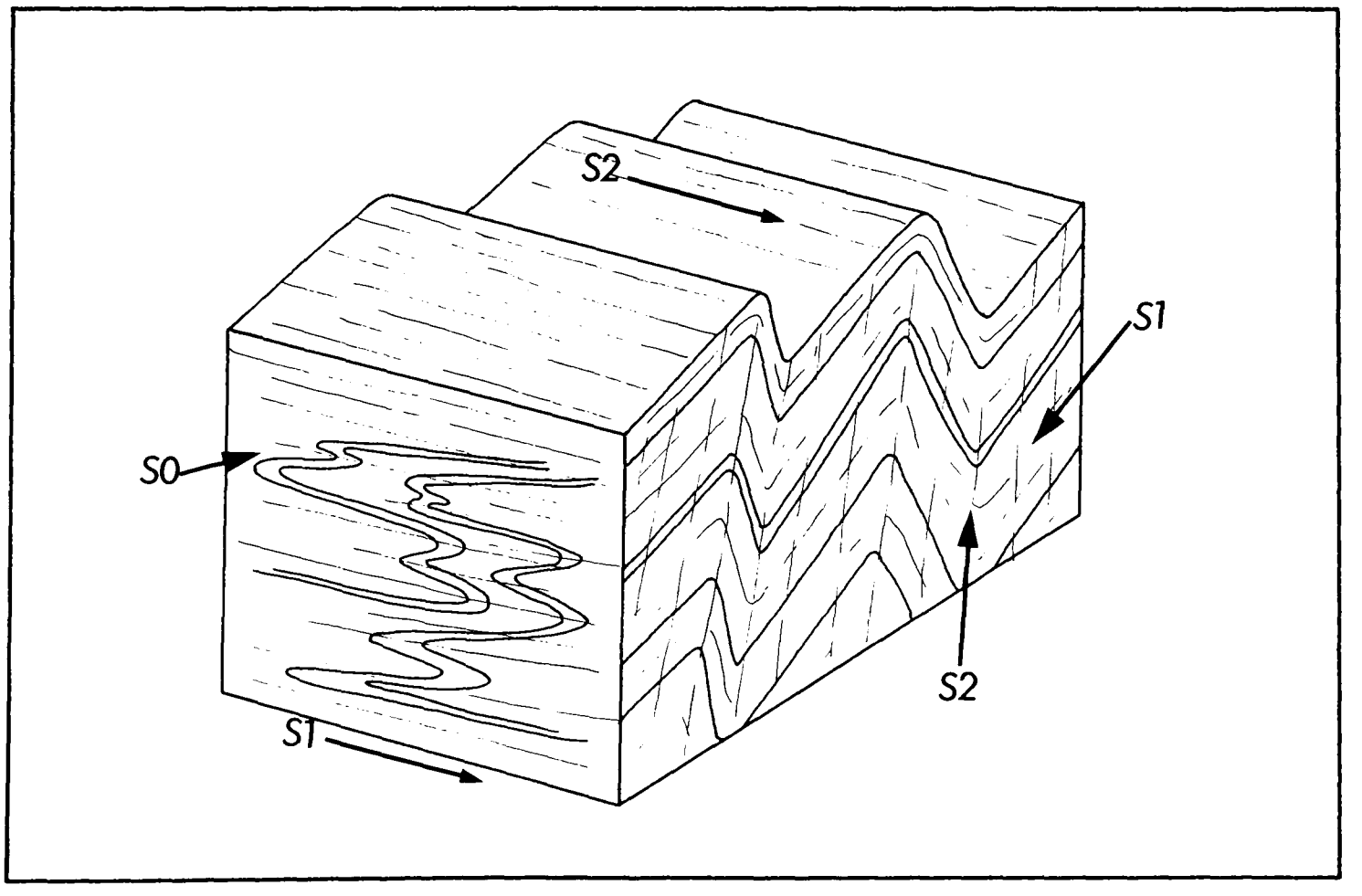


Figure 4.9 - Three-dimensional sketch of refolded fold structures within the Kastaneri Formation (locality 230a, southern Païkon Massif). The D1 folds and fabric are flat-lying and, on certain surfaces, D2 folds can be seen overprinting these structures.

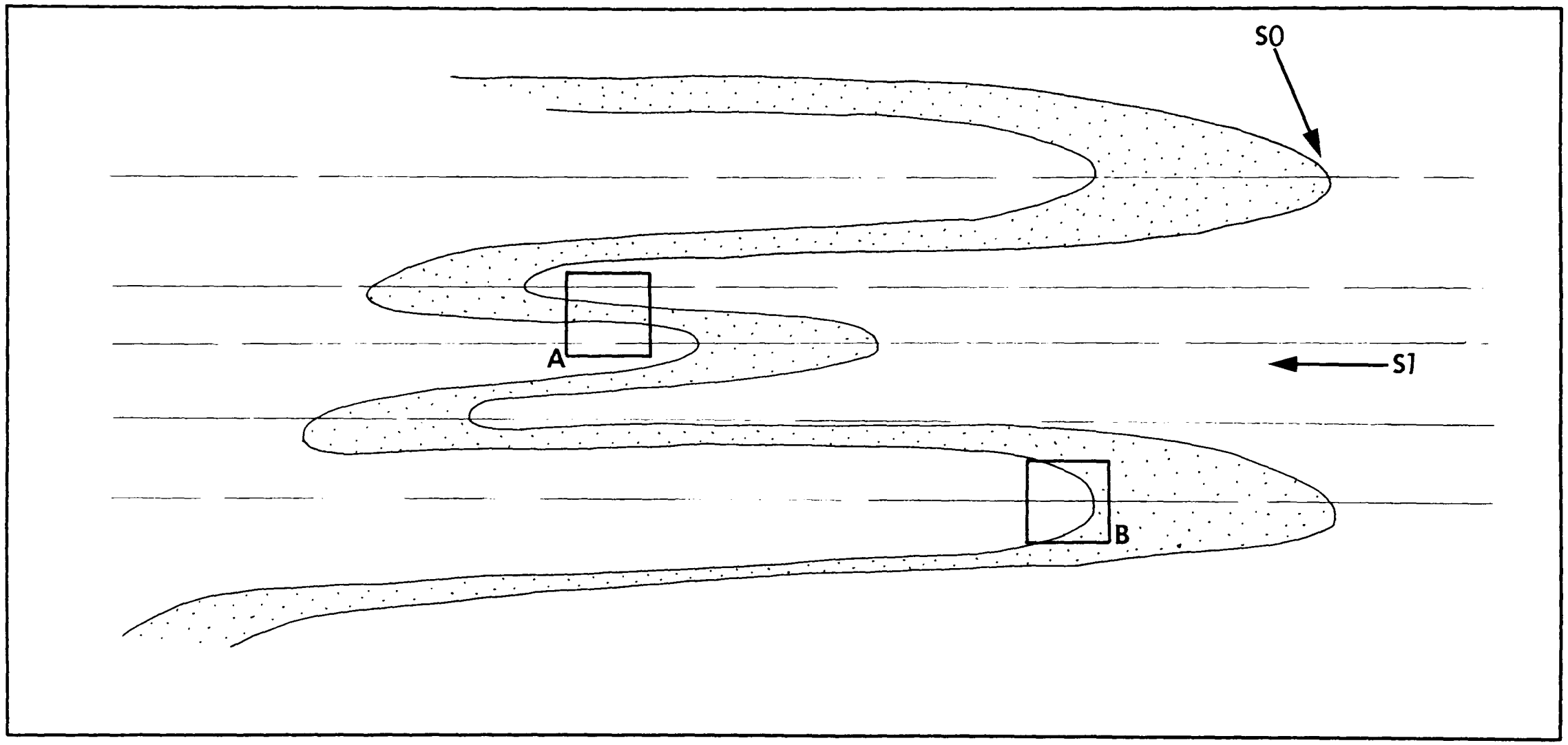
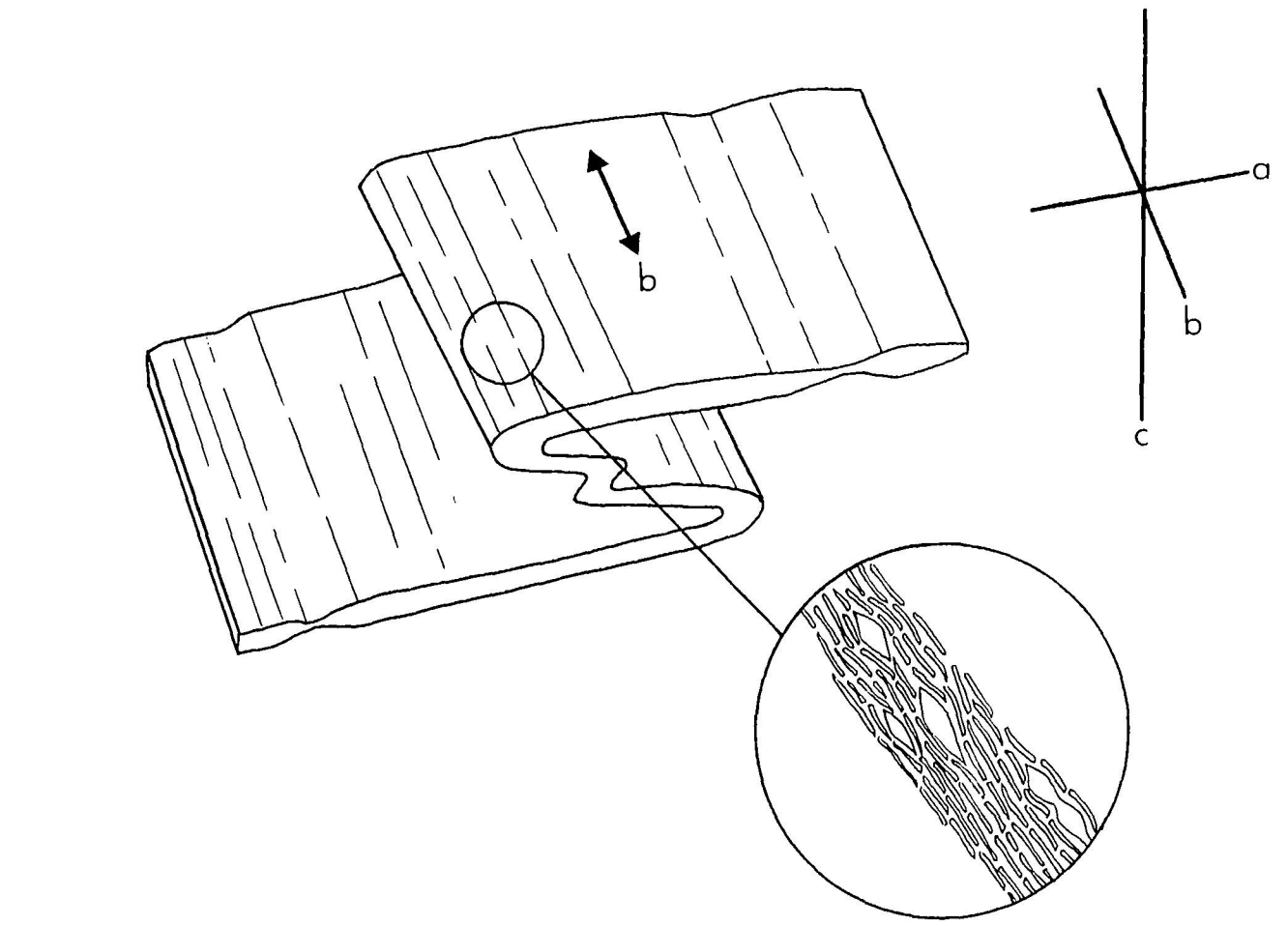


Figure 4.10 - Sketch showing the relationship between the S1 fabric and primary compositional layering (S0) for isoclinal folds developed during D1 compression. Box A - S0 and S1 are sub-parallel along fold limbs. Box B - S0 and S1 meet at high angles in the fold nose area.

to the b-tectonic axis of the isoclines (Figure 4.11). The D1 foliation is perpendicular to the lineation and parallel to the axial planes of D1 folds. Oriented thin-sections from the Gandatch Formation demonstrate the syn-deformational growth of foliation-parallel metamorphic minerals, such as phengitic mica, platy chlorite (Figure 4.12). The growth of porphyroblastic epidote and albite occurred concurrently with foliation development and consequently these minerals are also often slightly elongate parallel to the D1 lineation, indicating that it is a stretching lineation. The D1 foliation and lineation are best developed in phyllosilicate-rich S0 horizons. Conversely, the D1 lineation is relatively poorly-developed in horizons rich in quartz and calcite, but is still present as elongate, fold axis-parallel calcite crystals, deformed quartz grains and sparse micas. Figure 4.13 is a photomicrograph of an oriented thin section from the limb of a D1 fold. The thin section was cut perpendicular to the D1 foliation and parallel to the D1 lineation, and shows dynamically recrystallised calcite crystals, strained quartz and secondary micas aligned parallel to the lineation, which is parallel to the axes of D1 folds.

As described above, the axial directions of D1 folds parallel the D1 lineation and are not perpendicular to it as might be expected. In other words, D1 folds have been rotated until parallel to the dominant transport direction (i.e. parallel to the stretching lineation). Similar structures have been reported from the Oman Mountains (Le Métour *et al.*, 1990; see section 4.2.2 below) and the Caledonides (Escher & Watterson, 1974). The rotation is largely due to the ductile nature of the crustal regime in which the structures were generated (i.e. high pressure, low-moderate temperature). Under ductile conditions, rotation proceeds by simple shear and occurs when flattening and shearing are the dominant processes of deformation. In this case, resultant D1 fold axes have become aligned parallel to the D1 stretching lineation at most localities. Due to this rotation, the polarity, or vergence, of D1 folds is impossible to determine. The D1



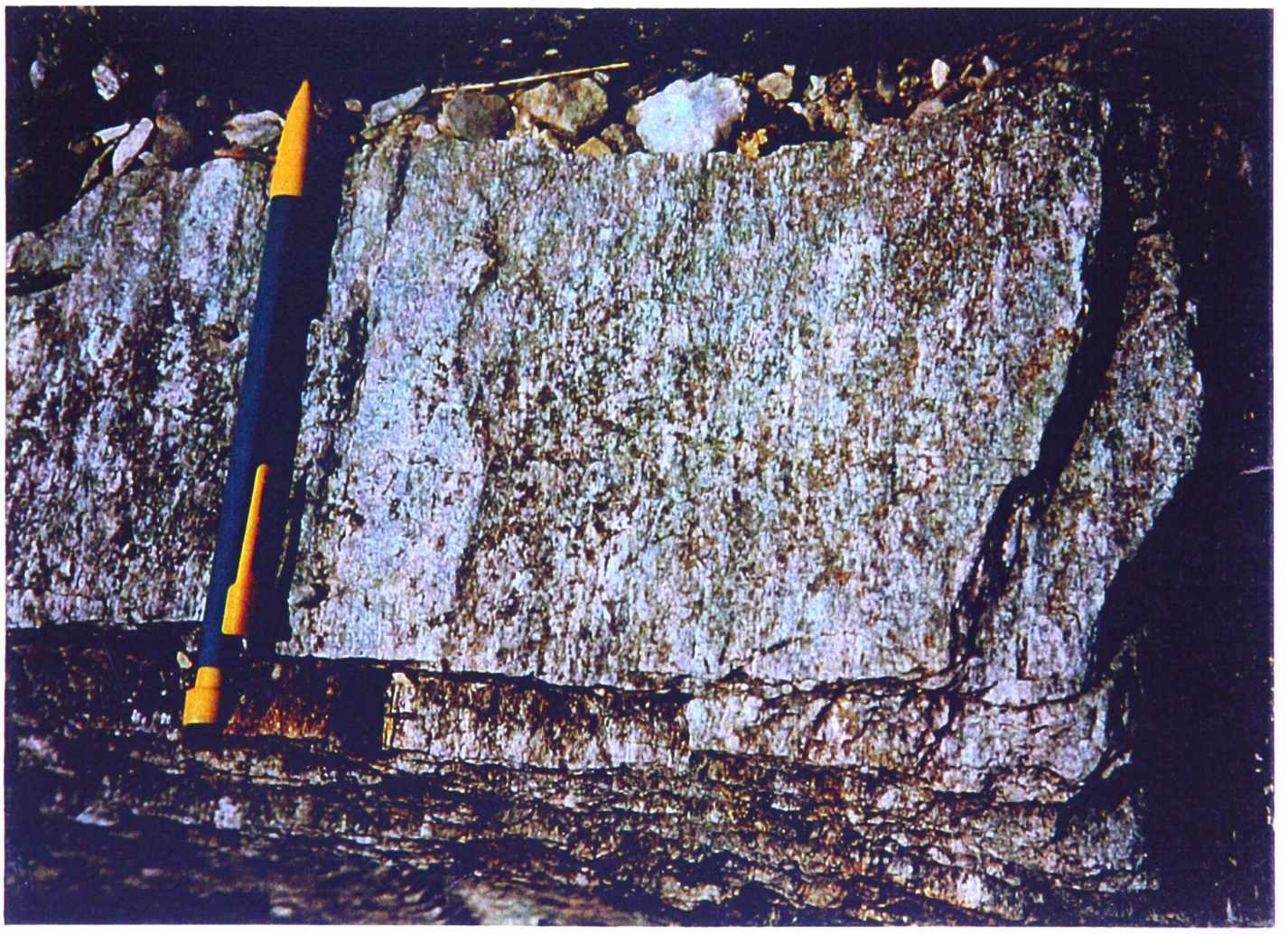


Figure 4.11 - Sketch of the style of folding associated with D1, and the D1 stretching lineation generated parallel to the b tectonic axis of those folds. Asymmetrical isoclines often have attenuated long limbs but are crenulated along their short or overturned limbs. The stretching lineation (inset circle) is defined by plates of chlorite and mica and elongate, lensoid crystals of quartz, feldspar and epidote. The photograph shows the D1 lineation in the field at locality 21 (east of Micra Livadia).

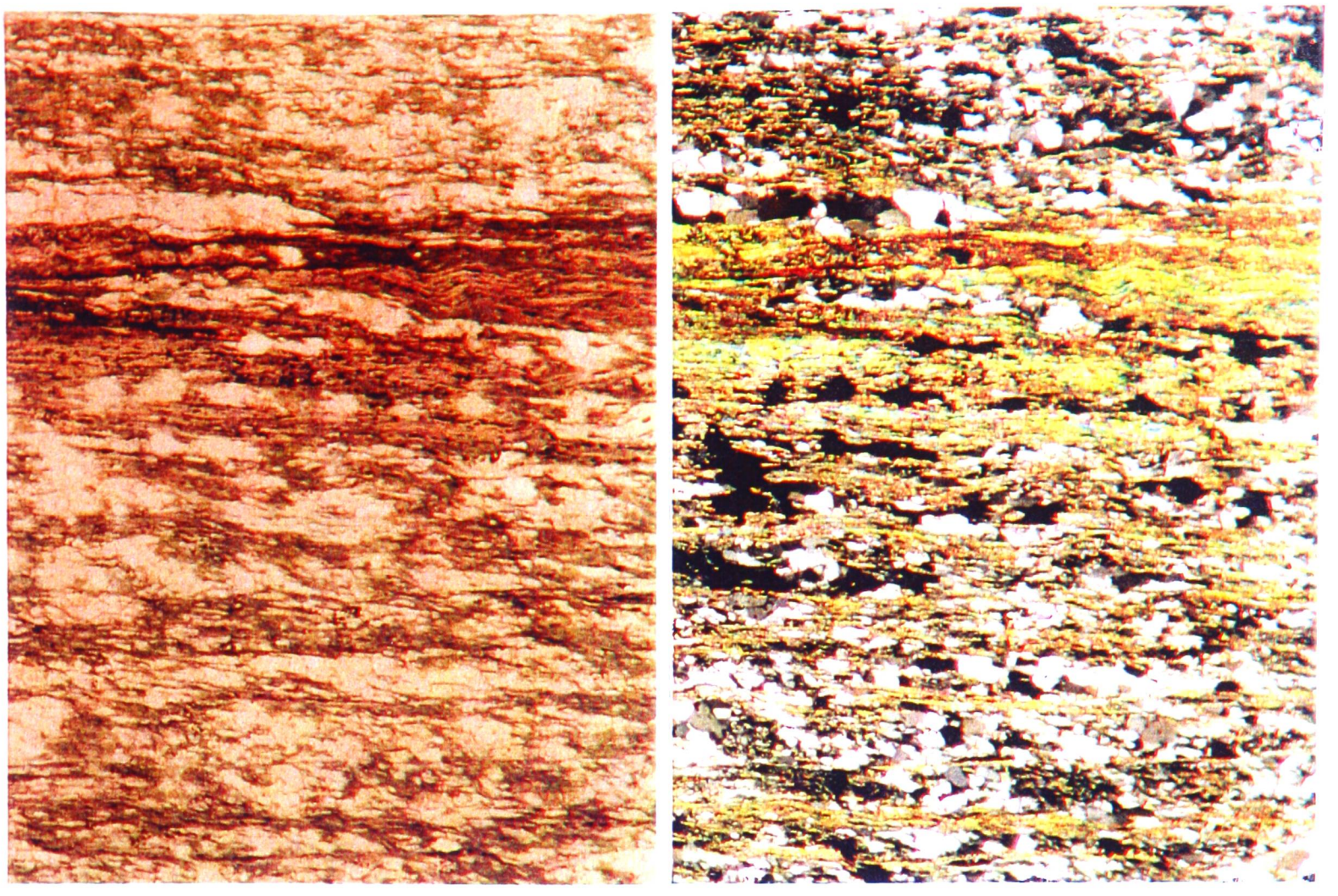


Figure 4.12 - Photomicrograph of an oriented thin section from a horizon of chloritic schists within the Gandatch Formation (locality 262, east of Archangelos village). The S1 fabric is oriented horizontally and is defined by platy phyllosilicate minerals such as chlorite and mica. Strained quartz crystals are slightly elongate parallel to the S1 fabric also.

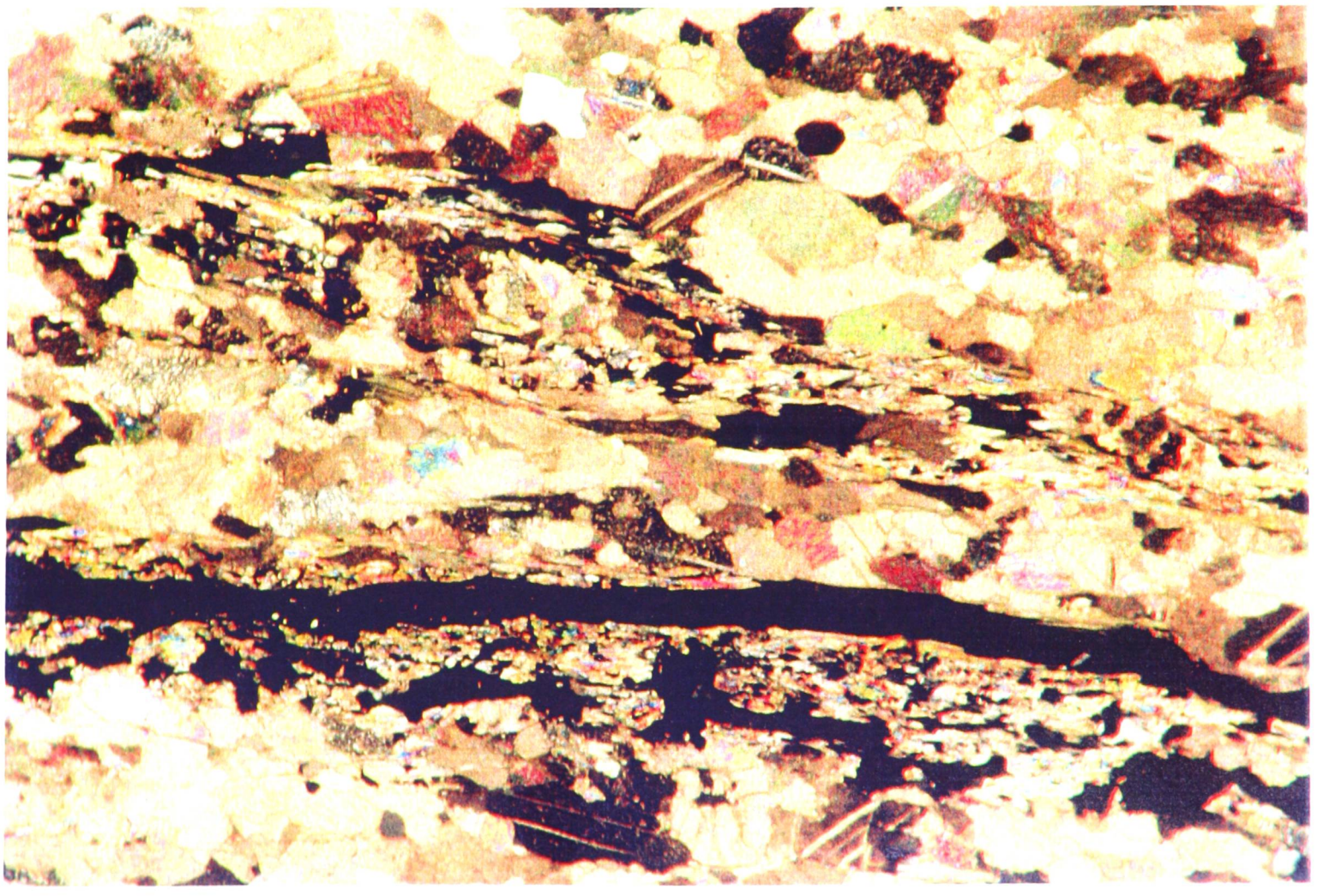


Figure 4.13 - Photomicrograph of an oriented thin section from the limb of a D1 fold in the Gandatch Formation (locality 335, near Meghala Livadia). Calcite crystals are aligned parallel to the D1 stretching lineation, as are elongate plates of chlorite and mica.

lineation, however, trends consistently east-west and is very likely to represent the principal direction of transport during this contractional phase, although it is not clear from structural data alone whether transport was directed westward or eastward.

Fold structures associated with D1 are rarely preserved within the Livadia Formation, which reflects the relatively low competency of this unit compared to the bedded schists and carbonates of the Gandatch Formation. Nevertheless, the associated D1 lineation is common throughout the Livadia Formation. The lineation again trends east-west, as demonstrated in Figure 4.14, and cleavages/foliations are pervasive, refracted and aligned parallel to the axial planes of D1 folds preserved in the Gandatch Formation.

The volcanics and volcaniclastics of the Kastaneri Formation display a wide variety of D1 structures. As with the Gandatch Formation, the Kastaneri Formation is isoclinally folded about E-W axes, though scarcely, and exhibits a well-developed axial-planar cleavage and axis-parallel lineation. Rudaceous debris-flow horizons, which crop out at locality 401 (1 km north of Khromni village; Figure 4.3), preserve vestiges of the early D1 fabric within competent siliceous clasts, while the succeeding D2 fabric dominates the schistose matrix (chapter 4.6). Evidence of both D1 and D2 events are recorded in the clasts, some of which have been rotated (Figure 4.15).

4.2.2 - *Discussion*

The conclusions of this work support Vergely's (1984) recognition of a major Upper Jurassic phase of compressional folding within the Païkon Massif and it is concluded here that the JE1 event of Vergely (1984) is equivalent to the D1 event of this study.

D1 compression was characterised by deep-crustal, ductile deformation under blueschist

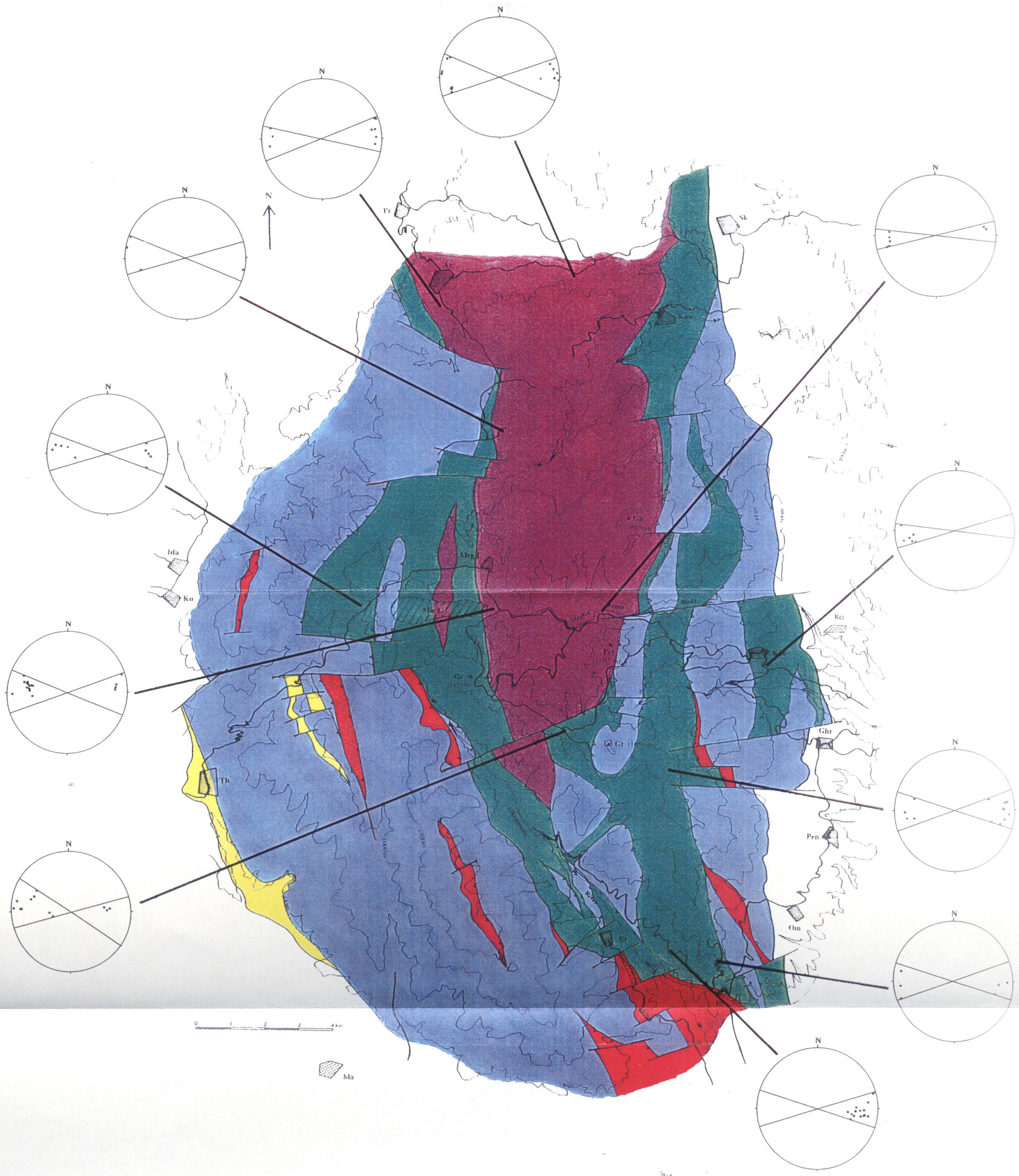
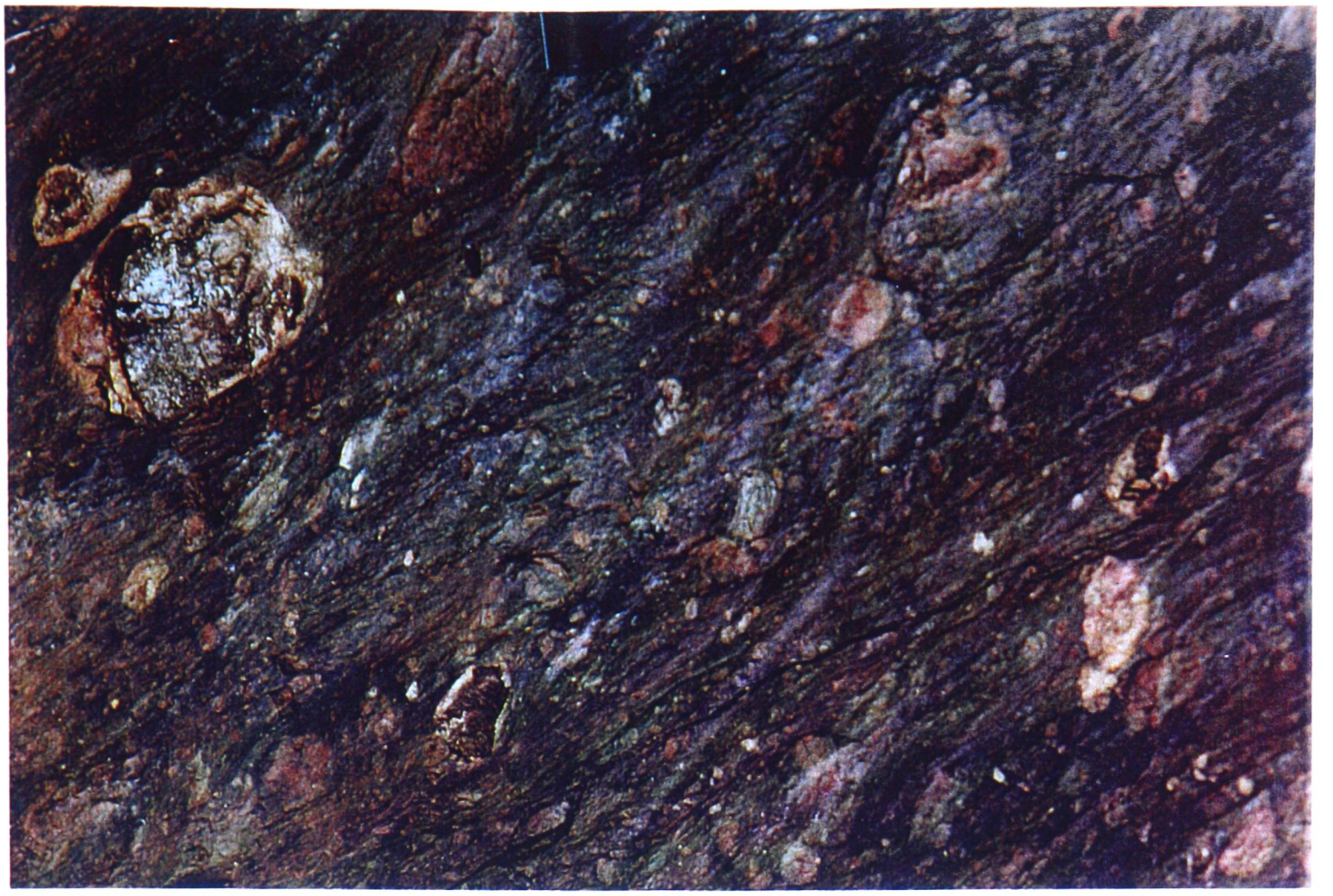


Figure 4.14 - Geological map of the Païkon Massif with stereographic projections showing the orientation of the D1 lineation from various localities. The D1 lineation is quite consistently east-west-trending and is represented by small full circles.



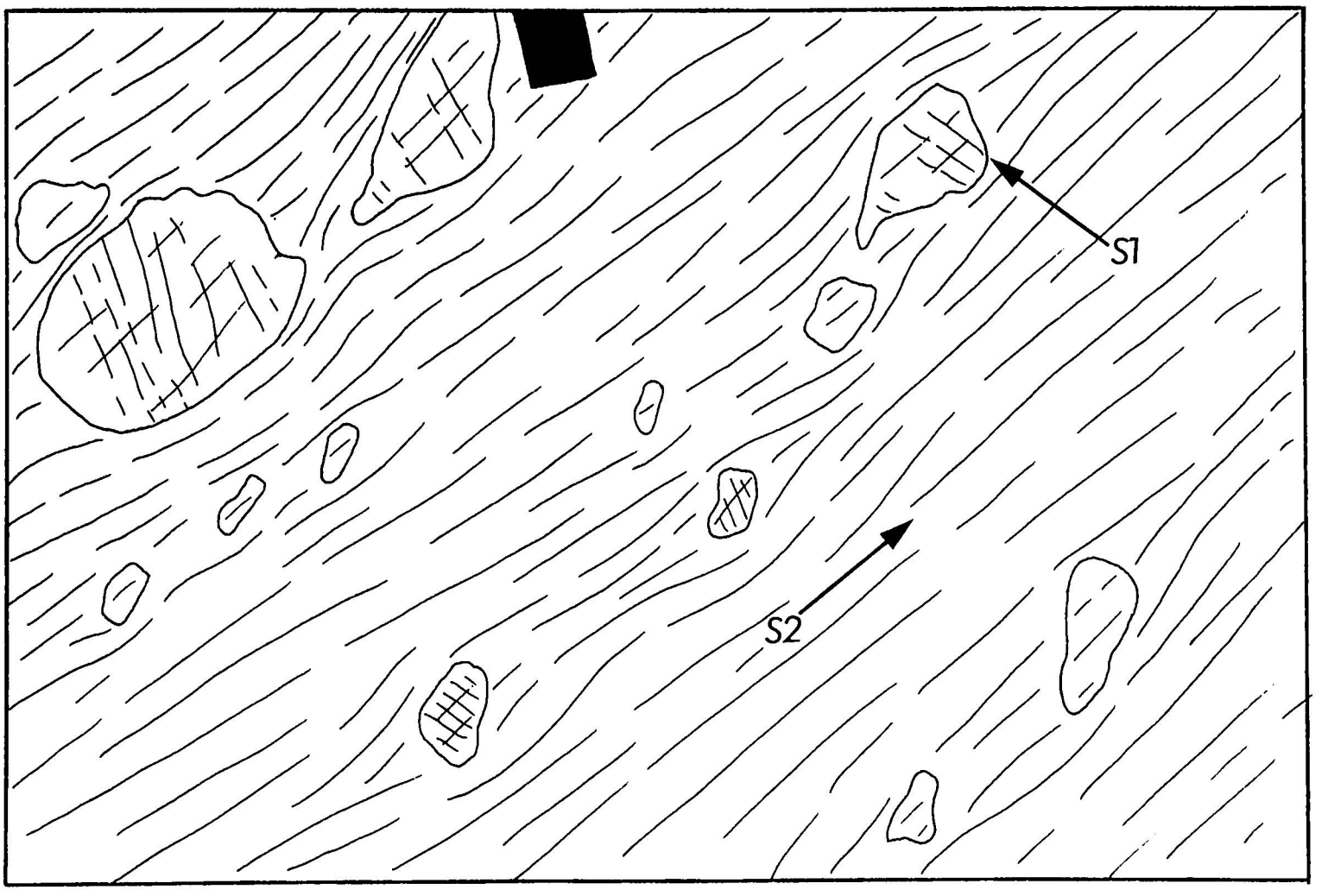


Figure 4.15 - Sheared breccio-conglomerate horizon from the Kastaneri Formation (locality 401, north of Khromni village). The clasts are highly competent and silicious and are set in a fine-grained, schistose matrix. The main fabric runs from top right to bottom left in the photograph and dominates the matrix. However, an earlier fabric can also be picked out in the silicious clasts, trending from top left to bottom right. The early fabric was generated during D1 deformation and the dominant, later fabric formed during the D2 event.

to upper greenschist facies conditions, as indicated by lawsonite and biotite-stilpnomelane-bearing assemblages respectively. A significant amount of burial and/or tectonic overburden is required to generate such metamorphic conditions in the Païkon Massif at this time. Although there is no direct evidence from within the Païkon Massif of what caused this compression event, the tectonic evolution of neighbouring regions (e.g. the Pelagonian and Almopias zones to the west, Sharp, 1995; the Peonias zone to the east, Vergely, 1984) indicate that compression was taking place throughout the Internal Hellenides at this time. Therefore, it is possible that either the Guevgueli Ophiolite (to the east) or the Almopias Ophiolite (to the west) was obducted onto the Païkon Massif as these ocean basins closed and the Serbo-Macedonian and Pelagonian continents began to collide with the southern margin of Eurasia (see chapter 7 for a full discussion). Late Jurassic structures from the Guevgueli Ophiolite indicate westward vergence (Bebien *et al.*, 1986), which may indicate that it was this eastern ophiolite which overrode the Païkon Massif during D1. D1 compression is thus a result of an Upper Jurassic regional collisional event, during which the Païkon Massif underwent tectonic burial.

Metamorphic mineral assemblages present within the lower Païkon megasequence suggest that the Gandatch Formation records higher temperature and pressure conditions (co-existing stilpnomelane and biotite; ~450°C and 5-7 kb) than the Kastaneri Formation (lawsonite; <330°C and 3-6 kb) (Baroz *et al.*, 1987). This suggests that the stratigraphically lower Gandatch Formation was buried for longer and/or to a deeper level than the Kastaneri Formation, resulting in upper greenschist facies assemblages in the former and blueschist facies conditions in the latter. Baroz *et al* (1987) conclude that these assemblages are likely to have developed either in a subduction zone setting or due to the tectonic over-pressure of an obducting nappe.

A similar structural and metamorphic event to that of D1 in the Païkon Massif, has been documented from the Oman Mountains (El Shazly & Coleman, 1990). The continental

margin of Oman was overridden and tectonically buried by the obducting Semail Ophiolite in the late Cretaceous. As a result, the underlying continental margin (e.g. region 3 of the Saih Hatat window; El Shazly & Coleman, 1990) underwent blueschist to eclogite facies metamorphism in an A-type subduction zone (Hodges *et al.*, 1982). The buried rocks were folded, and the ductile folds were progressively rotated with increasing strain until their axial directions were in parallelism with the dominant transport direction (Métour *et al.*, 1990). These structures are comparable to those that characterise the D1 event in the Païkon Massif.

In Oman, an amphibolite grade metamorphic sole marks the base of the obducted Semail Ophiolite. Such a metamorphic sole, along with the entire overriding nappe, has presumably been removed from the Païkon Massif by post-obduction denudation, as there is no remaining evidence of these units within the present-day study area.

4.3 - UPPER JURASSIC EXTENSION - E0

4.3.1 - *Tectonic Unroofing and Core Complex Exhumation*

In order to preserve blueschist facies mineral assemblages, as are present in the Kastaneri Formation of the lower Païkon megasequence (i.e. lawsonite), it is necessary to uplift or exhume the high P-low T rocks before higher temperature mineral assemblages stabilise during thermal re-equilibration. Such uplift has obviously affected the lower Païkon megasequence, which is locally lawsonite-bearing, and is likely to have ensued by extension along low angle detachment faults, resulting in core complex formation (Platt, 1986). This extension occurred subsequent to the D1 compression event that generated the high P-low T phases, but prior to Kimmeridgian/Portlandian deposition of the Khromni Limestones (Brown & Robertson, 1994, in press). The youngest possible age of unroofing is thus limited by

the unconformably overlying Khromni Limestones (i.e. pre-Kimmeridgian). In order to surficially expose rocks which have very recently undergone ductile deformation, the phase of extension responsible (here termed E0) must have been substantial and fairly rapid, removing many kilometres (~20 km) of overburden from the buried lower Païkon megasequence.

Within the Païkon Massif, as it is presently, no extensional structures relating to this major pre-Kimmeridgian exhumation event have been identified. Similarly, no vestiges of the overlying rock pile, presumably emplaced onto the Païkon unit during D1 compression, remain within the Païkon Massif and must therefore have been completely removed by extension and denudation during and immediately following the E0 event. The only evidence of the E0 event is the fact that ductile, blueschist rocks must have been uplifted over a relatively short period of time and to a sufficiently high level to allow shallow-water carbonates to accumulate upon them.

4.3.2 - *Discussion and Regional Implications*

As stated in section 4.2.3, D1 compression is likely to have caused the westward obduction of the Middle Jurassic Guevgueli Ophiolite onto the lower Païkon megasequence resulting in ductile, blueschist deformation. The rapid change in regional stress regime from contractional (D1) to extensional (E0) is likely to reflect tectonic processes operating in the developing North Atlantic ocean (Robertson & Dixon, 1984).

Outwith the Païkon Massif there is clear evidence of a like-aged extensional event in the Pelagonian and Almopias zones to the west and in the Peonias subzone to the east, and in the more northerly Voras Massif (chapter 6). The eastern Pelagonian and Almopias zones record evidence of transtensional faulting and blueschist exhumation at

this time, and extension in these areas is sealed by transgressively overlying carbonates of Kimmeridgian age (Sharp, 1995). Recent work in the Pelagonian and Almopias zones (*op. cit.*) indicates that transtensional faulting is associated with acidic volcanism (the Liki and Klissochori Units) and ultimately the formation of the Upper Jurassic to Lower Cretaceous-aged Meglenitsa Ophiolite (Stais, 1994; Sharp, 1995) in a dextral pull-apart setting in the eastern Almopias subzone (Sharp, 1995). Similar transtensional faulting and associated sequences have been reported from the northern extension of the Pelagonian zone in former Yugoslavia (Dimitrijevic & Dimitrijevic, 1976).

In short the Meglenitsa Ophiolite of the eastern Almopias zone formed in the Upper Jurassic-Lower Cretaceous due to E0 extension (Stais, 1994; Sharp, 1995). A similar tectonic setting and age is also envisaged for the Ano Garefi Ophiolite of the Voras Massif to the north (see chapter 6) and possibly for some of the ophiolitic bodies of the Peonias subzone to the east (the Innermost Hellenic Ophiolite Belt or IMHOB; Haenel-Remy & Bebien, 1985; Bebien *et al.*, 1986; see chapters 1 and 7). More specifically, it is feasible that the western part of the Guevgueli Ophiolite, and possibly the Sithonia Ophiolite to the south, formed by dextral transtension at this time (Uppermost Jurassic - pre-Kimmeridgian). WNW-ESE-oriented transtension in the western Guevgueli Ophiolite (Bebien & Gagny, 1978; Jung & Mussallam, 1984; Bebien *et al.*, 1986; Bebien *et al.*, 1987) roughly corresponds to Uppermost Jurassic extensional stress regimes envisaged for the Pelagonian and Almopias zones (e.g. during the formation of the Meglenitsa Ophiolite; Sharp, 1995), whereas the SW-NE extension characteristic of the eastern Guevgueli does not (Bebien *et al.*, 1987).

The Guevgueli Ophiolite as a whole is interpreted to be late Middle to Upper Jurassic in age (166-146 Ma) based on radiometric dates obtained from the ophiolite itself (Spray *et al.*, 1984) and the coeval Fanos Granite (Borsi *et al.*, 1966; Makris, 1977; Jung *et al.*, 1980; Spray *et al.*, 1984 and Bebien *et al.*, 1987), and biostratigraphical dates obtained from overlying radiolarian cherts (Danelian *et al.*, 1996). It is widely accepted that the

Guevgueli ocean basin completely separated the Païkon Massif from the Serbo-Macedonian Massif during this period (Mercier *et al.*, 1975; Bebien & Mercier, 1977; Dimitriadis & Asvesta, 1993; Stais, 1994). However, it is possible that the 166-146 Ma dates only correspond to the eastern part of the present day Guevgueli Ophiolite and that the western part of the Guevgueli complex is somewhat younger. For example, the western part of the Guevgueli Ophiolite has a completely different structural organisation (Haenel-Remy & Bebien, 1987) and is in faulted contact with the eastern part of the complex (Figure 4.16, Bebien & Mercier, 1977; Bebien, 1977; Bebien, 1982). Moreover, the western and eastern parts of the Guevgueli complex differ significantly in their geochemical characteristics; the western part being more akin to the Meglenitsa and Sithonia Ophiolites to the east and south respectively (i.e. Mid-Ocean Ridge Basalts) than to the eastern Guevgueli rocks (i.e. Calc-Alkaline Basalts; Bebien, 1977; Bebien, 1982; Bebien *et al.*, 1986; Bebien *et al.*, 1987). These geochemical discrepancies have been attributed to spreading taking place along a dextral transtensional shear zone (i.e. to form the majority of the IMHOB) with the contemporaneous development of small pull-apart basins (i.e. the Guevgueli and Sithonian Ophiolites; Bebien *et al,* 1987). However, the difference in geochemical signature between pre-D1 "Eohellenic" ophiolites and later-formed "Neohellenic" transtensional pull-apart basins has been noted in many other parts of the Internal Hellenides (Smith, 1993). It should also be noted that the western part of the Guevgueli complex does not have an intrusive relationship with the Middle-Upper Jurassic Fanos Granite, the two units always being separated by a significant fault.

In an attempt to more accurately date the western part of the Guevgueli Ophiolite, radiolarian fauna from within red cherts at the top of the western volcanic complex were extracted and studied during the course of this work. However, due to post-depositional deformation no accurate age constraints could be obtained (T. Danelian, pers.comm., 1995) and thus a two-stage spreading history for the Guevgueli Ophiolite complex is

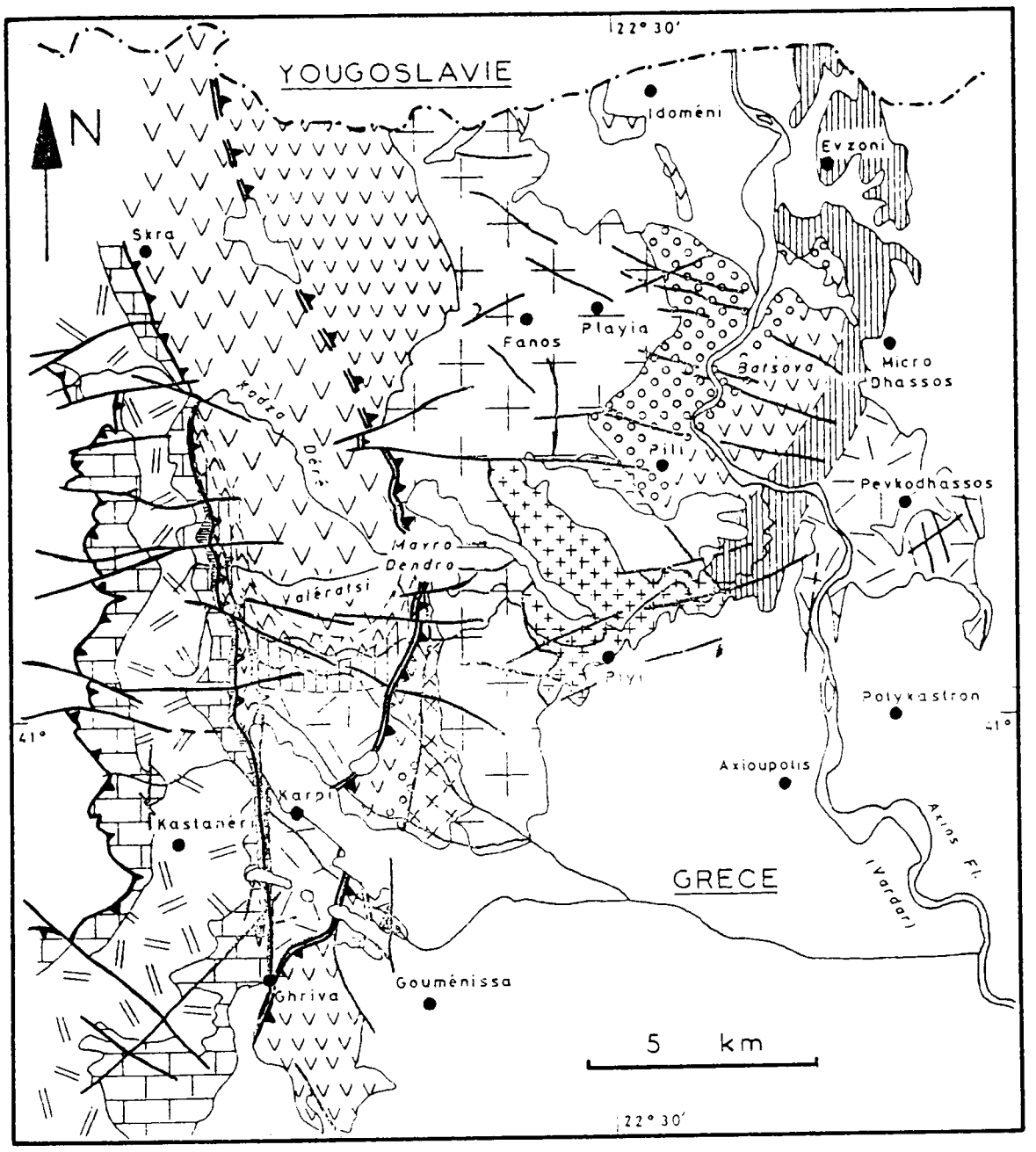


Figure 4.16 - Simplified map of the Guevgueli Ophiolite (Peonias subzone), after Bebien (1982). The map shows the western and eastern sides of the Guevgueli Ophiolite separated by a major reverse fault which runs from the Yugoslavian border in the north to Ghriva village (Païkon-Guevgueli contact) in the south.

conjectural at this stage and further biostratigraphical, structural and geochronological investigations on the western side of the Guevgueli complex are required to either support or refute this hypothesis, which will be discussed further in chapter 7.

It is thus likely that the blueschist facies rocks of the lower Païkon megasequence were exhumed during a major phase of regional extension (E0) which affected the whole of the Internal Hellenides and produced secondary oceanic crustal rocks to both the east and the west of the Païkon Massif; further discussion in chapter 7.

4.4 - LOWER CRETACEOUS COMPRESSION - A JE2 EVENT ?

4.4.1 - *Previous Conclusions*

Mercier (1968) documented the existence of the "Calcaires de Khromni" (Khromni Limestones of this work) and "Le Flysch Éocrétacé" (Ghrammos Formation of this work) in southwestern parts of the Païkon Massif only. In light of this, Mercier concluded that the Cretaceous Transgressive Limestones unconformably overlie the Kastaneri Formation in northern parts of the Massif and to the east (Figure 4.17). Following Mercier's work, Vergely (1984) described a second phase of compressional deformation of Lower Cretaceous age, postulated to have occurred subsequent to Upper Jurassic (D1 and E0) deformation, which he named JE2 (Figures 4.1 & 4.2). Vergely also identified this Lower Cretaceous JE2 event in the Pelagonian and Almopias zones to the west, and concluded that it was a compressional event of regional significance which affected the whole of the Internal Hellenide belt. The JE2 is evidently characterised by brittle E- to SE-verging thrusts and folds generated by the overthrusting of Almopias units from the west (Vergely, 1984).

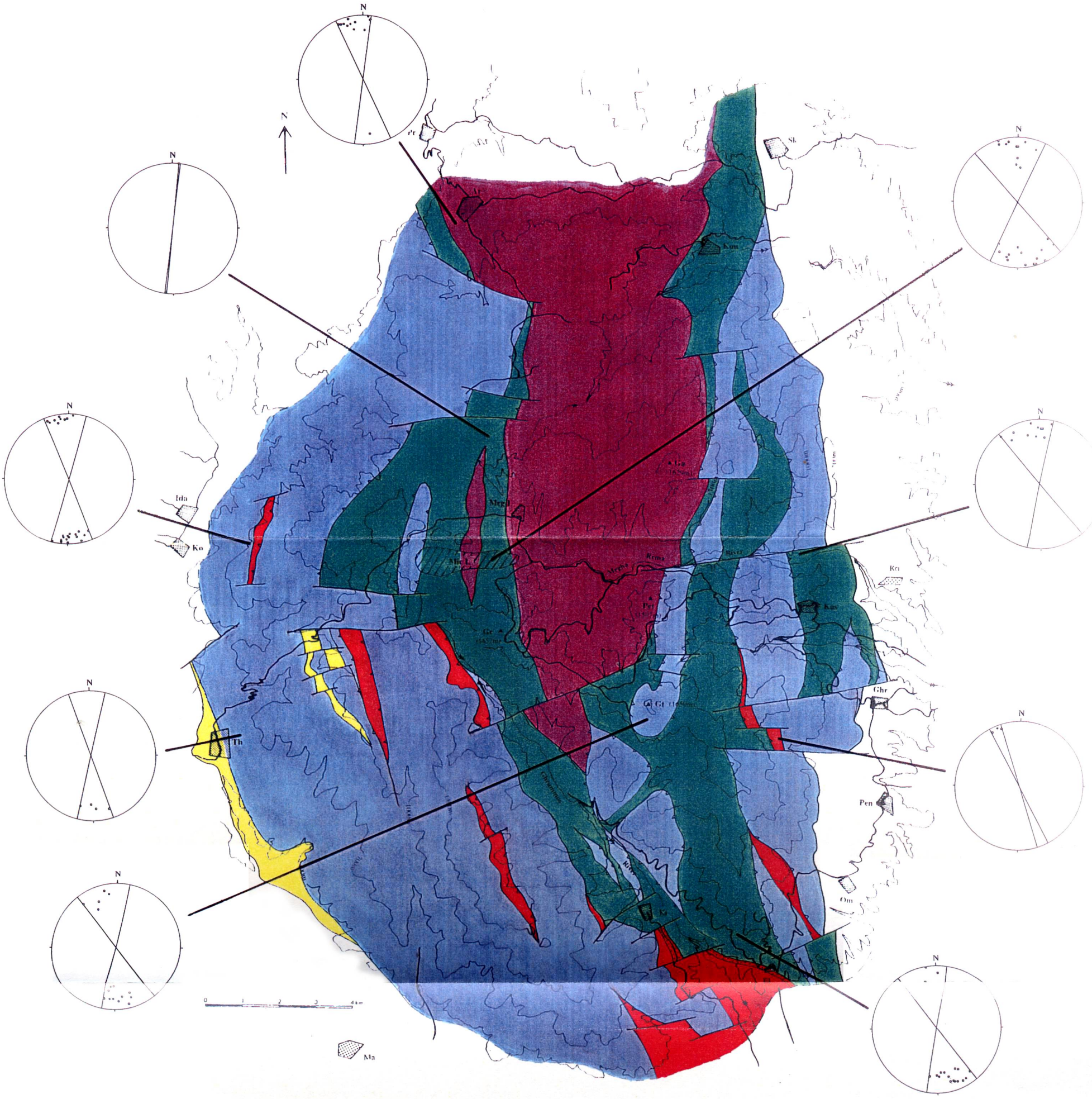


Figure 4.17 - Geological map of the Païkon Massif with stereographic projections showing the orientation of the D2 lineation from various localities. The D2 lineation trends variably from NW to NNE and is represented by small full circles.

4.5.2 - *Recent Findings and New Key Localities*

New key localities studied during the course of this work reveal, contrary to the findings of Mercier (1968), that the Ghrammos Formation extends over the entirety of the study area, from north to south, on both eastern and western sides of the Païkon Massif (Brown & Robertson, in press; chapter 3.8). It has also been shown (chapter 2.2.5 and 2.2.6) that gradational, depositional contacts exist between the Khromni Limestones and the Ghrammos Formation (Figure 2.15) and between the Ghrammos Formation and the Cretaceous Transgressive Limestones (Figures 2.16a & b). Thus it is concluded here that field observations at key localities (e.g. 3 km south of Khromni village, localities 439 and 440; Figure 4.3) indicate that a regional scale unconformity does not separate the Cretaceous Transgressive Limestones from underlying lithological units, and that the passage from the Kimmeridgian-Portlandian Khromni Limestones to the Ghrammos Formation and from the Ghrammos Formation to the Cretaceous Transgressive Limestones is conformable. Where minor discordances do occur, they are likely to represent localised non-deposition in the Ghrammos fluvial system or minor, localised uplift and subsidence as opposed to a penetrative compressional event of regional scale.

In order for the existence of a JE2 event to be supported, the Khromni Limestones and Ghrammos Formation must have been subjected to a phase of folding which does not extend into the Cretaceous Transgressive Limestones or any of the other upper Païkon megasequence stratigraphic units. Vergely (1984) described these JE2 folds as chevrons with E to SE vergence. During this study, such E- to SE-verging chevron folds were indeed observed within the Khromni Limestones and Ghrammos Formation on the western side of the Païkon Massif, but they were also observed in the overlying Cretaceous Transgressive Limestones, Buff Pelagic Carbonates and Tchouka Flysch, and were seen to fold the contacts between the Cretaceous Transgressive Limestones and both the Ghrammos Formation below and the Buff Pelagic Carbonates above

(Sharp & Robertson, 1992; Sharp, 1995; Brown & Robertson, 1994, in press). It is therefore unlikely that these folds were generated during a compressional event of Lower Cretaceous age, and a Tertiary age for these fold structures is proposed. In fact, all fold structures assigned by Vergely (1984) to the JE2 event are characteristic of, and can be confidently attributed to, the early Tertiary D2 compression event in the western Païkon Massif (see section 4.6). Importantly, all stratigraphic units of the upper Païkon megasequence, from the Khromni Limestones to the Tchouka Flysch, have undergone identical structural histories and no evidence exists to support Vergely's proposal of an additional contractional event of Lower Cretaceous age.

4.5.3 - *The Regional Picture*

As stated above, Vergely concluded that JE2 affected the whole of the Internal Hellenides. However, recent work by Sharp (1995) has, in accordance with this work, concluded that no evidence of a JE2 event could be found in the Pelagonian or Almopias zones and Vergely's JE2 structures can again be assigned to Tertiary tectonism. The Upper Jurassic to Lower Cretaceous Meglenitsa Ophiolite of the eastern Almopias subzone is unconformably overlain by carbonates of Aptian/Albian age, but this discordance has been attributed to localised deformation along the western margin of the eastern Almopias and not a regional scale event (Sharp, 1995). Further research is still required to either support or refute the existence of a JE2 event within areas more "internal" than the Païkon Massif; such structural investigations were outside the scope of this work.

Hence, in light of the new observations made during this study, it is here concluded that no evidence exists within the Païkon Massif for a "JE2 event" and that all compressional structures which formed subsequent to D1 can be attributed to Tertiary tectonism (D2 and D3; chapters 4.6 and 4.7 respectively). The upper Païkon

megasequence was therefore deposited free of significant compressive stress during the Upper Jurassic and Cretaceous.

4.5 - UPPER CRETACEOUS (TURONIAN) EXTENSION - E1

4.5.1 - *Platform to Basin Transition : the Cretaceous Transgressive Limestones and Buff Pelagic Carbonate.*

As described in chapter 3.9 and 3.10, the shallow-water platform carbonates of the Cretaceous Transgressive Limestones gave way to deeper-water pelagic carbonates (the Buff Pelagic Carbonates) over a relatively short interval. The transition from the Cretaceous Transgressive Limestones to the Buff Pelagic Carbonates is marked by a significant hiatus in deposition and an ubiquitous ferruginous crust surface (up to 5 cm thick) overlying a locally-occurring intraformational limestone conglomerate at the top of the Cretaceous Transgressive Limestone carbonate platform succession (Sharp & Robertson, 1992; Sharp, 1995; Brown & Robertson, in press). The extensional event which took place subsequent to deposition of the Cretaceous Transgressive Limestones (chapter 3.9) and prior to deposition of the Buff Pelagic Carbonates (chapter 3.10) has been termed E1 by Brown & Robertson (in press). The ferruginous crust surface is overlain by deeper-water, *Globotruncana*-bearing limestones of the Buff Pelagic Carbonates (Sharp & Robertson, 1992; Sharp, 1995; Brown & Robertson, in press).

It was initially proposed that the ferruginous crust formed during a period of non-deposition which occurred during extensional collapse of the Aptian/Albian to Turonian platform to a deeper-water, pelagic setting (Sharp & Robertson, 1992). However, the more recent identification of rhizoliths and *Microcodium* within the red ferruginous crust indicate that the crust formed during subaerial exposure (T. Scoffin, pers. comm. to I. Sharp, 1993), suggesting that a period of uplift and emergence immediately preceded collapse of the platform (Cretaceous Transgressive Limestones) and a

corresponding switch to basinal sedimentation (Buff Pelagic Carbonates and Tchouka Flysch).

4.5.2 - *Eustatic Versus Tectonic Controls*

The rapid change from platformal to basinal facies can be explained by tectonically-induced extensional collapse or a rapid eustatic sea-level rise. The Turonian stage has been documented as a period of global sea-level high-stand (Haq *et al.*, 1987; Hall, 1988) and so eustatic drowning is likely to have played a role in this deepening event. However, regionally significant extension, although not directly evident from the Païkon Massif, affected much of the Hellenic orogenic belt at this time, and so, Turonian deepening cannot be rationalised by eustasy alone. For example, the Turonian stage in Argolis and Euboea (respectively of Clift, 1990 and Robertson, 1990a) is characterised rifting, sea-floor spreading and ophiolite genesis, while subsidence on a regional scale has been documented throughout other parts of the Hellenides (Fleury, 1980; Thiebault, 1982; Harbury, 1986 and Robertson *et al.*, 1991). In northern Greece, this extensional event has also been recognised within the neighbouring Pelagonian and Almopias zones, where syn-sedimentary normal faulting and the onset of deep-water carbonate deposition have been documented (Sharp, 1995). Therefore the Turonian E1 event is likely to reflect a regional extension event which occurred in conjunction with a global sea-level high-stand. Notably, this regional subsidence event predates the first evidence of compression-related flexural subsidence in the Eastern ("internal") Hellenides of Early Tertiary age, i.e. D2 of Brown & Robertson (in press).

4.5.2 - *Discussion and Conclusions*

The Turonian stage in the Païkon Massif involved a short period of uplift and subaerial exposure followed by regional extensional collapse and drowning of the earlier Cretaceous carbonate platform. Initial subaerial exposure may reflect a brief period of

flexural footwall uplift which occurred prior to rift-related subsidence (Sharp, 1995; this work). For the first time, this work has identified the E1 deepening event on the eastern side of the Païkon Massif as well as on the west, indicating that both flanks of the anticlinal Païkon Massif have undergone identical structural histories.

As noted in chapter 3.10, Mercier (1968) locally identified a shallow-water faunal assemblage of Maastrichtian age from western parts of the Païkon Massif. These findings may reflect normal faulting at this time, resulting in basinal areas undergoing pelagic/flysch deposition (as seen in southern Païkon Massif), while coeval shallow-water deposition was concentrated on locally-occurring platform highs.

4.6 - EARLY TERTIARY COMPRESSION - D2 "Neohellenic" Deformation

4.6.1 - *Introduction*

The earliest Tertiary phase of compression (D2 of Brown & Robertson, in press) is probably the most significant deformation event to have affected the study area in terms of the present-day configuration of lithological units within the Païkon Massif. The structures which formed during D2 have not only resulted in considerable thrust-imbrication, folding and disruption of the stratigraphic column, but are responsible for folding the entire Païkon subzone (chapter 1) into a broad, upright, south-plunging anticline which spans the entire Païkon Massif.

D2 structures are common throughout the study area, but are most conspicuous in western and central areas than in the extreme east. This is due to overprinting by structures associated with the subsequent D3 compressional deformation phase along the Païkon-Guevgueli margin (section 4.7). On the western side of the Païkon Massif, the majority of fold and thrust structures associated with D2 deformation have a

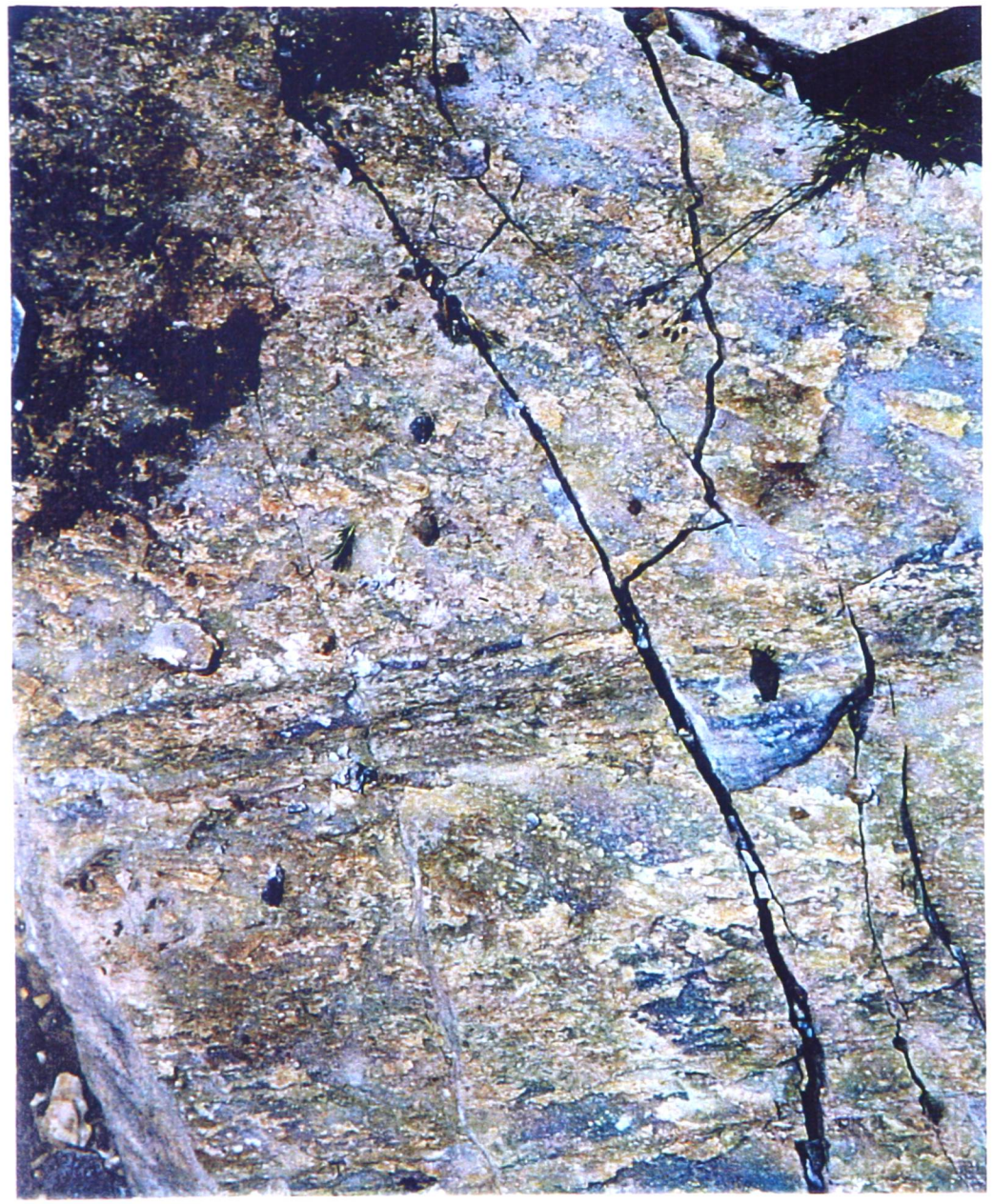
northeastward polarity, whereas those seen on the eastern side of the Païkon (i.e. between Kastaneri and Micra Livadia, Figure 4.3) have roughly westward vergence; this dual vergence is related to overthrusting of the Meglenitsa and Guevgueli Ophiolites respectively, and will be discussed in section 4.6.4 below, and in chapter 7.

4.6.2 - *Field Observations*

Post-Maastrichtian deformation saw the re-instigation of compressive stresses in the Païkon Massif, resulting in D2 structures. All stratigraphic units within the Païkon Massif, from the Gandatch Formation to the Tchouka Flysch, were greatly affected by this phase of contractional deformation. During D2, an extensive fold-and-thrust belt developed across the Païkon Massif, characterised by dual-vergent fold and fault structures and a 295°N to 010°N-trending, axis-parallel lineation (Figure 4.18). Every unit in the area was affected by this phase of deformation and, at key localities, D2 structures overprint those of D1, such as at the structural type locality between Micra and Meghala Livadia (central Païkon, Figures 4.3 and 4.19).

At the structural type locality (Figure 4.19), folds resulting from both D1 and D2 events are present. Those of D1 are ductile and tight to isoclinal in nature and display a consistent E-W-trending axis-parallel lineation, as described in section 4.2. These D1 folds were then refolded about the roughly NNW-trending axes of brittle, flattened chevron folds typical of D2. The D1 lineation is similarly folded. At this locality the SSW-trending lineation of the D3 compressional event (chapter 4.7) can be seen overprinting all earlier structures.

North of Khromni village (locality 401; Figure 4.3), a remnant D1 fabric is preserved



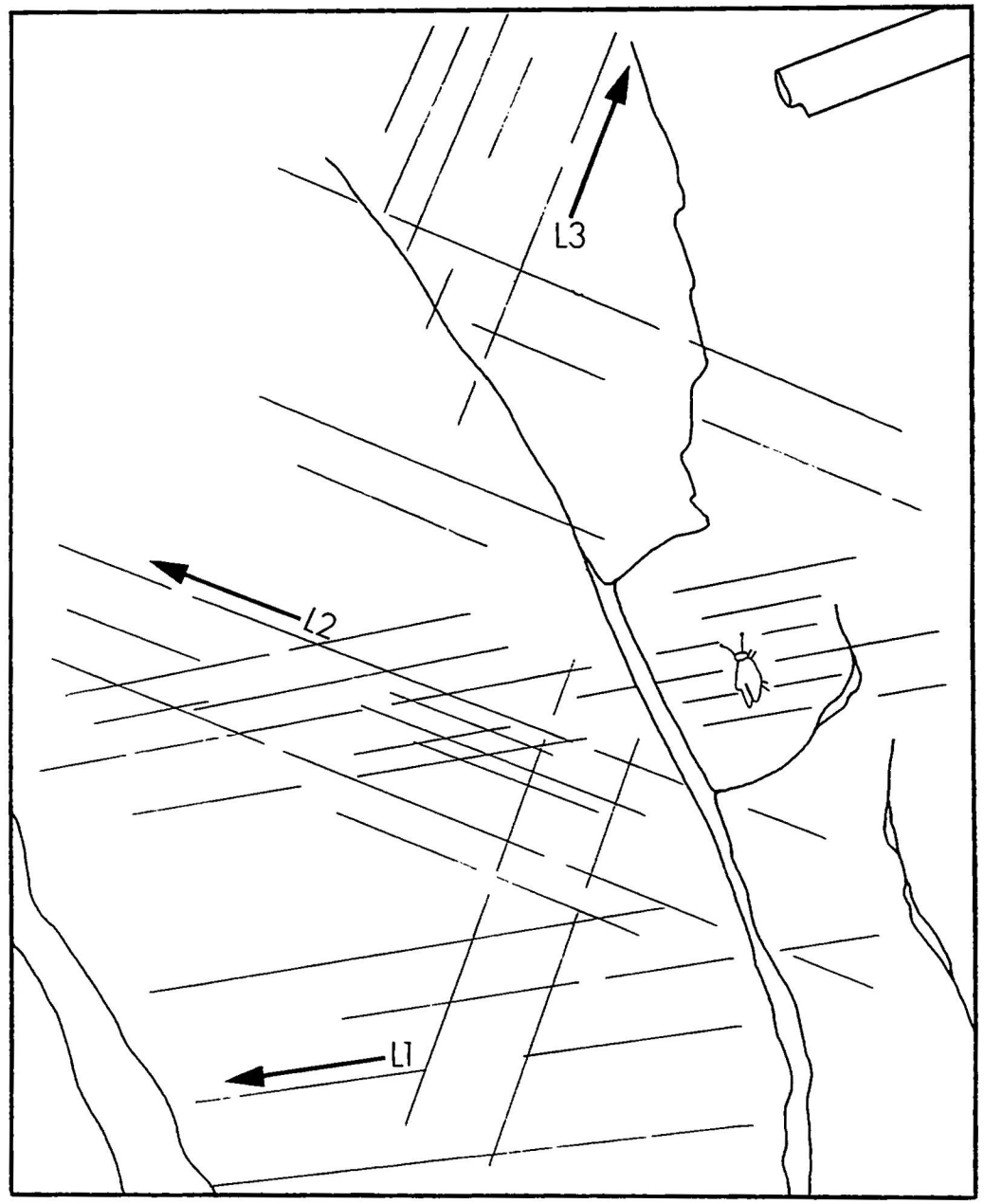


Figure 4.18 - Field photograph showing the lineations that have been generated during the three main compressional events in the Païkon Massif. The lineations are on a primary bedding surface within the marbles of the Gandatch Formation. The D1 lineation is most prominent, trending sub-horizontally across the photograph. The D2 lineation trends diagonally from bottom right to top left and the D3 lineation, which is very faint here, trends from top right to bottom left (see adjacent sketch for clarification).



Figure 4.19 - Field photograph and sketch of the structural type locality between Micra and Meghala Livadia, central Païkon Massif (see Figure 4.3). In the foreground, east-west-trending isoclinal folds can be picked out and are refolded by D2 non-cylindrical, tight to chevron folds in the middle ground. The D2 folds are warped by open D3 folds which are not obvious in the photograph. S0 surfaces at this locality display three distinct lineations that correspond to D1 (east-west), D2 (northwest-southeast) and D3 (northeast-southwest) deformation events.

within competent siliceous clasts, set in a less competent, schistose matrix in which the original E-W D1 fabric has been completely obliterated by the NNW-trending D2 fabric. The D2 fabric is also seen in the clasts, but only crenulates the D1 fabric there (see Figure 4.15).

Folds

All folds associated with D2 contraction are characteristic of structures formed in a high-level, brittle crustal regime. Chevron, box and open folds prevail, particularly in the more competent carbonate units, while reverse faults, duplex structures and a penetrative schistosity (S2) dominate less competent units (e.g. Livadia, Kastaneri and Ghrammos Formations).

The interbedded marbles and schists of the Gandatch Formation vary in fold style depending on the carbonate:clastic ratio at any given locality. At locality 296, for example, the Gandatch Formation comprises dominantly marbles (Stratotype 1, chapter 3.4) and is folded into inclined chevron folds (Figure 4.20). At this locality, chevron folds are not similar, and S0 compositional layering surfaces display bedding-parallel slickenside structures indicating that layer-parallel shear has taken place along D2 fold limbs. The axial directions of the folds plunge towards 200-208°N and fold asymmetry indicates dominant vergence towards the ESE. Thin (<1 cm) schistose interbeds preserve a remnant S0-parallel S1 foliation, which has been folded about the hinges of D2 folds and crenulated by the D2 fabric. Mixed carbonate-clastic areas (Stratotype 2, chapter 3.4), on the other hand, tend to form folds which are more open and have less angular hinge zones, as observed west of Kastaneri village at locality 422 (Figure 4.21). In this area, D2 folds are open and upright to slightly inclined in orientation. The folds are slightly asymmetrical towards the northeast, but no definitive vergence direction was noted. Fold hinges trend towards the northwest and axial surfaces dip 37-76° towards 247-261°N.

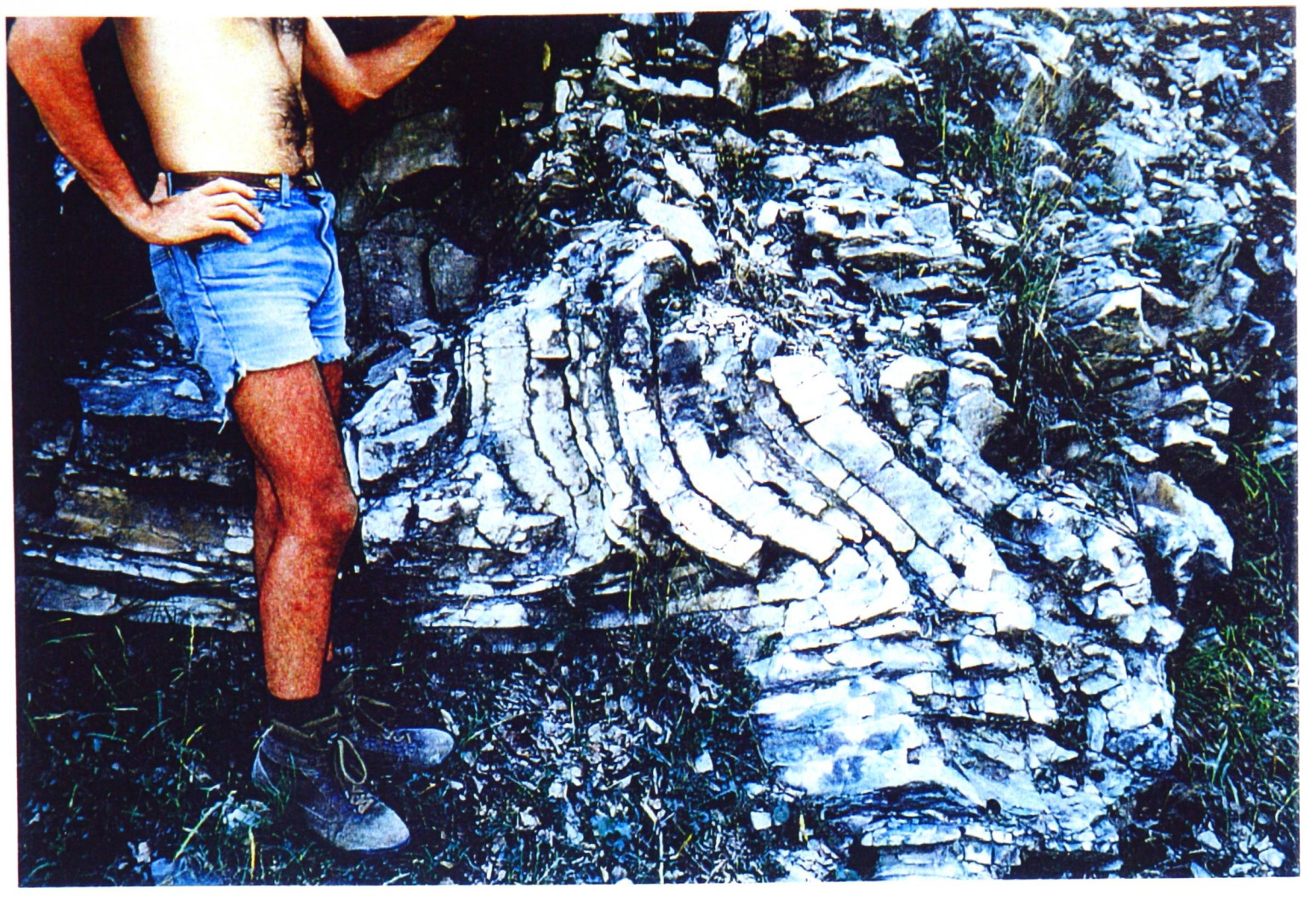


Figure 4.20 - Field photographs of chevron folds typical of D2 deformation in the marbles of the Gandatch Formation (locality 296, by Micra Livadia). In the upper photograph the chevron folds have undergone layer-parallel shear and the fold nose is slightly flattened as a consequence.

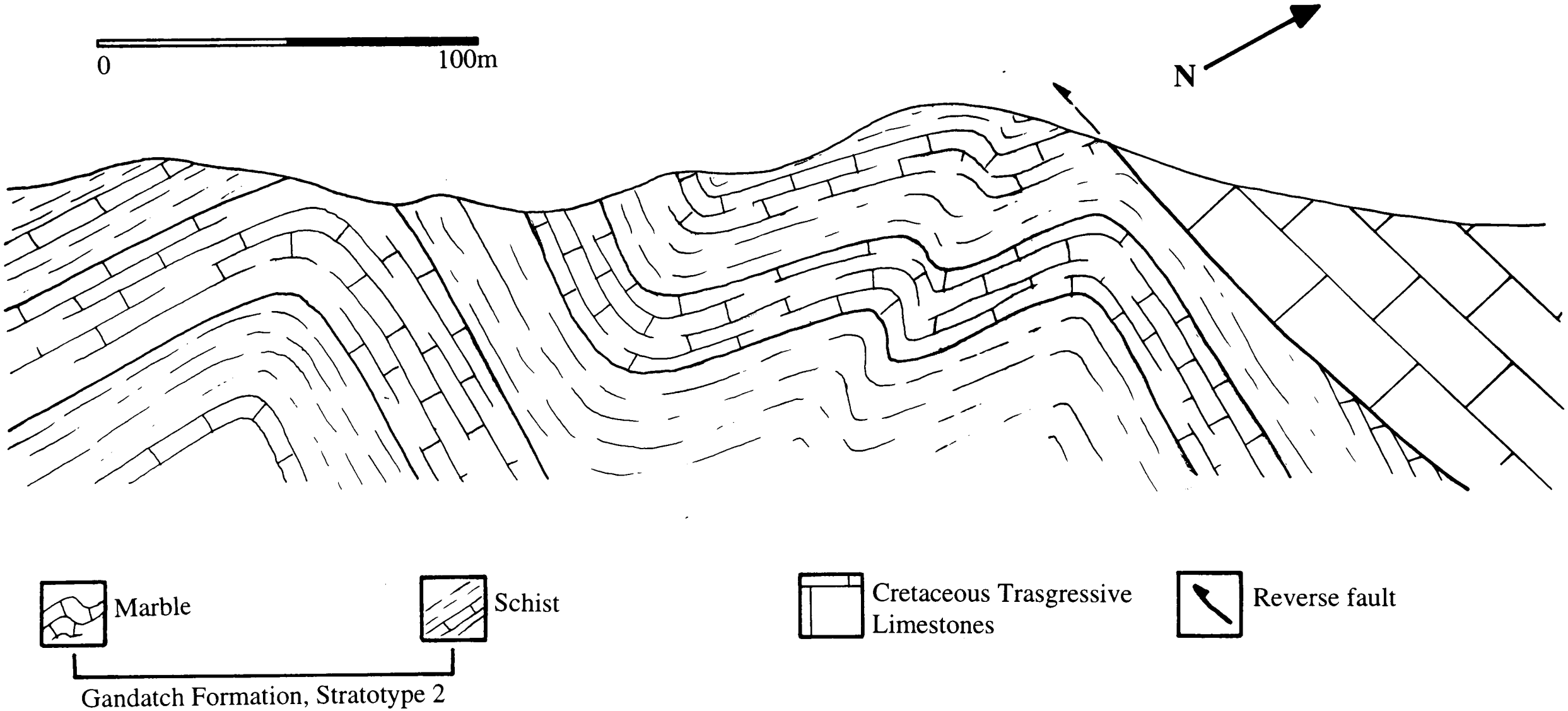


Figure 4.21 - Field sketch of D2 folds within Stratotype 2 of the Gandatch Formation (locality 422, by Mount Petrades, central Païkon Massif). The Gandatch meta-sediments are overlain, with an east-dipping reverse fault, by an imbricate of the Cretaceous Transgressive Limestones. D2 folds are asymmetrical, inclined and open to tight with rounded fold noses.

The Cretaceous Transgressive Limestones contain very few clastic horizons and are thus very competent. Consequently, the governing style of folding in this unit is brittle, open chevron and box folding, coupled with extensive reverse faulting. These structures are best observed on the western margin of the Païkon Massif (Figure 4.22). Due to the competent and brittle nature of this unit, jointing is pervasive and, as a result, D2 folds are difficult to pick-out in many areas. Therefore, fold structures are most easily recognised where the Cretaceous Transgressive Limestones contact the Buff Pelagic Carbonates or the Tchouka Flysch, or where less competent clastic interbeds occur. In such areas the outcrop pattern reveals the D2 fold structures that are less evident elsewhere.

D2 folds were also observed within the Kastaneri Formation, although less commonly. These consist of upright to inclined open folds. In most areas, however, the relatively incompetent volcanics and volcaniclastics of this unit deform by faulting and by forming penetrative C-S and schistosity fabrics, duplex structures and shear zones (Figure 4.23). At locality D (Figure 4.3), a single, meso-scale, open fold pair deform the volcaniclastics of the Kastaneri Formation. There is a high degree of angular discordance between the D2 axial-planar fabric and the S0/1 layering, and vergence is towards the WSW. Both D2 and D3 lineations are evident.

All folding associated with D2 compression, regardless of fold style, is non-cylindrical. Fold hinges die out laterally, as wavelength, amplitude and displacement diminish along strike, generating pinch-and-swell-like structures (Figure 4.24 and 4.19). Consequently, the apparent vergence of D2 folds varies between NE and SE in the western Païkon Massif, and SW and NW in the eastern Païkon Massif, although the dominant transport direction is to the ENE and WSW, respectively (Figure 4.25).

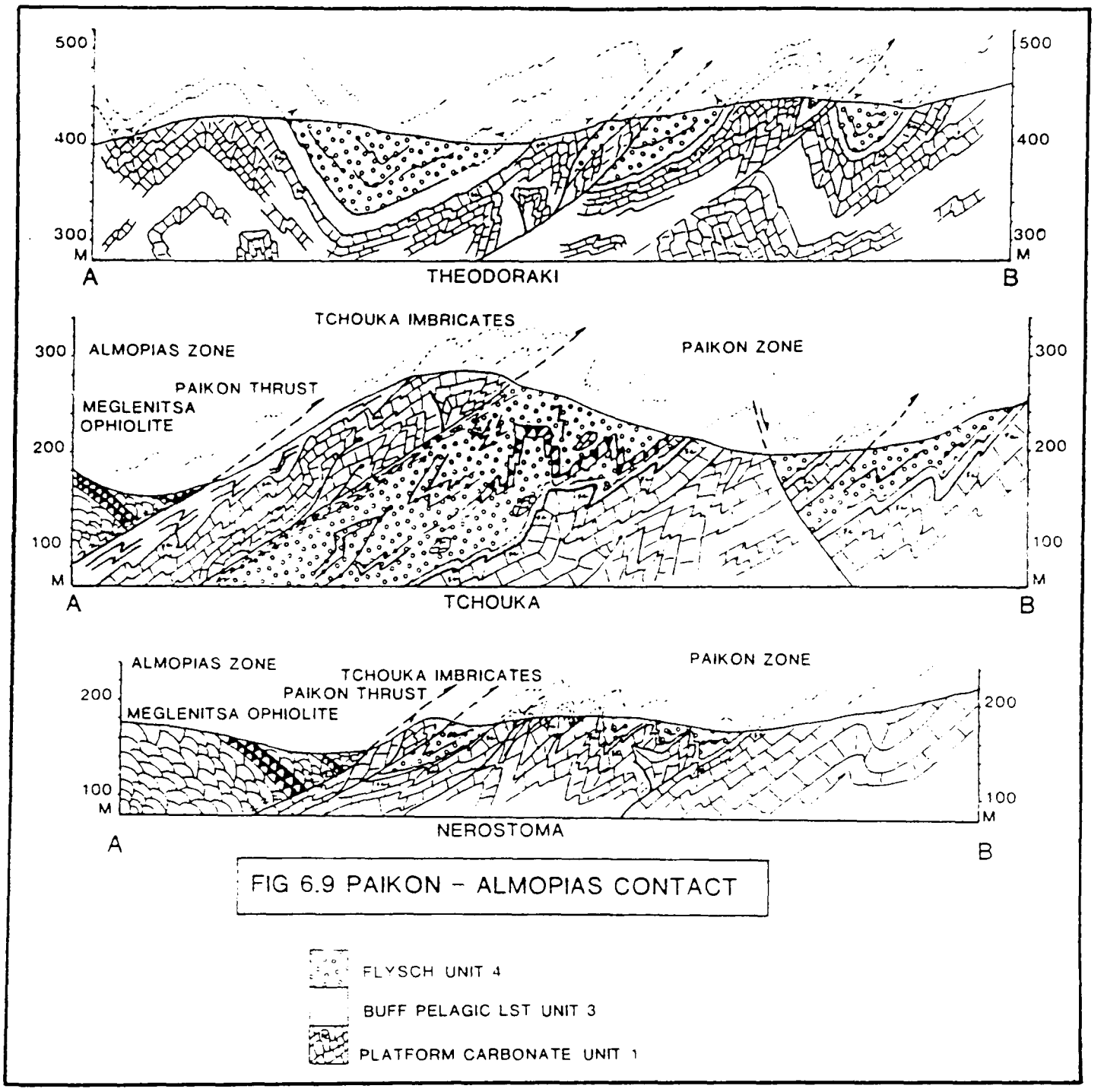
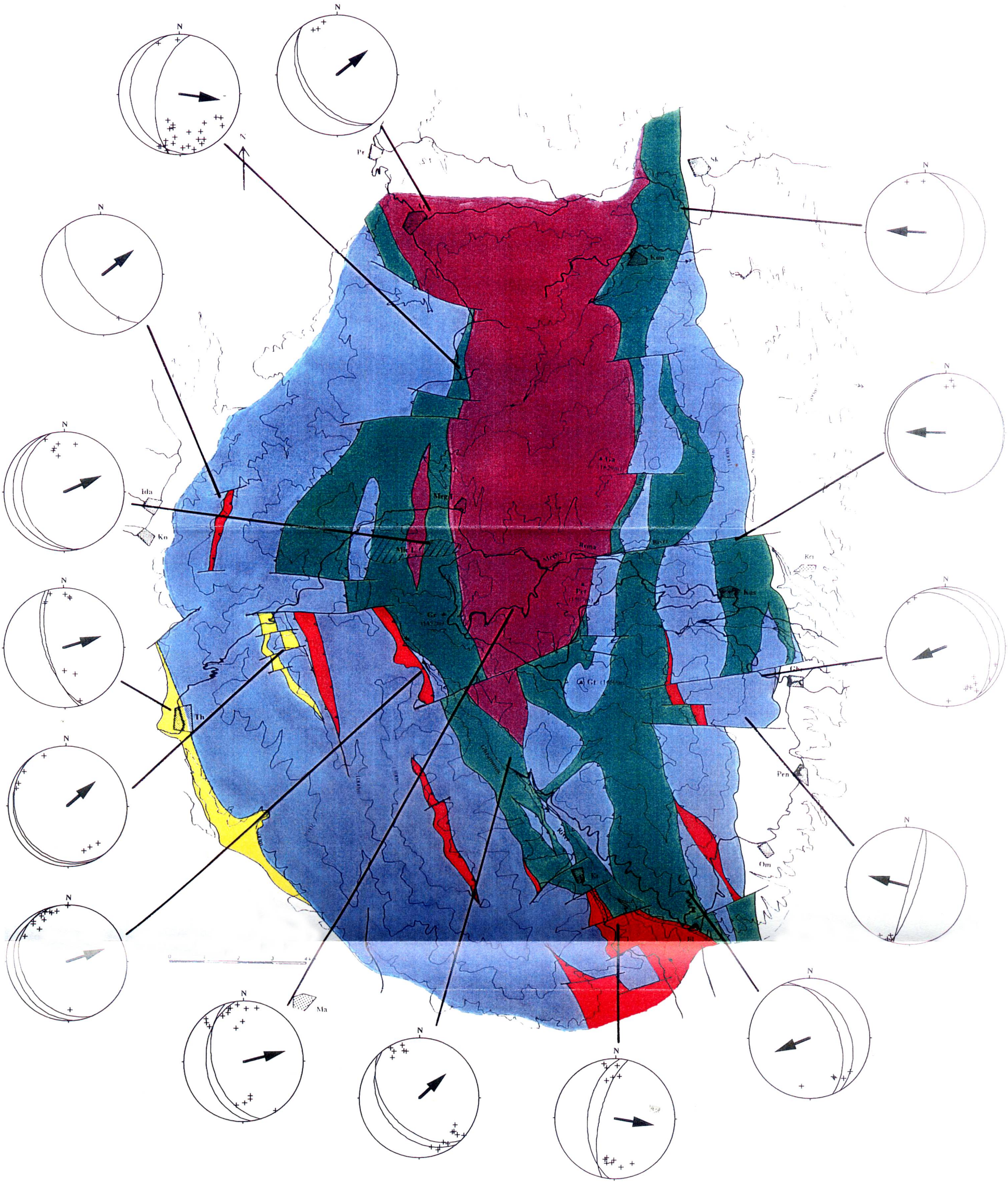


Figure 4.22 - Three cross-sections through the western margin of the Paikon Massif (after Sharp, 1995). In these areas (Theodoraki, Tchouka and Nerostoma, Figure 4.3) the Cretaceous Transgressive Limestones, Buff Pelagic Carbonates and Tchouka Flysch are chevron and box folded, reverse faulted and repeated by Tertiary D2 deformation. All structures indicate that the dominant direction of transport is towards the east and northeast.


N
Ida
Ko
Th
Ma
Kun
Kes
Prn
Om
Sk
Pr
Rema
Mega
Ali
Ki
Ku
Ta
Pet
Gr
Ch
Ri
Ba
Ha
Ta
Ka
Ma
Ta
Ka
Ta
Ka
Ta
Ka

Lineation. D2 folds are associated with an axis-parallel lineation, which trends ~295°N to 010°N in all parts of the Païkon Massif (Figure 4.18). Unlike the lineation generated during ductile D1 deformation, the lineation associated with D2 does not indicate the dominant transport direction, but is aligned perpendicular to it (i.e. parallel to the b-tectonic axis). Therefore, it is likely that the D2 lineation developed at the junction between the S2 foliation and the S0 compositional layering and is thus an intersection lineation (Passchier & Trouw, 1996; Figure 4.26). The relationship between the D2 foliation, the primary layering (S0) and the D2 lineation is well exposed at locality 23 (east of Micra Livadia; Figures 4.3 and 4.26). Here, the Gandatch Formation (Stratotype 2) is folded by ESE-verging flattened chevron folds which have a strong axial-planar fabric and a fold axis-parallel lineation. Three-dimensional surfaces show that the D2 lineation is generated along the intersection between S2 and S0/1 foliations. This phenomenon has also been reported from Tertiary structures in the Pelagonian zone to the west (Sharp, pers. comm, 1993).

Planar Structures. D2 thrusting and tear-faulting are ubiquitous, affecting all stratigraphic units from the basal Gandatch Formation to the topmost Tchouka Flysch. As described for D2 fold structures, D2 reverse faults propagate in opposite directions on either side of the study area: westward-directed thrusting predominates on the eastern side of the Païkon Massif, while essentially eastward-directed thrusting is typical on the western side, as evidenced by duplex structures (Figure 4.27a). Tear faults are generally aligned perpendicular to the direction of thrust propagation.

Reverse faulting is most prevalent in the less competent Livadia, Kastaneri and Ghrammos Formations and in the Tchouka Flysch, in which shearing is commonplace and the development of duplex structures widespread (Figure 4.27 and 4.27a). On the western flank of the Païkon Massif, all D2 planar structures dip at moderate angles towards 245

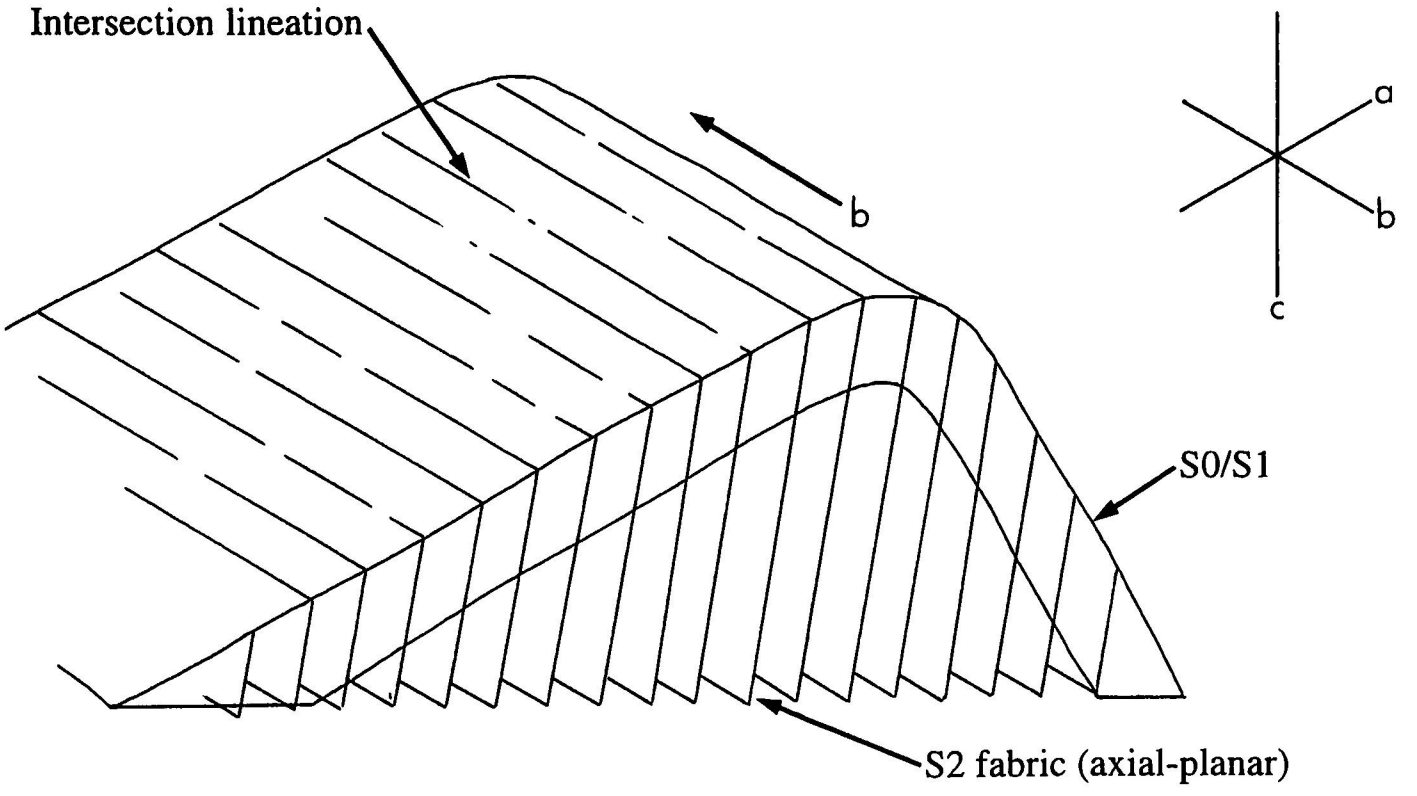


Figure 4.26 - Sketch diagram showing the geometric characteristics of the D2 lineation. The schistose fabric (S2) associated with D2 compression is axial-planer to D2 folds. The lineation occurs at the intersection between the folded foliation (S0/S1) and the S2 faric. It is thus an intersection lineation.



Figure 4.27 - Field photograph of a compressional duplex which was generated in the Ghrammos Formation sediments during D2 deformation (locality 278, south of Khromni village).



Figure 4.27a - Structural map of the Païkon Massif showing orientation data for the dip of bedding, the trend of lineations and the dip (and hence vergence) of duplex structures.

Bedding D1 lineation D2 lineation D3 lineation

Duplex structures

to 295°N and indicate that the overall transport direction is towards the ENE. In contrast, planar structures on the eastern side of the Païkon anticline dip at high to moderate angles towards 060 to 110°N, suggesting that transport in this area was dominantly towards the west.

In most areas, the Kastaneri and Livadia Formations are pervasively foliated, as are some horizons of the Gandatch Formation, the Khromni Limestones, the Ghrammos Formation and the Cretaceous Transgressive Limestones. Along D2 fold limbs this D2 fabric is at a high angle to S0/1 as demonstrated in Figure 4.28. At locality 1 (north of Eliftherohori), complex C-S fabrics and duplex structures affect the highly sheared Kastaneri Formation. "C" (shear) planes generally dip at high angles towards the west, while "S" (schistosity) planes dip steeply towards the east. This suggests high angle top-to-the-east shearing, although C-S fabric orientations were highly variable in this area. Where more competent horizons occur, sigmoidal duplex structures have formed between the spaced S planes and these also indicate a top-to-the east sense of shear. Similar duplex packages formed within the Ghrammos Formation (e.g. at locality 278; Figure 4.27), where shearing was concentrated in zones spaced between 0.5 and 2 m apart. Between the shear zones, sigmoidal, piggy-back duplex packages dip at moderate angles (30-60°) towards 265°N. Each sigmoidal "fish" in the duplex is in thrust contact with those above and below. Slickenside structures on such thrust contacts, and the geometry of the duplex as a whole, indicate top-to-the-east compressional movement.

Thrust-Imbrication and Flexural Foredeep Deposition

The most striking large-scale effect of D2 compression is extensive thrust-imbrication, which causes both repetition and shortening of the stratigraphic sequence, and the emplacement of thrust-bound sheets within and between stratigraphically unconnected units. In the vicinity of the Ghrammos River valley (southern central Païkon Massif),



Figure 4.28 - Field photographs showing the relationship between the D2 cleavage, or foliation, and primary compositional layering (S0). Due to the open to tight, chevron style of folding that characterises D2, S2 and S0/1 often meet at high angles. The Upper photograph shows the D2 fabric developed in a calc-schist horizon within the Gandatch Formation. The lower photograph shows the high-angle D2 faric within a marl horizon in the Cretaceous Transgressive Limestones.

thick (up to 200 m) laterally extensive (0.5 to 5 km) slices of Cretaceous Transgressive Limestones have been tectonically incorporated into the Kastaneri Formation (Figure 4.29) and along the Kastaneri/Livadia contact (Figure 4.30). Due to the northeast-directed thrusting process, the southwest-dipping Cretaceous imbricates are highly recrystallised, often strain-hardened and silicified, while the host volcanics/volcanoclastics are severely sheared and weathered (Figure 4.31).

A similar thrust relationship between the Cretaceous Transgressive Limestones and the Kastaneri Formation is seen on the eastern side of the Païkon Massif. The carbonates are again extremely recrystallised and the volcanics sheared, but duplex structures and C-S fabrics on the east side of the Païkon Massif indicate westward fault propagation. For example, Figure 4.33 shows such west-verging imbricate structures in the vicinity of Karpi and Ghriva villages.

In the vicinity of Micra Livadia (central Païkon Massif, Figure 4.3), meso- and macro-scale asymmetrical D2 flattened chevrons fold the contact between the Gandatch and Livadia Formations (Figure 4.34). The Gandatch marbles preserve D2 fold structures, while D2 axial-planar cleavages are all that remain in the schistose Livadia volcaniclastics. In the southern central Païkon Massif, similar thrust-imbrication and repetition can be observed between the Ghrammos Formation and the Cretaceous Transgressive Limestones (Figure 4.35), while in the extreme west, near the Païkon/Almopias contact at Theodoraki, imbrication of the Tchouka Flysch, the Buff Pelagic Carbonates, the Cretaceous Transgressive Limestones and occasionally the Ghrammos Formation occurs (Figure 3.65).

In a few key areas (e.g. locality 454, north of Eliftherohori village, southern central Païkon), chaotic mélange deposits underlie thick thrust-imbricates of Cretaceous Transgressive Limestone (Figure 4.36). The mélange deposits are derived partly from

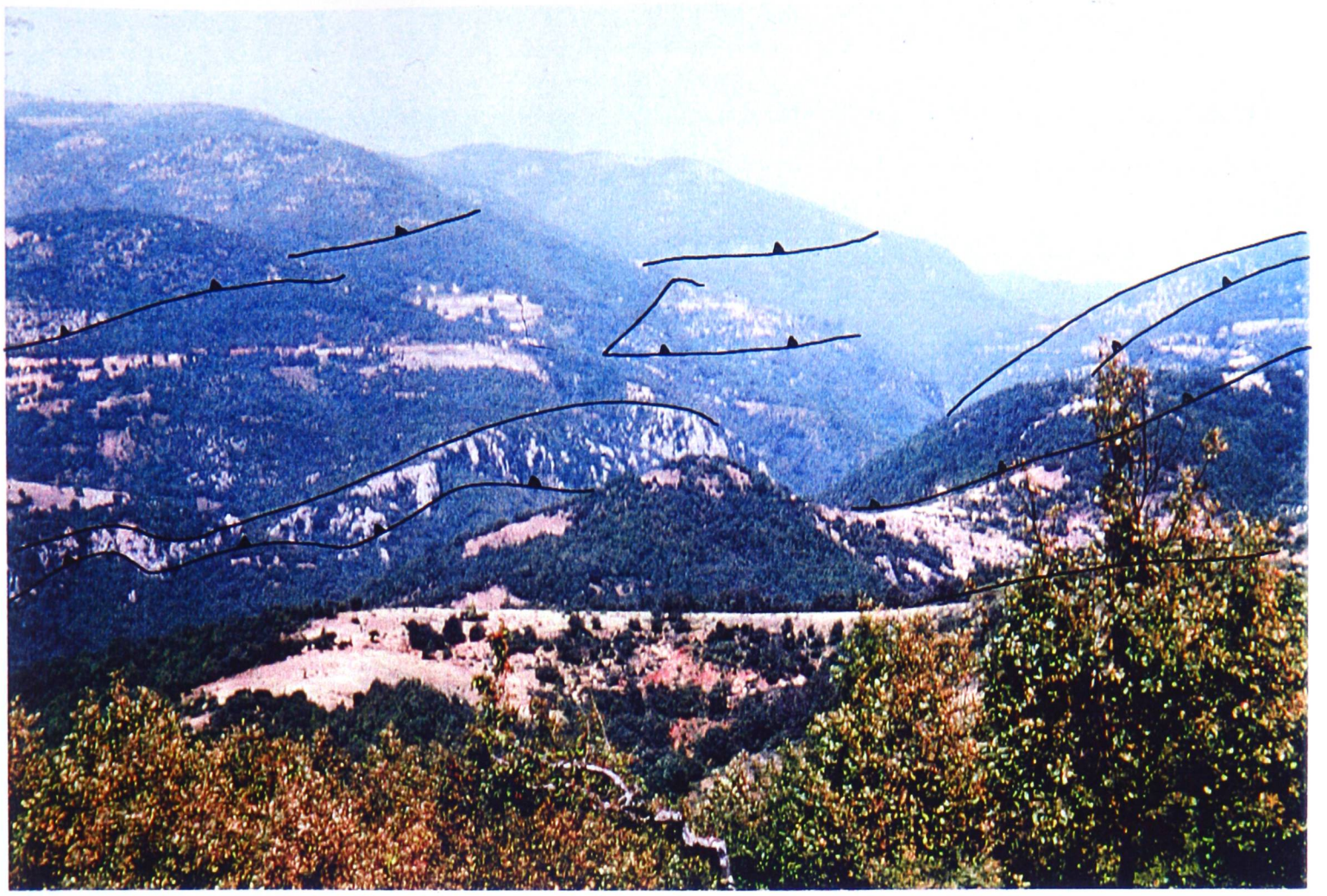


Figure 4.29 - Thrust imbricates of the Cretaceous Transgressive Limestones within the Kastaneri Formation (Ghrammos River valley, southern central Païkon Massif). The imbricates reach up to 1 kilometre thick and 10's of kilometres long.



Figure 4.30 - Thrust imbricate of Cretaceous Transgressive Limestone overlying the highly-folded Gandatch Formation (Micra Livadia, central Païkon Massif). The Cretaceous Transgressive Limestone is more rheologically competent than the Gandatch Formation and has thus avoided the intense folding which can be seen in the Gandatch Formation.



Figure 4.31 - Field photograph of an iron-stained thrust contact between the Kastaneri Formation (brown) and an imbricate of Cretaceous Transgressive Limestone (grey). Proximal to the thrust contact, the limestone is completely recrystallised and has been intensely veined and silicified. The brown volcanic rocks are highly sheared.

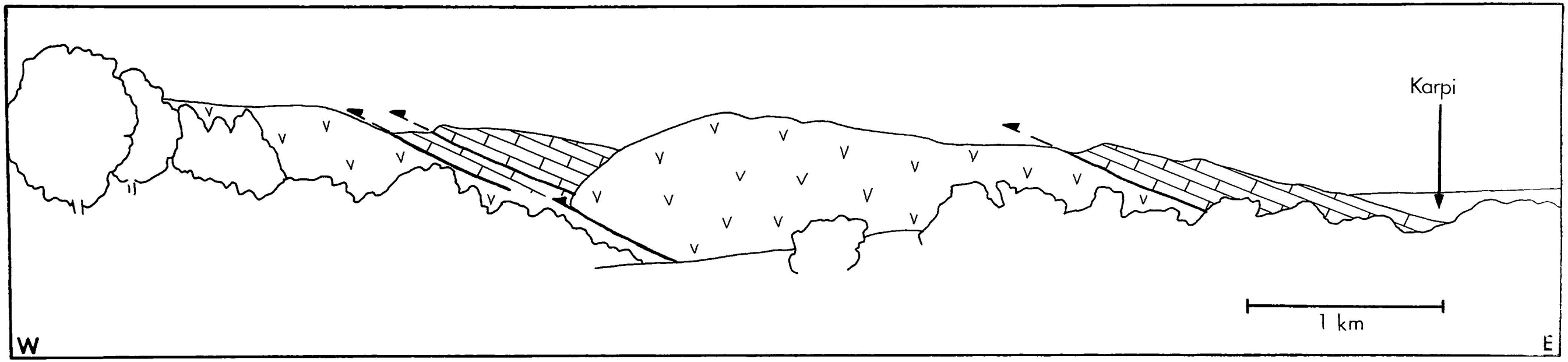
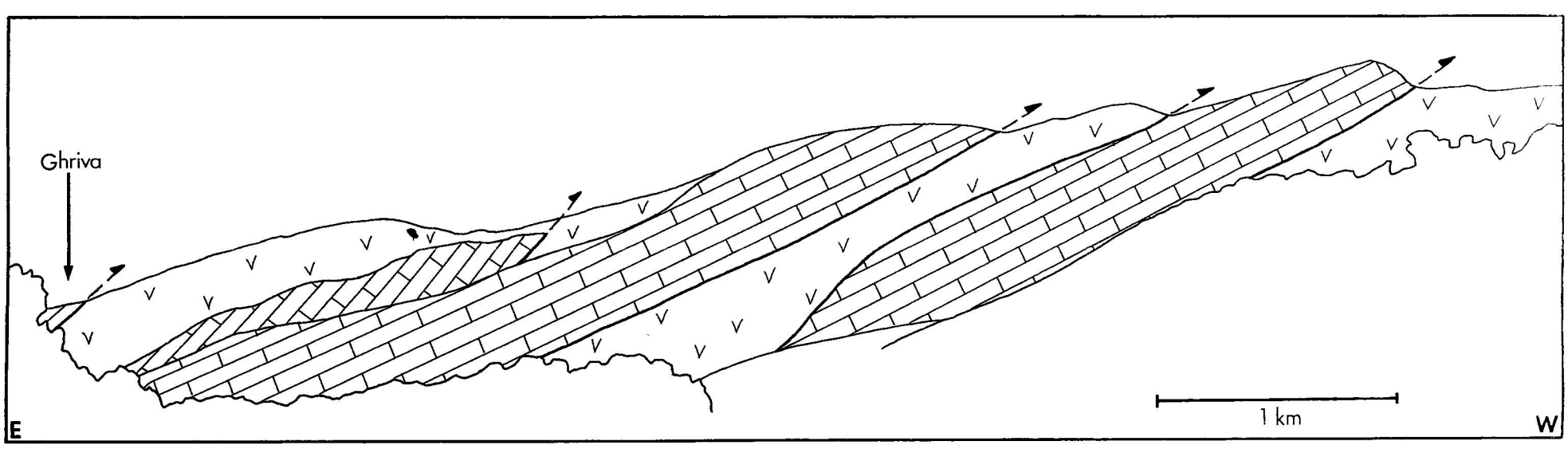


Figure 4.33 - Field photographs and corresponding sketches illustrating thrust imbricates of Creaceous Transgressive Limestone on the eastern side of the Païkon Massif. The upper photograph/sketch is taken looking north (Karpi village is down on the plain to the right) and shows limestone imbricates (brick patten) within the volcanics of the Kastaneri Formation (v pattern). The lower photograph is taken looking south and again shows imbricates within the Kastaneri Formation volcanics. In both cases the direction of thrust propagation is westward.







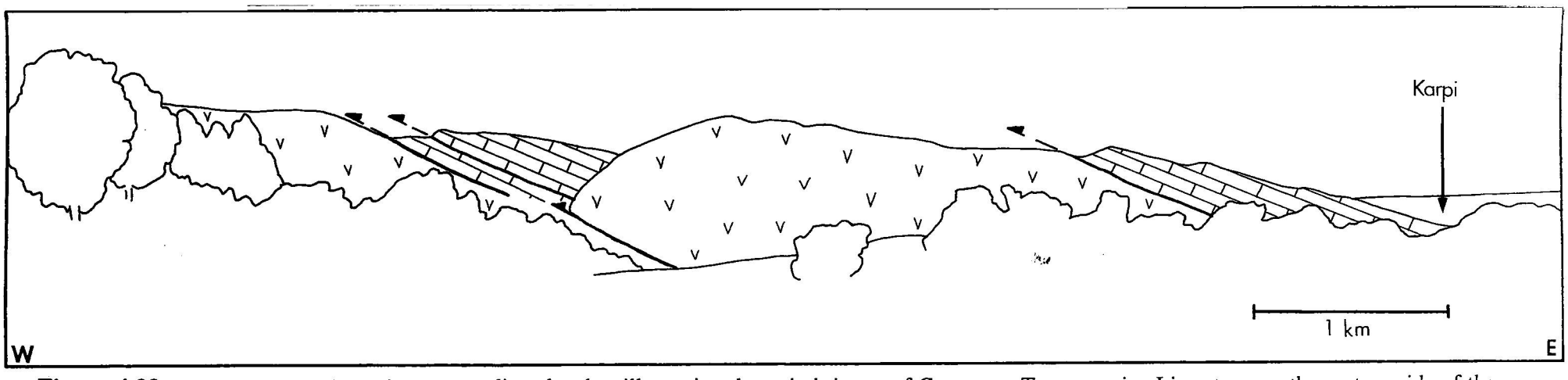


Figure 4.33 - Field photographs and corresponding sketches illustrating thrust imbricates of Creaceous Transgressive Limestone on the eastern side of the Païkon Massif. The upper photograph/sketch is taken looking north (Karpi village is down on the plain to the right) and shows limestone imbricates (brick patten) within the volcanics of the Kastaneri Formation (v pattern). The lower photograph is taken looking south and again shows imbricates within the Kastaneri Formation volcanics. In both cases the direction of thrust propagation is westward.

FIGURE 4.34 D



Figure 4.34

A - Geological map of the Micra Livadia area, central Païkon Massif; **B** - Cross-section from A to B showing open D3 folds which warp and refold the D2 structures; **C** - Cross-section from X to Y showing D2 chevron folds which, in this area, are east-verging; **D** - Field photo-montage of the eastern part of the Micra Livadia area (roughly from B to Y).

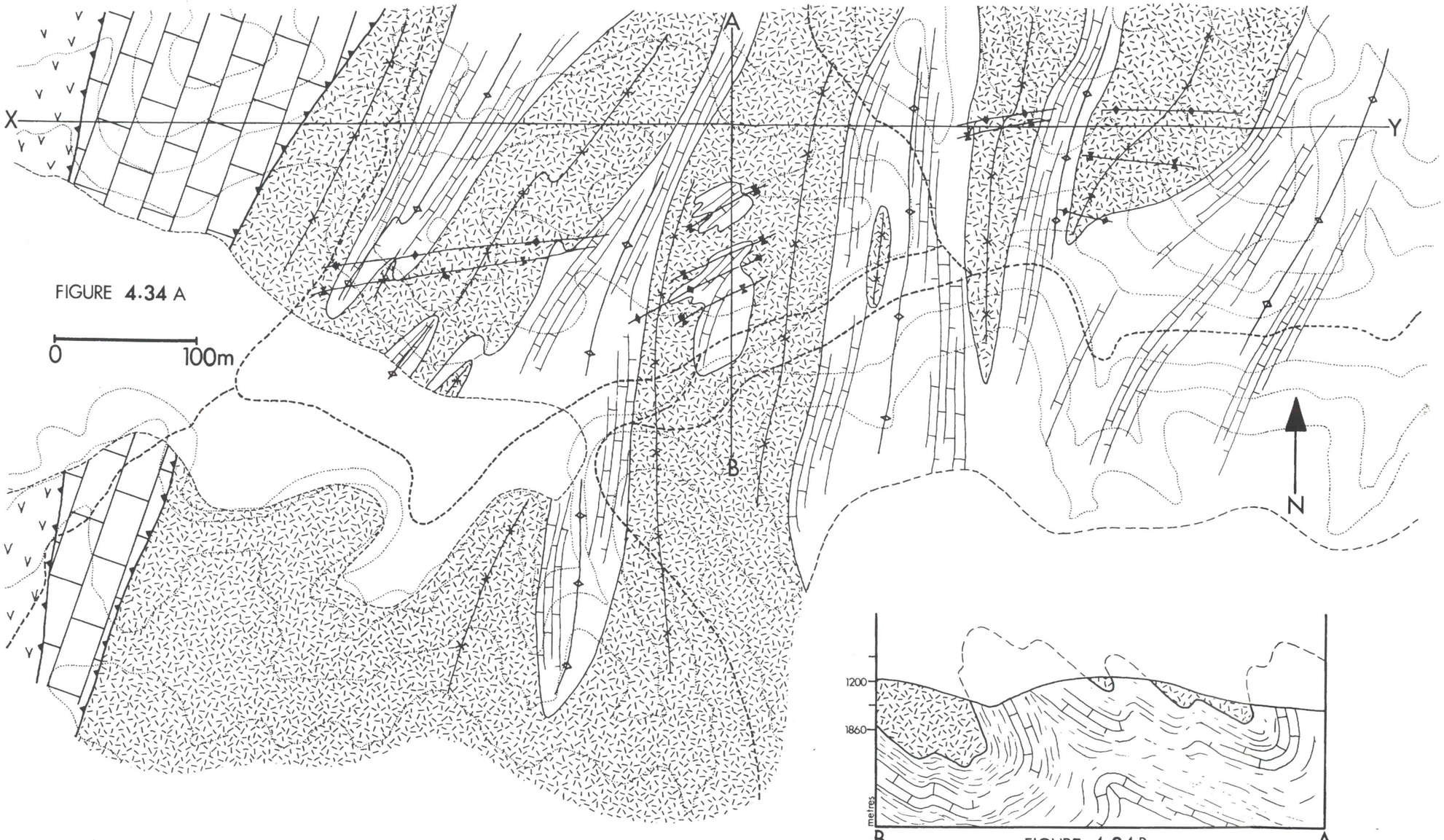


FIGURE **4.34** A

FIGURE **4.34** B

FIGURE **4.34** C

Kastaneri Fm
Cret. Trans. Lstn
Gandatch Fm
Livadia Fm
D2 anticline
D2 syncline
D3 anticline
D3 syncline
Thrust
Stratigraphic contact
Topo contour
Dirt track
Limit of exposure

Figure 4.34 - Continued on next page.....

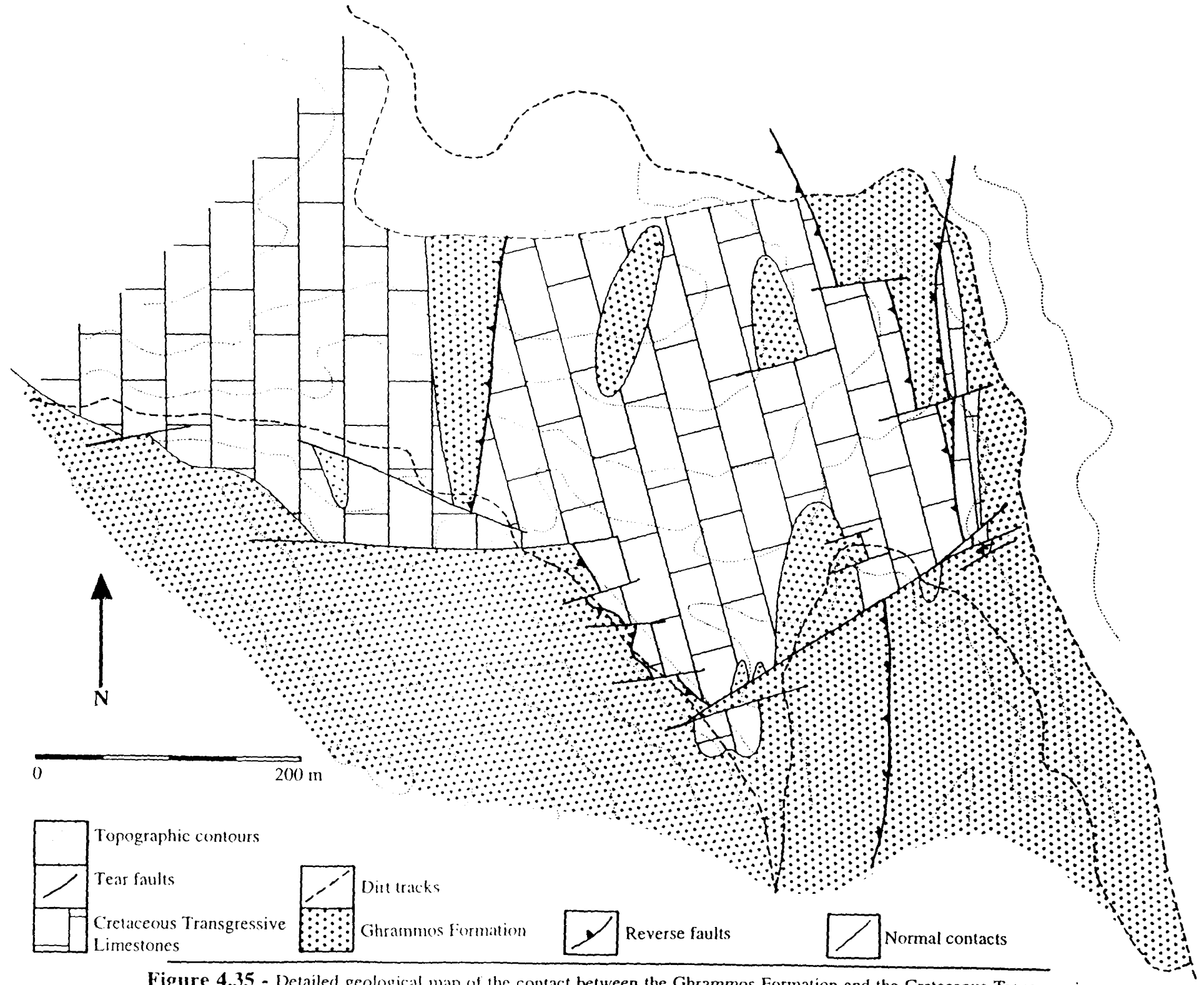


Figure 4.35 - Detailed geological map of the contact between the Ghrammos Formation and the Cretaceous Transgressive Limestones (locality 282, central, southern Paikon Massif). In this area the normal stratigraphic succession has been disrupted and repeated by D2 fold and reverse fault structures, which are themselves off-set by roughly E-W-trending tear faults.

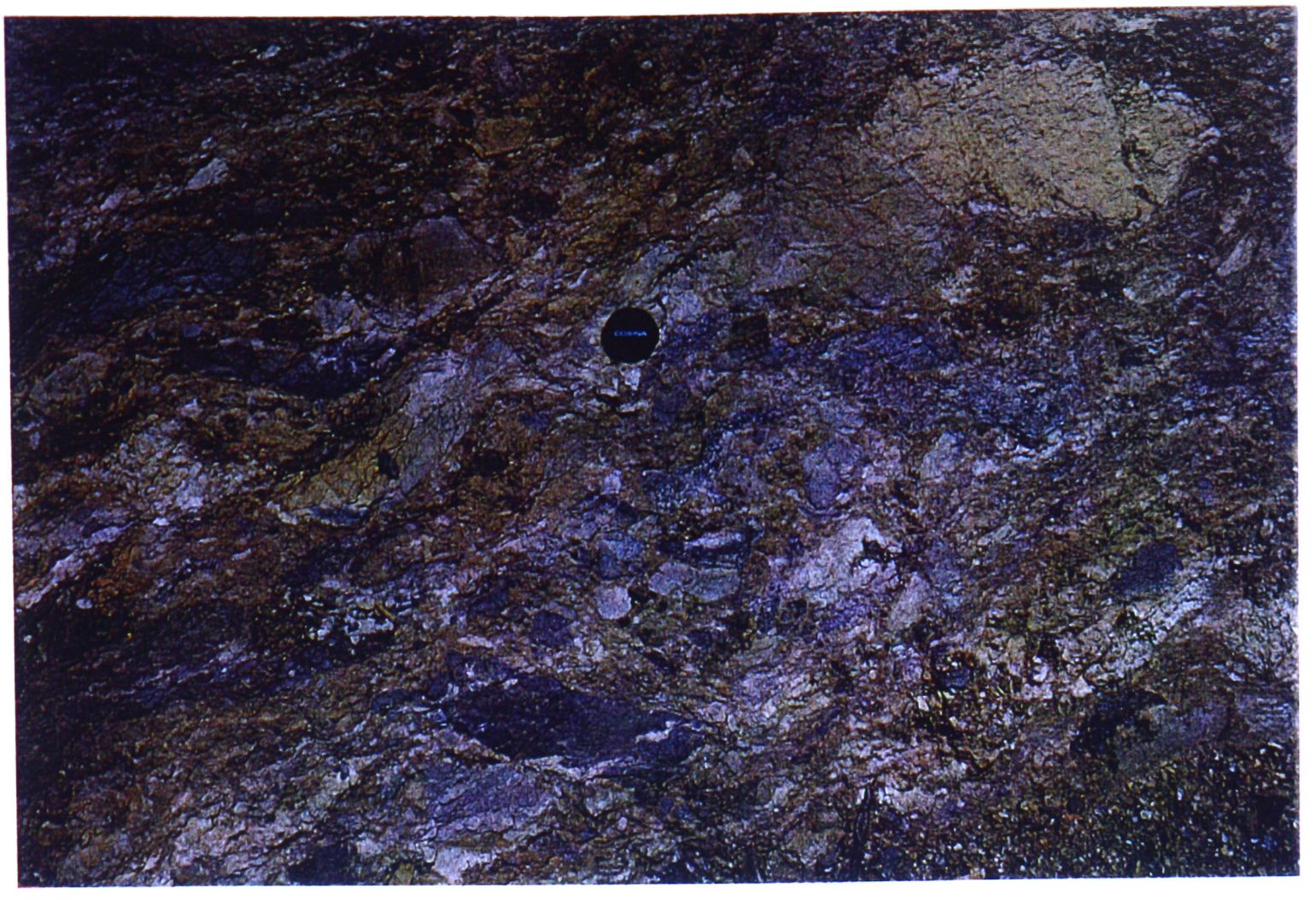


Figure 4.36 - Field photograph of mélange that was produced during thrust-imbrication of the Cretaceous Transgressive Limestones. Pebbles and boulders of limestone, acidic tuff, quartz-porphyry and andesitic volcanics predominate (locality 454, north of Eliftherohori).

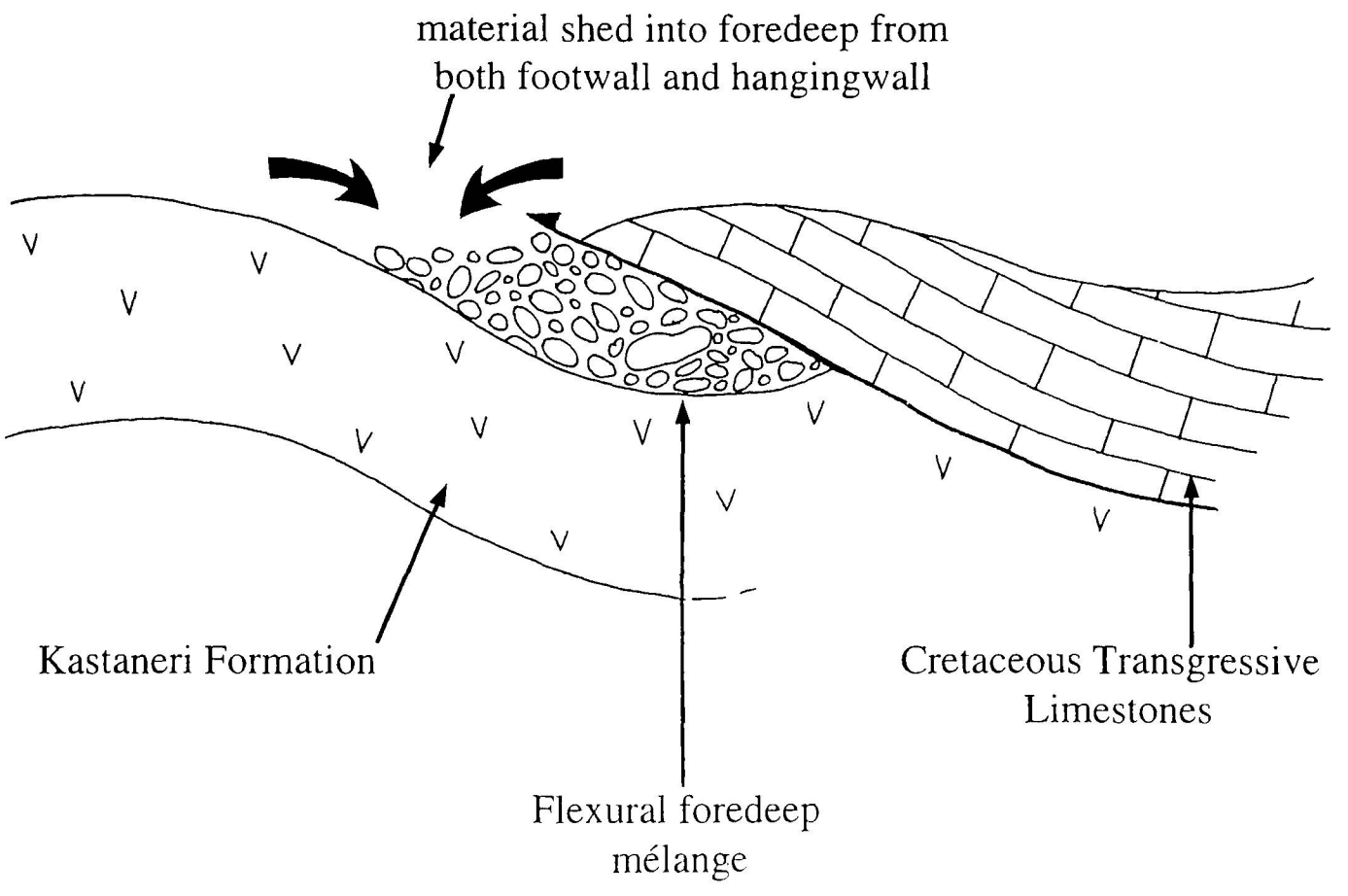


Figure 4.37 - Sketch diagram showing the development of a flexural foredeep mélange. The Cretaceous Transgressive Limestones are thrust over the volcanic rocks of the Kastaneri Formation generating a flexural depression. Detritus from both the hangingwall (limestone) and the footwall (volcanics) are shed into the basin producing a tectonic mélange (lithospheric flexure is exagerated in this figure)

the overlying para-autochthonous imbricate and partly from the underlying Kastaneri Formation, and are postulated to have been deposited in small flexural troughs which developed as the load exerted from the over-thrusted rock pile depressed the underlying autochthon (Figure 4.37).

4.6.3 - *Petrological Observations and Metamorphism*

All mineral assemblages generated during D2 compression are characteristic of metamorphism under greenschist facies conditions. The paragenesis of mica, epidote, quartz and albite is commonplace throughout the volcanic rocks of the Livadia and Kastaneri Formations and within clastic horizons of the Gandatch Formation. In these three units the D2 metamorphic minerals overprint those generated during D1 deformation and platy minerals (e.g. mica and chlorite) have grown parallel to the dominant D2 axial-planar schistosity (S2). Microscopic D2 folds crenulate the S1 schistosity, as shown on Figure 4.38. The photomicrograph (Figure 4.38) is of an oriented thin section from Stratotype 2 of the Gandatch Formation (chapter 3.4) at locality 336 (Figure 4.3) where the D2 crenulation foliation, comprising micas, chlorite, quartz and lesser feldspar and epidote, is oriented parallel to the axial planes of the micro-folds. In the fold nose area, the remnant D1 foliation is kinked and overprinted by the D2 crenulation foliation. Away from the fold nose, the D2 foliation domains are spaced and many of the intervening microlithons (Passchier & Trouw, 1996) preserve the remnant D1 foliation.

Figure 4.39 is a photomicrograph of an oriented thin section from the Gandatch Formation. The thin section has been cut parallel to the D1 foliation and clearly shows D2 folds crenulating the D1 schistosity. A sheared D1 foliation (horizontal) is the dominant fabric in this slide and is defined primarily by micas in the D1 cleavage

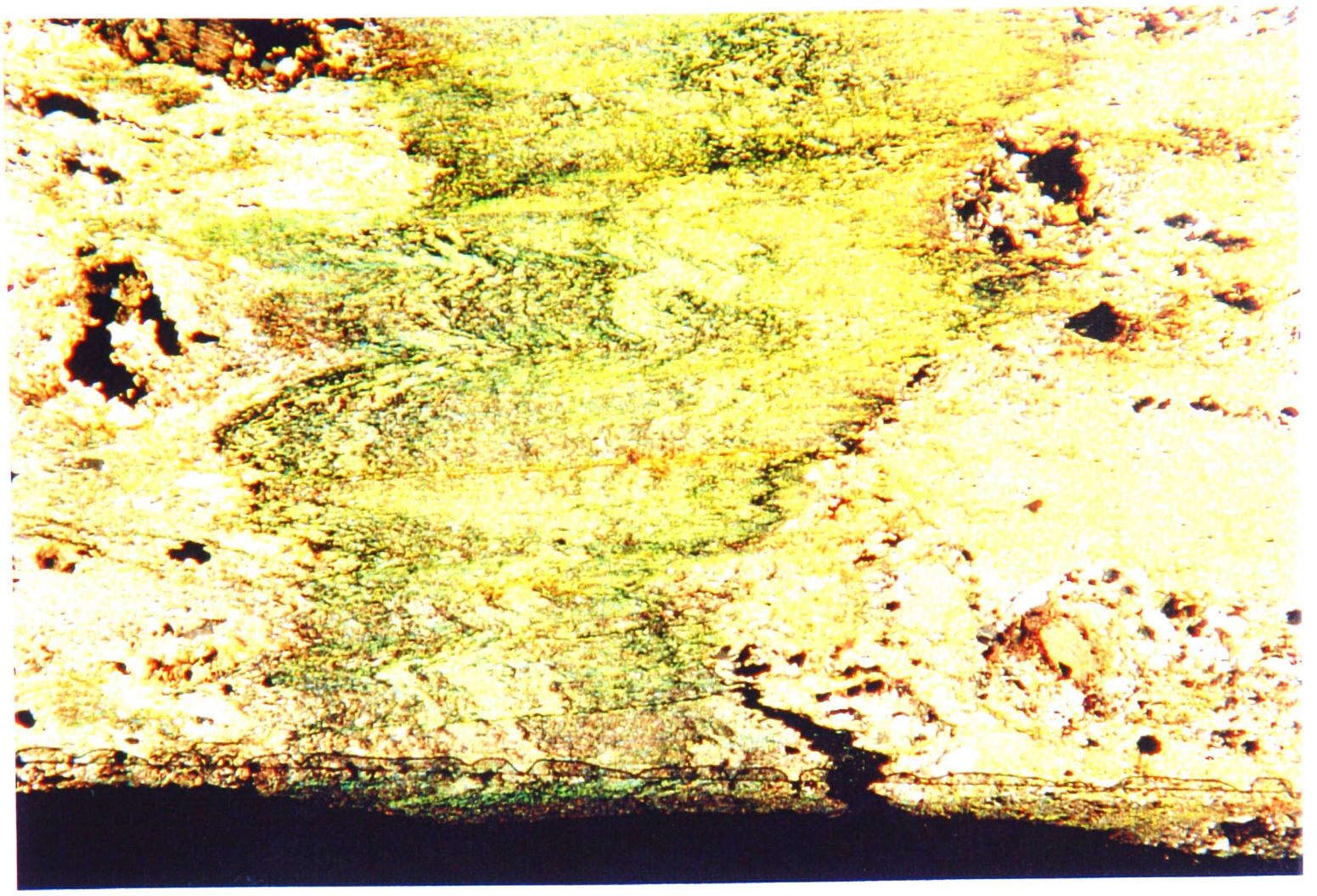


Figure 4.38 - Photomicrograph of the D1 fabric (very fine-grained mica and chlorite) being folded by D2 folds and overprinted by the horizontally-oriented D2 phyllosilicate minerals (namely mica). The D1 fabric has been preserved in a layer of chlorite-mica-schist within the Gandatch Formation (Stratotype 2) but is no longer present in the phyllosilicate-poor layers around it. Magnification x30.

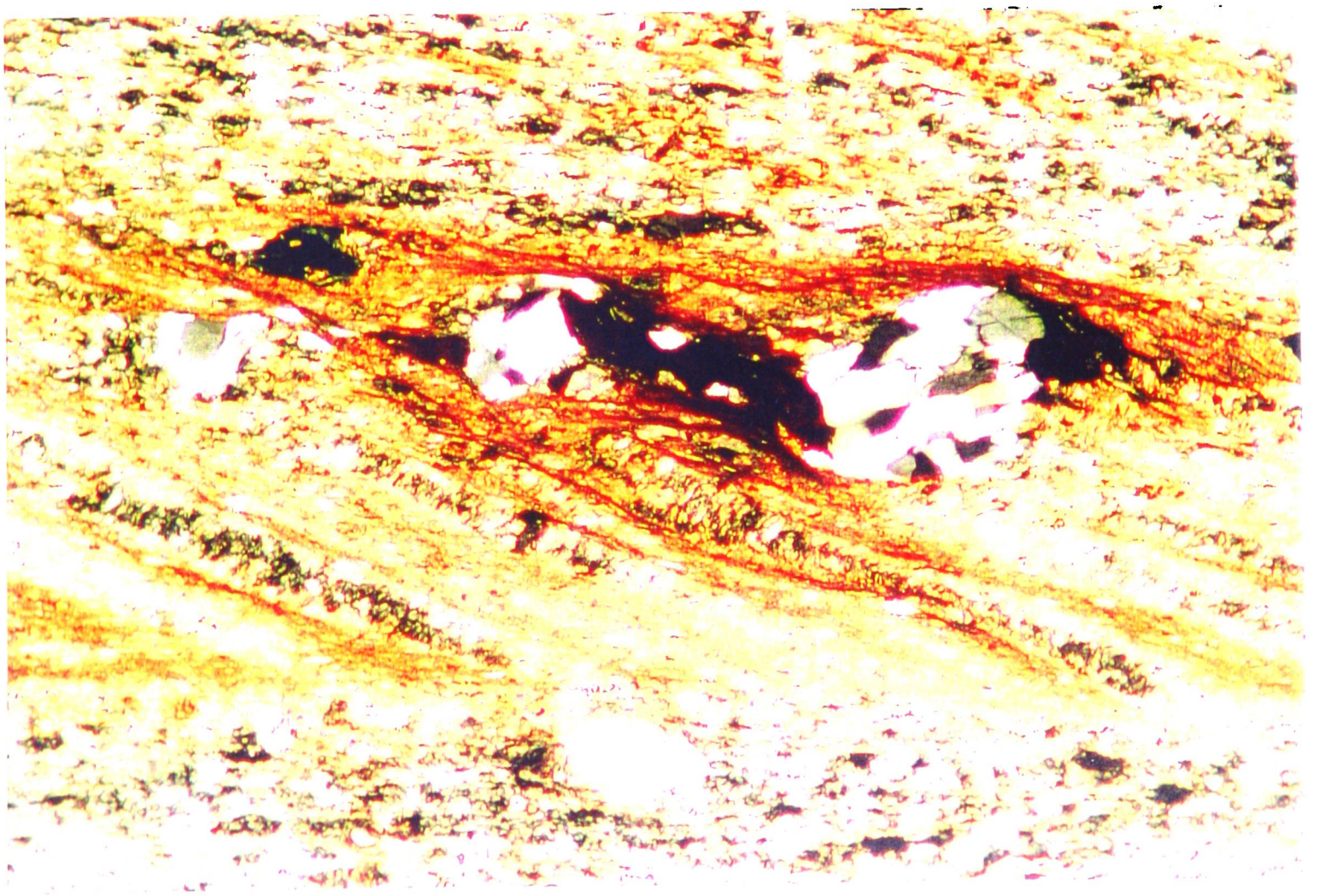


Figure 4.39 -Photomicrograph of cross-cutting fabrics within the Gandatch Formation. The D1 fabric is oriented horizontally and has sheared the layer-parallel quartz porphyroblasts into a mantled σ structures. The D2 fabric crenulates S1 and trends from top left to bottom right in the picture. Magnification x30.

domain, with less deformed microlithons of quartz, albite, mica and rare chlorite. Mantled porphyroblasts of quartz have been sheared by the D1 foliation into σ-type morphologies (Passchier & Trouw, 1996), indicating a dextral sense of shear (Figure 4.39). The D1 fabric is folded about D2 fold axes, which are oriented from top left to bottom right in the photograph. The largest sigmoidal quartz grain has been slightly displaced on its right hand side (pushed upwards) by the D2 folds. Similarly, Figure 4.40 is an oriented thin section from the Gandatch Formation showing the weak D1 foliation (very faint in photograph) being overprinted by the well-defined D2 foliation. This slide also illustrates that the Gandatch Formation has been affected, at least locally, by the D3 deformation event (section 4.7). The fabric associated with D2 is clear, but the remnant D1 fabric is scarce and D3 only slightly overprints the D2 schistosity.

Figure 4.41 is a photomicrograph and sketch of a strained quartz grain from the volcaniclastics of the Kastaneri Formation at locality 334 (north of Khromni; Figure 4.3). The quartz grain was overgrown by small, secondary micas during D1 and both the micas and the host quartz were subsequently folded during D2. D1 micas have been bent and fractured along the hinges of the D2 folds, suggesting that the folding regime was brittle.

In the marbles of the Gandatch Formation (Stratotype 1) and the Cretaceous Transgressive Limestones, the S2 fabric is defined by elongate calcite crystals (and rare micas and/or platy chlorites). Pelagic foraminifera (*Globotruncaca sp.*) within the Buff Pelagic Carbonates are commonly replaced by secondary quartz and albite, an assemblage characteristic of greenschist facies metamorphism (Figure 4.42).

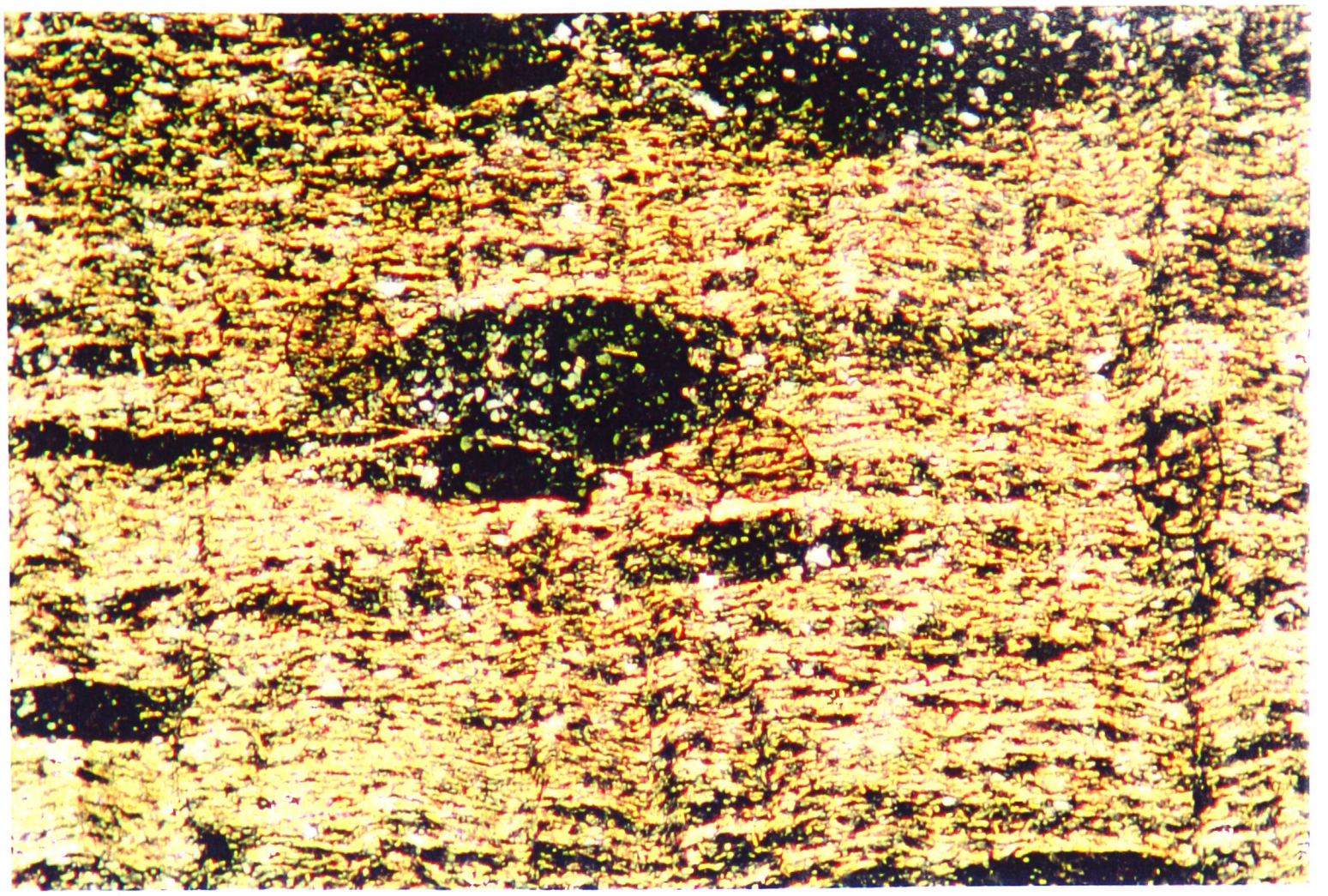


Figure 4.40 -Photomicrograph of a sample from the Gandatch Formation (magnification x30) showing some cross-cutting fabrics. The dominant fabric, oriented horizontally, is S2 which is primarily defined by micas in this instance. The later-formed S3 fabric is quite faint but can be picked out trending vertically in the picture. S3 is marked by small laths of mica and chlorite and is associated with small kink folds (e.g. bottom centre). The S1 fabric is very faint at this magnification, but remnants of it can be seen between the S2 fabric which is overprinting it.

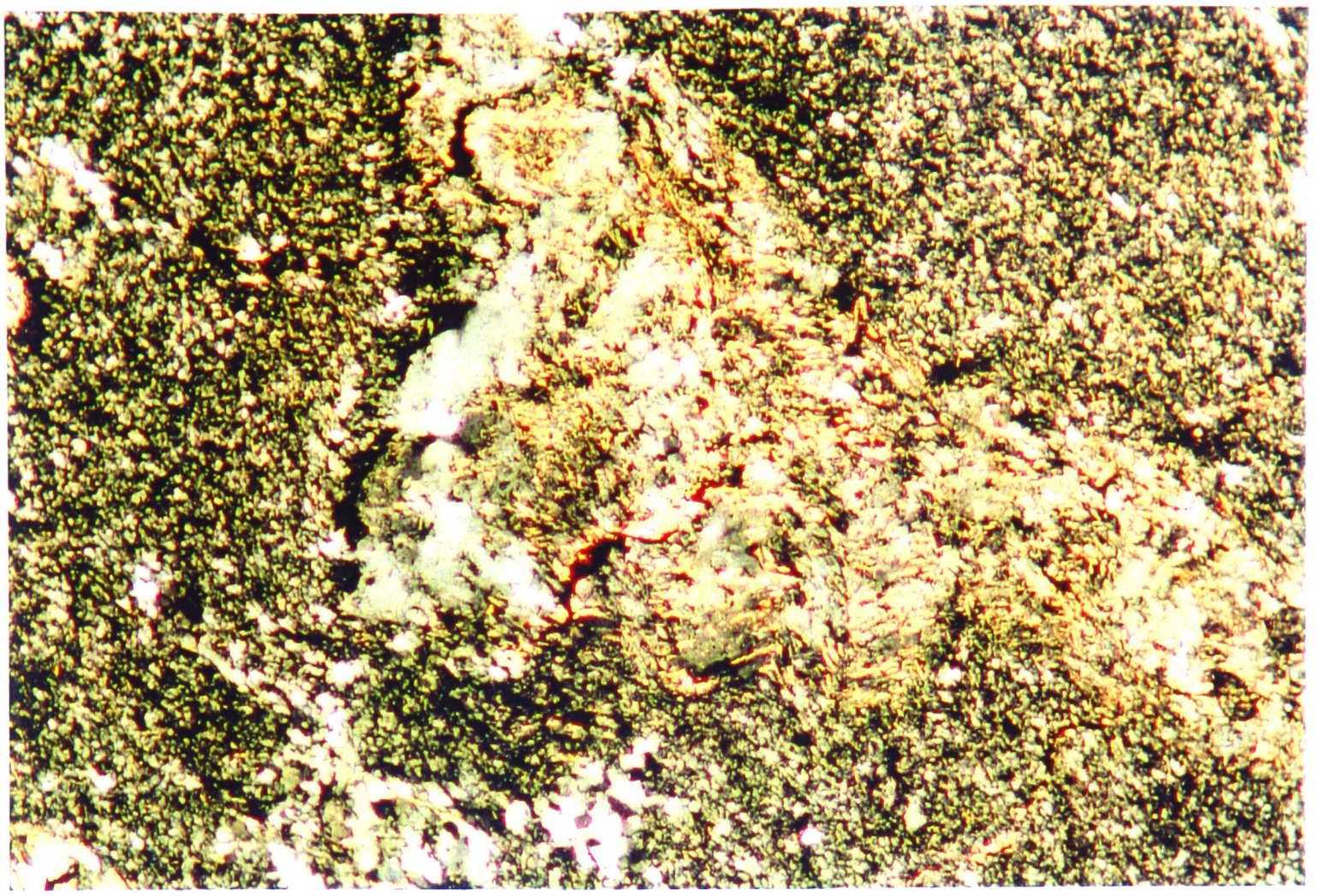


Figure 4.41 -Photomicrograph of a deformed quartz grain within a volcaniclastic sample of the Kastaneri Formation (magnification x20). The irregular outline of the quartz grain is due to small folds which cause the extinction of the quartz to undulate regularly. Within the quartz, later-formed micas are also folded, and close inspection of the fold hinge area reveals that the micas have been brittley fractured during folding.

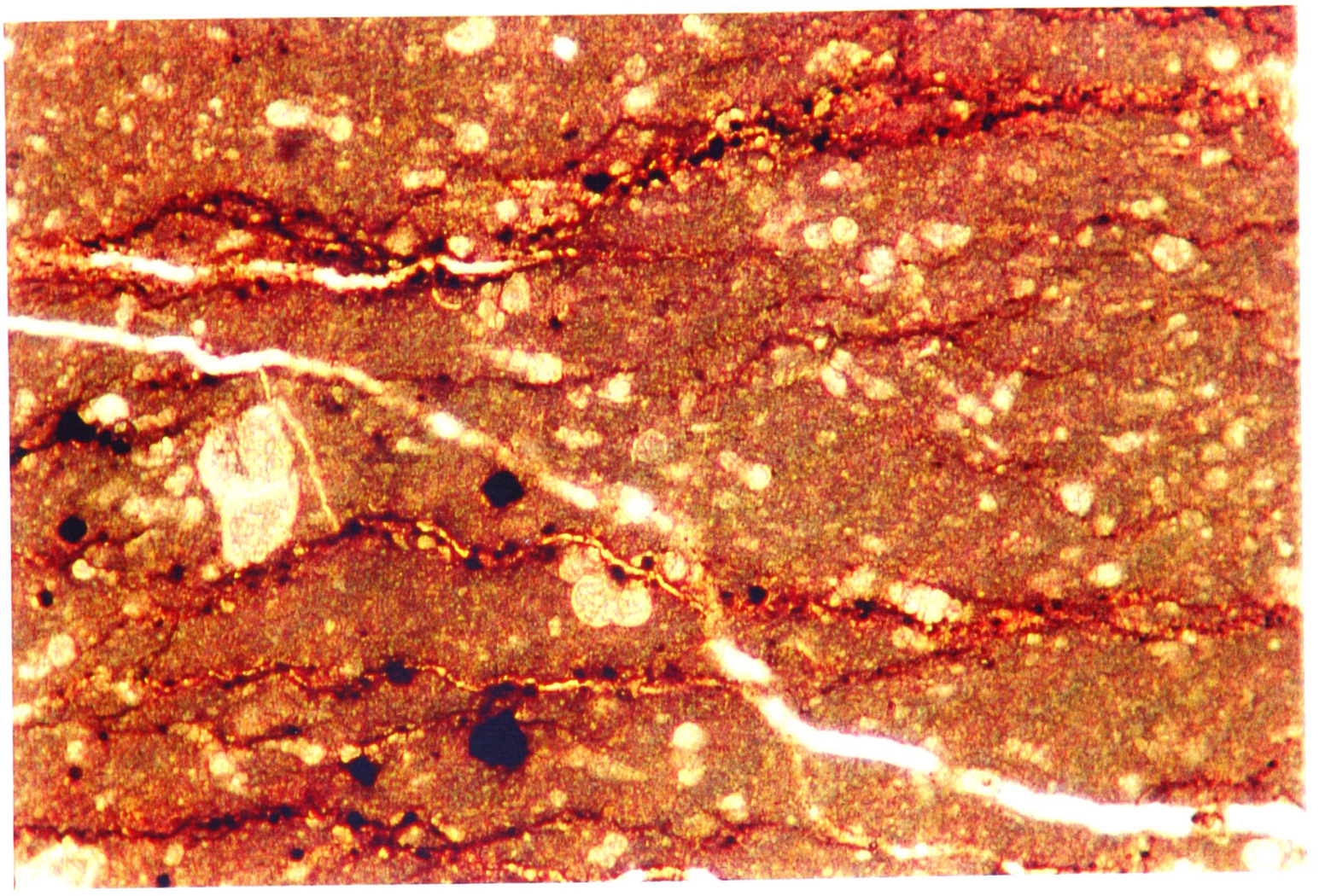


Figure 4.42 -Photomicrograph (x30 magnification) of the Buff Pelagic Carbonates from near Theodoraki village, western Païkon Massif. The bulbous, rounded *Globotruncana sp.* have been replaced by microcrystalline quartz and albite during D2 deformation (greenschist facies alteration).

4.6.4 - *Discussion and Conclusions*

The dual vergence of structures associated with D2 deformation is the result of coeval compression on the eastern and western sides of the Païkon Massif. Structural studies of the contact between the Païkon subzone and the adjacent Almopias subzone (to the west) suggest that D2 contractional deformation in the western Païkon Massif results from northeastward overthrusting of the Meglenitsa Ophiolite onto the Païkon Massif (Sharp & Robertson, 1992; Sharp, 1995; Brown & Robertson, in press). It is postulated here that the westward vergence, which affects the eastern side of the Païkon Massif, was probably generated during westward overthrusting of the Guevgueli Ophiolite onto the eastern Païkon margin (Brown & Robertson, in press). The Païkon Massif thus behaved as a "pop-up" between two converging ophiolite units, and it is very likely that the present, regional-scale, NNW-SSE-trending Païkon anticline developed during this stage (Mercier, 1968; Vergely, 1984; Brown & Robertson, in press). Regionally, the D2 compressional event occurred in response to complete closure and suturing of Neohellenic ocean basins (resulting in ophiolite obduction) as the Hellenic continental fragments (e.g. the Pelagonian block) were accreted onto the southern margin of Eurasia (further discussion in chapter 7).

This work confirms the importance of a Tertiary compressional event (D2) equivalent to the CT1-2 of Vergely (1984), however, the D2 event is more complex than previously proposed. Vergely (1984) documented that D2 (CT1-2) structures verge only towards the west throughout the Païkon Massif. In contrast, it has been shown here that only eastern parts of the Païkon Massif contain D2 structures with SW to NW vergence, while the whole of the western Païkon Massif is characterised by northeast-verging D2 structures. It is proposed, however, that the southeast-vergent JE2 structures described by Vergely (Figures 4.1 & 4.2) from the western Païkon Massif may actually be early Tertiary D2 structures which have been wrongly assigned to a Lower Cretaceous event.

4.7 - LATER TERTIARY COMPRESSION - D3

4.7.1 - *Field Relations*

The third phase of compressional deformation to influence the Païkon Massif occurred at some, poorly constrained, time in the Tertiary after D2, but prior to Neogene-Quaternary extension (E2, section 4.8). D3 structures are almost exclusively developed along the eastern margin of the Païkon Massif, near the Païkon-Guevgueli contact, although a D3 lineation can be recognised throughout the Massif, affecting all lithological units therein. This pervasive stretching lineation, which plunges consistently towards the SSW to SW (Figure 4.43), is the most conspicuous evidence of D3 deformation. From east to west, the lineation becomes progressively more faint, but can still be seen intersecting and overprinting the E-W and NNW-SSE-trending lineations of D1 and D2 respectively.

In more easterly areas (e.g. between Ghriva and Kastaneri, Figure 4.3), D3 deformation has given rise to strong SSW-trending mylonitic fabrics (Figure 4.44) that affect all stratigraphic units on the eastern side of the Païkon Massif. Mylonite fabrics are restricted to the Païkon-Guevgueli contact, where all pre-existing structures and/or original sedimentary features have been entirely obliterated.

In the Cretaceous Transgressive Limestones the D3 mylonitic fabric formed by the dynamic recrystallisation of calcite. Figure 4.46 is a photomicrograph of mylonitised limestone from locality 323 (Figure 4.3) cut perpendicular to the D3 foliation. Small sheared σ and sometimes δ structures (Hanmer & Passchier, 1991; Passchier & Trouw, 1996) can be picked out, both of which indicate a dextral, top-to-the SSW shear.

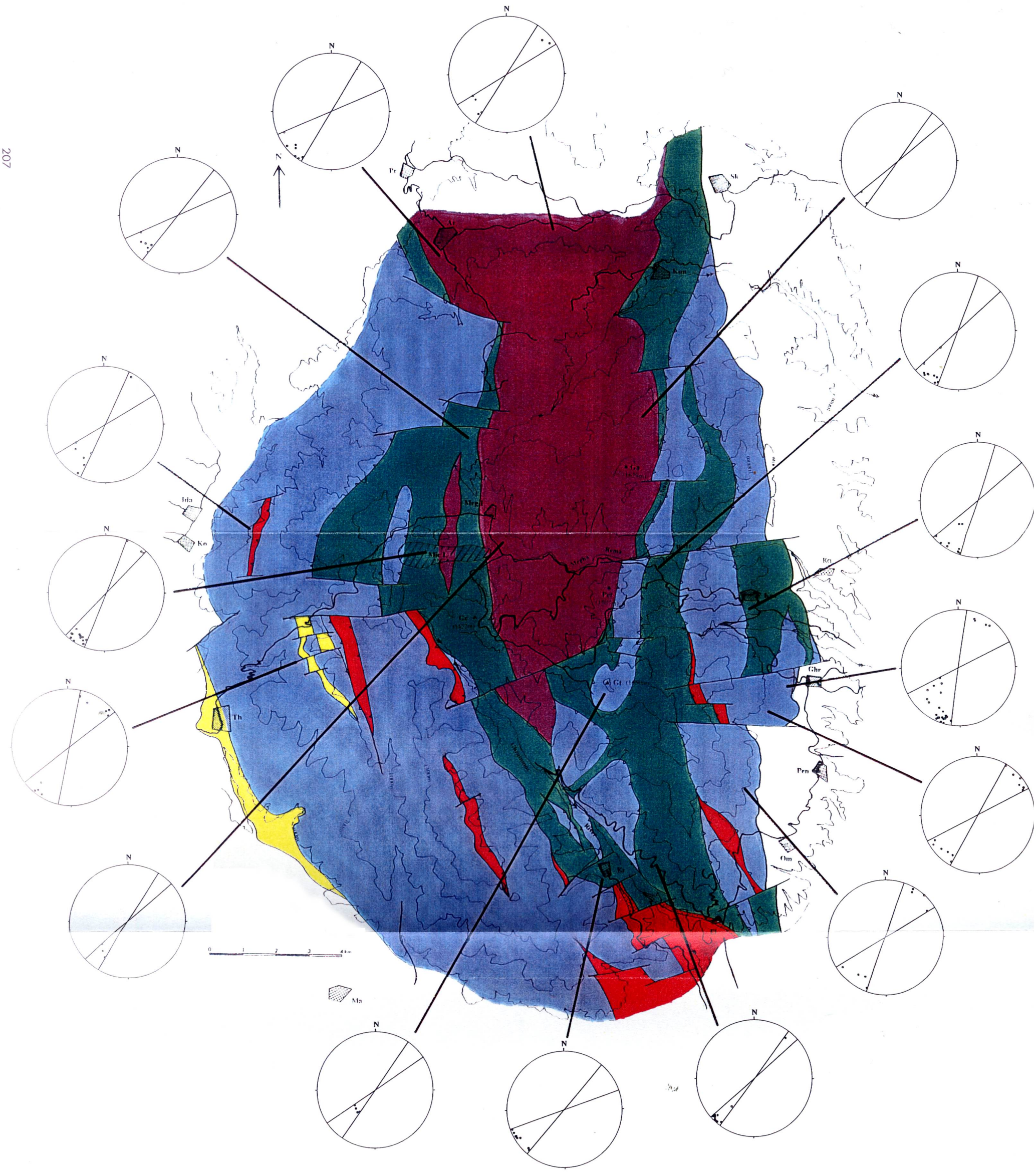


Figure 4.43 - Geological map of the Païkon Massif with stereographic projections showing the orientation of the D3 lineation from various localities. The D3 lineation trends quite consistently to the SW-NE and is represented by small full circles.



Figure 4.44 -Field photograph showing marble mylonites which were produced during D3 transpressional deformation in the Cretaceous Transgressive Limestones (by Ghriva village, easternmost Païkon Massif).

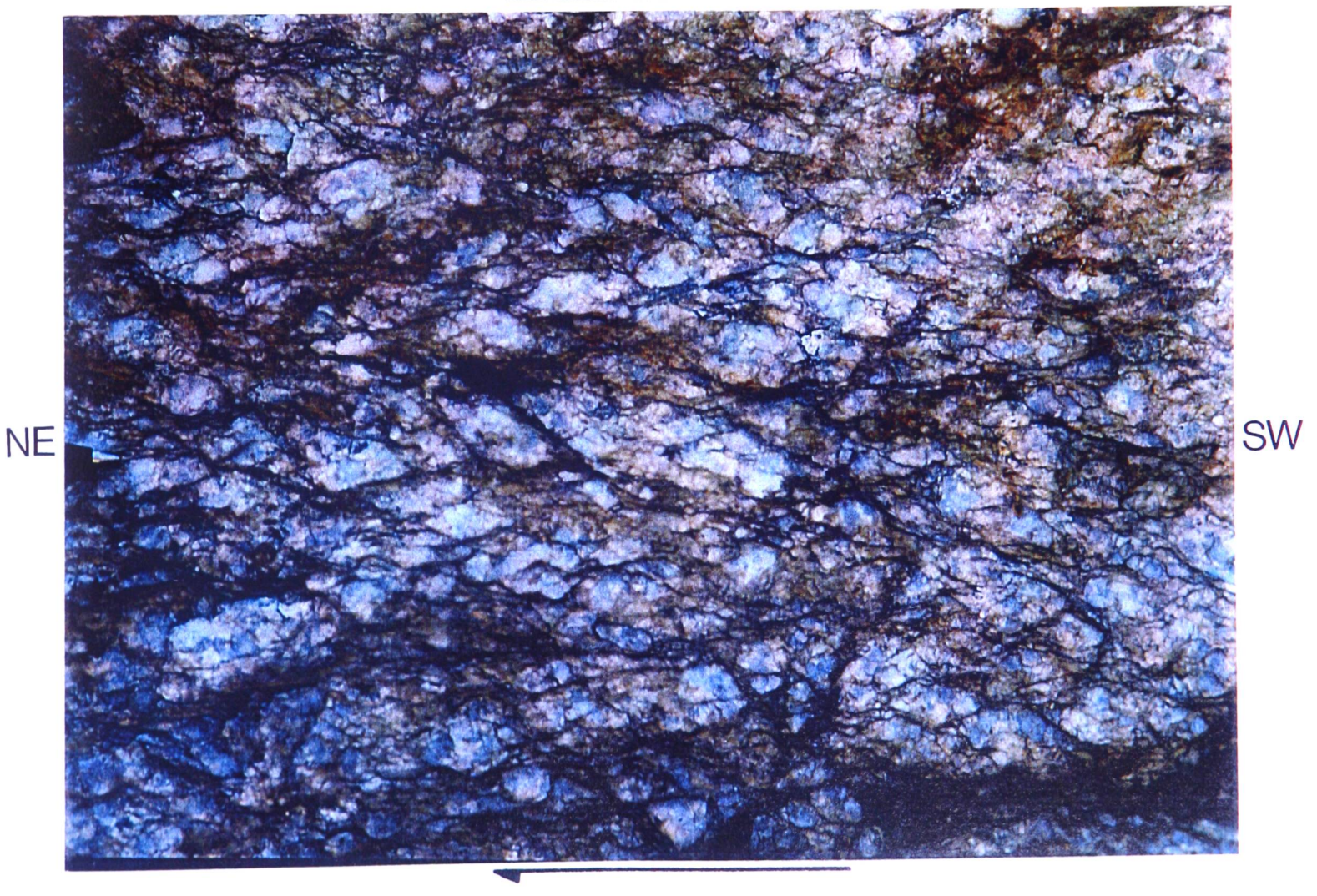


Figure 4.45 -Field photograph of sheared quartz porphyroblasts within the Kastaneri Formation (by Ghriva village). The porphyroblasts have been sheared into δ and σ structures during D3 deformation and indicate a top-to-the-SW sense of shear.

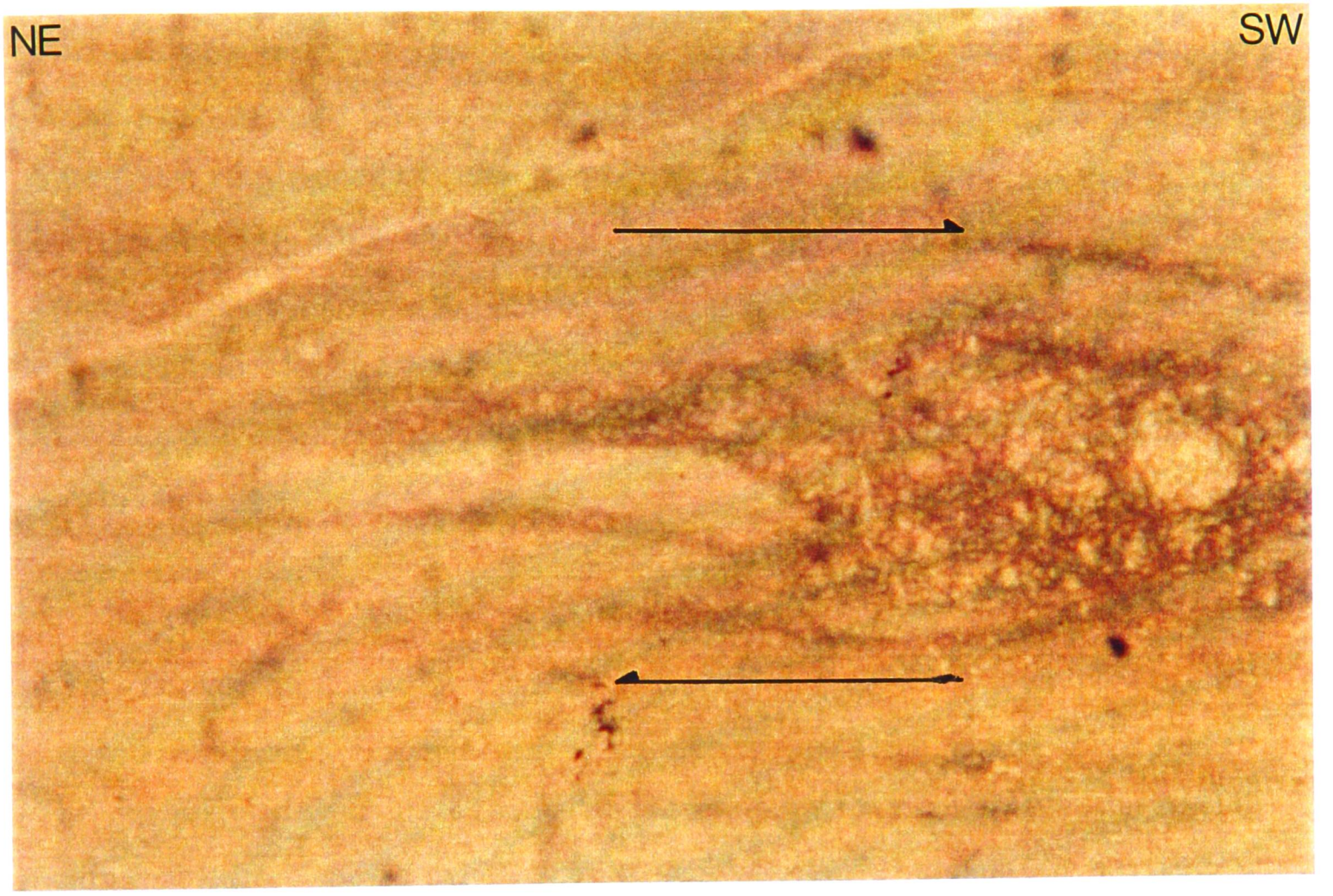


Figure 4.46 -Photomicrograph of a microcrystalline marble mylonite from the Cretaceous Transgressive Limestones near the Païkon-Guevgueli contact (Ghriva village, eastern Païkon Massif). Top-to-the-SW shearing is indicated by σ structures. Magnification x25.

Duplex structures and shear fabrics from the Tchouka Flysch and Kastaneri Formation (Figure 4.45) also indicate a top-to-the-SW shear sense, which suggests that dextral transpression as opposed to orthogonal compression was dominant in this area. Tangential WNW-directed thrusting and SSW-verging open folds are also associated with the transpressive stress of D3 and has formed a narrow fold and thrust belt (i.e. a strike-slip duplex) just west of Ghriva (Figure 4.47). D3 is also responsible for warping pre-existing structures into SW-trending open, overturned and kink folds, as seen at Micra Livadia (Figure 4.34a, b, c & d). More rheologically competent stratigraphic units, such as the Cretaceous Transgressive Limestones and the Buff Pelagic Carbonates, respond to D3 tectonism by warping into metre- to decametre-scale open to overturned folds, while phyllosilicate-rich lithologies (e.g. the Tchouka Flysch and Stratotype 3 of the Gandatch Formation) deform into coaxial kink folds. In other parts of the Païkon Massif D3 folds develop as large (10's of metres wavelength), open monoclines or small (0.1 m wavelength) WNW-ESE trending kink folds. Such folds are rare in more westerly areas of the Massif.

4.7.2 - *Discussion*

The intensely deformed Païkon-Guevgueli margin was originally thought to be conformable (Bebien, 1982; Figure 4.48), which is clearly not the case; this contact was later recognised as a "sheared margin", and attributed to tectonic suturing of the eastern Prepeonias subzone with the Guevgueli Ophiolite (Vergely, 1984; Figure 4.49). However, it is now clear that a significant phase of dextral transpressional deformation affected the whole of the Païkon Massif sometime after D2, although intense mylonitisation and the development of strike-slip duplex packages was restricted to the



Figure 4.47 - Detailed geological map of the Ghriva area (eastern Païkon Massif). The map shows the folded, faulted and repeated stratigraphic succession of the Cretaceous Transgressive Limestones, Buff Pelagic Carbonates and Tchouka Flysch, all tectonically overlain, with east-dipping thrusted contact, by the Guevgueli Ophiolite of the Peonias subzone.

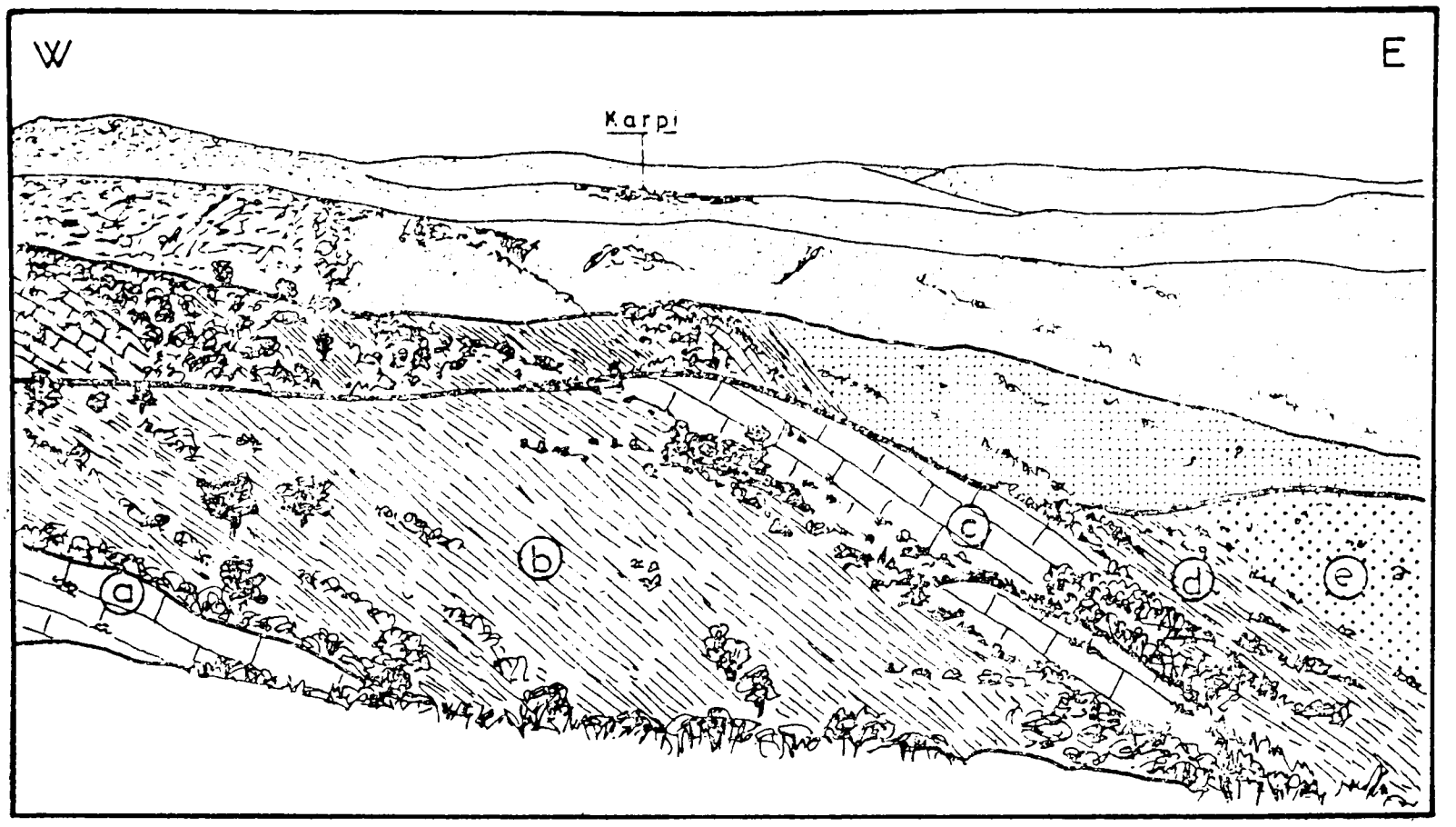


Figure 4.48 - Diagram from Bebien (1982) showing a normal, depositional contact between the Païkon and the Guevgueli Ophiolite (by Karpi, easternmost Païkon Massif).

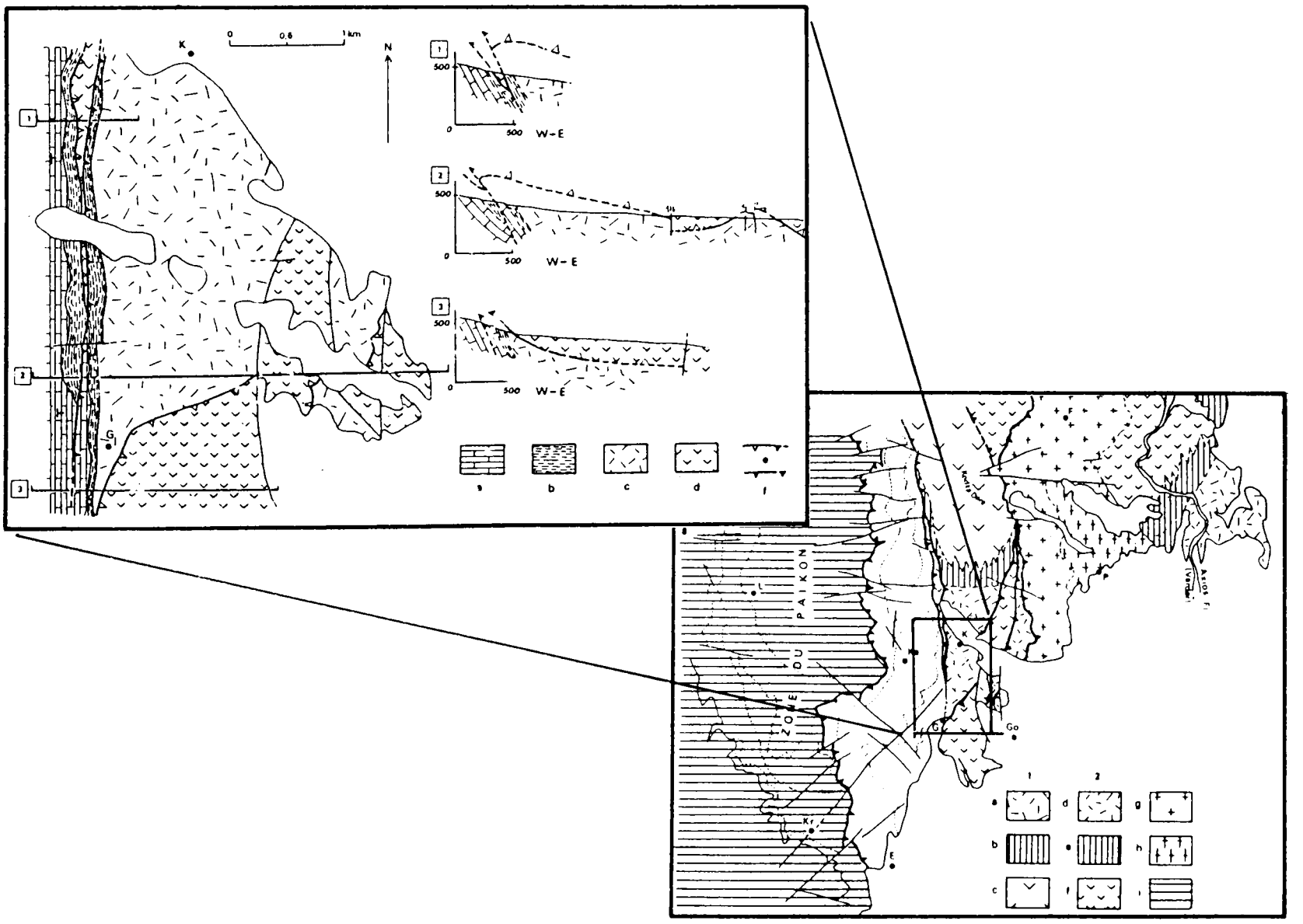


Figure 4.49 - Geological maps from Vergely (1984) showing a thrusted contact between the Païkon and the Guevgueli Ophiolite (westernmost Païkon Massif).

vicinity of the Païkon-Guevgueli margin. It is suggested that post-suture "tectonic escape", resulting from post-D2 regional transpression along the Païkon-Guevgueli contact, is a likely explanation.

Within the Hellenic orogenic belt, Tertiary "Neohellenic" compression commenced in the east (internal isopic zones) and progressed westward (external isopic zones). This diachronous compression reflects the docking of continents and intervening ocean basins with the southern margin of Eurasia, and took place earlier in the Internal Hellenides (e.g. the Païkon subzone) than in the External Hellenides due to the more northerly disposition of the former (Aubouin, 1970; Smith & Moores, 1974). For example, the main phase of Neohellenic compression and suturing in the Païkon Massif (Internal Hellenides) took place in the earliest Tertiary (post-Maastrichtian) whereas effectively D2 ophiolite obduction and tectonic juxtaposition of terranes did not occur until the Eocene in the Pindos zone to the west (External Hellenides; Robertson *et al.*, 1991; Degnan, 1992). Therefore it is likely that D3 compression in the Païkon Massif occurred in response to Neohellenic collisions still taking place much further to the present day west, which caused tightening to occur along the Païkon-Guevgueli contact, inducing SW-directed transpressional "tectonic escape".

Similar late-stage "tightening" structures (e.g. post-suture kink folds) have been observed in the Pelagonian and Almopias zones to the west (F3 of Sharp, 1995) and from the Voras Massif to the north (this work, chapter 6). Post-suture dextral transpression has also been concluded for these areas.

Undeformed *Nummulites*-bearing Eocene limestones in the Peonias zone (Mercier, 1968) provide an upper limit to the age of Neohellenic deformation (D2 and D3) in the Internal Hellenides.

4.8 - LATE-STAGE EXTENSION - E2

Subsequent to the Neohellenic orogenic episode (D2 and D3) the Païkon Massif, and indeed much of the Hellenide belt, was subjected to a series of "Neotectonic" extensional deformation events, here termed E2, which are still active to the present day. The detailed complexities of these events were not studied in detail during this work, however, in the Païkon Massif most E2 movements have been concentrated along previously formed structures and/or lines of weakness (for example thrust faults formed during D2 and D3) producing normal and dip-slip slickensides on fault planes. The E2 events also produced many NNW to N-trending, normal (dip-slip) faults, which can be seen cross-cutting all earlier structures; these generally follow the strike of Tertiary (D2) fold axis orientations and thrust faults. The dip-slip component of many of these Neotectonic faults is evidenced by the significant lateral displacement of inclined lithological boundaries (as seen in the southern, central Païkon Massif, Figure 4.3).

Throughout northern Greece the tensile crustal stresses induced by "E2" extension have resulted in extensive normal faulting, graben formation and the exhumation of deep-crustal rocks. For example Neotectonic faulting in Argolis (Clift, 1990) and the Gulf of Corinth (Jackson *et al.*, 1982) have resulted in the formation of graben and half-graben structures. Further north, extensional unroofing of metamorphic core complexes and the exposure of deep-seated Tertiary granites occurred in the Serbo Macedonian and Rhodope Massifs (Kolocotroni & Dixon, 1991; Hague, 1993; Dinter, 1994), while the exhumation of blueschist facies rocks generated during the Neohellenic phase of orogenesis (D2, D3) took place in the central Almopias subzone (Sharp, 1995). The Neotectonic period of extension is also associated with the widespread eruption of Pliocene volcanic rocks throughout northern Greece (Vougioukalakis, 1994).

The Neotectonic extensional regime so widely recognised throughout the Hellenides was induced in response to the onset of northwards subduction along the Hellenic arc,

some distance to the south and southwest (Figure 4.50; Robertson & Dixon, 1984; Meulenkamp *et al.*, 1988). The study area and environs are situated in a back-arc position with respect to the Hellenic arc (Jolivet *et al.*, 1994; Vougioukalakis, 1994), and it is estimated that the onset of subduction began sometime between the Oligocene (26 Ma; Meulenkamp *et al.*, 1988; Ligdas *et al.*, 1990), the Middle Miocene (13 Ma; Le Pichon & Angelier, 1979) and the late Middle Miocene (5 Ma; McKenzie, 1978; Mercier *et al.*, 1979).

4.9 - CONCLUSIONS

The Païkon Massif was subjected to three distinct phases of contractional deformation (D1, D2 and D3) and three phases of extensional deformation (E0, E1 & E2). The first compressive phase (D1) took place in the Upper Jurassic (~JE1 of Vergely, 1984) and is related to the initiation of ocean basin closure and ophiolite obduction in the Eastern ("internal") Hellenides, as Hellenic micro-continental blocks (such as the Pelagonian zone) docked with the southern margin of the Eurasian continent. At this time, pre-Kimmeridgian units of the Païkon Massif (lower Païkon megasequence) were subjected to ductile, isoclinal folding and now display an E-W-trending lineation, which possibly reflects transport direction. These structures developed, at least partly, under high confining pressures, capable of developing lawsonite (Baroz et al, 1987). D1 structures and high pressure-low temperature metamorphism do not affect the upper Païkon megasequence (i.e. the Khromni Limestones and succeeding units).

Soon after D1, a phase of rapid unroofing and extensional uplift (E0) must have taken place in the Païkon Massif in order to preserve the lawsonite-bearing blueschist facies assemblages of the Kastaneri Formation. No structural evidence for this event is



Figure 4.50 - Field photograph of an E2 extensional fault within an imbricate of the Cretaceous Transgressive Limestones (north of Eliftherohori village). Slickensides on the fault surface indicate dip-slip movement.

preserved within the Païkon Massif, primarily because pervasive Tertiary compressional deformation has overprinted it.

The existence of a "JE2" compressional event of Lower Cretaceous age (Vergely, 1984) was not confirmed within the Païkon Massif during the course of this work. Existence of the JE2 event in the Pelagonian and Almopias zones to the west has also been disproved (Sharp, 1995). Instead, tectonism during the Uppermost Jurassic and Cretaceous periods was comparatively quiescent, and the sedimentary successions of the upper Païkon megasequence were deposited free of compressive stress.

During the Turonian, the Païkon Massif underwent moderate uplift, as evidenced by *Microcodium*-bearing ferruginous crusts, followed by rift-related subsidence: E1. This led to the deposition of deep-water pelagic carbonates and radiolarites, as part of a regionally significant crustal extension event found elsewhere in the Eastern ("internal") Hellenides. These include the Eastern Pelagonian margin (Sharp et al, 1991; Sharp, 1994), Eastern Argolis (Clift, 1992) and Eastern Euboea (Robertson, 1990). Both western and eastern Païkon margins display identical collapse sequences, confirming that the Païkon Massif is a single, composite unit that was folded into a SSE-plunging anticline, as opposed to two distinct tectonostratigraphic terranes (the Païkon and Prepeonias subzones of Mercier, 1968), separated by a major reverse fault (chapters 1 & 2).

The second phase of compressive deformation (D2) is characterised by west-verging structures in the eastern Païkon Massif and northeastward verging structures in the western Païkon Massif. Vergely (1984) reported only westward vergence throughout the Païkon Massif as a whole (CT1-2). D2 compression is the result of NE-directed ophiolite emplacement from the Almopias subzone to the west (the Meglenitsa Ophiolite), and approximately east to west ophiolite emplacement from the Peonias subzone to the east (the Guevgueli Ophiolite). Earlier, D1, ductile folds were re-folded

about NNW-trending brittle fold axes (D2) and the whole of the Païkon Massif was warped into a broad, NNW-SSE-trending anticline. This does not support a recent proposal that the anticlinal Païkon Massif is a "tectonic window" of upfolded Pelagonian units, as proposed by Godfriaux & Ricou (1991; chapter 1).

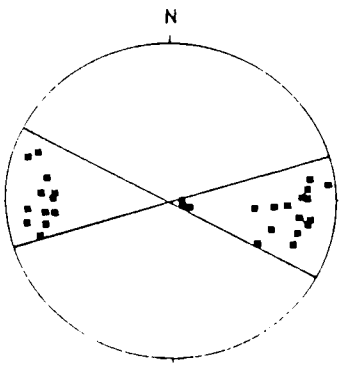
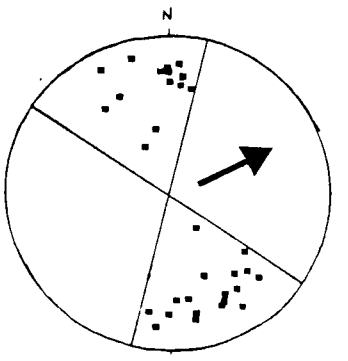
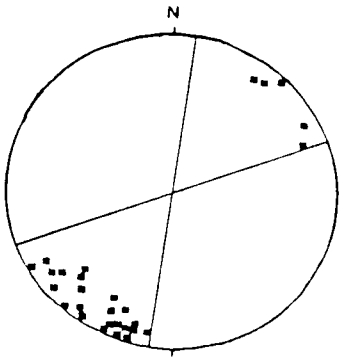
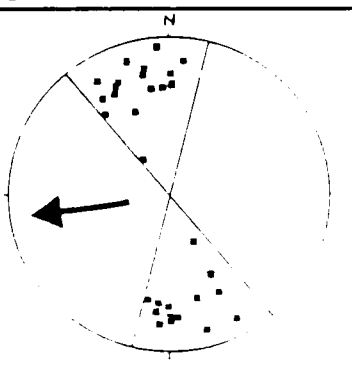
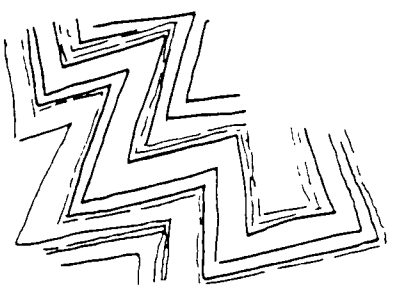
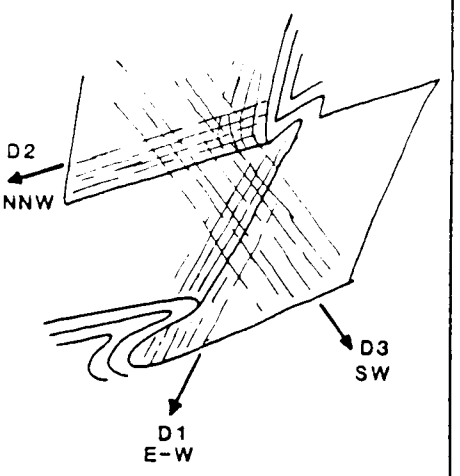
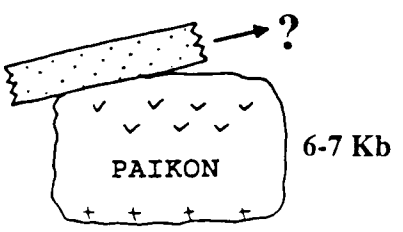
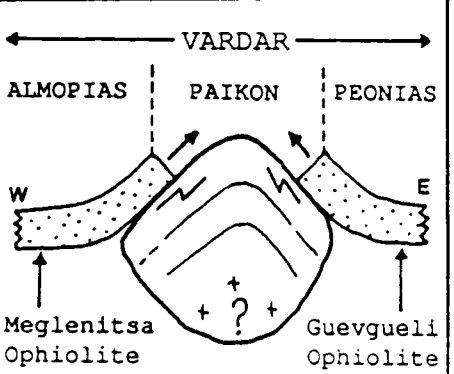
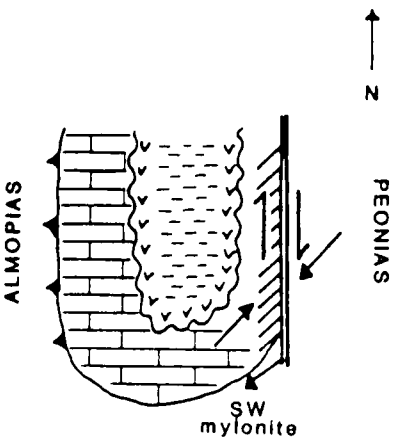
Later in the Tertiary, a SSW-trending mylonite fabric developed along the Païkon-Guevgueli contact, associated with a stretching lineation that developed throughout the Païkon Massif and SSW-verging folds. A possible explanation for these late-stage structures is dextral transpressional shear induced by post-suture "tightening" along the Païkon-Guevgueli contact. The Païkon Massif was finally affected by a series of Neotectonic events (E2) that commonly exploit older structures. Neotectonic structures are related to extensional stress induced in the back-arc region of the present day Aegean subduction zone (Jolivet *et al.*, 1994).

Concerning the geotectonic models outlined in chapter 1, it appears that significant modifications have to be made to each in the light of the new structural data presented here. The Juxtaposed Terranes model (Mercier, 1968) requires that western margin of the Païkon Massif overthrust the Almopias subzone with westward polarity during Neohellenic compression (i.e. D2). This is clearly not the case as all D2 structures on the western Païkon margin verge consistently towards the east. The Tectonic Window and Multi-shell models (respectively of Godfriaux & Ricou , 1991 and Bonneau *et al.*, in press) encounter similar problems due to this eastward-verging western Païkon margin, as both of these models require that ophiolitic rocks of Peonias subzone origin overthrust the Païkon Massif (or eastern Pelagonian margin according to these models; see chapter 1.3.2) with westward polarity. Although the ophiolitic rocks in the Almopias subzone do overlie the western Païkon margin, the polarity of movement along this contact is unequivocally eastward and *not* westward. The validity of these geotectonic models will be explored further in chapter 7.

4.10 - SUMMARY

Two distinct megasequences exist in the Païkon Massif, separated by an Upper Jurassic (pre-Kimmeridgian) unconformity. Three compressional (D1-3, Figure 4.51) and three extensional (E1-2) phases of deformation can be inferred. D1 (Upper Jurassic) occurred due to docking of the Hellenic microcontinents onto the Eurasian margin. Blueschist exhumation in the Upper Jurassic (E0) was followed by a long period of comparative tectonic stability, after which E1 (Upper Cretaceous) caused flexural uplift then rift-related collapse. D2 (Early Tertiary) compression was followed by D3 dextral transpressive shear, possibly caused by post-suturing "tectonic escape". Finally, E2 refers to Neotectonic (Neogene-Quaternary) extension. D1 is equivalent to the previously recognised JE1 event of Vergely (1984), but there is no evidence of a JE2 (Early Cretaceous) event in the Païkon Massif. Tertiary deformation is more complex than previously realised.

Figure 4.51 -Table illustrating the main structural features of each of the three main contractional deformation events (D1, Upper Jurassic; D2 early Tertiary; D3, later Tertiary) to affect the Païkon Massif.

EVENT	D1	D2	D3
TIME	LATE JURASSIC	EARLY TERTIARY	LATER TERTIARY
STRUCTURES	 Plot of the east-west trending lineation of D1 Central Paikon area.	 West Paikon D2 fold axes Vergence to the E-NE	 Plot of the D3 lineation Consistent SW trend.
		 East Paikon D2 fold axes Vergence to the WNW-W	
	 Sketch of D1, ductile, isoclinal folds from the Gandatch Formation.	 Sketch of D2, brittle, chevron folds from the Gandatch Formation.	 Sketch of structural type loc. by Micra Livadia
METAMO-RPHISM	BLUESCHIST FACIES DUCTILE	GREENSCHIST FACIES BRITTLE	GREENSCHIST FACIES MYLONITISATION
INTERPRETATION	? Polarity of obduction ?  Paikon subjected to high pressure, low temperature conditions	 Whole Paikon folded into a NNW-trending anticlinal structure	 Dextral transpression along Paikon-Guevgueli margin.
		FINAL CLOSURE AND SUTURING OF OCEAN BASINS TO EAST & WEST OF PAIKON	RENEWED COMPRESSION RESULTING IN POST-SUTURE "TECTONIC ESCAPE"

Chapter 5

Geochemistry

CHAPTER 5 - GEOCHEMISTRY

5.1 - INTRODUCTION AND PREVIOUS WORK

Preliminary geochemical studies of the Livadia and Kastaneri Formation volcanics have been carried out by two previous workers: Mercier (1968), Bebien (1982) and Bebien *et al.* (1994, in press). These workers concluded that the Païkon volcanic suites are of island arc origin and that they are of probable Jurassic age (see chapters 2 & 3). Mercier's work was carried out before the advent of modern geochemical analytical techniques and he concluded that the volcanic rocks of the Païkon Massif represent outpourings of arc affinity. Bebien (1982) similarly concluded an arc-type environment of eruption, but Bebien *et al* (1994, in press) interpreted the western and eastern sides of the Païkon Massif as belonging to different geochemical suites (i.e. the Païkon and Prepeonian subzones of Mercier, 1968). No comprehensive study of the volcanics has been undertaken to date and very little data or detailed information have been published concerning their geochemical character or tectonic environment of eruption.

This chapter details the results of over 100 whole-rock geochemical analyses from the Païkon Massif. The principal objectives are threefold:

- To establish the original character of the volcanics.

- To assess and characterise the effects of the metasomatic event that has influenced the Livadia and Kastaneri volcanics, and in so doing, determine which samples and elements are suitably unaltered to be of use in fulfilling the first objective.

- To determine the geotectonic environment of eruption of the Païkon volcanics; do they represent an arc sequence?

- To ascertain whether the Livadia and Kastaneri volcanic units are genetically related (e.g. by fractionation) or whether they represent two geochemically distinct volcanic suites.

5.2 - METHODOLOGY

As described in chapter 4, the pre-Kimmeridgian lower megasequence of the Païkon Massif has suffered several phases of contractional deformation characterised by blueschist to upper greenschist facies (D1) and greenschist facies (D2 and locally D3) deformation. A major hydrothermal event has also affected these largely Jurassic units, causing considerable chemical change. This event took place prior to the Upper Jurassic (D1) compressional event and probably during, or shortly following, eruption of the volcanic/volcaniclastic formations (see chapter 4). Pervasive weathering has more recently had its effect on the volcanic rocks which, in conjunction with the deformation and alteration events outlined above, have significantly influenced the geochemical character of the rocks.

It is well known that metamorphism and fluid infiltration are among the most common causes of geochemical alteration in volcanic rocks and, consequently, it is the most fresh and unaltered samples that are sought for analysis. The principal reason for this is element mobility. Many of the major, minor and trace elements which form the principal constituents of most igneous (and indeed sedimentary and metamorphic) rocks are mobile under blueschist/greenschist facies and/or weathering conditions and can become highly unstable when subjected to the throughflow of hydrothermal fluids (Rollinson, 1993). For this reason, and given the intense deformation that the volcanics of the Païkon Massif have undergone, it is necessary to assess not only which samples but also which elements retain their primary geochemical signatures/concentrations and will thus yield reliable information concerning the tectonic setting of eruption.

5.2.1 - *Screening Samples*

In the field, well over 100 samples of both the Livadia Formation and the Kastaneri Formation were collected for whole-rock geochemical analysis by X-Ray Fluorescence (XRF). Samples were collected from all parts of the Païkon Massif but predominantly from the south where both exposure and preservation are good. The most fresh, basic rocks were sampled preferentially, although a complete suite from basic to acidic rocks was collected to constrain the low pressure fractionation paths. Once trimmed, crushed and powdered the samples were analysed using the XRF technique outlined in the Appendix (Fitton & Dunlop, 1985) for major and trace elements.

Elimination of Sedimentary Samples

Samples plotting in the "sedimentary" field on the Zr/TiO_2 versus Ni diagram of Winchester and Max (1982) were eliminated.

Elimination of Highly Altered Samples

The intensity of alteration varies markedly from locality to locality and so it is important to eliminate, as far as possible, those samples most severely affected by secondary processes. Metasomatism in the Païkon Massif probably took place during or immediately subsequent to the eruption of the volcanics but prior to D1 deformation, because the intensity of alteration varies across D1 structures and is not concentrated along them. The variation may be due to one of three factors (or a combination of them):

a) Hydrothermal fluids have been channelled along certain horizons, possibly those with relatively high porosities, resulting in a correspondingly high degree of alteration in such horizons.

b) The effects of the hydrothermal fluids were originally concentrated in a limited area (i.e. proximal to a vent) and have subsequently been dispersed over a wider area due to tectonism.

c) The areas most severely affected by the hydrothermal process were originally restricted to a limited stratigraphic position (e.g. the uppermost eruptives) and have, again, been more widely distributed by later folding and faulting.

A simple Harker plot of Al_2O_3 versus SiO_2 suggests that silica is enriched by some hydrothermal process (Figure 5.1). It is widely accepted that the maximum SiO_2 concentration in most naturally-occurring primary igneous rocks is 75%, and it can be seen from Figure 5.1 that a cluster of samples, denoted by open circles, lie above this value. Included in this cluster are 26 samples from localities 134, 179, 182, 184, 214, 239, 326 and 330 (see Appendix). Because these rocks cannot have formed by

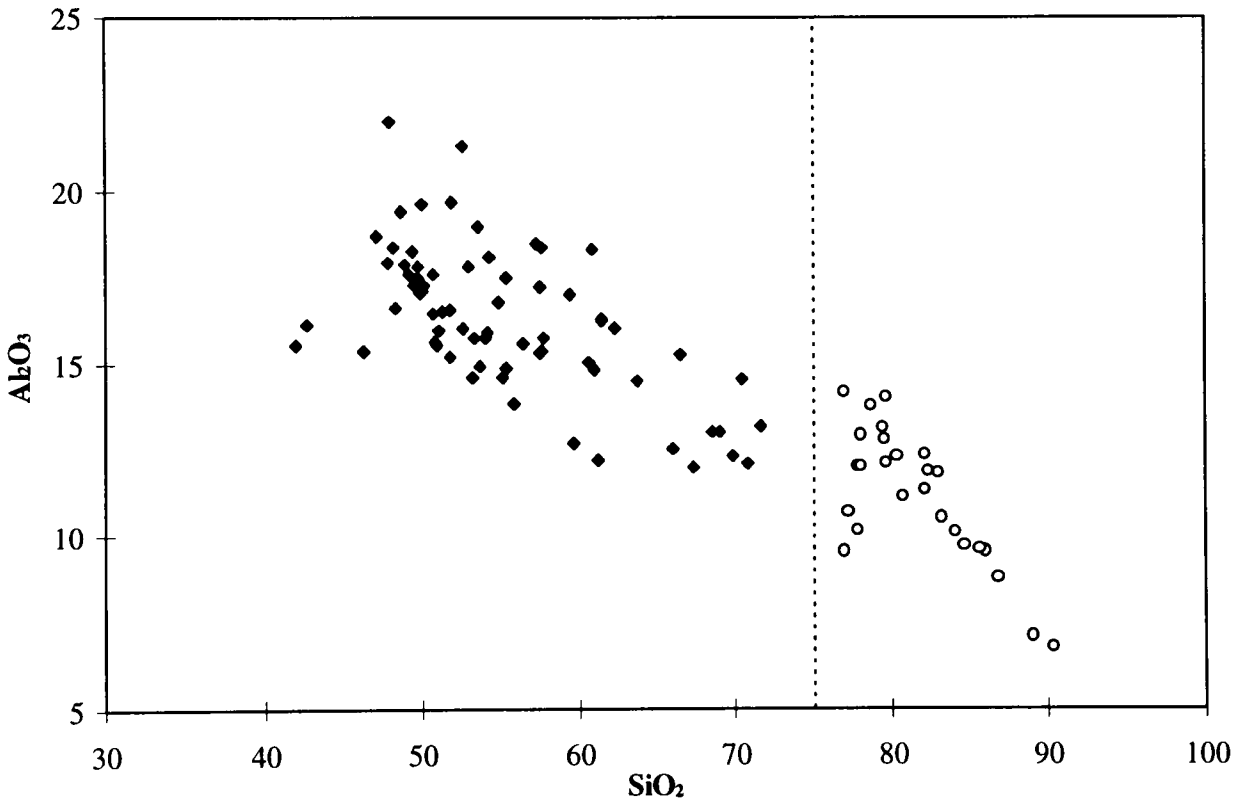


Figure 5.1 - Harker plot of Al_2O_3 versus SiO_2 for all samples analysed from the Païkon Volcanic Group. Those samples with over 75% silica cannot have formed as natural differentiates and have thus been eliminated from further consideration.

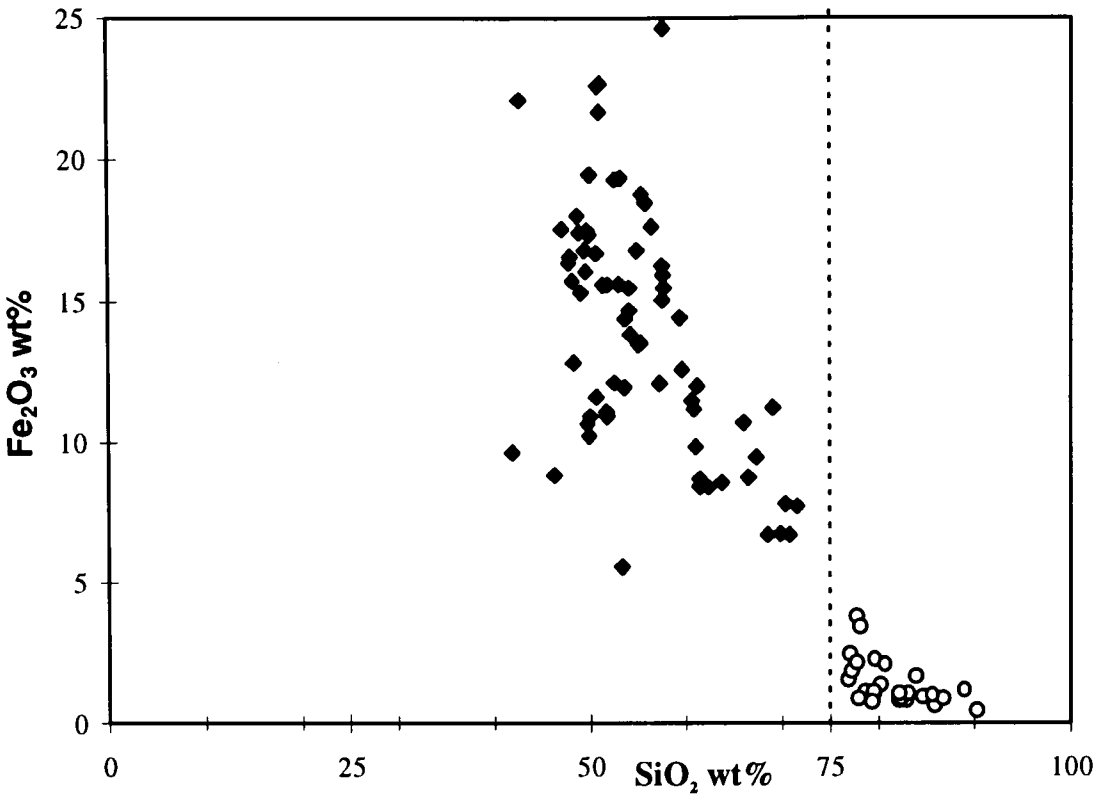


Figure 5.2a. Harker plot of Fe_2O_3 v's SiO_2 for all samples from the Païkon Massif.

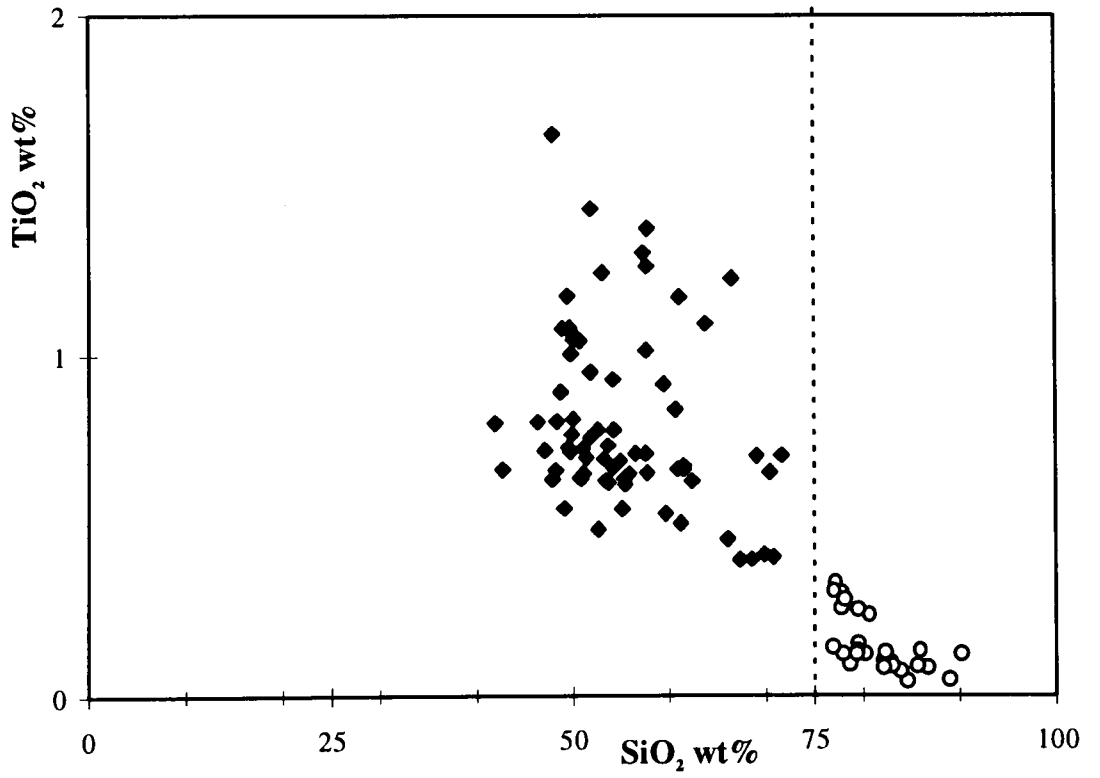


Figure 5.2b - Harker plot of TiO_2 v's SiO_2 for all samples from the Païkon Massif.

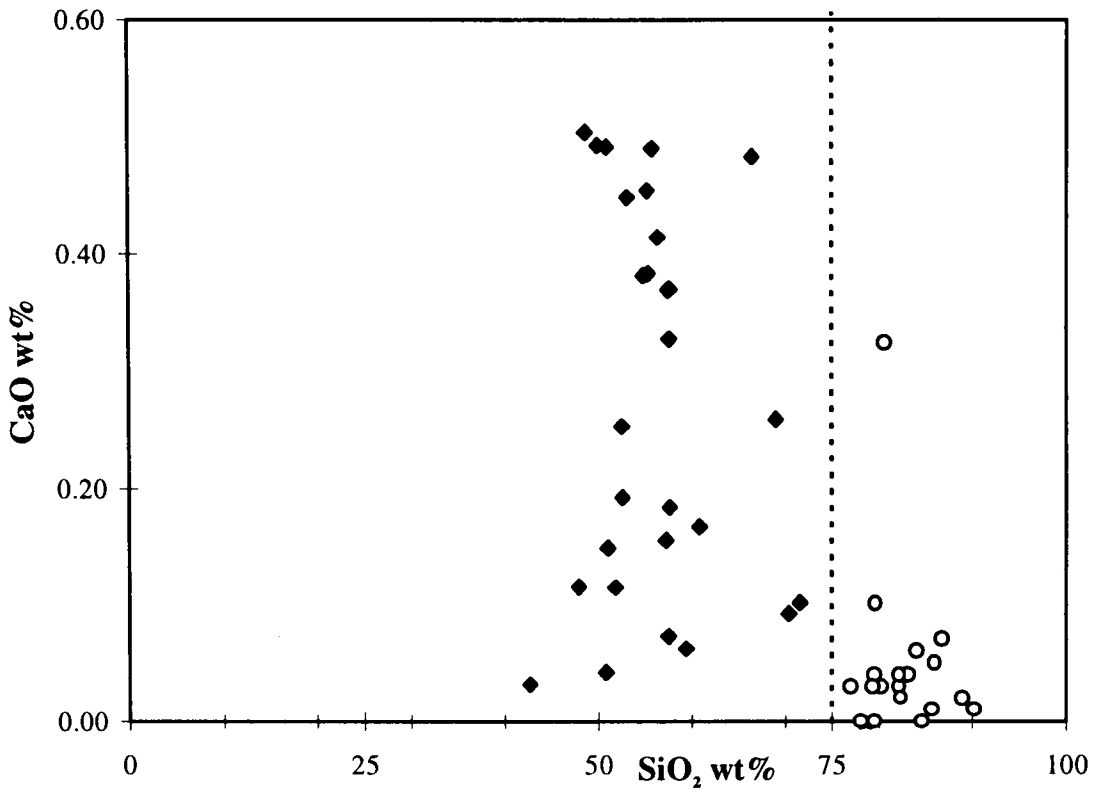


Figure 5.2c - Harker plot of CaO v's SiO_2 for all samples from the Païkon Massif.

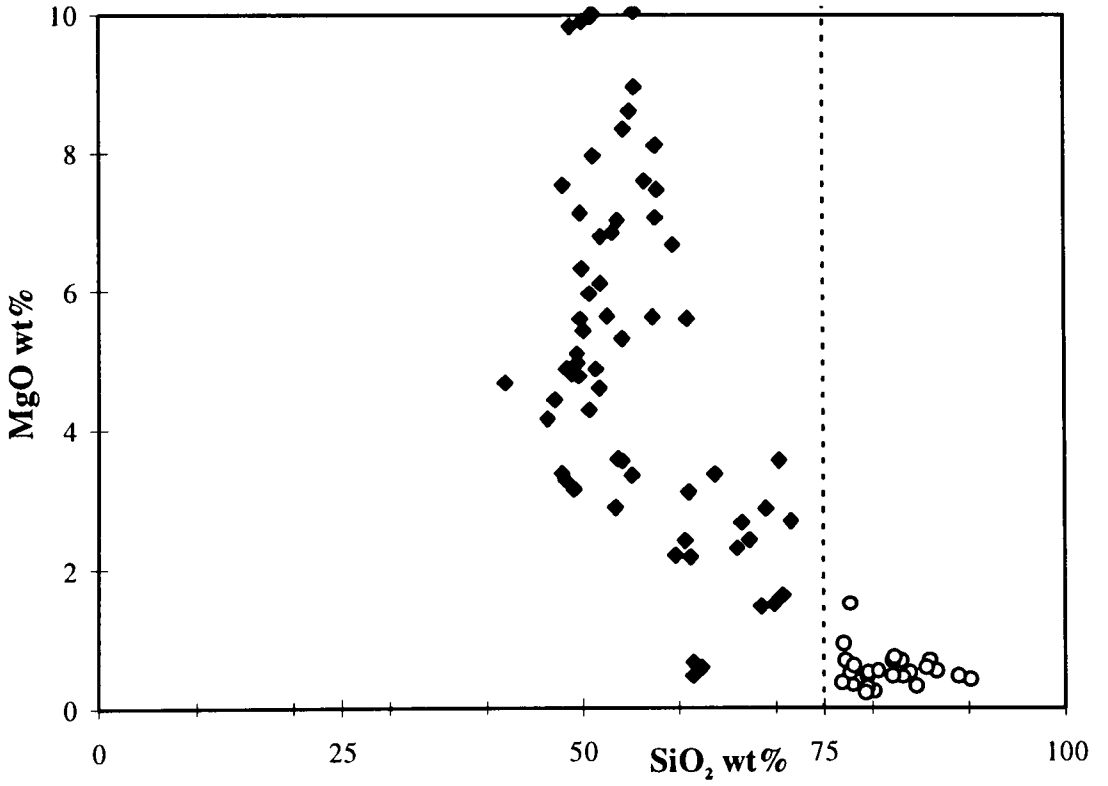


Figure 5.2d - Harker plot of MgO v's SiO_2 for all samples from the Païkon Massif.

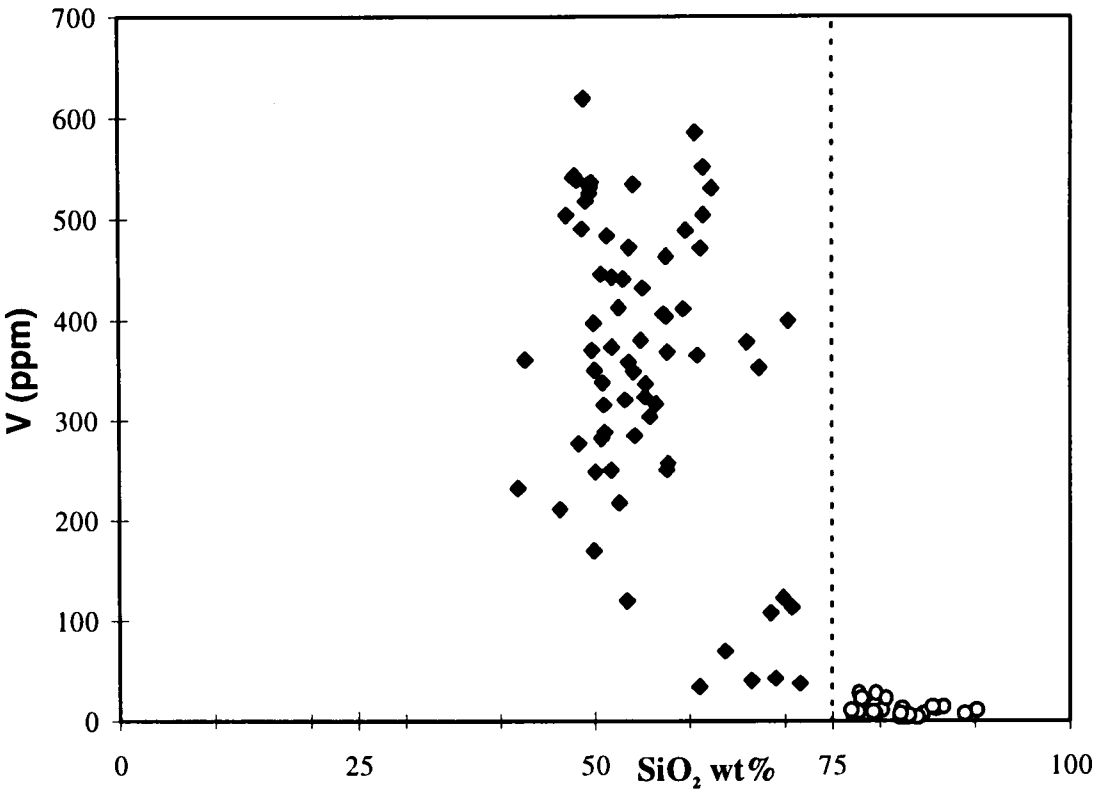


Figure 5.2e - Harker plot of V (ppm) v's SiO_2 for all samples from the Païkon Massif.

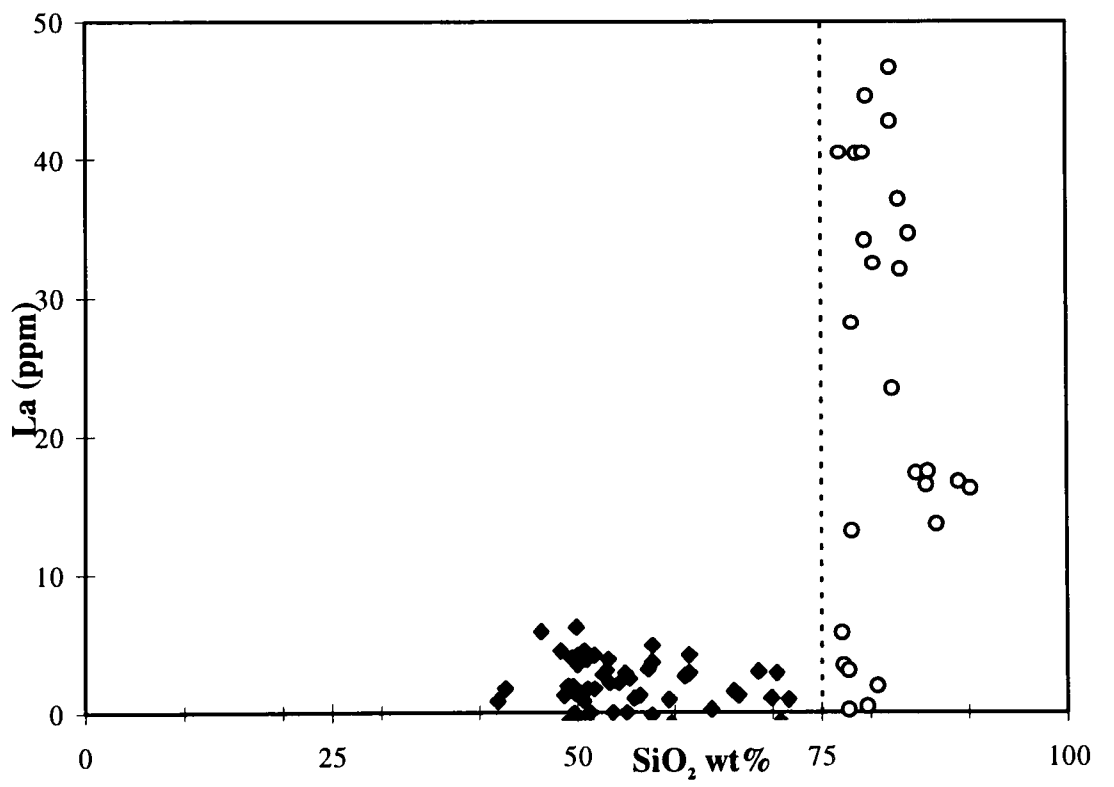


Figure 5.2f - Harker plot of La (ppm) v's SiO_2 for all samples from the Païkon Massif.

primary igneous processes, and are thus the result of secondary activity, they cannot be relied upon to yield primary geochemical signatures and must therefore be treated with caution. They have not been included in the geotectonic discrimination processing which follows.

These samples *are* of use, however, to help determine the geochemical nature of the hydrothermal event discussed above. Figures 5.2a-f demonstrate some of the prevalent effects of the metasomatism, namely a significant decrease in many major element concentrations (e.g. Fe_2O_3, Figure 5.2a; TiO_2, Figure 5.2b; CaO, Figure 5.2c and MgO, Figure 5.2d), except SiO_2 which shows a notable increase. A similar decrease in certain trace elements (such as V, Figure 5.2e; Ni, Cr, Sc and Cu) is also characteristic, although many trace elements are present in considerably higher concentrations in the ultra-acidic samples than in any of less altered samples (e.g. La, Fig. 5.2f; Rb, Zr, Nb, Ba, Pb, Th, Ce and Nd). The consequences of this hydrothermal alteration will be discussed further in section 5.4 (Discussion and Conclusions).

The addition of up to 30 wt% SiO_2 to a suite of volcanic rocks (which has almost certainly taken place in some of the ultra-acidic samples) must affect the weight % concentration of the other major element oxides in the rock simply by dilution. In order to assess whether or not this is the only reason for a consistent concentration decrease in other major elements of the ultra acidic samples, a method of determining the expected decrease in oxide concentration for a given increase in SiO_2 has been derived (Figure 5.3). The relationship can be defined by the following simple equation:

$$\%\Delta C_2 = -\left(\frac{100 * \Delta C_1}{100 - C_1^o}\right)$$

where :

C_1^0 is the original SiO_2 concentration of the protolith

ΔC_1 is the change in SiO_2 wt% during metasomatism

ΔC_2 is the change in wt% of the other element

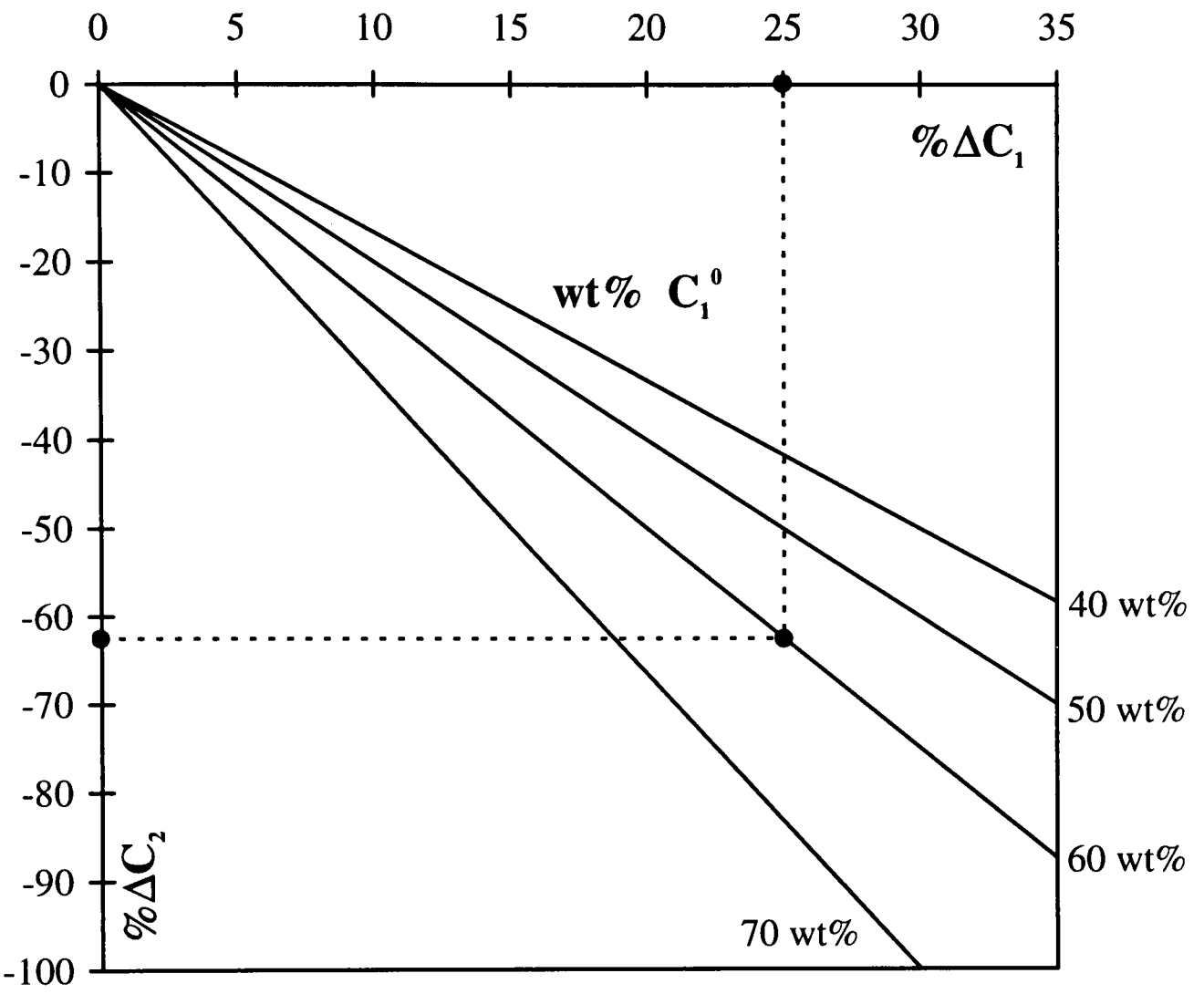


Figure 5.3. Diagram to show the expected dilution that any given element would expect to endure following a given increase in silica concentration. The X axis represents the percentage increase in silica during metasomatism, and the corresponding dilution of other elements (%) can be read off the Y axis. The diagonal lines represent the original silica concentration of the rock.

From Figure 5.3 it can be seen that a rock with an originally andesitic composition (~60 wt% SiO_2) would expect to lose 62.5 wt% of each of its other major elements if a 25 % increase in SiO_2 were to take place (i.e. increase from 60 - 85 wt% SiO_2). This means that an element which started at 5 wt% in the original rock would decrease by 62.5 % to 1.875 wt % in the modified rock, if dilution due to silica input were the only reason for its concentration fall. The data presented in the Appendix

clearly show that all elements whose concentrations have dropped markedly in the highly acidic samples do so by several orders of magnitude more than would be anticipated due to dilution alone. This strongly implies that the hydrothermal fluids responsible for this metasomatic phase are not only enriched in SiO_2, K_2O and sometimes MgO and selected trace elements (namely Rb, Nb, Ba, Pb, Th, La, Ce and Nd) but that they also strip the host igneous rock of many of its other major and trace element components (majors - CaO, Na_2O, MnO, P_2O_5 and occasionally MgO and Fe_2O_3; traces - Ni, Cr, Sc and Cu).

It may be noted that a spurious "fractionation trend" is present in these high-silica samples in that progressive dilution will produce a systematic relationship between SiO_2 and all other elements. If general positive correlations exist between silica enhancement and the depletion of other elements these will appear as pseudo-fractionation trends.

5.2.2 - *Screening Elements*

All of the samples now remaining have less than 54% SiO_2 and have been used to determine the geochemical signature of the Livadia and Kastaneri Formations and hence to deduce their tectonic environment of eruption. All samples have undergone a phase of blueschist facies metamorphism, a phase of greenschist facies metamorphism, weathering and have almost certainly been affected by hydrothermal alteration to some degree. It is thus very important to attempt to determine mobility or immobility of each of their constituent elements establish which can be used as indicators of primary magmatic character.

The conclusions of previous geochemical studies of element mobility (e.g. Loughnan, 1969; Cann, 1970; Bloxham & Lewis, 1972; Pearce & Cann, 1973; Pearce, 1975 and Pearce, 1983) reveal which elements are suitable for use in tectonic setting discrimination diagrams.

Major Elements

As indicated above, and in the Appendix, the most common major elements analysed during whole rock XRF analysis, and expressed as wt% oxides, are SiO_2, Al_2O_3, Fe_2O_3, MgO, CaO, Na_2O, K_2O, TiO_2, MnO and P_2O_5. According to previous workers, the majority of these oxides are mobile under either greenschist or blueschist facies conditions and/or during weathering. Their stability can be summarised as follows:

During regional metamorphism up to greenschist facies grade, the only major element that remains immobile is TiO_2, all others are susceptible to concentration changes due primarily to mineralogical transformations (Pearce, 1975). Further major element mobility takes place during weathering processes where all the major oxides except Al_2O_3, and perhaps TiO_2 are unstable (Pearce, 1975). Even P_2O_5, which can remain immobile during both metamorphism and weathering, becomes unreliable when the host rock is influenced by hydrothermal fluids, as many of these rocks certainly have been. As a result it cannot be assumed that the concentrations of any of the ten major elements, other than possibly TiO_2 and Al_2O_3, are presently at the same concentration as they were at the time of extrusion. Inevitably, the possibility of gain or loss of major elements other than TiO_2 and Al_2O_3 means that the absolute values of these two will not be necessarily original and, strictly, only their ratio might be preserved.

Trace Elements

As with the major oxide elements some trace elements are susceptible to the effects of weathering, metamorphism and hydrothermal alteration, which may result in their preferential removal or concentration in the host volcanics. The stability of trace elements largely depends on their ionic potential, which determines their mobility in aqueous fluids. It has been documented that trace elements with either low (<3) or high (>12) ionic potentials are mobile, whereas those intermediate are more stable (Pearce, 1983). The most mobile trace elements are those with low ionic potential (the LFSE or LILE) which include Rb, Ba and Sr. All are extremely mobile in aqueous fluids (Loughnan, 1969) and are thus not suitable for use on many tectonic

setting discrimination diagrams from areas such as the Païkon Massif, which rely on altered samples. Those elements which remain stable during weathering (Cann, 1970) and post-eruption alteration are the HFS elements such as Ti, Zr, Y and Nb (Pearce & Cann, 1971 & 1973; Pearce, 1975). Cr is also stable under most conditions (Bloxham & Lewis, 1972; Pearce & Cann, 1973) and so, occasionally, are the rare earth elements (Pearce, 1975; Rollinson, 1989). Therefore, according to such literature, the most reliable trace elements to use are Ti, Zr, Y, Nb, Cr, Ni, V and with caution the rare earth elements.

5.3 - TECTONIC DISCRIMINATION

5.3.1 - *Screening Discrimination Diagrams*

The concept of petrogenetic provinces was initially developed by Judd (1886) and Harker (1909) long before the underlying mechanisms connecting tectonic processes with magma character were recognised. Since then the subject has been expanded greatly by the empirical investigation of correlations between character and setting, notably by Cann, Pearce and Winchester. Rollinson (1993) summarises the majority of this work. The empirical distinctions are now more securely based on an appreciation of the more fundamental controls of mantle source characteristics and extents of melting inferred for different tectonic settings. These, however, are outside the scope of the present study. Thanks to this research it is now possible to determine the tectonic environment of eruption of a suite of volcanic rocks by using simple discrimination diagrams based on the concentrations and/or concentration ratios of certain immobile trace elements. For this study, only discrimination diagrams which utilise those elements deemed to be stable within the Païkon volcanics, as assessed in section 5.2, will be considered here, all others have been dismissed. Figure 5.4 lists the discrimination diagrams which are of potential use, summarises their relative strengths and weaknesses in relation to this study and assesses their functional value on a scale of 1 to 3.

It is important to appreciate that tectonic settings form a continuum without inherently sharp domains, just as the totality of mantle source characteristics, melting histories, crustal assimilation and fractional crystallisation generates a continuum of chemical composition of igneous rocks. The "discrimination" is a fuzzy process and is ultimately only as good as the original identifications of setting and the assessment of the attribution of the magmatic rocks sampled to that setting.

PLOT	AUTHORS	USE	RATING
Ti - Zr - Y	Pearce & Cann, 1973	Discriminates WPB, IAT, CAB	1
Ti - Zr (lin)	Pearce & Cann, 1973	Discriminates IAT, CAB, MORB	1
Ti - Zr (log)	Pearce, 1982	Discriminate VAB, MORB, WPB	1
Zr/Ti - Nb/Y	Winchester & Floyd, 1977	Indicates degree of fractionation; involves Nb which may be mobile	2-3
Zr/Y - Ti/Y	Pearce, 1975; Pearce & Gale, 1977	Best for WPB; large overlap between IAT and MORB	2
Ti - Cr	Pearce, 1975	Discriminates MORB & IAT	1-2
Cr - Y	Pearce & Wanming, 1988	Discriminates VAB & MORB	1
Ti/Y - Nb/Y	Pearce, 1982	Good for WPB, poorer for VAB; involves Nb which may be mobile	3
Zr/Y - Zr (1)	Pearce & Norry, 1979	Discriminate VAB, MORB, WPB	2
Zr/Y - Zr (2)	Pearce, 1983	Discriminates Oceanic Arc from Continental Arc	1
Ti/Cr - Ni	Beccaluva *et al.*, 1979	Discriminates MORB & IAT	1-2
TiO_2 - Y/Nb	Floyd & Winchester, 1975	Separates Alkali from Tholeiite; poorer for VAB	3
V - Ti/1000	Shervais, 1982	Discriminates IAT, MORB, Alkali Basalts; poor for CAB	2
V - Cr	Miyashiro & Shido, 1975	Discriminates CAB & IAT	1-2
Nb - Zr - Y	Meschede, 1986	Best for WPB, poorer for VAB; involves Nb which may be mobile	3

Figure 5.4 - Table listing the tectonic discrimination diagrams which are of potential use during this study. Highlighted discrimination diagrams are those which have been used.

5.3.2 - *The Livadia Formation*

After undertaking the screening processes outlined above, 33 samples of volcanic rock from the Livadia Formation remain and have been plotted onto suitable discrimination diagrams (highlighted in Figure 5.4) which utilise the immobile elements outlined in sections 5.2.2 above. All remaining samples are basalts or basaltic-andesites (<54% SiO_2) and are thus adequate for use in the chosen discrimination diagrams.

Figure 5.5a is a ternary plot involving Ti, Zr and Y, which was devised by Pearce & Cann (1973). The samples of the Livadia Formation mostly lie in or near to the IAT (Island Arc Tholeiite) or IAT plus MORB (Mid Ocean Ridge Basalt) fields. On the linear Ti versus Zr plot of Pearce & Cann (1973; Figure 5.5b) the majority of Livadia samples plot comfortably within the IAT field, with only a few plotting outside the template area (samples 328/3, 328/4, 291/2, 291/3 & 291/4). Similar results are obtained using the logarithmic Ti versus Zr plot (Pearce, 1982; Figure 5.5c), where the Livadia suite plots within the VAB (Volcanic Arc Basalt) field.

The Ti versus Cr and Ti/Cr versus Ni plots of Pearce (1975; Figure 5.5d) and Beccaluva *et al.* (1979; Figure 5.5e) respectively, discriminate solely between MORB and IAT, where all samples analysed fall neatly within the IAT field. The Cr versus Y plot (Pearce & Wanming, 1988; Figure 5.5f) largely corroborates this with only one sample plotting in the MORB domain (sample 328/2); the rest reveal entirely IAT abundances.

Two templates which utilise the Zr/Y versus Zr relationship have been used during this study. That of Pearce & Norry (1979; Figure 5.5g) is useful for separating VAB from MORB and WPB (Within Plate Basalt) settings, whereas the template of Pearce (1983; Figure 5.5h) discriminates between continental and oceanic arc settings alone.

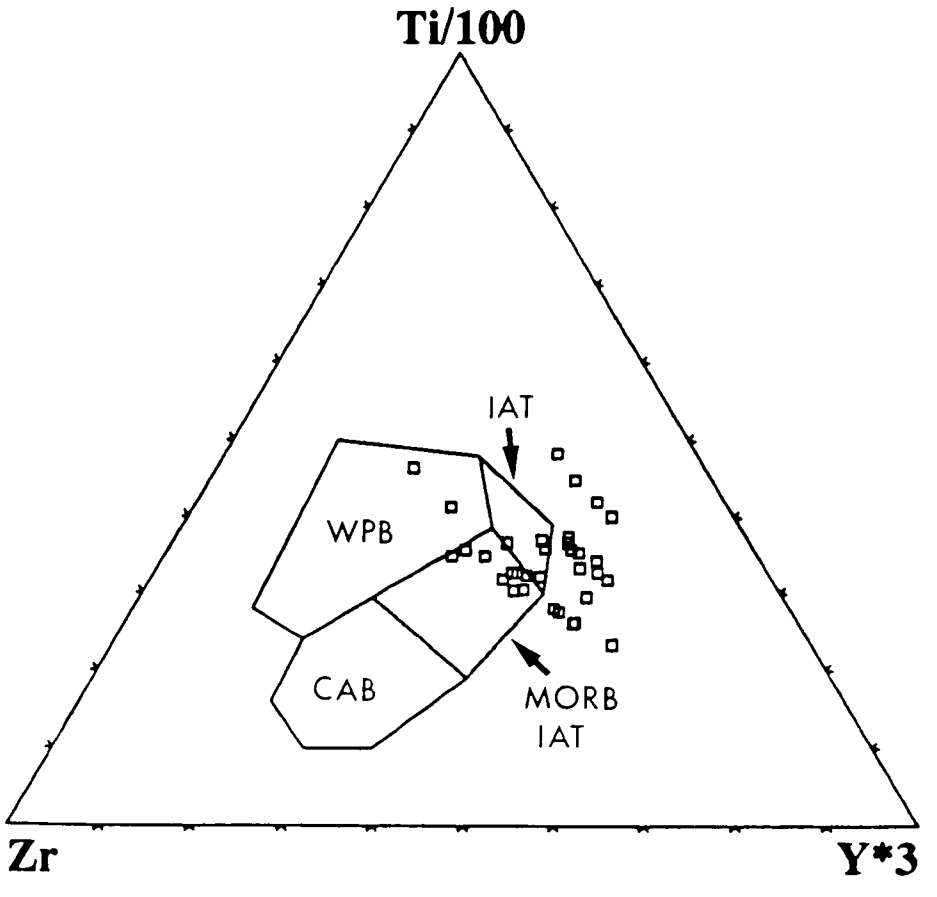


Figure 5.5a - Ternary plot of Ti-Zr-Y (after Pearce & Cann, 1973) for the remaining samples from the Livadia Formation.

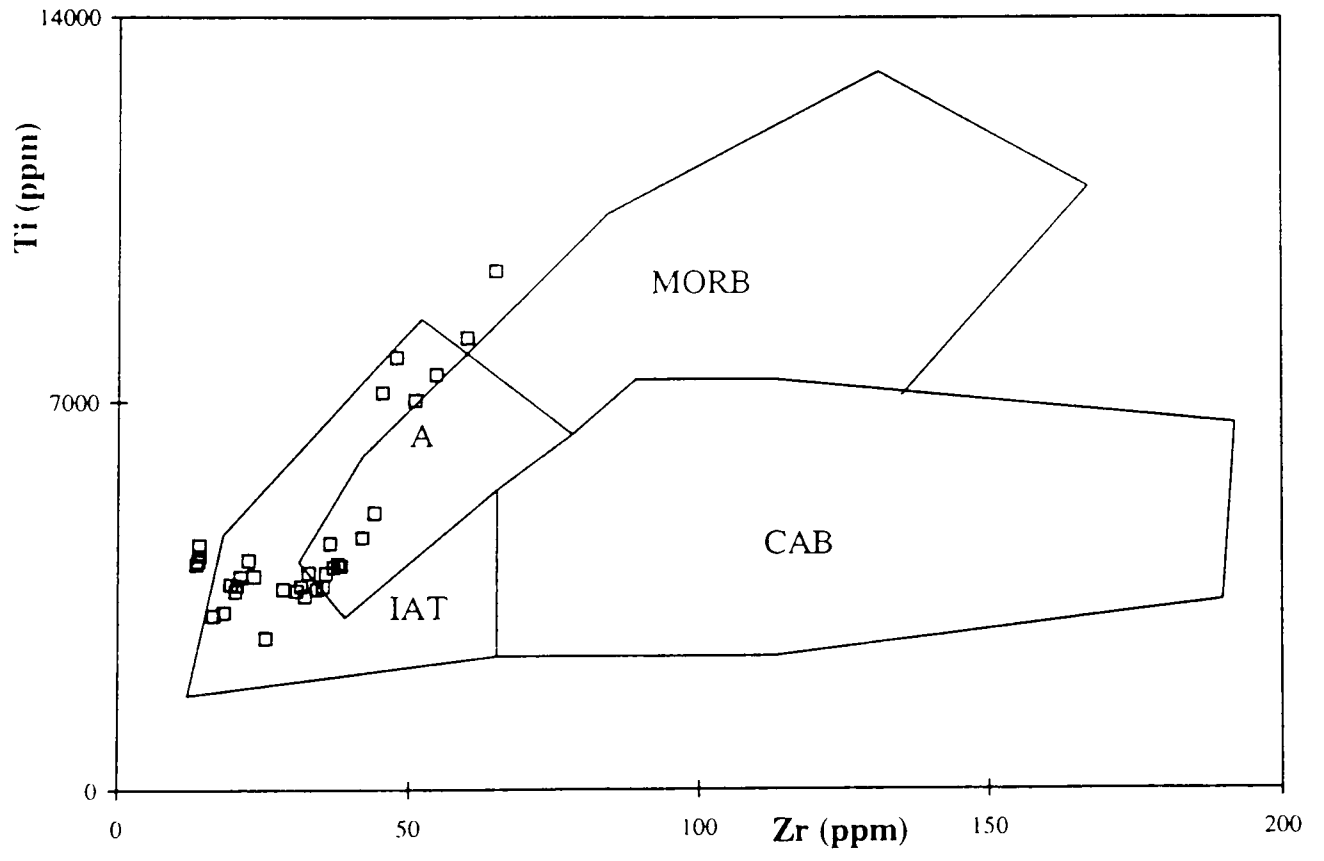


Figure 5.5b - Plot of Ti v's Zr (after Pearce & Cann, 1973) for the Livadia Formation.

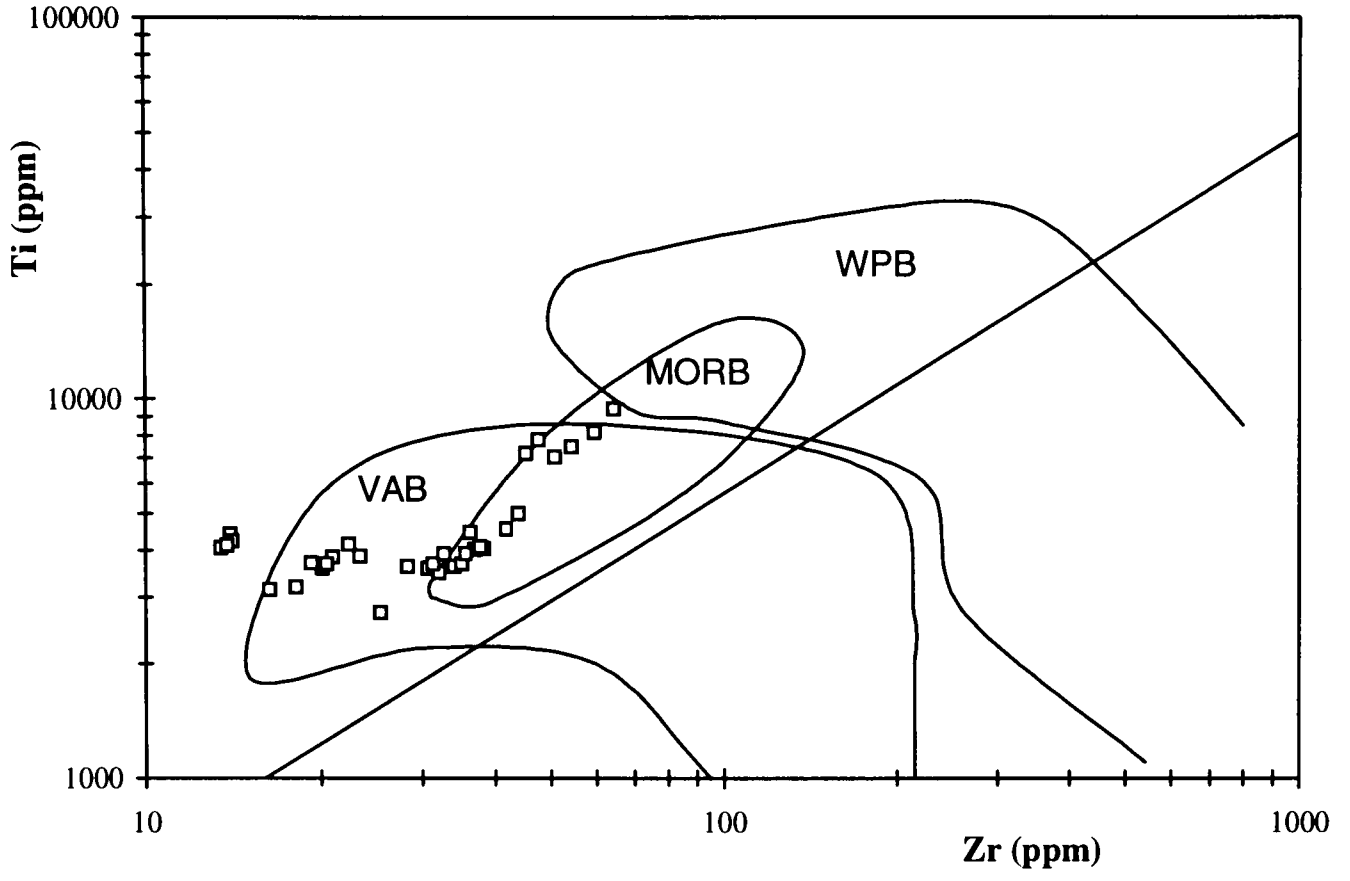


Figure 5.5c - Plot of Ti v's Zr (after Pearce, 1982) for the Livadia Formation.

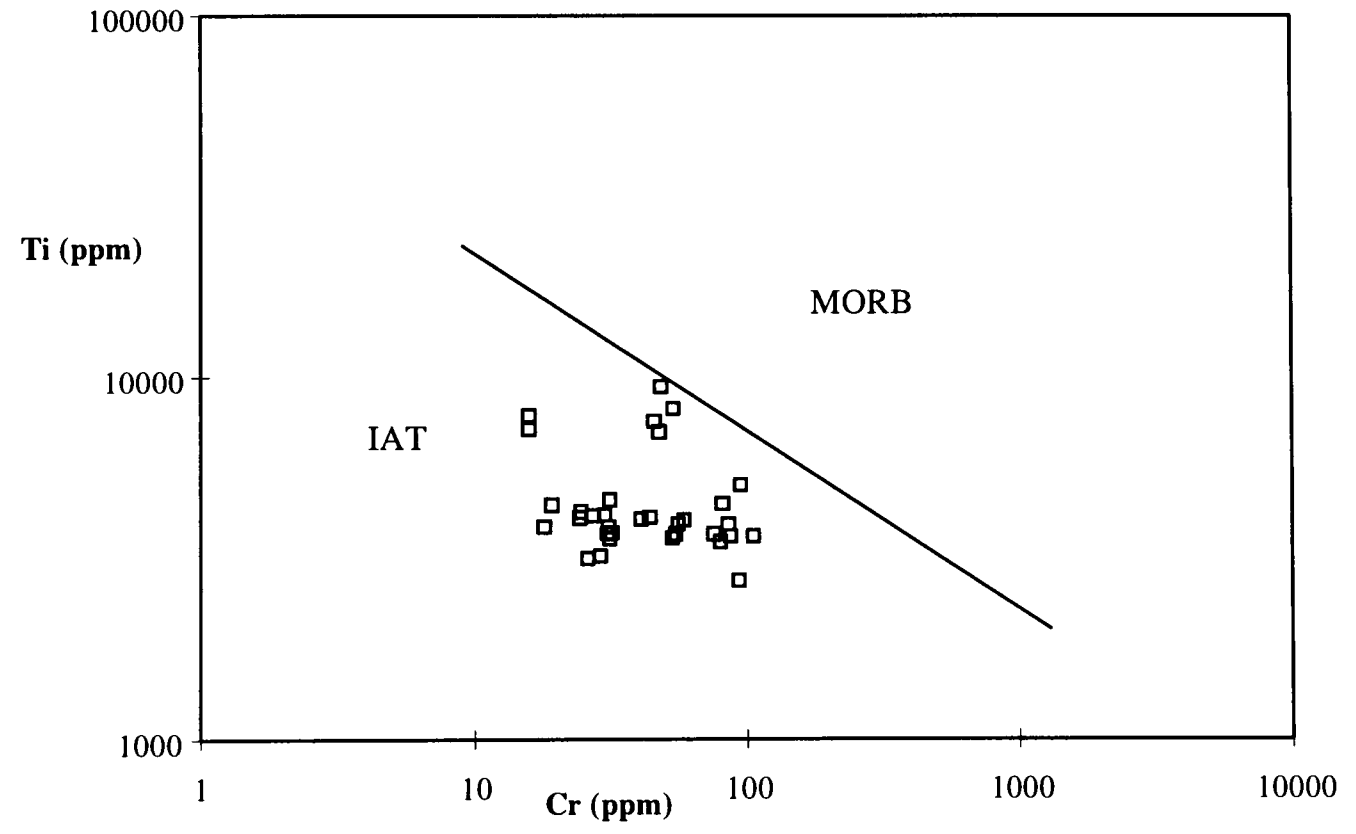


Figure 5.5d - Plot of Ti v's Cr (after Pearce, 1975) for the Livadia Formation.

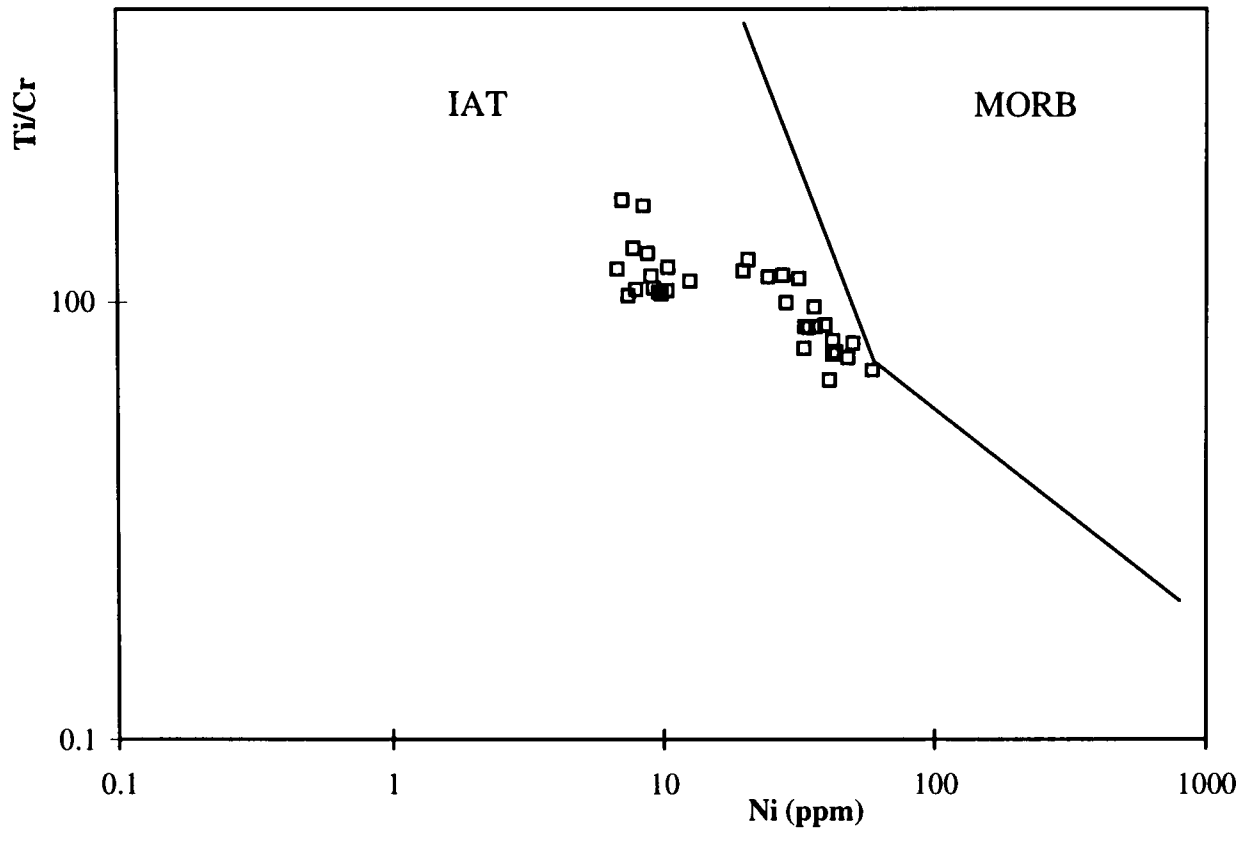


Figure 5.5e - Plot of Ti/Cr v's Ni (after Beccaluva *et al.*, 1979) for the Livadia Formation.

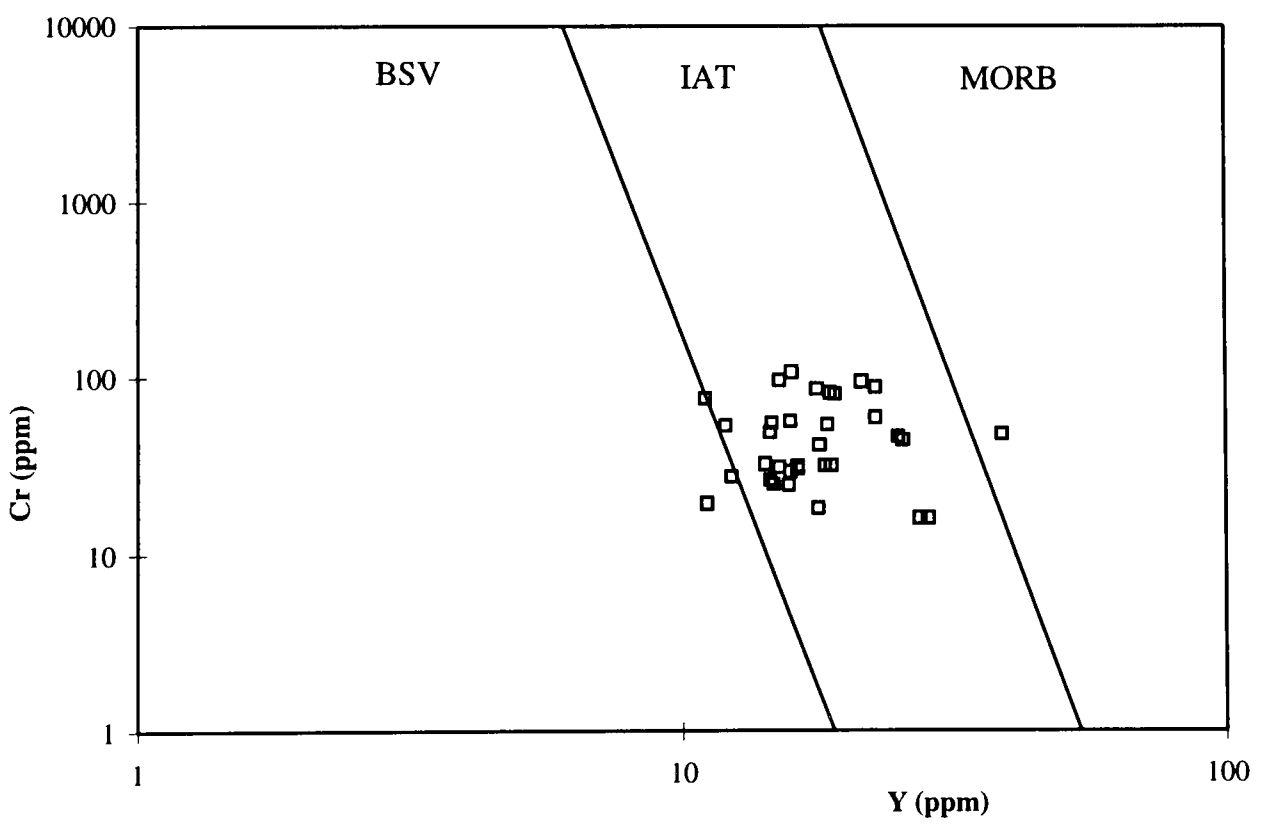


Figure 5.5f - Plot of Cr v's Y (after Pearce & Wanming, 1988) for the Livadia Formation.

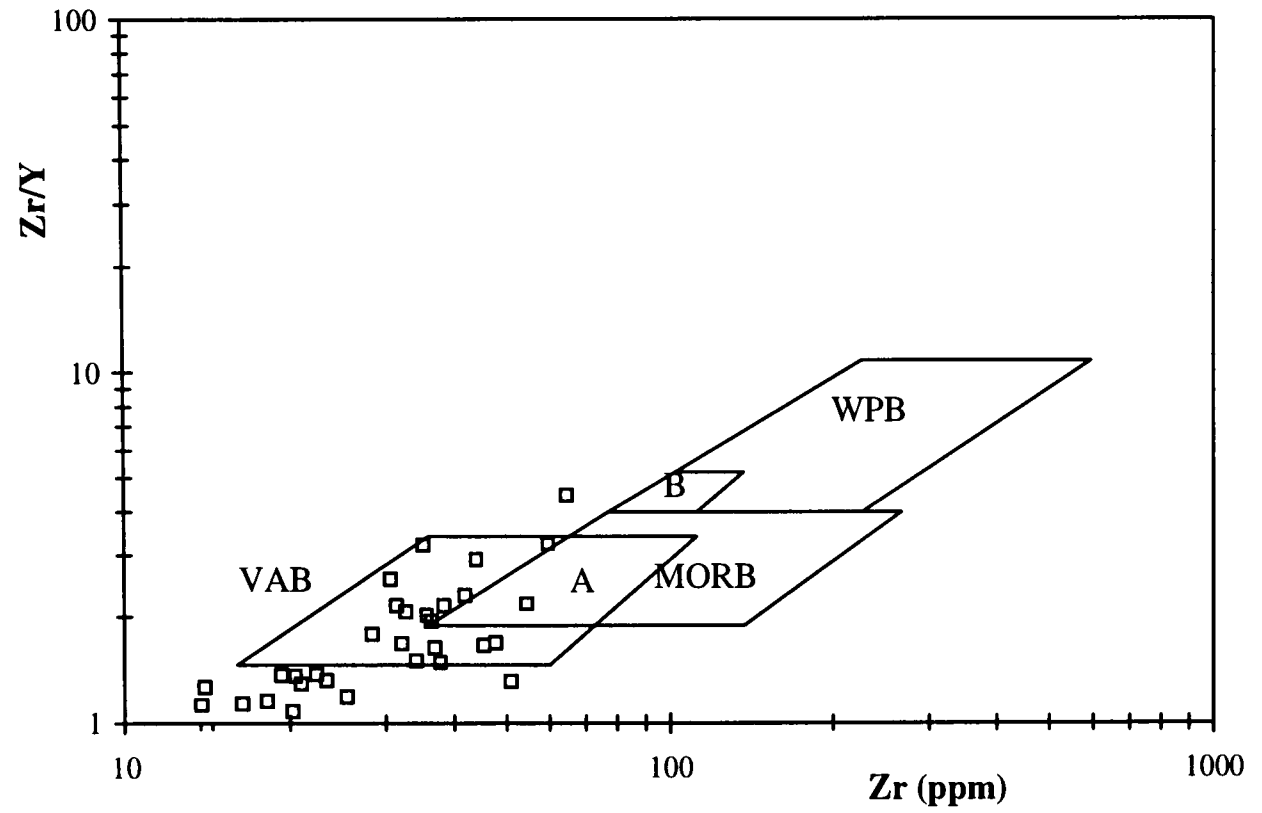


Figure 5.5g - Plot of Zr/Y v's Zr (after Pearce & Norry, 1979) for the Livadia Formation. Field A = VAB plus MORB; field B = WPB plus MORB.

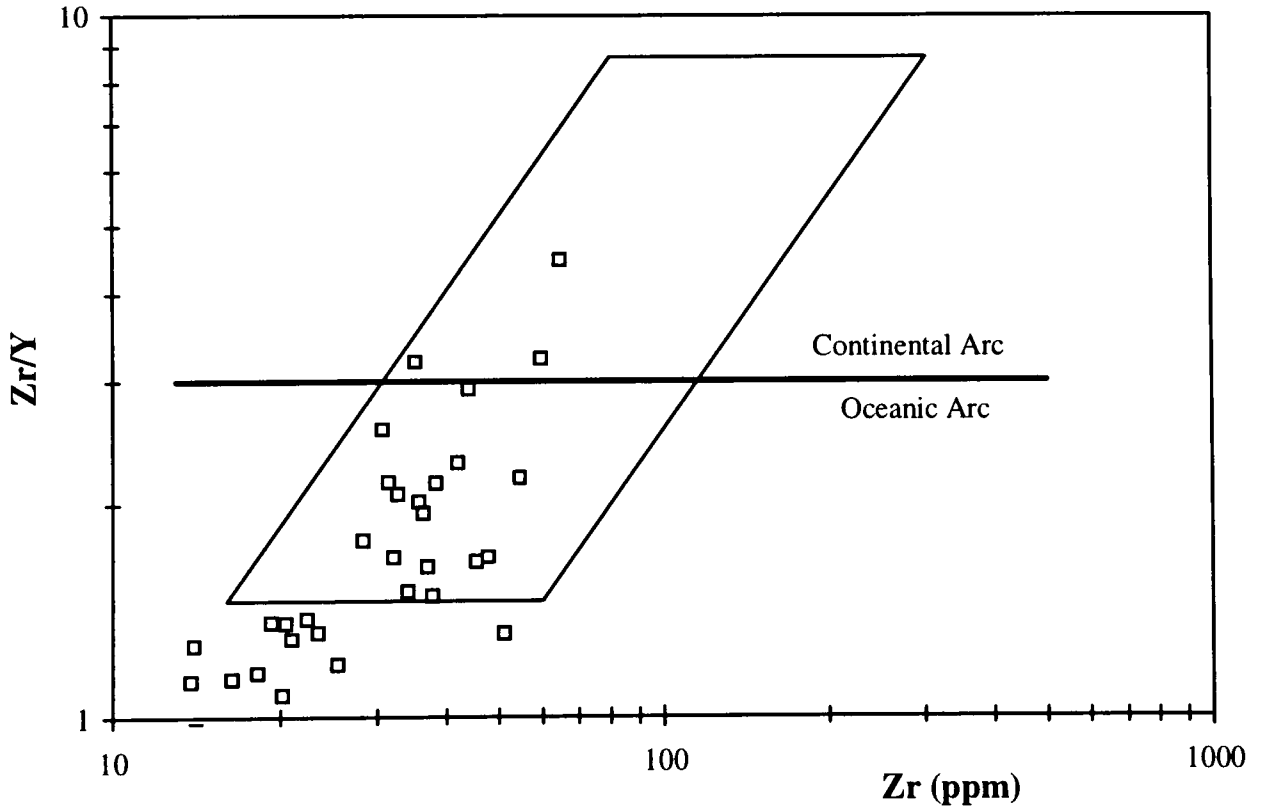


Figure 5.5h - Plot of Zr/Y v's Zr (after Pearce, 1983) for the Livadia Formation.

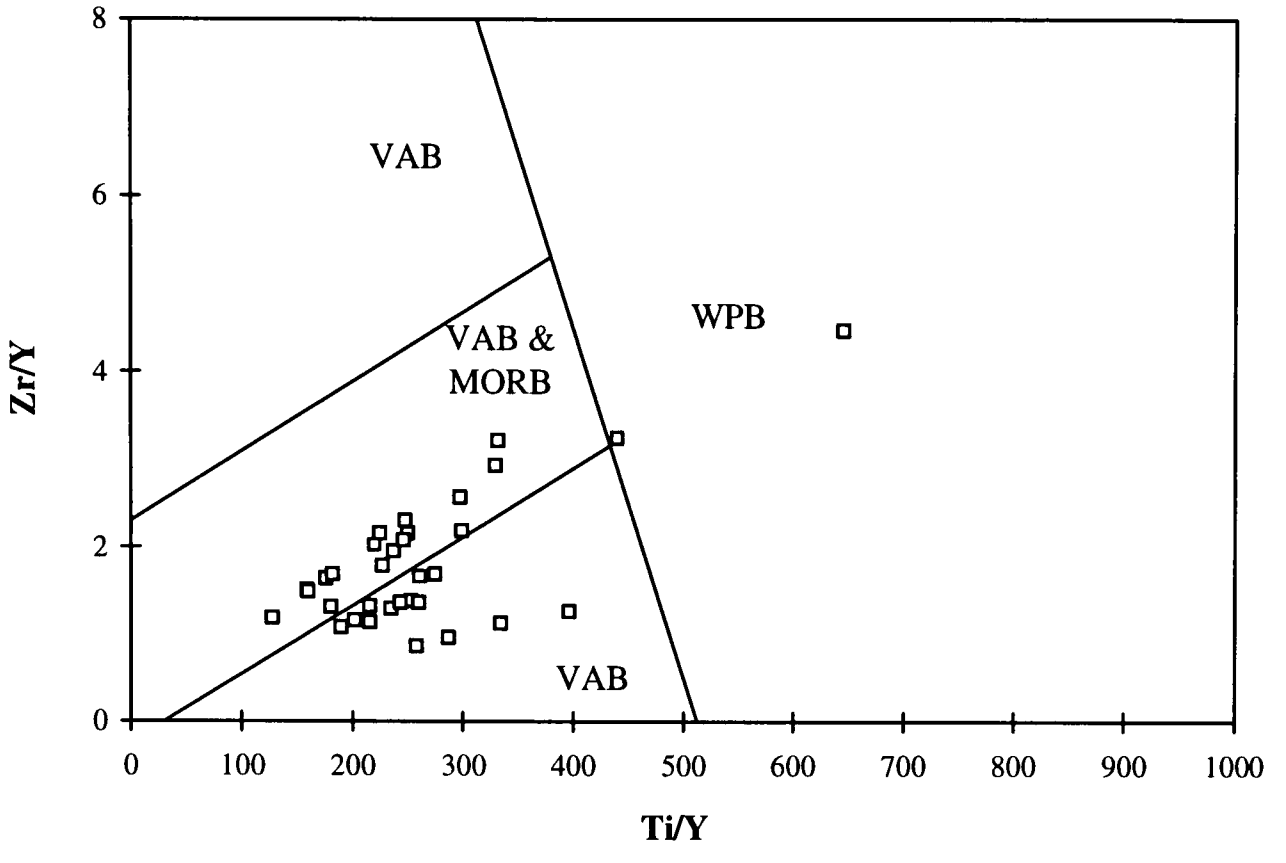


Figure 5.5i - Plot of Zr/Y v's Ti/Y (after Pearce, 1975; Pearce & Gale, 1977) for the Livadia Formation.

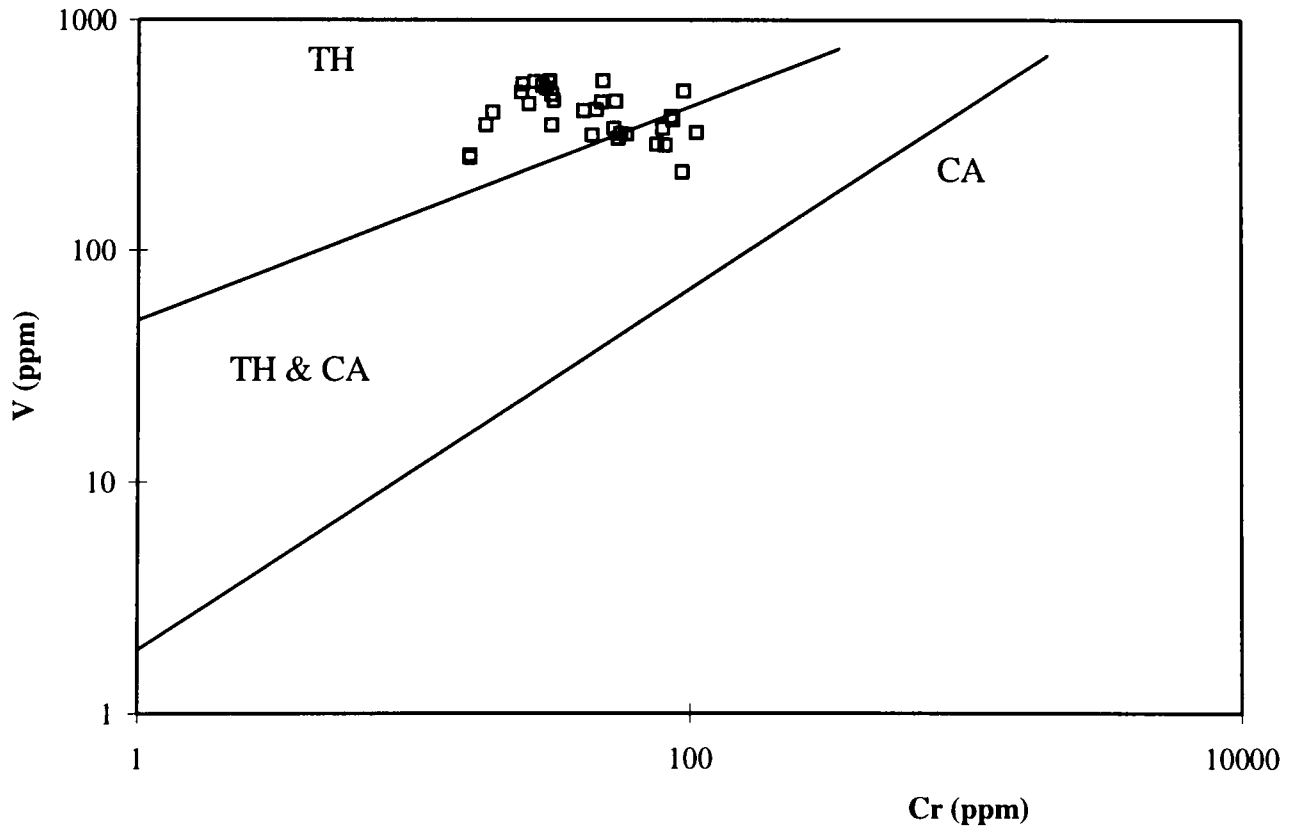


Figure 5.5j - Plot of V v's Cr (after Miyashiro & Shido, 1975) for the Livadia Formation.

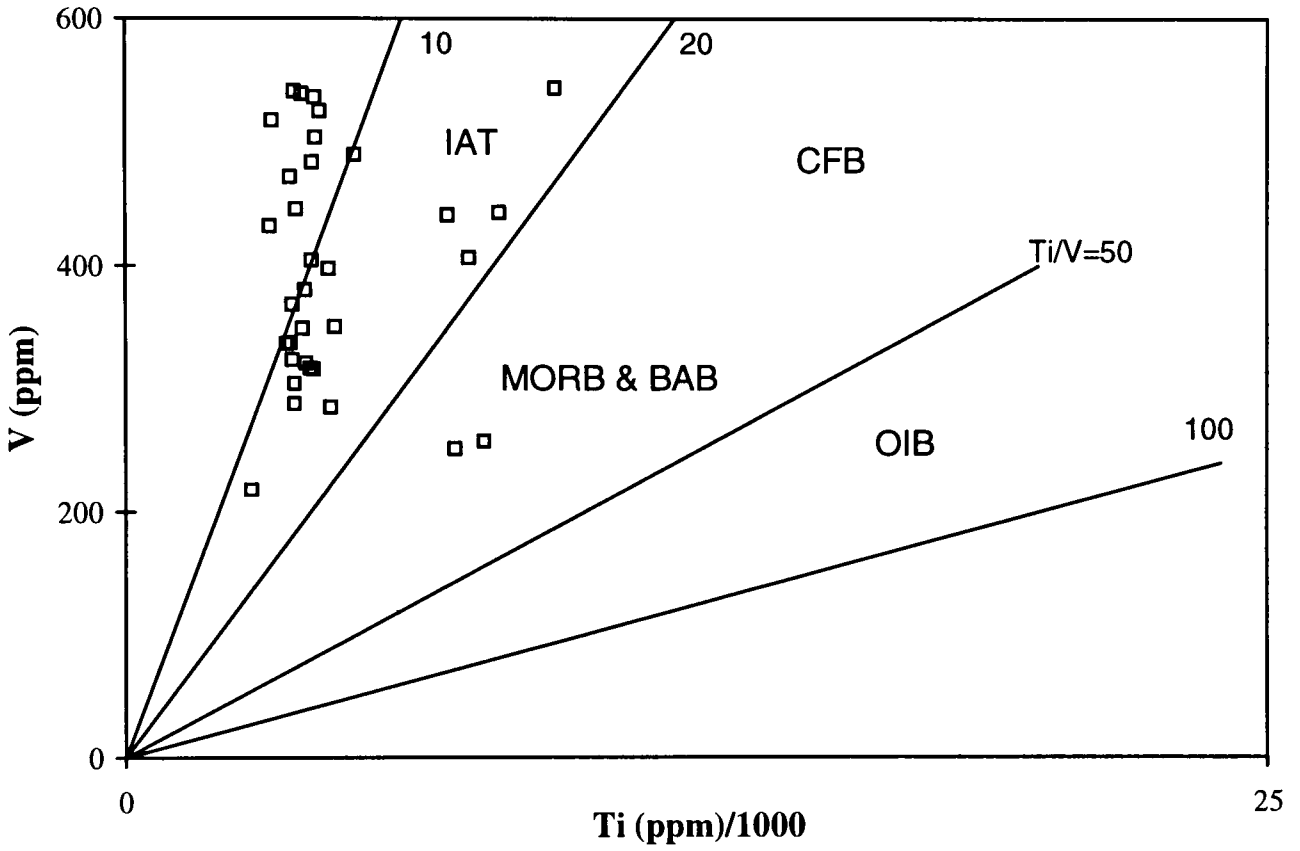


Figure 5.5k - Plot of V v's Ti/100 (after Shervais, 1982) for the Livadia Formation.

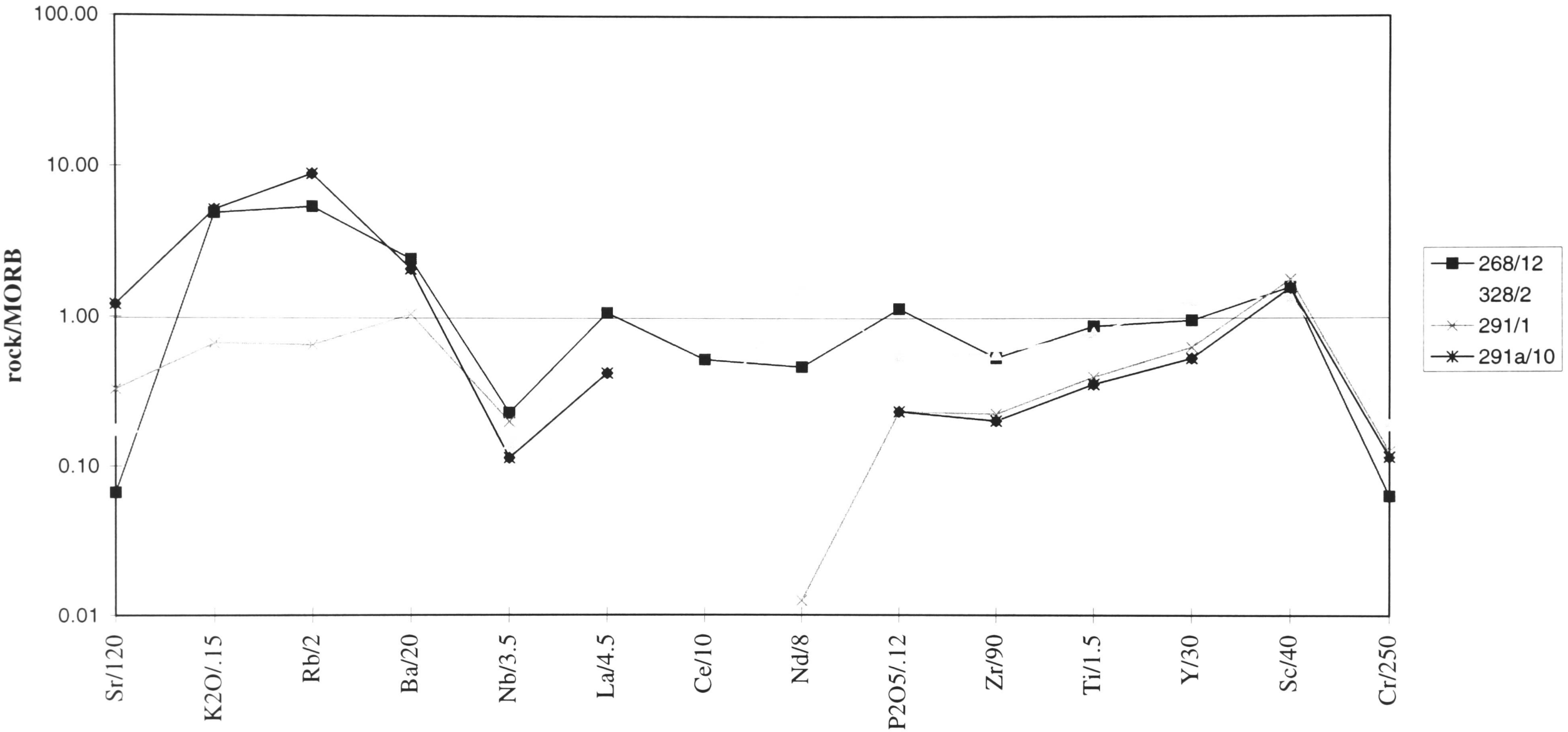
In the former, many samples plot in or near the VAB field, although several lie outside the template area. This is due to a combination of slightly high Y and/or slightly low Zr values in the samples compared to the rest of the suite. This phenomenon affects the latter Zr/Y versus Zr plot also. Here the Livadia volcanics are shown to be of predominantly Oceanic Arc derivation, but not exclusively so as 3 samples (328/3, 328/4 & 268/9) plot in the continental arc field. Only two samples (again samples 328/3 & 328/4) plot outside the VAB field in Figure 5.5i (Zr/Y versus Ti/Y), although a large overlap does exist between the VAB and the VAB plus MORB fields in this diagram. This means that the result from this discrimination diagram alone cannot be used to infer either of these two settings definitively.

Miyashiro & Shido (1975) devised a plot to discriminate between tholeiitic and calc alkaline basalts using V and Cr (Figure 5.5j). Samples from the Livadia Formation are grouped largely within the tholeiite field with only a slight overlap into the calc-alkaline plus tholeiite field. Finally, the V versus Ti/1000 diagram (Shervais, 1982; Figure 5.5k) is rather less well constrained than those discussed so far. The IAT field extends a little way to the left of the Ti/V=10 line (see Rollinson, 1993) but many samples still plot to the left of this. A combination of low Ti and, more commonly, high V are responsible.

When considered together Figures 5.5a-k show conclusively that the Livadia Formation volcanics are almost wholly Volcanic Arc Basalts and even more precisely that they are Island Arc Tholeiites. Only a handful of samples deviate from this trend due possibly to higher degrees of alteration in these samples, which can be considered as exceptions to the norm.

In addition to the discrimination diagrams described above, tectono-chemical information can be gleaned from MORB-normalised multi-element spidergrams (Pearce, 1982). A selection of such spidergrams from the Livadia Formation is displayed in Figure 5.6. The Livadia Formation volcanics show variable enrichment

Figure 5.6 - MORB-normalised trace element spidergrams for selected samples from the Livadia Formation



in Large Ion Lithophile (LIL) elements (e.g. Rb, K, Sr and Ba), which is a characteristic feature of the subduction zone environment and is attributed to the slab flux. However, due to the extremely mobile nature of these elements, this phenomenon cannot be used on its own to infer arc volcanism as it can be mimicked by hydrothermal alteration. Other spidergram features do back up this discrimination though. The High Field Strength (HFS) elements Y, Zr, Ti and Nb mostly show significant depletion relative to MORB, which indicates that higher degrees of partial melting of the source mantle took place. A notable feature is the relative depletion of Nb compared to the adjacent light rare earth elements. This is a particularly characteristic geochemical feature of arc volcanism. The incompatible elements from La onwards have generally flat depletion patterns more typical of Island Arc Tholeiites than Volcanic Arc basalts, which typically show a more spiky pattern of selective enrichments and depletions relative to MORB.

5.3.3 - *The Kastaneri Formation*

14 samples from the Kastaneri Formation survived the screening process and have been plotted on the same discrimination diagrams as the Livadia Formation to allow comparison between the two units. Many of the geochemical characteristics of the two formations are comparable, with only minor differences which are discussed below.

On the ternary Zr-Ti-Y plot of Pearce and Cann (1973; Fig. 5.7a) the Kastaneri Formation samples reveal largely IAT signatures. Figures 5.7b & c plot Ti versus Zr and show that all samples but 2 (414a/1 & 412a/4) plot in the IAT field. There is a degree of overlap into the IAT plus MORB field but none of the samples lie in the solely MORB domain. This is not the case in Figures 5.7d & e which plot Ti versus Cr and Ti/Cr versus Ni respectively. In these templates 2-4 samples (438/1, 438/2 & 447a/2) are excluded from the IAT field, where the rest of the Kastaneri suite lie, and plot within the MORB field. However, they do lie very close to the IAT/MORB boundary and therefore may not be true MORB rocks.

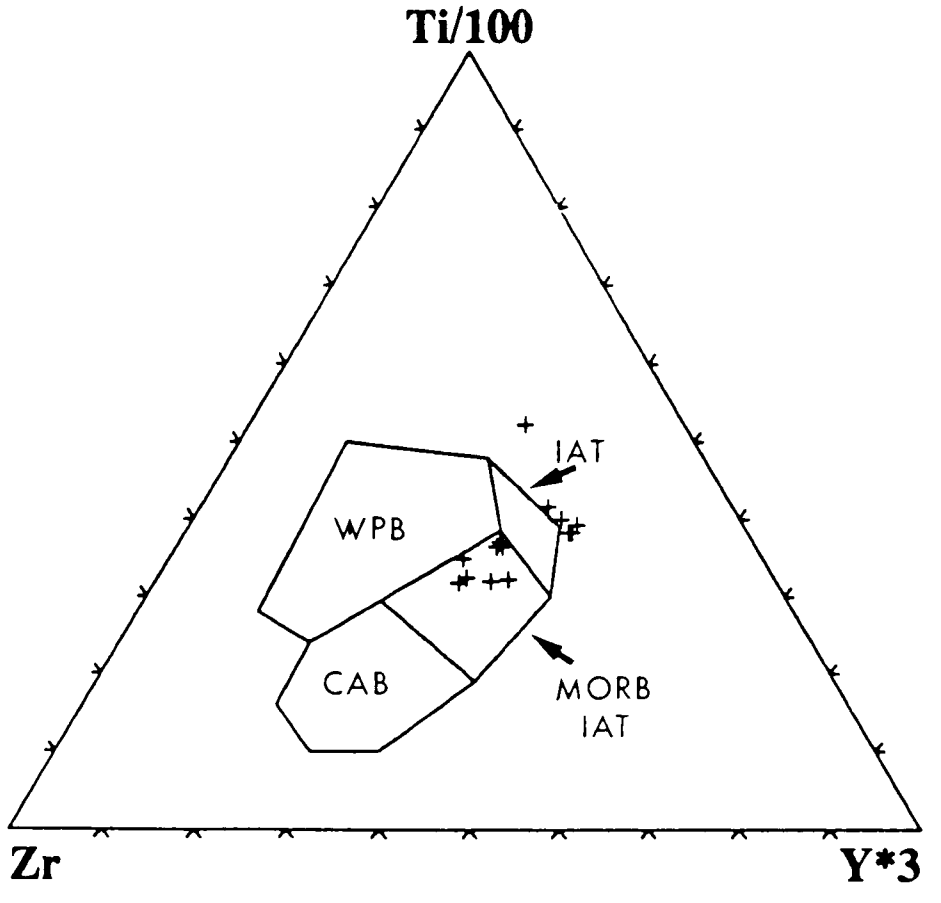


Figure 5.7a - Ternary plot of Ti-Zr-Y (after Pearce & Cann, 1973) for the remaining samples from the Kastaneri Formation.

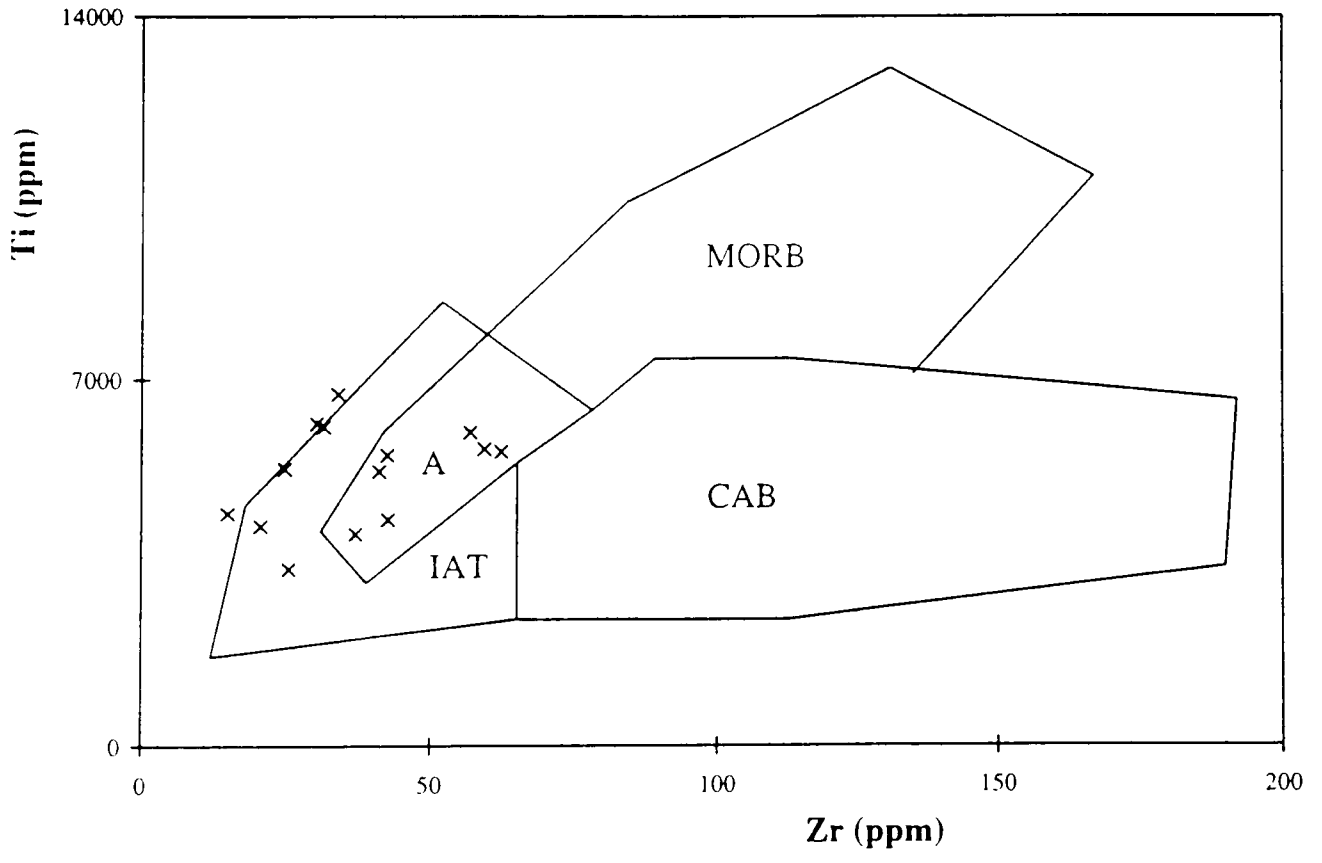


Figure 5.7b - Plot of Ti v's Zr (after Pearce & Cann, 1973) for the Kastaneri Formation.

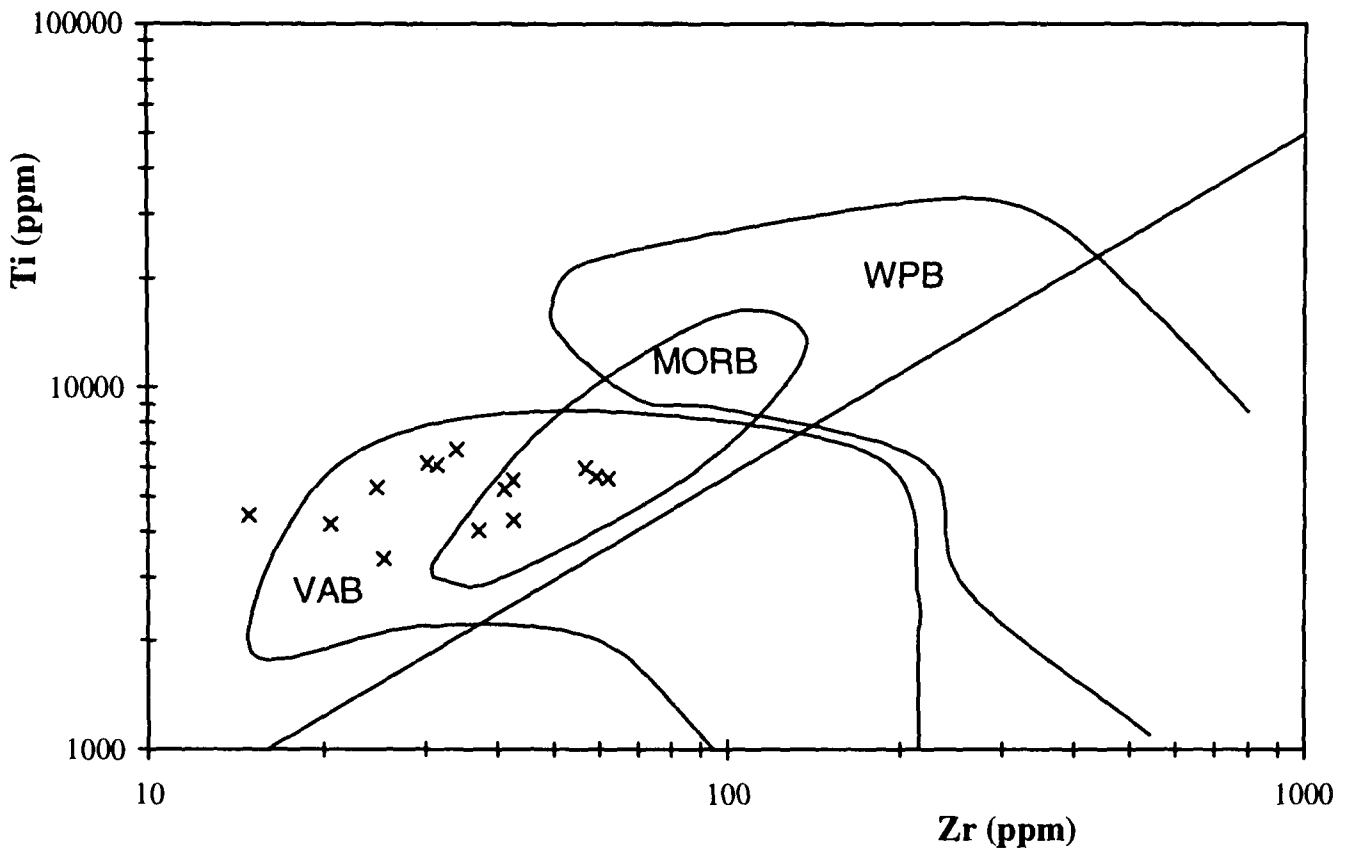


Figure 5.7c - Plot of Ti v's Zr (after Pearce, 1982) for the Kastaneri Formation.

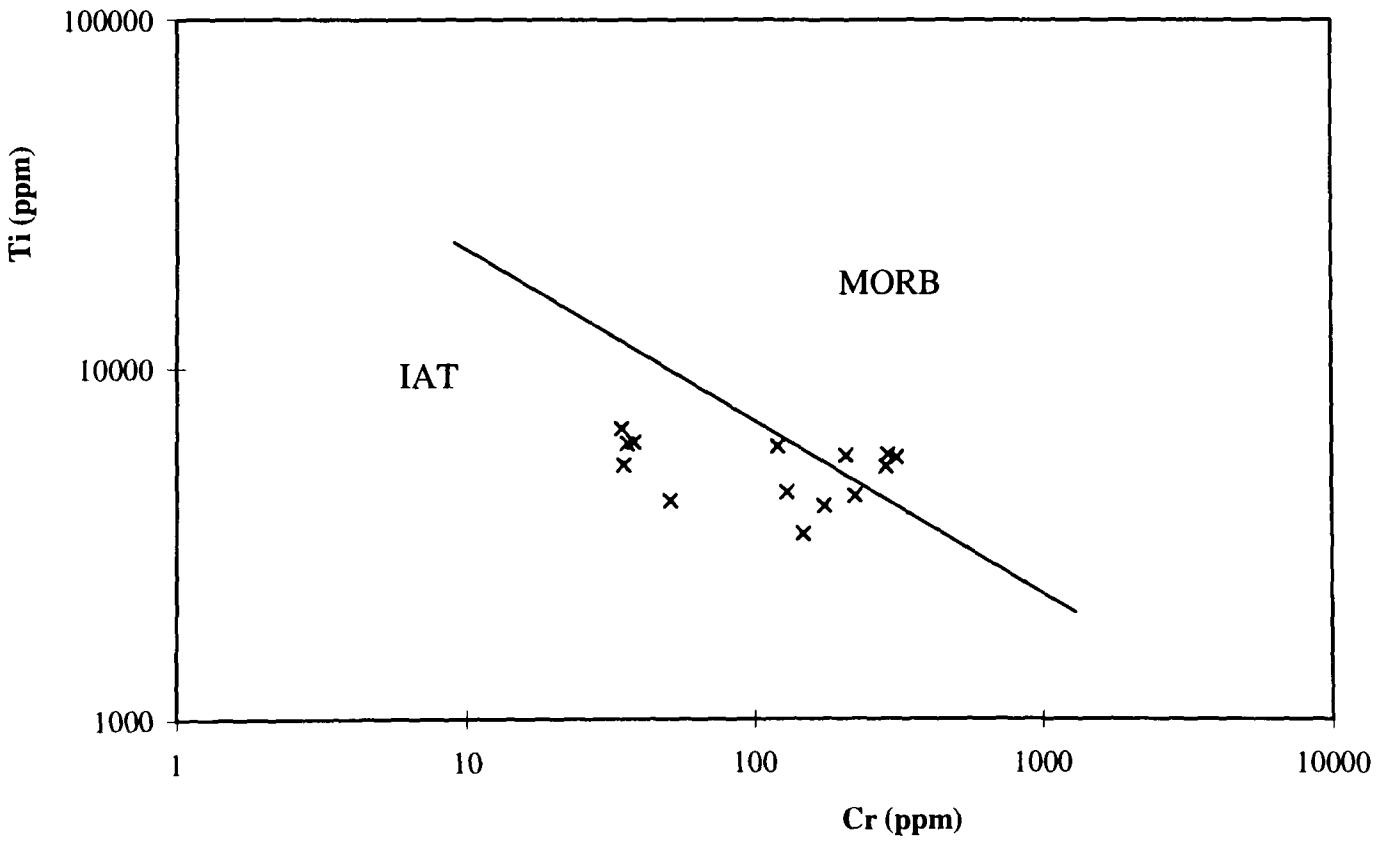


Figure 5.7d - Plot of Ti v's Cr (after Pearce, 1975) for the Kastaneri Formation.

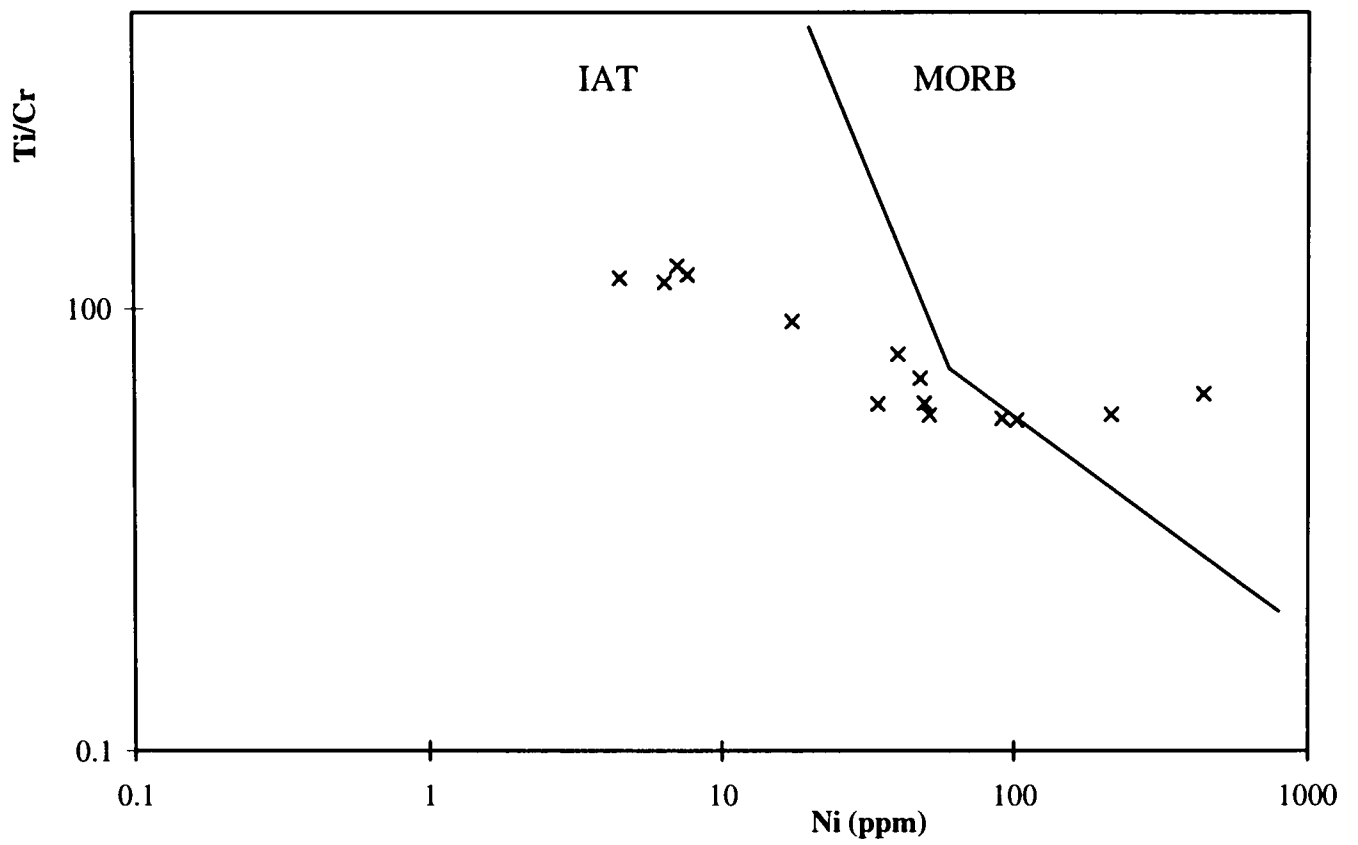


Figure 5.7e - Plot of Ti/Cr v's Ni (after Beccaluva *et al.*, 1979) for the Kastaneri Formation

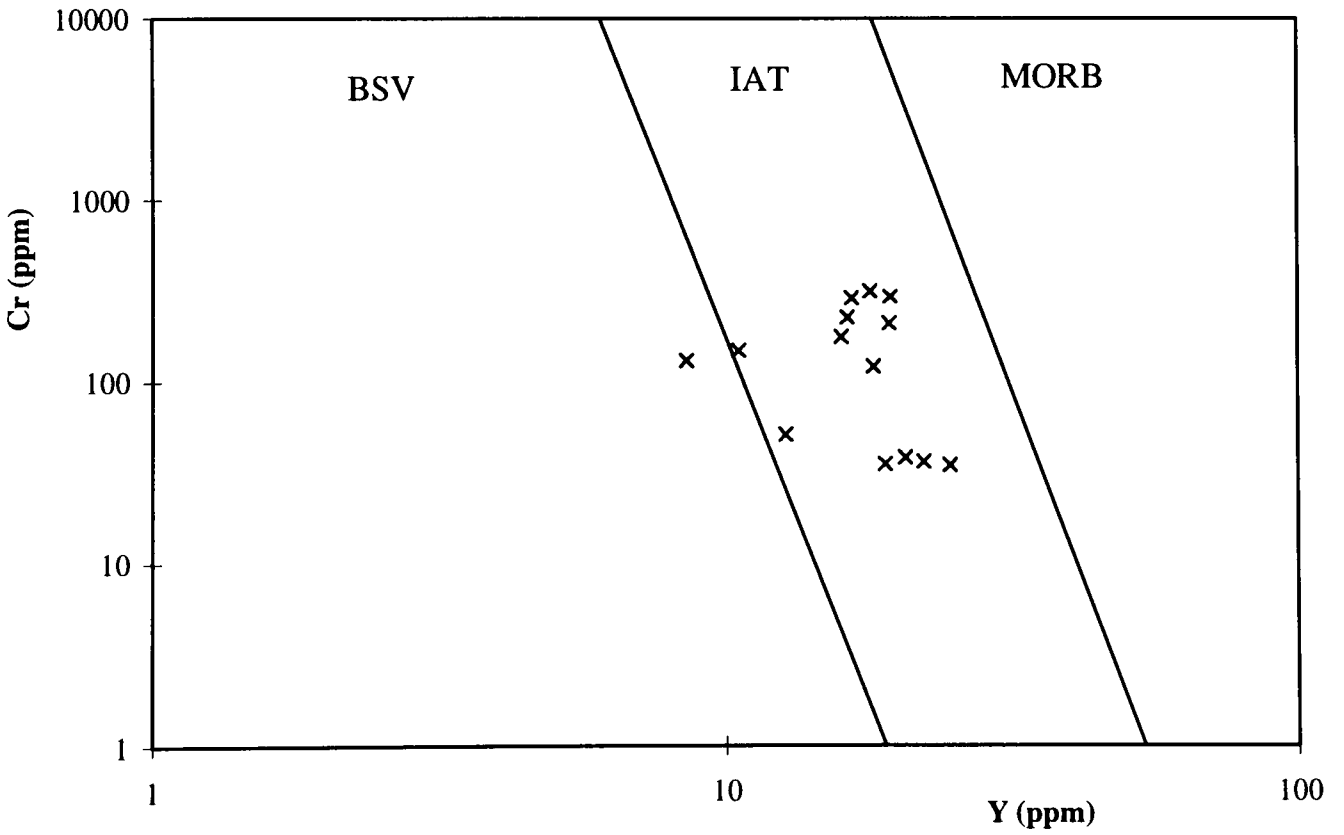


Figure 5.7f - Plot of Cr v's Y (after Pearce & Wanming, 1988) for the Kastaneri Formation

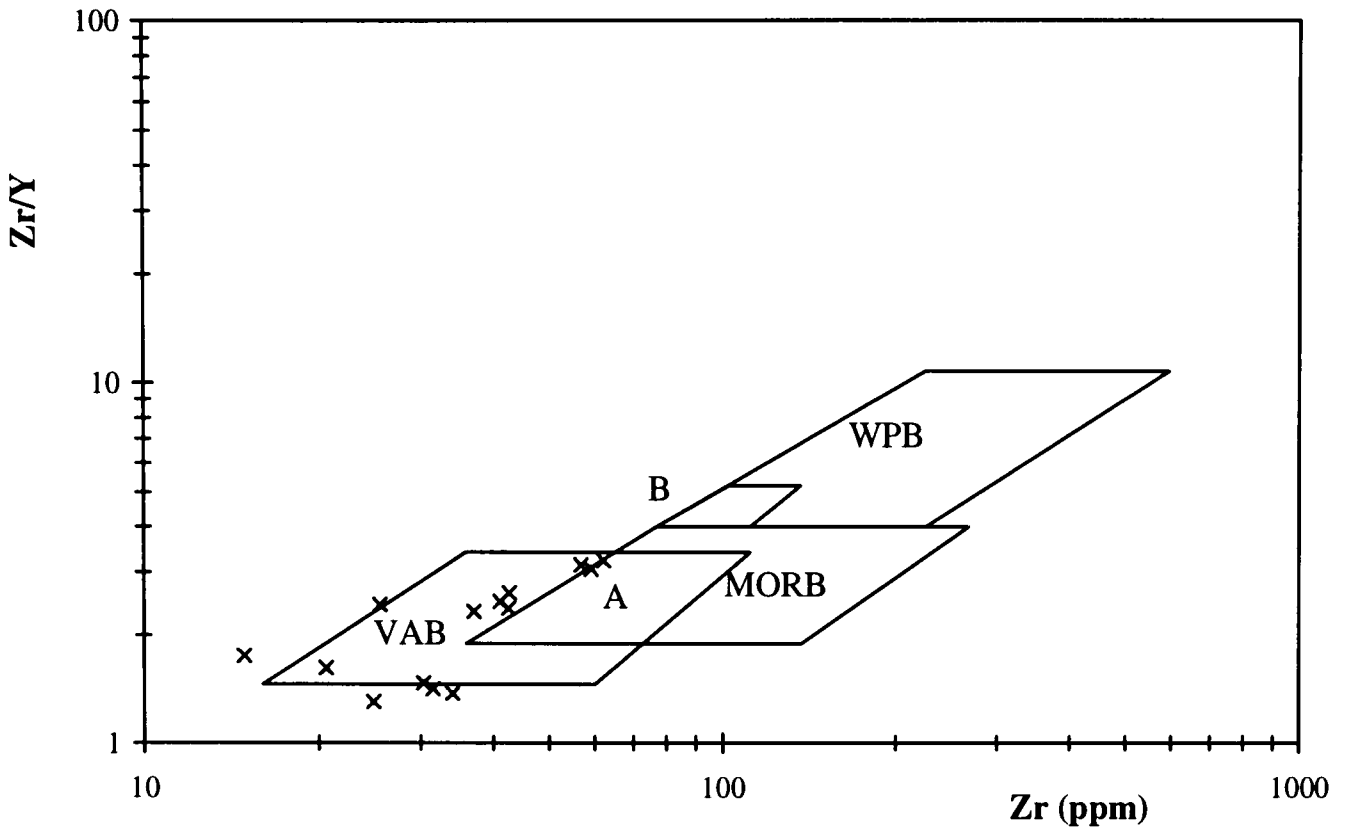


Figure 5.7g - Plot of Zr/Y v's Zr (after Pearce & Norry, 1979) for the Kastaneri Formation. Field A = VAB plus MORB; field B = WPB plus MORB.

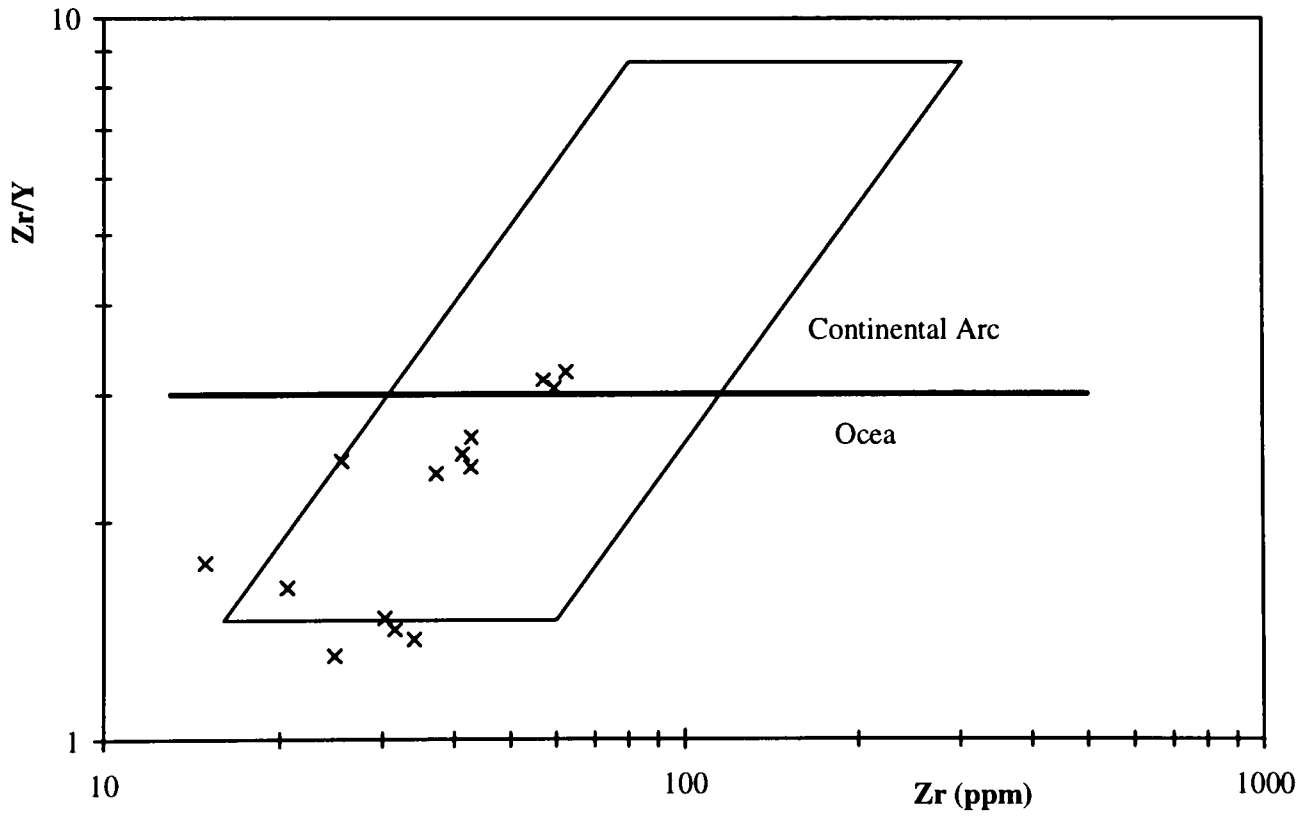


Figure 5.7h - Plot of Zr/Y v's Zr (after Pearce, 1983) for the Kastaneri Formation.

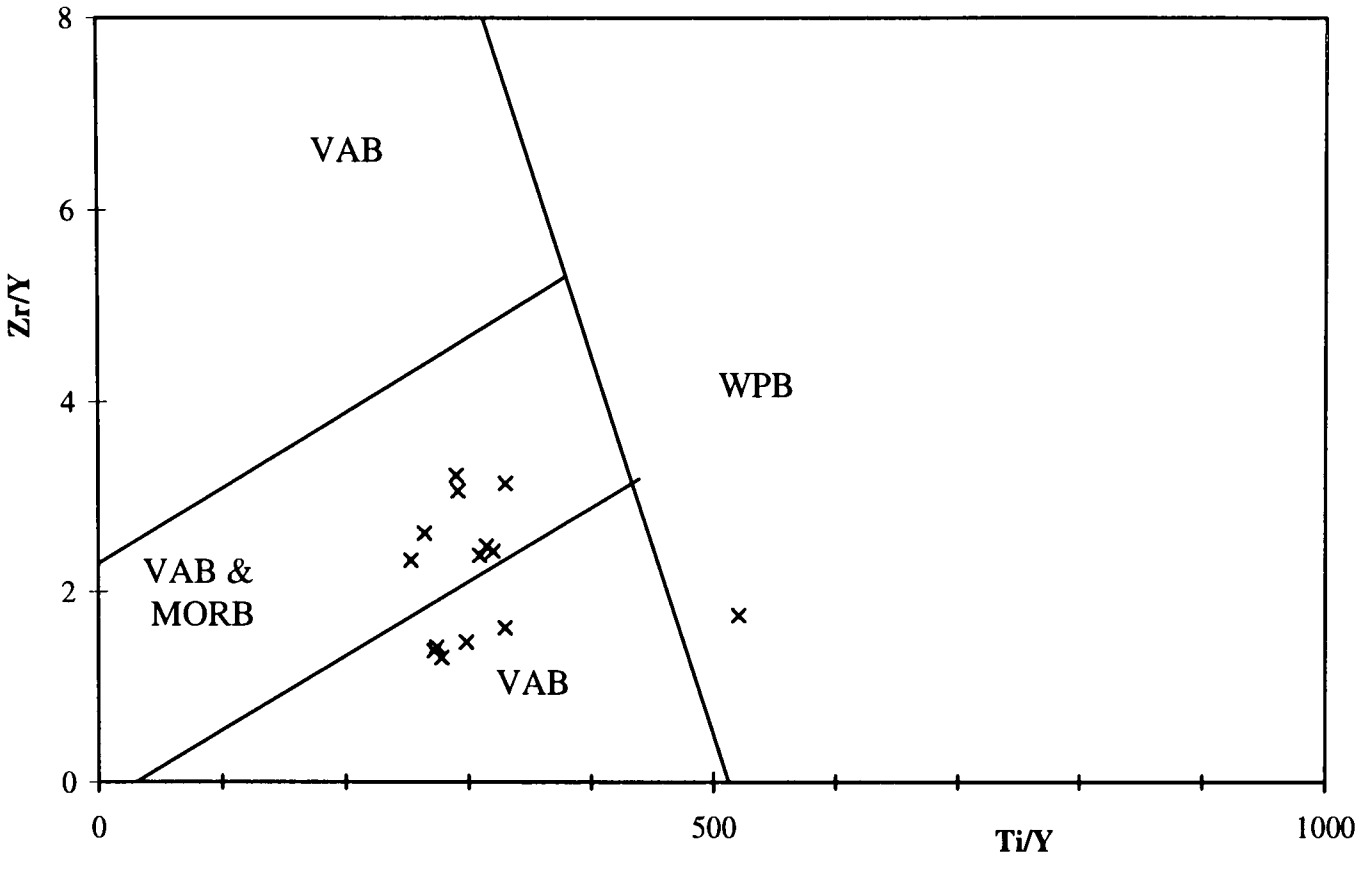


Figure 5.7i - Plot of Zr/Y v's Ti/Y (after Pearce, 1975; Pearce & Gale, 1977) for the Kastaneri Formation.

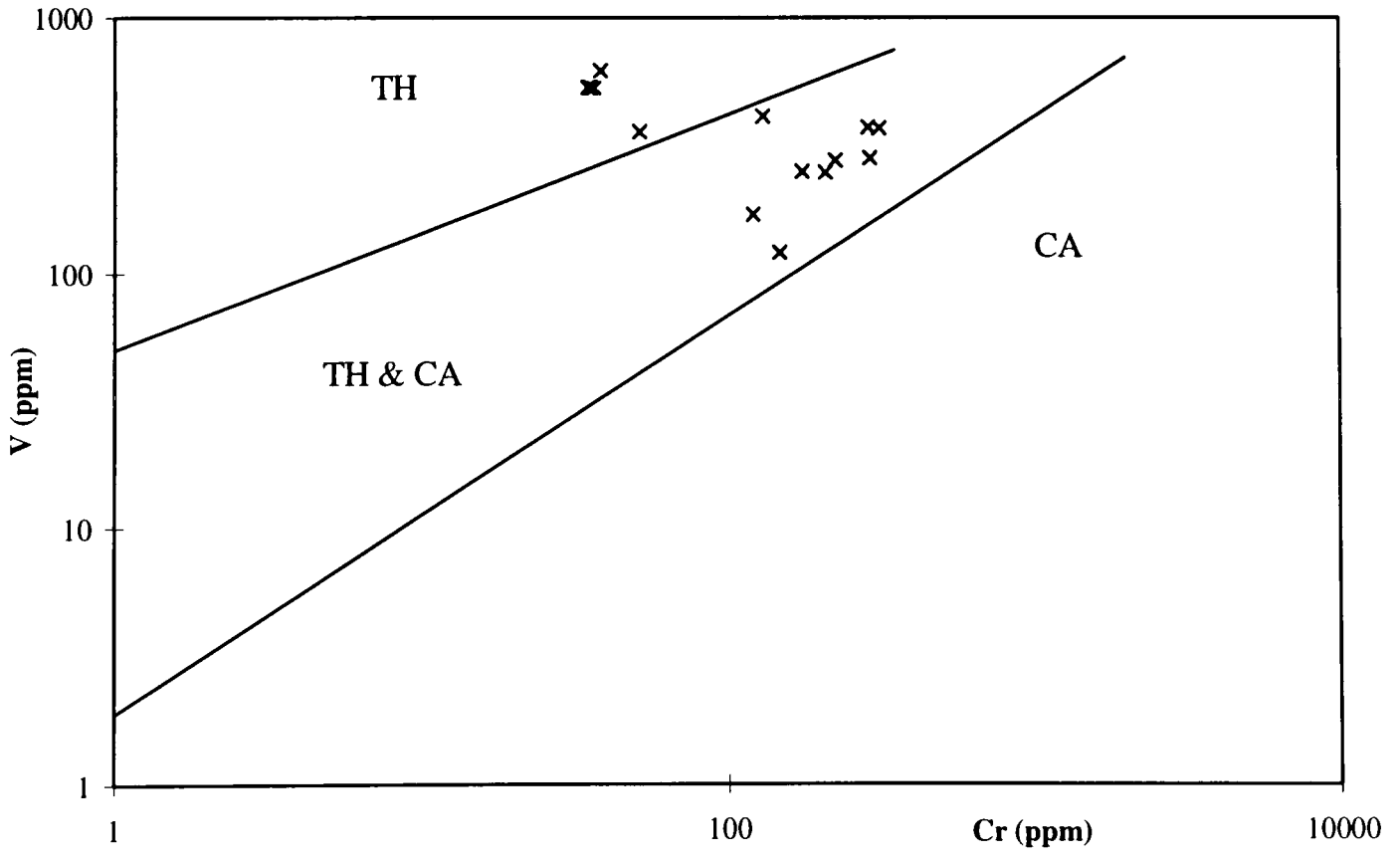


Figure 5.7j - Plot of V v's Cr (after Miyashiro & Shido, 1975) for the Kastaneri Formation

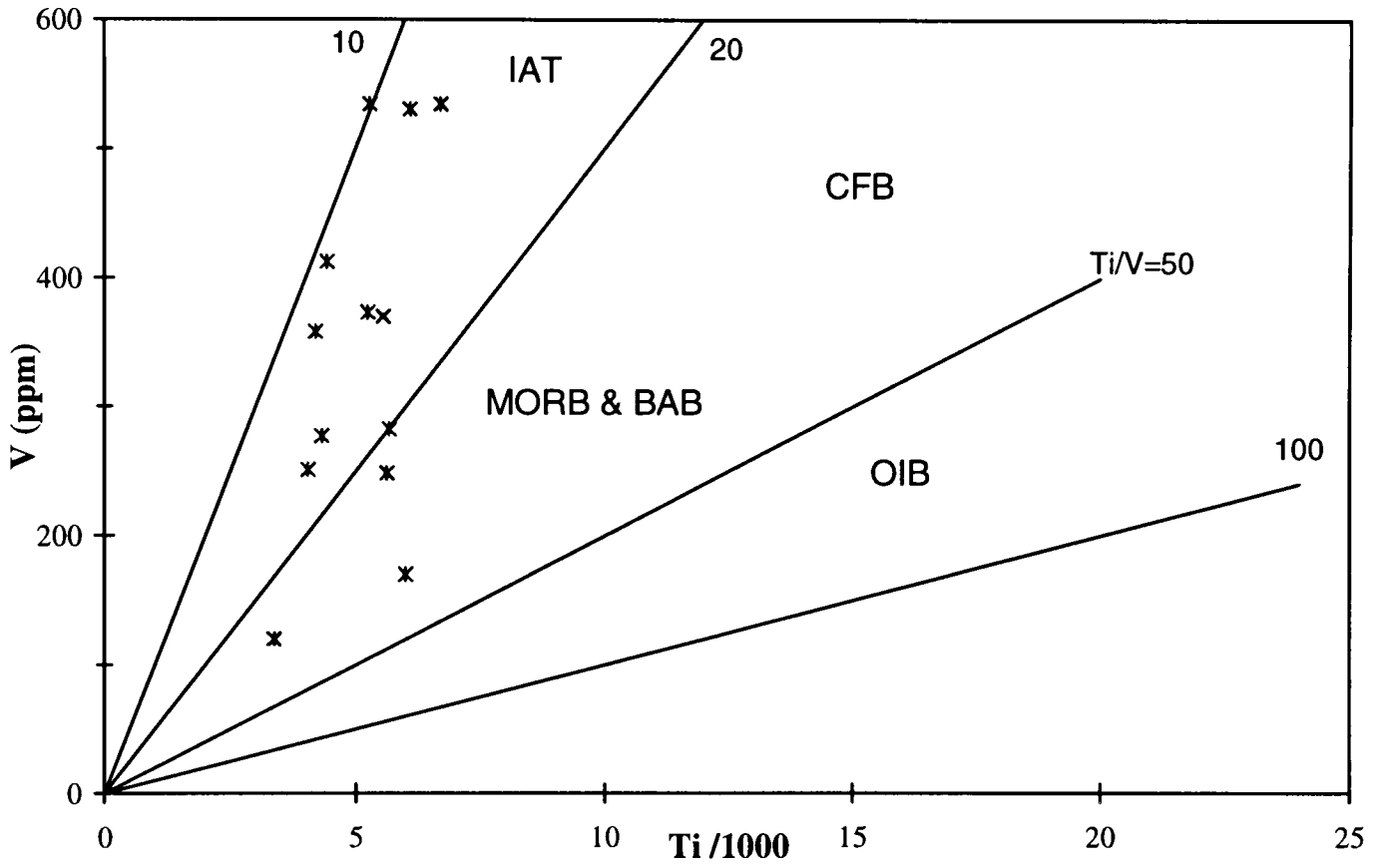


Figure 5.7k - Plot of V v's Ti/100 (after Shervais, 1982) for the Kastaneri Formation.

A clear cluster of points plotting in the IAT field are again displayed on Figure 5.7f (Cr versus Y). The two Zr/Y versus Zr schemes (Figures 5.7g & h) are virtually identical to those plotted for the Livadia Formation, with the great majority of samples showing VAB characteristics and a small group of low Zr/high Y samples plotting just below the template boundaries. The same information can be gleaned from the Zr/Y versus Ti/Y plot (Figure 5.7i) in which one solitary sample deviates from the VAB field to fall just inside the WPB domain.

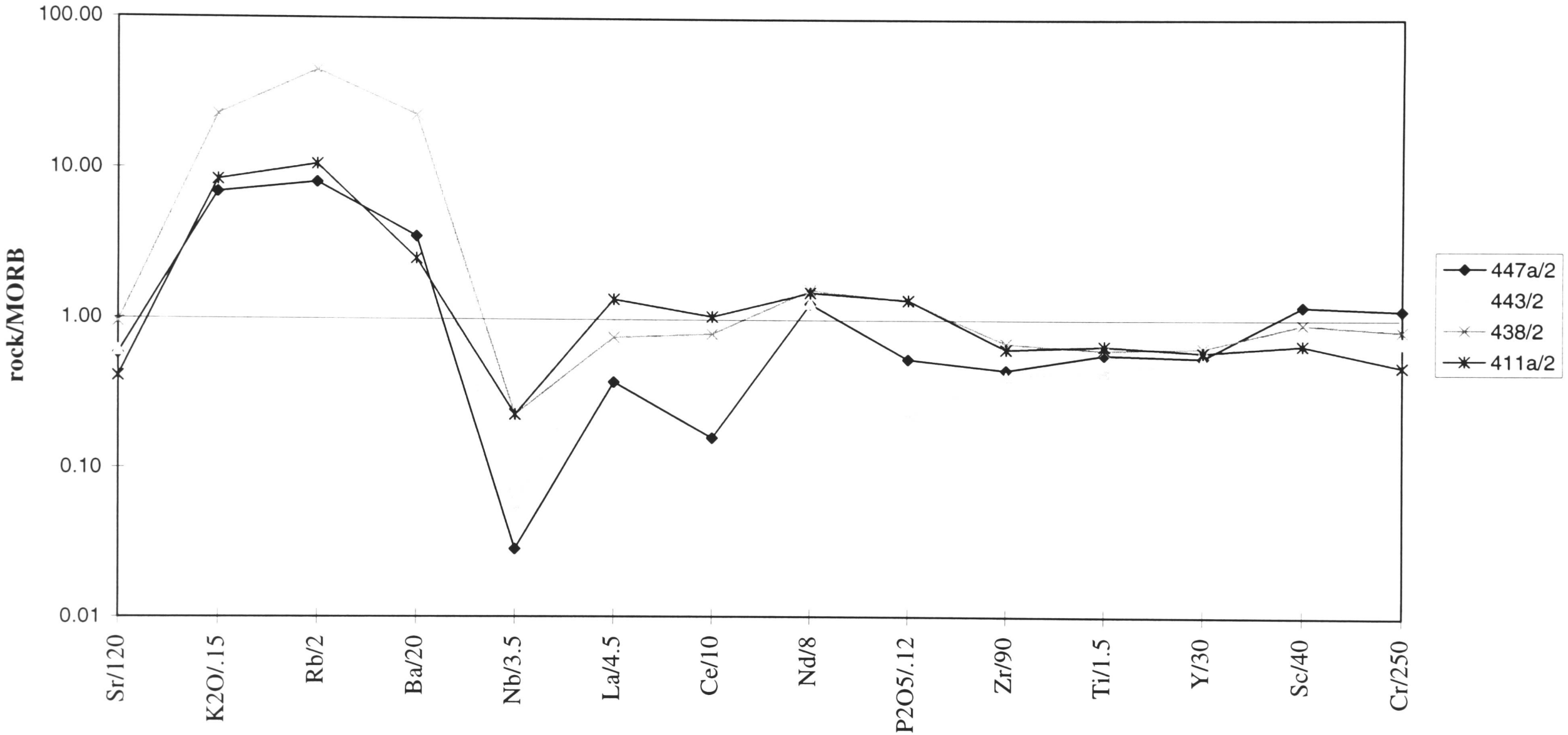
The Kastaneri samples which plot on the V versus Cr diagram of Figure 5.7j are displaced slightly to the right compared to the Livadia Formation samples. All still plot wholly within the tholeiite or tholeiite plus calc alkaline field, although Cr concentrations are generally higher in these samples than in their Livadia counterparts. The V versus Ti/1000 plot (Figure 5.7k) is again rather diffuse, although to a lesser degree than the Livadia samples. Most samples plot in the IAT field with a small group of low V samples extending into the MORB and OIB segments.

Multi-element spidergrams (Figure 5.8) for a selection of Kastaneri samples again show features which indicate subduction zone involvement and a high degree of partial melting; all consistent with an arc setting. The Kastaneri Formation volcanics show a suggestion of greater slab involvement in the form of higher LILE and LREE levels but the ratio of most-to-least incompatible elements is similar (i.e. flat) and comparable to MORB.

5.4 - DISCUSSION AND CONCLUSIONS

After careful screening of samples, elements and discrimination diagrams, the whole-rock geochemical data from 47 samples (33 Livadia and 14 Kastaneri) has been used

Figure 5.8 - MORB-normalised trace element spidergrams for selected samples from the Kastaneri Formation



to determine that the Païkon Volcanic Group formed in a supra-subduction, volcanic arc setting. The rocks most closely resemble island arc tholeiites, but eruption onto a microcontinental sliver or a continental margin arc setting cannot realistically be eliminated. It is not possible to distinguish between an oceanic arc and a continental margin (i.e. Andean-type) arc using the data available.

The data presented strongly suggest that the Livadia and Kastaneri Formation volcanics are members of the same IAT geochemical suite, although the chemical nature of the alteration processes which each formation has endured is different. The rock samples from the Kastaneri Formation have undergone much more extensive hydrothermal leaching, and corresponding silicification, than those of the Livadia Formation, hence many more samples collected from the Kastaneri Formation were unsuitable for this study. This may be due to the higher proportion of permeable volcaniclastic horizons within the Kastaneri Formation, which would allow hydrothermal fluids to be channelled along them, leaching many elements and causing considerable chemical alteration. On the other hand, the Livadia Formation has experienced higher degrees of depletion with respect to CaO and Sr than has the Kastaneri Formation. This may be due to the kaolinitisation of calcic feldspars. Initial IAT eruptives are more likely to produce Ca-rich plagioclase feldspars, while later eruptives in the same magmatic suite may have evolved to Andesine feldspar compositions, which have less Ca to lose, the additional Ca being caught up in more stable mineral phases. As a result, leaching of Ca and Sr during the metasomatic process will more greatly affect the Livadia Formation than the Kastaneri Formation.

Certain samples from the Livadia Formation are extremely rich in iron (up to 23%, sample 268/4) and hence it is possible that haematitisation or pyritisation of these samples has taken place and, as documented in chapter 3, altered samples from both the Kastaneri and Livadia Formations are often associated with disseminated pyrite deposits. This mineralisation, together with the geochemical character of the volcanics as a whole, suggest that Kuroko-style alteration prevailed during or shortly

following volcanism. This style of alteration is common in such arc settings (Garson & Mitchell, 1977; Mitchell & Bell, 1973; Pearce & Gale, 1977).

With respect to the recent work of Bebien *et al* (1994, in press) it seem unlikely, given the results of this work, that the western and eastern sides of the Païkon Massif comprise volcanic rocks which belong to different geochemical suites, as samples collected from all parts of the study area during this work are very similar in character. For example, samples from locality 328 (eastern Païkon Massif) show similar trends and elemental concentrations as samples from locality 268 (central Païkon Massif) and locality 444 (western Païkon Massif). See the Appendix for raw data.

Chapter 6

The Voras Massif

CHAPTER 6 - THE VORAS MASSIF

6.1 - INTRODUCTION

The Voras Massif (Figure 6.1) is situated directly to the north and northwest of the Païkon Massif and forms an east-west-trending mountainous ridge along the frontier between Greece and former Yugoslavia. A reconnaissance study of the Voras Massif from Loutraki Gorge in the west to the former Yugoslavian border in the extreme east was carried out, focusing on the regional tectono-stratigraphic significance of this area in order to test the various hypotheses of previous workers. Geochemical analyses of key volcanic successions were undertaken, as these were previously lacking, and petrological, palaeontological and structural investigations of all units were performed. Detailed mapping of this area was, however, outwith the scope of this thesis.

6.2 - PREVIOUS WORK

The Voras Massif was first studied by Mercier (1968, 1973), who produced a map and outlined the general geology of the area. He concluded that the Voras Massif comprised rocks of Pelagonian zone affinity in the west (the Kaimaktchalan Massif), rocks of Païkon subzone affinity in the east (the Pinovon Unit) and three stacked, west-verging Tertiary thrust-imbricates of Almopias subzone rocks in-between (the Ano Garefi, Peternic and Loutra Pozar Units, from east to west respectively; Figure 6.2). Mercier's work was later modified by Migiros and Galeos (1990) and Galeos *et al.* (1994) who established a regional tectono-stratigraphy based on a remapping of the area. Migiros & Galeos envisaged the Voras Massif as comprising two palaeo-marginal basin successions (the Ano Garefi and Kali Pediada Units), which formed within continental crust of wholly Pelagonian zone affinity (Figure 6.3). No rocks of Païkon, Peonias or Serbo-Macedonian affinity are considered in this model.

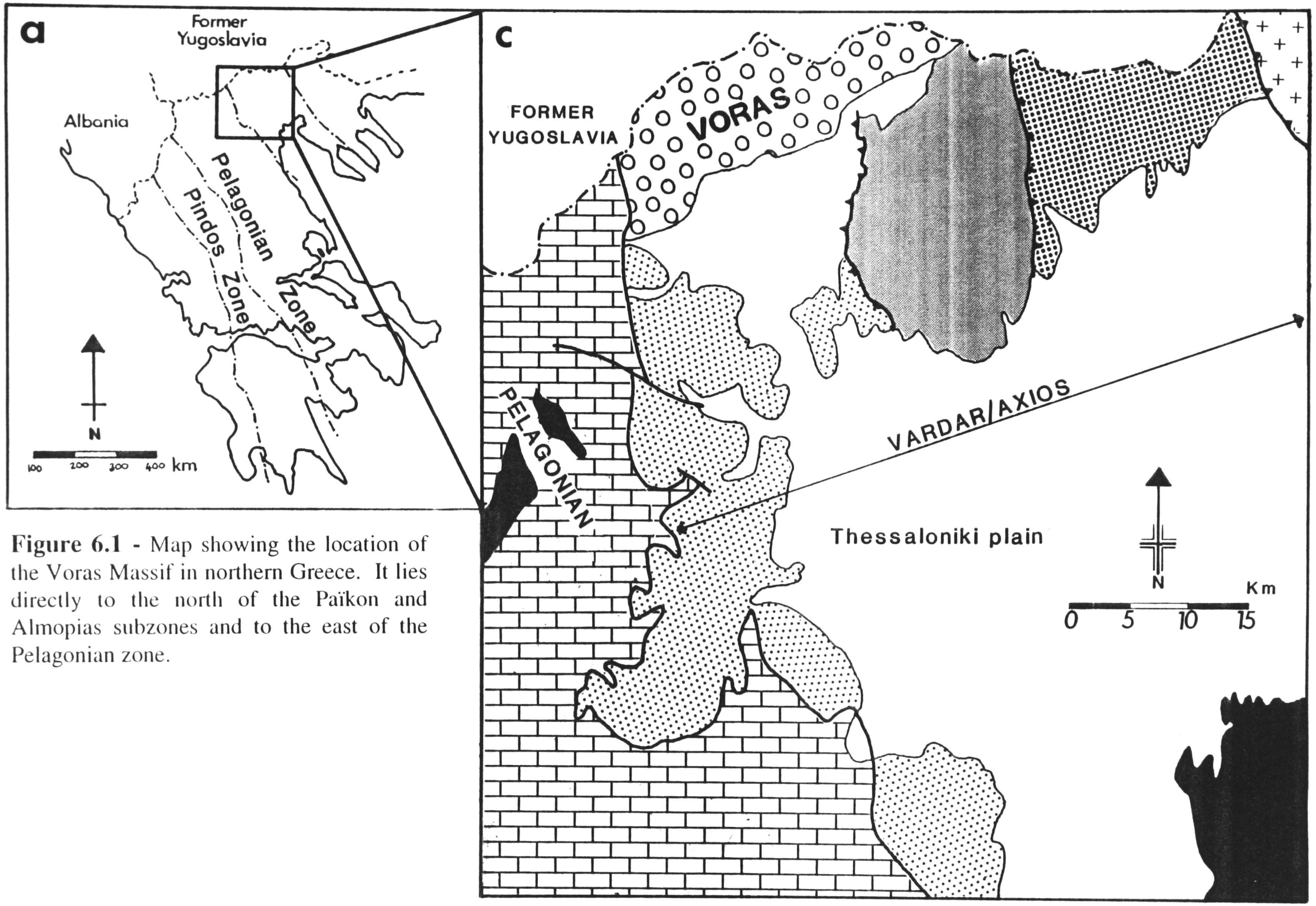


Figure 6.1 - Map showing the location of the Voras Massif in northern Greece. It lies directly to the north of the Païkon and Almopias subzones and to the east of the Pelagonian zone.

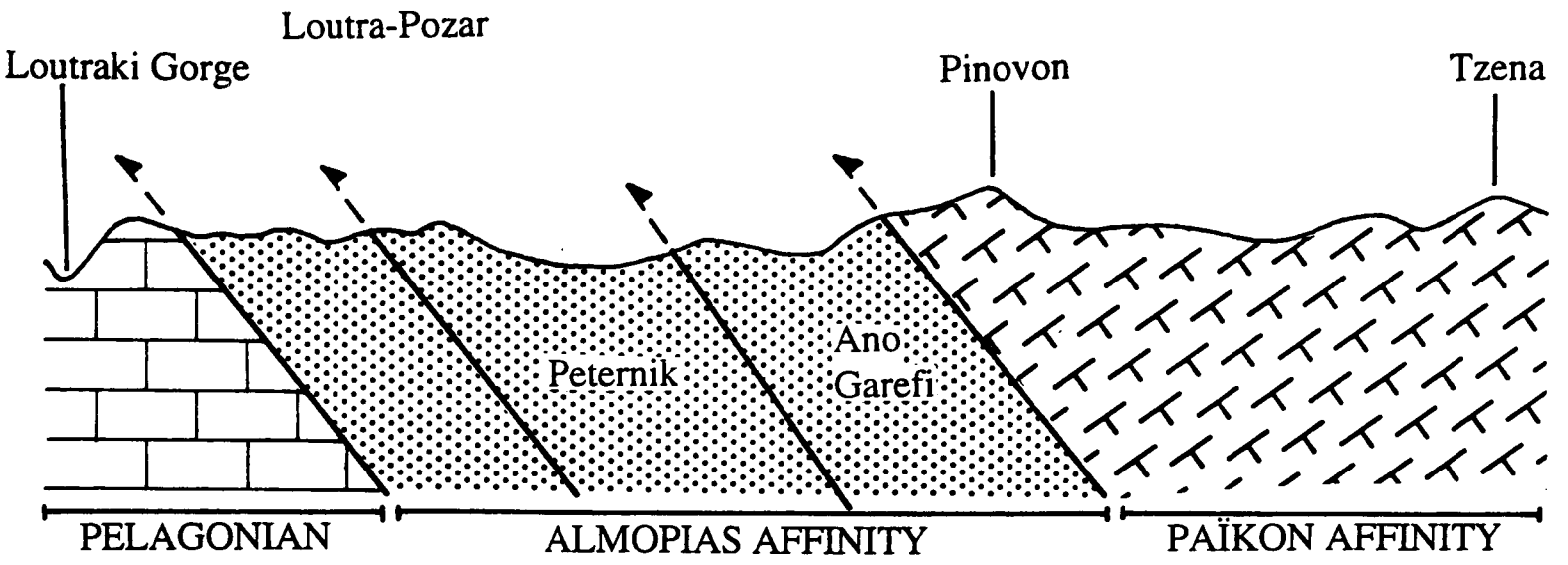


Figure 6.2 - Mercier's geotectonic model of the Voras Massif. The Kaimakchalan Massif (Pelagonian affinity) is overlain by three imbricates of Almopias affinity (Loutra-Pozar, Peternik & Ano Garefi) which are, in turn, overlain by the Païkon-related Pinovon Unit.

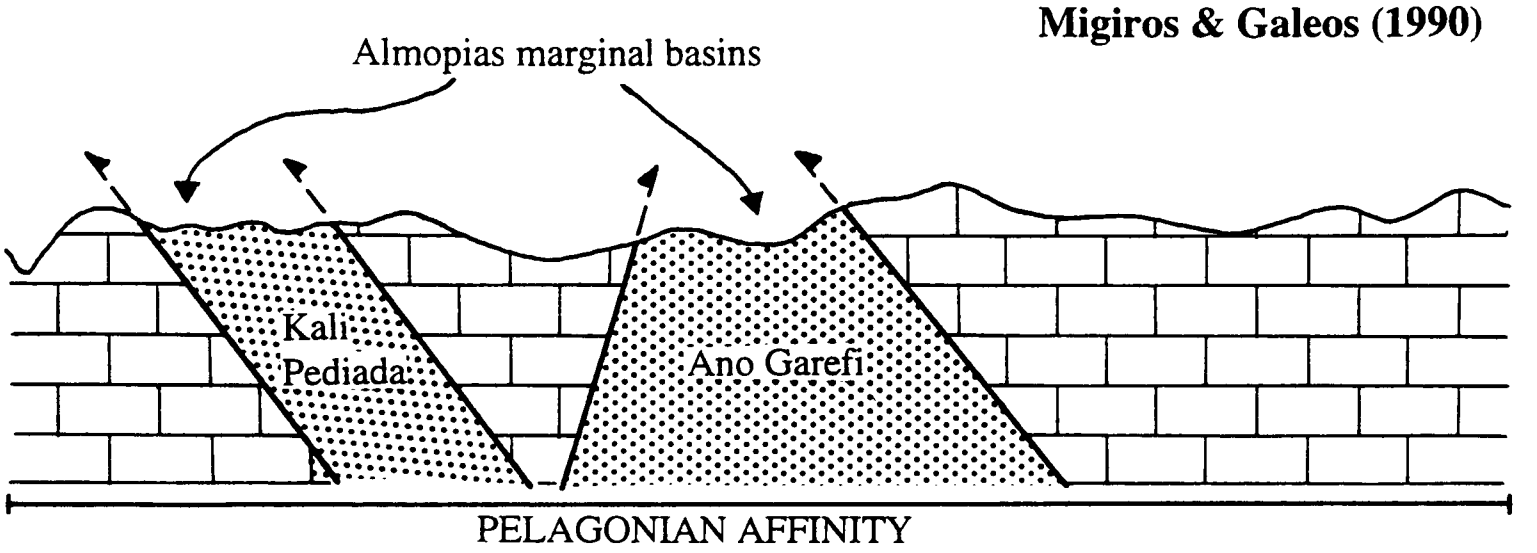


Figure 6.3 - Geotectonic model of the Voras Massif as proposed by Migiros & Galeos (1990). The Voras Massif is dominantly of Pelagonian affinity with two marginal basins therein (Kali-Pediada & Ano Garefi).

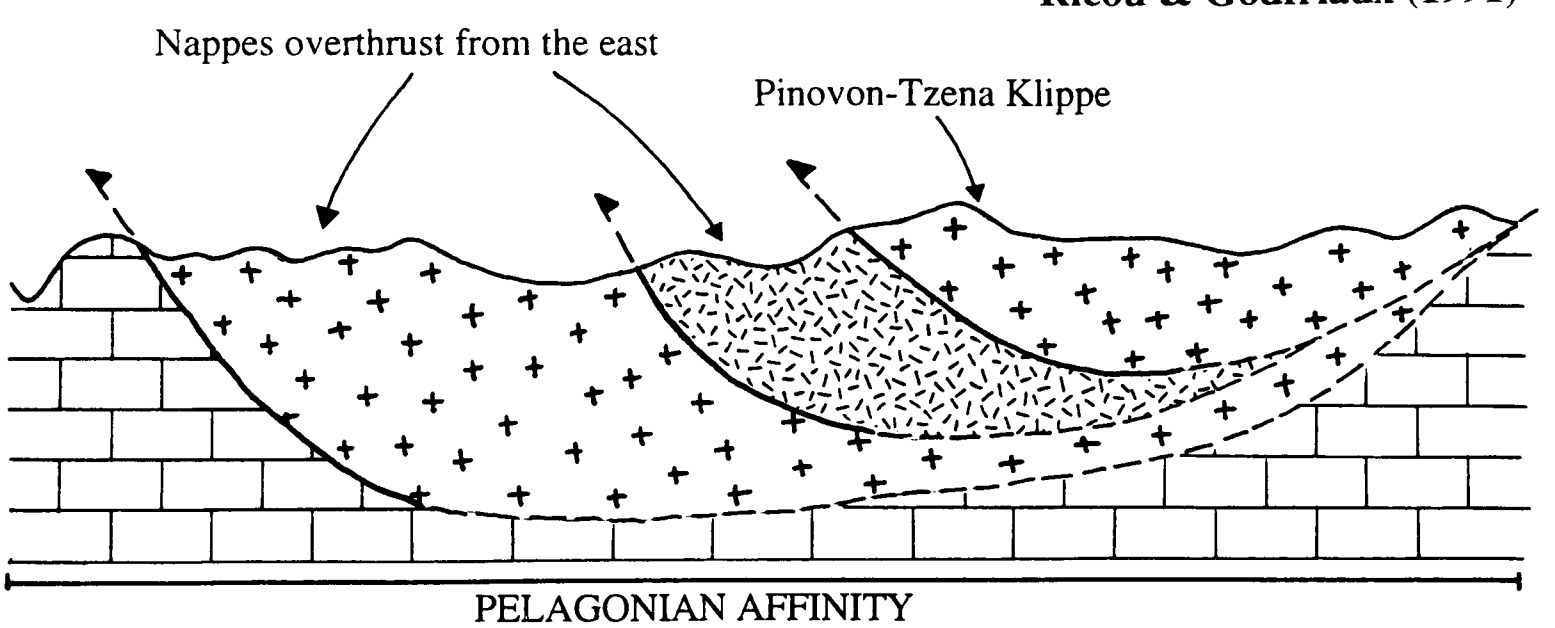


Figure 6.4 - Model of the Voras Massif proposed by Ricou & Godfriaux (1991). Pelagonian rocks floor the Voras Massif and are overlain by nappes of Serbo-Macedonian and Peonias affinity and a klippe a Serbo-Macedonian affinity (Pinovon-Tzena klippe).

In a recent tectonic interpretation, Ricou & Godfriaux (1991) proposed that the Voras Massif comprises a major Tertiary thrust slice of Serbo-Macedonian-type continental basement and cover sediments, which was emplaced towards the southwest onto basement rocks of the Pelagonian zone. According to this model (Figure 6.4), the Pelagonian basement rocks reappear as a "tectonic window" in the Païkon Massif. This interpretation (Ricou & Godfriaux, 1991) was incorporated into a palaeogeographical reconstruction of the evolution of Tethys as a whole (Decourt *et al.*, 1993), in which the entire Voras Massif was thought to be derived from the Serbo-Macedonian zone to the east.

This chapter presents new data collected during this study to test the two alternative hypotheses outlined above and focuses on the question of whether the Voras Massif represents an allochthonous regional westward continuation of the Serbo-Macedonian zone, as proposed by Ricou & Godfriaux (1991), or whether it is an essentially autochthonous, composite unit comprising rocks of Pelagonian, Almopias and/or Païkon zone affinities.

There are five tectono-stratigraphic zones with which the rocks of the Voras Massif have been compared: 1) The continental Pelagonian zone in the west, 2) The ophiolitic Almopias subzone; 3) The volcanic arc Païkon subzone, 4) The ophiolitic Peonias subzone and 5) The continental Serbo-Macedonian zone in the east (see chapter 1; Figure 6.1). The essential stratigraphic features of these five units are outlined in Figure 6.5 and in chapter 1. There now follows a brief description of each of the six thrust-bound units which constitute the Voras Massif, based on reconnaissance field observations carried out during this study, and conclusions concerning their regional significance will be drawn from these findings.

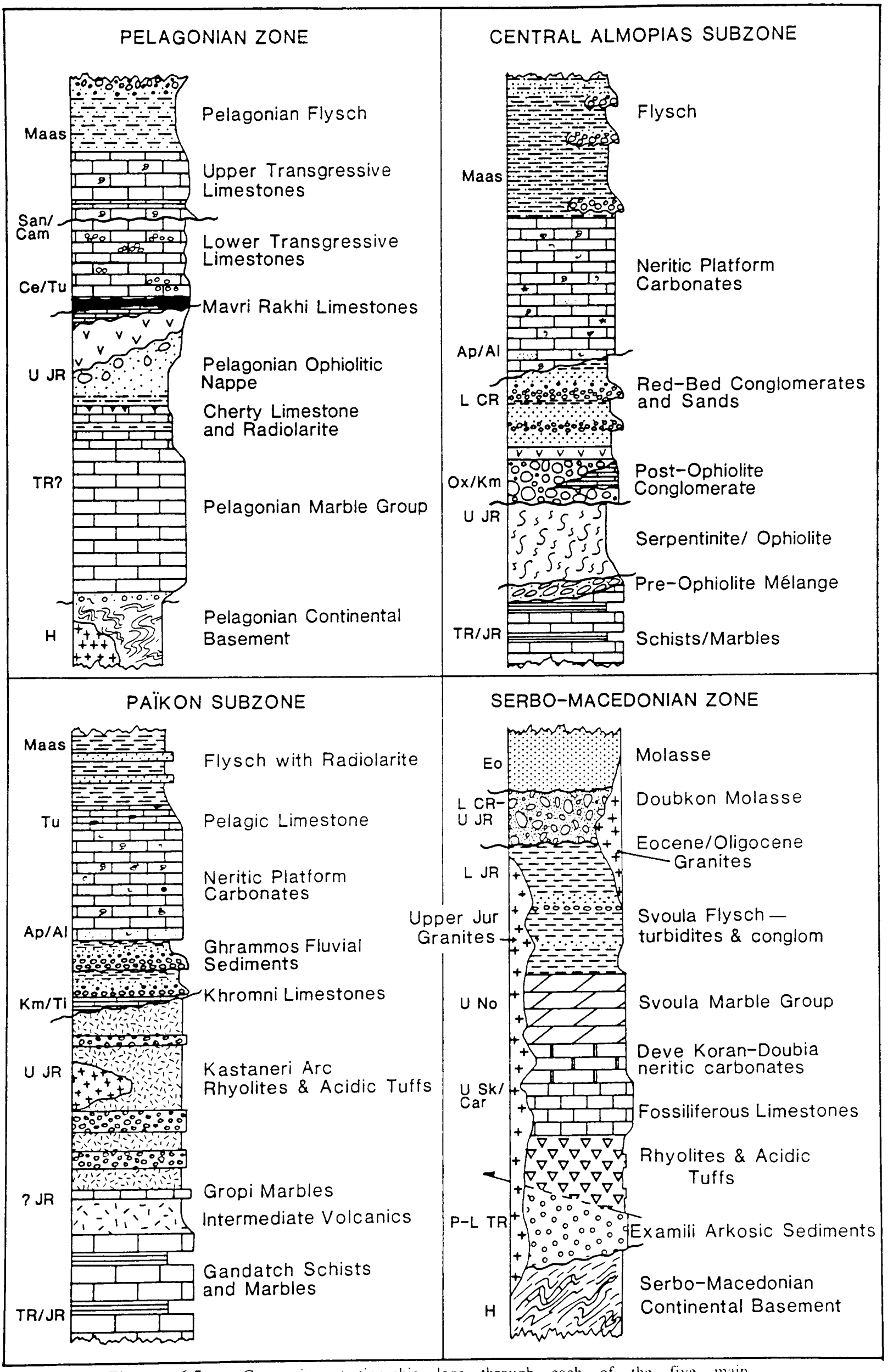


Figure 6.5 - Composite stratigraphic logs through each of the five main tectonostratigraphic terranes with which the rocks of the Voras Massif have been compared.

Continued on the next page.....

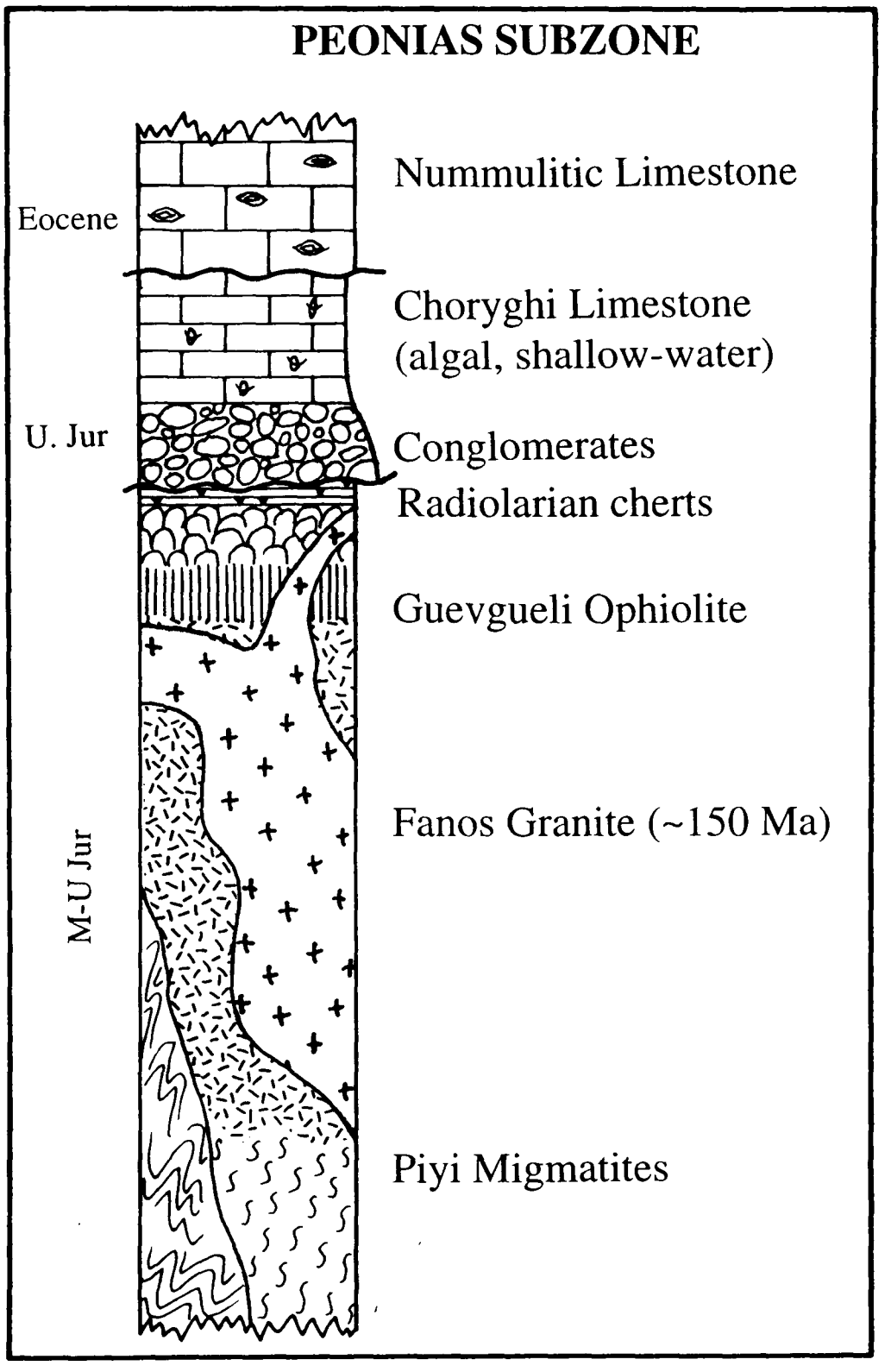


Figure 6.5 - ....continued. (data from various sources)

6.3 - TECTONO-STRATIGRAPHY OF THE VORAS MASSIF

Based on the field relationships observed during this reconnaissance study, the Voras Massif can be sub-divided into six tectono-stratigraphic units, here referred to as Units 1 to 6, from west to east respectively; each is separated from those adjacent by major Tertiary tectonic contacts (Figure 6.6). The most westerly of these units (Unit 1 - the Loutra-Arideas Unit) overthrusts a sequence of gneisses, marbles, limestones and flysch of known Pelagonian affinity (the Kaimaktchalan Massif; Mercier, 1968; Sharp, 1995) with a northeast-dipping Tertiary tectonic contact (Figures 6.6 and 6.7). The stratigraphy of each of these six units will now be outlined in turn, beginning with those in the west and proceeding eastwards. Each of the thrust-bound units is described from its stratigraphic base upwards.

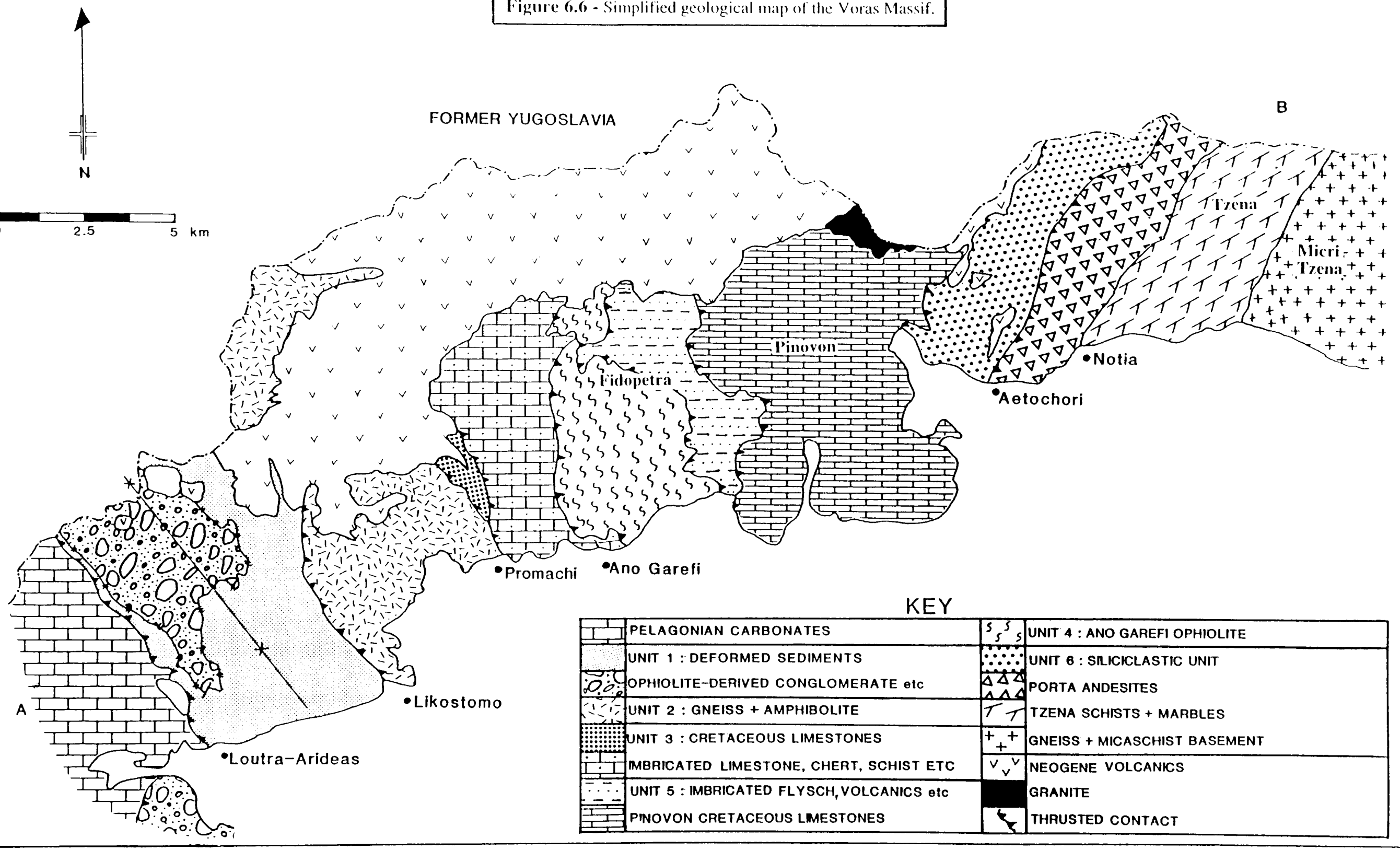
6.3.1 - *Unit 1 - the Loutra-Arideas Unit*

Stratigraphy, Petrology and Field Relations

Unit 1, the Loutra-Arideas Unit (Figures 6.6, 6.7 and 6.8a) essentially corresponds to the Loutra Pozar Unit of Mercier (1968; Figure 6.2), the Loutra-Arideas and Kali Pediada Units of Migiros & Galeos (1990; Figure 6.3) and the Ano Loutraki Unit of Ricou & Godfriaux (1991). It extends eastwards from Loutraki Gorge to just west of Promachi village (Figure 6.6).

At its base, the generally east-dipping Loutra-Arideas Unit comprises a thick, strongly folded sequence of schists, thin-bedded sandstones, detrital carbonates and conglomerates (Figure 6.9), that have been metamorphosed to greenschist facies grade (chlorite and epidote). The schists are rich in fine-grained quartz, secondary chlorite, sericite and epidote and contain disseminated cubes of pyrite. The sandstones are

Figure 6.6 - Simplified geological map of the Voras Massif.



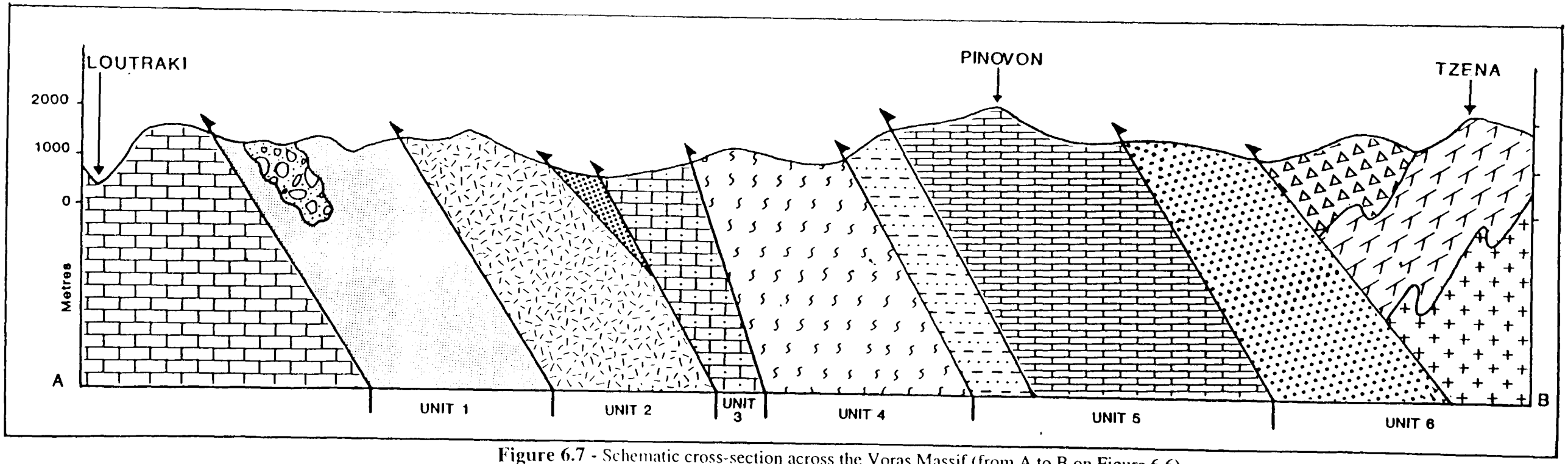


Figure 6.7 - Schematic cross-section across the Voras Massif (from A to B on Figure 6.6).

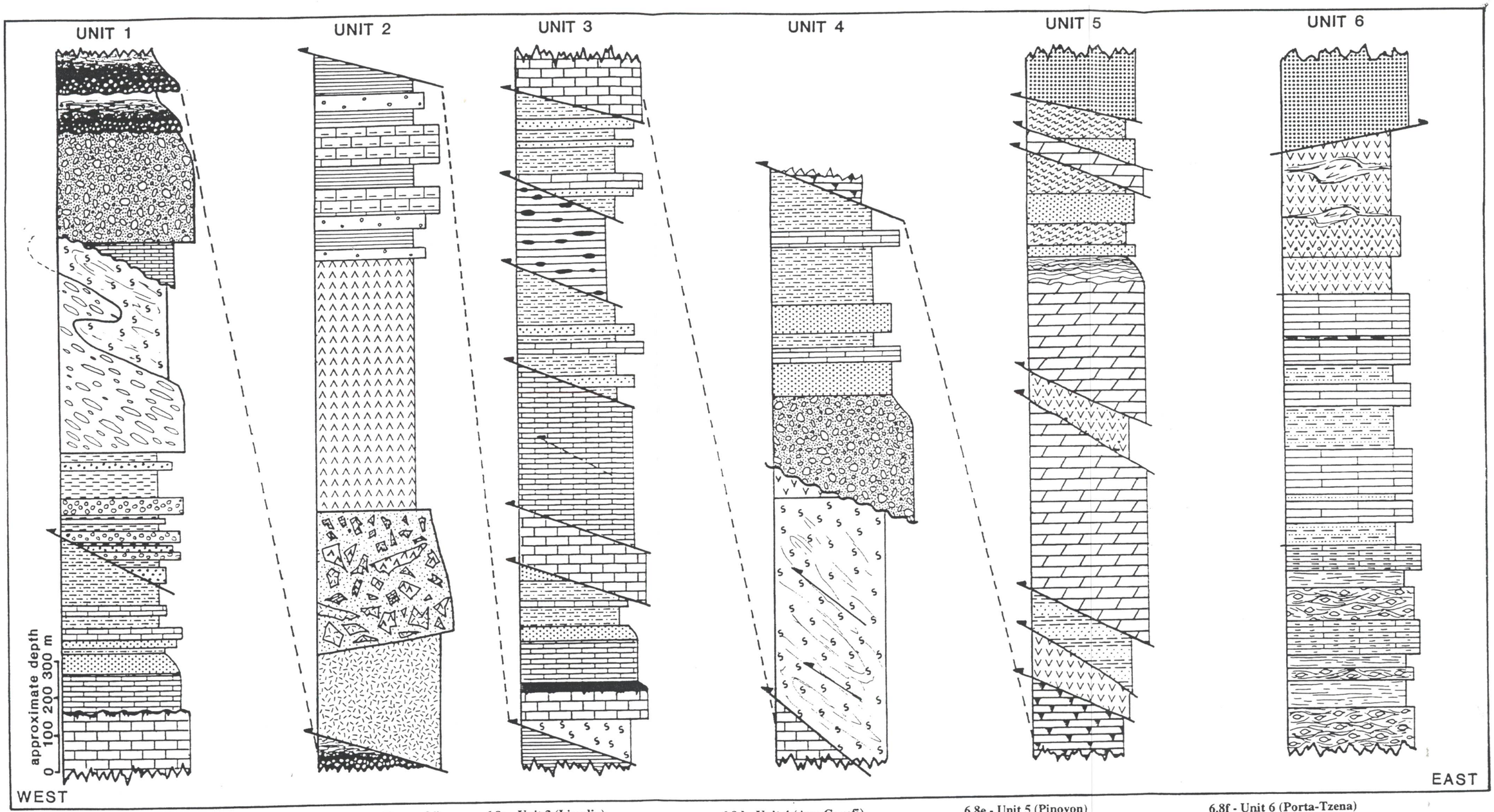


Figure 6.8 - Composite logs through each of the six main thrust-bound units of the Voras Massif. **6.8a** = the Loutra-Arideas Unit; **6.8b** = the Likostomo-Promachi Unit; **6.8c** = the Livadia Unit; **6.8d** = the Ano Garefi Unit; **6.8e** = the Pinovon Unit; **6.8f** = the Porta-Tzena Unit.

somewhat coarser-grained but are of comparable composition. Both of these lithologies are strongly foliated, with secondary chlorite and mica plates oriented parallel to the dominant schistosity. Carbonate horizons are relatively subordinate and contain recrystallised quartz and calcite with minor white mica and chlorite.

The only preserved sedimentary structures observed were in strained conglomerate horizons, up to 1 m thick, which display normal grading. The conglomerates invariably pass gradationally upwards into sandstones and ultimately schists, although significant layer-parallel shear has disrupted these graded units. Clasts within the conglomerates are poorly-sorted and range in size from 2 mm-10 cm and have been derived, almost wholly, from basic volcanic (Figure 6.10) and continental basement sources (e.g. amphibolitic schist, chloritised vesicular basalts, serpentinite). All clasts have been strongly flattened and are now elongate parallel to an early lineation in the rocks, which trends towards 325-355°N (Figure 6.11). The abundance of conglomeratic horizons increases steadily up-section to where it makes contact with a serpentinitic unit above. The whole of this interbedded schist, carbonate, conglomerate unit has been strongly folded and thus the original thickness of the unit is impossible to determine.

The top of the meta-sedimentary sequence is overlain by a thick unit of serpentinised dunites and harzburgites, with a sheared, folded contact (Figure 6.12). At the contact, the meta-sediments are a pale purple colour and are rich in clasts of chloritised basalt and serpentinite. It is therefore likely that the basal meta-sediments have been at least partly derived from the tectonically overlying serpentinite. The dunites and harzburgites display polygonal hydration textures typical of serpentinisation (i.e. tortoise-shell texture) and are present as large clasts, blocks and boulders (up to 30 m diameter) within a wholly serpentinised matrix: a serpentinitic mélange. Towards the stratigraphic top of the serpentinite (i.e. to the east), a chaotic unit of highly chloritised and epidotised medium-grained meta-basic (Figure 6.13) and meta-gabbroic blocks occurs. The epidosites have a sheet-like appearance, with local fine-grained,



Figure 6.9 - Field photographs of the basal chloritic schists/conglomerates of the Loutra-Arideas Unit. The top photograph shows a typical outcrop of thinly-bedded, highly-foliated chlorite schists interbedded with thin horizons of detrital carbonate. The lower photograph is of a sheared conglomeratic horizon within the chloritic schists.

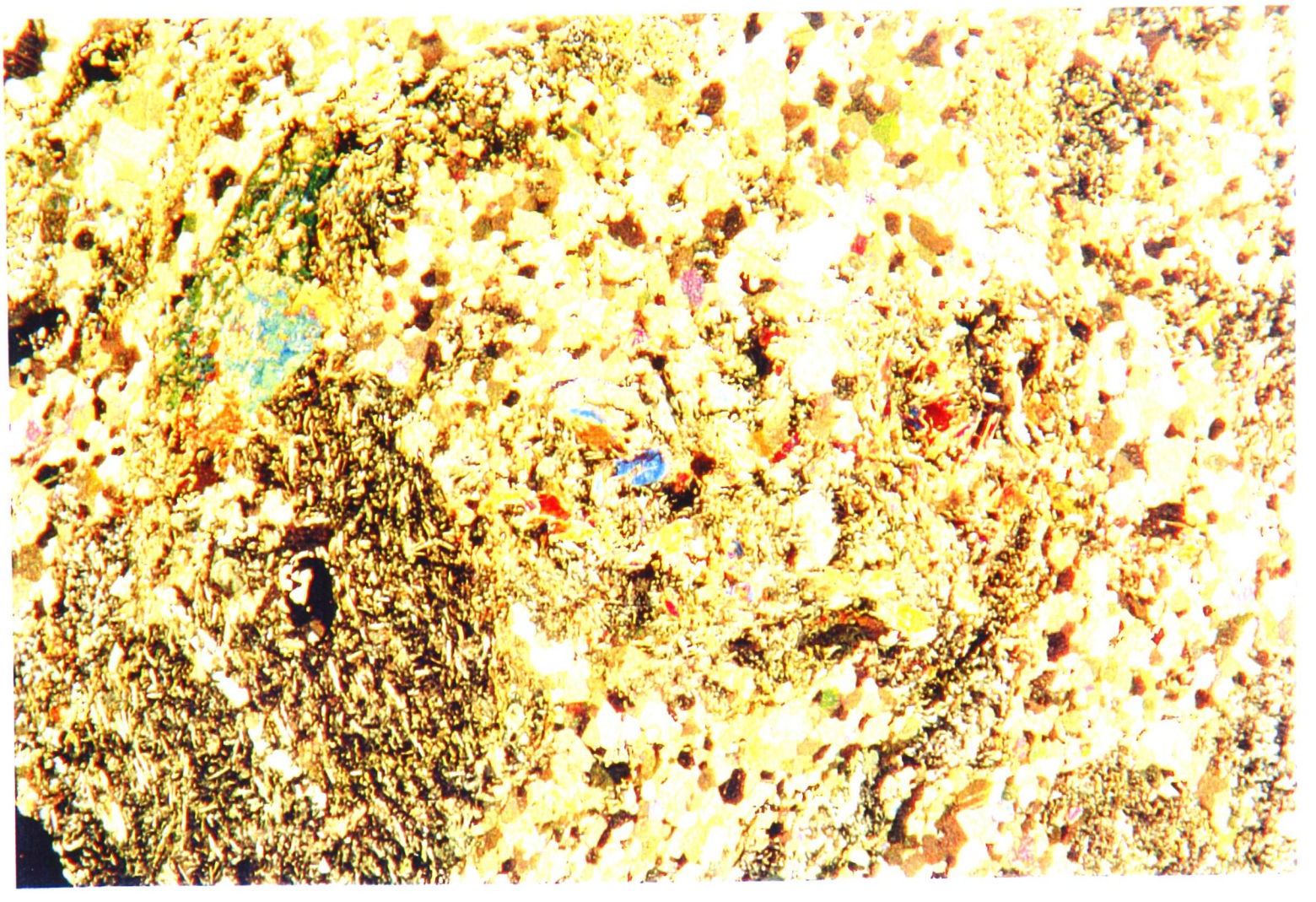


Figure 6.10 - Photomicrograph of an altered basalt clast within the basal chloritic schists/conglomerates of the Loutra-Arideas Unit. The original feldspar-phyric texure of the basalt can still be recognised, although much alteration to phyllosilicate minerals and epidote has occurred.

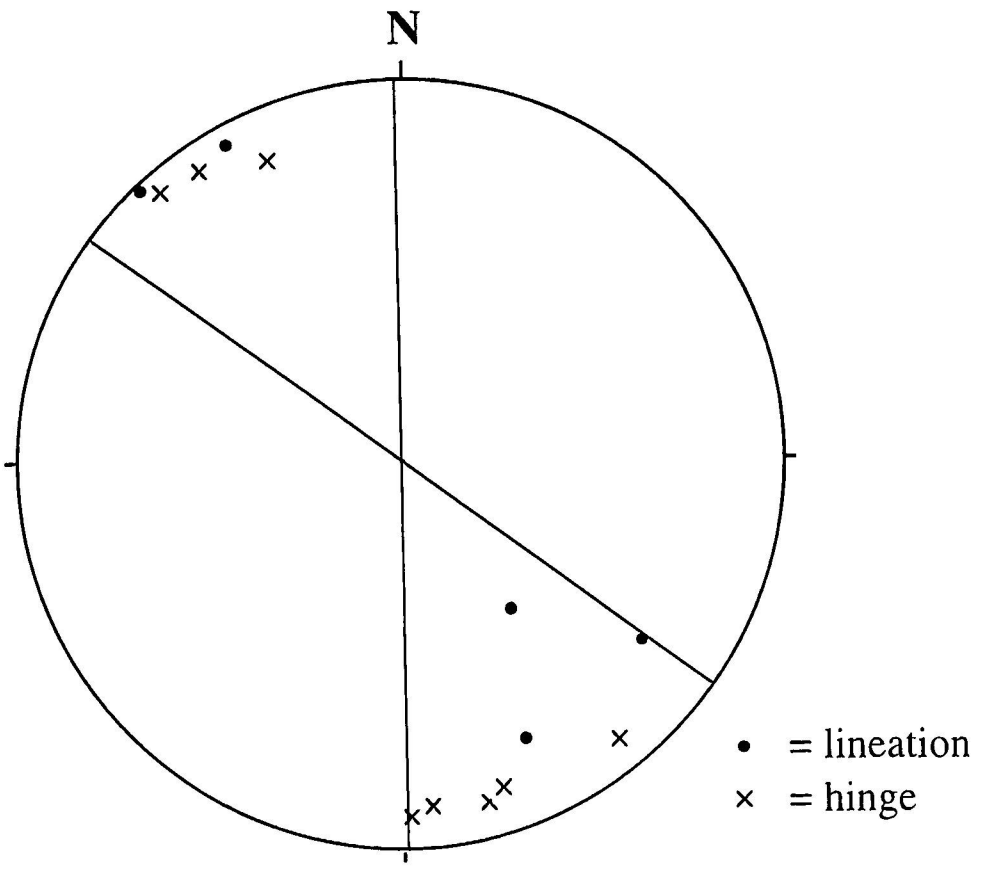


Figure 6.11 - Stereographic projection of the northwest-southeast-trending lineation present within the basal schists/conglomerates of the Loutra-Arideas Unit. The lineation corresponds to an Upper Jurassic phase of compression (see section 6.3.1 - **Structure**).



Figure 6.12 - Field photograph of sheared and serpentinised ultrabasic rocks (dunites and harzburgites) from the Loutra-Arideas Unit.

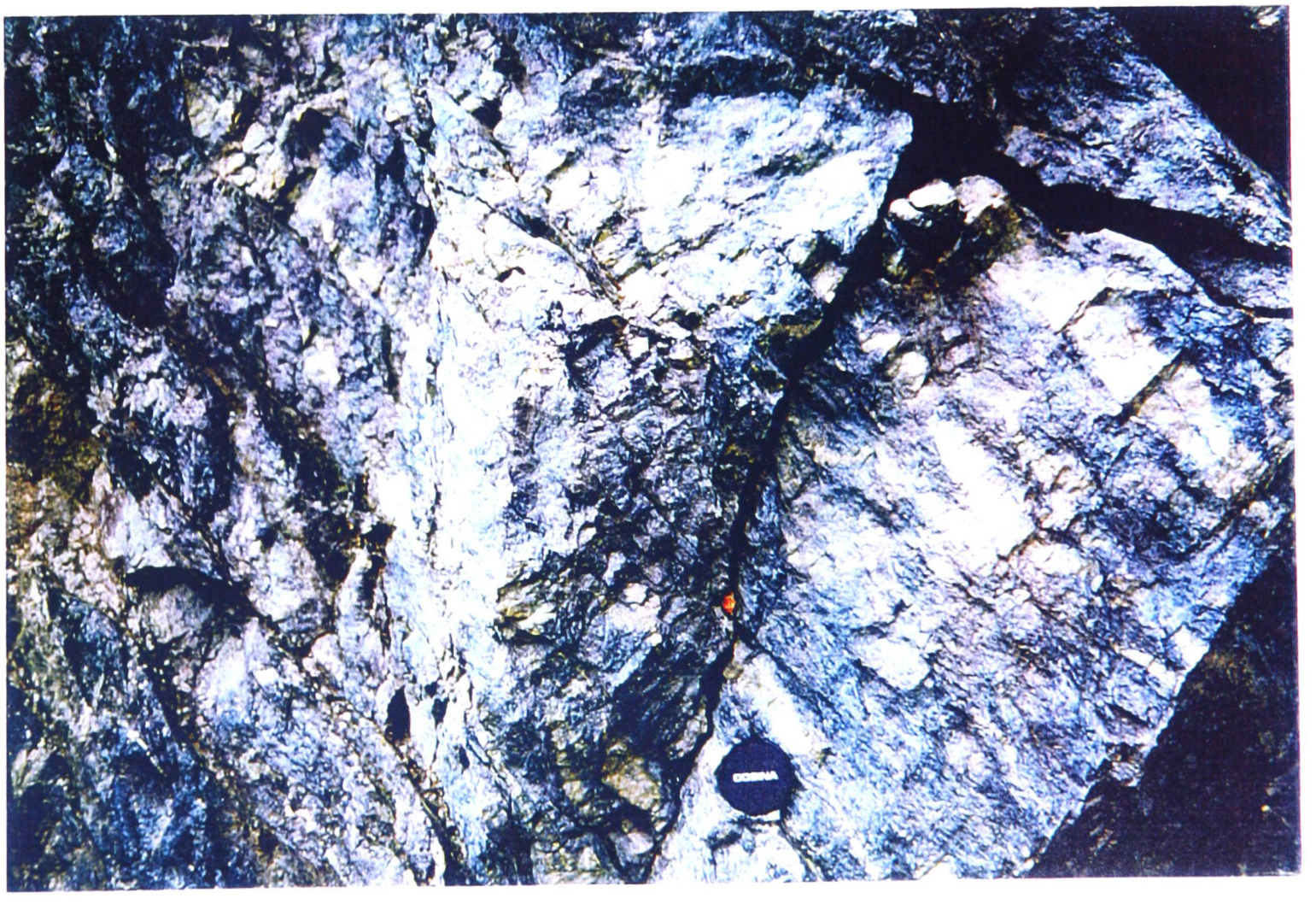


Figure 6.13 - Epidotised fine-grained meta-basic rocks from the Loutra-Arideas Unit. The epidote veins are aligned parallel to what may be chilled margins and are intimately associated with discontinuous blocks of meta-gabbro.

dark layers up to 3 cm wide, which may represent altered chilled contacts. Neither the serpentinised unit, the meta-gabbros nor the meta-volcanics display the prominent NE-SW-trending lineation which is so prominent in the underlying meta-sedimentary succession.

Considering the rock types which constitute the serpentinitic mélange (i.e. altered dunites, harzburgites, gabbros and meta-basites), it is concluded here that the serpentinites, and the serpentinitic mélange, represent the altered remnants of a dismembered ophiolite.

The serpentinitic mélange is unconformably overlain by a relatively undeformed sequence of shallow-water carbonates, interdigitated with well-rounded, coarse conglomerates and sandstones of mainly ophiolitic derivation (the Kali Pediada Unit of Migiros & Galeos, 1990; Figure 6.14). This is evidenced by clasts of serpentinised dunites and harzburgites, chloritised basalts (Figure 6.15) and epidosites within a fine, sandy, serpentinite-rich matrix. The limestones (Figure 6.16A & B) have been dated as Upper Jurassic (~Kimmeridgian) based on a fauna comprising *Cladocoropsis sp.* algae (this work) and reefal corals of similar age (Galeos *et al.*, 1994). The reefal limestones are limited in extent and are rich in ophiolitic detritus (serpentinite). The ophiolite-derived conglomerates contain well-rounded clasts of fossiliferous limestone which are lithologically identical to the reefal carbonates with which the conglomerates are associated (i.e. Upper Jurassic ?*Cladocoropsis*-bearing; Figure 6.17). The clasts of reef limestone are themselves rich in clasts of ophiolitic detritus, which suggests that the reef limestones and the well-rounded conglomerates were deposited contemporaneously above the serpentinites.

The ophiolite-derived conglomerates and reef limestones pass conformably upwards into a thick (~100 m) sequence of red-bed conglomerates, sandstones and siltstones.

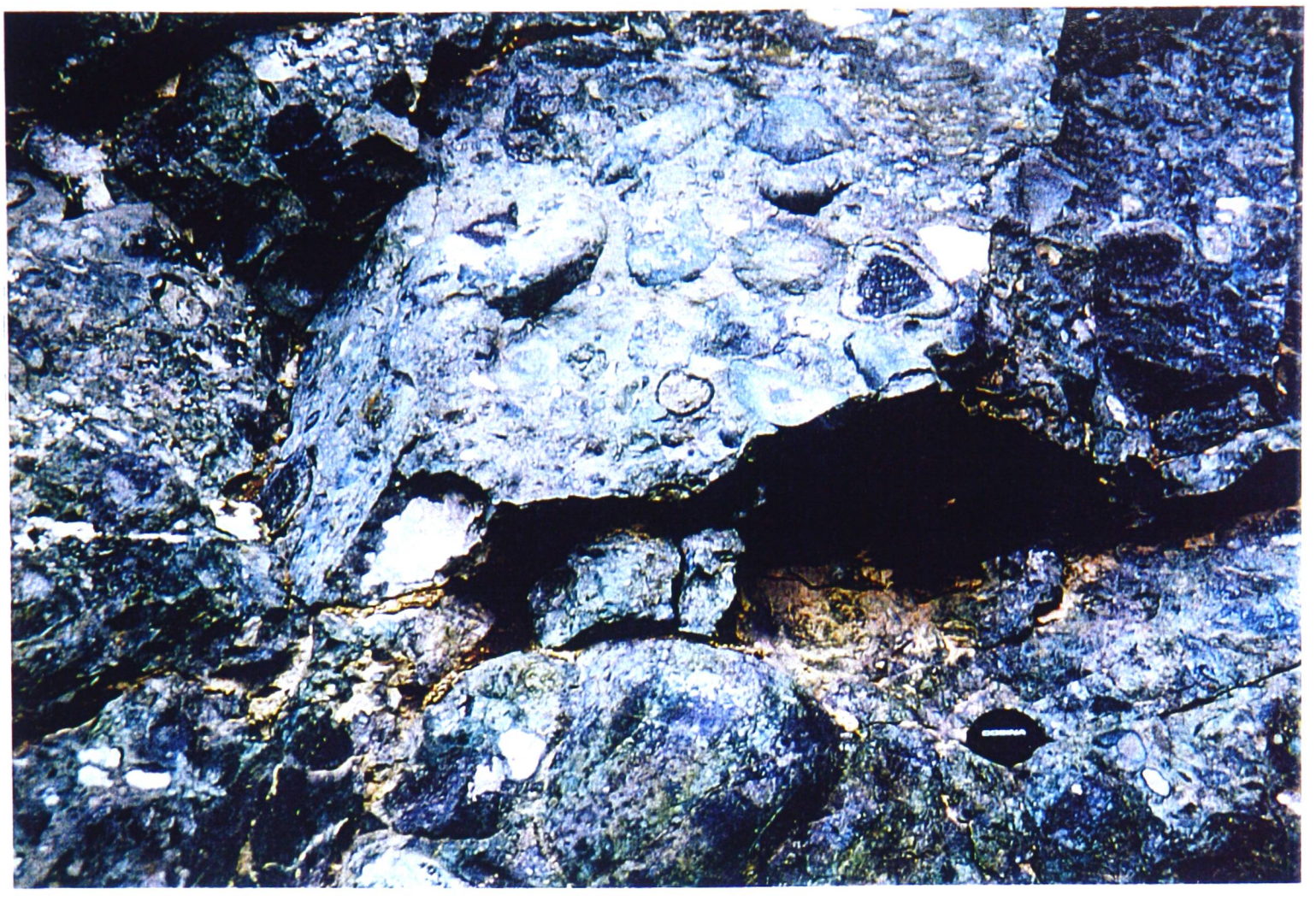


Figure 6.14 - Field photograph of the well-rounded, largely ophiolite-derived conglomerate of the Loutra-Arideas Unit. The conglomerate comprises clasts of serpentinised ultramafics, altered basalt and minor limestone (white clasts) and overlies the serpentinite unit shown in Figure 6.12.

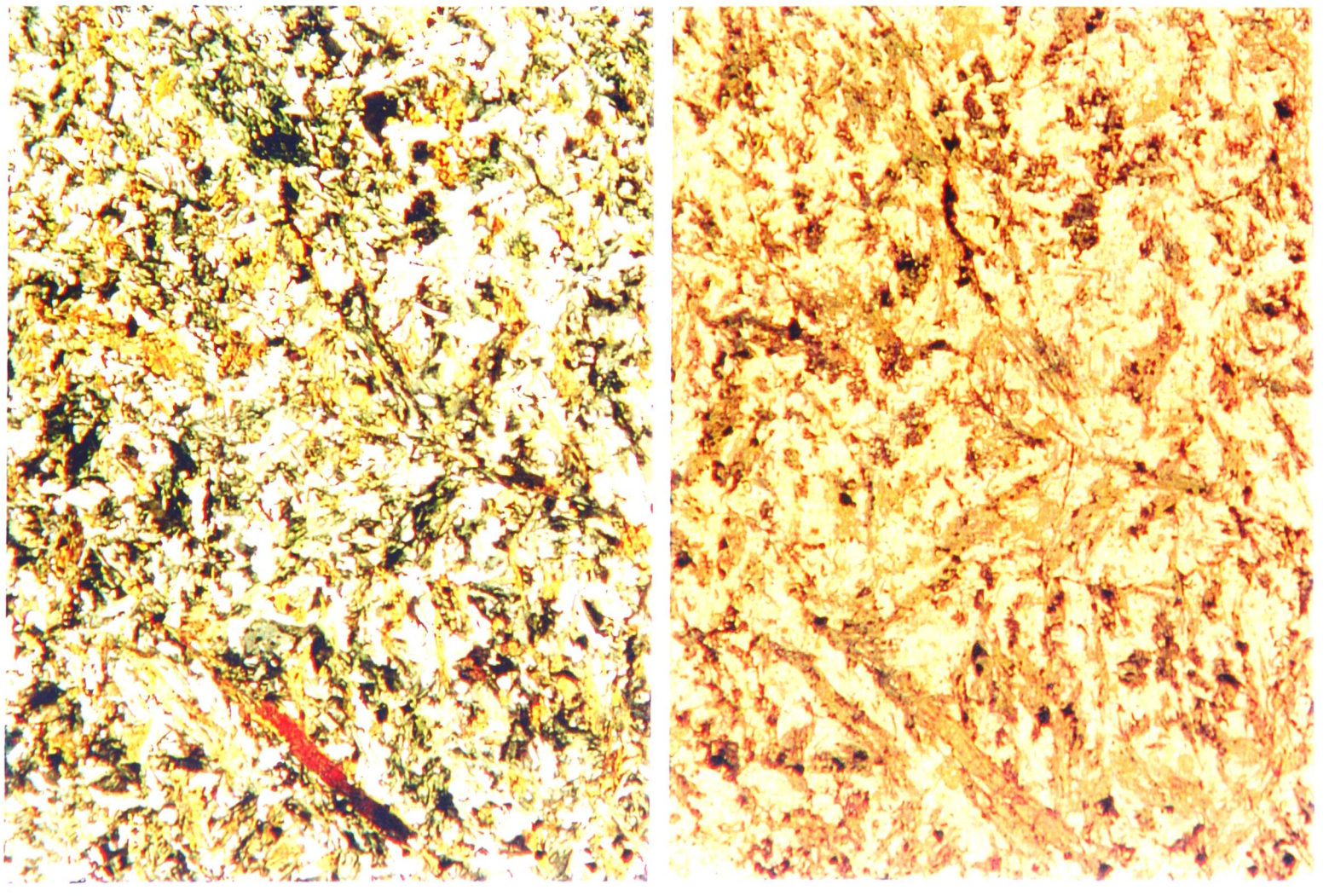


Figure 6.15 - Photomicrograph of a clast of altered basalt from the rounded conglomerates of the Loutra-Arideas Unit. The original porphyritic texture can still be clearly seen.



Figure 6.16A - Field photograph of shallow-water limestones from the Loutra-Arideas Unit. The limestones occur locally above the serpentinite unit and contain corals of Upper Jurassic age and possibly *Cladocoropsis* algae.



Figure 6.16B - Field phtotgraph of the top of the Upper Jurassic limestones of the Loutra-Arideas Unit. The limestones are topped by a strained, sub-rounded intraformational conglomerate which contains coral debris.



Figure 6.17 - Field photograph of a clast of Upper Jurassic limestone (see Figure 3.16A & B) within the rounded ophiolite-derived conglomerate of the Loutra-Arideas Unit. Some clasts of limestone contain clasts of serpentinite.

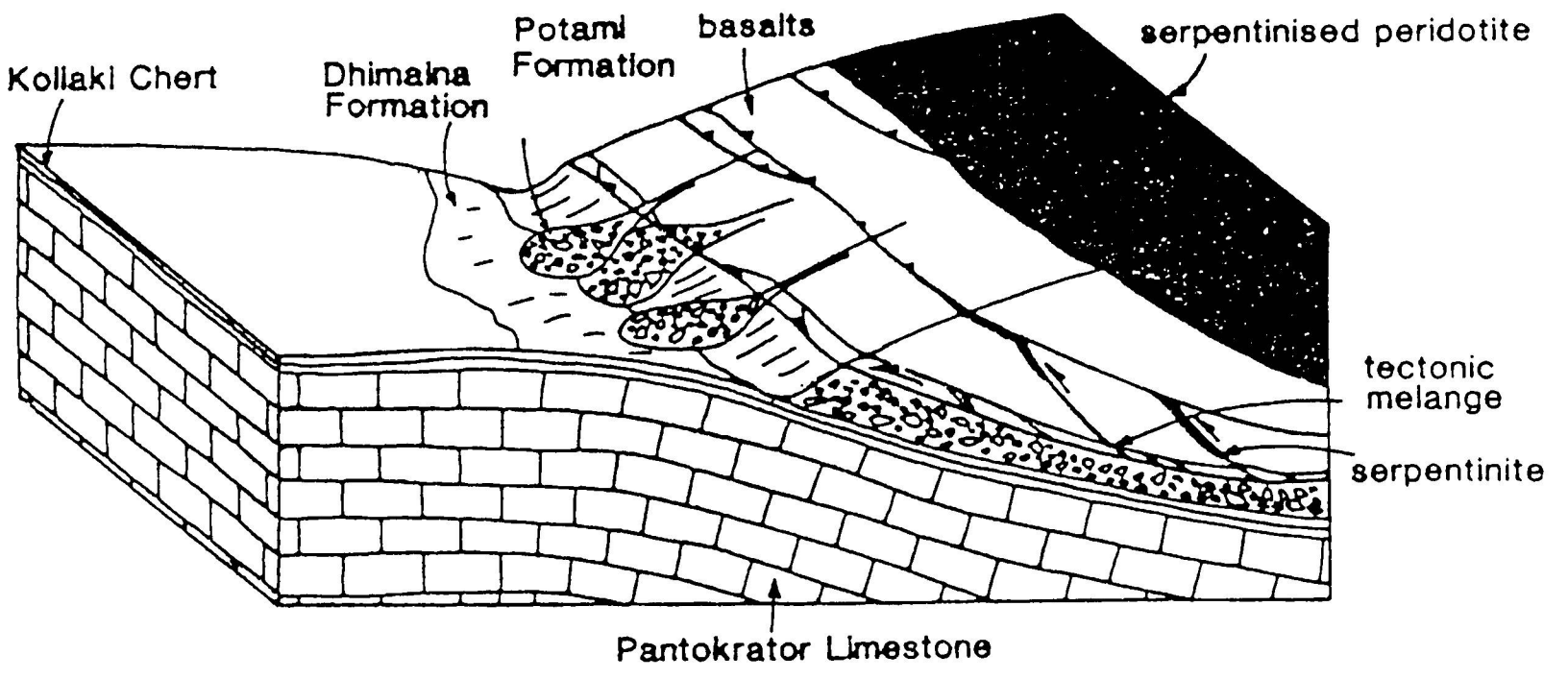


Figure 6.18 - Block diagram showing the development of a flexural foredeep in advance of an emplacing ophiolite. As the foredeep forms it is filled with a mélange deposit which is derived mostly from the overriding ophiolite. After Clift (1990)

The sediments are post-Upper Jurassic in age at their base while the upper levels of the sequence have been dated as Aptian/Albian by Galeos *et al.* (1993) based on pollen extracted from thin black phyllite interbeds. The sediments are thick-bedded, and erosive-based conglomerates tend to form the lowermost deposits of cyclical fining-up units. On the whole, the red-bed sedimentary succession fines upwards, as evidenced by a progressive decrease in conglomeratic horizons up-section, into dominantly sands and silts.

The top of the Loutra-Arideas Unit comprises dark grey neritic carbonates containing large *Nerineid* gastropods. A detailed palaeontological study of this unit was carried out by Galeos *et al.* (1993) who inferred an Aptian-Albian age.

Interpretation

The basal chloritic-schist/flattened-conglomerate succession of the Loutra-Arideas Unit was largely derived from continental basement and ophiolite sources, as evidenced by abundant mica-schist, serpentinite, altered basalt and marble clasts. The relatively thick-bedded, graded conglomerate horizons may have been deposited by high-density turbidity currents or debris flows, whereas the thinner bedded chloritic schists, sandstones and detrital carbonates could represent lower-density turbidites, derived from a continental margin and carbonate platform.

The schists/conglomerates are overlain by the altered remains of an ophiolite (i.e. serpentinised dunite and harzburgite, epidosite (?sheeted dykes), chloritised basalts and gabbros) and therefore the basal meta-sediments may have been deposited in a foredeep or foreland basin (Beaumont, 1981) generated in advance of an obducting ophiolite, now represented by the overlying serpentinitic mélange (this work, also Galeos *et al.*, 1993). Comparable foredeep deposits have been documented from Argolis (the Potami and Dhimaina Formations; Baumgartner, 1985; Clift, 1990), where debris flows and turbidites derived from the obducting Migdhalitsa Ophiolite were deposited as a

tectonic mélange in a foredeep setting (Figure 6.18). Similar foredeep deposits have also been documented from Euboea (south-eastern Greece; Robertson, 1990a), from Oman during the obduction of the Semail Ophiolite onto the Oman continental margin (Robertson, 1987), and from Newfoundland (Canada), where the Milan Arm Mélange, rich in serpentinite, basalt and gabbro clasts, was deposited in a foreland basin in advance of the obducting Bay of Islands Ophiolite (Williams, 1975).

This phase of ophiolite obduction in the Voras Massif is probably responsible for flattening clasts within the basal Loutra-Arideas schist/conglomerate unit, and for generating the early NW-SE-trending lineation (see **Structure** below).

As stated above, the serpentinites (hydrated dunites and harzburgites), meta-gabbros and epidosites (?sheeted dykes) overlying the deformed schists/conglomerates, represent the remains of a dismembered ophiolite, now preserved as a very coarse, mélange. Comparable mélange is present in the Arnissa area of the Pelagonian zone to the southwest, where large (up to 100 m diameter) blocks of altered peridotite, lava, gabbro and diorite are set in a sheared serpentinite matrix and interpreted as a dismembered ophiolite (Sharp, 1995).

In contrast to the ophiolite-derived meta-sediments which lie below the dismembered ophiolite, the ophiolite-derived conglomerates which unconformably overlie the ophiolite have not been strongly flattened and deformed, suggesting that they were deposited subsequent to ophiolite obduction. Galeos *et al.* (1993) interpret these overlying ophiolite-derived conglomerates as having formed contemporaneously with erosion of an ophiolitic source area, and the observations made during this study support this interpretation. The Upper Jurassic reefal limestones were deposited contemporaneously with the ophiolite conglomerates, probably only forming in areas where clastic sedimentation was minimal, such as on topographic highs in a shallow-marine setting.

The red-bed conglomerates at the top of the Loutra-Arideas Unit are interpreted by Galeos *et al.* (1993) as having been deposited in a fluvial environment subsequent to ophiolite emplacement and erosion. The sediments are similar in facies to the Ghrammos Formation of the Païkon Massif which are interpreted (chapter 3.8) as braided fluvial deposits; thus the interpretation of Galeos *et al.* (1993) seems appropriate. The red-beds also very closely resemble similar deposits described from the western Almopias subzone, namely the base of the Kerassia Unit of Sharp (1995).

Regional Comparisons

The stratigraphic succession described from the Loutra-Arideas Unit bears a striking similarity to that described from the Pelagonian zone and the western Almopias zone to the southwest (Sharp, pers. comm, 1993; Sharp, 1995). In the Pelagonian zone, Triassic marbles are overlain by ophiolite-derived debris flows interpreted to have been deposited in a foreland basin, in front of an advancing ophiolite of either Almopias or Pindos derivation (Figure 6.19). The ophiolite, which was obducted in the Upper Jurassic (Vergely, 1984; Sharp, 1995), is now represented by a mélange of ophiolite-derived blocks within a serpentinite matrix. In the Nisi area (Figure 6.1), the dismembered ophiolite is unconformably overlain by a well-rounded ophiolite conglomerate, which contains fossiliferous clasts of Oxfordian-Kimmeridgian limestone, and in other areas the ophiolite is directly overlain by the limestones themselves, which are rich in ophiolite-derived detritus (e.g. the Basal Kerassia Unit of the western Almopias subzone; Sharp, 1995).

In the Païkon subzone, the Kimmeridgian-aged Khromni limestones crop out and pass conformably upwards into the red-bed fluvial sediments of the Ghrammos Formation, which is comparable to the Upper Jurassic limestone and red-bed conglomerate succession of the Loutra-Arideas Unit. However, none of the ophiolite-derived or

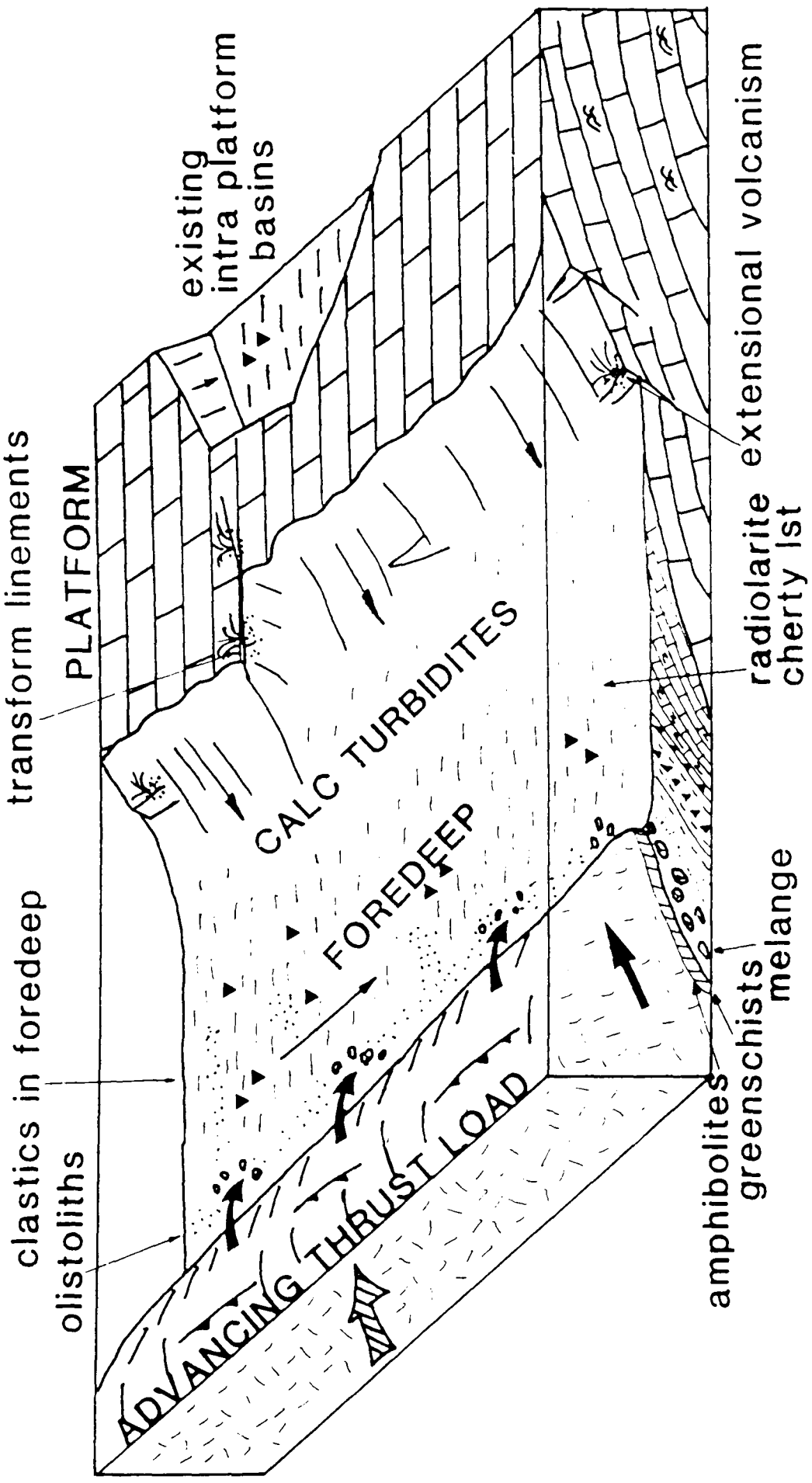


Figure 6.19 - Schematic block diagram of the emplacement of the Pelagonian Ophiolite Nappe and the development of the foredeep sequence at the top of the Pelagonian platform (after Sharp, 1995).

ophiolitic units observed in the Loutra-Arideas Unit are seen anywhere in the Païkon Massif and, thus, it is concluded here that the Loutra-Arideas Unit is unlikely to be of Païkon subzone affinity. Similarly, the Peonias zone contains a few lithological units which resemble those described from the Loutra-Arideas Unit (e.g. the Kimmeridgian Choryghi Limestones), but other than this there is little comparison.

Structure

All lithological units present in the Loutra-Arideas Unit have been affected by a phase of compressional deformation characterised by west-verging, asymmetrical, open to tight folds and a prominent fold axis-parallel lineation which plunges towards the NE (i.e. 027°N to 049°N; Figure 6.20). This deformation event must have taken place sometime after the Aptian/Albian, as it affects the topmost neritic limestones of the Loutra-Arideas Unit. An identical NE-SW-trending lineation and roughly west-verging asymmetrical fold structures characterise early Tertiary compression in the Pelagonian subzone to the south (F2 fold phase of Sharp, 1995; CT2 fold phase of Vergely, 1984; Figure 6.21), and it is therefore concluded here that these Loutra-Arideas structures formed during the same event.

The lowermost meta-sediments (chloritic schists, sandstones, detrital carbonate and conglomerates) of the Loutra-Arideas Unit exhibit an earlier lineation and were strongly flattened prior to generation of the Tertiary fold structures, suggesting that they were subjected to an additional, earlier phase of deformation. The NE-SW-trending Tertiary lineation overprints an earlier lineation which trends towards the NW-SE (Figure 6.11). This NW-SE lineation is characteristic of Upper Jurassic compression in the Pelagonian zone (Sharp, pers. comm., 1993; Sharp, 1995; Figure 6.22). In the Loutra-Arideas Unit this early lineation is parallel to the direction of maximum elongation of clasts within conglomerate horizons, indicating that it is a stretching lineation, which is again characteristic of the Upper Jurassic lineation in the Pelagonian zone (Vergely, 1984;

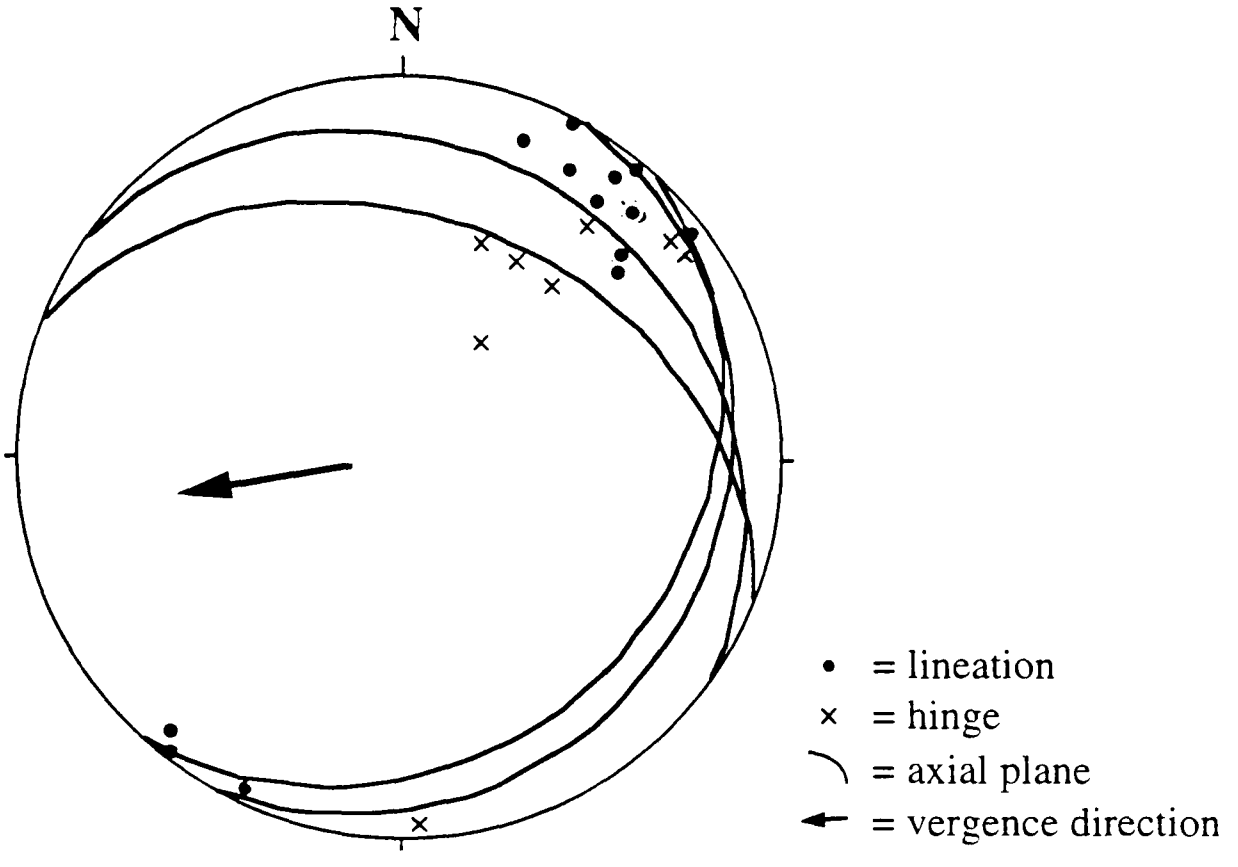


Figure 6.20 - Stereographic projection showing the NE-SW-plunging fold axes and axis-parallel lineation which affects all lithologies within the Loutra-Arideas Unit. These structures closely correspond to Tertiary structures recorded from the Perlagonian zone to the southwest (see Figure 6.21 below).

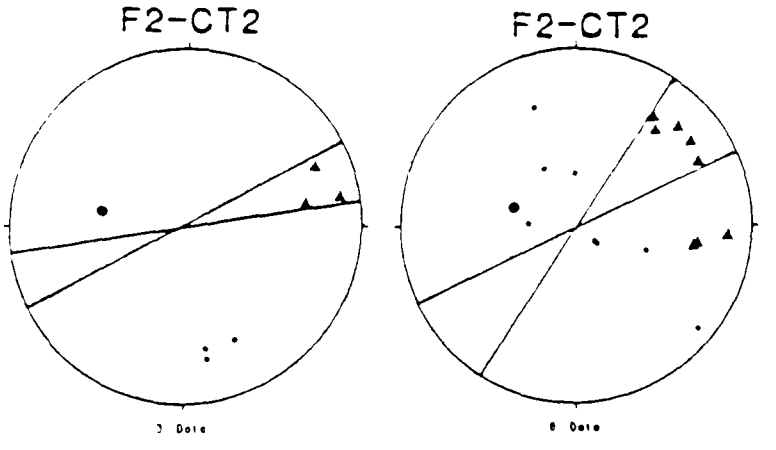


Figure 6.21 - Stereographic projection of NE-SW-trending Tertiary structures (F2) from the Pelagonian zone (after Sharp, 1995).

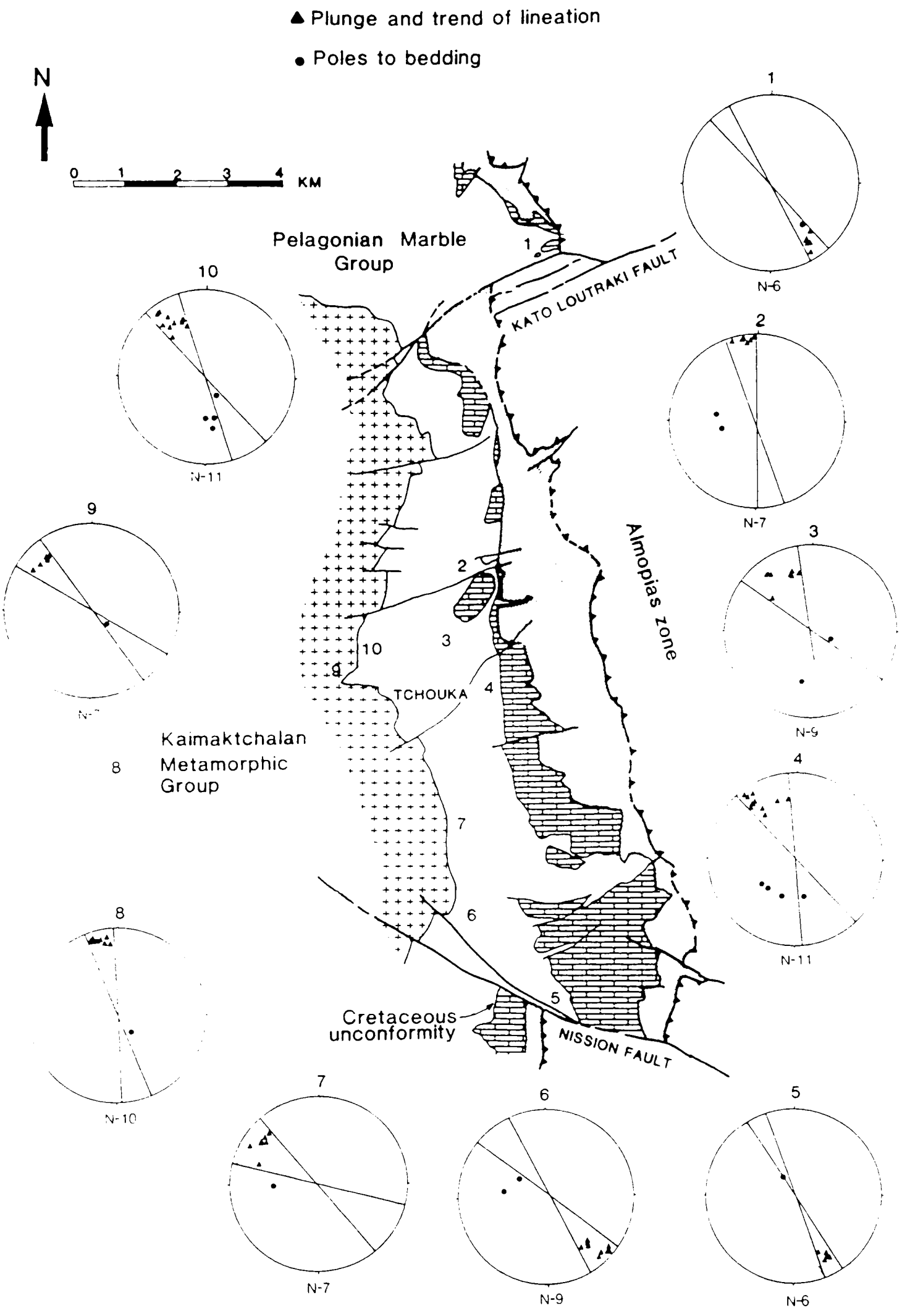


Figure 6.22 - Stereographic projection of NW-SE-trending Upper Jurassic structures (F1) from the Pelagonian zone (after Sharp, 1995).

Sharp, 1995). Notably, the Kimmeridgian to Aptian-Albian succession of the Loutra-Arideas Unit effectively "seals" this early phase of compressional deformation, which is associated with the obduction of an ophiolitic nappe onto the Pelagonian continental margin.

Subsequent, "thin-skin" overthrusting during the early Tertiary emplaced more easterly units (i.e. the Likostomo-Promachi Unit) onto the Loutra-Arideas Unit that was warped into a broad N-S-trending synclinal structure (Migiros & Galeos, 1990; Galeos *et al,* 1993; this work, Figure 6.7).

Summary

It is concluded here that the Loutra-Arideas Unit of the Voras Massif most closely resembles the stratigraphic succession created along the contact between the continental Pelagonian zone and the ophiolitic Almopias subzone, as exposed in the southwest. The Loutra-Arideas Unit bears little similarity to the Païkon and Peonias zones and is in no way comparable to the Serbo-Macedonian Massif.

6.3.2 - *Unit 2 - the Likostomo-Promachi Unit*

The eastern limit of the Loutra-Arideas Unit is overthrust, with westward polarity, by a thrust slice of augen gneiss which is overlain to the east, with questionable contact (probably faulted), by garnet-mica-schists and amphibolites. The amphibolites are, in turn, overlain to the east by marbles and micaceous sandstones, exposed to the north and northwest of Promachi village (Figure 6.6). These lithologies constitute the Likostomo-Promachi Unit (Figure 6.8b). The Likostomo-Promachi Unit corresponds to the western part of the Livadia Unit of Migiros & Galeos (1990), the western part of the Peternik Unit of Mercier (1968) and the Aridea Metamorphics of Ricou & Godfriaux (1991).

Stratigraphy, Petrology and Field Relations

The augen gneiss is medium-grained and comprises dominantly strained quartz, feldspar and white mica with minor chlorite, which generate a gneissose fabric that dips consistently down towards the east (Figure 6.23). The white mica content of the gneiss increases towards the contact with the amphibolites to the east. The gneisses and amphibolites are separated by a breccia unit (well exposed in road cuts due NW of Promachi), which has been almost wholly derived from the adjacent gneiss and amphibolite rocks, together with a minor amount of garnet-mica-schist and marble clasts (Figure 6.24). The gneiss, garnet-mica-schist and amphibolite clasts all contain a well-developed high-grade fabric, as seen in the adjacent units, and are set in a lower grade (possibly meta-pelitic), siliceous matrix. East (on top) of the breccias, the amphibolites (Figures 6.25 & 6.26) and garnet-mica-schists are interbedded and often contain retrogressive chlorite and epidote (Figure 6.27). Retrogression is most prevalent in the garnet-mica-schists and along fracture zones within the amphibolites, which presumably channelled the retrogressing fluids.

Still further east, the amphibolites pass upwards, with questionable contact, into micaceous marbles which become interbedded with micaceous psammites up-section (to the east). No faunal or sedimentary structures remain in these rocks and they exhibit a S0-parallel foliation which is roughly parallel to that observed in the amphibolites. In the east, the psammites and micaceous marbles are overthrust by rocks of Unit 3 - the Livadia Unit.

Structures

The augen gneisses, garnet-mica-schists and amphibolites have all been poly-phase deformed and contain a high-grade metamorphic fabric, marked by either a foliation defined by amphibole laths (amphibolites) or an augen gneissic fabric (gneisses), and have mineralogical assemblages indicative of high (amphibolite) grade metamorphism (e.g. amphiboles, garnet, muscovite).

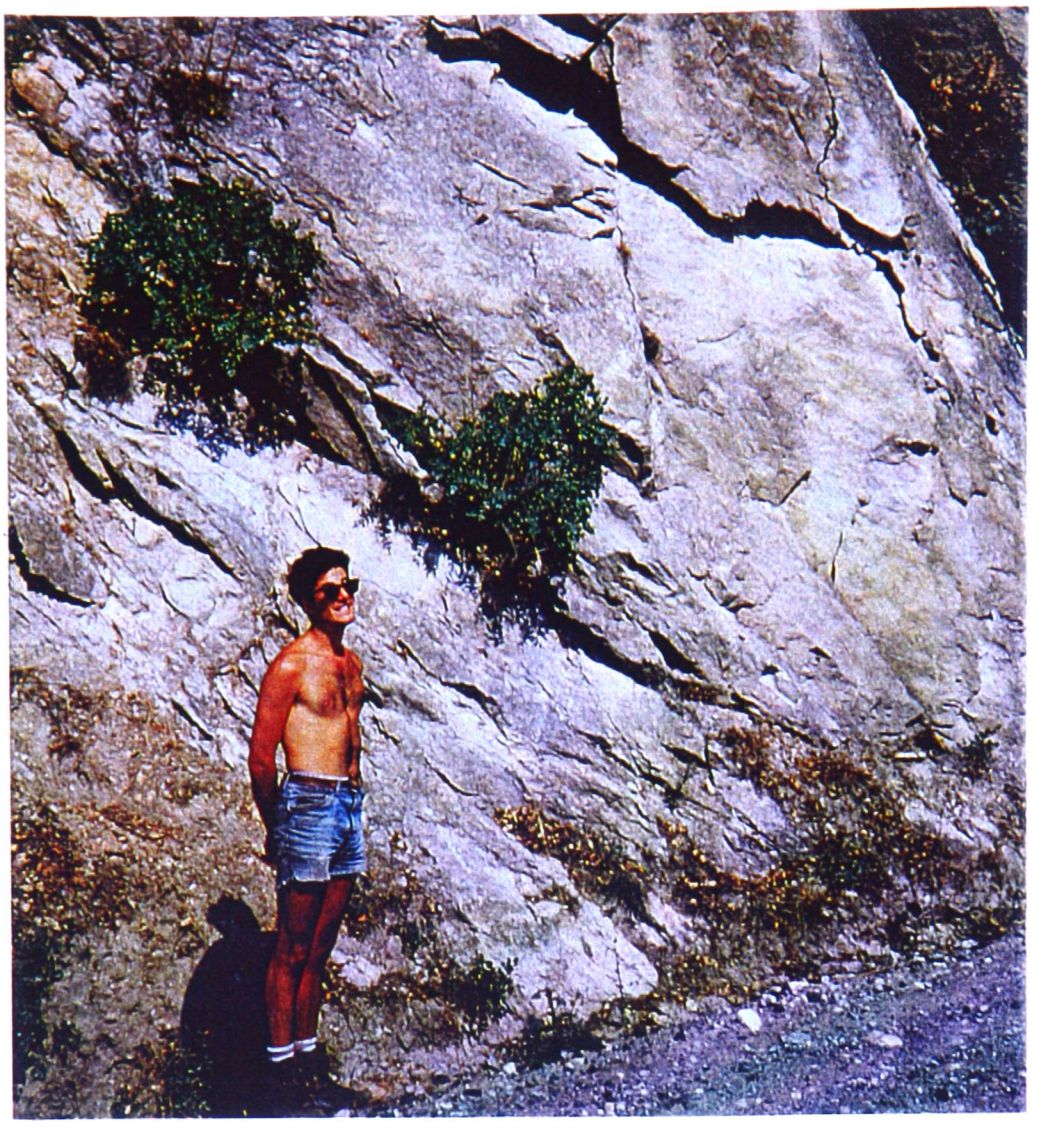


Figure 6.23 - Field photograph of the quartzo-feldspathic augen gneiss (Likostomo Gneiss) of the Likostomo-Promachi Unit. The gneissose fabric dips down towards the east (top left to bottom right in photograph).

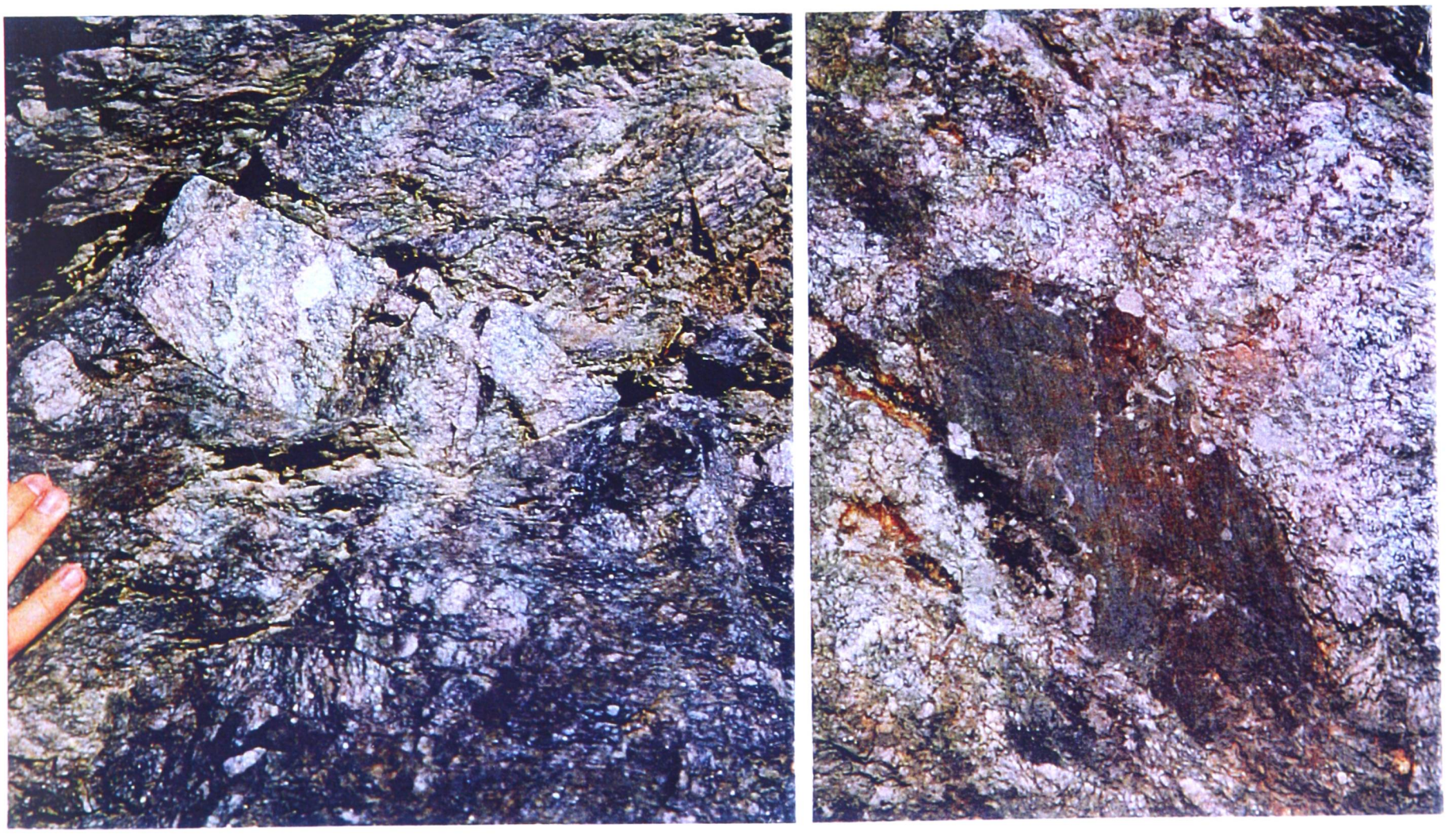


Figure 6.24 - Field photographs of the breccia unit which separates the augen gneisses from the amphibolites of the Likostomo-Promachi Unit. The high-grade fabric of the clasts does not continue into the breccia matrix. The large, dark clast is 20 cm long.



Figure 6.25 - Field photograph of the amphibolites of the Likostomo-Promachi Unit. The high-grade fabric is clearly picked out by foliation-parallel retrogressed layres and by foliation-parallel quartz veins.

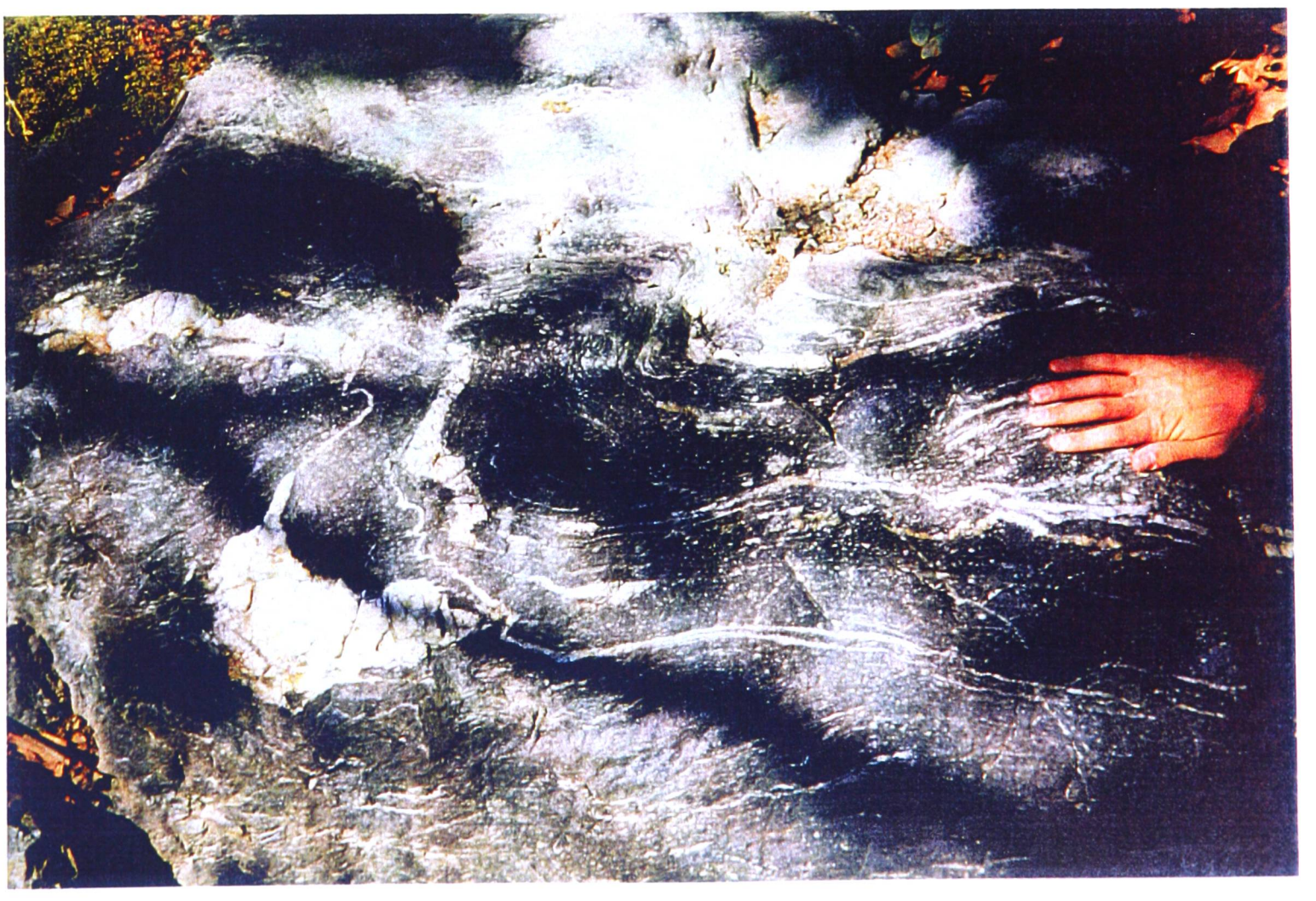


Figure 6.26 - The amphibolites of the Likostomo-Promachi Unit. In this photograph the high-grade fabric of the amphibolites is being folded by ductile, tight to isoclinal folds (see section 6.3.2 - **Structures**).

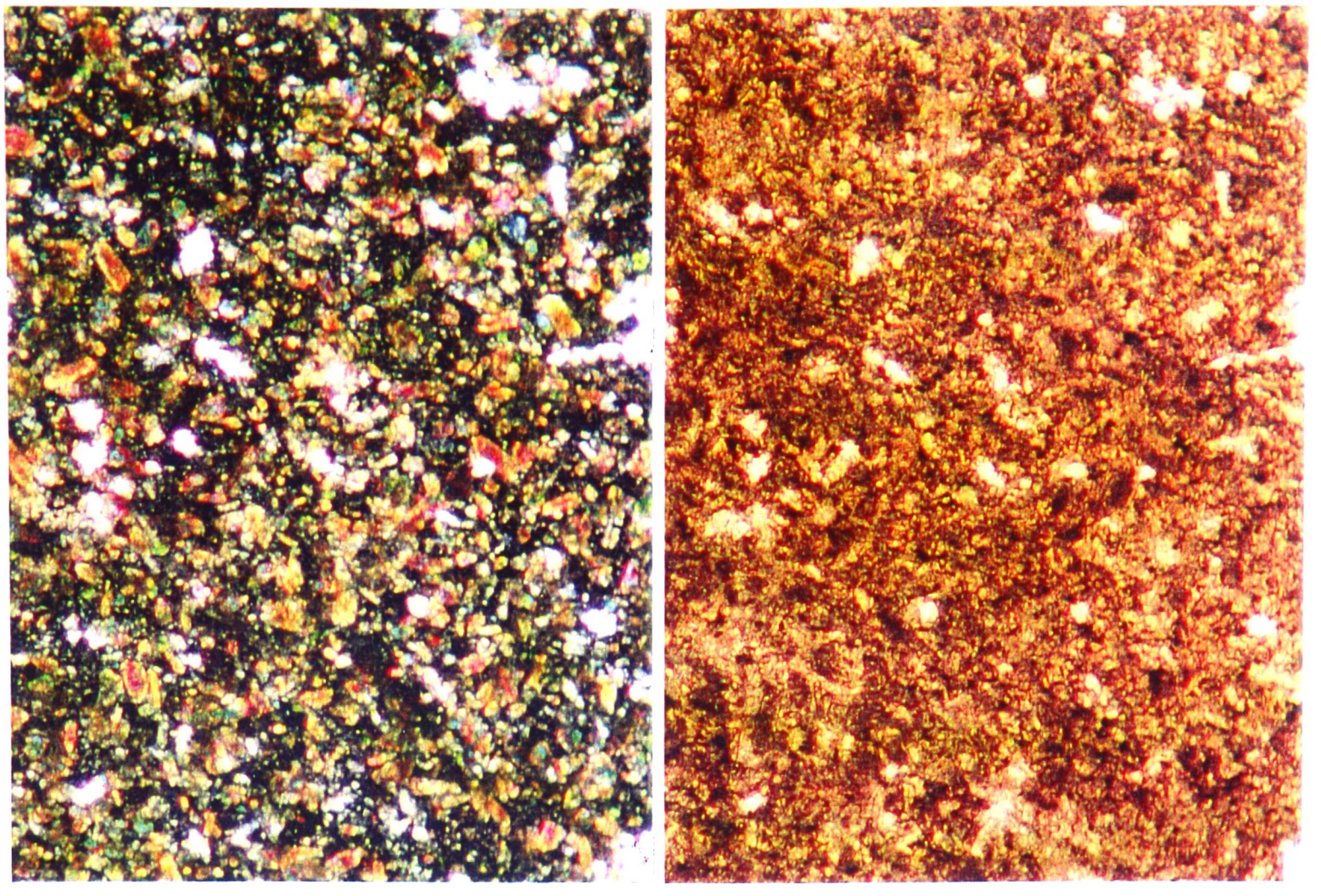


Figure 6.27 - Photomicrograph of the Likostomo-Promachi amphibolites that have been retrogressed to chlorite and epidote (greenschist facies). In horizons where retrogression has occurred, the high-grade fabric is less obvious. Both ppl (left) and xpl (right) are shown.

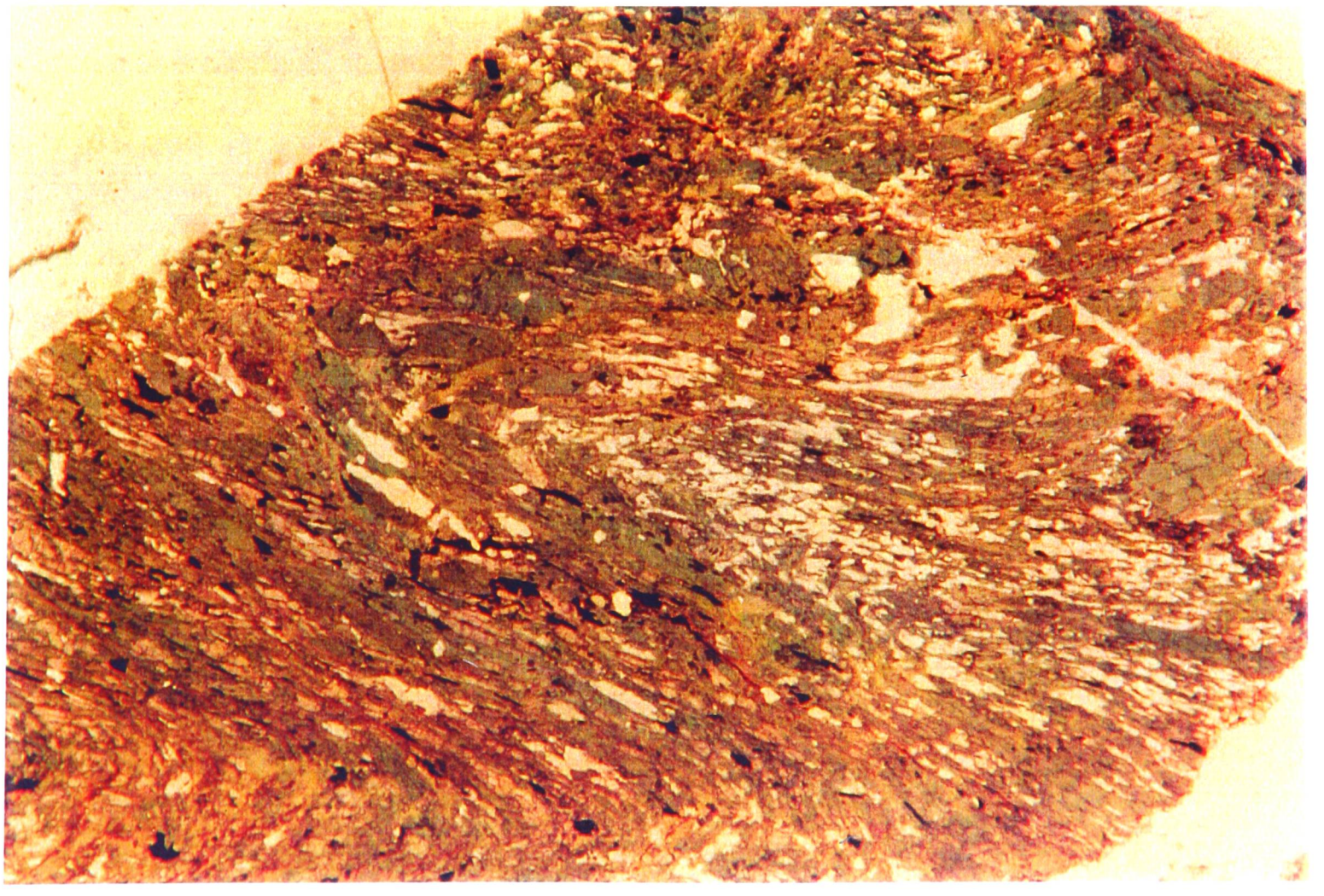


Figure 6.28 - Photomicrograph of the high-grade fabric of the amphibolites (Likostomo-Promachi Unit) being isoclinally folded. These folds are likely to have been generated by an Upper Jurassic phase of ductile compression.

In addition to this high-grade fabric, the gneiss/schist/amphibolite association and the overlying micaceous marbles and psammites of the Likostomo-Promachi Unit have been affected by three phases of compressional deformation. The first of these is characterised by tight to isoclinal folding. These structures fold the high-grade fabric in the amphibolites, as demonstrated in Figures 6.26, 6.28 and 6.29. The second compressional phase is preserved as open to tight folds associated with a fold axis-parallel lineation, which trends towards the NE (i.e. 026°N to 072°N; Figure 6.29). Overprinting and crenulating these structures are a later generation of kink folds, characterised by hinges trending towards 330°N to 352°N and west to southwest-directed vergence (Figure 6.30).

The latter two compressional events are characteristic of Tertiary compression within the Pelagonian zone (Sharp, 1995). The first corresponds to the F2 Tertiary deformation of Sharp (1995; and CT2 of Vergely, 1984), as described from the Loutra-Arideas Unit to the west (Figures 6.20 and 6.21), and the second relates to the later F3 Tertiary kink-folding event of Sharp (1995; and CT3 of Vergely, 1984; Figure 6.31). The first phase of isoclinal folding is therefore likely to correspond to the Upper Jurassic "Eohellenic" deformation event (JE1 of Vergely, 1984; F1 of Sharp, 1995; D1 of Brown & Robertson, in press).

Interpretation

The augen gneisses described above are remarkably homogeneous in composition and comprise a mineralogy (quartz, feldspar, white mica, chlorite) which suggests that their protolith is granitic. The mineralogy of the garnet-mica-schists, on the other hand, suggests a protolith of pelitic composition, while the amphibolites are likely to represent meta-basic rocks.

In addition to the high-grade metamorphic fabric in the gneiss/mica-schist/amphibolite

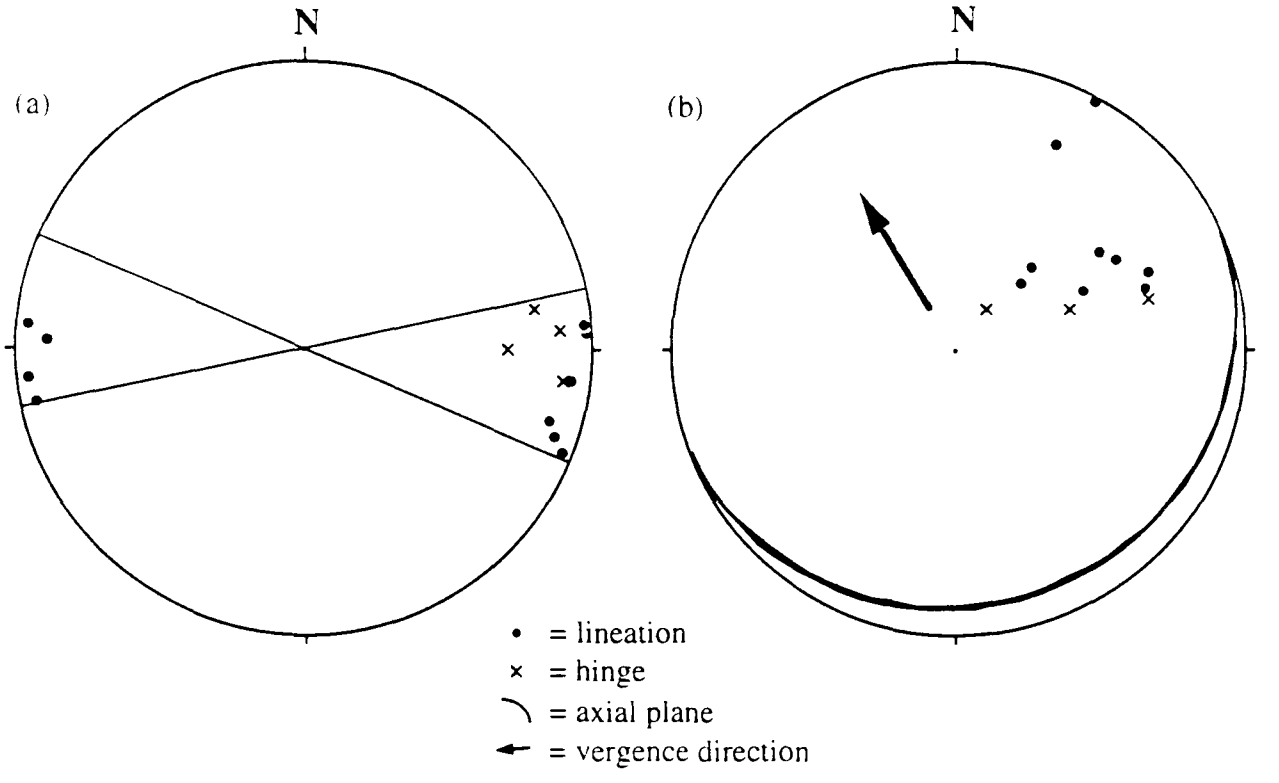


Figure 6.29 - Stereographic projections from the Likostomo-Promachi Unit showing the E-W-oriented structures of the first post-high-grade folding event (A) and the NE-SW-trending fold axes and axis-parallel lineations of the second folding event (B). These structures are comparable in style and orientation to those generated during Tertiary tectonism (F2) in the Pelagonian zone (see Figure 6.21).

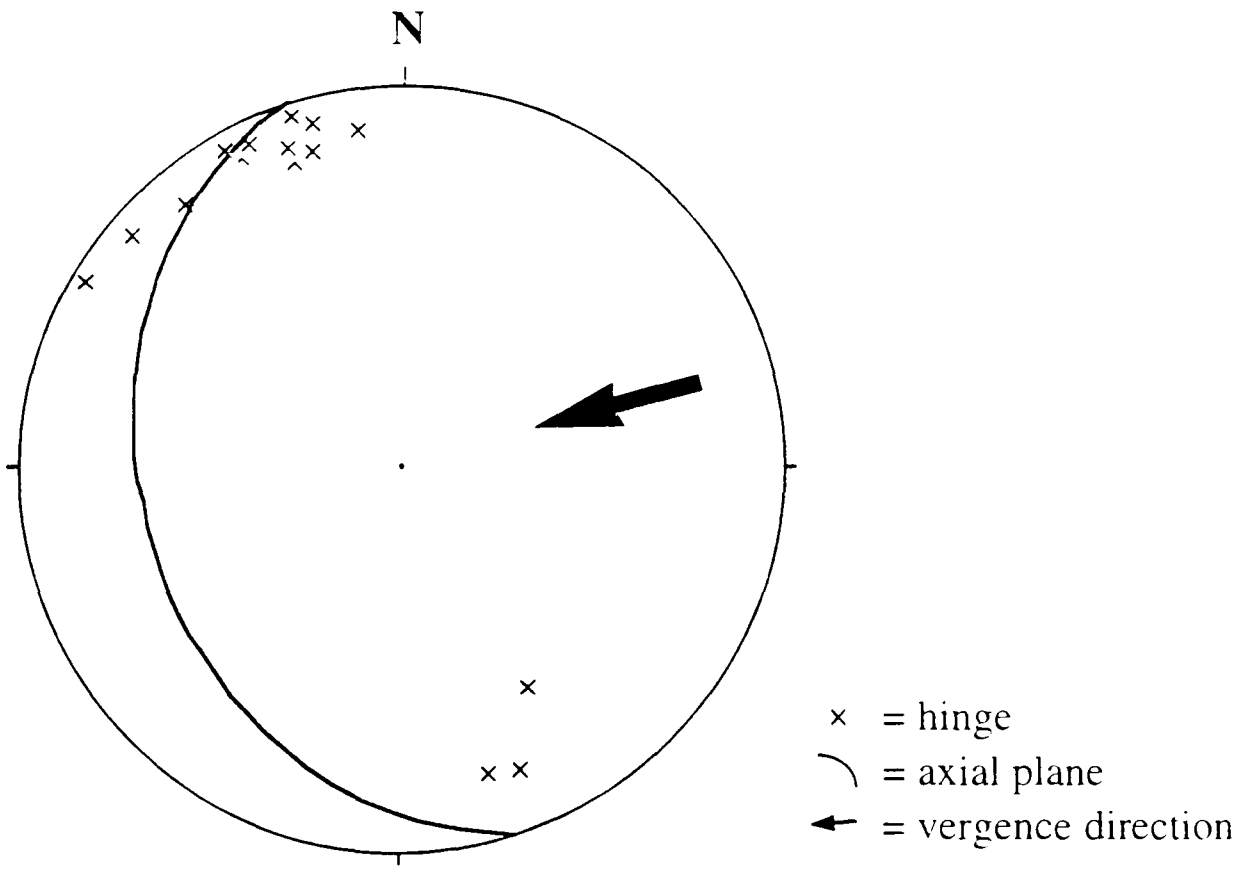


Figure 6.30 - Stereographic projection of the late-stage kink folds which affect the Likostomo-Promachi Unit. The kink fold axes trend towards the NNW and verge southwestward (c.f. Figure 6.31).

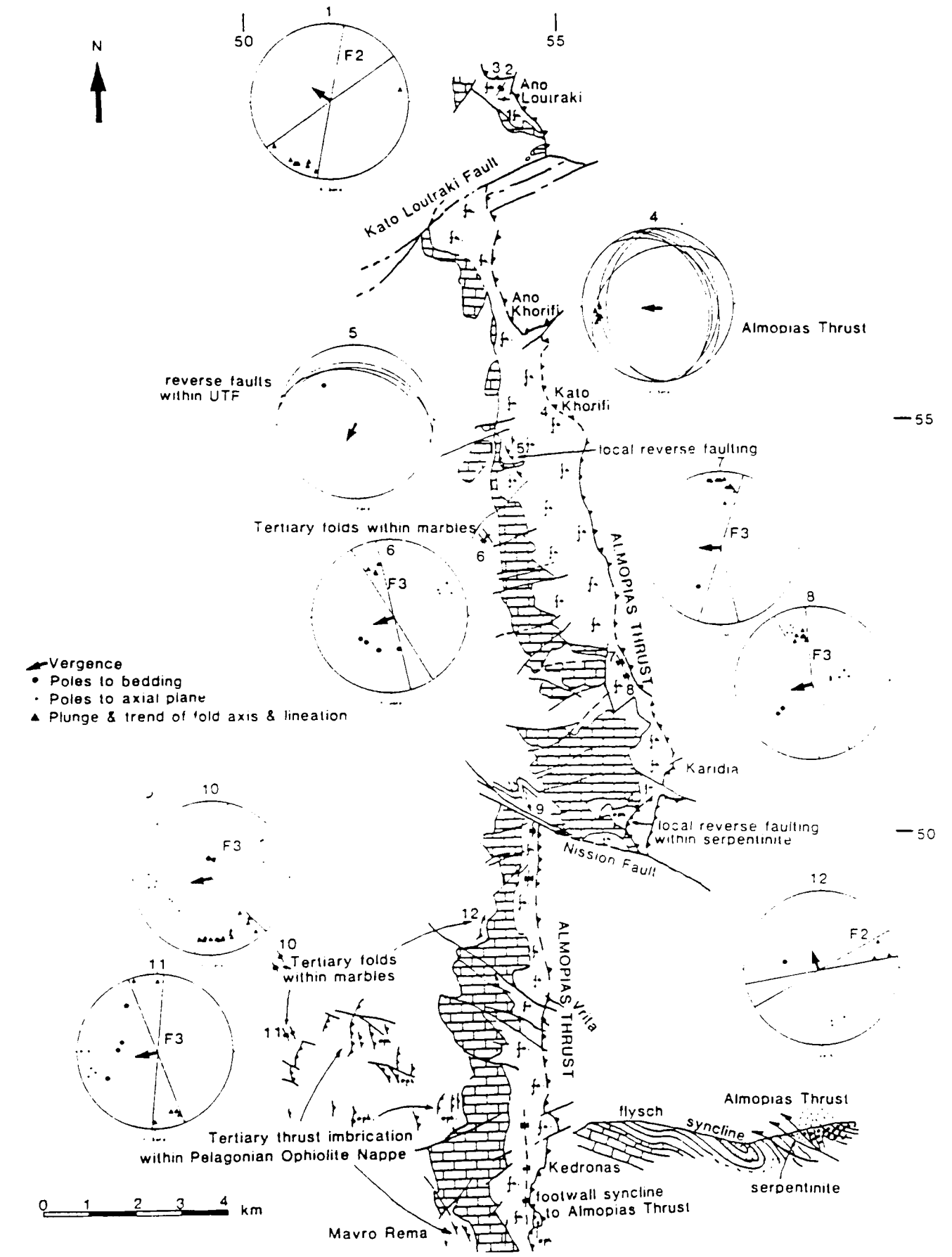
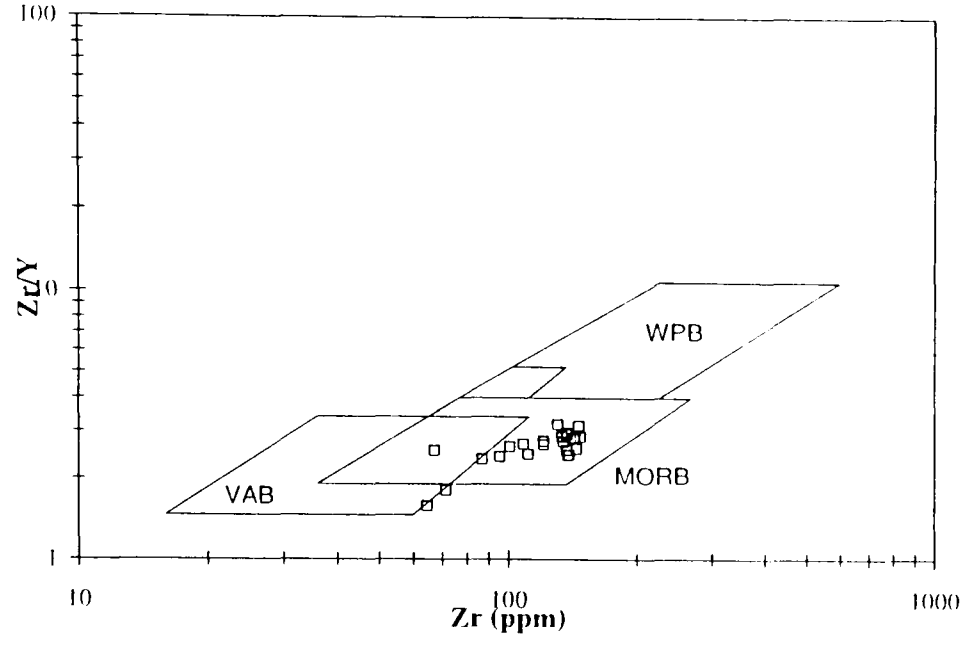


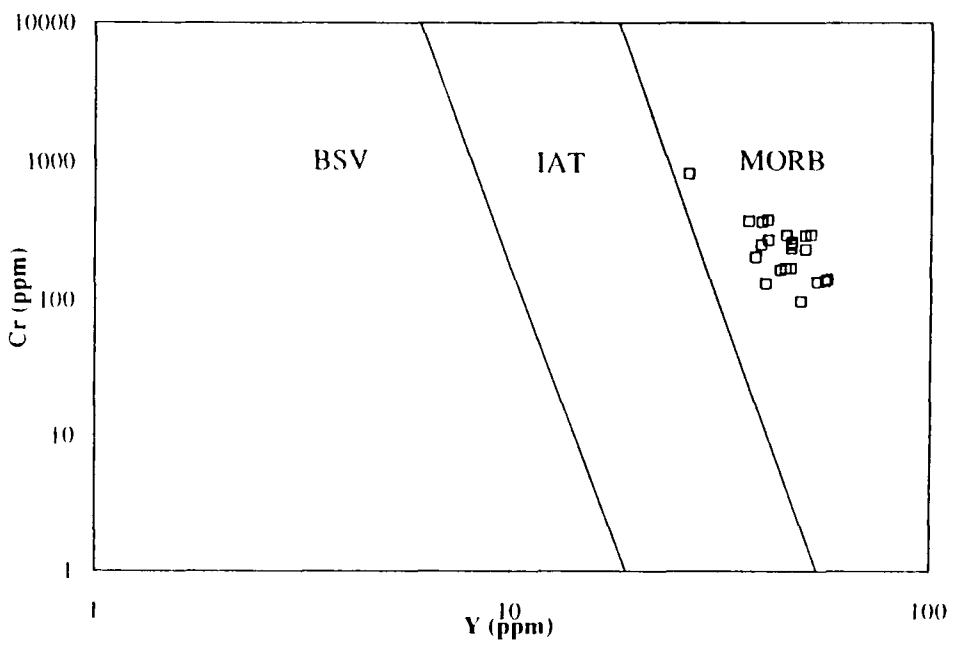
Figure 6.31 - Diagram showing structures associated with Tertiary deformation in the Pelagonian zone. F2 structures trend NE-SW, while F3 kink folds and associated structures trend NNW-SSE, which is comparable to similar structures recorded from the Likostomo-Promachi Unit (see Figure 6.30). After Sharp (1995).

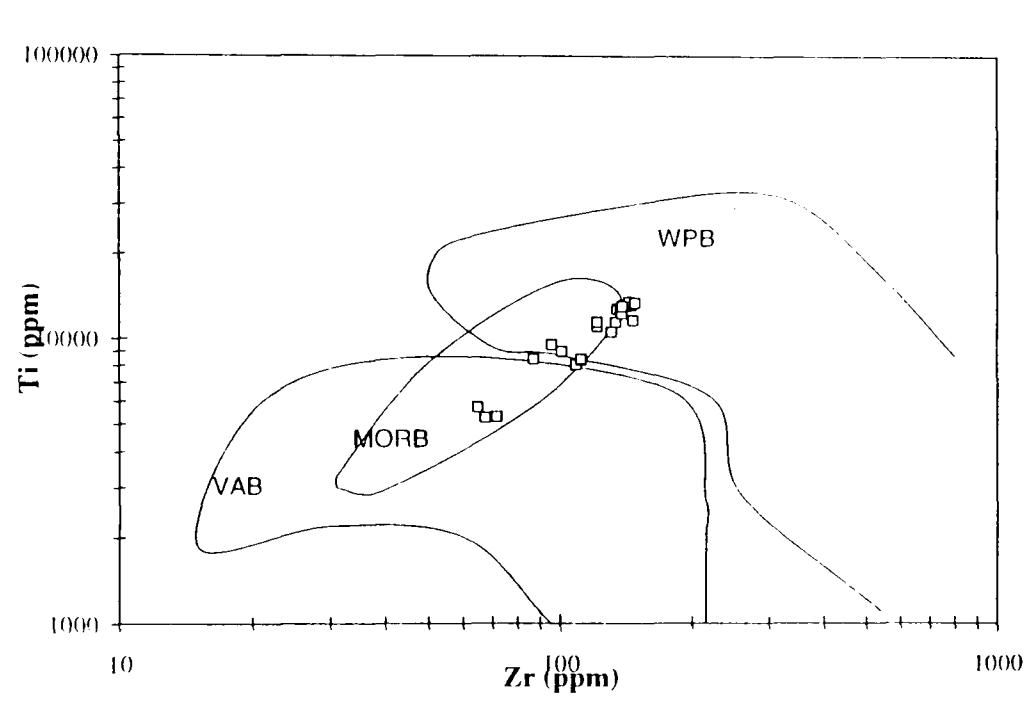
association there is also evidence that these units were subjected to the Upper Jurassic and Tertiary deformation events described from the Loutra-Arideas Unit (see **Structures** section above). No rocks of Mesozoic age, from anywhere in the Internal Hellenides, contain an early high-grade fabric such as this, and they have only been affected by Upper Jurassic and Tertiary compressional events (Sharp, 1995; this work, chapter 4). This implies that the high-grade event, which is responsible for the high-grade fabric, occurred prior to the Mesozoic. The gneisses, garnet-mica-schists and amphibolites are therefore interpreted to be of pre-Mesozoic age.

Migiros & Galeos (1990) suggested that the amphibolites represent a "metamorphic sole" which was generated by the obduction of the Ano Garefi Ophiolite (see section 6.3.4) during Upper Jurassic regional compression. Geochemical analyses carried out during this study indicate that the amphibolites are of Mid Ocean Ridge Basalt (MORB) composition (Figure 6.32), which resembles the MORB/Within Plate Basalt (WPB) geochemical signature of the Ano Garefi Ophiolite. However, the Upper Jurassic Ano Garefi Ophiolite (section 6.3.4) could not have been emplaced in pre-Mesozoic time and so this hypothesis is unlikely. Alternatively, it is suggested here that the gneiss/mica-schist/amphibolite association may represent a slice of pre-Mesozoic-aged continental basement which was tectonically incorporated into the Voras Massif during Tertiary thrusting.

The breccia unit which lies between the gneisses and the interbedded garnet-mica-schists and amphibolites was definitely deposited subsequent to pre-Mesozoic high (amphibolite) grade deformation, as the high-grade fabric still prevalent in the breccia clasts does not extend into the matrix (Figure 6.33). No evidence of the Upper Jurassic phase of deformation was observed in the breccia unit either, therefore it is possible that the breccia was generated along a fault zone of either Tertiary or younger age.







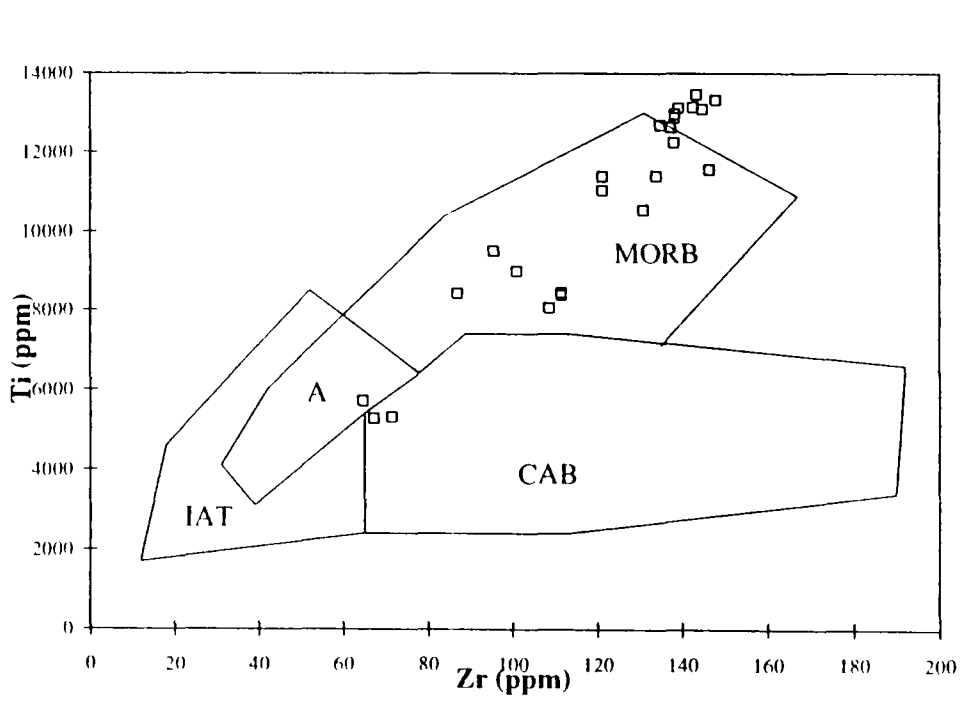


Figure 6.32 - Templates showing the geochemical characteristics of the Likostomo-Promachi amphibolites. See chapter 5 for details of the templates and their authors

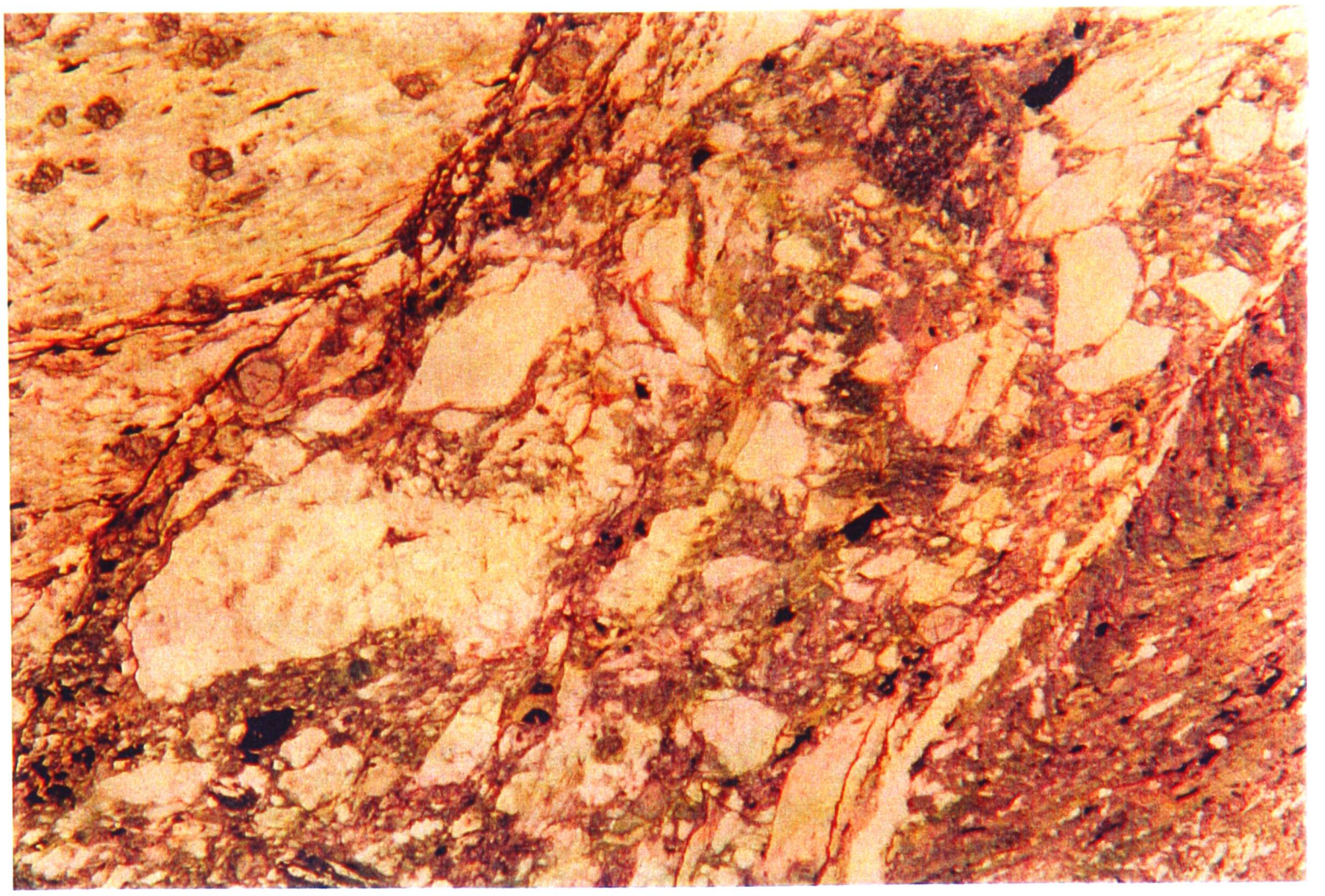


Figure 6.33 - Photomicrographs showing the high-grade fabric of the Likostomo-Promachi amphibolites being truncated by the lower-grade breccia matrix. The upper photograph is taken in plane polarised light (ppl) and the lower is taken under crossed polars (xpl).

The interbedded micaceous marbles and micaceous psammites are not likely to form part of the high-grade continental basement sequence, as they contain no evidence of an early high-grade fabric. They do, however, record all of the Upper Jurassic and Tertiary contractional deformation events. This implies that they were deposited some time after high-grade deformation of the gneiss/amphibolites, possibly as an early Mesozoic sedimentary cover to the continental basement rocks. In future, detailed mapping of contact between the gneiss/amphibolite and psammite/marble units might shed light on their relationship, be it thrusted, conformable or depositional.

Regional Correlations

The gneisses, garnet-mica-schists and amphibolites of the Likostomo-Promachi Unit can be correlated with continental basement rocks of the Pelagonian zone, as exposed in the Kaimaktchalan Massif to the west (Sharp, pers comm, 1993; S. Dimitriadis pers. comm., 1993; Mountrakis, 1984; Sharp, 1995); this comprises ortho- and augen gneisses, amphibolites and mica-schists of pre-Upper Palaeozoic age (Mountrakis, 1982, 1984), depositionally overlain by Triassic marbles of the Pelagonian Marble Group (Sharp, 1995). The continental basement rocks of the Pelagonian zone have a sedimentary protolith (Brunn, 1956), which was intruded by Late Carboniferous granites (Yarwood and Aftalion, 1976). The micaceous marbles are thus likely to be equivalent to the Triassic basement cover rocks of the Pelagonian Marble Group. The Likostomo-Promachi basement rocks are, however, quite different from the continental basement of the Serbo-Macedonian zone, to the east (S. Dimitriadis, pers. comm., 1993), which comprises banded, coarse, garnetiferous gneisses, marbles, biotite-rich schists, quartzo-feldspathic schists and amphibolites (Batty, 1993).

The younger breccia unit bears a strong similarity in protolith and stratigraphic position to the Lower Tectonic Mélange of the Klissohori Unit of the Almopias zone (Vergely, 1984; Sharp, 1995), interpreted to have formed along a palaeo-fault line. Given the

present day situation of the Likostomo-Promachi Unit breccia, a similar tectonic environment of formation is possible and indeed the breccia may have been generated along the major normal fault which runs all along the southern margin of the Voras Massif; the along-strike continuation of the Kato Loutraki fault south of the Kaimaktchalan Massif.

Summary

The Likostomo-Promachi Unit comprises pre-Mesozoic continental basement rocks of Pelagonian zone affinity, which are ?depositionally overlain by early Mesozoic marbles and psammites, which are temporal, stratigraphic and partly facies equivalents of the Pelagonian Marble Group. All of these lithologies were incorporated into a tectonic breccia unit, which may have formed due to faulting along the southern margin of the Voras Massif. All units exposed in the Likostomo-Promachi Unit are also very similar to the Klissochori Unit (Sharp, 1995) of the eastern Pelagonian zone.

6.3.3 - *Unit 3 - the Livadia Unit*

At its structural base, the Livadia Unit (Figures 6.6, 6.7 and 6.8c) exhibits an east-dipping slab of augen gneiss overlain to the east by marbles, sheared serpentinite and Cretaceous limestones, which are in turn overlain to the east by imbricates of sugary marble, chloritic schist, bedded chert and buff, nodular limestone. The Livadia Unit is equivalent to the eastern part of the Peternik unit of Mercier (1968) and the eastern part of the Livadia unit of Migiros & Galeos (1990).

Stratigraphy, Petrology and Field Relations

At the base of the Livadia Unit, a thin sliver of white augen gneiss is thrust south-westward onto the eastern margin of the Likostomo-Promachi Unit. The overlying marbles are folded and recrystallised and exhibit pink, nodular, possibly palaeokarstic

surfaces (c.f. Sharp, 1995), which are likely to represent S0 surfaces, well exposed, for example, in river sections north of Promachi, Figure 6.6. The marbles have been overthrust by a sliver of serpentinite, which is highly sheared at its base and unconformably overlain by a deformed succession of carbonates, which are pale grey and thick-bedded at their base and rudist-bearing at their top. The unconformity surface is marked by a thick lateritic and bauxitic surface. The base of the grey limestone succession contains *Orbitolina sp.* foraminifera, which indicate an Aptian/Albian age and an outer platform setting (Sartorio & Venturini, 1988; Figure 6.34), and the uppermost limestones contain strained and sheared *Vaccinites sp*, rudists, which are characteristic of the Upper Cretaceous (Turonian-Maastrichtian; Moore, 1969; Figures 6.34 & 6.35). The rudist-bearing limestones pass conformably upwards into thin-bedded sands, silts and mudstones interbedded with detrital carbonates, potentially of uppermost or post-Upper Cretaceous age.

Further east, the silts, sands and mudstones are structurally overlain by a northeast-dipping, thrust-imbricate stack led by a sheet of grey, coarse-grained micaceous augen gneiss. Marble slices within the imbricate stack are clean, blue-white, wholly recrystallised and often sugary (Figure 6.36). They contain S0-parallel boudins of dolomitic material and what appear to be the remains of fenestral textures and algal fiammé. Parallel to S0, the marbles also exhibit horizons which are pink/white and highly fractured; possibly palaeokarstic surfaces. Interfolded and thrusted with the white marbles are lenses and sheets of green schists, which are rich in chlorite, white mica and quartz (strained) with lesser amounts of feldspar (?albite) and epidote. Bedded red cherts are also present as thin thrusted sheets within the Livadia Unit, as are more detrital striped grey and white marbles.

Limestone thrust slices are darker, less internally deformed and are characterised by an invading network of buff, muddy partings which give the limestone a nodular



Figure 6.34 - Grey Cretaceous limestones from the Livadia Unit. The rock on the left hand side of the photograph contains two large, deformed rudist bivalves (possibly *Vaccinites sp.*, top left) and the rock to the bottom right is *Orbitolina*-bearing.

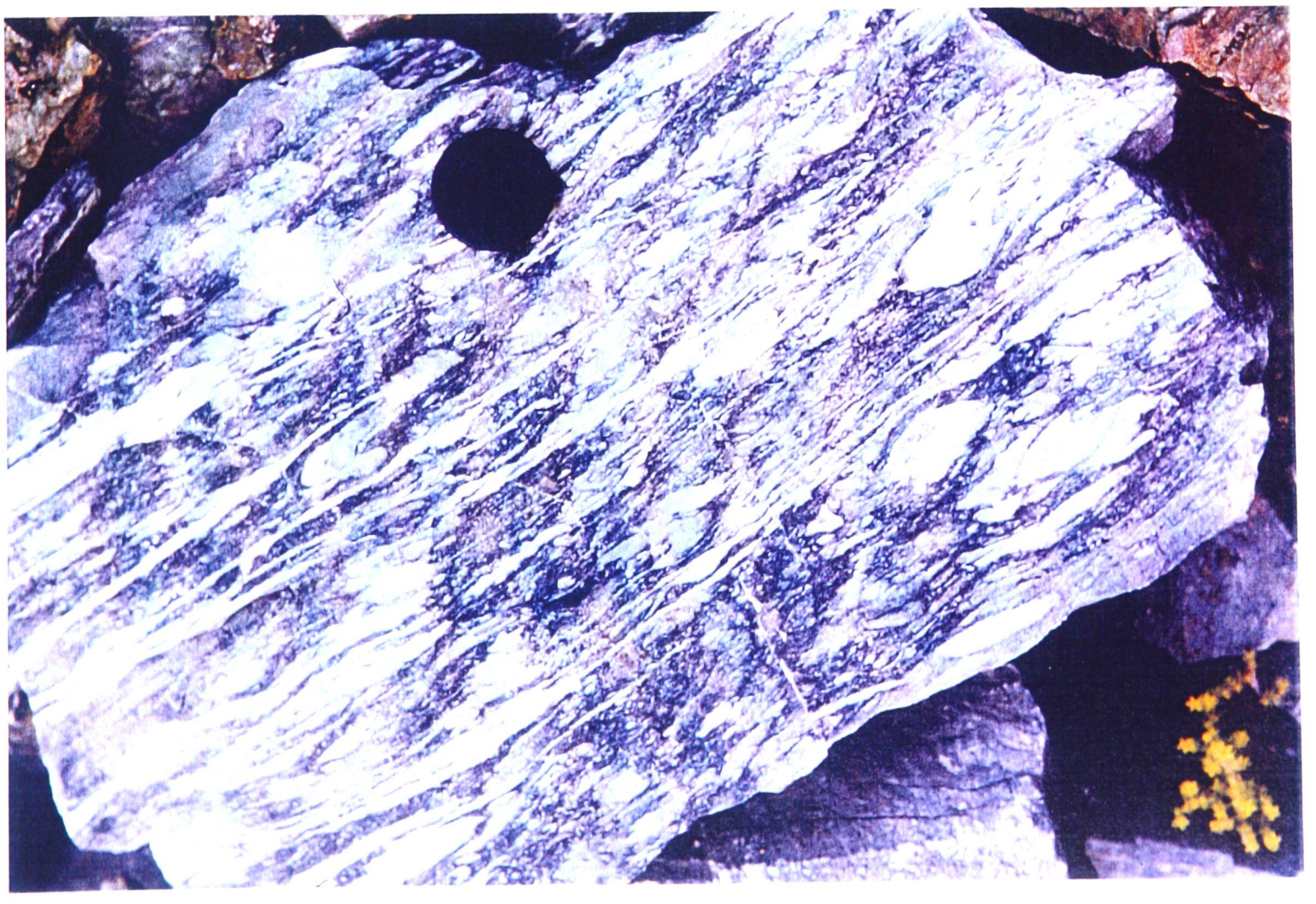


Figure 6.35 - Limestone from the top of the shallow-water Cretaceous limestones of the Livadia Unit. The rock comprises the highly sheared remains of rudist bivalves.



Figure 6.36 - Field photograph of white sugary marbles which have been tectonically incorporated into the Livadia imbricate stack.



Figure 6.37 - Field photograph of the marbles of the Livadia Unit. The marbles have been tightly folded around asymmetrical isoclines whose axes trend towardsthe northeast.

appearance. No fauna are preserved in these limestones. Slices of fine-grained clastic sediments are also present in the Livadia Unit imbricate stack and these often contain thin horizons of micritc limestone and deformed cherts, within which the remains of deformed radiolarian tests were observed.

Interpretation and Regional Correlations

Thrust slices of micaceous and augen gneiss within the Livadia Unit are lithologically identical to those described for the Likostomo-Promachi Unit and are interpreted as upthrusted continental basement slivers of Pelagonian zone affinity. The serpentinite is almost certainly derived from hydrated oceanic peridotite, and the unconformably overlying *Orbitolina*- and rudist-bearing limestones were deposited in a relatively shallow-water (outer platform) marine environment, as indicated by their fauna. The thin-bedded sediments which the limestones pass up into may represent a phase of deepening, characterised by low-density gravity flow (i.e. turbidity) deposits.

The Peonias subzone does not comprise comparable lithologies to those observed in the Livadia Unit, and hence the Livadia Unit is unlikely to be affiliated with this tectonostratigraphic unit. The Cretaceous Transgressive Limestones and the Tchouka Flysch of the Païkon Massif resemble the Aptian-Albian to Turonian-Masstrichtian shallow-water limestones and overlying post-Upper Cretaceous sediments of the Livadia Unit in their age and environment of deposition, although the limestone fauna and sedimentary facies of these units are not directly comparable. The Cretaceous limestone succession does not unconformably overlie ophiolitic rocks in the Païkon Massif as is evident in the Livadia Unit. None of the lithologies present in the Livadia imbricate stack are seen anywhere in the Païkon subzone. The Serbo-Macedonian zone comprises continental basement rocks overlain by fossiliferous Triassic marbles, but these are very different to the augen gneisses and palaeokarstic marbles of the Livadia Unit. It is unlikely, therefore, that the Livadia Unit is genetically related to any of these tectono-stratigraphic units.

However, the sequence, from gneisses to highly deformed marbles, serpentinite, Cretaceous limetones and ultimately post-Upper Cretaceous flysch, is identical to parts of the Mesozoic sequence of the Pelagonian zone, as exposed in the Arnissa region and to the Klissochori and Nea Zoi Units of the central Almopias zone (Sharp, 1995). In the Arnissa region, continental basement rocks are depositionally overlain by deformed marbles which show well-preserved palaeokarstic surfaces. The marbles are overlain by volcanic-derived schists and cherts, which are in turn overlain by the serpentinised remains of a dismembered ophiolite. The serpentinite is then unconformably overlain by *Orbitolina*- and *Vaccinites*-bearing Cretaceous limestones, which ultimately pass up into a deep-water flysch of post-Upper Cretaceous age.

The lithologies within the Livadia imbricate stack are also similar to rock types that have been described only from the Pelagonian zone. The white, sugary marbles correspond to the lowermost marbles of the Pelagonian Marble Group (Sharp, 1995), which similarly comprise dolomitic S0-parallel boudins and algae (Gryphoporella Curvata, Norian; Mercier, 1968). The chloritic schists and bedded cherts of the Livadia Unit imbricates may be equivalent to volcanic-derived schists and bedded cherts of the Kato Grammatiko Formation of the Pelagonian zone, and, finally, the dark grey, muddy limestones seen in the Livadia Unit correspond very closely to the Buff Nodular Carbonates of the Kerassia Formation of the Almopias subzone.

Structure

Two distinct phases of compressional deformation are identified in the Livadia Unit. The first phase is only observed in the marble and chlorite-schist lithologies and is characterised by ductile, isoclinal folds whose axial directions trend towards 038°N to 050°N (Figure 6.37), and a remnant schistosity defined in the chlorite-schists by chlorite and mica (Figure 6.38). An axis-parallel lineation is associated with these folds and similarly trends towards the NE-SW (Figure 6.39). These structures are identical in

style to Upper Jurassic structures documented from both the Pelagonian zone (JE1 of Vergely, 1984; F1 of Sharp, 1995) and the Païkon Massif (D1 of this work, chapter 4.2), although their orientation is rather different to both of these areas. The intense Tertiary thrusting and folding of the later compressional event may account for this discrepancy. The fact that these structures only affect the marble and chlorite-schist units (thought to be equivalent to the Triassic Pelagonian Marble Group and the Kato Grammatiko Formation, respectively) supports an Upper Jurassic age for this event, as none of the younger, Cretaceous lithologies have been affected by it.

The second phase of compression to affect the Livadia Unit was observed in all lithological units, from Triassic to Uppermost Cretaceous, suggesting a Tertiary or later age for this deformation event. The structures associated with this event are very different in style to those of the Upper Jurassic phase outlined above. Folds are brittle chevron and box folds (characteristically non-cylindrical) and are associated with intense brittle reverse faulting. Fold hinges trend variably towards 130°N to 162°N and an axis-parallel intersection lineation trends similarly towards the NW-SE (Figure 6.40). The structural style of this deformation event closely resembles the early Tertiary compressional events documented from the Pelagonian, Almopias and Païkon subzones; however, the polarity of the structures (i.e. fold and lineation orientations and vergences) correspond most closely to early Tertiary deformation within the Païkon Massif (i.e. D2, see chapter 4). An axial planar foliation is also associated with Tertiary deformation and this fabric crenulates and folds the Upper Jurassic foliation, as shown in Figure 6.38.

The intense thrust-imbrication which pervades the Livadia Unit is contemporaneous with early Tertiary chevron folding, and duplex structures generated along fault zones indicate west to southwest propagation (Figure 6.41).

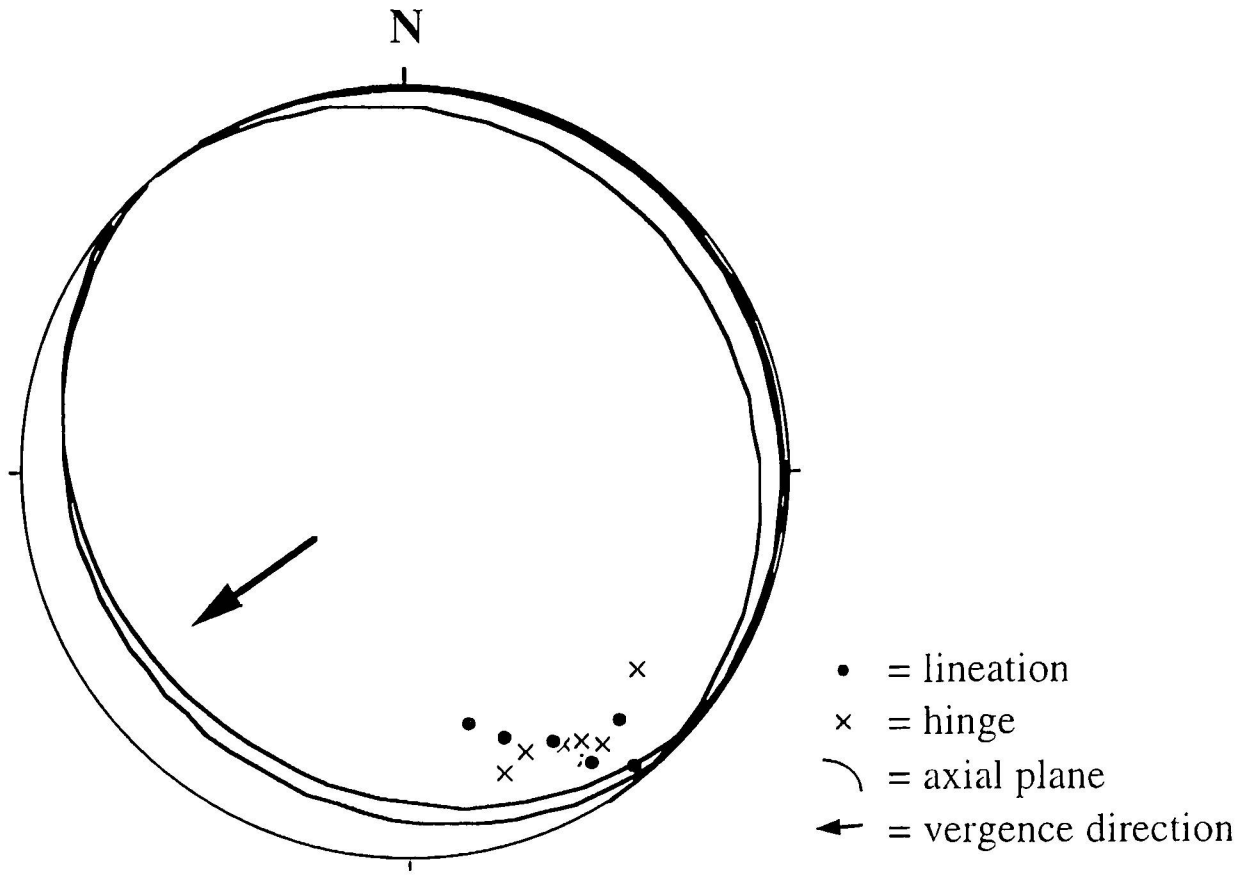


Figure 6.40 - Stereographic projection of Tertiary brittle structures (lineations, fold axes and axial planes) recorded from all lithological units within the Livadia Unit. The structures trend towards the NW-SE, which correspond closely to Tertiary (D2) structures in the Païkon Massif (see chapter 4.6).

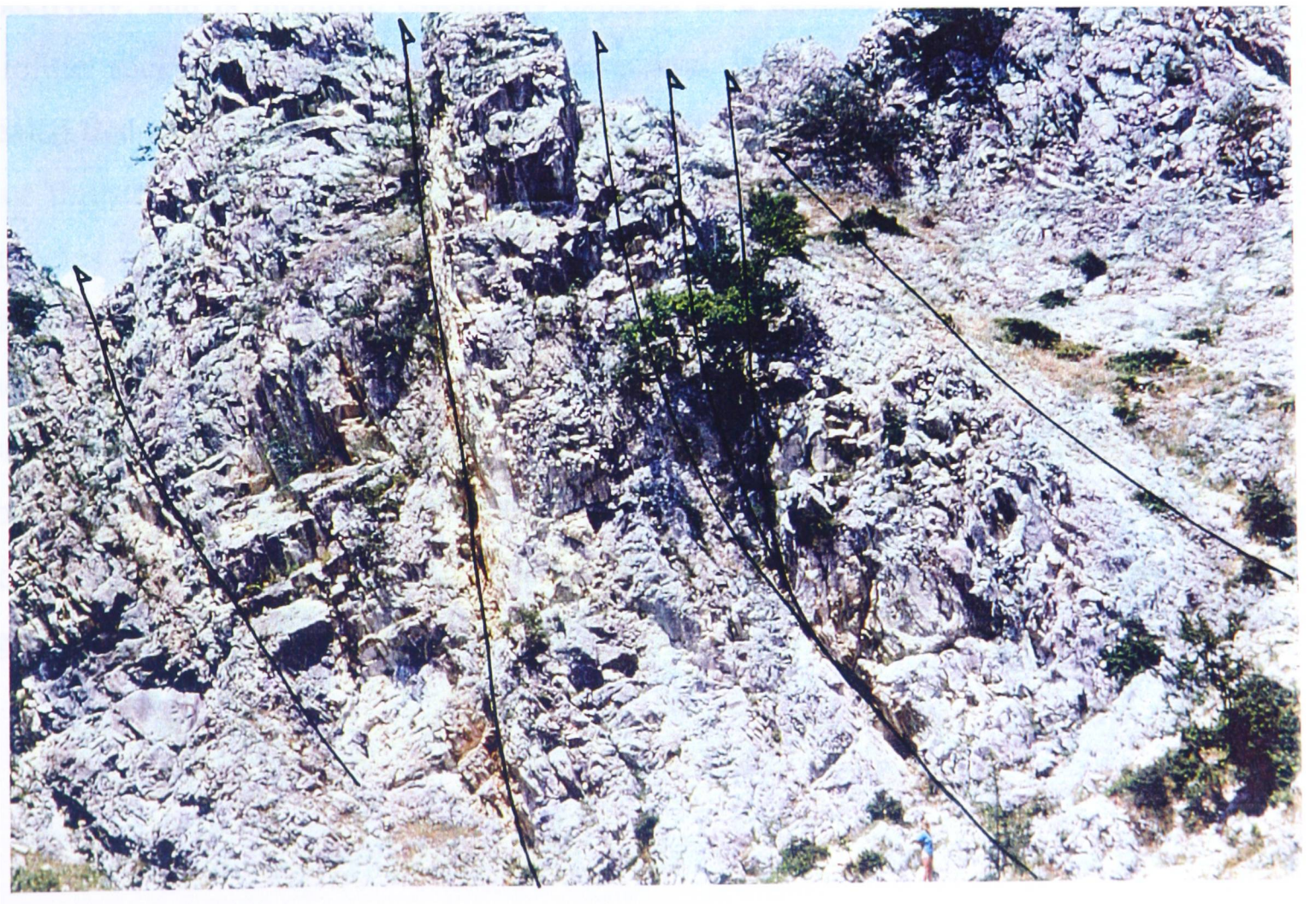


Figure 6.41 - Field photograph of Tertiary thrust faults within imbricates of marble from the Livadia Unit. Slickenside and duplex structures along the thrust surfaces indicate transport towards the west and southwest.

Summary

The lithologies of the Livadia Unit all bear a striking resemblance in both facies and age to units exposed within the Pelagonian zone to the southwest. Marbles and chloritic schists within the Livadia Unit have been affected by a phase of ductile compression of Upper Jurassic age, while all other units record only brittle Tertiary deformation.

6.3.4 - *Unit 4 - the Ano Garefi Unit*

In essence, the Ano Garefi Unit comprises an ophiolitic succession and unconformably overlying cover sediments. The Ano Garefi Unit is equivalent to the Ano Garefi Units of Mercier (1968) and Migiros & Galeos (1990) and the Fidopetra Ophiolitic Unit of Ricou & Godfriaux (1991). The best exposure of the unit can be found directly to the north of Ano Garefi village (Figures 6.6 & 6.42).

Migiros & Galeos (1990) suggested that the Ano Garefi Unit is tectonically overlain to both the west and east, by the Livadia Unit and the Pinovon Unit of this work respectively, and is therefore essentially exposed as a tectonic window of underlying ophiolitic rocks. However, a detailed structural investigation of the contact has revealed that this is not the case. The eastern limit of the Livadia Unit is marked by a major thrusted contact along which the Livadia Unit is tectonically overlain by the lithologies of the Ano Garefi Unit. The contact between these two units is highly sheared and dips steeply towards the east (Figure 6.43). Asymmetrical folds with NNE-trending axes, duplex structures and slickensides within the fault zone all indicate westward vergence (Figure 6.44). These structures are most prominent within deformed serpentinite of the ophiolitic component of this unit and within sheared sandstones and siltstones with which the ophiolite is in contact. Local east to northeast-verging back-thrusts were also



Figure 6.42 - Looking east onto the Ano Garefi Ophiolite (middle ground) and the Pinovon Massif (far ground) from the west. Most of the red/brown rocks of the Ano Garefi Ophiolite shown in this photograph are serpentinised dunites and harzbrgites.



Figure 6.43 - Field photograph of highly sheared Ano Garefi cover sediments where they contact with the Livadia Unit further west. The dominant fabric dips down towards the east (top right to bottom left). Duplex and shear structures indicate top-to-the west transport.

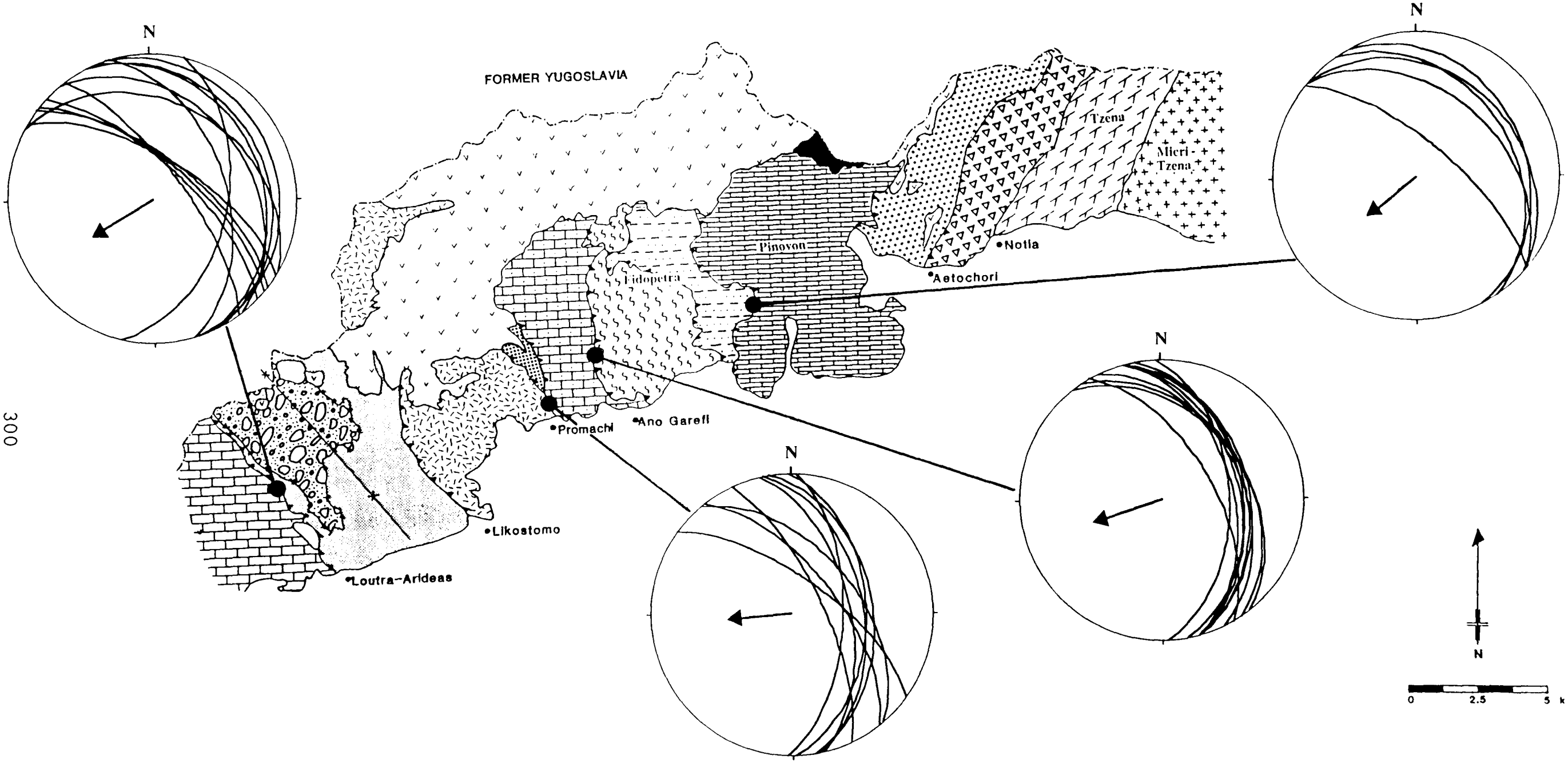


Figure 6.44 - Simplified geological map of the Voras Massif with stereographic projections showing the polarity of thrusting along some of the major contacts. Contact between, A = the Kaimaktchalan Massif and Loutra-Arideas Unit; B = Likostomo-Promachi Unit and Livadia Unit; C = the Livadia Unit and Ano Garefi Unit; D = the Ano Garefi Unit and Pinovon Unit. All conatcts verge roughly towards the W to SW.



Figure 6.45 - Field photograph of felsic dykes within the serpentinised ultramafic rocks of the Ano Garefi Ophiolite. Similar felsic dykes intrude the Meglenitsa Ophiolite which lies directly to the south (see section 6.3.4 - **Interpretation and Regional Correlations**).

Towards the western margin of the Ano Garefi Unit, the altered peridotites of the ophiolite are unconformably overlain by a conglomeratic unit, comprising predominantly well-rounded, ophiolite-derived clasts (serpentinite, dunite, tectonised harzburgite). These conglomerates are very similar to the ophiolite-derived conglomerates described from the Loutra-Arideas Unit (section 6.3.1), in that they are well-rounded, mostly ophiolite-derived and unconformably overlie ophiolitic lithologies (Figures 6.46 & 6.47). Also, limestone clasts within the ophiolite conglomerates are similarly rich in ophiolite detritus, as described from the Loutra-Arideas Unit. However, limestone clasts containing *Orbitolina. sp* within this conglomerate indicate a probable Aptian/Albian age for the cover sediments (Sartorio & Venturini, 1988), in contrast to the Upper Jurassic age postulated for the conglomerates of the Loutra-Arideas Unit.

In a limited area, limestones containing deformed rudist fragments (possibly *Monopleuridae*) overlie the ophiolite, and possibly the ophiolite conglomerate, with questionable contact (Figure 6.48). Rudists indicate that the limestones were deposited in a shallow-water environment during the Upper Cretaceous (Moore, 1969). In most areas, however, the ophiolite is in east-dipping thrust contact over an extensive unit of thin-bedded sandstones, siltstones, mudstones and detrital carbonates, with locally-occurring, thick interbeds of coarse conglomerate. To the west these sediments pass conformably down into limestones containing *Nerineid* gastropods and deformed rudists, which indicate a Cretaceous age. The sediments and limestones are strongly interfolded and are ultimately thrust on top of the Livadia Unit (to the west) with an east-dipping contact (as discussed above).

To the north, towards the former Yugoslavian border, the serpentinised ophiolite overlies a deformed conglomeratic unit with an east-dipping, thrust contact. The conglomerate comprises clasts of almost wholly ophiolite derivation, although clasts of



Figure 6.46 - Well-rounded, ophiolite-derived conglomerates which overlie the Ano Garefi Ophiolite. Clasts are dominantly of serpentinite and altered basalt, although clasts of shallow-water limestones occur locally.

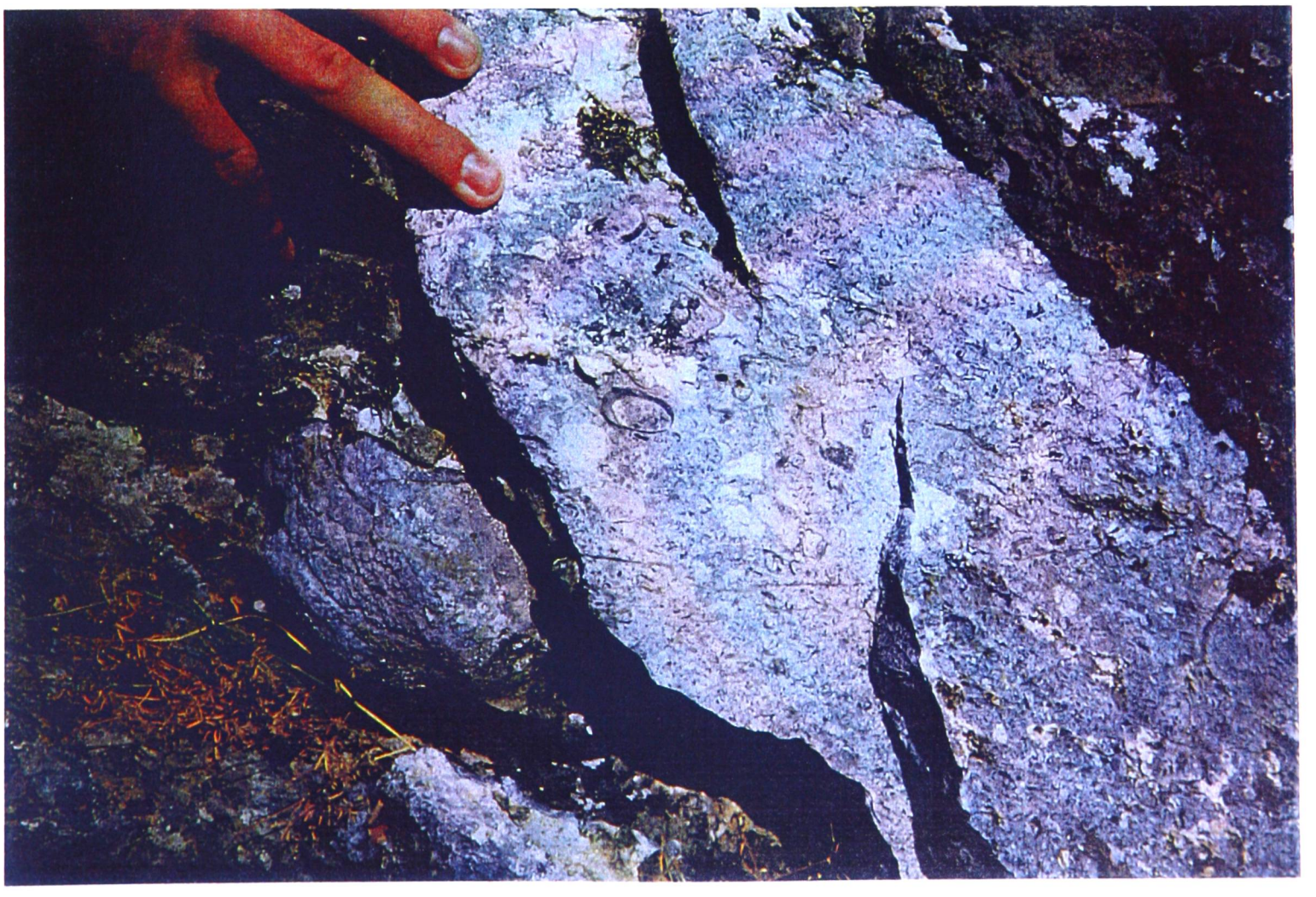


Figure 6.47 - Close-up photograph of a limestone clast within the ophiolite-derived conglomerate of the Ano Garefi Unit. The limestone contains bivalves, gastropods and *Orbitolina sp.* (Aptian/Albian). Some limestone clasts also contain ophiolitic detritus.



Figure 6.48 - Field photograph of the bauxitic, possibly unconformable contact between the Ano Garefi Ophiolite and overlying shallow-water (rudist-bearing) limestones of Cretaceous age.

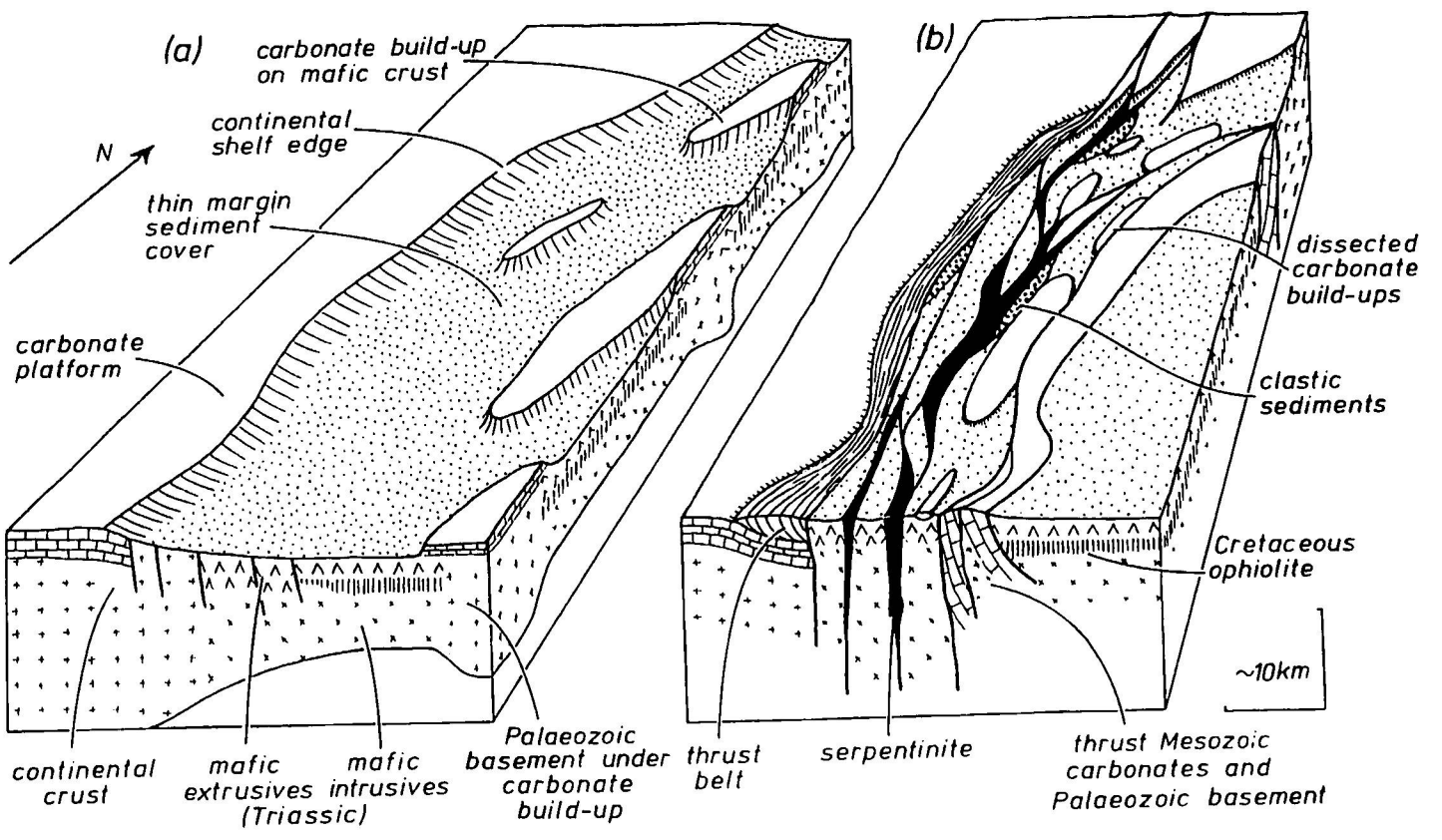


Figure 6.49 - Schematic block daigram showing the formation of ophi-calcite deposits during transtension along the Anatalya margin in the Jurassic-Cretaceous (a) and the latest Cretaceous-Miocene (b). After Woodcock & Robertson (1982).

Nerineid gastropod-bearing limestones occur, and this conglomerate is comparable in facies and stratigraphic position to the basal schist/conglomerate unit of the Loutra-Arideas Unit (section 6.3.1). Clasts in the deformed conglomerate are again elongate, but this time in a roughly east-west orientation. Unlike the schists/conglomerates of the Loutra-Arideas Unit, however, the deformed conglomerates of the Ano Garefi Unit have been subjected to only one phase of compressional deformation and not two (see **Structures** section below).

In contrast to the cover succession just described, further north around Fidopetra (Figure 6.6), the ultrabasic rocks of the Ano Garefi ophiolite are overlain by metre-scale, calcite-filled fissures, which are in turn overlain by thin-bedded, deeper-water clays and calc-turbidites which pass conformably upwards into thin-bedded, micritic limestones. In this area the peridotites are intercalated with significant amounts of clastic sediments.

Interpretation and Regional Correlations

The serpentinites, dunites, harzburgites, gabbros and lavas of the Ano Garefi Unit are all interpreted as the obducted remains of oceanic crust and mantle, representing an ophiolite. The MORB to WPB geochemical signature of the ophiolitic lavas (Migiros & Galeos, 1990) suggest that this ophiolite may have formed in a back-arc basin (Wood *et al.*, 1980) or during the formation of a small ocean basin along a continental margin (Pearce, 1980; Migiros & Galeos, 1990). The tectonic environment of formation of the Ano Garefi Ophiolite will be discussed further in chapter 7.

As stated above, the sedimentary units which both underlie and overlie the ophiolite bear a close resemblance to those described from the Loutra-Arideas Unit to the west. With this in mind, it is very likely that the deformed conglomerates which tectonically underlie the ophiolite in the west may have formed in advance of the ophiolite as it was obducted. This is supported by the fact that the deformed conglomerates are derived

almost wholly from the ophiolite and its cover limestones (*Nerineid* gastropod-bearing). The unconformably overlying, undeformed ophiolite-derived conglomerates are also similar to those reported from the Loutra-Arideas Unit (section 6.3.1) and are, therefore, also likely to have been generated during post-obduction erosion of the ophiolite. However, both the syn- obduction and post-obduction ophiolite-derived conglomerates vary greatly in age with respect to those of the Loutra-Arideas Unit. An Aptian-Albian age (*Orbitolina sp.*) is estimated for the ophiolite conglomerates which overlie the Ano Garefi Ophiolite, as opposed to an Upper Jurassic age for those in the Loutra-Arideas area. Furthermore, in the Ano Garefi area, the syn-obduction, deformed conglomerates are likely to be post-Upper Cretaceous in age (i.e. they contain Cretaceous *Nerineid* gastropod and deformed rudist clasts), while those of the Loutra-Arideas area are pre-Upper Jurassic. These age discrepancies suggest that the Ano Garefi ophiolite formed subsequent to Upper Jurassic regional compressional deformation and was emplaced in post-Upper Cretaceous times. This conclusion is supported by structural data (see **Structures** below).

The westerly limestones and overlying sediments may originally have formed part of the Upper Cretaceous ophiolite cover succession, but a conformable relationship is no longer preserved, and the ophiolite vestiges are now thrust over the sediments and limestones with westward polarity. In the north, the calcite-filled fissures in the peridotite may be ophi-calcite or ophi-carbonate deposits which formed due to the tectonic fragmentation of oceanic basement rocks and the subsequent infilling of voids with carbonate (Bernouilli & Weissert, 1985; Bogoch, 1987). There are four main tectonic settings in which ophi-calcite associations can form; along oceanic spreading ridges (Aumento & Loubat, 1971); along transform faults (Bonatti *et al.*, 1974); along compressional intra-oceanic ridges (La Gabrielle & Auzende, 1982) and along transtensional margins (Woodcock & Robertson, 1982). Given that the Vardar zone has a history of transtensional tectonics in the Upper Jurassic-Lower Cretaceous (chapters 1, 4 & 7) it is suggested here that the ophi-calcite association in the Ano Garefi Unit is the

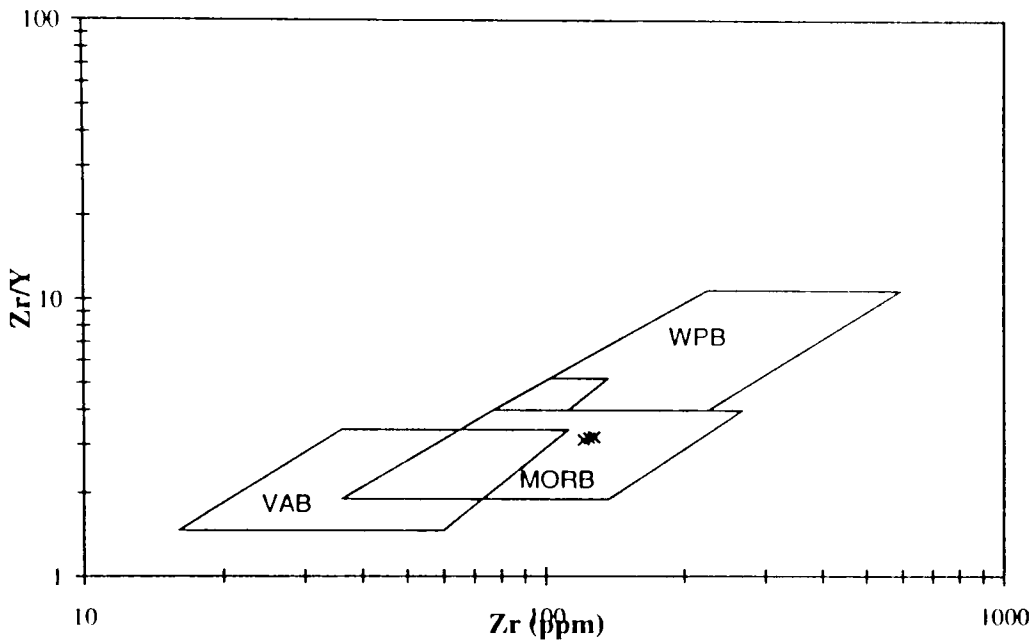
result of transtensional pull-apart, as described, for example, from the Terikova Ophiolite in Anatalya, Turkey (Woodcock & Robertson, 1982; Figure 6.49). The abundance of sedimentary material within the ophi-calcitic peridotites supports this small pull-apart basin model. As stated above, the ophi-calcite association is overlain by deep-water distal turbidites and thin-bedded carbonates (pelagic) and it is possible that this sequence records unconformable deposition taking place in deep parts of the basin while the ophiolite conglomerate and neritic carbonates were being deposited simultaneously at the basin margins.

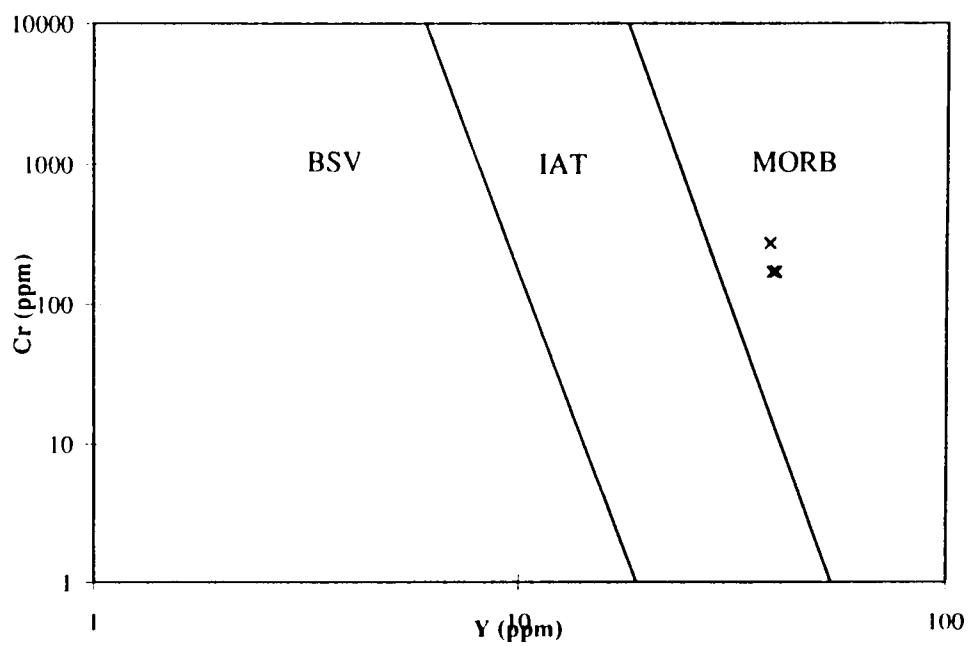
The Ano Garefi Ophiolite could be equivalent to either the Upper Jurassic dismembered ophiolite, which has already been ruled out, the uppermost Jurassic-Lower Cretaceous Meglenitsa Ophiolite or the more easterly Guevgueli Ophiolite. In order to be of Guevgueli Ophilolite affinity, the Ano Garefi Ophiolite is required to have been transported westward as a nappe over the entire Païkon Massif during the Tertiary, as suggested by Ricou & Godfriaux (1991). However, no evidence exists in the Païkon Massif to support this Tertiary nappe model, as the Païkon Massif underwent only high-level, brittle compressional deformation at this time (chapter 4). Additionally, there are no ophiolitic rocks or "metamorphic sole" rocks of Tertiary age within the Païkon Massif, as would be expected had an ophiolitic nappe been overthrust (Woodcock & Robertson, 1977). It is most likely, therefore that the Ano Garefi Ophiolite is comparable to the Meglenitsa Ophiolite of the eastern Almopias subzone. Both the Meglenitsa and Ano Garefi Ophiolites are unconformably overlain by rocks of Aptian/Albian age and both are likely to have formed in transtensional pull-apart basins in the Upper Jurassic to Lower Cretaceous. Additionally, both the Meglenitsa and Ano Garefi Ophiolites have been intruded by fine-grained felsic dykes, a feature Sharp (1995) suggested was common to several Neotethyan ophiolites formed subsequent to Eohellenic contractional deformation.

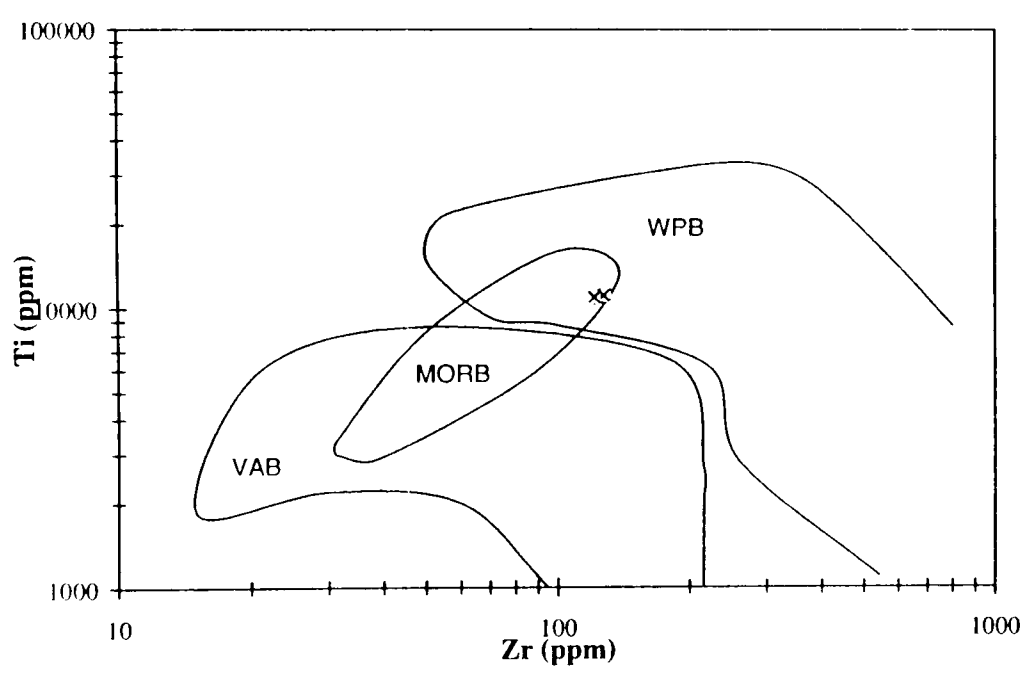
structures, occasional asymmetric folds and the moderate eastward dip of most thrust packages indicate westward thrust propagation (Figure 6.44). Structurally above and to the west of the imbricate stack, the spectacular cliffs of the Pinovon Massif provide excellent exposure of a thick, structurally-repeated grey limestone succession, which passes up into pink, micritic carbonates and ultimately interbedded sandstones, siltstones and detrital carbonates.

Lava flows within the imbricate stack were analysed using the X-Ray Fluorescence technique outline in the Appendix, and the immobile trace elements were then used to determine their tectonic environment of eruption. The geochemical signatures of the imbricate lavas correspond very closely to the lavas analysed from the top of the Ano Garefi Ophiolite to the east (Migiros & Galeos, 1990; Figure 6.51), thus it is possible that these lavas were derived from the ophiolitic unit and incorporated into the thrust-stack during Tertiary deformation (see **Structures** section below). In fact, all lithologies present in the thrust-stack may have been derived from the top of the ophiolite and its cover sequence (i.e. red cherts, limestones, bedded clastics and lavas). Overlying the imbricate zone is an area of intense shearing and mylonitisation (Figure 6.52), presumably formed due to Tertiary overthrusting of the Pinovon limestones onto the Ano Garefi Ophiolite and its cover sediments.

The grey limestones of the Pinovon Massif are characterised by thick (up to 1.5 m) beds of sparse-biomicrite, bioclastic-packstone and lesser calcarenite, with thin interbeds of detrital pink calcilutite. The faunal assemblage of this limestone unit is dominated by benthic foraminifera (e.g. *Miliolidae, Cuneolinae* and *Textulariidae*), bivlaves, *Nerineid* gastropods and rudist bivalves (*Monopleurida sp.*; this work, and *Hippurites sp*; Mercier, 1968), which indicate an Upper Cretaceous age and a shallow-water setting. Locally, thin pink calcilutite horizons were observed within the neritic limestone







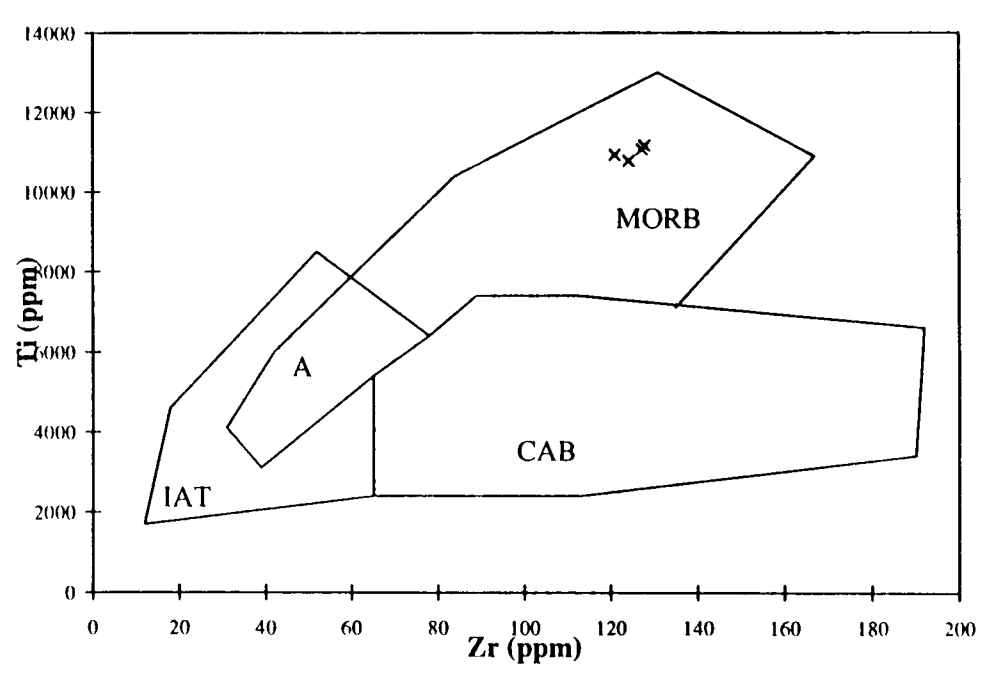


Figure 6.51 - Templates showing the geochemical characteristics of the volcanic rocks between the Ano Garefi Unit and the Pinovon Unit. 4 samples were analysed. See chapter 5 for template details.



Figure 6.52 - Field photograph of mylonitic rocks along the east-dipping contact between the Ano Garefi Unit and the Pinovon Unit. The mylonites were probably produced when the thick Pinovon limestones overthrust the Ano Garefi Ophiolite during Tertiary compression.

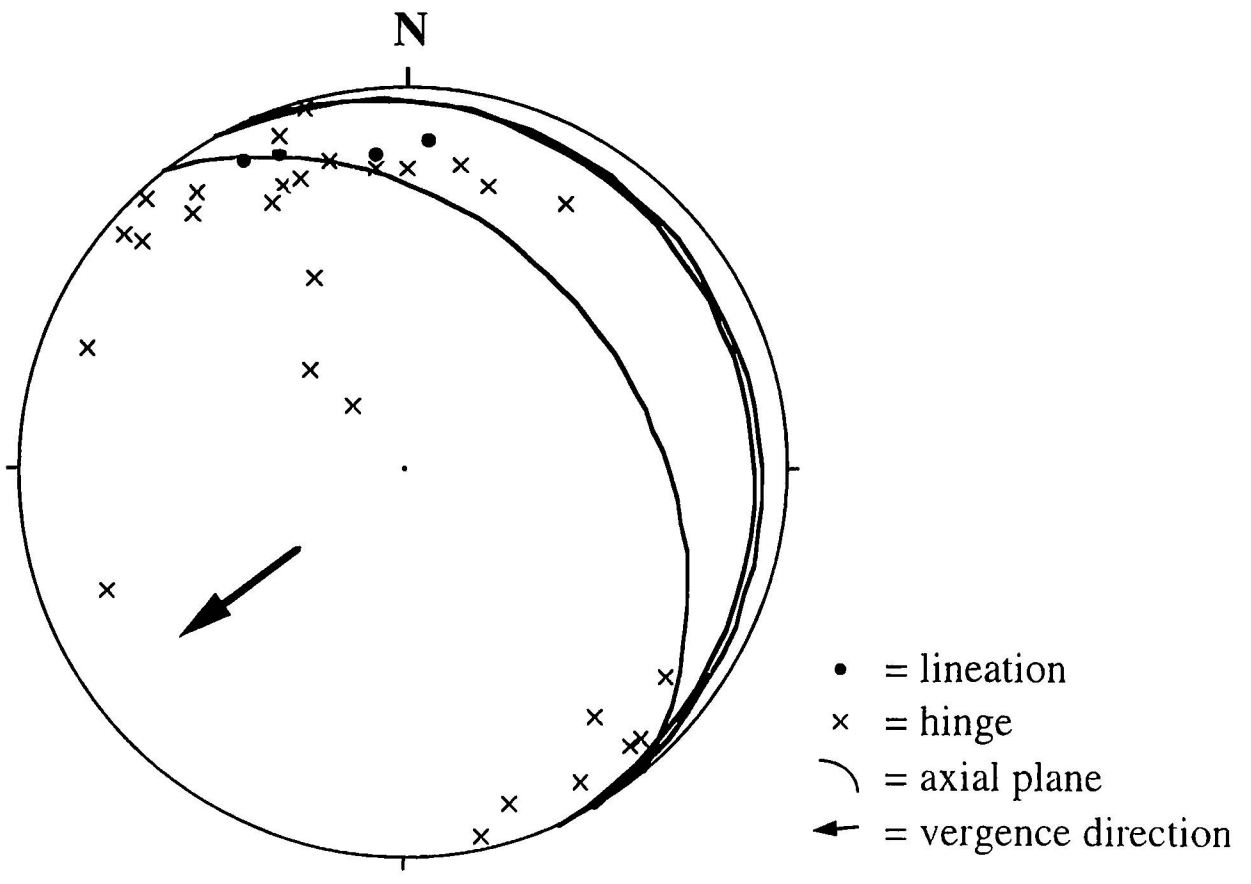


Figure 6.53 - Stereographic projection of lineations and fold structures recorded from the Pinovon Unit. The structures affect lithologies of Upper Cretaceous age and were thus most probably produced during the Tertiary or latest Cretaceous.

succession. These horizons are highly bioturbated and often culminate in a thin ferruginous cap. Due to intense chevron folding and thrust-imbrication, a complete transect through this unit from base to top was not possible.

Towards the summit of Pinovon, particularly on its northwestern side, limited outcrops of thin-bedded, pink pelagic limestone and a conformably overlying mixed carbonate-clastic sequence are exposed. The pelagic limestones contain the recrystallised remains of *Globotruncana linnei, G. arca, G. gr. stuarti-stuartiformis, G. gr. arca-convexa, g. convexa* and *G. calciformis*, which indicate a Campanian-Maastrichtian age (Mercier, 1968). The overlying mixed carbonate-clastic succession is thin-bedded and often normally-graded into fining-upwards units of 2-10 cm thickness. Carbonate interbeds (up to 2 cm thick) are detrital and parallel laminated.

Rarely, upfolded and/or upthrusted slices of a siliceous, volcaniclasitc unit crop out; these are highly indurated and altered to chlorite, sericite, epidote and secondary albite. Most primary textures have been destroyed, although rare igneous (i.e. porphyritic) textures remain in some of the clasts.

Interpretation and Regional Correlations

An open platform setting is envisaged for the grey neritic limestones which constitute the bulk of the Pinovon Massif, based on the fauna and facies observed. The platform was sporadically subjected to periods of non-deposition and increased clastic input, indicated by pink, bioturbated calcilutite horizons. At its stratigraphic top, the Upper Cretaceous shallow-water platform gave way to deeper-water pelagic sedimentation (*Globotrunana*-bearing carbonates), which in turn was followed by mixed carbonate-clastic deposition, probably by way of proximal turbidity currents as indicated by Bouma-type graded and parallel-laminated interbeds (Einsele, 1992).

The rapid transition from neritic to pelagic deposition is likely to indicate that the area underwent extensional subsidence in the Upper Cretaceous. Similar neritic to pelagic successions from elsewhere in the Internal Hellenides support this hypothesis. In the Argolis Peninsula, for example, Upper Cenomanian platform carbonates pass into pelagic carbonates and flysch deposits over a relatively short interval (Philip *et al.*, 1989; Clift, 1990), and this succession has been attributed to a major lithospheric extensional event which took place in the Hellenides during the Turonian (Fleury, 1980; Thiebault, 1982; Hall, 1988; Clift, 1990; Sharp, 1995; this work, chapter 4.5).

All of the lithologies described from the Pinovon Unit can be correlated with the Uppermost Jurassic to Upper Cretaceous of the Païkon Massif which lies directly to the south. The grey neritic limestones of the Pinovon Unit resemble the Cretaceous Transgressive Limestones (chapter 3.9) of the Païkon Massif in facies, fauna and age, and have undergone similar structural repetition (see **Structures** section below). In the Pinovon Unit, the neritic limestone pass conformably up into pink, *Globotruncana*-bearing carbonates and ultimately thin-bedded turbidites and this is mirrored exactly in the Païkon Massif. In the Païkon Massif, the Cretaceous Transgressive Limestones pass upwards into Buff Pelagic Carbonates (*Globotruncana*-bearing; chapter 3.10) which in turn grade up into the turbiditic deposits of the uppermost Cretaceous Tchouka Flysch (chapter 3.11).

Structures

The Upper Cretaceous carbonates and clastic sediments of the Pinovon Unit have been affected by one phase of brittle deformation, which is attributed to the early Tertiary phase of deformation which affects the whole of the internal Hellenides (phase D2 of this study; see chapter 4.6). The deformation is characterised by meso- and macro scale chevron and box folding, as observed on the south-facing cliffs of the Pinovon Massif, and extreme thrust-repetition. As a consequence the apparent thickness of the limestone succession has been significantly increased making its absolute thickness difficult to

assess. Thrust and fold vergence is consistently directed towards the west (Figures 6.44 & 6.53).

6.3.6 - *Unit 6 - the Porta-Tzena Unit*

The most easterly unit of the Voras Massif extends, from base to top, from the former Yugoslavian border in the east to north of Aetochori village in the west (Figures 6.6 & 6.7). The unit is floored by the Kalivia Socrati gneisses, which pass upwards with depositional contact into the meta-sedimentary sequence of Mount Tzena. The contact is folded by large, kilometre-scale asymmetrical folds, which consistently verge towards the east (Figure 3.3). The Tzena meta-sediments then pass conformably up into a thick succession of volcanics and volcaniclastics (the Porta andesites) which form the western limit of the Porta-Tzena Unit. The Porta-Tzena Unit is equivalent to the Tzena and Aetochori Units of Migiros & Galeos (1990) and to the eastern part of the Pinovon-Tzena Klippe of Ricou & Godfriaux (1991).

The basal Kalivia Socrati gneisses are well exposed along a road which winds NE from just outside Notia village (Figure 6.6). They comprise coarse garnetiferous gneisses, mica-schists, marbles and meta-basites which are interbedded on a 5-10 m scale. A detailed metamorphic and petrological study of these basement units was outside the scope of this thesis, and the following is a brief description of the broad structural and petrological features of the unit. The gneisses and schists have been subjected to poly-phase deformation and display a high grade, folded gneissic/schistose fabric delineated by amphibole laths and garnet porphyroblasts (Figure 6.54). The high-grade fabric has been subsequently folded during two phases of deformation and much of the original amphibolite grade mineralogy has been retrogressed to epidote, albite and chlorite, which overprint the high-grade fabric and form secondary fabrics parallel to the axial planes of later folds. The marbles are highly recrystallised, with sutured, stylolitic

calcite crystals and white mica laths oriented parallel to their dominant gneissosity. Meta-basic rocks are common and their mineralogy is dominated by biotite, amphibole and garnet with secondary epidote, chlorite and large albite porphyroblasts.

The contact between the Kalivia Soctrati mica-schists/gneisses and the Tzena meta-sediments is exposed at the top of Micri Tzena (see Figure 3.2). Mercier (1968) noted the concordance between these two units (Figure 6.55) and close examination of the contact during the course of this work confirmed this hypothesis. The top of the Kalivia Socrati basement succession is marked by mica-schists and lesser micaceous marbles. On the south-facing cliffs of Micri Tzena these schists and marbles are overlain by relatively thick-bedded marbles of the Tzena meta-sediments and the fabrics of the two units are concordant. The contact has been folded by flat-lying isoclines (the dominant fabric in this area is axial-planar to these folds) and refolded by more open, asymmetrical folds which verge towards the east (Figure 6.58). The high-grade fabric, which characterises the gneiss and mica-schists further down hill, has been overprinted by the retrogressive fabric which dominates along the contact. No evidence of this high-grade fabric was seen anywhere in the Tzena meta-sediments.

The Tzena meta-sediments comprise a highly deformed succession of interbedded marbles, chloritic schists, calcarenites and calcilutites (Figure 6.56). The sediments have been completely recrystallised; thus any fauna and/or sedimentary structures that may have been present originally, have been completely destroyed. The marbles are white to grey and have a sugary texture. They are variably micaceous and their mica content increases markedly towards more schistose interbeds, which are chlorite- mica- and epidote-rich.

Structures associated with the deformation of these sediments indicate that two distinct phases of compressional deformation have taken place. The first produced tight,

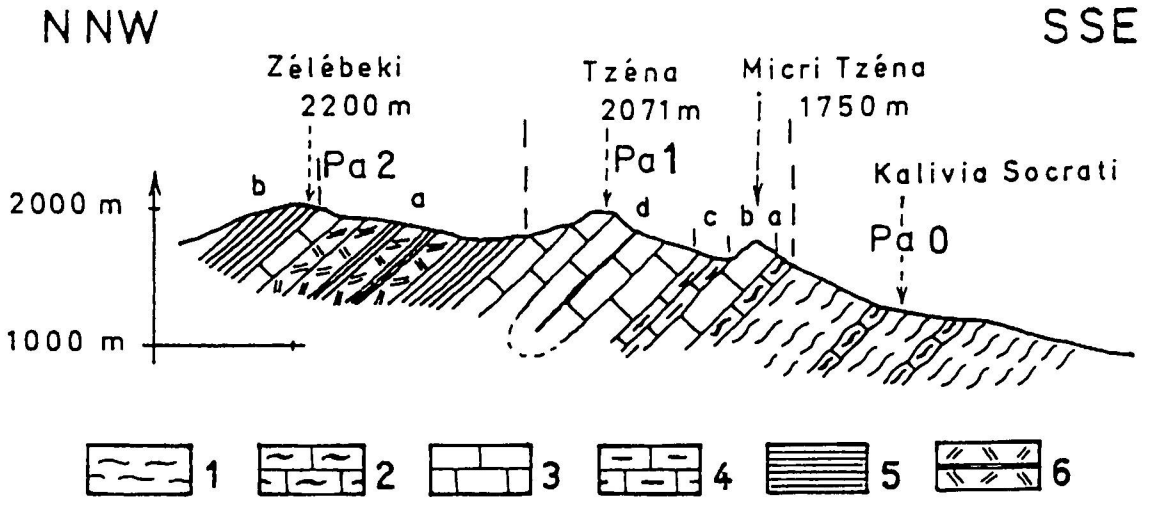


Figure 6.55 - Schematic cross-section of the depositional contact between the Kalivia Socrati Gneisses and the Tzena Meta-sediments in the easternmost Voras Massif (after Mercier, 1968). 1 = Mica-schists; 2 = Calc-schists; 3 = Marbles; 4 = Chloritic, micaceous calc-schists; 5 = Chloritic schists; 6 = Porta Andesites.

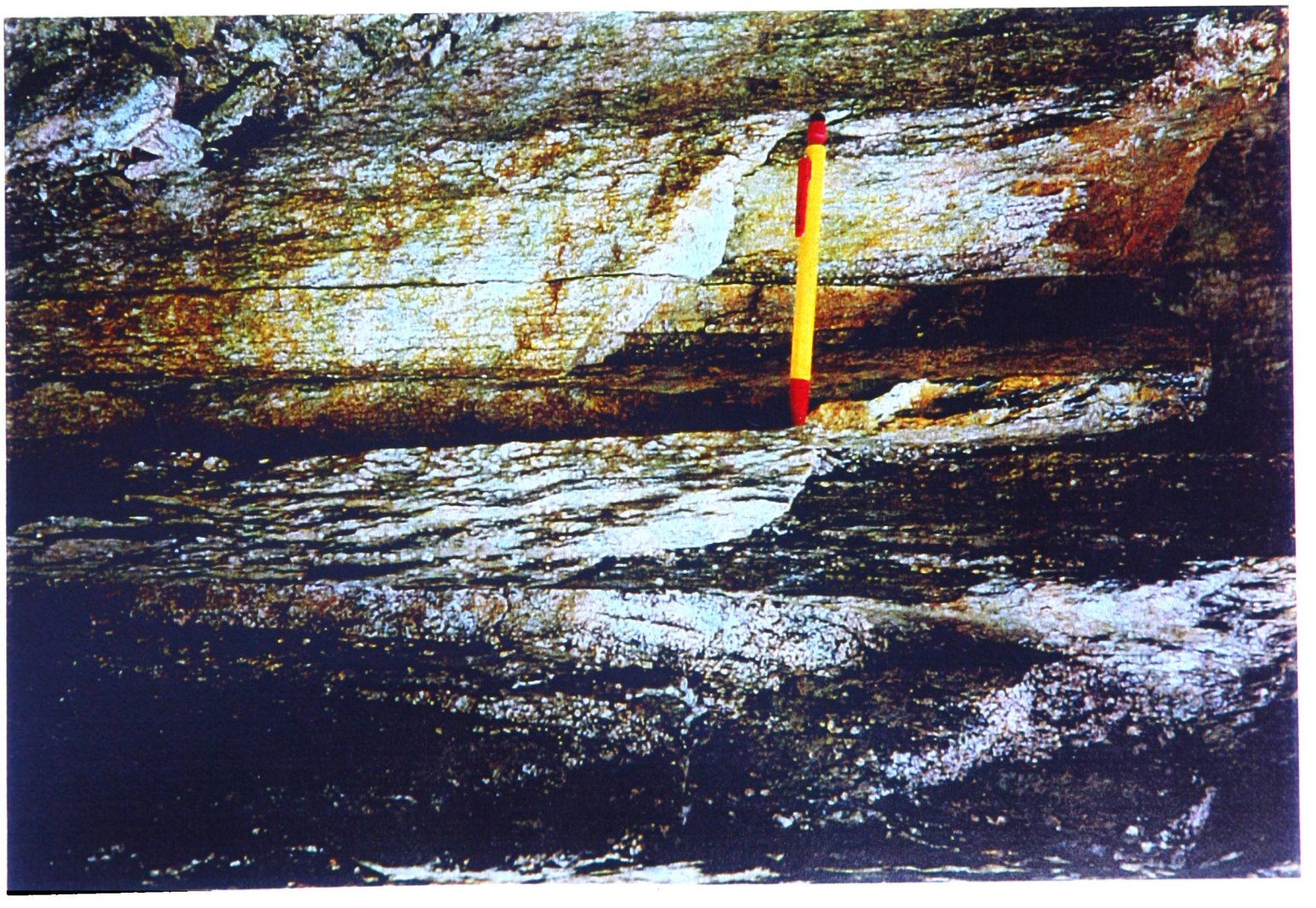


Figure 6.56 - Field photograph of the Tzena Meta-sediments of the Porta-Tzena Unit. Bedded marbles, micaceous calc-schists and chloritic schists predominate.

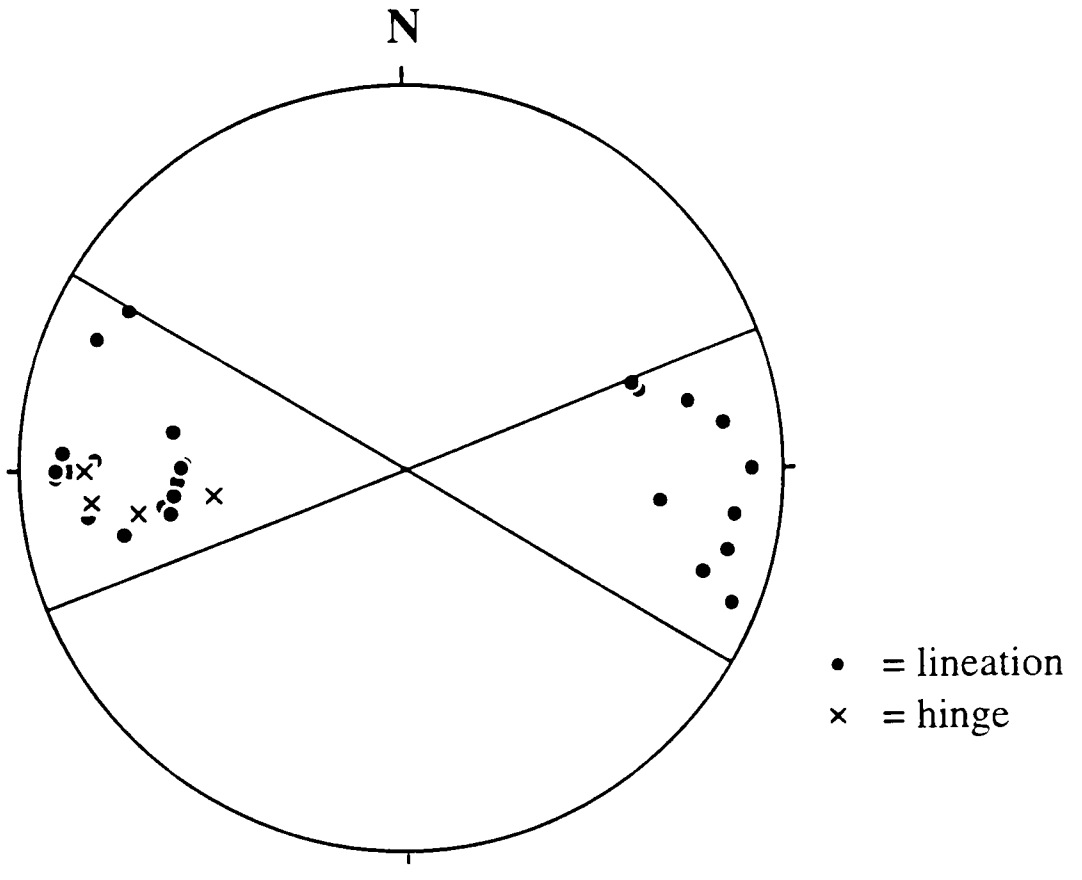


Figure 6.57 - Stereographic projection of the primary structures (Upper Jurassic) recorded within the Tzena Meta-sediments. The lineations and fold hinges are invariably oriented roughly east-west. Vergence is questionable due to subsequent deformation.

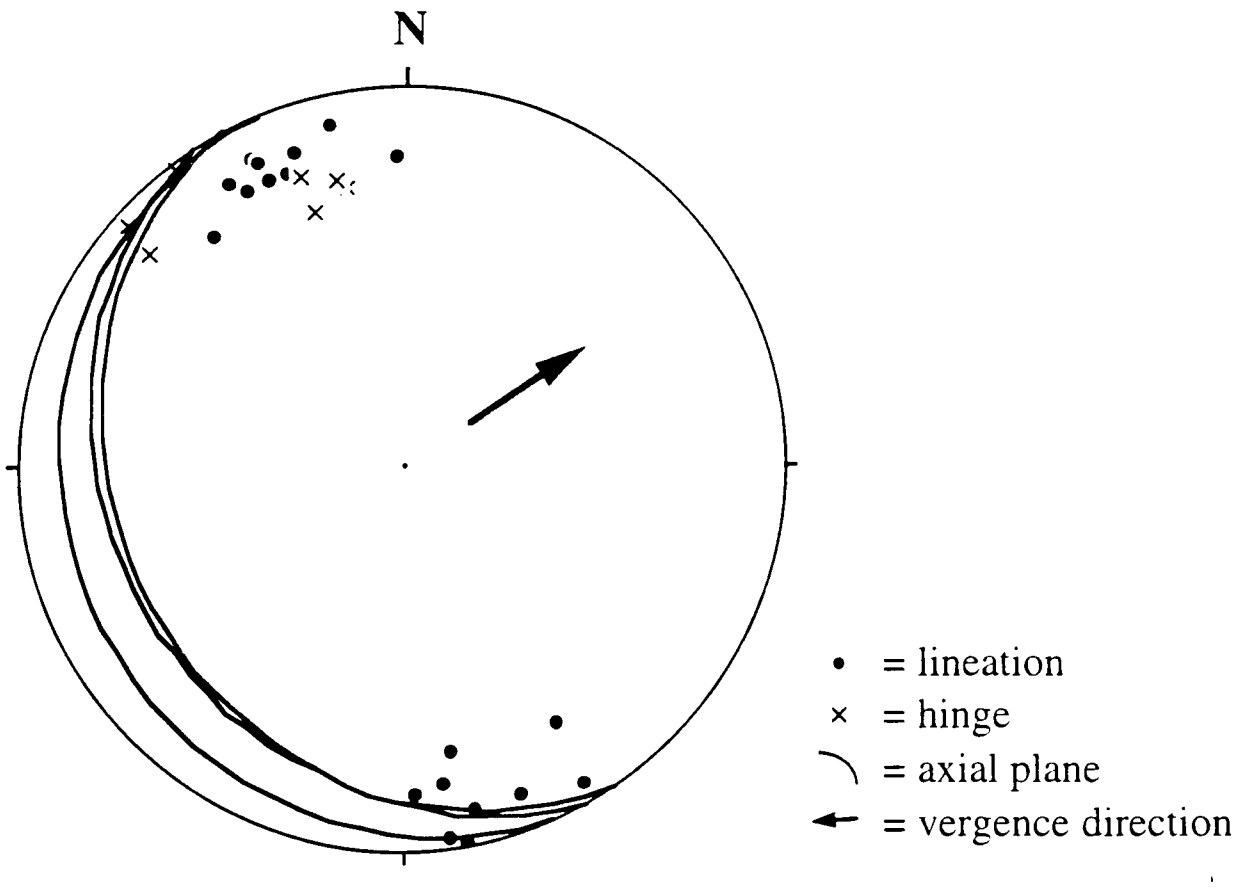


Figure 6.58 - Stereographic projection of the seconday structures (Tertiary) observed within the meta-sediments of the Porta-Tzena Unit. These brittle structures (folds and lineations) trend between NW-NNE and SE-SSW which is very similar to Tertiary folds from the Païkon Massif to the south (see chapter 4). The folds verge eastwards.

isoclinal folds which have an associated E-W-trending lineation (Figure 6.57), and the second, later event developed brittle, chevron folds with non-cylindrical fold axes trending between 330°N and 010°N (Figure 6.58).

To the west, the contact between the Porta andesites and the Tzena meta-sediments is exposed along a track which heads north out of Notia. The contact is gradational and marked by a transitional black schist. The overlying Porta andesites comprise a thick, folded pile of highly sheared intermediate-composition volcanics and volcaniclastics (Figure 6.59). Sheared volcanic flows (andesites) form by far the majority of the unit and although much of this formation has been highly deformed, small sigmoidal lenses of relatively undeformed andesite occur (Figure 6.60). The majority of lava horizons have been altered to chlorite and epidote, and the prevailing fabric comprises platy chlorite laths in rough parallelism, wrapped around large euhedral porphyroblasts of epidote (Figure 6.61). Volcaniclastic interbeds are relatively minor and vary between very fine-grained tuffaceous schists, now largely altered to chlorite, epidote and mica, and breccio-conglomeratic rudites (Figure 6.62), comprising sub-angular to sub-rounded, flattened clasts of altered chlorite schist and porphyritic lavas and acidic tuffs.

The whole of the Porta andesite succession has been shot through with thin (up to 1.5 cm) veins of epidote. The veins have been intensely deformed by both isoclinal and kink folding and are often strongly attenuated parallel to the dominant schistosity (Figure 6.63). Due to the intensity of their deformation it is probable that they were injected prior to the compressional deformation events that have affected the Porta-Tzena Unit (see **Structures** section below). Much of the volcanic succession has been impregnated with disseminated sulphide (pyrite), although areas of intense alteration are restricted to certain zones.

The sigmoidal lenses of less deformed volcanic material were sampled and analysed

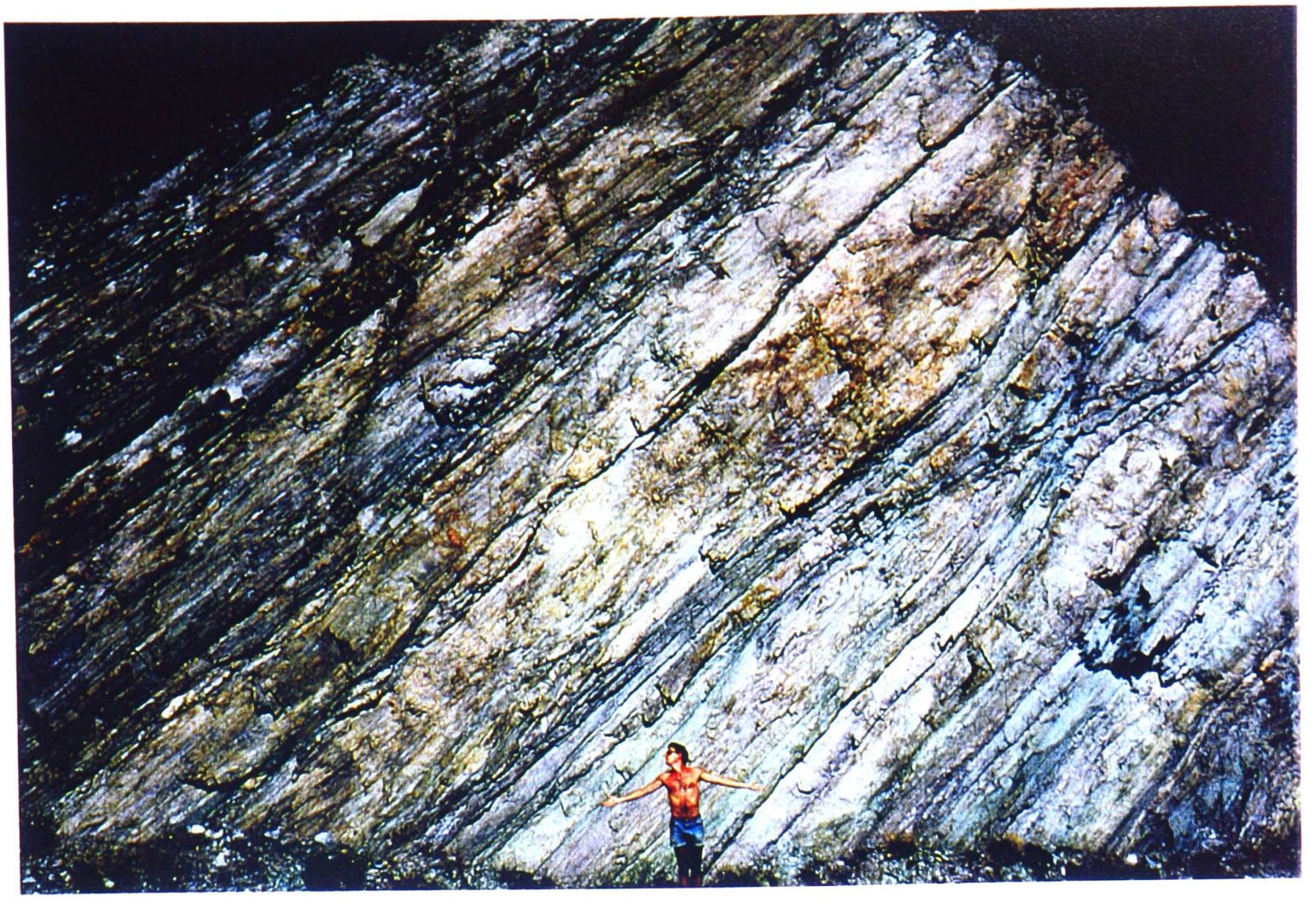


Figure 6.59 - Typical outcrop of the Porta Andesites from the Porta-Tzena Unit. Highly sheared andesitic lavas are dominant and interbedded with deformed volcaniclastic horizons. The Porta Andesites are rich in secondary chlorite and epidote.

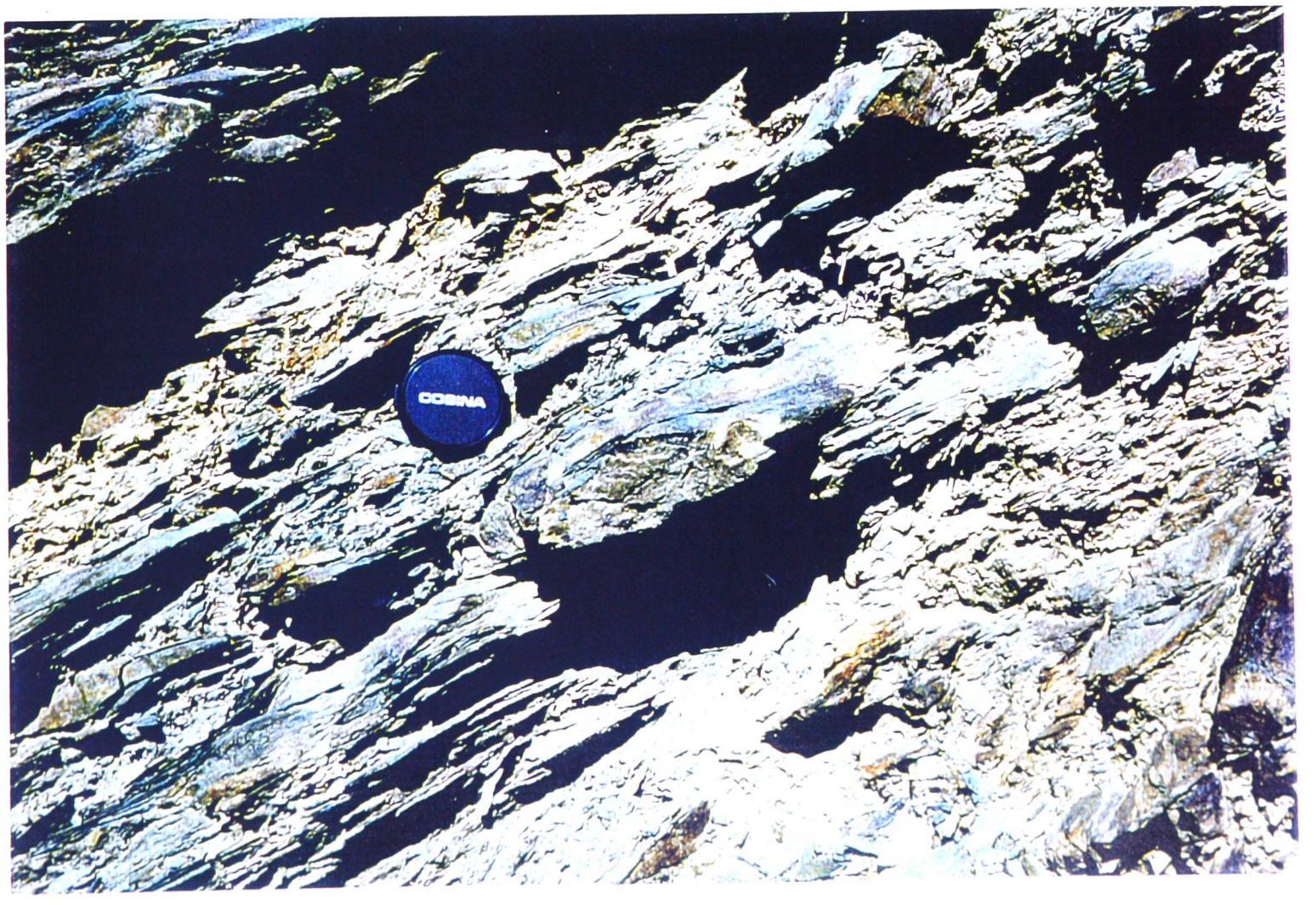


Figure 6.60 - Sigmoidal lenses of relatively undeformed andesite surrounded by highly sheared rock. Remnant igneous textures can still be seen in these lenses.

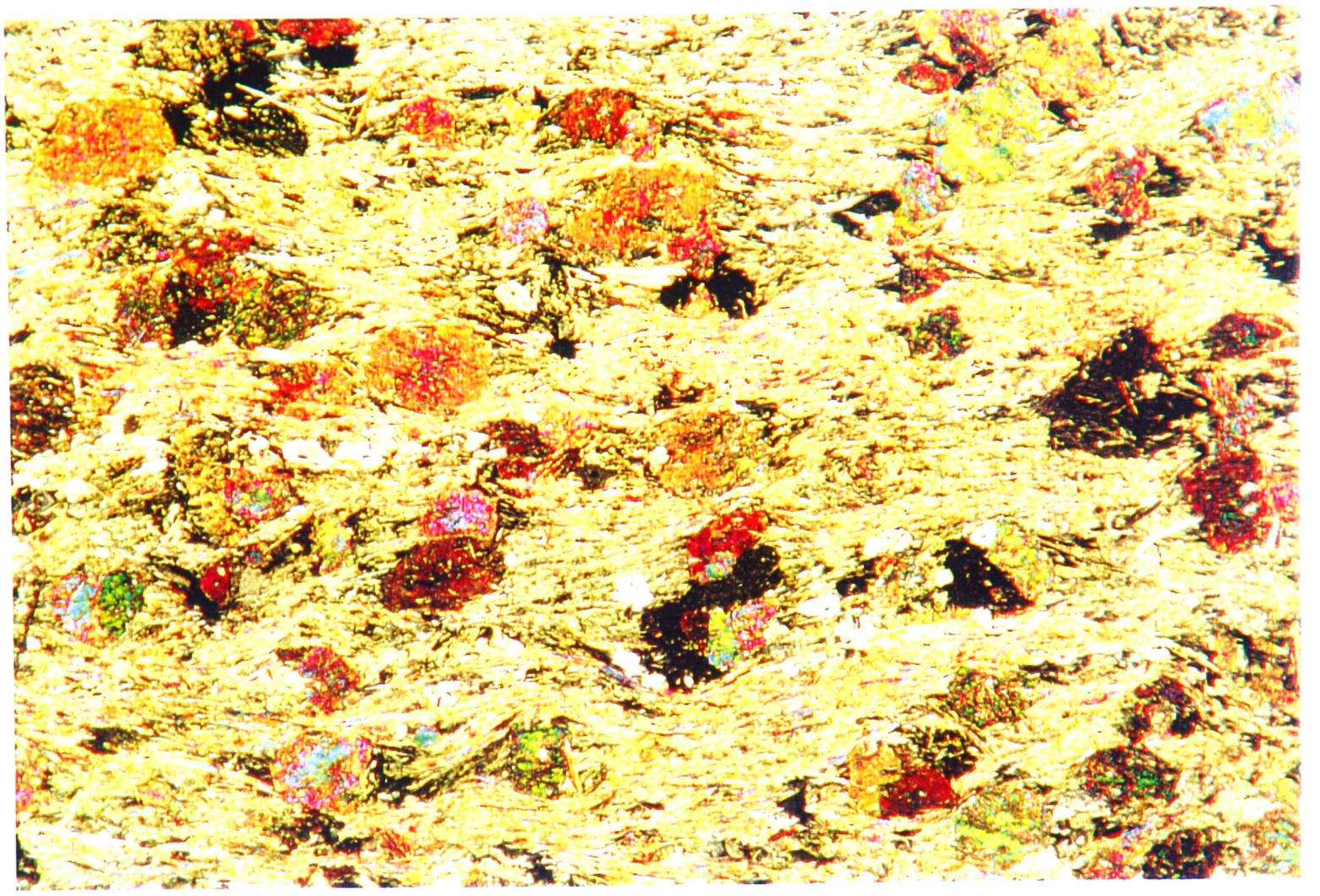


Figure 6.61 - Photomicrograph of the Porta Andesites. The andesites have been metamorphosed to greenschist facies. The dominant schistosity is defined by chlorite plates, and sometimes micas, and these often wrap around large, coeval epidotes.



Figure 6.62 - Field photograph of a deformed rudite horizon within the Porta Andesites of the Porta-Tzena Unit. Clasts are wholly volcanic and set in a fine- to medium-grained tuffaceous matrix. They were porbably formed by mass flow deposits either during (pyroclastic) or shortly following (epiclastic) volcanism.

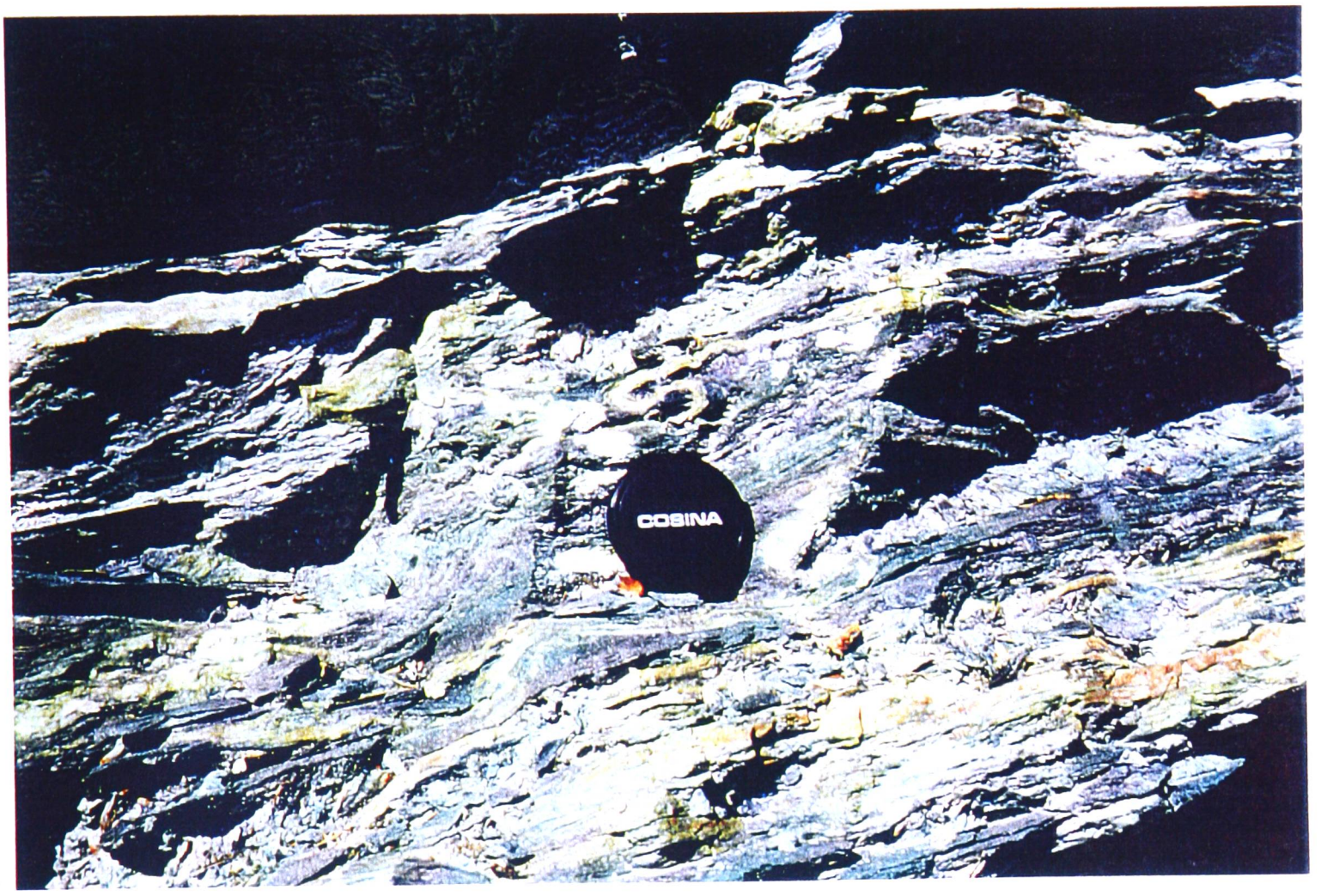


Figure 6.63 - Tightly folded epidote veins within the Porta Andesites. The epidote veins often pick out isoclinal folds that would otherwise be less obvious. The isoclines are associated with an early fabric, both of which are folded by later (Tertiary) deformation.

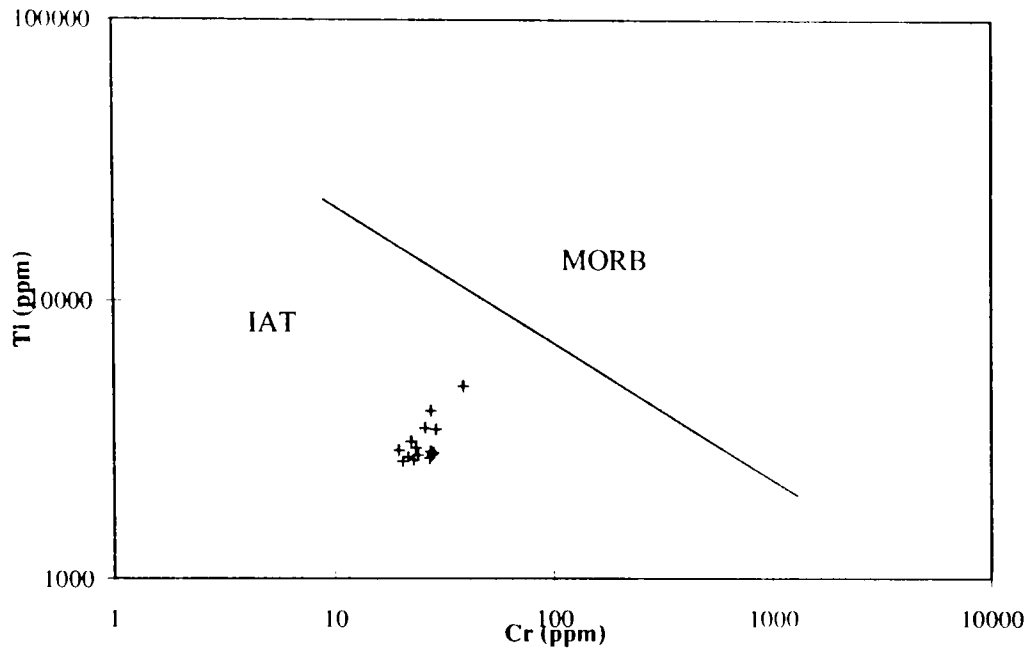
using the X-Ray Fluorescence technique outlined in the Appendix , along with samples of more deformed volcanics for comparison. Sample and trace element screening was carried out as detailed in chapter 5 and the suitable data were plotted on the discrimination diagrams shown on Figure 6.64. The data indicate that the Porta andesites are likely to be of Island Arc Tholeiite (IAT) type[1].

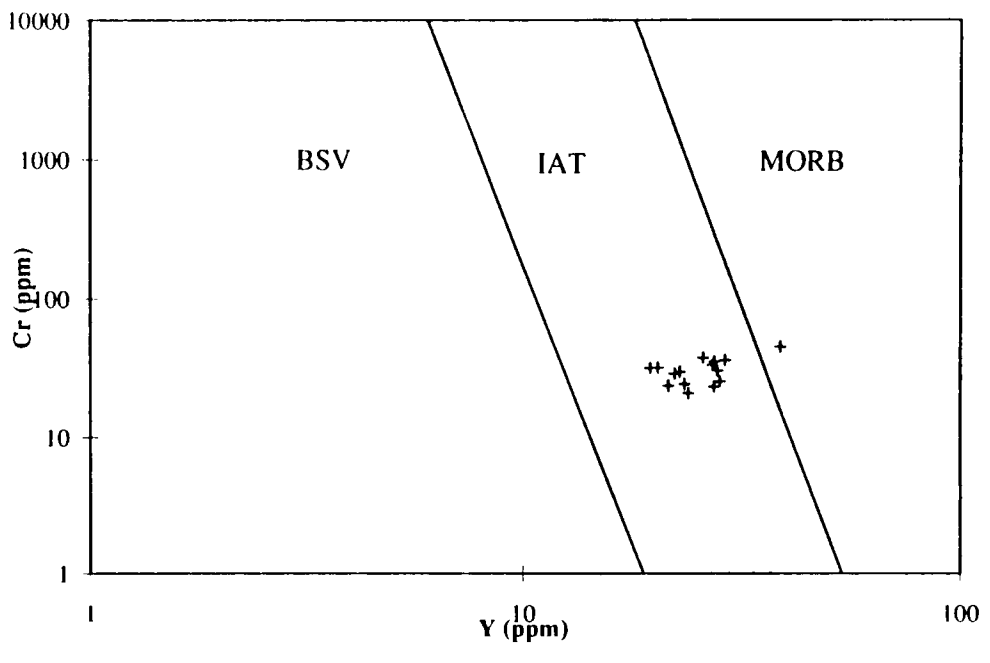
Interpretation and Regional Correlations

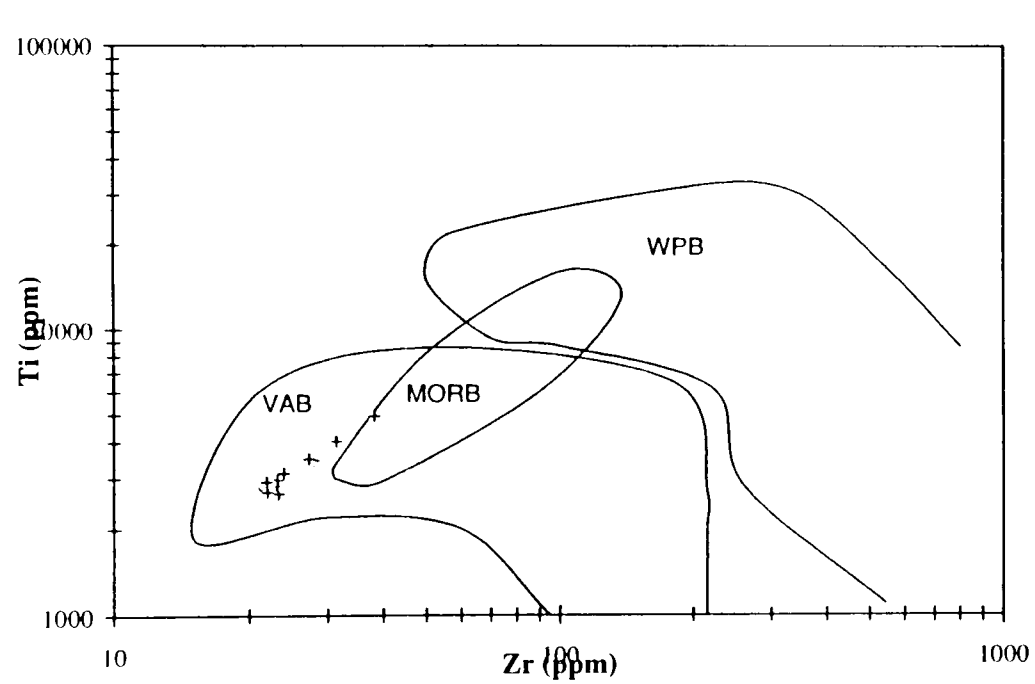
The poly-phase deformation history and distinctive high-grade fabric of the Kalivia Socrati gneisses suggests that they represent pre-Alpine continental basement. The gneisses are, however, quite different to the continental basement described from the Pelagonian zone (with which the Likostomo gneisses are affiliated) in that they contain strongly banded garnetiferous gneisses and abundant biotite-rich mica-schists which have not been described from the Pelagonian basement (Mountrakis, 1984, Sharp, 1995). They also lack meta-granitic gneisses, which are abundant in the Pelagonian Kaimaktchalan Massif (Yarwood & Aftalion, 1976; Sfeikos, 1992; Sharp, 1995). However, the Kalivia Socrati gneisses bear a much closer resemblance to the continental basement rocks of the Serbo-Macedonian zone to the east (S. Dimitriadis, pers. comm., 1993; Batty, 1993; Dixon & Dimitriadis, 1984) and it is therefore concluded here that the Kalivia Socrati gneisses were originally part of the Serbo-Macedonian Massif and were separated from it during the formation of the Innermost Hellenic Ophiolite Belt (IMHOB; Peonias subzone), more specifically the Guevgueli ocean basin, during the late-Middle and Upper Jurassic (see chapter 4.5).

The basement rocks are depositionally overlain by the Tzena meta-sediments, which are in turn overlain by the Porta andesites to the west. The thin interbeds of marble, calcschist and chloritic schist which constitute the Tzena meta-sediments closely resemble deep-water gravity flow deposits (i.e. turbidites) which characterise the slope

[1] It must be pointed out that the samples analysed from the Porta andesite succession all contain between 60 and 65 % SiO2 and are therefore not ideal for plotting on tectonic discrimination diagrams. The data is the best available, but the results, unfortunately, should be treated with some degree of caution







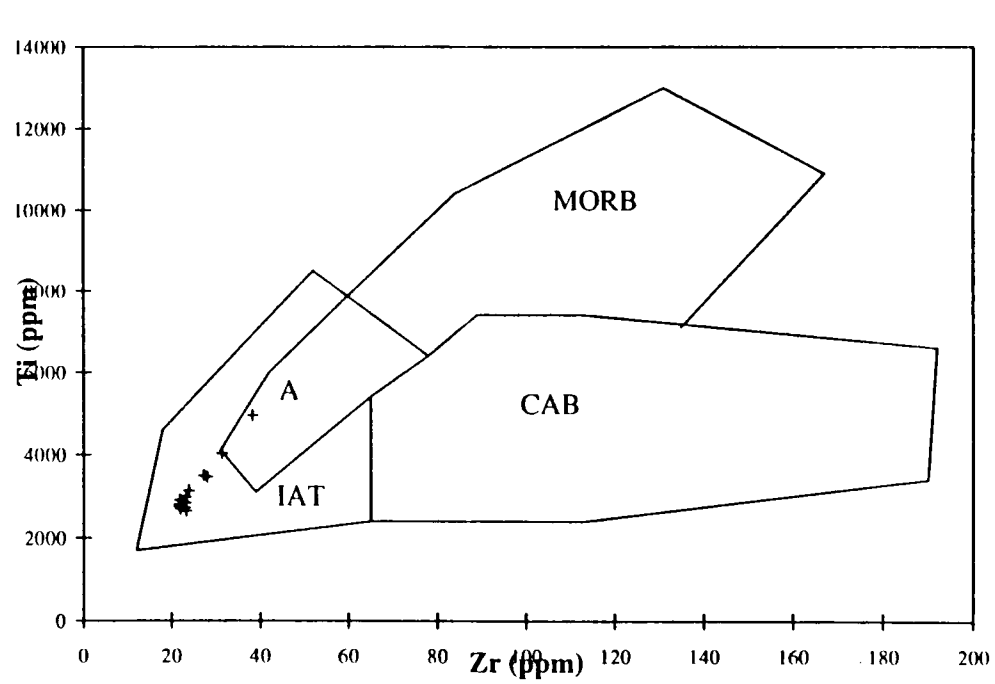


Figure 6.64 - Tectonic discrimination diagrams for the Porta Andesites (Unit 6, Voras Massif). The volcanics appear to be Island Arc Tholeiites. See chapter 5 for template details

deposits of the Poros Formation of the Argolis Peninsula (southern Greece), where redeposited carbonates are interbedded with thin interbeds of chlorite and mica-rich terrigenous clays (Clift & Robertson, 1989a; Clift, 1990; Clift & Robertson, 1990b). The Tzena meta-sediments are also strikingly similar to the slope deposits of the Gandatch Formation (chapter 3.4) in both facies association and deformation history (see **Structures** section below). Furthermore, in both areas (i.e. the Païkon Massif and the Porta-Tzena Unit of the Voras) the slope carbonates pass conformably upwards into a succession of intermediate-composition volcanics and volcaniclastics of Island Arc Tholeiite affinity, postulated to be of late-Middle to Upper Jurassic age (Mercier, 1968; this work, chapters 3 and 4). It is therefore concluded that the Porta-Tzena Unit of the Voras Massif is equivalent to the Gandatch, Livadia and Kastaneri Formations of the Païkon Massif which lies directly to the south. This hypothesis is supported by structural data from both areas (see **Structures** section below). That the Porta-Tzena Unit and the lowermost units of the Païkon Massif are equivalent implies that the Gandatch Formation of the Païkon Massif is underlain by pre-Alpine continental basement of Serbo-Macedonian zone affinity. In addition, the Porta andesites comprise a significantly higher proportion of primary lava flow deposits than do either the Livadia and Kastaneri Formations of the Païkon Massif. This might possibly suggest that the Porta andesites of the Voras Massif were erupted in closer proximity to a central volcanic centre, while the Païkon volcaniclastic succession was deposited some distance away on the flanks of the volcano.

Between the Tzena-Porta Unit (Unit 6) and the Pinovon Unit (Unit 5), a deformed silici-clastic unit crops out (Aetochori Formation of Migiros & Galeos, 1990). It comprises indurated and sheared interbedded sandstone and siltstone horizons, with a probable volcano-sedimentary origin (this work). All original sedimentary structures have been obliterated. This meta-sedimentary package is in thrust contact with both adjacent units and in both cases the contact dips steeply to the east. Structures within this sequence appear to record only one deformation phase and those structures

observed give no conclusive information concerning polarity of movement. Considering the Païkon subzone affinity of both the Porta-Tzena (to the east) and Pinovon (to the west) Units, it is possible that this sedimentary unit can be correlated with the Ghrammos Formation of the Païkon Massif which has also been derived from a volcanic source and has suffered only Tertiary deformation. Therefore, the eastern Voras Massif includes an almost complete transect through the stratigraphy of the Païkon Massif from the Gandatch Formation (Porta-Tzena Unit) to the Tchouka Flysch (Pinovon Unit).

Structures

Structural data (lineations, foliations, folds, σ and δ structures, duplex structures and reverse faults) indicate that the whole of the Porta-Tzena Unit has undergone two distinct phases of compressional deformation as seen in the Tzena meta-sediments (Mercier, 1973, this work, Figures 6.57 & 6.58). In addition, the basal Kalivia Socrati gneisses have been subjected to at least one significantly higher-grade deformation event which occurred prior to deposition of the Tzena meta-sediments or the Porta andesites. The first event to affect the whole Porta-Tzena Unit is most commonly seen within the Porta andesite succession, picked out by deformed epidote veins. This event is distinguished by ductile, isoclinal folding about roughly east-west axes (Figure 6.65). Many of these folds have been flattened and show signs of hinge thickening and limb attenuation. Where these folds are not preserved (i.e. in highly sheared zones in the Porta andesites), the early ductile deformation can still be identified as a stretching lineation oriented parallel to the axes of associated isoclinal folds (Figure 6.66).

The second phase of contractional deformation to affect the Porta-Tzena Unit is more pervasive and is associated with brittle, non-cylindrical chevron folds. The secondary folds are more obvious and have very variable axial directions which, in the Porta Andesites trend towards 300°N to 010°N (Figure 6.67). A roughly axis-parallel lineation occurs in conjunction with the chevron folds and similarly trends with

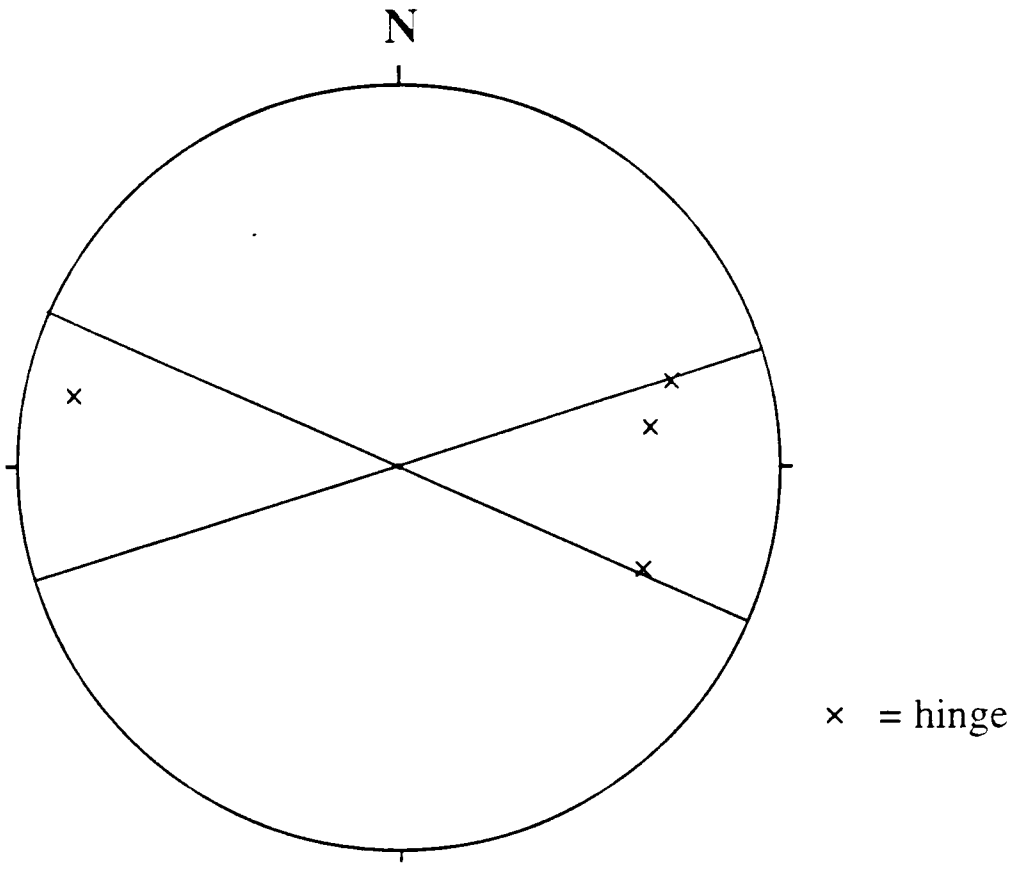


Figure 6.65 - Stereographic projection showing the orientation of early folds within the Porta Andesites. The early folds (Upper Jurassic) trend roughly east-west.

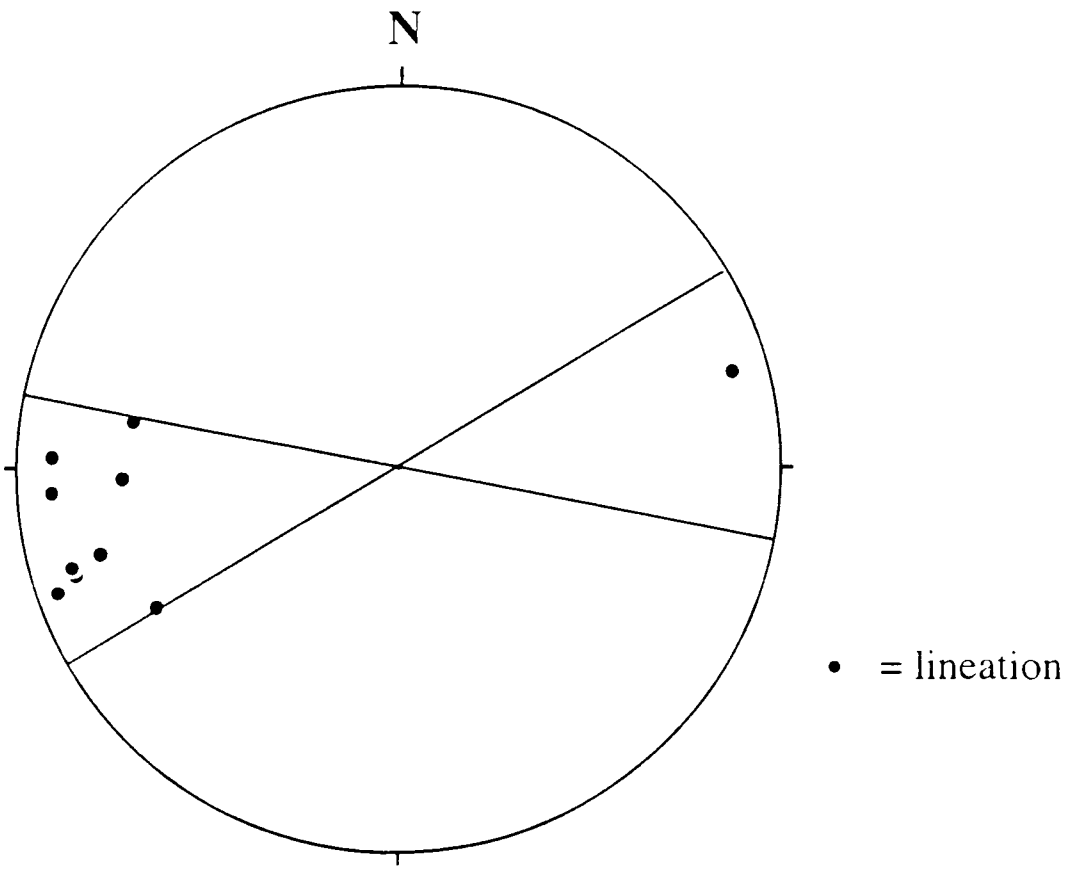


Figure 6.66 - Stereographic projection showing the orientation of an early lineation within the Porta Andesites. As the early folds (see Figure 6.65), the early (Upper Jurassic) lineation trends roughly east-west.

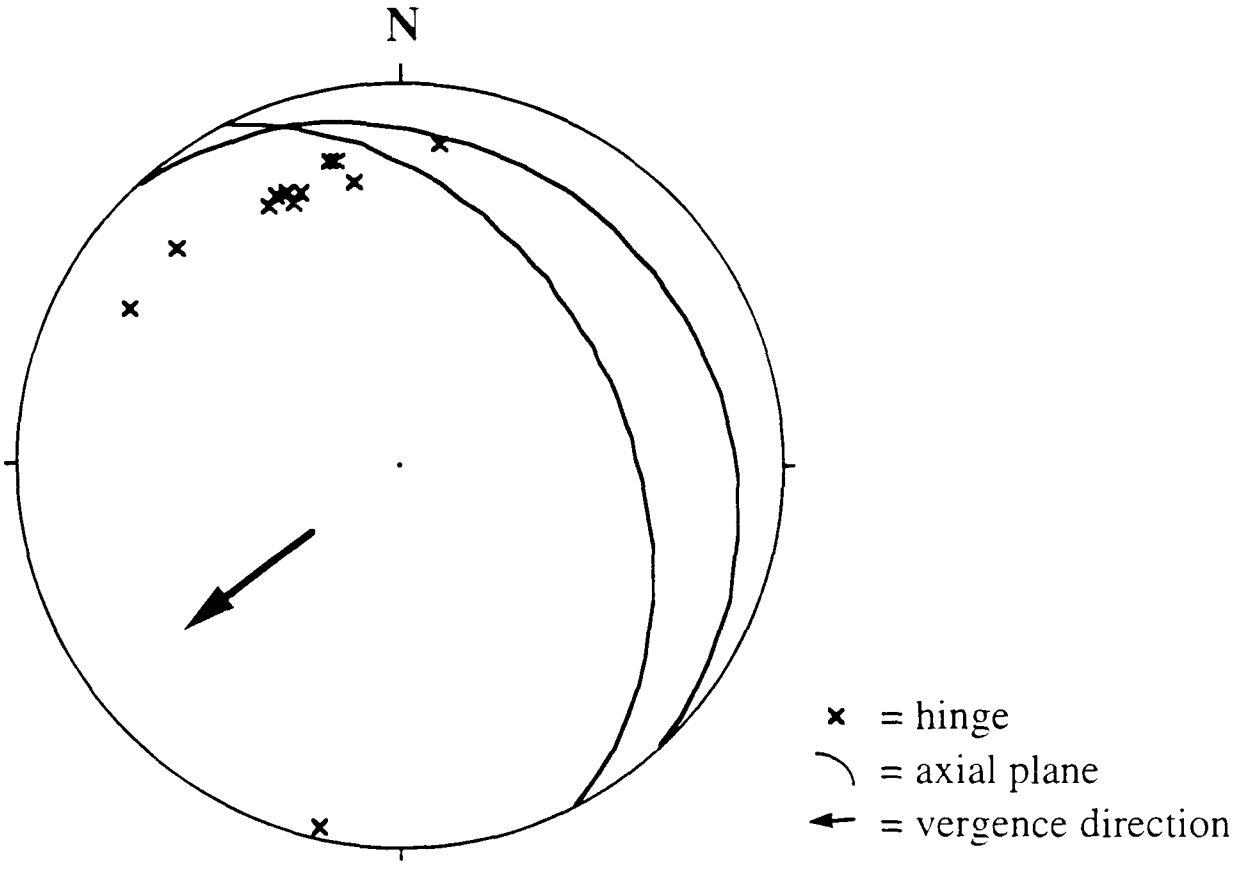


Figure 6.67 - Stereographic projection showing the orientation of a second phase of folds (Tertiary) from the Porta Andesites. The folds are brittle, non-cylindrical and trend between NW-NNE and SE-SSW.

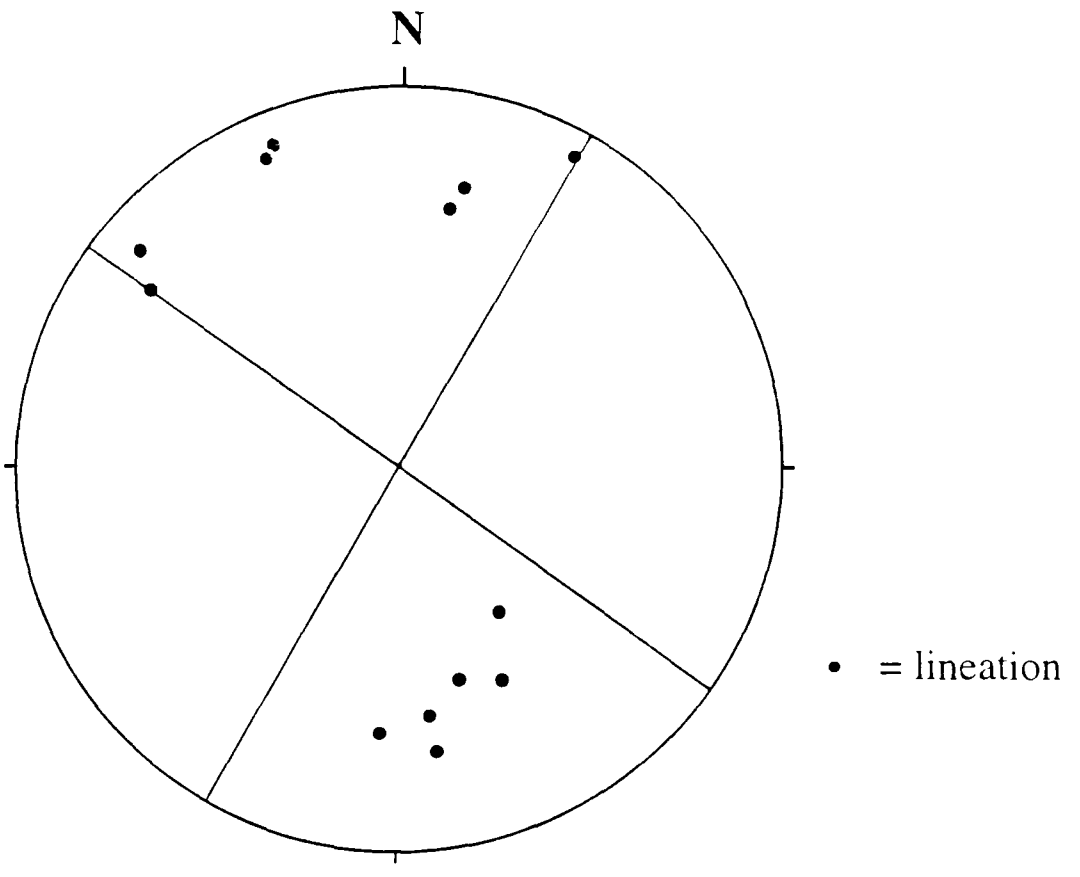


Figure 6.68 - Stereographic projection showing the orientation of the Tertiary lineation within the Porta Andesites. The lineation is roughly parallel to the fold axes shown in Figure 6.67, trending NW-NNE and SE-SSW.

great variability towards the NW to NE (Figure 6.68). Together with the variable trend there is a change in vergence direction from locality to locality. It does appear, however, that the Porta andesites in the west generally verge towards the NW to SW, while the Tzena meta-sediments and the Kalivia Socrati gneisses verge consistently towards the NE and E (Figures 6.67 and 6.58 respectively).

In this area it is not possible to date the deformation events based on the ages of the units that they affect as all lithological units are postulated to have been deposited prior to the Upper Jurassic (Mercier, 1968; this work). It is therefore necessary to use the characteristics of the deformation events themselves to assess their timing. The ductile, isoclinal event is comparable in style to the Upper Jurassic contractional event described from elsewhere in the Voras Massif (e.g. the deformed ophiolite conglomerates of the Loutra-Arideas Unit, the amphibolites of the Likostomo-Promachi Unit and the marbles and chloritic schists of the Livadia Unit), and it is similar in both style and orientation to the Upper Jurassic (D1) event in the Païkon Massif (this work, see chapter 4.2). The isoclinal folding event associated with east-west-trending axes and lineations is therefore assigned to the Upper Jurassic. The second folding event closely resembles early Tertiary deformation observed in the rest of the Voras Massif (F2 of Sharp, 1995 and D2 of this work) but most closely parallels the D2 event described from the western Païkon Massif where D2 deformation verges to the east and northeast (as in the Tzena meta-sediments and Kalivia Socrati gneisses), which is not seen anywhere else in the generally west-verging Voras Massif. A similar early Tertiary age is thus concluded for the chevron folds of the Porta-Tzena Unit.

6.4 - DISCUSSION

The Voras Massif comprises six main structurally bound units, each containing a more or less competent or related succession. The contacts between the units are Tertiary thrusts which verge consistently towards the west and southwest.

After having outlined a modified stratigraphy and structural history for each of the six units of the Voras transect (section 6.3.1 to 6.3.6), the implications for the geological evolution of the area will now be discussed.

In the westernmost Voras Massif, the succession exposed in Unit 1 (the Loutra-Arideas Unit) essentially comprises deformed, interbedded schists, Triassic-Jurassic marbles and clastics, then deformed ophiolitic rocks unconformably overlain by Upper Jurassic (~Kimmeridgian) limestones, ophiolite-derived conglomerate and red-bed conglomerate (Aptian-Albian). This is a classic Pelagonian/western Almopias-type sequence, as exposed south of the Loutraki fault (I. Sharp, pers. comm., 1993), and particularly resembles the Kerassia Unit of the western Almopias zone. Indeed, the deformed arenites and conglomerates, which occur towards the top of the Triassic-Jurassic marbles/schists of Unit 1 are similar to the Arnissa Passage Beds Member of the Pelagonian Zone (Sharp, 1995). These meta-clastics mark the top of the Pelagonian Marble Group throughout the Pelagonian zone of northern Greece and are interpreted to represent a syn-ophiolite-emplacement, foredeep "flysch", which was shed off, and subsequently over-ridden by, an obducting ophiolite. The post-emplacement erosional cover to the ophiolite in Unit 1 is represented by unconformably overlying, ophiolite-derived conglomerates with well-rounded clasts and local reefal limestones of Upper Jurassic (~Kimmeridgian) age.

The unconformable nature of this contact is postulated here to indicate that, in this area, the ophiolitic assemblage was deformed and emplaced onto the eastern margin of the

Pelagonian zone prior to the Upper Jurassic Pre-Kimmeridgian), when the conglomerates and limestones which seal this event were deposited. This Upper Jurassic compressional deformation event can be correlated with the regional JE1 event of Vergely (1984), the F1 event of Sharp (1995) and the D1 event of Brown & Robertson (1994, in press). However, there is no evidence in the study area to support the existence of a later, JE2 event documented by Vergely (1984), and all structures which occur subsequent to the Pre-Kimmeridgian event (JE1) can be attributed to Tertiary tectonism.

The gneisses of the Likostomo-Promachi Unit were interpreted by Ricou & Godfriaux (1991) to represent a slice of Serbo-Macedonian continental basement, carried over the Païkon Massif as an allochthonous nappe. However, the gneisses are petrologically and genetically comparable to the metamorphic continental basement rocks of the Pelagonian zone, as exposed in the Kaimaktchalan Massif to the west, and bear little resemblance to the high-grade continental basement rocks which crop out in the Serbo-Macedonian Massif to the east. Therefore, the gneisses are postulated here to be upthrust slices of the Pelagonian zone continental basement and not an allochthonous slice of Serbo-Macedonian basement as Ricou & Godfriaux suggest (1991).

Two models can account for the amphibolites of the Likostomo-Promachi Unit. Firstly, the amphibolites may represent part of a metamorphic basement sequence of Pelagonian zone affinity, as discussed in section 6.3.2, or the amphibolites may have formed as an ophiolitic "metamorphic sole", which would suggest that they are affiliated with the Almopias zone (Migiros & Galeos, 1990). However, as discussed in section 6.3.2, the high-grade mineralogy and fabric of the amphibolites, and indeed of the associated gneisses and garnet-mica-schists, are cut and deformed by the Upper Jurassic structures (i.e. phase JE1 of Vergely, 1984; D1 of Brown & Robertson, in press; F1 of Sharp, 1995) with which ophiolite emplacement is associated (see section 6.3.1). This implies that the amphibolites and the high-grade fabric pre-date ophiolite emplacement and

therefore cannot be metamorphic sole rocks. Also, no ophiolitic rocks were observed in contact with the amphibolites, or associated with them, as expected if they were the metamorphic sole of an obducting ophiolite.

The breccia unit found between the gneisses and amphibolites post dates both of these lithologies and is very similar in composition and character to the Klissohori Mélange, which crops out near the village of Klissohori, 2 km north-east of Edessa (Mercier & Vergely, 1974; Vergely, 1984; Sharp, 1995). In the south the Klissohori Mélange has been inferred to occur along the strike of a palaeo-transform fault (the extension of the Nission Fault? in the Pelagonian zone; Vergely, 1984; Sharp, 1994). Similarly, the breccia described from the Likostomo-Promachi Unit crops out along strike of the Kato Loutraki Fault, and thus may have been generated during fault movement along this lineament during the Mesozoic. If this is the case, then the breccia unit, as the adjacent gneisses, can be assigned to the Pelagonian zone.

As concluded for the Likostomo-Promachi Unit, the gneisses cropping out in the Livadia Unit are probably related to the continental basement of the Pelagonian zone, as opposed to the Serbo-Macedonian zone, due to their petrographic and compositional characteristics (I. Sharp, pers. comm., 1993; S. Dimitriadis, pers. comm., 1993; Mountrakis, 1984; Batty, 1993). Similarly, the serpentinite-decolled Triassic, palaeo-karstic marbles and Cretaceous limestones, as well as the imbricated marbles, limestones, chloritic schists and bedded cherts east of the Livadia Unit, show a striking similarity to lithologies which crop out in the Pelagonian zone and the western/central Almopias subzone (e.g. the Kilssochori Unit). The rocks of the Livadia Unit have no direct equivalents in the Serbo-Macedonian zone. For example, the palaeo-karstic marbles seen in the study area are identical to the ?Triassic (Norian) Pelagonian marbles well exposed in both the Arnissa area and in the Klissochori Unit of the central Almopias subzone (Sharp, 1995). The unconformable relationship between these marbles and the overlying Cretaceous limestones in Unit 3 of the study area is identical

to that seen immediately to the west of Loutraki Gorge, which is well known to be of Pelagonian affinity (Mercier, 1968; Sharp, 1995).

Unit 4, the Ano Garefi ophiolite, itself is bound on either side (i.e. between the Livadia Formation in the west and Pinovon Massif in the east) by major thrust contacts. In both cases these contacts dip to the east, suggesting west to south-westward vergence, which is inferred to have developed during the Tertiary. Local, late-stage back-thrusts verge towards the east along the western contact. Perhaps the most important structural observation of this western tectonic contact is that Unit 3 (Livadia) does not overthrust the Ano Garefi Ophiolite, from west to east forming a tectonic window, as recently suggested by Ricou & Godfriaux (1991), but rather the ophiolitic rocks of Unit 4 are thrust south-westwards over Unit 3. This is in keeping with the original mapping of Mercier (1968).

The *Orbitolina*-bearing, ophiolite-derived conglomerates, which unconformably overlie the Ano Garefi Ophiolite in the west, suggest that the ophiolite underwent uplift to near sea-level, or above, prior to Aptian/Albian times. Tertiary deformation then resulted in final westward thrusting, which placed the ophiolite structurally on top of Unit 3 to the west, and structurally below the Cretaceous limestones of Unit 5 to the east.

The carbonate and clastic lithologies of Unit 5 are identical in age, faunal assemblage and facies to the Middle and Upper Cretaceous sequences which crop out in the Païkon subzone to the south. In the Païkon, shallow-water, rudist-bearing limestones of Aptian/Albian age (Mercier, 1968) pass with a normal contact upwards into pink, pelagic, *Globotruncana sp.*-bearing limestone and ultimately deep-water flysch of Turonian to Maastrichtian age (Sharp & Robertson, 1992; Sharp, 1995; Brown & Robertson, in press); this is identical to the succession observed in Unit 5 of the study area. Similarly, the volcaniclastic rocks cropping out locally within the Pinovon Massif

(Unit 5) are strikingly similar in both petrology and geochemistry (work in progress) to volcaniclastics exposed in the Païkon subzone (Kastaneri Fm).

Unit 6 exposes a sequence which passes conformably from gneisses, marbles and schists, through slope metasediments to sheared andesites and intermediate volcaniclastics. Unlike the gneisses of Units 2 & 3, those exposed in this area bear more resemblance to the metamorphic basement rocks of the Serbo-Macedonian zone than those of the Pelagonian zone (S. Dimitriadis, pers. comm, J.E. Dixon, pers. comm., I. Sharp, pers.comm).

The conformable succession seen above the gneisses and micaschists in the study area (i.e. from interbedded marbles, chloritic schists and calcarenites to highly-deformed andesites and volcaniclastics of probable island arc affinity) is identical to that exposed directly to the south, within the Païkon subzone. As in the Païkon Massif, the marble/schist unit and the volcanic/volcaniclastic unit both exhibit structures which indicate two phases of compressional deformation; one early, ductile and associated with an east-west trending lineation, the other later and brittle with north-south trending fold axes. This is identical to the structural history exhibited within the Voras Massif. Because these metasedimentary/meta volcanic successions are similar in the Voras and the Païkon it is taken here that the underlying gneiss/micaschist unit exposed in the Voras also exists below the Païkon Massif forming its metamorphic basement, as suggested by Mercier (1968). This suggests, therefore, that the Païkon subzone is floored by continental metamorphic basement of Serbo-Macedonian affinity, from which it must have rifted some time in the past (possibly during back-arc basin formation - the Peonias subzone ophiolitic rocks, Bebien, 1987; Stais, 1994; Sharp, 1995). Hence this island arc initially formed along a continental, Andean-type margin, probably during the eastward subduction of the Palaeotethyan Vardar ocean beneath the Serbo-Macedonian continent.

The meta-volcanic unit exposed in Unit 6 is, however, considerably thicker than that seen in the Païkon (due partly to fold and thrust repetition) and also contains a much greater proportion of andesitic rocks relative to volcaniclastics than the Païkon equivalents. This may indicate that the arc edifice lies to the north of the Païkon and possibly even north of the Voras. The Païkon volcaniclastics (Livadia Formation) are therefore postulated as more distal equivalents of the Unit 6 volcanics (Porta andesites).

Recent work (Sharp, 1994; Sharp & Robertson, in press) shows that the Meglenitsa ophiolite comprises a thick pile of MORB-type ophiolitic volcanics with no exposed basement. These volcanics are overlain by deep-water sediments, including radiolarian mudstones, turbidites and redeposited limestones of Lower-Mid Cretaceous age (Stais & Ferriere, 1991; Sharp, 1995). Petrographic studies suggest that the provenance of the ophiolitic sedimentary cover was both from the Pelagonian zone to the west and from the Païkon subzone to the east (Mavrolokkos unit, Sharp & Robertson, in press). The Meglenitsa ophiolite, which is relatively undeformed, contrasts significantly with the deeply eroded ophiolites of the Pelagonian zone to the west, which are overlain by Upper Jurassic-Lower Cretaceous shallow-water carbonates.

It appears, therefore, that two distinct phases of ophiolite evolution have taken place; the first occurred in pre-Upper Jurassic and is unconformably overlain by Kimmeridgian/Tithonian limestones, and a second, post-compression pull-apart phase which is relatively undeformed and overlain by Aptian/Albian sediments. Sharp & Robertson (in press) inferred that a collision took place in the Late Jurassic (JE1 of Vergely, 1984) closing the Mesozoic Almopias (western Vardar/Axios) ocean and that this was followed by the re-opening of a pull-apart basin in the Early Cretaceous (Meglenitsa Ophiolite). This younger ocean was then unconformably overlain by cover sediments of Aptian/Albian age.

In the study area both postulated stages of ophiolite development can be seen. In Unit 1 deformed ophiolitic rocks are overlain by Kimmeridgian limestones (c.f. Almopias ophiolites), and in Unit 4 the relatively undeformed Ano Garefi Ophiolite is overlain by Aptian/Albian conglomerates (c.f. the Meglenitsa Ophiolite). A similar inference was made by Jacobshagen & Wallbrook (1984) further south on the Aegean island of Syros.

6.5 - CONCLUSIONS.

The Voras Massif comprises six tectonostratigraphic units which are separated by west to southwest verging thrust faults of Tertiary age. Units 1, 2, 3 and 4 all expose rocks of Pelagonian and/or Almopais (western Vardar-Axios) subzone affinity, while Units 5 and 6 are lithologically and stratigraphically identical to the Païkon subzone (central Vardar-Axios). Other than the gneiss/micaschist unit seen in the extreme east of Voras, none of the units are similar to the more easterly Serbo-Macedonian zone.

Two phases of contractional deformation have affected the Voras Massif. The first involved pre-Kimmeridgian, ductile deformation associated with the initial obduction of the Almopias ophiolites onto the Pelagonian continent to the east. The second took place in the early Tertiary and entailed brittle thrusting, chevron folding and telescoping of the stratigraphic sequences present. An intervening phase of extension and pull-apart basin formation took place. This structural history mirrors that described recently for the Pelagonian, Almopias (Sharp & Robertson, in press) and Païkon Units (Brown & Robertson, in press).

Therefore, the results as a whole indicate that the Voras Massif comprises imbricated units of Pelagonian and Vardar-Axios affinity and thus refutes the concept of a far-travelled, Serbo-Macedonian nappe (Ricou & Godfriaux, 1991).

Chapter 7

Conclusions

CHAPTER 7 - CONCLUSIONS

7.1 - INTRODUCTION

This thesis presents significant new stratigraphic, petrological, structural and geochemical data which leads to an important tectonostratigraphic re-evaluation of the critical Païkon unit in the Hellenide orogenic belt. During the course of this study, as presented in chapters 2 to 6, it has become apparent that major modifications have to be made to the geotectonic models of the Païkon Massif proposed by previous workers, as the data presented here does not corroborate these theories. There now follows a discussion of each previous model (Figures 7.1A, B & C), with respect to its applicability to the Païkon Massif, followed by a synopsis of the revised tectonic evolution of the study area as proposed here.

7.2 - PREVIOUS MODELS

7.2.1 - *The Thrust-Imbricate Model (Mercier, 1968)*

The Thrust-imbricate model, as illustrated on Figure 7.1A, envisages the Païkon Massif as part of a west-verging imbricate stack of tectonostratigraphic units, generated during Tertiary compression. In this model, the Païkon Massif is separated into two distinct isopic zones (the Païkon and Prepeonias subzones) which are separated by a major east-dipping Tertiary thrust contact. The data collected during this study do not wholly support this model in that :

1 - The Païkon Massif represents an anticlinal structure, created during early Tertiary deformation (D2), which comprises identical stratigraphic successions on either flank. Additionally, each side of the Païkon anticline has undergone a similar

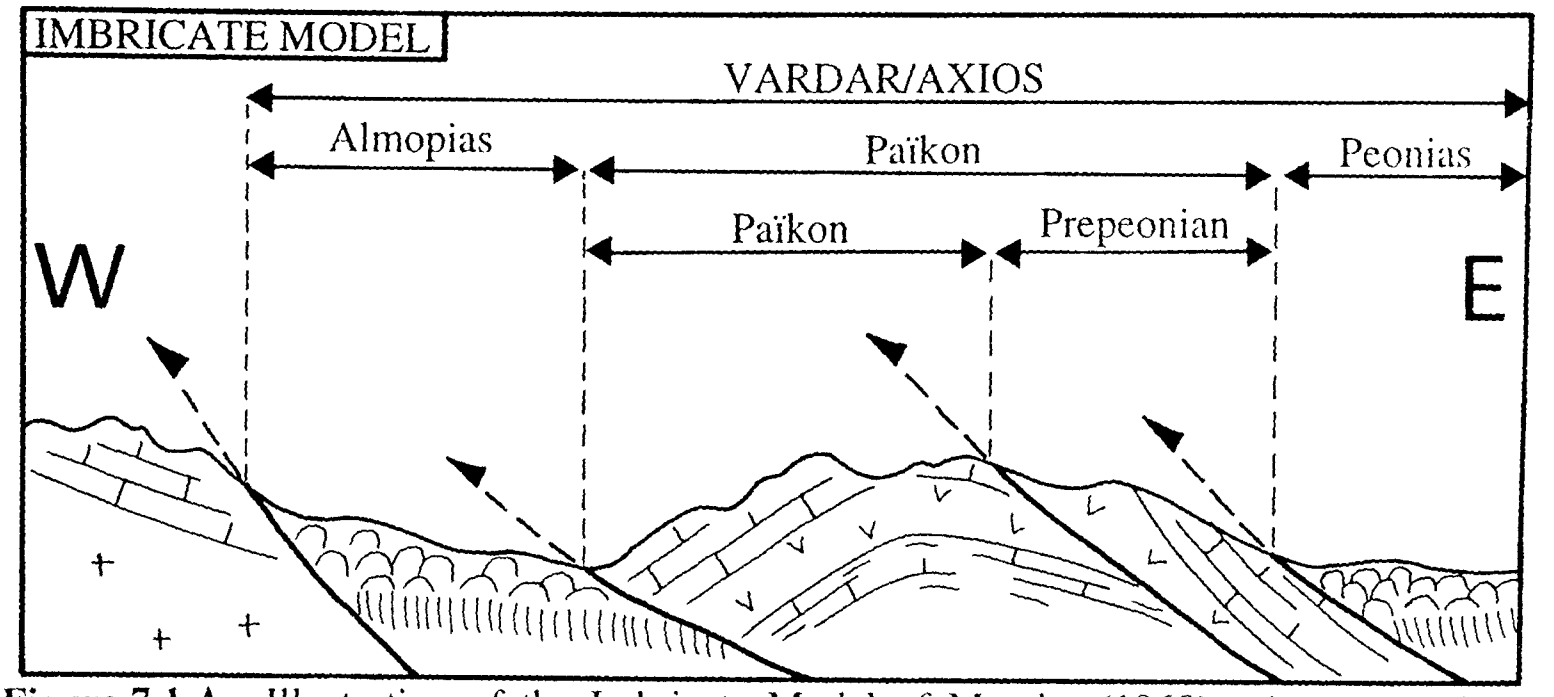


Figure 7.1 A - Illustration of the Imbricate Model of Mercier (1968). A westward-propagating thrust stack was envisaged across the Internal Hellenides.

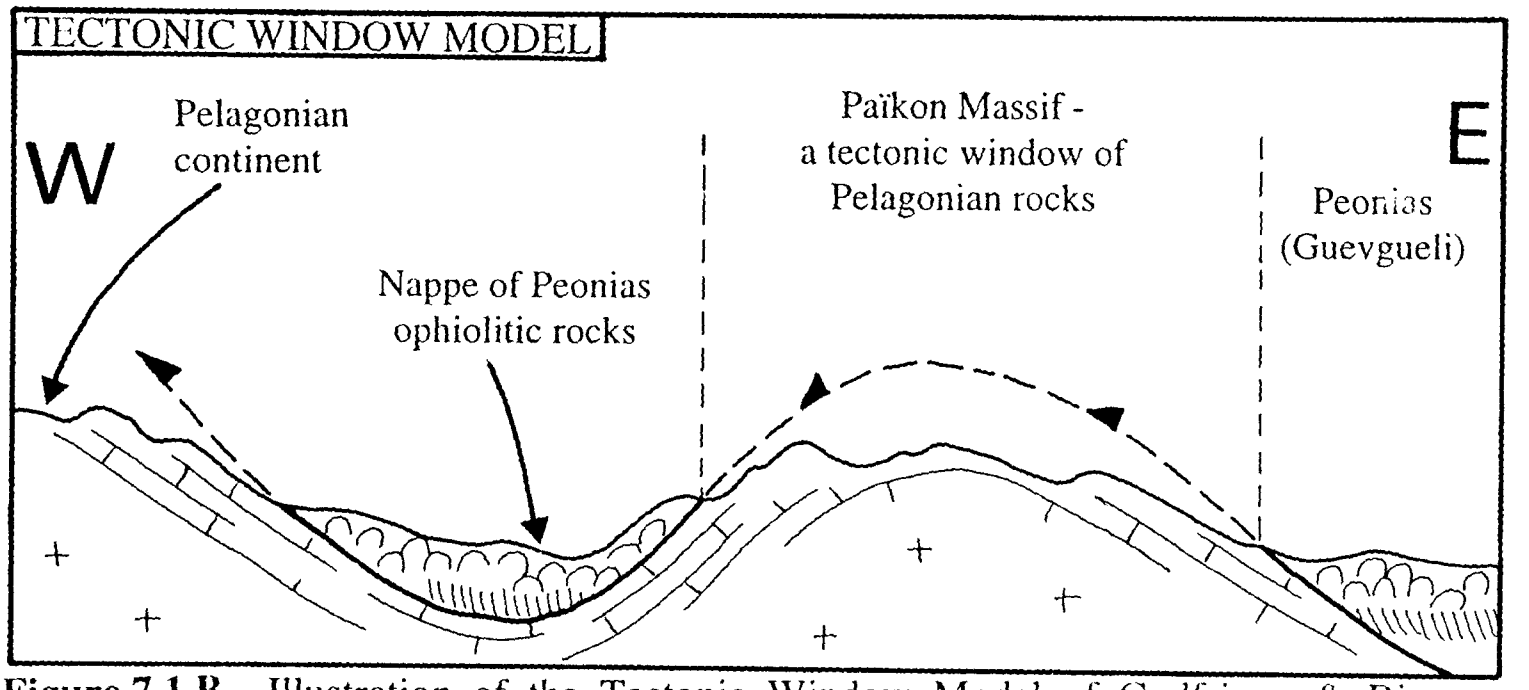


Figure 7.1 B - Illustration of the Tectonic Window Model of Godfriaux & Ricou (1991). An ophiolitic "nappe" overlies the western Païkon with west-verging contact

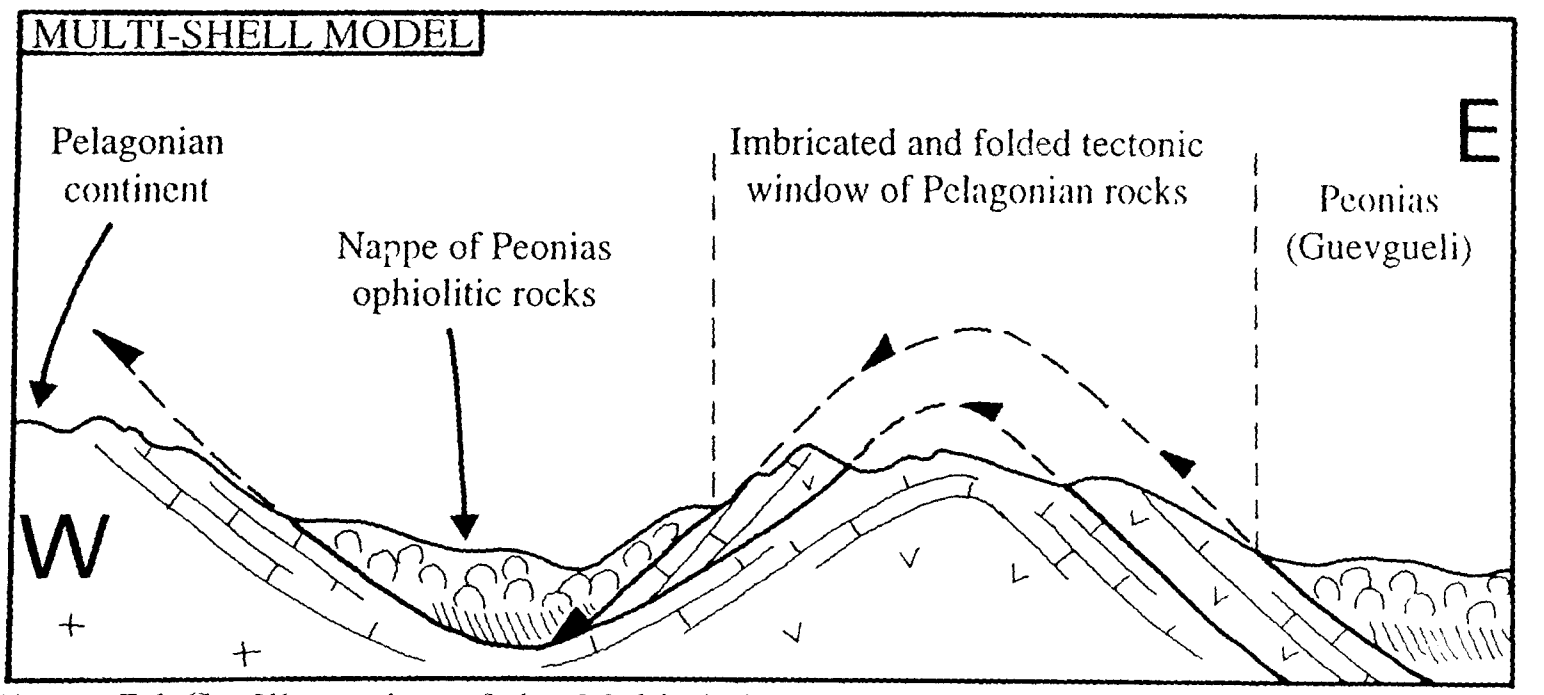


Figure 7.1 C - Illustration of the Multi-shell Model (Bonneau *et al.*, in press). The Eastern Pelagonian zone is exposed as an upfolded and imbricated window beneath a nappe of ophiolitic rocks derived from the Peonias subzone.

deformation history to the other. Therefore, it is not likely that the Païkon Massif represents two distinct tectonostratigraphic units, juxtaposed along a N-S-trending reverse fault.

2 - Although the Guevgueli Ophiolite of the Peonias subzone *does* tectonically overlie the eastern margin of the Païkon Massif (as the Thrust-imbricate model suggests), the western margin of the Païkon Massif *does not* tectonically overlie the Almopias subzone. Instead, it has been shown here that the western margin of the Païkon Massif is overlain by the Almopias subzone by way of an east-verging reverse fault of Tertiary (D2) age. The west-verging imbricate stack of Mercier is therefore not confirmed.

3 - Although much thrust-imbrication is evident within central parts of the Païkon Massif (as described in chapters 2, 3 and 4), no major west-verging tectonic contact exists within the Païkon Massif separating the Païkon subzone from a theoretical Prepeonian subzone. All such reverse faults are local and laterally discontinuous.

4 - The result of geochemical analyses presented in chapter 5 indicate that the volcanic rocks exposed on the eastern and the western sides of the Païkon Massif have indistinguishable geochemical signatures. Both areas contain volcanic rocks that are likely to represent island arc tholeiites and have been subjected to similar degrees and styles of chemical alteration. Thus, these data cannot be used to support the Thrust-imbricate model.

7.2.2 - *The Tectonic Window Model (Godfriaux & Ricou, 1991)*

The Tectonic Window model (Figure 7.1B) sees the Païkon Massif as an anticline of Pelagonian rocks which are exposed as a "window" beneath a Tertiary nappe of ophiolitic rocks derived from the Peonias subzone. As for the Thrust-imbricate

model above, certain data collected during this study conflict with a model of this kind:

1 - The Tectonic Window model requires the Païkon Massif to have been overridden by an ophiolitic nappe during the Tertiary, which implies that Tertiary structures in the study area (D2) should be consistently west-verging, with the rocks of the Almopias subzone overlying the western Païkon Massif. This is clearly not the case: although the Almopias subzone *does* overlie the Païkon Massif, the polarity of the structures along this contact (and far into the Païkon Massif) indicate an east to northeast transport direction. These data are not consistent with the Tertiary nappe hypothesis.

2 - The style of D2 deformation is not consistent with the obduction of an ophiolitic nappe during this time. The study of ophiolite emplacement in other parts of the world (e.g. Oman, California and in the Pelagonian zone) indicate that ophiolite-obduction is often associated with the formation of amphibolite to upper greenschist facies metamorphic soles and high-strain, ductile deformation. The Cretaceous rocks of the Païkon Massif have not undergone this style of deformation and have, instead, thin-skin brittle deformation under lower greenschist facies conditions. Additionally, given that the topmost units of the Païkon Massif are exposed on both eastern and western sides of the Païkon Massif, it is unlikely that a metamorphic sole, if there ever was one, has been completely removed by denudation.

3 - The rocks of the Païkon Massif and the Pelagonian zone cannot be realistically compared in that the Pelagonian zone does not contain a thick, stratigraphically important succession of Middle to Upper Jurassic volcanic and volcaniclastic rocks of island arc tholeiite composition. Additionally, the continental basement rocks inferred to underlie the Païkon Massif (as exposed in the Voras Massif) do not resemble those of the Pelagonian zone (Gondwanan) and are much more closely associated with the Serbo-Macedonian metamorphic basement

(Eurasian). It is therefore unlikely that the Païkon Massif was derived from the same continental mass as the Pelagonian zone, let alone attached to it under the ophiolitic rocks of the Almopias subzone.

4 - Stratigraphic units exposed on top of the ophiolitic rocks of the Almopias subzone and the adjacent Pelagonian zone indicate that the ophiolite now present in the Almopias subzone must have been emplaced (if indeed they were at all) at least 30 Ma before they could have been thrust over the Cretaceous rocks of the Païkon Massif, as both are unconformably overlain by rocks of middle Cretaceous age (Mercier & Vergely, 1994). Similarly, Sharp (1995) infers that the Upper Jurassic to Lower Cretaceous Meglenitsa Ophiolite of the Almopias subzone formed *in situ.* Again, this information is not in keeping with the emplacement of an ophiolitic complex from the Peonias subzone during Tertiary compression.

7.2.3 - *The Multi-shell Model (Bonneau et al., in press)*

As the Multi-shell model (Figure 7.1C) is an adaptation of the Tectonic Window model discussed above, all the points which refute the Tectonic Window model also apply to the Multi-shell model. Therefore, on these grounds alone it is very unlikely that the Multi-shell model can be successfully applied to the Païkon Massif.

The Multi-shell model was based on the discovery of Cretaceous fauna in rocks previously dated as Middle Jurassic (i.e. the Gropi Formation, which has been abandoned during this work). This information was interpreted to suggest that the Païkon Massif comprises at least two stratigraphically coherent, superposed units of Pelagonian affinity. Although these Cretaceous dates have been confirmed (and expanded) during this work, it is not evident from the data collected that each occurrence of Cretaceous Transgressive Limestone represents the uppermost rocks of a stratigraphically-coherent unit. In fact, most occurrences of the Cretaceous Transgressive Limestones in central parts of the study area are thrust-bound

imbricates which have been incorporated into stratigraphically much lower units. Hence, Cretaceous rocks within the central Païkon alone do not support a multi-shell model.

7.3 - PROPOSED TECTONOSTRATIGRAPHIC EVOLUTION OF THE STUDY AREA

7.3.1 - *Introduction*

The Païkon Massif can be subdivided into two essentially conformable stratigraphic parts; the lower Païkon megasequence, which comprises the Gandatch, Livadia and Kastaneri Formations, and the upper Païkon megasequence, which comprises the Khromni Limestones, Ghrammos Formation, Cretaceous Transgressive Limestones, Buff Pelagic Carbonates and Tchouka Flysch. The two megasequences are separated by an important structural and metamorphic discontinuity of pre-Kimmeridgian age. The lower Païkon megasequence crops out in central parts of the Païkon Massif and is poorly dated as uppermost Triassic/Jurassic (Gandatch Formation) to late-Middle to Upper Jurassic, or pre-Kimmeridgian (Kastaneri Formation) in age. The upper Païkon megasequence constitutes the flanks of the Païkon Massif anticline and is much better constrained, in terms of age, as Kimmeridgian (Khromni Limestones) to Maastrichtian (Tchouka Flysch).

An important conclusion of this thesis, derived from both field and laboratory observations, is that both the eastern and western flanks of the anticlinal Païkon Massif reveal the same stratigraphic successions and have undergone identical deformation histories from the Triassic/Jurassic onwards. The Païkon Massif can therefore be seen simply as a single tectonostratigraphic unit which was folded into an anticlinal structure during Tertiary deformation (i.e. folded subsequent to the deposition/formation of all principal stratigraphic units).

7.3.2 - *?Triassic-Jurassic Continental Margin Deposits and the Onset of Arc Volcanism*

As discussed in chapter 6, the rocks exposed in the eastern Voras Massif (i.e. the Porta-Tzena and Pinovon Units) are interpreted here to be of Païkon subzone affinity and include stratigraphic units which are equivalent to the Gandatch Formation (Tzena meta-sediments), the Livadia and Kastaneri Formations (the Porta andesites) and the Cretaceous Transgressive Limestones, Buff Pelagic Carbonates and Tchouka Flysch (the Pinovon Unit) of the Païkon Massif. Work in the Voras Massif has also revealed that these Païkon-related stratigraphic units are underlain by continental basement rocks and, hence, it is inferred here that the Païkon Massif is also floored by similar pre-Alpine metamorphic rocks. The continental basement rocks likely to underlie the Païkon Massif are lithologically distinct from those exposed in the Pelagonian zone to the west, but quite closely resemble the metamorphic basement of the Serbo-Macedonian zone to the east. It is likely, therefore, that the Païkon Massif was originally closely associated with the Serbo-Macedonian continent in some way, and not with the Pelagonian zone.

Biostratigraphic investigations carried out by Stais & Ferriere (1991) and Stais (1994) suggest that the Innermost Hellenic Ophiolite Belt (or IMHOB), which constitutes the Peonias subzone, originally formed as an aulacogen within the Serbo-Macedonian continental basement during the Triassic. This is evidenced by dates obtained from radiolarian cherts, which indicate the presence of a deep-water basin. Meanwhile, complete continental rifting, sea-floor spreading and the creation of oceanic lithosphere was taking place further to the west in the Vardar/Axios ocean, due to the break-up of the north African (Gondwanan) margin.

The Guevgueli Ophiolite of the IMHOB (Peonias subzone) now separates the Païkon Massif from the Serbo-Macedonian Massif. However, biostratigraphical (Danelian *et al.*, 1996) and geochronological (Borsi *et al.*, 1966; Makris, 1977; Jung *et al.*, 1980;

Spray *et al.*, 1984 and Bebien *et al.*, 1987; De Wet, 1989) data indicate that this belt of oceanic crustal rocks was not generated until the late-Middle to Upper Jurassic. Thus, it is proposed that the early stratigraphic units of the Païkon Massif were deposited on the rifted, thinned continental margin of the Serbo-Macedonian Massif, and it should be possible to correlate these early Païkon stratigraphic units across the Peonias subzone into the Circum-Rhodope and Serbo-Macedonian zones in the east.

The age constraints for the lower Païkon megasequence are poor, therefore it is not immediately obvious which stratigraphic units were deposited before the generation of the IMHOB. However, close investigation of rocks of pre-late-Middle to Upper Jurassic age exposed within the Serbo-Macedonian and Circum-Rhodope zones assist such correlations and indicate probable time ranges for the generation of their Païkon equivalents.

The Gandatch Formation includes meta-sedimentary rocks (schists, marbles and conglomerates) that have been interpreted here as lower slope apron or base-of-slope apron detrital carbonates and clastics (see chapter 3.3). Given the regional position of the Païkon Massif at their time of deposition, the Gandatch Formation was most probably deposited on the thinned, west to southwest-facing continental margin of the Serbo-Macedonian Massif. The Gandatch Formation meta-sediments are quite distal with respect to the carbonate platform from which they are inferred to have been derived and they may therefore represent distal equivalents of the Svoula Group (including the Svoula Flysch) which was deposited on the Serbo-Macedonian margin (i.e. the present-day Circum-Rhodope zone) during the latest Triassic to Middle Jurassic (Kauffmann et al., 1976; Mussallam, 1991; Dimitriadis & Asvesta, 1993). The Svoula Group overlie shallow-water, platformal marbles of Triassic age, which may partly be the source for both the Svoula Group and the Gandatch Formation.

7.3.3 - *The Onset of Subduction, Arc Volcanism and Back-arc Basin Genesis*

The Gandatch Formation of the Païkon Massif is conformably overlain by the Livadia Formation of the Païkon Volcanic Group. Geochemical analyses of the Livadia Formation (chapter 5) indicate that they are likely to represent island arc tholeiites which were erupted in a supra-subduction, volcanic arc setting. A comparable unit to the Livadia Formation has been described from the opposing side of the IMHOB in the Circum-Rhodope zone: The Chortiatis Group. The Chortiatis Group occupies a similar straigraphic position to the Livadia Formation and correspondingly comprises volcanic rocks that are interpreted to be of arc affinity (Mussallam & Jung, 1986). The Chortiatis Group volcanic rocks are dated as Middle Jurassic in age, which may possibly suggest a similar age for the Livadia Formation.

Considering the tectonic evolution of volcanic arcs elsewhere in the world (e.g. the Tonga arc; Clift, 1993), it is possible that the Chortiatis Group represents the remnant or outer arc of the Païkon arc *sensu stricto*, which ceased to erupt when the main volcanic centre (near the Païkon Massif) became separated from the Serbo-Macedonian Massif during the opening of the Guevgueli Ophiolite in late-Middle to Upper Jurassic times.

Arc volcanism continued in the Païkon Massif throughout the Middle Jurassic, and probably into the Upper Jurassic, with the eruption of the Kastaneri Formation, while the inferred Guevgueli back-arc basin, began to spread in the Peonias subzone (i.e. to the east) during the late-Middle to Upper Jurassic. The Kastaneri Formation is derived from the same island arc tholeiite magmatic suite as the Livadia Formation and comprises basic, intermediate and ultra-acidic volcanic rocks, interdigitated with great thicknesses of fine- to coarse-grained volcaniclastics. Both sides of the Païkon Massif contain volcanic rocks of very similar chemical character.

The arc volcanism represented by the Livadia and Kastaneri Formations of the Païkon Massif, and the associated back-arc spreading in the Peonias subzone (the Guevgueli

Ophiolite), are likely to depict the destruction, by eastward subduction, of the Triassic/Jurassic Neotethyan ocean of the Vardar/Axios beneath the western margin of the Païkon Massif (or the thinned-Serbo-Macedonian continental crust as it still was when subduction commenced).

The basic igneous rocks of the Guevgueli back-arc basin (or Guevgueli Ophiolite as it is now) is intimately associated with migmatites and granites of the same age. This rock association is inferred to be the result of magma mixing during the opening of the Guevgueli oceanic basin (De Wet, 1989; Dimitriadis *et al.*, 1994, in press). The basic component is derived from the mantle in response to an extensional crustal regime generated in the back-arc region, and the acidic component has been derived from anatexis of the thinned continental crust. The resultant effect is the simultaneous creation of basic oceanic lithosphere (Guevgueli Ophiolite) and the intrusion of granitic plutons (e.g. Fanos granite), which meet along zones of magma mixing represented by migmatites.

Thick volcanic arc successions present in the Païkon Massif and a sizeable back-arc basin in the Peonias subzone suggest that the Triassic/Jurassic Vardar/Axios ocean must have been relatively wide and subduction long-lived.

7.3.4 - *Eohellenic Deformation - the D1 event*

Initial collision between the Pelagonian zone (western side of the Vardar/Axios ocean), the Païkon Massif (eastern side of the Vardar/Axios ocean) and the southern margin of the Eurasian continent (of which the Serbo-Macedonian zone may be part) occurred in the Upper Jurassic. This led to a regional contractional deformation event (D1) which took place in the study area prior to the Kimmeridgian. During D1 deformation the stratigraphic units of the lower Païkon megasequence were subducted to deep crustal levels (~20 km) where they were subjected to pervasive ductile deformation under blueschist and upper greenschist facies conditions (i.e.

lawsonite and biotite/stilpnomelane assemblages respectively). The Gandatch, Livadia and Kastaneri Formations were all isoclinally folded and developed an associated E-W-trending lineation. In high-strain, ductile domains, folds rotate their axes into the direction of maximum strain and therefore do not record the polarity of deformation. However, the contemporaneous stretching lineation *is* likely to represent the dominant transport direction associated with D1, although whether transport was from west to east or from east to west is not clear from this information alone. The D1 compressional event of this work is essentially equivalent to the JE1 event of Vergely (1984) from the whole of the Internal Hellenides and the F1 event of Sharp (1995) from the Pelagonian zone and the Almopias subzone.

The analysis of structures in the Peonias and Almopias subzones, and to some extent in the Pelagonian zone, suggest that Upper Jurassic transport predominantly proceeded from east to west, therefore the subducting Vardar/Axios ocean was overridden by the Païkon Massif to the east, which, in turn, was overridden and deeply-buried by the ophiolitic rocks of the Peonias subzone and the western margin of the Serbo-Macedonian continent.

7.3.5 - *Extensional exhumation and pull-apart basin formation*

Soon after D1 compression, a phase of regionally-significant extension is inferred to have ensued. This event (E0) led to the extensional or transtensional unroofing and uplift of blueschist facies assemblages in the Païkon Massif (i.e. the lawsonite-bearing Kastaneri Formation) and in the eastern Pelagonian zone and the Almopias subzone to the west. No structural evidence for this E0 extensional event remains within the Païkon Massif due to the effects of subsequent deformation events, namely D2 and D3. This extension/transtension is also characterised by acidic volcanism in the Pelagonian and Almopias zones, and the Klissochori-Rhizarion block of the eastern Pelagonian margin was rifted from the eastern margin of the Pelagonian block via leaky transform faults, with associated acidic volcanism (Vergely, 1984; Sharp,

1995). As discussed in chapter 7, it is likely that some of the units exposed in the Voras Massif (i.e. the Likostomo-Promachi and Livadia Units) are similar to the Klissochori-Rhizarion block and, thus, are likely to have been transtensionally separated from the Pelagonian zone *sensu stricto* during this event also.

E0 is also inferred to have generated a pull-apart basin floored by oceanic crustal rocks in the eastern Almopias subzone (Meglenitsa Ophiolite) and it is suggested here that similar processes were operating in the Peonias subzone at this time (i.e. generation of the western Guevgueli Ophiolite and the Sithonia Ophiolite). It is also proposed here that the ophiolitic rocks of the Ano Garefi Unit in the Voras Massif formed in a similar pull-apart setting during this event. All of these ophiolitic complexes are comparable in their structural arrangements, which consistently indicate their formation under a dextral transtensional regime (i.e. dyke orientations and structural framework). Additionally, all of these ophiolites are characterised by MORB (Meglenitsa, Sithonia) and sometimes MORB plus WPB (Ano Garefi) signatures, whereas earlier-formed crust (e.g. the eastern Guevgueli and indeed the majority of the IMHOB) are characterised by MORB transitional to supra-subduction zone signatures.

Evidence of this Upper Jurassic to Lower Cretaceous extensional event has been reported far to the north in the Pelagonian zone in former Yugoslavia and to the south of Greece in the vicinity of the Argolis peninsula.

7.3.6 - *Upper Jurassic and Lower Cretaceous Transgressions*

In the Païkon Massif, the now highly-deformed and metamorphosed lower Païkon megasequence was uplifted during E0, and the Kastaneri Formation exposed at the surface. There then followed a period of erosion and subaerial exposure, of indeterminate length, during which lateritic deposits were laid down on the Kastaneri Formation. The volcanic rocks were subsequently transgressed and unconformably overlain by the shallow-water, Kimmeridgian to Portlandian Khromni Limestones. These limestones record the youngest possible age for the D1 event, which is otherwise poorly-constrained in the Païkon Massif, and seal the obducted and eroded Pindos, ?Vardar/Axios and Peonias Ophiolitic complexes.

The Kimmeridgian Khromni limestones are characterised by rapidly-changing facies rich in shallow-marine fauna (bivalves, gastropods, benthic foraminifera etc.) and periodic clastic input. A distinctive feature of these limestones is their abundance of *Cladocoropsis mirabilis* algae, which are important time and facies indicators. It is possible that the Khromni Limestones were deposited only in southerly parts of the Païkon Massif, as they have only been encountered in the vicinity, and to the south, of Khromni village and, for the first time during this work, south of Omalou village in the southeastern Païkon Massif. It is possible, however, that their lack of exposure in more northerly areas is not due to restricted deposition area, but is the result of tectonic cut-out.

Contemporaneous transgressive deposits have been reported from many other areas in the Internal Hellenides; for example Oxfordian-Kimmeridgian ophiolite-derived conglomerates and shallow-water limestones in the Pelagonian zone, and contemporaneous but more basinal facies in the western/central Almopias subzone. To the east, Kimmeridgian shallow-water, *Cladocoropsis*-bearing limestones also unconformably overlie the Guevgueli Ophiolite; the Choryghi Limestones (Mercier, 1968), which likewise provide the upper age limit for D1, or Eohellenic, deformation in this part of the Internal Hellenides. In the Voras Massif the dismembered ophiolitic

melange of the Loutra-Arideas Unit is unconformably overlain by ophiolite-derived conglomerates and shallow-water limestones, which were likened, in chapter 6 of this work, to the transgressive units described from the Pelagonian zone. An Upper Jurassic (corals; Galeos et al, 1994) and possible Kimmeridgian (? *Cladocoropsis* algae; this work, chapter 6) age has been assigned to these units also.

Therefore, regional scale transgression in the Internal Hellenides, which commenced in the Oxfordian/Kimmeridgian provides a fairly consistent uppermost age limit for the Eohellenic compressional deformation event (D1).

7.3.7 - *Portlandian-Aptian/Albian Fluvial Deposition*

After the deposition of the Khromni Limestones in the Païkon Massif, regression ensued, resulting in a switch from shallow-marine to fully continental conditions and the deposition of the fluvial Ghrammos Formation. Although it is very likely that the sediments of the Ghrammos Formation were reworked from the underlying Kastaneri Formation and Khromni Limestones, it is unclear from which direction they were derived, as no palaeocurrent indicators remain.

In order for underlying rocks of the Kastaneri Formation and Khromni Limestones to be a source, some kind of relative uplift of the source region must have taken place. This uplift may have occurred in response to continued, regional-scale E0 extension in neighbouring areas (i.e. the formation of the Meglenitsa, Ano Garefi and western Guevgueli Ophiolites may still have been going on in the uppermost Jurassic or lowermost Cretaceous) or to more localised small-scale extensional faulting within the Païkon Massif.

As discussed in chapter 3, the Ghrammos Formation is likely be a more proximal equivalent to Mavrolokkos Flysch of the central Almopias subzone. The Ghrammos Formation and the Mavrolokkos Flysch have a similar age and both were largely

derived from a siliceous volcanic source (?the Kastaneri Formation of the Païkon Volcanic Group and/or the acidic volcanics of the Klissochori-Rhizarion block to the west) and deposited by a fluvial system.

7.3.8 - *Lower Cretaceous Compressional Deformation (JE2)?*

Vergely (1984) described a second phase of penetrative compressional deformation within the Païkon Massif, and indeed the Internal Hellenides as a whole, which was inferred to have taken place in the Lower Cretaceous; the JE2 event. This event was evidently characterised by SE-verging folds and affected only the Ghrammos Formation and underlying units. During the course of this work no evidence was discovered to support the existence of such a Lower Cretaceous compressional event, as all SE-verging structures observed within the Ghrammos and underlying formations affect the Cretaceous Transgressive Limestones, Buff Pelagic Carbonates and Tchouka Flysch, which are Aptian/Albian to Maastrichtian in age. These structures have therefore been attributed to Tertiary deformation (i.e. D2). The existence of a "JE2" compressional event of Lower Cretaceous age (Vergely, 1984) in the Païkon Massif was not confirmed during the course of this work. As described in chapter 4, this JE2 event has also been rejected in the Pelagonian and Almopias zones to the west (Sharp, 1995). Instead, tectonism during the uppermost Jurassic and Cretaceous periods was comparatively quiescent, and the sedimentary successions of the upper Païkon megasequence were deposited free of significant compressive stress.

7.3.9 - *Aptian/Albian Transgression*

Mercier (1986) described a major unconformity in the Païkon Massif between the Ghrammos Formation and the Cretaceous Transgressive Limestones, which was supported by Vergely's recognition of a JE2 event. However, the fluvial sediments of

the Ghrammos Formation are conformably overlain by the shallow-marine, platform carbonates of the Cretaceous Transgressive Limestones which are Aptian/Albian to Turonian in age. The global sea-level high stand responsible for this marine transgression continued throughout the Middle Cretaceous (Haq *et al.*, 1987). Both sides of the Païkon Massif posess identical platformal sequences, although those on the eastern flank are considerably more deformed than those on the west, and these limestones were, of course, deposited prior to the formation of the main Païkon anticline and were thus both part of a continuous platform which covered the whole of the Païkon Massif at this time.

The base of the Cretaceous Transgressive Limestone platform is Aptian/Albian in age and grades conformably up from the underlying Ghrammos Formation. It is marked by a basal calcarenitic unit which reaches up to 20 m in thickness. The calcarenites pass up into a nodular, lagoonal limestone unit, then the rest of the limestone succession above is dominated by neritic carbonates rich in shallow-marine benthic fauna. Similar carbonate platforms built up throughout the Hellenides at this time, for example in the southern Pelagonian zone (Argolis peninsula, Greece; Clift, 1990), the northern Pelagonian zone and western/central Almopias subzone (northern Greece; Sharp, 1995) and in western Turkey (the Menderes Metamorphic Massif and the Bey Daglari Unit; Dürr, 1976; Poisson, 1977; Collins, 1997).

7.3.10 - *Turonian Regional Extension and Platform Collapse*

During the Turonian, the Païkon Massif is interpreted to have been subjected to subaerial exposure due to a relative drop in sea-level, as evidenced by *Microcodium*-bearing ferruginous crusts at the top of the Cretaceous Transgressive Limestone platform. A subsequent relative sea-level rise, marked by a switch in sedimentation from platformal to pelagic, is then inferred to have taken place, with both western and eastern margins of the Païkon Massif recording identical deepening sequences. The Turonian stage is widely interpreted as a time of globally high sea-level (Haq *et*

al., 1987) and the transition from platform to basinal deposition throughout the Hellenides at this time may be, at least partly, a consequence of this phenomenon. However, considering the regional tectonic set-up in the Hellenides (and beyond) at this time, the Turonian deepening event cannot be solely attributed to eustasy. As described in chapter 4.3, this event, which is manifest in the Païkon Massif simply as a deepening event, is marked in other areas by syn-sedimentary faulting (i.e. the Kerassia Unit of the Pelagonian Sharp, 1995) and by rifting, sea-floor spreading and ophiolite genesis (i.e. in Argolis and Euboea; Clift, 1990; Robertson, 1990a), while subsidence on a regional scale has been documented throughout other parts of the Hellenides (Fleury, 1980; Thiebault, 1982; Harbury, 1986 and Robertson *et al.*, 1991). Similar platformal collapse sequences have also been described from outside the Hellenide belt at this time, for example in the Apennines of Italy (Montanari *et al.*, 1989; Bosellini, 1989). It is therefore likely that the Turonian deepening event reflects a phase of extensional tectonism of regional-significance (i.e. E1 of Brown & Robertson, in press), which occurred in conjunction with a global sea-level high-stand. Notably, this regional subsidence event predates the first evidence of compression-related flexural subsidence in the Internal (eastern) Hellenides of Early Tertiary age, i.e. D2 of Brown & Robertson (in press).

Therefore, the shallow-water carbonate platforms of the Hellenides, Apennines and Taurides persisted, without significant tectonic disturbance, until the Turonian, when regional-scale extension commenced and caused the widespread collapse of the neritic platforms and the deposition of deeper-water sediments and the formation of oceanic crust. This extensional event is also associated with a major extinction event (Kauffmann & Johnson, 1988; Scott, 1988).

7.3.11 - *Uppermost Cretaceous Flysch Deposition: Fault Scarp Degradation and Foreland Basin Formation.*

Some time later in the Upper Cretaceous (Maastrichtian) the Buff Pelagic Carbonates of the Païkon Massif were superseded by deep-water turbidites and radiolarite deposits (the Tchouka Flysch), which reflect the input of terrigenous clastic material into a deep-water basin. The redeposited sediments of the Tchouka Flysch were derived mostly from lithologies present in the underlying Païkon Massif, particularly the Kastaneri Formation, the Ghrammos Formation and the Cretaceous Transgressive Limestones, but some degree of input from an ophiolitic source is also evident.

Turbiditic flysch deposition largely reflects the generation of a flexural foredeep, generated due to the onset of ophiolite obduction in the early Tertiary (i.e. as a result of the D2 event). Such transition-to-flysch sequences (coupe de passage; Mercier, 1968) of similar age have been described from elsewhere in the Internal Hellenides, for example the Kipsari Passage Member of the Pelagonian zone (Sharp, 1995) and the early Tertiary transition from platform carbonates to flysch in the Argolis Peninsula (Clift, 1990). The flysch units in both of these areas are similarly interpreted to reflect foreland basin development due to Tertiary compression and ophiolite obduction.

7.3.12 - *Neohellenic Deformation: The D2 Event*

The second phase of compressive deformation to affect the Païkon Massif (D2) is characterised by west-verging brittle structures in the eastern Païkon Massif and east to northeast-verging brittle structures in the western Païkon Massif. The dual vergence of structures associated with D2 deformation is the result of coeval compression on the eastern and western sides of the study area. Vergely (1984) reported only westward vergence throughout the Païkon Massif during the Tertiary (CT1-2). During the D2 event, earlier, D1, ductile folds were re-folded about NNW-

trending brittle D2 fold axes and the whole of the Païkon Massif was upfolded into a broad, NNW-SSE-trending anticline.

Structural studies of the contact between the Païkon subzone and the adjacent Almopias subzone suggest that D2 contractional deformation in the western Païkon Massif results from northeastward overthrusting of the Meglenitsa Ophiolite onto the Païkon Massif (Sharp & Robertson, 1992; Sharp, 1995; Brown & Robertson, in press). It is proposed here that the westward vergence, which affects the eastern side of the Païkon Massif, was probably generated during westward overthrusting of the Guevgueli Ophiolite onto the eastern Païkon margin (Brown & Robertson, in press). The Païkon Massif thus behaved as a "pop-up" fold between two converging ophiolite units, and it is very likely that the present, regional-scale, NNW-SSE-trending Païkon anticline developed during this stage (Mercier, 1968; Vergely, 1984; Brown & Robertson, in press). Regionally, the D2 compressional event occurred in response to complete closure and suturing of Neohellenic ocean basins (resulting in ophiolite obduction) as Hellenic continental fragments (e.g. the Pelagonian block) began to accrete onto the southern margin of Eurasia.

This work confirms the importance of a Tertiary compressional event (D2) equivalent to the CT1-2 of Vergely (1984); however, the D2 event is more complex than previously proposed. Vergely (1984) documented that D2 (CT1-2) structures verge only towards the west throughout the Païkon Massif. In contrast, it has been shown here that only eastern parts of the Païkon Massif contain D2 structures with SW to NW vergence, while the whole of the western Païkon Massif is characterised by northeast-verging D2 structures. It is proposed, however, that the southeast-vergent JE2 structures described by Vergely (Figures 4.1 & 4.2) from the western Païkon Massif may actually be early Tertiary D2 structures which have been wrongly assigned to a Lower Cretaceous event.

7.3.13 - *Renewed Contraction in the later Tertiary: D3 Transpression*

Throughout the Cretaceous and Tertiary the entire southern margin of the Eurasian continent was characterised by active subduction (Robertson & Dixon, 1984). As the numerous Neotethyan ocean basins closed (e.g. the Vardar/Axios and Pindos oceans), the microcontinental blocks which now constitute Greece and Turkey were progressively accreted onto southern Eurasia. The northeastern Neotethyan oceans (Vardar/Axios) closed first, due to their relative proximity to the Eurasian continent, and the deformation associated with their closure propagated southwestward as the ophiolitic suture zones locked up. The Vardar/Axios ophiolites closed in the early Tertiary (causing the D2 event in the Païkon Massif) therefore deformation was transferred to the more southwesterly Pindos ocean, which did not close until the Eocene (Degnan, 1992). It is postulated here that final closure of the Pindos ocean and docking of the Apulian continent with Eurasia caused the later Tertiary D3 event in the Païkon Massif. After Eocene suturing of the Pindos ocean, deformation was transferred to the Ionian zone, which is still being actively deformed. This on-going deformation is related to subduction along the Hellenic arc-trench system located to the south and west of Crete (Robertson *et al.*, 1991).

The D3 deformation event in the study area produced a SSW-trending mylonite fabric along the Païkon-Guevgueli contact and associated stretching lineations and SSW-verging folds developed throughout the Païkon Massif. These late-stage structures were formed under a dextral transpressional regime, induced by post-suture "tightening" along the Païkon-Guevgueli contact.

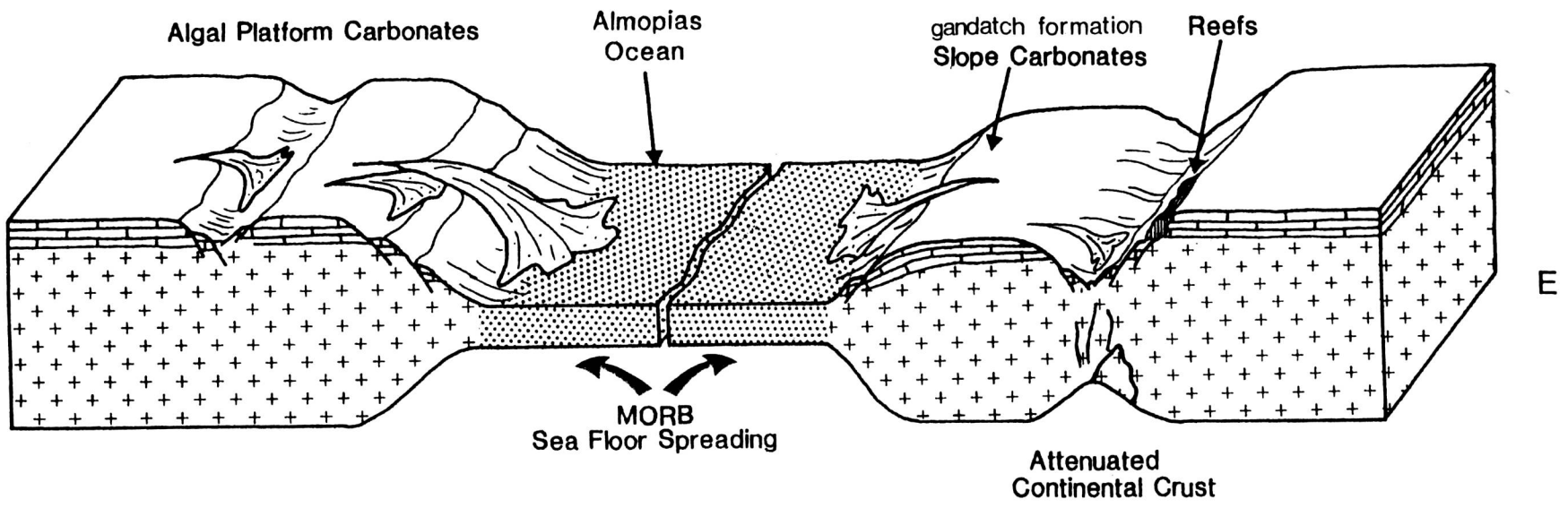
7.3.14 - *Neotectonic Extension*

The most recent event to affect the Païkon Massif is a series of Neotectonic extensional/transtensional events (E2) that commonly exploit older structures. In many parts of the Internal Hellenides, including the Voras Massif, this extensional

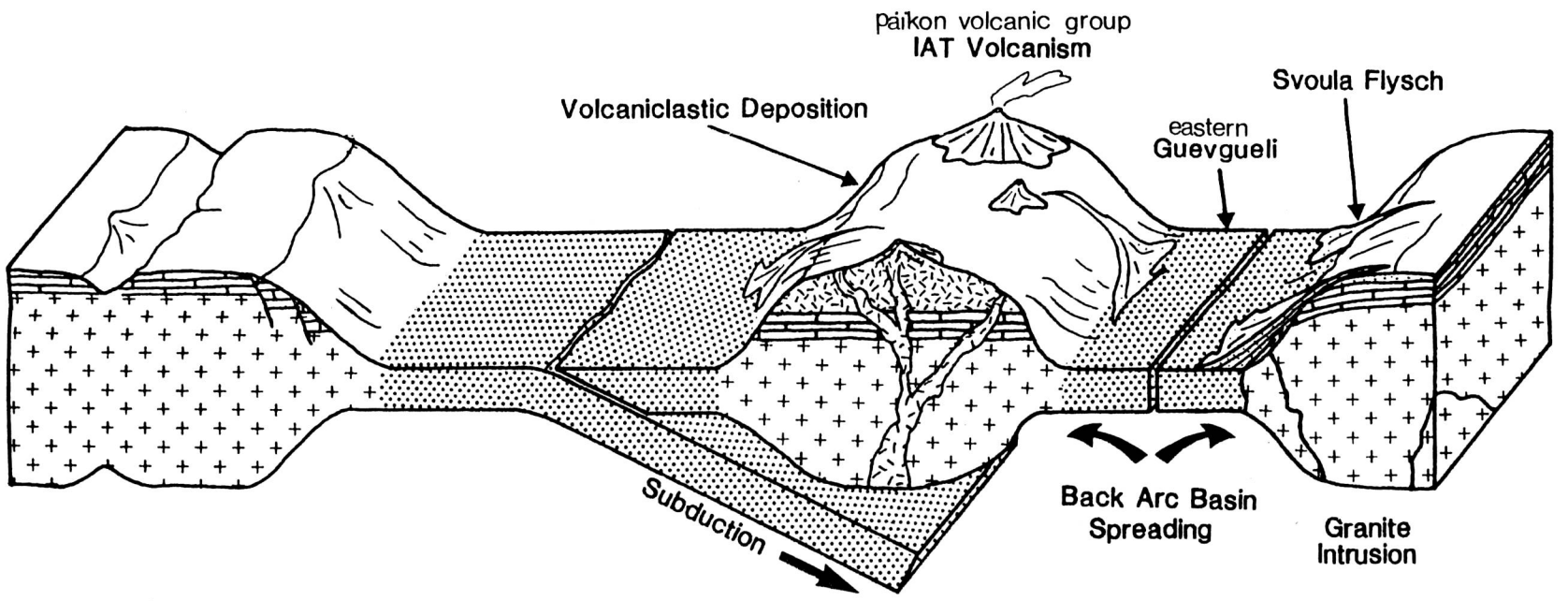
FIGURE 7·2 - CARTOONS SHOWING THE TECTONIC EVOLUTION OF THE PAÏKON MASSIF

PELAGONIAN | ALMOPIAS | PAÏKON | PEONIAS | SERBO-MACEDONIAN

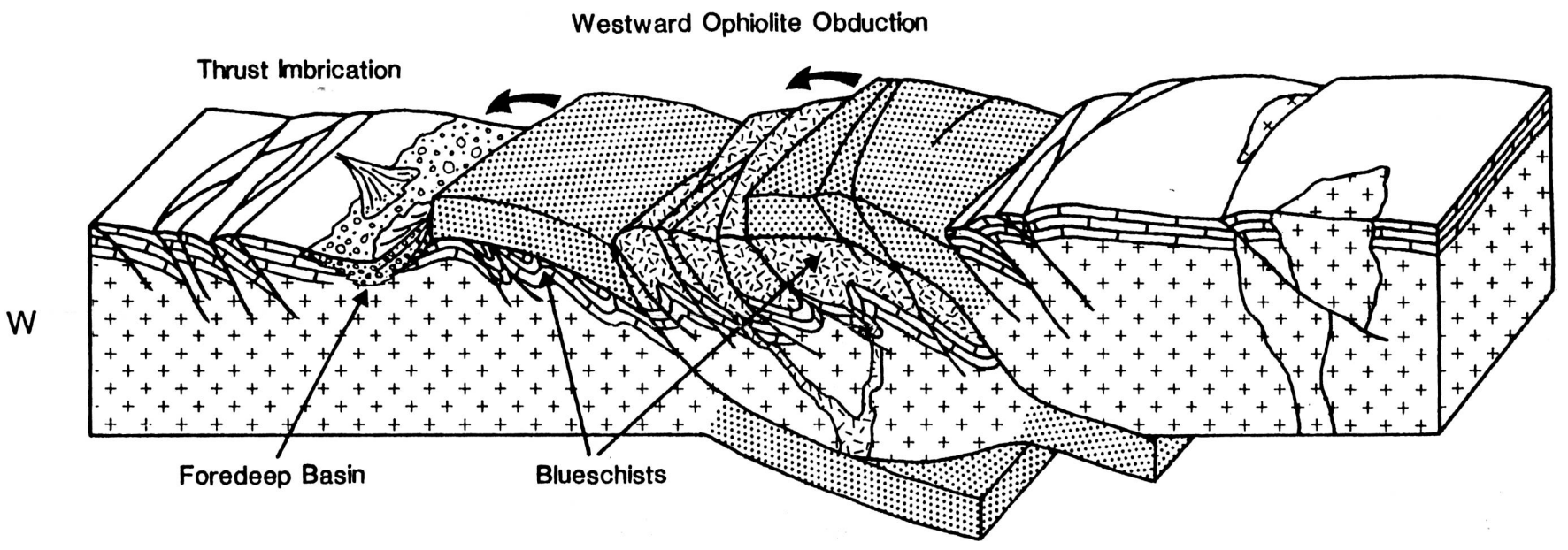
A TRIASSIC - LOWER JURASSIC



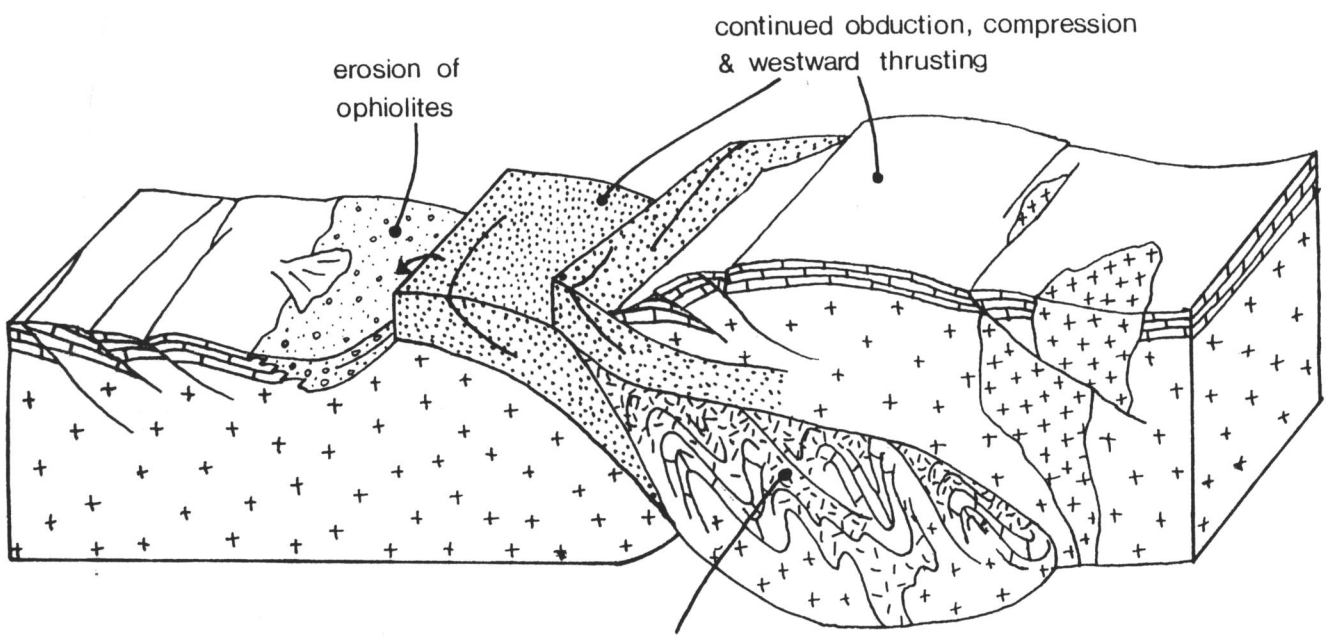
B. MID - UPPER JURASSIC



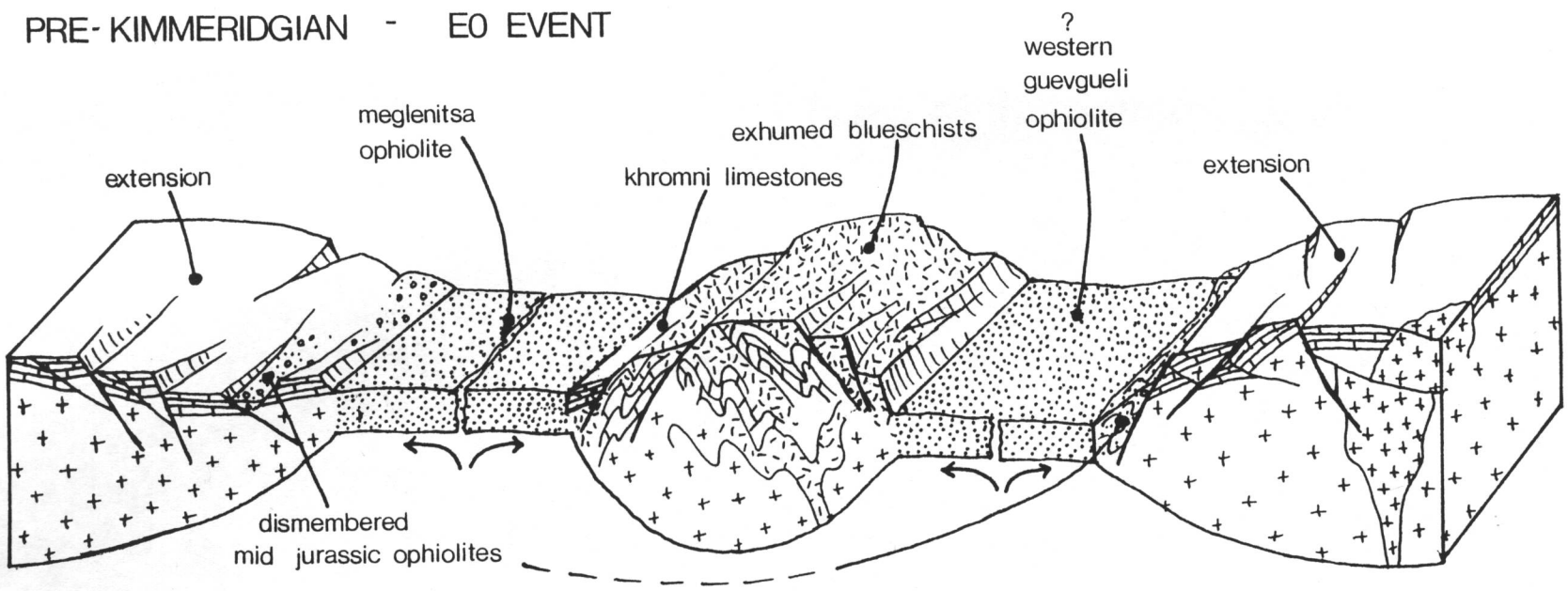
C EARLY UPPER JURASSIC



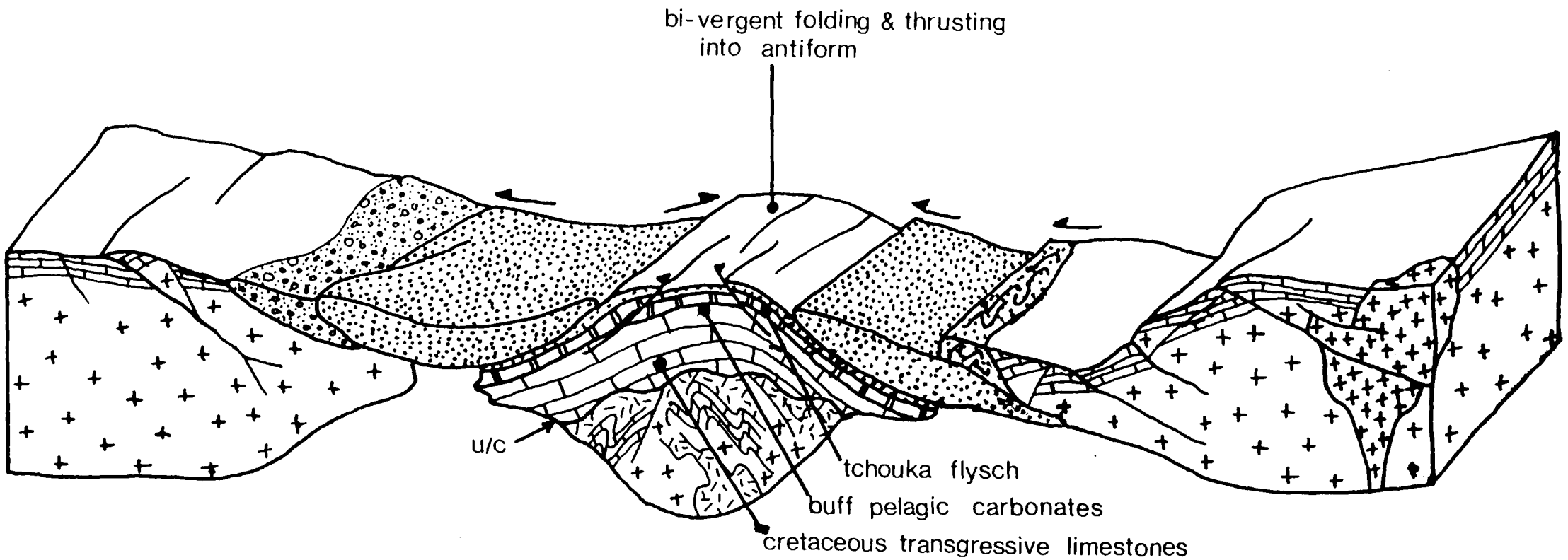
D UPPER JURASSIC - D1 EVENT



E PRE-KIMMERIDGIAN - E0 EVENT



F TERTIARY - D2 EVENT



Limestones. A major unconformity separates these two stratigraphic units. The Meglenitsa, Ano Garefi and possibly western Guevgueli Ophiolites formed during this extensional event (Figure 7.2D).

5 - Relative sea-level drop resulted in deposition of the fluvial Ghrammos Formation, which was then conformably overlain by the platform carbonates of the Cretaceous Transgressive Limestones. No regional compressional event of Lower Cretaceous age (JE2) was identified in the Païkon Massif.

6 - Renewed extension in the Turonian (E1) resulted in collapse of the Cretaceous carbonate platform and the deposition of the Buff Pelagic Carbonates. The Tchouka Flysch was then deposited in a flexural foreland basin formed due to the initiation of Tertiary deformation.

7 - D2 compression then followed in the early Tertiary due to the final closure and suturing of the ocean basins in the Almopias and Peonias subzones. The ophiolitic rocks of the Almopias subzone were overthrust onto the western margin of the Païkon Massif and the Guevgueli ophiolite was thrust onto the eastern Païkon margin. The Païkon Massif was thus folded into a large NNW-SSE-trending anticline and underwent bi-vergent brittle deformation (Figure 7.2E).

8 - Closure of the more southwesterly Pindos ocean in the Eocene caused dextral transtensional tectonism (D3) along the already-sutured Païkon-Guevgueli contact.

9 - E2 Neotectonic extension in the Païkon Massif is a result of on-going subduction in the Hellenic trench/arc/back-arc system to the south.

7.5 - WIDER IMPLICATIONS

The significant arc system of the Païkon and Voras Massifs is the only unit of its kind described from the Hellenide orogenic belt. This fact has great implications for potential palaeogeographic reconstructions of this part of the Tethyan region. The presence of a volcanic arc associated with the subduction of the Neotethyan Vardar/Axios Ocean implies that this ocean basin was wide enough, and its subduction sustained for long enough, to generate melting in the mantle wedge for a period in the order of 20 to 30 million years. The presence of the arc in this particular area also implies that the Vardar/Axios Ocean formed *in situ* and is not likely to have been transported into its present geographical position due to subsequent tectonic processes. The *in situ* generation of the Guevgueli back-arc basin, which formed between the Païkon arc *sensu strico* and the remnant arc (Chortiatis Group), also supports the idea of a wide, *in situ* Vardar/Axios ocean during the Jurassic.

An equivalent unit to the Païkon Massif of the Internal Hellenides may be the Çangaldag Complex of the Pontides in northern Turkey (Ustaömer, 1993). The Çangaldag Complex is of similar age to the volcanic rocks of the Païkon Massif and is also inferred to be of arc affinity. Should these units be equivalent, which is likely, this work can be used to further the correlations already suggested between the tectonostratigraphic zones of Greece and Turkey.

Structural data collected during this study do not support the presence of a compressional JE2 event of Lower Cretaceous age. This event was previously inferred to pervasively affect the entire Hellenide region and, therefore, its refutation in the Païkon subzone, and also in the Almopias subzone and the Pelagonian zone, has profound implications for the tectonic evolution of this part of the Tethyan belt.

Finally, the recognition of transtensional and transpressional structures within the Païkon Massif, and neighbouring areas of the Vardar/Axios zone, during the Cretaceous and Tertiary, strongly suggest that this region was dominated by strike-

slip processes throughout much of its Mesozoic history. This again has strong connotations concerning palaeogeographic reconstructions of the Tethyan realm.

7.6 - POSSIBLE FUTURE WORK

Despite the significance of the new data collected and presented during the course of this study, geological investigations, which were outside the scope of this particular research project, may be very beneficial to furthering our understanding of the tectonic evolution of the Vardar/Axios zone and the Hellenic orogen as a whole. Detailed structural, sedimentological, palaeontological and geochemical work would be of great benefit in the Voras Massif, and tracing the Païkon/Voras volcanic arc into Former Yugoslavia may prove invaluable.

References

References

Aktas, G. and Robertson, A.H.F. 1984. The Maden Complex, SE Turkey; Evolution of a Neotethyan active margin. In: The Geological evolution of the eastern Mediterranean. (Dixon, J.E., Editor et al). Geol. Soc. Spec. Publ. 17, 373-402.

Aramaki, S. and Ui, T. 1982. Orogenic andesites and related rocks. In: Thorpe, R.S. (Editor). Andesites, John Wiley and Sons.

Aubouin, J. 1959. Contribution a l'étude géologique de la Gréce Septentrionnale: Les confins de l'Epire et de la Thessallie. Ann. géol. pays Héll., 10. 483pp.

Aubouin, J., Bonneau, M., Celet, P., Charvet, J., Clement, B., Degardin, J.M., Dercourt, J., Ferriere, J., Fleury J.J., Guernet, C., Maillot, H., Mania, J., Mansy, J.L., Terry, J., Thiebault, P., Tsoflias, P., and Verrieux, J.J. 1970 Contribution à la géologie des Hellenides: Le Gavrovo, le Pinde et al Zone Ophiolitique Subpelagonian. Annales de la Societé Géologique du Nord, 90, 277-306.

Aumento, F. and Loubat, H. 1971. The Mid-Atlantic ridge near 45°N; XVI, Serpentinised ultramafic intrusions. Canadian Journal of Earth Sciences. 8(6), 631-663.

Baroz, F., Bebien, J. and Ikenne, M. 1987. An example of high-pressure low-temperature metamorphic rocks from an island-arc: the Paikon Series (Innermost Hellenides, Greece). Journal of Metamorphic Geology. 5, 509-527.

Bathurst, R.G.C. 1995. Burial diagenesis of limestones under simple overburden. Stylolites, cementation and feedback. Bull. Soc. Geol. France., t. 166 (2), 181-192.

Batty, S.J. 1993. Structural and tectonic evolution within the envelope and margins of the Volvi Complex, N.E. Greece. Unpublished Ph.D. thesis. University of Edinburgh. 439pp.

Baumgartner, P.O. 1985. Jurassic sedimentary evolution and nappe emplacement in the Argolis Peninsula (Peloponnesus, Greece). Memoire de la Societé Helvetique pour la Science Naturelle, p.111.

Beaumont, C. 1981. Foreland Basins. Geophysical Journal of the Royal Astronomical Society, 65, 291-329.

Bebien, J. 1977. Mafic and ultramafic rocks associated with granites in the Vardar zone. Nature, 270, 232-233.

Bebien, J. 1982. L'association ignée de Guevgueli (Macedoine Grèque): Expression d'un magmatisme ophiolitique dans une déchirure continentale. Thèse présentée a l'Université de Nancy. 470pp.

Bebien, J. and Mercier, J. 1977. Le carde structural de l'association ophiolites-migmatites-granites de Guévgueli (Macédoine, Grèce): Une croûte de bassin inter-arc? Bull. Soc. Géol. Fr., (7), XIX, 927-934.

Bebien, G. and Gagny, C. 1978. Influence de phenomenes de decrochement sur l'organisation du magmatisme dans l'association ophiolites-granites de Guevgueli

(zone du Vardar, Macedoine, Grecque). C. R. Acad. Sci. Paris, 286, serie D, 815-818.

Bebien, J., Dubois, R. and Gauthier, A. 1986. Example of ensialic ophiolites emplaced in a wrench zone: innermost Hellenic ophiolite belt (Greek Macedonia). Geology, 14, 1016-1019.

Bebien, J. Baroz, F., Capedri, S. and Ventureli, G. 1987. Magmatismes basiques associés a l'ouverture d'un bassin marginal dans les Hellénides internes au Jurassic. Ofioliti, 12, 53-71.

Bebien, J., Platevoet, B. and Mercier, J.-L. 1994. Geodynamic significance of the Paikon Massif in the Hellenides. Contribution of the volcanic rock studies. . 7th Cong. Geol. Soc. Greece. Thessaloniki, May, 1994. Abstracts p41

Bebien, J., Platevoet, B. and Mercier, J.-L. In press. Geodynamic significance of the Paikon Massif in the Hellenides. Contribution of the volcanic rock studies. Bull. Geol. Soc. Greece.

Beccaluva, L., Ohnenstetter, D. and Ohnenstetter, M. 1979. Geochemical discrimination between ocean-floor and island arc tholeiites-application to some tholeiites. Can. J. Earth Sci., 16, 1874-1882.

Bernouilli, D. and Weissert, H. 1985. Sedimentary fabrics in Alpine ophicalcites, South Pennine Arosa zone, Switzerland. Geology, 13, 755-758.

Best, M.G. 1982. Igneous and metamorphic petrology. W.H. Freeman and Co., San Fr., C.A., U.S.A., 630pp.

Bloxham, T.W. and Lewis, A.D. 1972. Ti, Zr and Cr in some British pillow lavas and their petrogenetic affinities. Nature, Phys. Sci., 237, 134-136.

Bogoch, R. 1987. Classification and genetic models of ophicarbonate rocks. Ofioliti, 12(1), 23-36.

Bonatti, E. et al. 1974. Ultramafic carbonate breccias from the equatorial mid-Atlantic ridge. Marine Geology, 16, 83-102.

Bonneau, M., Godfriaux, I, Moulas, I., Fourcade, E. and Masse, J.P. 1994. Imbricate structure of the Paikon window (Macedonia, Greece). New biostratigraphical data. - 7th Congr. geol. Soc. Greece, Thessalonique, Abstract, p. 43.

Bonneau, M., Godfriaux, I., Moulas, Y., Fourcade, E. and Masse, J-P. in press. Stratigraphie et structure de la bordure orientale de la double fenetre du paikon (Macédoine, Grèce). Bull. Geol. Soc. Greece., No. 7.

Borsi, S., Ferrara, G. and Mercier, J. 1966. Mesure d'age par la methode Rb/Sr des granites filoniens de Karathodoro (zones internes des Hellenides, Macedoine centrale, Grece). Cong. des geol. Yougoslaves, 2, 5-10.

Bosellini, A. 1989. Dynamics of Tethyan carbonate platforms. In controls on carbonate platform and development, SEPM Spec. Publ. No. 44, 3-13.

Bouma, A.H. 1962. The sedimentology of some flysch deposits. Elsevier, Amsterdam.

Bouma, A.H., Normark, W.K. and Barnes, N.E. 1985. Deep sea fans and related turbidite sequences. Springer-Verlag.

Brown, S. and Robertson, A.H.F. 1994. New structural evidence from the Mesozoic-Early Tertiary Paikon Unit, north-eastern Greece. 7th Cong. Geol. Soc. Greece. Thessaloniki, May, 1994. Abstracts p45.

Brown, S. and Robertson, A.H.F. in press. New structural evidence from the Mesozoic-Early Tertiary Paikon Unit, north-eastern Greece. Bull. Geol. Soc. Greece.

Brown, S., Sharp, I. and Robertson, A.H.F., in prep. Tecton-stratigraphic evolution and significance of the Voras massif, Eastern Hellenides, Macedonia (NW Greece).

Brunn, J.H. 1956. Etude géologique du Pinde septentrional et de la Macédonie occidentale. Annales Géologiques des Payes Hélleniques, 8, 1-358.

Brunn, J. 1959. Zone du Vardar et zone Pélagonienne en Grece. C. R. Somm. Soc. Géol. Fr., 6, 138-139.

Cann, J.R. 1970. Rb, Sr, Y, Zr, Nb in some ocean-floor baslatic rocks. Earth and Planetary Science Letters, 10, 7-11.

Cas, R.A.F. and Wright, J.W. 1987. Volcanic successions, modern and ancient; a geological approach to process, products and successions. Allen and Unwin, London, U.K., 578pp.

Celet, P. 1962. Contribution à l'étude geologique du Parnasse-Kiona et d'une partie des régions méridionales de la Grèce continentale. Annales Géologiques des Pays Helléniques, tome XIII, p. 425.

Celet, P. and Ferrière, J. 1978. Les Héllenides interne: Le Pélagonien. Eclogae Geologicae Helvetiae, 73, 467-495.

Clews, J., 1989. Structural controls on basin evolution: Neogene to Quaternanry of the Ionian zone, western Greece. J. Geol. Soc. Lond., 146, 447-457.

Clift, P.D. 1990. Mesozoic/Cenozoic sedimentation and tectonics of the southern Greek Neothethys (Argolis Peninsula). Unpub. Thesis. Univ. Edinburgh. 336pp.

Clift, P.D. 1992. The collision tectonics of the southern Greek Neotethys. Geologische Rundachau, 81, 669-679.

Clift, 1993. The tectonic evolution of vocanic arcs and marginal basins. Post-doctoral final report, University of Edinburgh (1990-1993).

Clift, P.D. and Robertson, A.H.F. 1989a. Tectonic reinterpretation of the Argolis (South Hellenides) in the light of isopic zone and terrane hypotheses. Terra Abstracts, 1, No.1, European Union of Geosciences V, Strasbourg, March 1989, 57.

Clift, P.D. and Robertson, A.H.F. 1990b. A Cretaceous Neotethyan carbonate margin in Argolis, southern Greece. Geological Magazine,

Cole, J.W. 1981. Genesis of lava of the Taupo volcanic zone, North Island, New Zealand. J. Volcanol. Geotherm. Res. 1, 317-337.

Collins, A.S. 1997. Tectonic evolution of Tethys in the Lycian Taurides, southwest Anatolia. Unpublished PhD thesis, University of Edinburgh. 458pp.

Collins, A.S. and Robertson, A.H.F. 1997. Lycian melange, southwestern Turkey: An emplaced Late Cretaceous accretionary complex. Geology, 25(3), 255-258.

Collinson, J.D. 1986. Alluvial sediments. In: Sedimentary environments and facies, Reading, H.G. (ed). Blackwell Scientific Publications, U.K. 20-54.

Cook, H.E. 1983. Ancient carbonate platform margins, slopes and basins. In: Carbonate depositional environments. Scholle, P.A., Debout, D.G. and Moore, CH. (eds). AAPG memoir 33, Tulsa,

Cook, H.E. and Mullins, H.T. 1983. Basin Margins. In: Carbonate depositional environments. Scholle, P.A., Debout, D.G. and Moore, CH. (eds). AAPG memoir 33, Tulsa, 539-618.

Cook, H.E., McDaniel, P.N., Mountjoy, E.W. and Pray, L.C. 1972. Allochthonous carbonate debris flows at Devonian bank ("reef") margins, Alberta, Canada. Bull. Can. petrol. Geol., 20, 439-497.

Crevello, P.D. 1978. Sedimentary record of longitudinal transport in late Pleistocene-Holocene of Bahamian Trough [abstr.]: Am. Assoc. Pet. Geol., Bull., 62(3), 507-508.

Crevello, P.D. and Schlager, W. 1980. Carbonate debris sheets and turbidites, Exuma Sound, Bahamas. Journal of Sedimentary Petrology, 50(4), 1121-1147.

Danelian, T., Robertson, A.H.F. and Dimitriadis, S. 1996. Age and significance of radiolarian sediments within basic extrusives of the marginal basin Guevgueli Ophiolite (northern Greece). Geological Magazine, 133 (2), 127-136.

De Wet, A.P. 1989. Geology of part of the Chalkidiki Peninsula, Northern Greece. Unpub. Thesis, Cambridge Univ.

Dewey, J.F., Pitman, W.C. III, Ryan, W.B.F. and Bonnin, J. 1973. Plate tectonics and the evolution of the Alpine system. Bulletin of the Geological Society of America, 84, 3137-3180.

Dercourt, J., Ricou, L.E. and Vrielynck, B. (eds) 1993. Atlas Tethys Plaeoenvironmental Maps, Beicip-Franlab, 1992.

Degnan, P.J. 1992 Tectono-sedimentary evolution of a passive margin: The Pindos zone of the NW Peloponnese, Greece. Unpub. Thesis, Univ. Edinburgh. 400pp.

Dercourt, J., Zonenshain, L.p>, Ricou, L.E. Kazmin, V.G., Le Pichon, X., Knipper, A.L., Grandjacquet, C., Sborrrtshikov, I.M., Geyssant, J., Lepvrier, C., Pechersky, D.H., Boulin, J., Sibuet, J.C., Savostin, L.A., Sorokhtin, O., Westphal, M., Bazhenov, M.L., Laver, J.P., and Biju-Duval, B. 1986. Geological Evolution of the Tethys Belt from the Atlantic to the Pamirs since the Lias. Tectonophysics, 123, 241-315.

Dimitriadis, S. and Asvesta, A. 1993. Sedimentation and magmatism related to the Triassic rifting and later events in the Vardar-Axios zone. Bull. Geol. Soc. Greece. Vol. XXV111/2, 149-168.

Dimitriadis, S., Zahariadou, S. and Asbesta, A. 1994. Involvement of asthenospheric, lithospheric and subduction components in the generation of basalts at a back-arc marginal basin setting. The late Jurassic dykes of Piyi-Latomi-Evzoni (Guevgueli complex) Greek Macedonia. 7th Cong. Geol. Soc. Greece. Thessaloniki, May, 1994. Abstracts p48.

Dimitriadis, S., Zahariadou, S. and Asbesta, A. in press. Involvement of asthenospheric, lithospheric and subduction components in the generation of basalts at a back-arc marginal basin setting. The late Jurassic dykes of Piyi-Latomi-Evzoni (Guevgueli complex) Greek Macedonia. Bull. Geol. Soc. Greece.

Dimitrijevic, M.D. and Dimitrijevic, M.N. 1976. The polyphase melangs of the Vardar zone. Bull. Geol. Soc. France, (7), t XVIII, N2, 205-208.

Dinter, D.A. 1994. Tertiary structural evolution of the southwestern Rhodope metamorphic province: A fundamental revision. 7th Congr. geol. Soc. Greece, Thessaloniki, abstract volume, 71.

Dixon, J.E. and Dimitriadis, S. 1984. Metamorphosed ophiolitic rocks from the Serbo-Macedonian zone, near Lake Volvi, north-east Greece. In: The geological evolution of the eastern Mediterranean. Spec. Pub. Geol. Soc. Lond., 17, 603-619.

Donovan, D.T. 1966. Stratigraphy; an introduction to principles. Thomas Murby and Co., London, 199pp.

Dürr, S., Altherr, R., Keller, J., Okrusch, M and Siedel, E. 1978. The median Aegean Crystalline belt: Stratigraphy, structure, metamorphism, magmatism. In: Alps, Apennines, Hellenides (Cloos, H., Roeder, D. and Schmidt, K., editors). Schweizerbart'sche Verlagsbuchandlung, Stuttgart.

Einsele, G. 1992. Sedimentary basins, evolution, facies and sedimentary budget. Springer Verlag. 627pp.

El-Shazly, A.K. and Coleman, R.G. 1990. Metamorphism in the Oman Mountains in relation to the Semail ophiolite emplacement. In: The geology and tectonics of the Oman Region (Robertson, A.H.F. convenor, et al.). Geol. Soc. Spec. Publ., 49, 473-493.

Escher, A. and Watterson, J. 1974. Stretching fabrics, folds and crustal shortening. Tectonophysics, 22, 223-231.

Ferriere, J. 1974. Etude géologique d'un secteur des zones helléniques internes subpelagonienne et pelagonienne (massif de l'Othrys-Grece continentale). Importance et signification de la période orogénique anté-Crétacé superieur. Bulletin de la Société Géologique de France, XVI, 543-562.

Ferriere, J. 1976. Sur la signification des séries du massif de l'Othrys (Grèce continental): la zone isopique maliaque. Annales de la Societé Géélogique de Nord, 96, 121-134.

Filbrandt, J. 1985. Tectonic evolution of the Vardar Zone in Chalkidiki, northeastern Greece. PhD Thesis, University of Wales.

Fisher, R.V. and Scmincke, H-U. 1984. Pyroclastic rocks. Springer-Verlag, Berlin, Federal Republic of Germany, 477pp.

Fitton, J.G. and Dunlop, H.M. 1985. The Cameroon line, West Africa, and its bearing on the origin of oceanic and continental alkali basalts. Earth and Planetary Science Letters, 72, 23-38.

Fleury, J.-J. 1980. Les zones de Gavrovo-Tripolitza et du Pinde-Olonos (Grèce continentale et Péloponnese do Nord). Evolution d'une platforme et d'un bassin dans le cdre alpin. Societé Géologique du Nord, publication, 4, p. 645. Villeneuve d'Ascq.

Floyd, P.A. and Winchester, J.A. 1975. Magma type and tectonic setting discrimination using immobile elements. Earth and Planetary Science Letters, 27, 211-218.

Galeos, A., Pomoni-Papaioannou, F., Tsaila-Monopolis, S., Turnsek, D. and Ioacim, Chr. 1994. Upper Jurassic-Lower Cretaceous "molassic-type" sedimentation in the western part of the Almopia subzone, Aridhea Loutra Unit (northern Greece). 7th Cong. Geol. Soc. Greece. Thessaloniki, May, 1994. Abstracts p 54.

Garson, M.S. and Mitchell, A.H.G. 1977. Mineralisation at destructive plate boundaries: A brief review. In: Volcanic processes in ore genesis (anaonymous), 81-97. Inst. Mining. Metallurgy, London, U.K.

Gill, J. 1981. Orogenic andesites and plate tectonics. A. El Goresy and W. Von Engelhardt (eds), 390pp

Godfriaux, I. and Ricou, L.E. 1991. Le Paikon, une fenêtre dans les Hellénides Internes (Macédoine, Gréce). C. R. Acad. Sci. Paris, 1. 313, Serie II, 1479-1484.

Green, T.J. 1982. Structural and sedimentological studies of the Pindos Zone, central Greece. Unpublished Ph.D. thesis, University of Cambridge.

Haenel-Remy, S. and Bebien, J. 1985. The Oreokastro Ophiolite (Greek Macedonia): an important component of the innermost Hellenic ophiolite belt. Ofioliti, 10, 279-296.

Haenel-Remy, S. and Bebien, J. 1987. Basalts et dolerites riches en magnesium dans l'association ignee de Guevgueli (Macedoine Greque): les temoins d'une evolution depuis des tholeiites abyssales jusqu'a des basaltes continentaux? Ofioliti, 12 (1), 91-106.

Hague, P.F. 1993. The structural and volcanic evolution of Tertiary basins along the southern margin of the Rhodope Massif, NE Greece. Unpub. Thesis Univ. of Southampton. 227pp.

Hall, R. 1988. Basement and cover rock history in western Tethys: HT-LP metamorphism associated with extensional rifting of Gondwana. In Audley-Charles, M. and Hallam, A. (eds) Gondwana and Tethys. Geol. Soc. London Spec. Publ., 37, 41-50.

Hanmer, S. and Passchier, C.W. 1991. Shear sense indicators: A review. Geological survey of Canada, special paper 90, 1-71.

Haq, B.U., Hardenbol, J. and Vail, P.R. 1987. Chronology of fluctuating sea levels since the Triassic. Science, 235, 1156-1167.

Harbury, N. 1986. The stratigraphy and structural evolution of the SE Aegean. Unpub. Thesis, Unversity of London.

Harker, A. 1909. The natural history of igneous rocks. New York: Macmillan.

Hedberg, H.D. 1976. International Stratigraphic Guide. Wiley. New York.

Hodges, Bartley and Burchfiel. 1982. Structural evolution of an A-type subduction zone, Lofoten Rombak area, Northern Scandinavian Caledonides. Tectonics, 1, 441-462.

Jackson, J.A., Gagnepain, J., Houseman, G., King, G., Papadimitriou, P., Soufleris, S. and Virieux, J. 1982. Seismicity, normal fault faulting and the geomorphological evolution development of the Gulf of Corinth (Greece): the Corinth earthquakes of February and March 1981. Earth and Planetary Science Letters, 57, 377-397.

Jacobshagen, V. and Wallbrecher, E. 1984. Pre-Neogene nappe structure and metamorphism of the North Sporades and the southern Pelion peninsula. In: Dixon, J.E. and Robertson, A.H.F. (eds). The geological evolution of the Eastern Mediterranean. Geol. Soc. London Spec. Publ., 17, 591-602.

James, N.P. 1983a. Reef. In: Carbonate depositional environments, Schole, P.A., Debout, D.G. and Moore, CH (eds), AAPG memoir 33.

James, N.P. and Ginsburgh, R.N. (eds) 1979. The seaward margin of Melize barrier and atoll reefs; morphology, sedimentology, organism distribution and Late Quaternary history. Int. Assoc. Sedimentol. Spec. Publ. No. 3, 191pp.

Jenkyns, H.C. 1986. Pelagic Environments. In Reading, H.G. (Editor), Sedimentary Facies and Environments and Facies, second edition, Blackwells Scientific Publications, Oxford.

Johns, D.R. 1978a. The geology of the area around Galaxidion, central Greece. Unpublished Ph.D. thesis, University of Cambridge, p.276.

Jolivet, L., Daniel, J-M., Truffert, C. and Goffe, B. 1994. Exhumation of deep crustal metamorphic rocks and crustal extension in back-arc regions. In: Tectonics, metamorphism and magmatism in island arcs (Arculus, R.J. editor et al). Lithos, 33(1-3), 3-30.

Jones, G. 1990. Tectono-stratigraphy and evolution of the Mesozoic Pindos ophiolite and associated units, northwestern Greece. Unpub. Thesis, University of Edinburgh. 397pp.

Jung, D. and Mussallam, K. 1984. The Sithonia ophiolite; a fossil oceanic crust [abstr.]. In: Ophiolites through time; a comparison of ophiolitic basic-ultrabasic associations from Proterozoic to Late Cainozoic. Ofioliti, 9 (Suppl.). p35. Third

annual meeting of the Working Group on Mediterranean ophiolites, Nancy, France.

Jung, D. and Mussallam, K. 1985. The Sithonia ophiolite: a fossil oceanic crust. Ofioliti, 10, 329-342.

Jung, D., Mussallam, K., Burgath, K., Kockel, F., Mohr, G. and Raschka, H. 1979. Minerology and geochemistry of the Chalkidiki makic-ultramafic rocks. Abstr. Internat. Ophiolite symposium, Nicosia (Cyprus), 40-41.

Jung, D., Mussallam, K., Burgarth, K., Kockel, H., Mohr, F. and Raschka, H. 1980. Ultramafic and related rocks of Chalkidiki (northern Greece) [abstr.]. In: An international symposium on metallogeny of mafic and ultramafic complexes: the eastern Mediterranean - western Asia area, and its comparison with similar metallogenic environments in the world. UNESCO, Natl. Tech. Dep. Miner-Petrogr-Geol., Athens, Greece, 50pp.

Karig, D.E. 1971. Origin and development of marginal basins in the western Pacific. Journal of Geophysical Research, 76, 2542-2561.

Kaufman, E.G. and Johnson, C.C. 1988. The morphological and ecological evolution of Middle and Upper Cretaceous reef-building rudists. Palios, 1988, reffs issue V.3., 124-216.

Kauffmann, G., Kockel, F. and Mollat, H. 1976. Notes on the stratigraphic palaeogeographical position of the Svoula Formation in the innermost zone of the Hellenides (Northern Greece). Bull. Soc. Geol. Fr., 18, VII, 225-230.

Ketin, I. 1966. Tectonic units of Anatolian Asia Minor (in Turkish), MTA Bull., v66, 20-34.

Kockel, F., Mollat, H. and Walther, H.W. 1977. Erlauterungen zur geologischen karte der Chalkidiki und angrenzender Gebiete 1:100000 (Nord Griechenland). Bundesanstalt fur Geowissenschaften und rohstoffe, Hannover.

Kolocotroni, C.N. and Dixon, J.E. 1991. The emplacement and generation of I-type granites during extension: The Oligocene Vrondou pluton, NE Greece. Terra abstracts, Vol. 3, N1, 40-41.

Kosmatt, F. 1924. Geologie der zentral Balkenhalbinsel, mit uebersicht des dinarischen Gebirgsbaues. Die kriegschauplatze 1914-1918, geologisch dargestellt, 12, 198pp.

La Gabrielle, Y. and Auzende, J-M. 1982. Active in-situ disaggregation of oceanic crust and mantle on Gorringe Bank: Analogy with ophilitic massifs. Nature, 297, 490-493.

Le Metour, J., Rabu, P., Tegyey, M., Bechennec, F., Beurrier, M. and Villey, M. 1990. Subduction and obduction: two stages in the Eo-Alpine tectonometamorphic evolution of the Oman Mountains. In: The Geology and Tectonics of the Oman Region (Robertson, A.H.F., convenor, et al.). Geol. Soc. Spec. Publ., 49, 327-339.

Le Pichon, X. and Angelier, J. 1979. The Hellenic arc and trench system: a key to the neotectonic evolution of the eastern Mediterranean area. Tectonophysics, 60, 1-42.

Leeder, M.R. 1982. Sedimentology, process and product. George Allen & Unwin.

Ligdas, C.N., Main, I.G. and Adams, R.D. 1990. 3-D velocity structure and constraints on the nature of the coupled subduction-spreading process in the Aegean area from seismic tomography. Tectonophysics, Symposium S2, 25th General Assembly of IASPEI.

Logan, B.W., Harding, J.L., Alu, W.M., et al. 1969. Carbonate sediments and reefs, Yucatan Shelf, Mexico; Part 1, Late Quaternary carbonate sediments of Yucatan shelf, Mexico. Amm. Ass. Petrol. Geol. Mem. No. 11, 5-128.

Loughnan, F.C. 1969. Chemical weathering of the silicate minerals. American Elsevier, New York.

Makris, J. 1977. Geophysical investigations of the Hellenides. Hamburger Geophysik Einzelschriften, 34, Reiche A, 0-244.

McKenzie, D.P. 1978a. Some remarks on the development of sedimentary basins. Earth and Planetary Science Letters, 40, 25-32.

McKenzie, D.P. 1978b Active tectonics of the Alpine-Himalayan Belt: The Aegean sea and surrounding regions. Geophysical Journal of the Royal Astronomical Society, 55, 217-254.

Mercier, J. 1966. Paléogéographie, orogenèse, métamorphisme et magmatisme des zones internes des Héllénides en Macédonie (Grèce): vue d'ensemble. Bulletin de Societé Géologique de France, 8, 1020-1049.

Mercier, J. 1968. Etude géologique des zones Hellénides en Macédoine centrale (Grèce). Thèse. Ann. géol. Pays Héll. 20, 792pp.

Mercier, J. 1973. Plissements synmétamorphiques d'échelle kilométrique, d'age jurassique supérieur-éocrétacé dans les Hellénides internes (Macédoine, Grèce). C. R. Ac. Sc., Paris, 276, D, 2249-2252.

Mercier, J.-L, Vergely, P. and Bebie, J. 1975. Les ophiolites helleniques 2obductees2 au Jurassique superieur sontelles les vestiges d'un ocean tethysien ou d'une mer marginale peri-europeene? Soc. Geol. Fr. Bull., 17(4), suppl. 4, 108-112.

Mercier, J.L. and Vergely, P. 1994. Is the Paikon Massif a tectonic window in the Vardar Zone? (Internal Hellenides, Macedonia, Greece). 7th Cong. Geol. Soc. Greece. Thessaloniki, May, 1994. Abstracts p60.

Mercier, J.L., Delibassis, N.D., Gauthier, A.J., Jarrige, J.J., Lemeille, F., Philip, H., Sebrier, M. and Sorel, D. 1979. La Néotectonique de l'Arc Egéen. Rev. Géol. Dyn. Geogr. Phys. Spec. Publ. No. 21, 67-92.

Meschede, M. 1986. A method of discriminating between different types of mid-ocean ridge basalts and continental tholeiites with the Nb-Zr-Y diagram. Che. Geol., 56, 207-218.

Meulenkamp, J.E., Wortel, M.J.R., Van Wamel, W.A., Spakman, W. and Hoogerduyn Strating, E. 1988. On the Hellenic subduction zone and the

geodynamic evolution of Crete since the late Middle Miocene. Tectonophysics, 146, 203-215.

Migiros, G. and Galeos, A. 1990. Tectonic and stratigraphic significance of the Ano Garefi ophiolitic rocks, (Northern Greece). Ophiolites; oceanic crustal analogues. Proceedings of the Symposium "Troodos 1987". Edited by J.Malpas et al. 279-284.

Mitchell, A.H. and Bell, J.D. 1973. Island-arc evolution and related mineral deposits. Journal of Geology, 81(4), 381-405.

Miyashiro, A. and Shido, F. 1975. Tholeiitic and calc-alcaline series in relation to the behaviours of titanium, vanadium, chromium and nickel. Am. J. Sci., 275(3), 265-277.

Montanari, A., Chan, L.S. & Alvarez, W. 1989. Synsedimentary tectonics in the Late Cretaceous-Early Tertiary pelagic basin of the Northern Apennines, Italy. In Controls on carbonate platform and basin development, SEPM spec. publ. No. 44, 379-398

Moores, E.M. 1969. Treatise on Invertebrate Paleontology. Moore, R.C. (ed). Geological Society of America Special Publication.

Mountrakis, D. 1982. Emplacement of the Kastoria ophiolite on the western edge of the internal Hellenides, (Greece). Ofioliti, 7 (2/3), special issue, 397-406.

Mountrakis, D. 1984. Evolution of the Pelagonian zone in N.W. Macedonia. In Dixon, J.E. & Robertson, A.H.F. (eds), The Geological evolution of the Eastern Mediterranean. Geol. Soc. London. Spec. Publ., 17, 581-590.

Mountrakis, D. 1986. The Pelagonian Zone in Greece: a polyphase deformed fragment of the Cimmerian continent and its role in the geotectonic evolution of the eastern Mediterranean. J. Geol., 94, 335-347.

Mullins, H.T. and Cook, H.E. 1986. Carbonate apron models; alternatives to the submarine fan model for palaeoenvironmental analysis and hydrocarbon exploration. In: Carbonate aprons versus submarine fans (Mullins, H.T. et al. eds), Sedimentary Geology 48(1-2), 37-79.

Mullins, H.T., Heath, K.C., Van Buren, M. and Newton, C.R. 1984. Anatomy of a modern open-ocean carbonate slope: northern Little Bahama Bank. Sedimentology, 31, 141-168.

Mussallam, K. 1991. Geology, geochemistry and the evolution of an oceanic crustal rift at Sithonia, NE Greece. In: Ophiolite Genesis and Evolution of the Oceanic Lithosphere. Peters, T., Nicolas, A. and Coleman, R.G. (eds), Kluwer Academic Publishers, London, 685-704.

Mussallam, K. and Jung, D. 1986. Petrology and geotectonic significance of the salic rocks preceding ophiolites in the Eastern Vardar zone, Greece. TMPM Tschermaks Min. Petr. Mitt., 35, 217-242.

Mutti, E. and Ricci Lucchi, F. 1972. Le torbiditi dell'Appennino settentrionale: introduzione all'analisi di facies. Memoire Societe Geologie di Italia, 11, 161-199.

Nance, D. 1976. The Livadia mafic-ultramafic complex and its metamorphic basement, NE Greece. Unpub. Thesis, University of Cambridge. 183pp.

Neumayr, H. 1875. Zur Bildung der Terra rossa. Kohle und Kali Geologische Keischsanst Verhandlung, Wien, 3, 50-1.

Nicholls, I.A. 1971a. Santorini volcano, Greece; tectonic and petrochemical relationships with volcanics of the Aegean region. Tectonophysics, 11(5), 377-385.

Passchier, C.W. and Trouw, R.A.J. 1996. Microtectonics. Springer.

Pearce, J.A. 1975. Basalt geochemistry used to investigate past tectonic environments on Cyprus. Tectonophysics, 25, 41-67.

Pearce, J.A. 1980. Geochemical evidence for the genesis and eruptive setting of lavas from Tethyan ophiolites, In Panayiotou, A. (Editor), Ophiolites: Proceedings of the International Ophiolite Symposium, Cyprus 1979. Geological Survey of Cyprus, Nicosia, 261-271.

Pearce, J.A. 1982. Trace element characteristics of lavas from destructive plate boundaries. In: Thorpe, R.S. (Editor). Andesites, 57-75, John Wiley and Sons.

Pearce, J.A. 1983. The role of the sub-continental lithosphere in magma genesis at destructive plate margins. In Hawkesworth, C.J. and Norry, M.J. (Editors), Continental basalts and mantle xenoliths, 230-249, Nantwich, Shiva.

Pearce, J.A. and Cann, J.R. 1971. Ophiolite origin investigated by discriminant analysis using Ti, Zr and Y. Earth and Planetary Science Letters, 12, 339-349.

Pearce, J.A. and Cann, J.R. 1973. Tectonic settings of basic volcanic rocks determined using trace element analysis. Earth and Planetary Science Letters, 19, 290-300.

Pearce, J.A. and Gale, G.H. 1977. Identification of ore-deposition environment from reace-element geochemistry of associated igneous host rocks.

Pearce, J.A. and Norry, M.J. 1979. Petrogenetic implications of Ti, Zr, Y and Nb variations in volcanic rocks. Contributions to Mineralogy and Petrology, 69, 33-47.

Pearce, J.A. and Wanming, D. 1988. The ophiolites of the Tibetan Geotraverses, Lhasa to Golmud (1985) and Lhasa to Khathmandu (1986). Phil. Trans. Roy. Soc. London, 327, 215-238.

Philip, J. Mermighis, A. and Tronchetti, G. 1989. Nouvelles donnés stratigraphique et paléogéographiques sur le Crétacé supérieur de domaine Héllenique interne. Le Massif de l'Akros (Argolide, Grèce). Comptes Rendues de l'Acadamie Scientifique de Paris. t308, série II, 1379-1384.

Pickering, K.T., Hiscott, R.N. and Hein, F.J. 1989. Deep marine environments. Unwin Hyman, London.

Pickett, E.A. 1994. Tectonic evolution of the Palaeotethys ocean in NW Turkey. PhD Thesis, University of Edinburgh

Pickett, E.A., Robertson, A.H.F. and Dixon, J.E. The Karakaya Complex, N.W. Turkey: a palaeotethyan accretionary complex. In : Geology of the Black Sea Region. MTA, Ankara, in press.

Platt, J.P. 1986. Dynamics of orogenic wedges and the uplift of high pressure metamorphic rocks. Bulletin of the Geological Society of America, 97, 1037-1053.

Poisson, A. 1977. Récherches géologique dans les Taurides occidentales, Turquie. Thèse d'Etat (Unpublished), Université de Paris-Sud, Orsay, France, p.790.

Poisson, A. 1984. The extension of the Ionian trough into southwestern Turkey. In Dixon, D.E. and Robertson, A.H.F. (Editors). The Geological Evolution of the Eastern Mediterranean, Geological Society of London, special publication, 17, 241-249.

Papanikolaou, D.J. 1984. The three metamorphic belts of the Hellenides; a review and kienamtic interpretation. In: The Geological evolution of the eastern Mediterranean. (Dixon, J.E., Editor et al). Geol. Soc. Spec. Publ. 17, 551-561.

Ricou, L.E. and Godfriaux, I. 1991. Une coupe à travers les ophiolites et gneiss allochthones entre le massif Pelagonien et la fenêtre du Paikon (Grèce du Nord). C. R. Acad. Sci. Paris, t. 313, Série II, 1595-1601.

Robertson, A.H.F. 1987. The transition from a passive margin to an Upper Cretaceous foreland basin related to ophiolite emlpacement in the Oman Mountains. Bulletin of the Geological Society of America, 99, 633-653.

Robertson, A.H.F. 1989. Palaeoceanography and tectonic setting of the Jurassic Coast Range ophiolite, central California: evidence from the extrusive rocks and the volcaniclastic sediment cover. Marine and Petroleum Geology, 4(3), 194-220.

Robertson, A.H.F. 1990a. Late Cretaceous oceanic crust and Early Tertiary foreland basin development, Euboea, eastern Greece. Terra Nova, 2, 333-339.

Robertson, A.H.F. 1990b. Tectonic evolution of Cyprus: in : Malpas, J. et al (eds), Ophiolites, Oceanic Crustal Analogues, Proc. Symp. Troodos, 1987. Geol. Surv. Dep., Cyprus, 235-252.

Robertson, A.H.F. and Dixon, J.E. 1984. Introduction: apects of the geological evolution of the Eastern Mediterranean. In Dixon, J.E. and Robertson, A.H.F. (Editors), The Geological Evolution of the Eastern Mediterranean, The Geological Society of London, special publication, 17, 1-74.

Robertson, A.H.F. and Degnan, P.J. 1992. The palaeogeographic setting of the Parnassos carbonate platform in the Mesozoic Pindos Ocean: Evidence from the Kerassia-Milia Complex. 6th Cong. Geol. Soc. Greece, Athens.

Robertson, A.H.F., Clift, P.D., Degnan, P.J. and Jones, G. 1991. Palaeogeographic and palaeotectonic evolution of the Eastern Mediterranean Neotethys. Palaeogeog, palaeoclim, palaeoecol, 87, 289-343.

Rollinson, H. 1993. Using geochemical data: evaluation, presentation and interpretation. Wiley & Son. New York. 352pp.

Sandulescu, M. 1989. Structure and tectonic history of the northern margin of Tethys between the Alps and the Caucasus. In: Rakus, M., Dercourt, J. and Nairn, A.E.M. (eds) Evolution of the northernmargin of Tethys. Mémoire de la Societé Géologique de France, 154, III, 91-100.

Sartorio, D. and Venturini, S. 1988. Southern Tethys Biofacies. Agip S.p.A., S. Donato Milanese.

Schlager, W. and Chermak, A. 1979. Sedimentary facies: Platform-basin transition, Tongue of the ocean, Bahamas. Society of Economic Palaeontologists and Mineralogists, special publication, 27, 193-205.

Scoffin, T.P. 1987. An introduction to carbonate sediments and rocks. Blackie, Glasgow and London.

Scott, R.W. 1988. Evolution of Late Jurassic and Early Cretaceous reef biotas. Palios, 1988, V.3., reefs issue, 184-193.

Sellwood, B.W. 1986. Shallow-marine carbonate environments. In Reading, H.G. (Editor), Sedimentary Facies and Environments and Facies, second edition, Blackwells Scientific Publications, Oxford.

Sengör, A.M.C. 1979. Mid-Mesozoic closure of Permo-Triassic Tethys and its implications. Nature, 279, 590-593.

Sengör, A.M.C. 1984. The Cimmeride Orogenic system and the tectonics of Eurasia. Geological Society of America, Special Paper, 195, p.79.

Sengör, A.M.C., Cin, A., Rowley, D.B. and Shangyou, N. 1991. Magmatic evolution of the Tethysides: a guide to reconstruction of collage history. Palaeogeography, Palaeoclimatology, Palaeoecology, 87, 411-440.

Sengör, A.M.C. and Yilmaz, Y. 1981. Tethyan evolution of Turkey: a plate tectonic approach. Tectonophysics, 75, 181-241.

Sfeikos, A. 1992. Analysis of deformation and kinematics of the Pelagonian nappe system, Kamvounia mountains (North Thessaly, Greece). Thesis, University of Tubingen.

Sharp, I.R. 1994. The Mesozoic-Tertiary sedimentary, tectonic-sedimentary evolution of the Almopias zone, NW Greece. Unpublished Ph.D. thesis, University of Edinburgh.

Sharp, I.R. and Robertson, A.H.F. 1992. Late Jurassic-Lower Cretaceous oceanic crust and sediments of the eastern Almopias zone, NW Greece; implications for the evolution of the Eastern "internal" Hellenides. 7th Congr. geol. Soc. Greece, Thessaloniki, abstract volume, 71.

Sharp, I.R. and Robertson, A.H.F. a Evidence for Turonian rift related extensional subsidence and Tertiary backthrusting: The Almopias and Paikon isopic zones, Northern Greece. Bulletin of the Geological Society of Greece, in press.

Sharp, I.R. and Robertson, A.H.F. b Late Jurassic-Lower Cretaceous oceanic crust and sediments of the eastern Almopias Zone, N.W. Greece; implications for the

evolution of the Eastern 'internal' Hellenides. Bulletin of the Geological Society of Greece, in press.

Sharp, I.R., Robertson, A.H.F. and Dixon, J.E. 1991. Tectonic and sedimentary history of the Eastern margin of the Pelagonian zone, NE Greece. In: European Union of Geosciences EUG VI, Strasbourg, Terra Abstracts, 3, 323.

Shervais, J.W. 1982. Ti-V plots and the petrogenesis of modern and ophiolitic lavas. Earth and Planetary Science Letters, 59(1), 101-118.

Schunemann, M. 1985. Contributions to the geology, geochemistry and tectonics of the Chortiatis series metamorphic calc-alkaline suite, Chalkidiki, Northern Greece. Unpublished Ph.D. Thesis, University of Hamburg, 182pp.

Smith, A.G. 1971. Alpine deformation and the oceanic areas of the Tethys, Mediterranean and Atlantic. Bulletin of the Geological Society of America, 82, 2039-2070.

Smith, A.G. 1979. Othris, Pindos and Vourinos Ophiolites and the Pelgonian Zone. 6th Colloquium on the Geology of the Aegean Region. Institute of Geological and Mineralogical Exploration, Athens, 1369-1374.

Smith, A.G. 1993. Tectonic significance of the Hellenic-Dinaric ophiolites. In: Magmatic Processes and Plate Tectonics. Alabaster, H.M., Harris, T. and Neary, C.R. (eds). Geological Society Special Publication No. 76, 213-243.

Smith, A.G. and Moores, E.M. 1974. The Hellenides. In: Mesozoic and Cenozoic Orogenic belts. Spec. Pub. Geol. Soc. London., 4, 15-39.

Smith, A.G. and Roobol, M.J. 1982. Andesitic Pyroclastic Flows. in: Andesites, Thorpe, R.S. (ed), John Wiley and Sons, 415-433.

Smith, A.G., Hynes, A.J., Menzies, M., Nisbet, E.G., Price, I., Welland, M.J.P. and Ferrière, J. 1975. The stratigraphy of the Othris Mountains, eastern central Greece: a deformed Mesozoic continental margin sequence. Eclogae Geologicae Helveticae, 68, 463-481.

Smith, A.G., Woodcock, N.H., and Naylor, M.A. 1979. The structural evolution of a Mesozoic continental margin. Journal of the Geological Society, London, 136, 589-603.

Spray, J.G., Bébien, J., Rex, D.C. and Roddick, J.C. 1984. Age constraints on the igneous and metamorphic evolution of the Hellenic-Dinaric ophiolites. In Dixon, J.E. and Robertson, A.H.F. (Editors). The Geological Evolution of the Eastern Mediterranean, The Geological Society of London, special publication, 17, 629-645.

Stais., A. 1994. Evolution geodynamique des bassins Mesozoiques Vardariens (domaines de Peonias et d'Almopias), Hellenides orientales. Unpub. Thesis. University of Lille.

Stais, A. and Ferriere, J. 1991. Nouvelles données sur la paléogéographie Mésozoique du domain Vardarien: Les bassins d'Almopias et de Péonias

(Macédoine, Hellénides internes septentrionales). Bull. Geol. Soc. Gréce. Vol XXV/1, 491-507.

Stow, D.A.V. 1986. Deep clastic seas. In: Reading, H.G. (ed). Sedimentary environments and facies, 2nd edition, Blackwell, Oxford, 399-444.

Thiebault, F. 1982. Evolution geodynamique des Hellenides externes en Peleponnese meridional (Grece). Soc. Geol. Nord, Spec. Publ., 6, 574pp.

Thomson and Thommason 1969

Underhill, J. 1985. Neogene and Quaternary tectonics and sedimentation in western Greece. Unpublished PhD thesis, University of Wales, Cardiff.

Underhill, J.R. 1988. Triassic evaporites and Plio-Quaternary diapirism in western Greece. Bulletin of the Geological Society, London, 145, 269.

Underhill, J.R. 1989. Late Cenozoic deformation of the Hellenide foreland, western Greece. Bulletin of the Geological Society of America, 101, 613-634.

Ustaömer, T. 1993. Pre-Late Jurassic tectonic-sedimentary evolution of North Tethys: Central Pontides, N Turkey. Unpublished Thesis, University of Edinburgh, 389pp.

Vergely, P. 1976. Chevauchement vers l'Ouest et rétrocharriage vers l'Est des ophiolites: deux phases tectoniques au cours du Jurassique supérieur-Eocrétacé dans les Hellénides internes. Bull. Soc. Géol. France (7), t. XVIII, no. 2, 231-244.

Vergely, P. 1984. Tectonique des ophiolites dans les Hellenides Internes (deformation, métamorphismes et phénomènes sédimentaires). Consequences sur l'Evolution des Region Tethysiennes Occidentales. Thèse (Unpublished) Université de Paris-Sud, Orsay.

Vougioukalakis, G. 1994. Pliocene volcanics of Voras Mt., Macedonia. Greece. 7th cong. of the Geol. Soc. Greece, Thessaloniki, 25-27 May, abstracts vol., 186-187.

Walker, R.G. 1966. Deep channels in turbidite-bearing formations. Amer. Ass. Petrol. Geol., Bull. 50(9), 1899-1917.

Whittaker, A., Cope, J.C.W., Cowie, J.W., Gibbons, W., Hailwood, E.A., House, M.R., Jenkins, D.G., Rawson, P.F., Rushton, A.W.A., Smith, D.G., Thomas, A.T. and Wimbledon, W.A. 1991. A guide to stratigraphical procedure. J. Geol. Soc. Lon., 148, 813-824.

Williams, H. 1975. Structural succession, nomenclature and interpretation of transported rocks in Western Newfoundland. Canadian Journal of Earth Sciences, 12, 1874-1894.

Williams and Rust 1969. Sedimentology of a braded river. J. Sed. Petrol. 39, 649-679.

Wilson, J.L. 1975. Carbonate facies in Geologic History. p.417, Springer-Verlag, Berlin.

Wilson, M. 1989. Igneous petrogenesis: A global tectonic approach. Chapman and Hall, London

Winchester, J.A. and Floyd, P.A. 1977. Geochemical discrimination of different magma series and their differentiation products using immobile elements. Chem. Geol., 20, 325-343.

Winchester, J.A. and Max, M.D. 1982. The geochemistry and origins of the PreCambrian rocks of the Rosslare complex, SE Ireland. J. Geol. Soc. London, vol. 139, 309-319

Wood, P.A., Joron, J.L., Marsh, J.G., Tarney, J. and Treuil, M. 1980. Major and trace element variations in basalts from the North Phillipine sea drilled during Deep Sea Drilling Project. Leg 58: A comparative study of back-arc basin basalts with lava series from Japan and mid-ocean ridges: Initial Report of the Deep Sea Drilling Project: Washington, U.S. Goverment Printing Office, v. 58, 873-894.

Woodcock, N.H. and Robertson, A.H.F. 1977. Origins of some ophiolite-related metamorphic rocks of the "Tethyan" belt. Geology, 5, 373-376.

Woodcock, N.H. and Robertson, A.H.F. 1982. Wrench and thrust tectonics along a Mesozoic-Cenozoic continental margin: Antalya Complex, SW Turkey. J. Geol. Soc., Vol. 129 (2), 147-163.

Yarwood, G.A. and Aftalion, M. 1976. Field relationships and U-Pb geochronology of a granite from the Pelagonian zone of the Hellenides. Bull. Soc. Geol. France, 7, 259-264.

Zachariadou, S. and Dimitriadis, S. in press. Crustal extension and partial melting possibly related to the opening of a marginal basin. The Pelitic migmatites of Piyi and Karathodoro, Guevgueli complex, Macedonia, Greece. Bull. Geol. Soc. Greece.

APPENDIX

X-RAY FLUORESCENCE ANALYTICAL TECHNIQUE

Carefully chosen samples were collected from volcanic units of primary interest in the study area during field work (i.e. the Livadia and Kastaneri Formations of the Païkon Massif and the Likostomo-Promachi Amphibolites, Pinovon Imbricate Lavas and Porta Andesites of the Voras Massif). The most fresh, unveined and basic samples available were selected for analysis. At the Department of Geology & Geophysics, Edinburgh University, the samples were trimmed using a diamond saw to remove any traces of veining or weathering. The samples were then crushed and finely ground to a grain size not greater than 200 mm, before whole rock geochemical analyses (X-Ray Fluorescence or XRF) were undertaken in accordance with the techniques proposed by Fitton & Dunlop (1985). Major element oxide concentrations were obtained by analysing glass discs comprising measured quantities of powdered rock sample and lithium flux on a Philips PW 1480 dispersive XRF spectrometer. Trace element concentrations were obtained by analysing pressed powder discs on a Philips PW 1450/20 machine. Samples were calibrated using USGS and CRPG international standards, as described in Abbey (1980).

The data obtained from the above analytical process were rigorously screened to remove any highly evolved and/or altered samples from further consideration. Those samples used to determine tectonic environment of eruption, or to determine the nature of metasomatic alteration, are listed in the succeeding pages.

APPENDIX

THE LIVADIA FORMATION

	291/1	291/2	291/3	291/4	291/5	291/8	291a/1	291a/2	291a/3	291a/5	291a/7	291a/10	268a/1	268a/2
SiO2	51.17	49.79	47.81	47.81	52.6	47.69	45.09	51.91	46.52	46.13	48.81	47.6	54.48	49.15
Al2O3	14.21	15.99	16.35	16.7	13.95	16.75	17.89	15.27	17.71	17.3	15.85	17.04	14.51	14.93
Fe2O3	13.71	15.11	16.61	16.25	12.87	16.79	16.81	14.84	15.19	15.78	16.08	14.84	15.4	18.03
MgO	3.41	4.72	6.05	4.79	3.19	5.36	4.24	3.4	3.17	3.25	4.12	3.05	7.68	10.16
CaO	12.11	6.56	3.3	6.99	12.13	4.5	7.51	5.98	10.46	10.71	7.23	11.26	0.35	0.18
Na2O	0.11	4.09	4.38	3.42	0.14	4.12	2.35	2.89	2.02	1.68	3.39	1.91	0.5	0.04
K2O	0.1	0.18	0.243	0.154	0.12	0.291	1.289	0.918	0.935	0.89	0.188	0.773	0.746	0.177
TiO2	0.595	0.676	0.734	0.703	0.522	0.686	0.689	0.64	0.638	0.612	0.616	0.532	0.672	0.455
MnO	0.209	0.128	0.141	0.134	0.202	0.128	0.196	0.216	0.186	0.196	0.189	0.187	0.222	0.256
P2O5	0.028	0.032	0.022	0.025	0.022	0.023	0.028	0.024	0.027	0.025	0.017	0.028	0.053	0.028
LOI	4.65	3.05	4.21	3.36	4.53	4.06	4.23	4.08	3.44	3.54	3.72	3.06	5.31	6.58
Total	100.30	100.33	99.85	100.34	100.28	100.40	100.32	100.17	100.30	100.11	100.21	100.28	99.92	99.98
Ni	9.9	6.8	7.8	10.5	8	9.1	12.6	8.8	9.3	10.4	9.7	7.5	28.6	41.2
Cr	31.3	24.3	19.1	24.5	25.9	27.2	30	18	30.9	30.7	31.8	28.9	40.8	93.4
V	472.1	483.7	397.5	525.2	432.4	536.4	503.7	349.3	539	541	445.9	517.7	404.3	217.8
Sc	71.1	60.9	69.5	61.1	56.6	64.5	69.1	65.2	69.2	71.6	70.9	62.5	64	35
Cu	120.2	106.7	110.5	103.4	112	129.9	161.2	160.9	126.9	125.4	150	115.3	96.5	37.9
Zn	97.6	123.4	161.1	131.2	88.5	137.8	144.6	137.8	109.8	109.8	130.3	100.3	101.9	106.5
Sr	39.5	51.7	21.6	53	35	37.3	104.8	92.3	131.5	137.9	191.7	145.5	2.7	1.7
Rb	1.3	2.9	4.6	3.2	2.6	6.3	27.6	16.4	19.2	19.5	2.6	17.8	10.5	2.6
Zr	20.2	13.5	14	14.1	16.4	13.8	22.4	23.4	21	20.5	19.3	18.2	38.4	25.4
Nb	0.7	0	0	0	0.6	0	0.3	0.5	0.4	0.3	-0.1	0.4	0.8	0.9
Ba	20.8	3.4	9.6	1.9	24.8	18.5	57.3	108.5	46.4	40.3	11.5	41.6	44	15.6
Pb	1.7	1.2	0	1.4	0	1.4	3.8	1.8	8.5	5.9	1.6	7.5	2.9	2.6
Th	4.1	3	4	5.2	1.6	5.2	5.8	3.6	3.7	5.7	4.4	5.1	3.3	6.1
La	0	0	1.3	3.9	0	0	-1.7	-3.4	-4.2	-2.2	0.8	1.9	-3.5	2.7
Ce	0	0	0	0	0	0	-3.4	-4.1	-2.7	-6.4	-4.8	-5.5	6.8	2.6
Nd	0.1	3.1	0	1.9	0	0	3.2	0.5	-2.9	-3.3	-1.1	-1.9	6.7	2.3
Y	18.8	15.7	11.1	14.7	14.5	12.3	16.3	17.8	16.3	15.1	14.2	15.8	17.9	21.4

X-Ray Fluorescence data for samples from the Livadia Formation that were used in tectonic discrimination diagrams.

APPENDIX

THE LIVADIA FORMATION

	268/2	268/4	268/5	268/6	268/7	268/8	268/9	268/10	268/12	268/13	268/14	328/1	328/2	328/3
SiO2	54.49	53.1	53.1	47.71	47.63	47.8	45.42	46.66	54.61	51.79	52.02	54.96	49.92	45.37
Al2O3	14.53	16.88	14.67	14.54	14.64	14.92	18.09	15.96	14.87	15.84	13.95	17.71	16.77	20.81
Fe2O3	15.07	22.68	16.59	20.29	21.18	21.24	16.8	18.17	14.65	15.84	17.63	11.61	14.69	15.69
MgO	7.68	11.79	7.14	9.38	9.34	7.45	9.17	9.99	7.06	8.12	8.41	5.39	6.44	7.13
CaO	0.31	0.17	0.39	0.46	0.04	0.14	0.47	0.46	0.35	0.36	0.36	0.15	1.67	0.11
Na2O	0.76	-0.03	0.56	0.07		1.07	0.62	0.93	0.79	0.87	0.23	4.83	3.41	3.49
K2O	0.397	0.013	0.904	0.115	0.04	0.131	1.391	0.034	0.733	0.885	0.467	0.03	0.023	0.654
TiO2	1.193	0.601	0.667	0.678	0.018	0.61	0.831	0.757	1.3	0.649	0.581	1.248	1.17	1.562
MnO	0.184	0.284	0.196	0.271	0.596	0.195	0.214	0.23	0.176	0.19	0.215	0.114	0.103	0.132
P2O5	0.133	0.043	0.051	0.051	0.237	0.052	0.051	0.052	0.136	0.055	0.048	0.093	0.066	0.09
LOI	5.44	7.93	5.93	6.45	0.036	6.4	6.76	6.69	5.39	5.67	6.1	4.02	5.86	5.35
Total	100.18	100.16	100.2	100.05	100.12	100	99.81	99.92	100.06	100.27	100.01	100.16	100.12	100.39
Ni	8.5	48.2	33.4	36.1	36.8	33.3	50.4	31.8	7.1	43.7	42.5	19.9	24.5	20.8
Cr	15.8	86.8	58.7	43.9	52.9	75.6	95	31.3	15.8	85.4	79.7	45.6	47.4	48.2
V	251.2	368.5	317.1	316	337.9	288.2	490.4	350.4	257.4	380.2	337	406.5	441.1	543.5
Sc	51.5	48.8	49.3	42.7	43.5	45	79.4	43.1	63	55.1	43.7	54.8	54.3	87.4
Cu	46.8	91.8	143.6	90.4	82.4	61.7	15.1	47.2	41.6	78.8	69.8	15.1	216.3	66
Zn	67	171.9	80.9	118.6	112.9	128.8	106.1	137.9	60.9	96.6	102.2	126.3	186.2	253.8
Sr	5.8	0.8	6.2	6.1	2.2	6.2	3.9	6	8	4.5	5	19.9	21	16.8
Rb	6	0.8	12.5	1.9	1.2	2.1	19	0.8	10.8	12.4	7	1.3	0.5	19.8
Zr	45.4	34.1	37	37.8	30.7	35.2	44.1	42	47.8	35.7	32.1	54.5	51	64.7
Nb	0.8	0.6	0.7	0.6	0.5	0.6	1.2	0.8	0.8	0.8	0.8	0.9	0.5	0.8
Ba	27.9	12.5	77.1	3.8	2.3	17.5	77.1	21.3	48.5	68.7	46.4	12.4	6.9	83.4
Pb	3	0.1	2.4	4.6	2.4	6.1	0.8	1.4	1.8	0.1	1.5	7.1	3.2	7.4
Th	3.5	9.2	4.6	7.5	7.9	9.8	3.9	4.1	3.1	4.9	5.6	1	2.2	3.8
La	-0.2	3.6	1.2	3.8	-0.5	1.7	1.2	4.1	4.8	2.8	2.4	3.1	3	-4.8
Ce	-3.8	1.1	-1.9	4.8	1.5	6.9	0.6	5.4	5.2	0.9	4.2	5.9	2.2	1.9
Nd	2.1	3.5	3.3	4.7	2.8	3	0	2.5	3.7	4.6	5.6	7.2	12.6	3.2
Y	27.4	22.7	22.7	25.5	12	11	15.1	18.3	28.4	17.7	19.1	25	38.9	14.5

X-Ray Fluorescence data for samples from the Livadia Formation that were used in tectonic discrimination diagrams.

APPENDIX THE LIVADIA FORMATION

	328/4	168/94/1	168/94/2	168/94/4	168/94/6
SiO2	49.26	52.32	51.52	52.36	49.78
Al2O3	18.65	16.51	17.17	12.98	13.67
Fe2O3	14.81	12.8	13.14	17.32	18.11
MgO	6.44	9.5	7.93	9.65	10.23
CaO	0.11	0.43	1.01	0.46	0.42
Na2O	4.06	2.53	3.55	0.04	0.11
K2O	0.046	0.047	0.068	0.007	0.006
TiO2	1.359	0.602	0.74	0.61	0.65
MnO	0.226	0.161	0.177	0.168	0.181
P2O5	0.071	0.046	0.062	0.058	0.062
LOI	5.03	5.41	5.02	6.23	6.43
Total	100.06	100.36	100.39	99.88	99.65
Ni	27.7	59.4	42.5	34.6	39.8
Cr	53.5	105.7	81	54.7	55.8
V	443.1	323.8	285.3	304.3	321.1
Sc	56	51.5	45.7	37.4	41.2
Cu	38.9	42.9	194.5	69.4	84.4
Zn	742.4	77	76.6	78.6	84.9
Sr	10.6	10	16.9	3	2.9
Rb	1.2	0.5	1.1	0.1	0.4
Zr	59.8	28.3	36.4	31.4	32.7
Nb	0.9	0.9	0.6	0.8	1.1
Ba	19	17.4	-0.4	0.3	-5
Pb	10.2	1.3	0.5	0.6	1.2
Th	2.7	3.3	4.6	5	6
La	-2.7	-2	2.1	1	3.8
Ce	6.4	5.8	10.9	4	-4.1
Nd	8.8	3.3	10.5	5.6	0
Y	18.5	15.9	18.7	14.6	15.8

X-Ray Fluorescence data for samples from the Livadia Formation that were used in tectonic discrimination diagrams

APPENDIX

THE LIVADIA FORMATION

	291/6	291/7	291a/4	291a/6	291a/8	291a/9	291a/11	291a/12	268/1	268/3	268/11	168/94/3	168/94/5
SiO2	68.69	69.44	57.31	65.78	60.31	61.25	64.37	60.44	67.52	39.8	58.9	66.53	69.62
Al2O3	12.08	11.83	12.18	11.7	15.91	15.71	12.19	16.02	12.81	15.03	11.73	12.54	12.81
Fe2O3	6.64	6.59	12.1	9.27	8.54	8.26	10.44	8.29	6.62	20.61	11.56	10.84	7.53
MgO	1.47	1.59	2.11	2.36	0.45	0.57	2.24	0.64	1.44	10.72	2.09	2.76	2.61
CaO	5.66	4.8	10.65	4.25	7.84	7.11	2.68	7.24	5.82	0.03	9.52	0.25	0.1
Na2O	3.65	3.71	1.34	3.8	4.4	4.78	5.07	5.13	3.85	-0.02	1.59	0.45	3.75
K2O	0.024	0.027	0.13	0.308	0.034	0.067	0.172	0.075	0.053	0.011	0.135	2.191	0.194
TiO2	0.406	0.398	0.512	0.388	0.661	0.617	0.446	0.652	0.393	0.618	0.486	0.677	0.684
MnO	0.068	0.07	0.137	0.147	0.044	0.08	0.135	0.073	0.084	0.244	0.119	0.101	0.075
P2O5	0.048	0.036	0.022	0.04	0.047	0.036	0.017	0.044	0.04	0.037	0.01	0.045	0.022
LOI	1.68	1.92	3.87	2.29	1.86	1.75	2.52	1.68	1.49	6.75	3.74	3.65	2.78
Total	100.42	100.41	100.36	100.33	100.10	100.23	100.28	100.28	100.12	99.97	99.88	100.03	100.18
Ni	3	3.9	3.8	8.7	3.5	2.2	6.8	2.6	3.7	37.3	6.6	4.1	4.9
Cr	6.4	8.2	24	18.1	25.4	26.6	20.7	25.2	6.6	86.6	25.1	0.2	-1.1
V	123.2	113.7	489.1	353.3	551.6	530.7	378.9	504.3	108	360.8	471.6	42.4	37.2
Sc	24.1	19.5	54.8	43.3	67.9	67.4	50.9	61.9	22	48.2	53.2	22	15.5
Cu	15.7	18.2	73.5	82.2	20.8	27.8	90.7	26.3	14.9	56	96.6	11.1	20.4
Zn	60.5	62.8	78.8	66.1	45.5	53.8	73.5	48.8	54.7	147	83.1	31.2	41.7
Sr	79.5	67.6	120.2	52.9	174.4	158.8	43	168	100.4	1.3	22.1	9.7	11.6
Rb	0.6	0	3.6	11.5	0.4	1.3	2.7	1.1	1.2	0.8	4.7	28.7	2.3
Zr	43.3	40.6	14.5	14.6	18.4	18.6	13.8	18.3	39.9	33.2	15.7	76.8	83.1
Nb	0.5	0.5	0.5	0.6	0.2	0.4	0.4	0.2	0.3	0.7	-0.1	0.5	1
Ba	11.8	11.3	16	39	3.1	23.9	15.4	15.1	30.8	5.7	23.8	191.2	21.8
Pb	5.4	3.7	-0.1	2.7	3.4	1.9	1	1.9	4.1	1.2	1.9	2	-0.3
Th	0.4	0.7	2.2	1.3	1.6	0.3	2.2	1.3	-2.5	7.6	0.4	3.2	0.9
La	1	-0.7	-0.8	-3.2	4.1	-4.1	1.5	2.8	2.9	1.7	-7.4	-1.6	0.9
Ce	2.6	6	-3.6	-3.7	0	-3.1	-6.1	-1.4	12.4	1.3	7.6	12.8	9
Nd	4.2	6.8	2.7	0.3	4.4	0.3	-1.1	2.1	7.3	6.2	3	6.1	6.1
Y	27	26.5	15.1	10.58	23.3	19.1	10.4	23.6	25.3	3.8	17.5	20.2	26.3

X-Ray Fluorescence data for samples from the Livadia Formation that were discarded due to alteration and/or non-basaltic composition.

APPENDIX **THE KASTANERI FORMATION**

	447a/1	447a/2	443/2	443/3	414a/2	438/1	438/2	438/3	411a/1	411a/2	412a/2	412a/3	412a/4	412a/5
SiO2	45.84	47.59	45.97	43.17	51.02	45.99	44.78	49.8	47.48	46.9	51.4	46.59	47.12	46.49
Al2O3	16.42	15.22	13.5	14.85	18.04	15.95	15.45	20.2	13.99	18.4	14.95	16.33	17.39	16.99
Fe2O3	9.81	10.04	9.86	11.46	11.38	10.53	9.78	11.49	4.96	9.6	13.93	15.08	16.02	16.57
MgO	6.56	5.61	4.08	4.35	6.68	5.4	4.85	5.33	2.56	9.3	5.04	4.48	4.85	4.57
CaO	6.47	7.07	10.37	9.58	2.44	6.5	8.3	0.24	12.44	2.92	7.76	7.57	5.35	7.27
Na2O	5.21	4.04	2.58	3.1	0.93	1.36	1.44	0.43	6.01	4.28	1.1	2.56	2.91	1.91
K2O	0.341	1.038	1.713	1.841	4.106	3.545	3.429	6.232	0.616	1.259	0.004	0.015	0.017	0.027
TiO2	0.924	0.872	0.672	0.719	0.698	0.944	0.935	0.738	0.561	0.997	0.881	1.015	1.119	1.025
MnO	0.149	0.144	0.16	0.153	0.112	0.186	0.294	0.046	0.152	0.167	0.127	0.161	0.163	0.17
P2O5	0.015	0.065	0.027	0.038	0.011	0.095	0.16	-0.015	0.023	0.162	0.041	-0.021	-0.011	-0.017
LOI	7.89	8.16	11.15	10.69	4.84	9.31	10.56	5.25	11.05	6.08	5.01	6.07	4.65	4.92
Total	99.63	99.85	100.08	99.95	100.26	99.81	99.98	99.74	99.84	100.07	100.24	99.85	99.58	99.93
Ni	102.4	91.2	49.5	51.5	17.5	214.4	443.8	47.9	34.3	40.1	6.4	7.7	7.1	4.5
Cr	312	286.6	174.5	223.6	50.9	291.4	207.6	129.6	146.9	120.2	35	36	34.4	38
V	370.5	373.3	250.8	277.2	358.3	282.6	248.8	412.8	120	170.1	534.4	531	534.8	619.4
Sc	47.3	48.6	39.6	46.6	47.3	47.4	37	63.7	22.2	26.8	43.2	43.5	44	45.3
Cu	36.1	30.9	11.3	12.7	47.2	11.8	10.6	14.8	32.5	441.9	51.9	52.3	52.7	51.5
Zn	97	80.8	113.7	121	103.7	131.5	115.4	124.1	52	146.1	104	111.2	117	117.9
Sr	60.8	69.5	72.5	68.1	27.7	79.1	113	6.6	48.3	49.1	149	91.2	81.9	113.8
Rb	4.9	16.2	26.5	28.4	88.2	96.6	90.1	169.9	10.3	21.3	-0.7	0.6	0.2	0.3
Zr	42.6	41.2	37.1	42.7	20.6	59.4	62.3	14.9	25.5	56.9	24.8	31.5	34	30.3
Nb	0	0.1	0.2	0.6	-0.2	1.1	0.8	0.3	-0.3	0.8	0.2	-0.1	0.2	0.1
Ba	15.5	70.8	121.2	112.3	52.7	531.2	454.9	904.6	31.3	50.4	1.1	-8.1	-8.2	25.2
Pb	2.3	1.2	8.8	9.5	0.6	2.6	1.8	1.6	1.7	2.8	1.7	4.3	1.1	4.2
Th	1.8	1.8	2.7	2	2.7	2.8	2.2	2.8	1	2.8	2.9	4.5	4.8	4.7
La	-2.1	1.7	4.1	4.4	-1	4.4	3.4	-1.7	2.1	6.1	-5.2	1.9	-0.8	-0.8
Ce	6.8	1.6	16.4	10.5	7.3	14.4	8	6.5	11.3	10.4	6.6	9.9	3.8	-1
Nd	5.7	10.2	10.3	8.8	5.3	8.5	12.6	4.3	7.5	12.1	6.5	5.7	5.6	8.1
Y	17.9	16.6	15.9	16.3	12.7	19.4	19.3	8.5	10.5	18.1	19	22.2	24.7	20.6

X-Ray Fluorescence data for samples from the Kastaneri Formation that were used in tectonic discrimination diagrams.

APPENDIX

THE KASTANERI FORMATION

	444/1	444/2	330/1	330/2	330/3	326/1	326/2	326/3	326/4	214a	239a	239b	184a	184b
SiO2	39.7	35	64.62	61.11	57.3	56.5	57.99	67.96	54.57	83.41	81.52	80.58	84.39	85.52
Al2O3	13.16	12.96	14.82	13.91	13.88	16.14	17.41	14.04	16.33	9.54	11.6	12.1	9.37	8.61
Fe2O3	7.57	8.05	8.52	8.23	9.24	13.72	10.66	7.55	14.27	0.92	0.76	0.78	0.62	0.85
MgO	3.56	3.9	2.59	3.22	2.91	6.34	5.33	3.43	6.69	0.29	0.66	0.66	0.67	0.51
CaO	15.36	17.91	0.47	4.06	4.9	0.06	0.16	0.09	0.07	0	0.04	0.03	0.05	0.07
Na2O	4.48	3.85	3.93	3.33	3.83	0.22	0.79	0.36	0.44	0.12	0.07	0.05	0.04	-0.03
K2O	0.97	1.087	0.78	0.654	0.409	1.573	2.063	2.442	1.361	4.259	3.844	3.994	3.02	3.17
TiO2	0.688	0.668	1.19	1.047	1.098	0.869	0.632	0.632	0.961	0.039	0.091	0.097	0.126	0.078
MnO	0.192	0.222	0.127	0.156	0.21	0.123	0.087	0.105	0.148	0.015	0.006	0.002	0.002	0.004
P2O5	0.062	0.078	0.232	0.211	0.234	0.023	0.07	0.045	0.037	0.005	0.008	0.004	0.003	0.006
LOI	14.29	16.48	2.84	4.11	6.12	4.86	4.71	3.47	5.21	1.49	1.82	1.96	1.87	1.49
Total	100.03	100.21	100.12	100.04	100.13	100.42	99.9	100.12	100.08	100.09	100.42	100.26	100.16	100.28
Ni	67.9	72.7	3.8	28	4.4	16.4	38	15.7	9.6	1.6	1.5	1.4	2.2	3.6
Cr	244.2	242.2	-2.3	58.4	-0.5	25.1	83.3	64.9	26.7	-18.8	-19.8	-21	-13.5	-15.2
V	211.4	232.7	40.5	69.9	34.1	411.8	365.4	400.6	463.3	6.1	2.8	3.8	12.3	12.5
Sc	34.4	44	45.2	40.7	34.7	60.4	64.4	59.3	57	0.8	5.3	4.2	3.8	3.5
Cu	39.3	24.8	4.5	23.6	8.6	60.2	50.3	24.4	43.5	0.6	0	0.7	3.5	1.3
Zn	79.7	88.6	122.5	104.4	134.2	203.9	157.4	76.2	167	22.1	25	29.5	180.2	119.3
Sr	128.6	146.6	35.6	70.9	74.8	7	14.9	8.9	7.9	2.9	4.2	3.4	1.1	1.2
Rb	11	11.5	12	10.4	6.6	35.4	45.1	54.6	30.8	119.4	116.3	121.4	102.7	105.7
Zr	45.9	41.3	60.7	55.3	57.3	24.6	47.7	41.4	28.4	67.5	92.9	96.6	80.8	63.6
Nb	0.8	0.7	0.8	0.8	0.9	0.2	0.5	0.7	0.4	6.1	8.6	8.8	8	6.7
Ba	60.7	64	57.9	54.8	41.4	169.7	183.7	236.7	133.7	302.7	464.2	460.1	495.7	530.7
Pb	11.5	11.3	3.6	3.1	4.4	3.8	4	5.2	6.8	6	2.4	3.8	18.2	5.6
Th	0.7	1.4	-1.1	0.2	1.3	1.9	0.6	-2.2	2.9	8.8	9.4	9.6	15.2	12.5
La	5.8	0.8	1.2	0.2	2.6	0.9	-3.2	2.8	-3	17.2	37	46.6	17.4	13.5
Ce	14.2	20.3	7.5	3.4	0.6	2.4	8	0.5	3.5	46	70.7	80.8	40.5	33.5
Nd	10.7	13.3	8	9.5	10	3.9	3.4	0	6.3	19.9	31.4	34.9	15.9	13.2
Y	15.8	16	32.5	29.4	29.6	17.8	27.4	46.7	20	17.2	22.9	25.3	15.3	13.5

X-Ray Fluorescence data for samples from the Kastaneri Formation that were discarded due to alteration and/or non-basaltic composition.

APPENDIX

THE KASTANERI FORMATION

	184c	184e	184d	182a	182b	134/1	134/2	134/3	134/4	179a/1	179a/2	179a/3	179a/4	179a/5
SiO2	84.3	80.84	89.18	77.07	78.03	82.74	82.2	81.19	87.89	79.26	78.57	78.7	77.21	75.9
Al2O3	9.42	11.64	6.64	13.47	13.7	9.9	10.36	11.18	6.96	12.13	12.62	13.02	12.78	13.96
Fe2O3	0.94	0.83	0.43	1.11	1.03	1.6	1.04	1.03	1.13	1.32	1.11	0.75	0.88	1.49
MgO	0.56	0.7	0.39	0.36	0.43	0.48	0.43	0.45	0.44	0.23	0.28	0.2	0.31	0.35
CaO	0.01	0.02	0.01	-0.01	0	0.06	0.04	0.04	0.02	0.03	0.04	0.03	0	0.03
Na2O	0.05	-0.03	0.04	0.17	0.08	2.87	3.66	3.85	1.29	2.47	2.59	4.74	1.37	2.39
K2O	3.416	4.139	2.179	5.454	4.723	1.057	1.126	1.31	1.282	3.148	3.751	1.9	6.292	4.617
TiO2	0.084	0.12	0.119	0.087	0.146	0.071	0.084	0.081	0.044	0.117	0.126	0.118	0.116	0.136
MnO	0.007	0.008	0	0.002	0.004	0.004	0.005	0.004	0.006	0.008	0.005	0.005	0.007	0.004
P2O5	0.002	0.002	0.003	0.014	0.015	0.013	0.003	0.009	0.001	0.031	0.034	0.043	0.012	0.033
LOI	1.62	1.87	1.22	2.13	2.02	1.55	1.2	1.23	1.26	1.36	1.21	0.89	1.12	1.46
Total	100.4	100.14	100.21	99.86	100.18	100.35	100.15	100.37	100.32	100.1	100.34	100.39	100.11	100.38
Ni	5.8	2.8	3.1	2.9	3.9	3.8	3.5	3.1	1.8	2.6	3.4	1.5	1.4	3.7
Cr	-9	-16.3	-13.6	-19.9	-17.2	-3.3	-6	-6.4	-2.3	-18.4	-18	-18.6	-16.3	-18.2
V	13.6	10.8	9.3	7.1	14.5	3.6	5.5	7.2	6.3	10.5	7.3	8.8	9.8	10.1
Sc	5.2	3.7	6.5	5.8	9.3	5.5	0.8	2.7	1.6	7.4	4.5	8.8	7.3	5
Cu	5.6	3.3	16.1	5.7	3	-1	-0.3	-2.5	-2.7	2.4	3.4	2.3	3.3	6.3
Zn	160.2	125.2	170.3	150.4	20.1	62.8	35.7	31.2	33.8	118.8	43.3	8.8	82.7	76.4
Sr	1.6	1	2.8	22.7	2.3	17	18.3	20.6	13.5	6.8	14	10.2	7.6	13.5
Rb	112.2	69.7	130.7	173.5	156.8	38.3	42.5	49.6	51	98.7	141.7	59.4	113.4	127.5
Zr	81.8	136.6	83.3	97.4	150	85.2	96.5	92	64.2	101.4	110.6	110.8	110.9	118.6
Nb	7.7	12.8	11.1	7.5	6	9.6	12.6	9.7	4.8	6.7	7.2	5.4	7.4	9
Ba	575.5	358.4	767.3	3458.6	477	249.3	247.6	291.2	195.7	587.3	1402.8	370.3	650.5	1183.4
Pb	7.8	16.8	14.4	12.5	6.2	78.6	30	17.1	26.1	9.9	12.4	7.7	11.4	24.8
Th	12.4	14	17.7	16.4	13.5	14.4	15.7	18.2	10.6	11.3	13	13.4	12.8	13.7
La	16.4	23.4	16.1	40.3	44.5	34.6	32	42.7	16.6	32.4	34.1	40.4	28.1	40.4
Ce	25.4	48	25	66.5	85.7	64.3	62.8	64.8	28.6	66.2	56.4	78.2	60.5	73
Nd	13.8	23.9	13.1	23.1	37.6	29.2	23.1	31.2	11	26.3	24	30.6	27.5	28.9
Y	14.2	15	15.4	31.9	33	10.2	14.8	11.4	12.6	20.3	22.1	20.4	23.5	29.9

X-Ray Fluorescence data for samples from the Kastaneri Formation that were discarded due to alteration and/or non-basaltic composition.

APPENDIX

THE KASTANERI FORMATION

	451/1	451/2	451/3	449/2	449/4	449/5	450
SiO2	74.68	75.34	73.44	75.8	78.67	79.7	76.49
Al2O3	10.3	9.77	9.09	11.63	11.94	10.95	11.74
Fe2O3	1.76	3.65	2.35	2.09	2.21	2.04	3.34
MgO	0.65	1.44	0.87	0.49	0.5	0.52	0.59
CaO	3.46	2.73	4.76	1.95	0.1	0.32	0.62
Na2O	5.2	3.53	4.03	3.79	4.25	4.03	3.05
K2O	0.1	0.343	0.224	1.076	0.98	0.745	1.39
TiO2	0.316	0.289	0.288	0.248	0.247	0.231	0.274
MnO	0.047	0.044	0.059	0.049	0.03	0.035	0.058
P2O5	0.011	0.068	0.01	-0.009	-0.009	-0.011	-0.009
LOI	3.34	3.25	4.71	2.69	1.26	1.28	2.13
Total	99.86	100.45	99.83	99.80	100.18	99.84	99.67
Ni	3.2	2.8	2.5	2.4	2.2	2.3	3.2
Cr	-2.9	-3.5	-2.7	-0.7	-0.2	-0.1	-1.2
V	6	8.7	9.7	27.4	26.6	21.8	22.4
Sc	6.7	8.3	8.7	12.1	11.5	9.3	17.3
Cu	-0.5	1.4	2.3	-0.7	0.6	-2.1	2.2
Zn	50.2	85	55.7	38.8	39.7	40.6	65.1
Sr	38.3	31.6	51.4	52.6	29	30.1	57.1
Rb	0.9	4.2	2.8	15.9	14.4	10.7	21.4
Zr	57.6	52.9	52.3	82.9	81.4	76.9	103.1
Nb	0.2	-0.1	0.5	-0.1	0.1	0.2	0.2
Ba	9.9	38	15.6	102	93.7	72.6	156.8
Pb	2.9	1.6	2.7	1.3	2.8	1.6	4.1
Th	-1.7	-0.4	-1	-0.7	-1.1	-1	-0.2
La	3.3	0.1	5.6	2.9	0.4	1.9	13.1
Ce	14.2	5.9	11.2	9.7	4.9	8.3	32.5
Nd	6.6	8.3	5.9	7.8	4.3	8.9	26.5
Y	21.5	15.1	17.2	27.4	21.6	30.1	64.5

X-Ray Fluorescence data for samples from the Kastaneri Formation that were discarded due to alteration and/or non-basaltic composition

APPENDIX

THE LIKOSTOMO-PROMACHI AMPHIBOLITES

	V11-UM3	V11-T7	V11-LM2	V11-UM2	V11-T3	V11-LM3	V11-T2	V11-M3	V11-T4	V11-B3	V11-T5	V11-LM4	V11-LM1	V11-B6
SiO2	56.19	51.28	48.35	48.44	45.84	48.86	48.7	46.83	50.67	48.43	50.12	47.98	48.24	46.77
Al2O3	11.68	12.83	13.83	14.01	13.69	13.39	15.08	14.58	13.26	15.18	15.69	14.77	13.94	14.45
Fe2O3	10.58	12.4	13	14.29	14.73	14.32	10.64	11.1	12.77	11.87	9.94	13.12	12.15	12.52
MgO	4.43	7.38	5.62	6.89	7.59	6.56	8.41	8.82	7.19	8.14	7.77	8.13	8.05	7.98
CaO	8.57	7.8	9.62	9.12	8.97	8.66	10.45	11.6	8.33	8.46	9.83	8.24	9.14	9.52
Na2O	1.79	1.09	1.65	2.74	1.3	1.36	0.91	1.97	1.13	3.49	1.21	1.2	1.47	2.46
K2O	0.796	3.092	2.678	0.501	2.764	2.485	2.557	0.615	2.87	0.679	2.55	2.742	2.741	0.861
TiO2	1.343	1.839	2.115	2.187	2.181	2.108	0.952	1.404	1.899	1.758	0.883	1.584	1.499	1.901
MnO	0.482	0.288	0.166	0.224	0.312	0.214	0.217	0.217	0.275	0.208	0.199	0.19	0.19	0.192
P2O5	0.136	0.15	0.162	0.212	0.174	0.23	0.036	0.117	0.153	0.242	0.04	0.12	0.125	0.191
LOI	4.05	1.93	2.9	1.8	1.73	1.8	2.05	3.11	1.97	1.94	2.05	2.22	2.78	3.31
Total	100.05	100.07	100.09	100.42	99.29	99.99	100.01	100.36	100.52	100.4	100.27	100.28	100.33	100.16
Ni	70.1	81.4	52	71.6	74.5	53.7	158	149.3	70.2	59.6	154.7	94.6	82.2	84.9
Cr	130.3	164	96.9	140.4	135.3	133.5	378.2	372	169.6	271.7	365.1	251.3	204.1	250.2
V	288.5	372.2	472	484.5	453	471	254.1	321.2	406.9	372.5	244.9	408	350.9	396.8
Sc	27	52.5	51.2	52.8	57.6	50	43.9	43.6	48.3	46.9	38.4	56	47.3	47.8
Cu	84.3	11.6	49.7	65.6	24.8	46.9	9.7	197.3	16.4	35.8	12.2	30.4	39.8	67.4
Zn	109.7	143.6	117.9	122.1	166.3	121.6	114.1	97	135.7	167.1	105.5	114.5	104.7	121.7
Sr	187.2	91.9	248.3	151.6	118.8	264	183.4	154	120.4	104.9	180.8	92.8	120.9	99.8
Rb	24.8	82	86.4	13.2	69.7	78.3	69.4	15.3	75.5	19.6	70.5	93.1	85.7	23.4
Zr	108.7	121.2	134.8	139.2	144.8	137.2	64.6	87	121.2	130.9	71.5	95.6	101	133.9
Nb	5.2	3.8	3.2	3.1	4.1	4.3	2.9	2.5	3.6	5.7	3.8	2.5	3.9	3.6
Ba	152.3	683.3	358.5	53.2	649.2	370.3	510.8	40.7	640.2	32.5	495	364.5	348.7	74.1
Pb	13.1	4.5	16.9	8.5	2.9	12.4	13.8	2.2	4.5	0.8	8.3	6.7	5.5	4.5
Th	3.1	1.7	1.7	2.8	2.6	3.6	3.9	1.9	2.2	2.2	2.6	3	1.4	2.2
La	10.5	0.5	2.4	-2.8	6.4	0.9	4.7	-0.2	4.2	6.5	12.1	0.3	-1.5	-1.3
Ce	20.2	13.3	11.1	15	11.1	5.6	24.6	4.7	5.1	19.2	13.2	9.7	5.8	18.5
Nd	15.2	13.2	13	17.6	14.3	12.3	17.8	9.1	11	16.3	15.2	8.4	9.1	15.2
Y	40.6	44.1	49.2	56.9	56.2	53.8	41	37	45.3	41.2	39.8	39.7	38.5	46.8

X-Ray Fluorescence data for samples from the Likostomo-Promachi Amphibolites that were used in tectonic discrimination diagrams.

APPENDIX **THE LIKOSTOMO-PROMACHI AMPHIBOLITES**

	V11-B5	V11-M2	V11-UM1	V11-B8	V11-M1	V11-B4	V11-B2	V11-B7	V11-B1	V11-UM1	V11-M2
SiO2	47.76	47.53	47.52	47.13	44.05	48.45	45.91	49.38	45.68	47.78	47.45
Al2O3	14.4	15.01	13.57	14.47	14.01	13.64	14.26	13.85	14.08	13.6	14.99
Fe2O3	13.48	10.9	14.17	13.14	11.26	13.31	13.84	12.92	13.22	14.33	10.84
MgO	8.43	8.76	6.91	8.06	9.45	8.29	8.99	8.11	8.74	6.92	8.83
CaO	8.4	10.02	9.56	9.37	11.16	8.95	9.13	8.01	9.96	9.63	10.03
Na2O	2.77	2.42	2.63	3.43	2.68	2.96	3.08	3.25	2.22	2.63	2.38
K2O	0.515	0.903	0.53	0.498	0.478	0.366	0.362	0.292	0.685	0.529	0.899
TiO2	2.19	1.397	2.146	2.105	0.878	2.041	2.244	1.928	2.221	2.162	1.407
MnO	0.205	0.185	0.228	0.215	0.216	0.211	0.219	0.196	0.198	0.229	0.191
P2O5	0.141	0.1	0.205	0.188	0.079	0.159	0.151	0.178	0.168	0.206	0.1
LOI	1.76	3.09	2.17	1.87	5.99	1.86	2.03	1.79	3.08	2.12	3.06
Total	100.05	100.31	99.65	100.47	100.26	100.25	100.21	99.9	100.25	100.12	100.19
Ni	67.2	154.1	71.5	80.3	295.9	75.8	71.9	56.3	84.7	71.5	154.1
Cr	232.3	293.6	139.1	261	820.6	236.3	290	169.5	295.1	139.1	293.6
V	435	375.7	470.7	414.9	228.6	413.4	423.6	413.8	428.6	470.7	375.7
Sc	53.6	45.3	54.9	50.2	31.9	53.8	52.1	48.4	51	54.9	45.3
Cu	118.2	50.3	69.4	41.9	163.5	129.6	128.4	101.9	80.2	69.4	50.3
Zn	153.9	109	122.9	138.5	103.4	168.4	218	162.5	129.9	122.9	109
Sr	80.6	135.1	137.4	97.1	85.7	97.3	64.8	59.8	123.5	137.4	135.1
Rb	12.3	18.2	13.4	14.6	11.8	6.9	6	4.9	17.3	13.4	18.2
Zr	142.6	111.5	138.3	137.3	67.2	138	143.4	146.4	147.9	138.3	111.5
Nb	3.4	4	2.5	3.6	2.3	3.9	3	3	4.3	2.5	4
Ba	40	65.7	60.4	48.7	33.5	12.4	18.7	20.6	56	60.4	65.7
Pb	4.7	6.1	8.8	2.7	2.1	4.2	1.1	2.2	7	8.8	6.1
Th	2.9	1.3	2.8	2.3	3.1	2.5	2.5	1.4	3.4	2.8	1.3
La	-0.9	-1.3	-0.2	4.6	9.2	-0.2	-0.4	3.3	0.3	-0.2	-1.3
Ce	20.9	13.7	11.2	18.2	11.8	10	7.9	22	16.2	11.2	13.7
Nd	18.4	12.6	12.1	15.9	9.8	13.8	15.2	14.5	17.5	12.1	12.6
Y	50.5	45.4	56.7	46.9	26.6	46.7	50.4	46.6	51.9	56.7	45.4

X-Ray Fluorescence data for samples from the Likostomo-Promachi Amphibolites that were used in tectonic discrimination diagrams.

APPENDIX

THE PORTA-TZENA ANDESITES

	V156a/1	V156a/2	V156a/3	V156a/4	V156a/5	V156a/6	V156a/7	V156a/8	V156a/9	V156a/10	V156a/13	V156a/14	V156a/15	V156a/16
SiO2	63.63	50.97	60.63	64.68	61.95	67.28	69.25	68.46	63.73	65.81	59.82	65.71	62.22	68.9
Al2O3	12.26	15.88	13.03	11.64	12.56	11.35	10.03	10.27	12.72	11.64	13.09	11.22	12.28	10.53
Fe2O3	8.81	12.94	10.4	9.47	9.72	8.09	7.66	7.79	8.63	8.67	10.73	9.25	9.99	7.85
MgO	1.54	3.89	1.17	1.6	2.4	1.95	1.82	1.77	1.19	2.39	2.97	3.09	2.64	1.69
CaO	10.68	11.04	11.45	9.42	9.04	7.73	8.14	8.39	11.02	7.49	9.21	6.45	9.05	7.98
Na2O	0.13	0.23	0.27	0.25	0.62	0.81	0.12	0.16	0.36	0.91	0.38	0.65	0.19	0.47
K2O	0.017	0.149	0.007	0.025	0.059	0.034	0.002	0	0.01	0.033	0.039	0.082	0.054	0.009
TiO2	0.456	0.824	0.481	0.467	0.672	0.458	0.442	0.467	0.475	0.496	0.578	0.522	0.583	0.448
MnO	0.276	0.486	0.304	0.305	0.403	0.347	0.444	0.453	0.311	0.364	0.416	0.389	0.407	0.34
P2O5	0	0	0.012	0.001	0.002	0.002	0.01	0.001	0.001	0.002	0.002	0	0.001	0.001
LOI	1.99	3.32	2.29	2.15	2.38	1.86	1.94	1.86	1.75	2.21	2.83	2.46	2.48	1.88
Total	99.79	99.73	100.04	100.01	99.81	99.91	99.86	99.62	100.20	100.02	100.07	99.82	99.90	100.10
Ni	3.7	9.2	4.4	4.7	6.9	5.9	7.7	6.3	3.2	6.7	7.8	7.1	8.8	4.5
Cr	27.2	38.9	27.4	24	27.5	21.6	20.4	27.9	28.3	23.5	29.1	22.3	25.9	22.9
V	526.8	681.5	555.2	480.7	525.7	449.2	487.4	398.1	546.8	430.6	551.2	449.5	487.6	443.4
Sc	36.8	69.4	45	48	58.2	38.6	41.6	34.9	42.7	43.7	46.4	45.1	55.6	39.9
Cu	37.5	56.8	55	48.7	47.6	57.1	246.9	58.4	57.2	36.7	44.4	36.8	49.1	32.8
Zn	209.5	510.6	354.8	419.5	565.2	466	678.7	302.3	292.5	558.6	354.8	382.4	345.7	219.9
Sr	258.2	288.3	241.6	192.3	207.3	174	214.5	202.5	242.1	170.2	245	173.4	226.4	213.2
Rb	0.5	1.1	0.1	0.5	0.5	0.1	0.8	0.5	0.4	0.3	0.3	0.8	0.7	0.1
Zr	22.9	38.2	22.5	21.6	31.3	21.7	23.3	22	23.1	23.2	27.9	23.9	27.2	22
Nb	0.1	0.4	0.3	0.1	0.5	0.1	0.2	0.1	0.2	0.5	0.1	0.5	0.5	0.1
Ba	2.8	19.6	0.1	4	0.1	2.7	0.1	1.1	0.1	0.9	7	0.6	0.1	0.1
Pb	29	42.1	21.7	19.4	28.6	22.8	19	43.3	29.7	22.7	49.4	37.5	39	44.8
Th	2.2	4.9	2.5	3.1	1.2	1.1	1.5	1.5	1.7	1.2	3.2	0.7	2	0.1
La														
Ce	13	14.3	7	7.1	14.7	5.5	4.7	11.9	7.9	11.6	15	5.2	9.8	13.5
Nd	11.4	7.5	9.6	5.8	8.4	8.3	6.2	4.3	11.1	7.7	8.5	7.8	6.8	8.5
Y	32.8	44.3	23	20.7	34.7	23.3	31.4	30	25.1	24	35.5	28.5	36.9	29.3

X-Ray Fluorescence data for samples from the Porta-Tzena Andesites that were used in tectonic discrimination diagrams.

APPENDIX

THE IMBRICATE LAVAS BETWEEN PINOVON & ANO GAREFI

	V156a/17	PIL/1	PIL/3	PIL/5	PIL/7
SiO2	66.65	48.7	48.89	47.82	47.03
Al2O3	11.11	14.37	13.78	13.99	14.54
Fe2O3	8.69	12.51	12.53	12.66	12.39
MgO	2.18	7.03	7.37	7.62	6.76
CaO	7.96	8.27	8.14	8.68	8.7
Na2O	0.41	3.03	2.66	2.67	3.06
K2O	0.089	0.189	0.483	0.546	0.562
TiO2	0.486	1.796	1.861	1.844	1.821
MnO	0.336	0.18	0.182	0.185	0.236
P2O5	0.003	0.143	0.15	0.148	0.146
LOI	1.98	3.95	3.87	4.04	4.62
Total	99.9	100.17	99.92	100.20	99.87
Ni	7	54.2	54.5	58.7	92.7
Cr	19.6	169.9	171.2	169.2	275.4
V	391	349.2	338.9	343.3	338.6
Sc	32	44.6	45.9	45.7	47.1
Cu	338.9	47.1	64.9	70.8	71.1
Zn	658.6	102.7	101.7	103	111.9
Sr	194.5	27.8	42.7	49	52.2
Rb	0.3	5.8	13.6	16.4	17.2
Zr	21.9	124.3	127.9	127.3	121.1
Nb	0.2	3.8	4	3.9	3.7
Ba	4	13	30.9	32.2	38.8
Pb	20.8	1.1	0.2	1.5	1.3
Th	0.9	3.7	2.3	2.8	3.6
La		-0.2	2.4	1	-2.8
Ce	8.9	10.3	11.5	17.4	18.1
Nd	8.7	12.9	15.1	15.2	16.7
Y	31.2	39.2	40	39.9	38.7

X-Ray Fluorescence data for samples from the Pinovon Imbricate Lavas that were used in tectonic discrimination diagrams